NASA CR 137916
REPORT NUMBER MDC A4318
CONTRACT NUMBER NAS2-8655

WIND TUNNEL AND GROUND STATIC INVESTIGATION OF A LARGE SCALE MODEL OF A LIFT/CRUISE FAN V/STOL AIRCRAFT

MCDONNELL AIRCRAFT COMPANY

MCDONNELL DOUGLAS CORPORATION

NASA CR 137916

Copy number //

Report number MDC A4318

WIND TUNNEL AND GROUND STATIC INVESTIGATION OF A LARGE SCALE MODEL OF A LIFT/CRUISE FAN V/STOL AIRCRAFT

Issue date 2 August 1976

Contract number NAS2-8655

MCDONNELL AIRCRAFT COMPANY

Box 516, Saint Louis, Missouri 63166 – Tel. (314)232-0232

MCDONNELL DOUGLAS CORPORATION

SUMMARY

An investigation was conducted in the NASA Ames 40-foot by 80-foot Wind Tunnel and Outside Static Test Facility to determine the aerodynamic/propulsion characteristics of a Large Scale Powered Model of a Lift/Cruise Fan V/STOL Aircraft. The model, designed by McDonnell Aircraft Company under Contracts NAS2-5499 and NAS2-8655 for Ames Research Center, was equipped with three 36-inch diameter turbotip X376B fans powered by three T58 gas generators furnished by NASA. The lift fan was located forward of the cockpit area and the two lift/cruise fans were located on top of the wing adjacent to the fuselage. The three fans with associated thrust vectoring systems were used to provide vertical, and short, takeoff and landing capability. For conventional cruise mode operation, only the lift/cruise fans were utilized.

The data that were obtained include lift, drag, longitudinal and lateral-directional stability characteristics, and control effectiveness. Data were obtained up to speeds of 120 knots at one model height of 20 feet for the conventional aerodynamic lift configuration and at several thrust vector angles for the powered lift configuration. Outside static tests to investigate ground proximity effects were conducted at three model-above-ground heights (H/D = 1.02, 2.55, 6.45).

Significant test results include:

- Induced lift up to 10% of gross thrust and negative induced drag for operational powered lift configurations of the complete three-fan model,
- Large induced lift values (up to 170% of gross thrust) with the nose lift unit inoperative and the lift/cruise units operating at 90° vectoring angles,
- Less than 1% total lift loss due to ground proximity, and
- Strong effects on inlet hot gas reingestion levels by varying thrust vector and splay angles and inlet shield configuration, thus indicating availability of positive ways to eliminate any operational problems.

The results presented in this report show qualitative effects and trends which are applicable to higher pressure ratio fan systems.

TABLE OF CONTENTS

TABLE OF CONTENTS (Continued)

List of Pages

LIST OF FIGURES

LIST OF FIGURES (Continued)

LIST OF FIGURES (Continued)

LIST OF FIGURES (Continued)

LIST OF FIGURES (Continued)

LIST OF FIGURES (Continued)

LIST OF FIGURES (Continued)

LIST OF FIGURES (Continued)

LIST OF FIGURES (Continued)

SYMBOLS AND NOMENCLATURE

GENERAL SYMBOLS

Symbol	Description	Units
A_{HL}	Fan inlet highlight area	m^2 (ft^2)
A_N	Nozzle exit area	m^2 (ft^2)
A_O	Fan inlet capture area	m^2 (ft^2)
A_{TH}	Throat area	m^2 (ft^2)
ASW	Antisubmarine warfare	---
b	Wing span	m (ft)
B.L.	Butt line	m (in)
c	Chord	m (in)
$\bar{c}$	Mean aerodynamic chord	m (ft)
C_D	Drag coefficient (D/qS)	---
C_F	Thrust calibration coefficient $(F_S/\delta_A)/(F_I/\delta_A)$	---
C_ℓ	Rolling moment coefficient (ℓ/qSb)	---
C_{ℓ_β}	Lateral stability parameter ($\partial C_\ell/\partial\beta$)	per degree
C_L	Lift coefficient (L/qS)	---
C_m	Pitching moment coefficient about $\bar{c}/4$ ($m/qS\bar{c}$)	---
C_n	Yawing moment coefficient (n/qSb)	---
C_{n_β}	Directional stability parameter ($\partial C_n/\partial\beta$)	per degree
C_Y	Side force coefficient (Y/qS)	---
C_{Y_β}	Side force parameter ($\partial C_Y/\partial\beta$)	per degree
D	Drag or nozzle exit diameter	N (lb) or m (ft)
DF1	Distortion factor $(P_{T_{max}}-P_{T_{min}})/P_{T_{AVG}}$	---
F_G	Gross thrust at forward speed	N (lb)
$F_{G_{LC}}$	Gross thrust of lift/cruise unit	N (lb)
$F_{G_{NL}}$	Gross thrust of nose lift unit	N (lb)

Symbol	Description	Units
F_I	Ideal gross thrust	N (lb)
F_N	Net thrust	N (lb)
F_S	Static thrust	N (lb)
F.S.	Fuselage Station	m (in)
g	Acceleration of gravity	m/s^2 (ft/sec^2)
GE	General Electric	---
H	Model height above ground measured from lift cruise nozzle exit.	m (ft)
ℓ	Rolling moment	N-m (ft-lb)
L	Lift	N (lb)
LC	Lift cruise	---
LSAB	Large Scale Aerodynamics Branch	---
m	Pitching moment	N-m (ft-lb)
MCAIR	McDonnell Aircraft Company	---
n	Yawing moment	N-m (ft-lb)
N_F	Fan speed	RPM
N_{GG}	Gas generator fan speed	RPM
NPR	Nozzle total pressure ratio	---
P	Static Pressure	N/m^2 (psi)
P_A	Ambient static pressure	N/m^2 (psi)
P_T	Total pressure	N/m^2 (psi)
q	Freestream dynamic pressure ($1/2\rho_o V_o^2$)	N/m^2 (psf)
R	Radius	m (in)
RC	Reference Center	---
$RPM/\sqrt{\theta}_{T_O}$	Corrected fan rotational speed	---
S	Wing area	m^2 (ft^2)
T_T	Total temperature	°K(°R)
T/C	Thermocouple	---

Symbol	Description	Units
TEL/TER	Trailing edge left/right	---
TEU/TED	Trailing edge up/down	---
T_J	Jet total temperature	°C (°R)
V_J	Jet velocity	m/sec (ft/sec)
V_{TH}	Velocity at the throat	m/sec (ft/sec)
V_o	Freestream velocity	m/sec (ft/sec)
(V_o/V_J)	Jet velocity ratio	---
VTO	Vertical takeoff	---
V/STOL	Vertical/short takeoff and landing	---
$\dot{w}$	Airflow rate	kg/sec (lb_m/sec)
W.L.	Waterline	m (in)
W/M	Windmilling	---
Y	Side force	N (lb)

GREEK SYMBOLS

α	Angle of attack	deg
β	Angle of sideslip	deg
Δ	Incremental	---
Δ_{T_i}	Inlet temperature rise ($T_{T_2} - T_{T_0}$)	°C(°F)
ΔT_j	Jet temperature rise ($T_J - T_{T_0}$)	°C(°F)
δ_a	Aileron deflection (positive is TED)	deg
δ_{aL}	Left aileron deflection	deg
δ_{aR}	Right aileron deflection	deg
δ_A	Relative static pressure (P/14.696)	---
δ_f	Flap deflection (positive is TED)	deg
δ_H	Horizontal tail deflection (positive is TED)	deg
δ_{LC}	Lift cruise unit geometric deflection	deg

Symbol	Description	Units
δ_{NL}	Nose lift unit geometric deflection	deg
δ_R	Rudder deflection (positive is TEL)	deg
δ_S	Inlet shield deflection angle	deg
δ_T	Relative total pressure ($P_T/14.696$)	---
δ_Y	Nozzle yaw vane deflection (positive TEL)	deg
θ_J	Resultant thrust vector angle	deg
θ_{LC}	Lift cruise unit thrust deflection angle	deg
θ_{NL}	Nose lift unit thrust deflection angle	deg
θ_T	Relative total temperature ($T_T/518.7$)	---
$\Lambda_{c/4}$	Sweep angle	deg
ρ_o	Freestream density	deg

SUBSCRIPTS

0	Freestream
1	Inlet throat
2	Fan entrance
3	Fan exit

1. INTRODUCTION

1.1 BACKGROUND

McDonnell Aircraft Company (MCAIR), a division of McDonnell Douglas Corporation, over the past several years has conducted a comprehensive analysis of V/STOL aircraft designs. One of the configurations analyzed, a lift/cruise fan multimission aircraft with interconnected propulsion units, provides significant advancements in V/STOL aircraft performance and operational capabilities. Large improvements are provided in payload/range, speed, altitude, safety, reliability and maintainability which are not presently achievable in either rotary wing or other proposed V/STOL vehicles. This interconnected lift/cruise fan concept can satisfy the military needs for V/STOL multimission aircraft as well as many civil needs for utility aircraft for support of construction, lumbering, oil exploration or development sites located in areas difficult to reach rapidly by other modes of transportation.

The MCAIR lift/cruise fan aircraft is a fixed wing vehicle powered by three identical turbotip driven fans that are pneumatically interconnected to each other and to two (or three) gas generators (depending on the specific aircraft design) during the powered lift flight mode. During cruise mode operation the gas generators power only the two over-the-wing lift/cruise fans. This unique application of flight proven lift fans provides a variable bypass ratio propulsion system which maximizes lift and control during VTO, provides excellent short takeoff characteristics, allows efficient engine matching for cruise and loiter, and provides for retention of symmetrical thrust, good control margins and vertical landing capability during one-engine-out operation.

Recognizing the need for development of technology for such V/STOL multimission aircraft for Naval purposes that also may serve many future civil-utility aircraft requirements, the NASA Ames Research Center, with Navy support, contracted with MCAIR to design a large scale powered model for test in the NASA Ames 40 foot by 80 foot wind tunnel. The initial design work was performed under Amendment No. 19 to Contract NAS2-5499. The remainder of the effort was done under Contract NAS2-8655. The model was to be approximately 0.7 scale of a potential Navy multimission aircraft and was to utilize fans and gas generators already existing in the NASA test hardware inventory. In addition, the contract covered engineering liaison support during fabrication of the model in the NASA Ames shops, engineering and technical support during the active test phases, data reduction

and analysis, and reporting of the results. This document is the final report of these activities. In addition, a NASA data report (Reference 1) was published shortly after completion of the tests.

1.2 40' X 80' WIND TUNNEL TESTS

The main objectives of the tests in the 40' x 80' wind tunnel included assessment of:

- o Powered flight characteristics,
- o Aerodynamic flight characteristics, power on and off, tail on and off, and
- o Propulsion air induction system characteristics.

The powered lift test data, from zero speed through transition, were used to evaluate flight procedures and vectoring schedules during transition and to establish aerodynamic-propulsion induced effects and flow fields with varying fan thrust, thrust vector angles, jet velocity ratios, and combined powered and aerodynamic control inputs. Longitudinal and lateral-directional characteristics in the loiter and cruise flight modes were established from the aerodynamic test data. The propulsion system test data were used to establish distortion profiles and inlet performance throughout the test operating range. Test variables included angle of attack, sideslip angle, fan thrust, thrust vector angles, tunnel airflow velocity, aerodynamic control deflections, and simulated powered lift control inputs.

1.3 OUTSIDE STATIC TESTS

The outside static test program included ground effects testing and propulsion system calibration tests. The ground effects test program included tests at 21.0, 8.3, and 3.3 foot heights and measured the total installed lift loss and inlet re[illegible]gestion characteristics of the model. The calibration tests included the [illegible]ner[illegible]on of a fan performance map and tests of each lift unit for comparison with the static calibrations done in the 40' x 80' tunnel. Flow field visualization tests were also conducted utilizing smoke. Force and moment data, fan and gas generator performance data, and inlet performance data were recorded during the te[illegible]t program.

2. MODEL DESCRIPTION

The aircraft model tested in this program was a large scale (approximately 70%) powered model of a subsonic fixed wing lift/cruise fan V/STOL aircraft concept configured originally for the Navy ASW mission. This configuration was the result of several design compromises required to provide multimission adaptability for operational usage aboard the Navy's VSS, LHP, LHA, and DD 963. Aerodynamic refinements of this design were based on small scale model low speed and high speed wind tunnel test data. These data were incorporated into a mathematically accurate definition of the complete aircraft mold line surface through use of the MCAIR Computer Aided Design Drafting (CADD) interactive graphics system. While the standard construction functions were used to initiate this effort, it was refined through extensive use of the Parametric Cubic (PC) curve and PC patch routines to arrive at PC surface definition.

For the model design the full scale mold line definition was reduced to 70% of full scale. Model construction of a tubular truss type structure with local rings supporting the combination metal and fiber glass mold line skins was selected in order to reduce costs by allowing relatively loose tolerances of the structure with reasonably accurate control of the external mold line shapes. Cuts were made at appropriate stations as determined by the model layout drawings for headers, ribs, longerons, etc.; details and reference line information were added, and drawings were hard-copied on stable Mylar. Part number callouts, hole sizes, and parts list were added manually along with small detail cuts to obtain the level of information required for hardware manufacture and model assembly at NASA Ames. The main features of the model included three gas generator driven turbotip fans, and variable geometry for all control surfaces and vectoring system components. A photo of the model is shown in Figure 2-1. The size and detail design of the model were based on utilizing existing propulsion system components, including the gas generators, turbotip fans, and vectoring system components supplied by NASA Ames. The physical size and performance characteristics of the T58-GE-8B gas generator and low pressure ratio (1.08) GE-X376B turbotip fan were the predominant considerations in sizing the model. Based on performance estimates of this system, a model scale was selected to provide inlet velocity ratios (V_O/V_{TH}) typical of full scale higher pressure ratio fan systems during jet velocity ratio (V_O/V_J) excursions. A schematic of the model illustrating the major propulsion system components is shown in Figure 2-2. The model had an overall length of 10.26 meters (33.7 ft), a span of 8.68 meters (28.5 ft) and a height of 2.76 meters

FIGURE 2-1
LARGE SCALE POWERED MODEL OF A LIFT/CRUISE FAN
V/STOL AIRCRAFT CONCEPT

FIGURE 2-2

LARGE SCALE POWERED MODEL PROPULSION SYSTEM

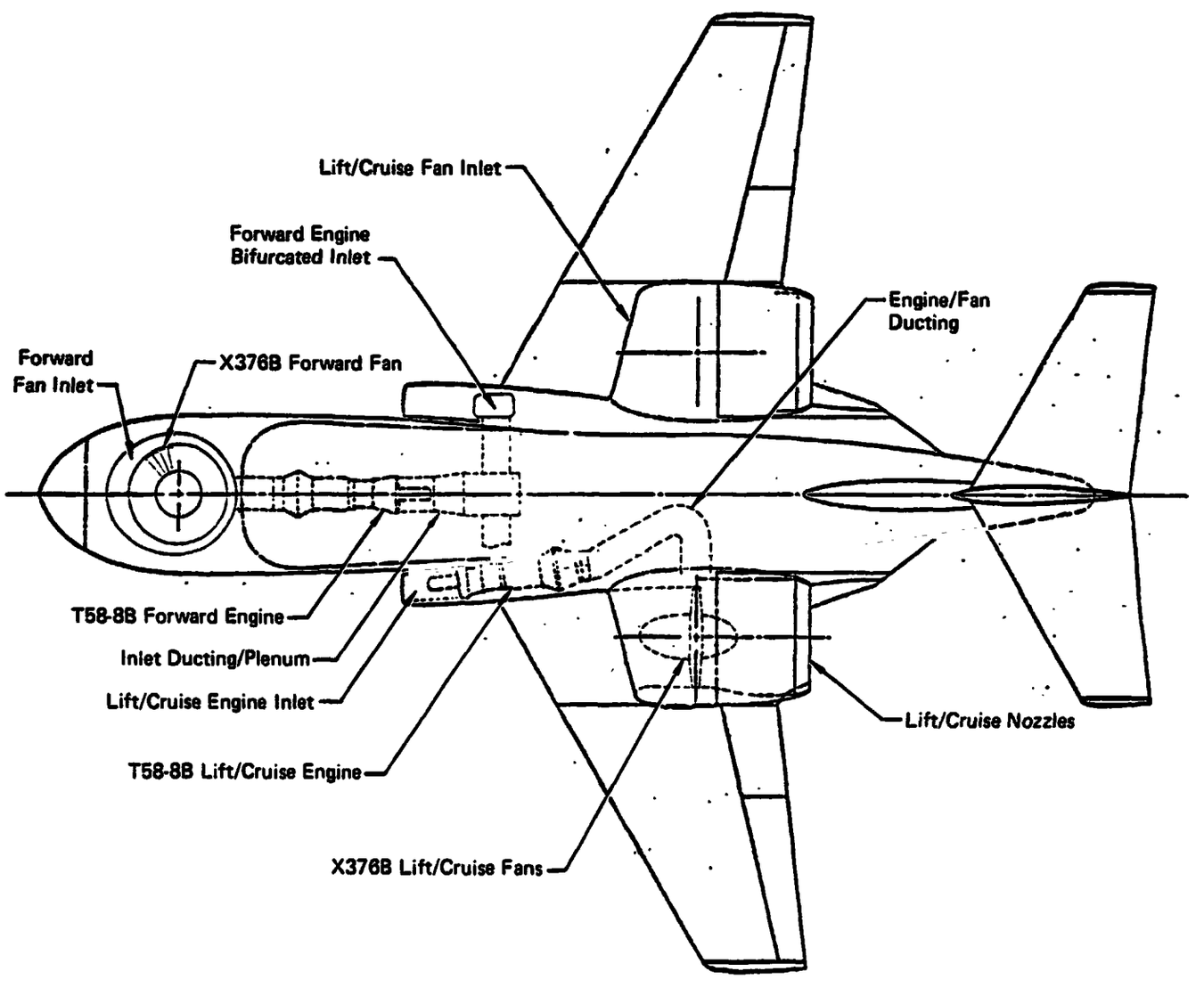

(11.9 ft). The basic geometry and overall dimensions of the model configuration are shown in Figure 2-3. Descriptions of the airframe and propulsion system components are presented below.

2.1 FUSELAGE

The basic fuselage shape of the aircraft accommodates side-by-side seating in the forward fuselage, and provides the necessary volume in the center fuselage for satisfying the needs of the multimission role. This wide bodied design allows for the installation of the lift fan unit in the forward fuselage section of the aircraft.

The fuselage section of the test model contained the main support truss, which in turn supported the wings, tail section, and turbotip fan units. The three gas generators, interconnect ducting, fuel distribution lines, lubrication system, instrumentation, fire extinguisher system and forced air cooling lines were all housed within the fuselage. Vent louvers were installed on the lower and upper surfaces of the fuselage to provide internal cooling air for the test model.

2.2 WING

The design concept incorporated a low wing with the lower surface flush with the bottom of the center fuselage. The basic wing had an aspect ratio of 4.5, a taper ratio of 0.30, and a quarter chord line sweep of 25°. Total wing planform area was 16.75 m^2 (180.3 ft^2). Further details of the wing geometry are given in Figure 2-3. The basic wing had different airfoil sections inboard and outboard of the lift/cruise fan nacelle/wing intersection. The inboard wing panel had an NACA 4416 airfoil section at B.L. 37.8, and the outboard wing panel used modified supercritical airfoil sections at root and tip. The transitions between these three specified stations were straight line elements. Coordinates of the wing airfoil sections are presented in Figure 2-4.

The control surfaces consisted of plain flaps and ailerons both hinged at the 75% chord line. The flaps had specific deflection angles of 0°, 15°, 30° and 45° and were manually positioned. The ailerons had a deflection range of ± 25° and were remotely operated.

2.3 EMPENNAGE

The aircraft empennage consisted of a "T" tail configuration with a movable horizontal stabilator and fixed vertical stabilizer. The geometry of the vertical and horizontal tail is presented in Figure 2-3. Both the vertical and horizontal tail components were detachable from the model for tail-off testing.

FIGURE 2-3
LARGE SCALE POWERED MODEL
Basic Geometry

	Wing	Horizontal Tail	Vertical Tail
Area, m^2 (ft^2)	16.572 (180.32)	4.006 (43.12)	3.096 (33.32)
Aspect Ratio	4.500	3.665	0.688
Taper Ratio	0.300	0.405	0.433
b_m (ft)	8.682 (28.49)	3.832 (12.57)	1.459 (4.787)
C_{Root_m} (ft)	2.968 (9.738)	1.488 (4.882)	2.960 (9.711)
C_{Tip_m} (ft)	0.890 (2.920)	0.603 (1.978)	1.282 (4.206)
$\bar{C}_m$ (ft)	2.116 (6.942)	1.108 (3.635)	2.232 (7.323)
Λ C/4	25.00°	25.20°	45.50°

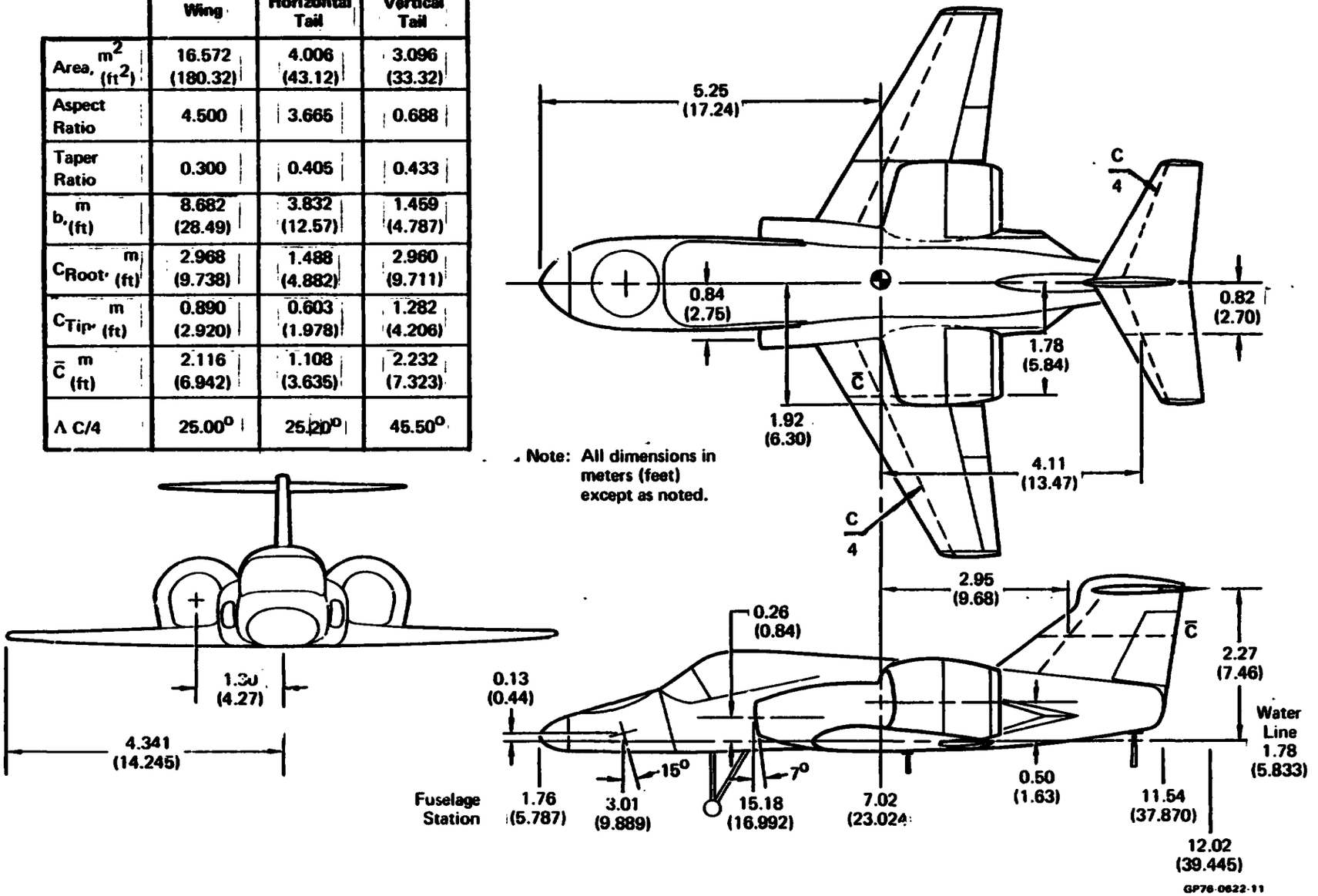

Note: All dimensions in meters (feet) except as noted.

FIGURE 2-4
LARGE SCALE LIFT/CRUISE FAN AIRCRAFT MODEL
Wing Airfoil Ordinates

Station	Exposed Root (0.221 $\frac{b}{2}$) NACA 4416		Wing Station (0.442 $\frac{b}{2}$) Modified, Supercritical, t = 14%c		Theoretical Tip (0.941 $\frac{b}{2}$) Modified, Supercritical, t = 8%c	
X, % Chord	Y_U, %c	Y_L, %c	Y_U, %c	Y_L, %c	Y_U, %c	Y_L, %c
0	0	0	0	0	0	0
1.25	3.275	−1.909	2.471	−2.467	1.422	−1.435
2.5	4.448	−2.645	3.233	−3.218	1.836	−1.840
5.0	6.123	−3.486	4.126	−4.069	2.307	−2.334
7.5	7.371	−3.957	4.729	−4.653	2.641	−2.678
10.0	8.363	−4.245	5.208	−5.099	2.902	−2.944
15.0	9.888	−4.459	5.945	−5.756	3.293	−3.335
20.0	10.933	−4.427	6.481	−6.177	3.569	−3.598
25.0	11.648	−4.245	6.878	−6.433	3.768	−3.766
30.0	12.000	−4.000	7.165	−6.560	3.904	−3.682
40.0	12.000	−3.467	7.478	−6.[illegible]5	4.029	−3.837
50.0	11.232	−2.901	7.494	−5.753	3.988	−3.531
60.0	9.920	−2.283	7.229	−4.503	3.789	−2.766
70.0	8.139	−1.653	6.662	−2.786	3.420	−1.465
80.0	5.920	−1.099	5.685	−1.091	2.829	−0.084
90.0	3.285	−0.608	3.980	−0.194	1.843	+0.496
95.0	1.781	−0.384	2.616	−0.210	1.090	0.342
100.0	0.171	−0.171	0.496	−0.447	0.108	0.214
LE Radius, %c	2.822		3.041		1.154	
Chord Length, m ft	2.409 (8.231)		2.049 (6.723)		0.891 (2.922)	
Incidence, deg	3.23		2.49		−2.77	

GP76-0862-253

The vertical tail utilized a basic NACA 65A010 airfoil section and was equipped with a moveable rudder. The rudder had nominal deflection angles of 0°, +10°, ±20°, and +30°, and was manually positioned.

The horizontal tail utilized a symmetrical NACA 64A0XX airfoil section with a thickness ratio of 0.10 at the root and 0.08 at the tip. The horizontal tail was a one-piece unit that was remotely operated, and had a deflection range of ±20°.

2.4 AIR INDUCTION SYSTEM

The model air induction system consisted of the lift/cruise fan inlets, the nose fan inlet, and gas generator inlets for each type fan installation as shown in Figure 2-3. A description of each inlet is presented below.

Lift/Cruise Fan Inlets

The lift/cruise fan inlets were located over the wing and adjacent to the fuselage in a fully integrated design concept. They were fixed geometry inlets with an internal contraction ratio (A_{HL}/A_{TH}) of 1.25. They had a 2:1 elliptical lip profile and cubic duct contours internally. A low drag modified elliptical cowl contour was used externally. The detailed geometry of the lift/cruise inlets is presented in Figure 2-5.

Lift/Cruise Gas Generator Inlet

The lift/cruise engine inlets were side mounted with fixed geometry. They also had an inlet contraction ratio of 1.25, a 2:1 elliptical lip shape internally, and low drag, modified elliptical cowl contours externally. For ease in fabrication, a straight-line-element conical duct was utilized internally. Parabolic boundary layer diverters were incorporated between the inlets and the fuselage. Details of the gas generator inlet geometry are presented in Figure 2-6. Details of the shields added as a means of reducing hot gas reingestion during operation at low ground heights are presented in Figure 2-7.

Nose Lift Fan Inlet

The nose fan inlet was located in the nose of the aircraft just downstream of the radome and forward of the canopy. It was a flush mounted inlet with an overall resultant contraction ratio (A_{HL}/A_{FAN}) of 2.09. The forward section of the inlet had a lip thickness ratio (Y/R_{HL}) of 0.30. [illegible]s decreased to a minimum thickness ratio of 0.20 at the sides, and remained a constant over the aft section of the inlet. Inlet turning vanes were not incorporated [illegible] design. It had a 1.4:1 elliptical lip profile at the leading [illegible] based to a 2:1 elliptical profile at the side. The 2:1 profile was [illegible] over the aft section of the inlet. Inlet closure doors were not included on this test model. For cruise

FIGURE 2-5
LIFT/CRUISE FAN INLET DESIGN GEOMETRY

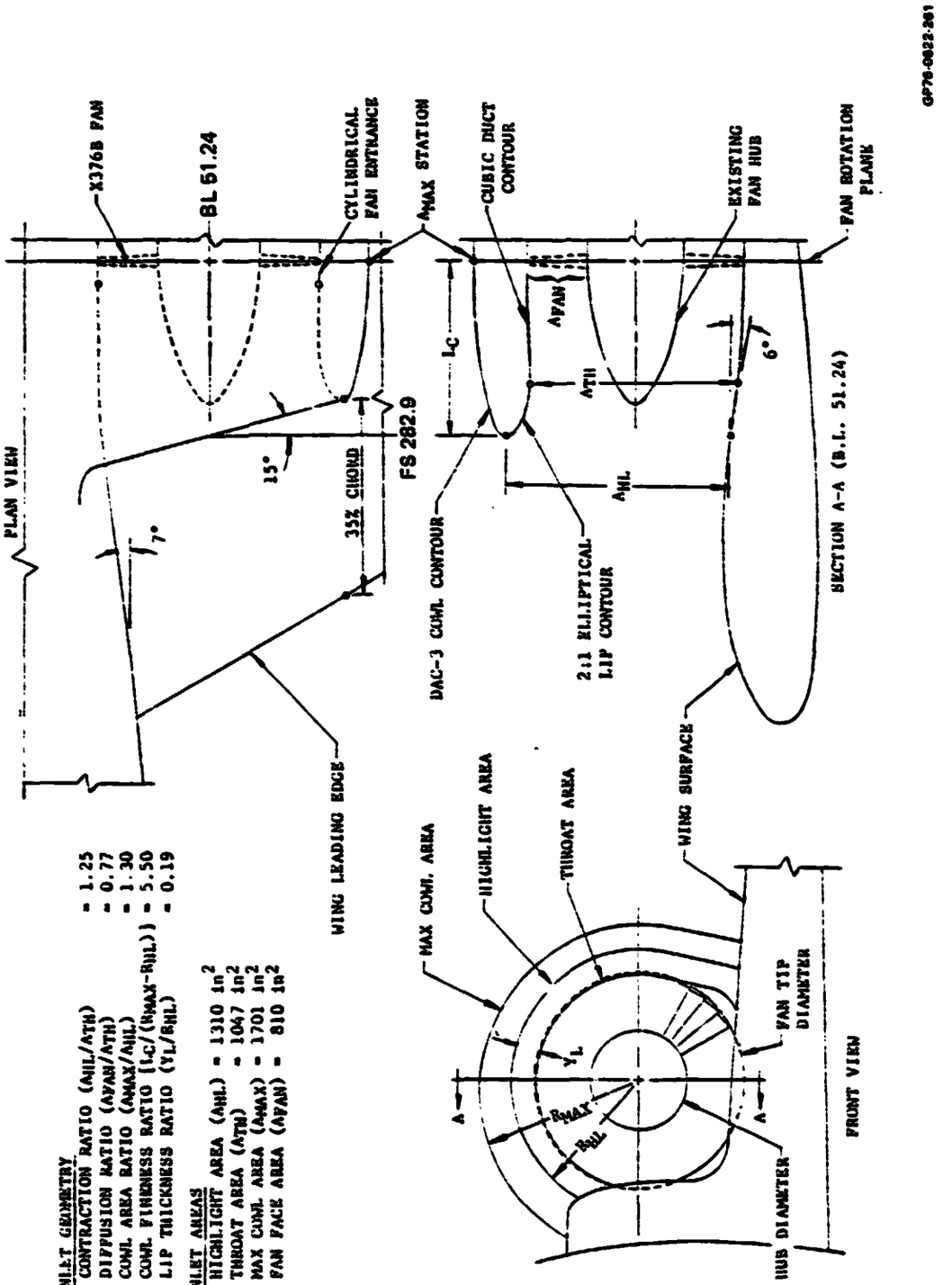

FIGURE 2-6
LIFT/CRUISE GAS GENERATOR INLET DESIGN GEOMETRY

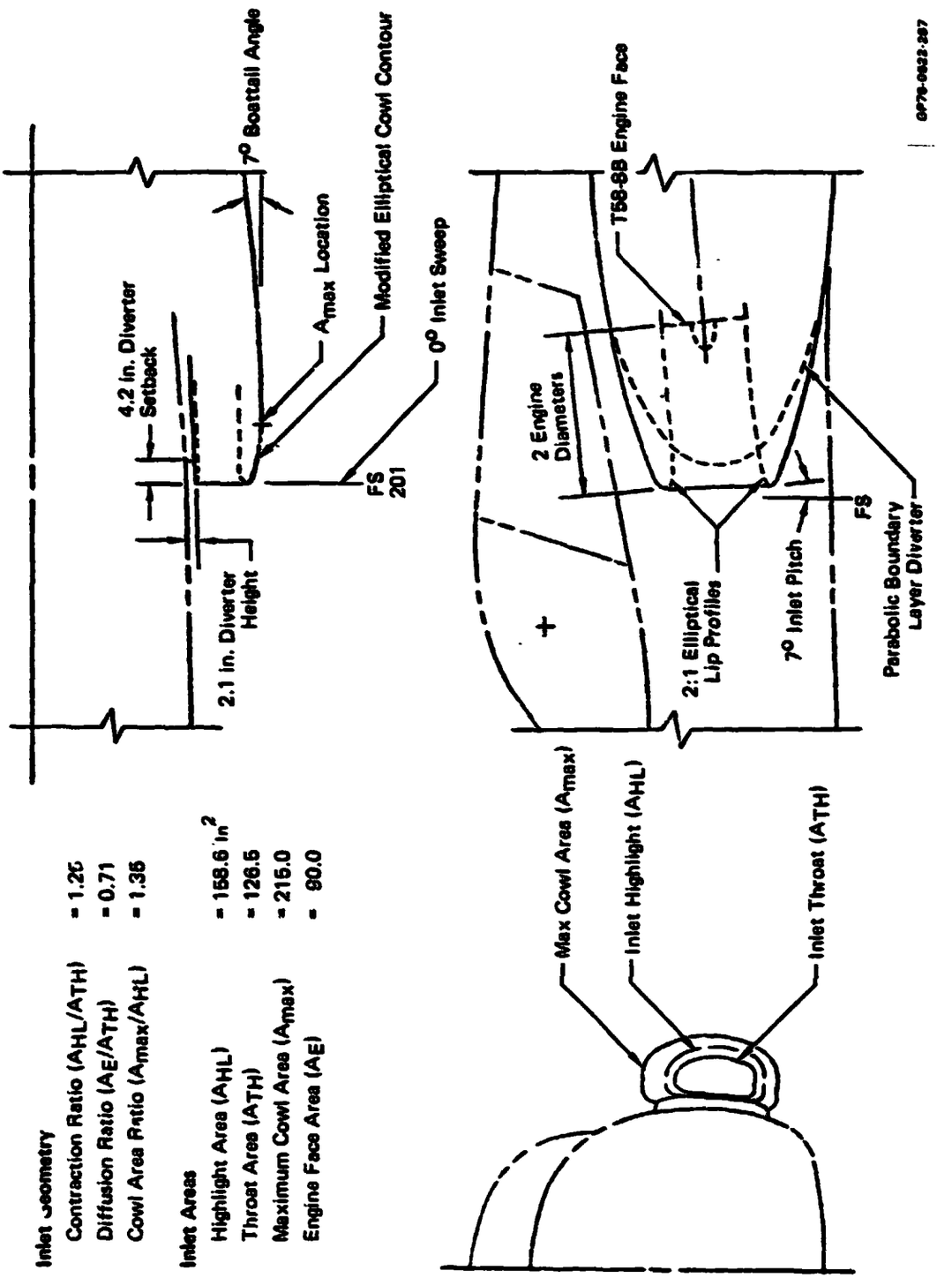

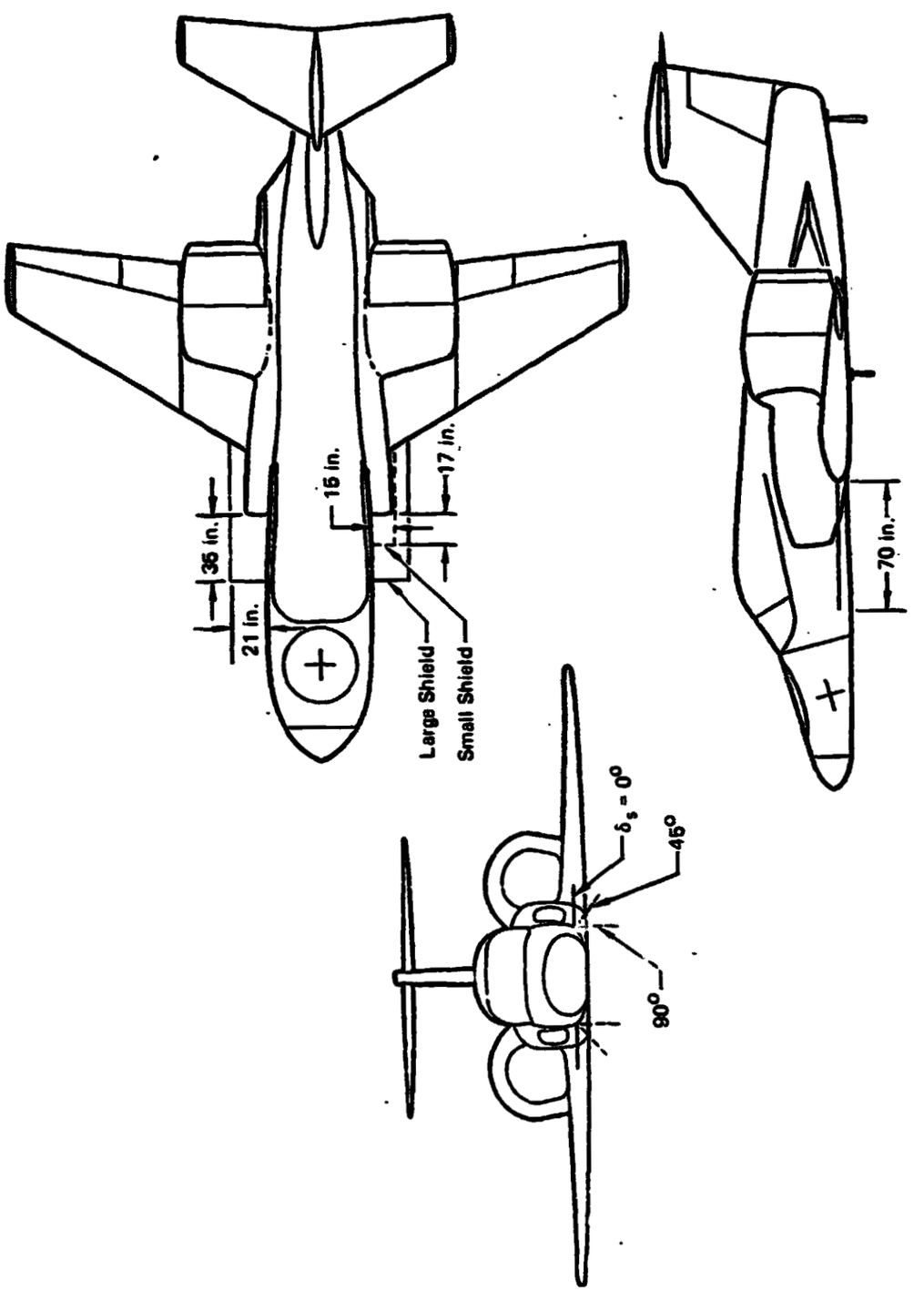

FIGURE 2-7
GAS GENERATOR INLET SHIELD GEOMETRY

mode testing (nose fan off), an inlet closure panel was installed on the inlet. Details of the nose lift fan inlet geometry are presented in Figure 2-8.

Nose Fan Gas Generator Inlet

The nose fan gas generator inlet design consisted of two flush mounted inlets, each ducted into a common plenum located upstream of the aft facing gas generator. The inlets were located on the upper surface of the lift/cruise gas generator nacelles at the approximate wing leading edge station. Each inlet had a contraction ratio (A_{HL}/A_{TH}) of 4.0 and a diffusion ratio (A_{PLENUM}/A_{TH}) into the plenum of 1.5. All inlet lip shaping consisted of 2:1 elliptical profiles with varying lip thickness around the periphery. For cruise mode testing, inlet closure panels were installed on each inlet. Details of the nose fan gas generator inlet geometry are presented in Figure 2-9.

2.5 GAS GENERATOR AND TURBOTIP FAN SYSTEM

Three identical 36" diameter GE-X376B turbotip fans were installed in the model, each one driven by a modified T58-GE-8B gas generator. The engine and fan for each lift unit were interconnected with steel ducts and bellows arranged as shown in Figure 2-2. The gas generators, turbotip fans, interconnect ducting and bellows were existing hardware items supplied by the Large Scale Aerodynamics Branch (LSAB) of NASA/Ames. The design characteristics of the gas generator and fan are presented in Figure 2-10. The performance values given are GE engine specification values, and are presented for reference only.

2.6 THRUST VECTORING SYSTEM

The exhaust nozzle thrust vectoring systems utilized on the nose lift unit and the two lift/cruise units were existing hardware components previously used and supplied by the LSAB of NASA/Ames. Descriptions of the lift/cruise vectored nozzles and the nose vectoring louvers are given in Figures 2-11 and 2-12, respectively, and are discussed below.

Lift/Cruise Vectored Nozzle

The lift/cruise vectored nozzle consisted of a fan exit diffuser, thrust vectoring hood segments, and a nozzle exit cone, as shown in Figure 2-11. The fan exit diffuser had a diffusion ratio ($A_{HOOD}/A_{FAN\ EXIT}$) of 1.50 and was used for both the vectored and nonvectored (cruise mode) test arrangements. Thrust vectoring was achieved with the fixed diameter detachable angular hood segments, so arranged as to provide geometric deflection angles (δ_{LC}) of 23°, 38°, 56°, 71° and 90°. The initial 23° hood segment was equipped with detachable cover panels on the upper surface, providing exhaust ports for simulating thrust reduction modulation. The

FIGURE 2-8
NOSE FAN INLET DESIGN GEOMETRY

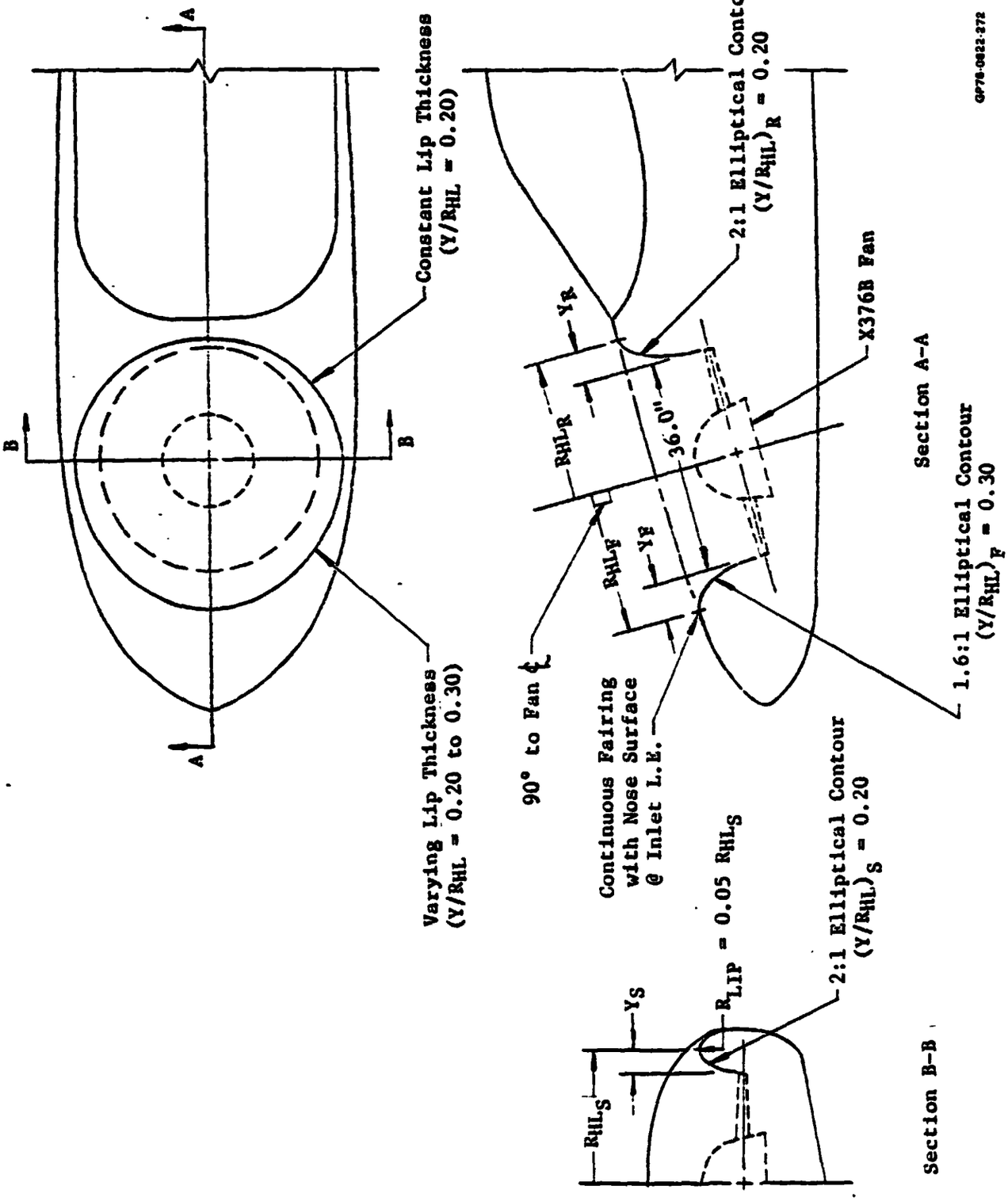

FIGURE 2-9
FORWARD ENGINE INLET DESIGN GEOMETRY

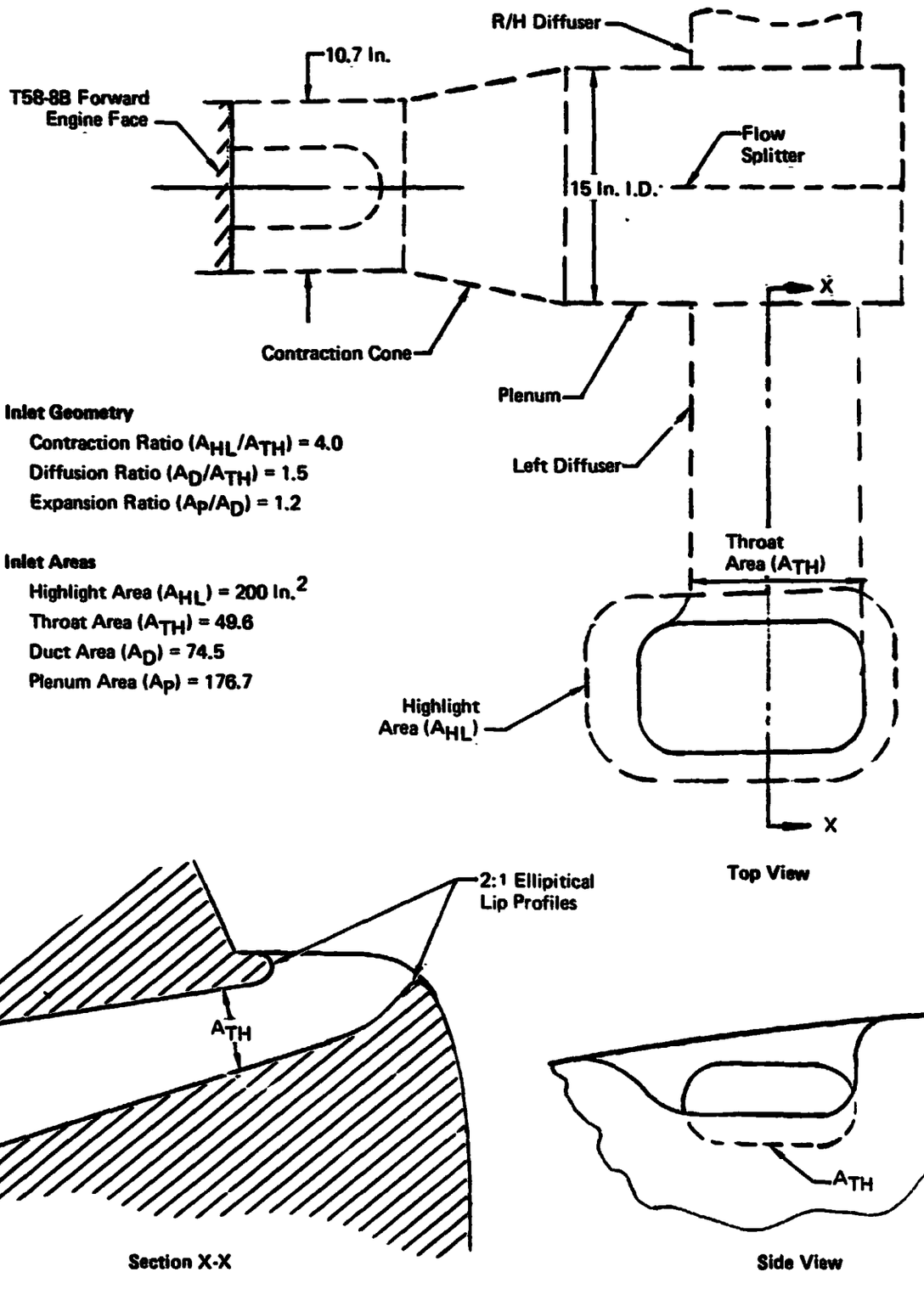

Inlet Geometry

- Contraction Ratio (A_{HL}/A_{TH}) = 4.0
- Diffusion Ratio (A_D/A_{TH}) = 1.5
- Expansion Ratio (A_P/A_D) = 1.2

Inlet Areas

- Highlight Area (A_{HL}) = 200 In.^{2}
- Throat Area (A_{TH}) = 49.6
- Duct Area (A_D) = 74.5
- Plenum Area (A_P) = 176.7

GP78-0822-282

FIGURE 2-10
GAS GENERATOR AND TURBOTIP FAN DESIGN CHARACTERISTICS

T58-GE-8B Gas Generator

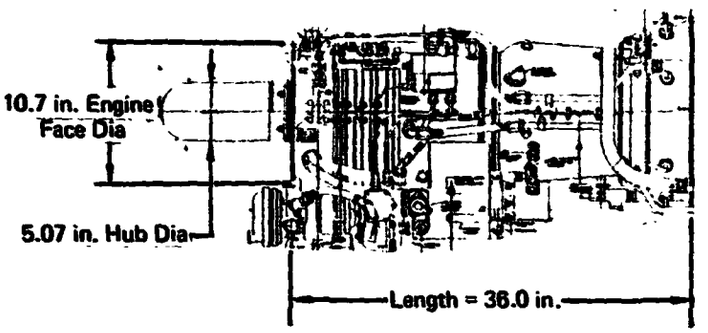

Design Point Performance (Intermediate Power)

Air Flow	12.4 lb/sec
Compressor Pressure Ratio	8.0:1
Turbine Inlet Temperature	1710°F
Exhaust Gas Temperature	1250°F
Engine Speed	19,500 rpm

GE-X376B Turbotip Fan

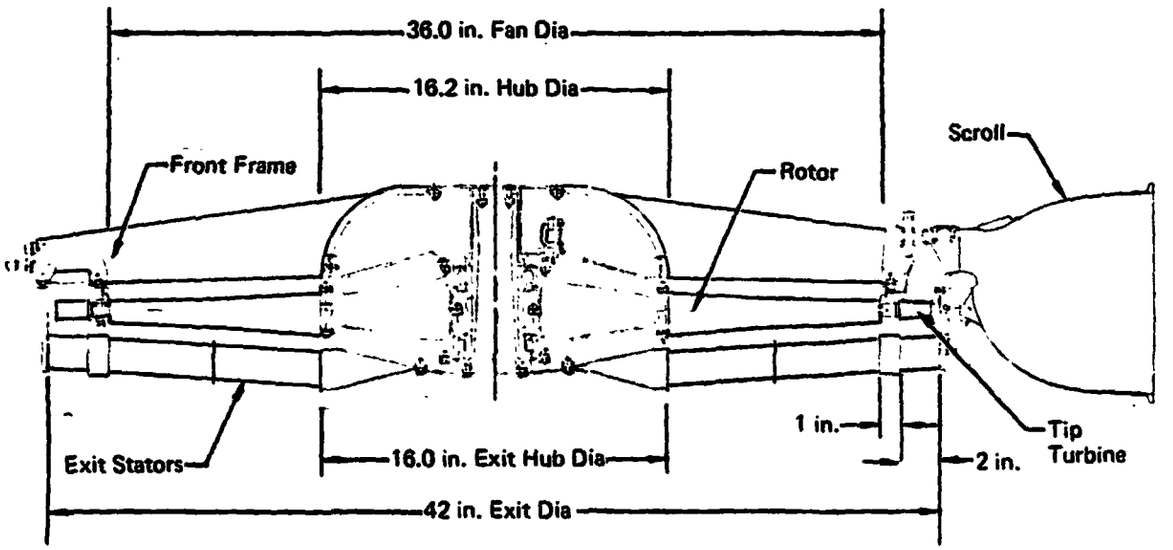

Design Point Performance (100% Speed)

Air Flow	153 lb/sec
Specific Flow	27 lb/sec-ft^2
Fan Pressure Ratio	1.08
Admission Arc	180°
Fan Speed (100%)	4074 rpm

GP78-0822-271

FIGURE 2-11
LIFT/CRUISE UNIT VECTORING SYSTEM GEOMETRY

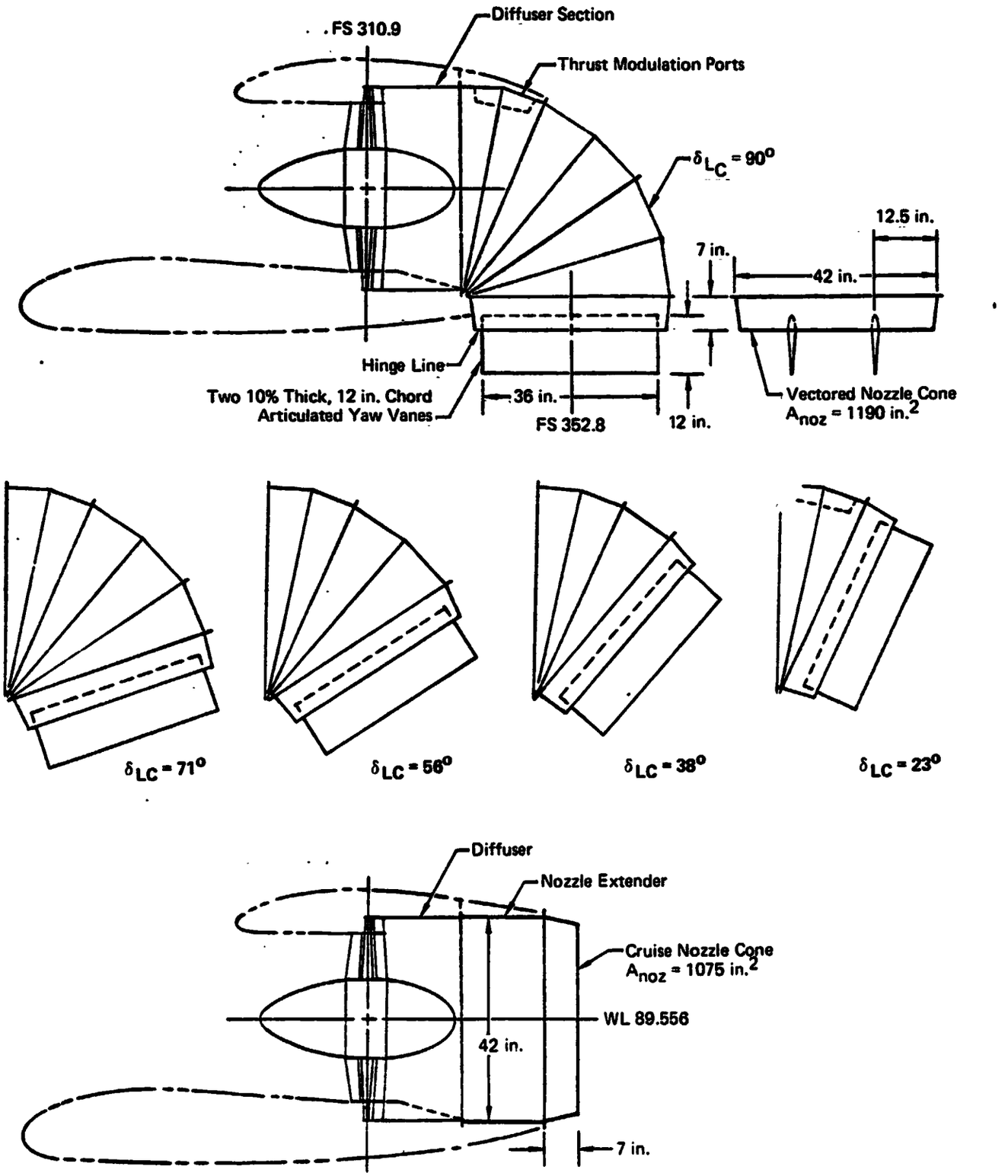

GP78-0822-277

FIGURE 2-12
NOSE LIFT UNIT VECTORING SYSTEM GEOMETRY

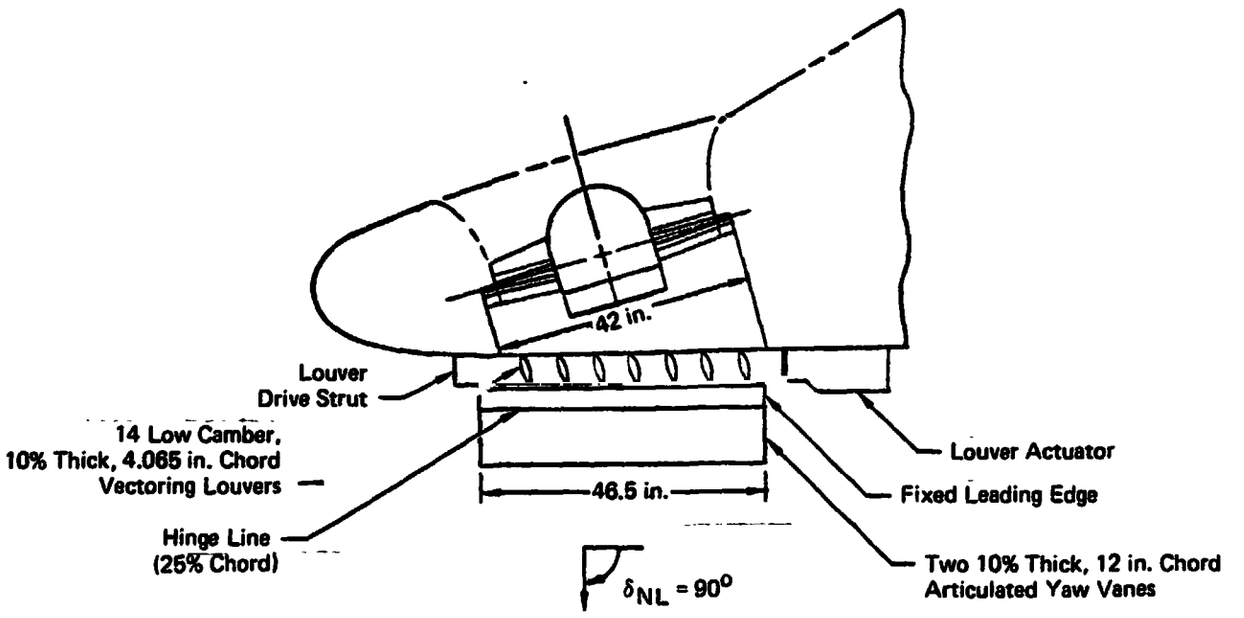

GP78-0822-274

thrust vectoring hood segments had constant area turning with a turning radius of 0.54 R/D. The nozzle exit cone was also detachable, and was equipped with two 10% thick, manually positioned, articulated yaw vanes. These vanes provided lateral vectoring of 0°, ±6° and ±12° to produce yawing moments. The nozzle cone had a fixed nozzle exit area of 0.7677 m^2 (1190 $in.^2$) with an exit contraction ratio (A_{HOOD}/A_{NOZ}) of 1.16.

For cruise mode testing (δ_{LC} = 0°), a 17 inch long constant area nozzle duct extension was installed downstream of the diffuser section. The cruise nozzle exit cone, which was attached to this extension, did not include exit yaw vanes. The cruise nozzle exit area was .6935 m^2 (1075 $in.^2$). An alternate cruise nozzle exit area of 0.6 m^2 (930 $in.^2$) was provided by a nozzle ring which attached to the exit cone. The cruise and vectored lift/cruise nozzles are shown in Figure 2-11.

Nose Lift Unit Vectored Nozzle

The nose lift unit thrust vectoring nozzle system utilized an existing, remotely activated louver and drive system. Fourteen low camber louvers, each with a thickness ratio of 10%, provided thrust vectoring over a range from 105° to 30°. Two 10% thick, manually positioned, articulated yaw vanes located beneath the louvers provided yaw vectoring of 0°, ±6° and ±12°. The yaw vanes were of the same design as those on the lift/cruise units, and were detachable from the model. For cruise mode testing, the complete louver and yaw vane vectoring system was removed and a lower surface nozzle unit cover panel was installed on the model. Details of the nose lift unit vectoring system are presented in Figure 2-12.

3. MODEL INSTRUMENTATION

The large scale powered model was fully instrumented with pressure and temperature pickups located at various positions on the airframe and propulsion system components. The quantity, type, and location of the instrumentation for each model component are described in the sections that follow.

3.1 AIRFRAME INSTRUMENTATION

A total of 105 static pressure ports were installed on the external surfaces of the wing and fuselage sections of the airframe. The locations of the pressure ports on each component are described below. No data from this instrumentation are included in this report due to problems encountered in the reduction process.

Wing

A total of 78 static pressure ports were installed on the left wing, aileron, and flap surfaces, distributed along butt lines located at four spanwise positions. Both the upper and lower left wing surfaces were instrumented. The locations of all wing pressure ports are presented in Figure 3-1.

Forward Fuselage

A total of 27 static pressure ports were installed on the forward fuselage of the model. This total included 16 ports on the left side of the nose section and 11 on the lower fuselage surface just downstream of the forward fan exhaust. The detailed locations are shown in Figure 3-2.

Empennage Flow Survey Rake

Dynamic pressure and flow direction were measured at the pivot axis of the horizontal tail plane by directional pitot static probes at the following six butt lines: 29.0, 42.1, 55.3, 68.4, 81.5, and 94.6.

3.2 PROPULSION SYSTEM INSTRUMENTATION

The propulsion system instrumentation included static pressure, total pressure, and total temperature measurements at various locations on the components of the three lift units. The components of the propulsion system that were instrumented included the following:

- o Left lift/cruise fan and gas generator inlets
- o Nose fan and gas generator inlets
- o Left and nose gas generator exits
- o Left, right, and nose fan and tip turbine exits
- o Left and nose fan nozzle exits.

FIGURE 3-1
LOCATION OF WING SURFACE STATIC PRESSURE PORTS
(Left Wing Only)

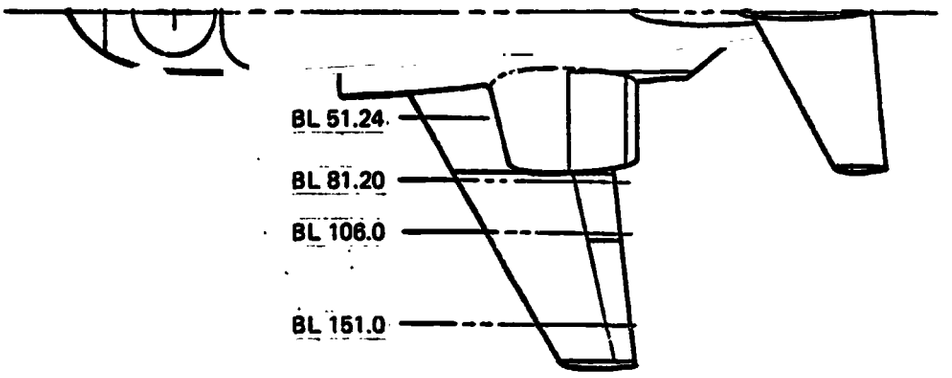

% Chord	Distance from Leading Edge (in.)							
	BL 51.24		BL 81.20		BL 106.0		BL 151.0	
	Upper Surface	Lower Surface	Upper Surface	Lower Surface	Upper Surface	Lower Surface	Upper Surface	Lower Surface
0	0.0	–	0.0	–	0.0	–	0.0	–
2.5	2.31	–	1.95	–	1.65	–	1.11	–
5.0	4.62	–	3.90	3.90	3.31	3.31	2.23	2.23
10.0	9.23	–	7.80	–	6.61	–	4.46	–
15.0	–	–	–	11.70	–	9.92	–	6.69
20.0	18.47	–	15.60	–	13.23	–	8.92	–
30.0	27.70	–	23.40	23.40	19.84	19.84	13.38	13.38
40.0	–	–	31.20	–	26.45	–	17.84	–
45.0	–	–	35.10	–	–	–	–	–
50.0	–	–	39.00	39.00	33.07	33.07	22.30	22.30
55.0	–	–	42.90	–	–	–	–	–
60.0	–	–	46.80	–	39.68	–	26.75	–
65.0	–	–	50.70	–	–	–	–	–
70.0	–	–	54.60	54.60	46.29	46.29	31.23	31.23
80.0	–	–	62.40	–	52.90	–	35.67	–
85.0	–	–	–	66.30	–	56.21	–	37.90
90.0	–	–	70.20	–	59.52	–	40.13	–
95.0	–	–	74.10	74.10	62.82	62.82	42.36	42.36
99.0	–	–	77.22	77.22	65.47	65.47	44.14	44.14
100.0	–	–	78.00	–	66.13	–	44.59	–

GP76-0622-264

FIGURE 3-2
LOCATION OF FORWARD FUSELAGE STATIC PRESSURE PORTS

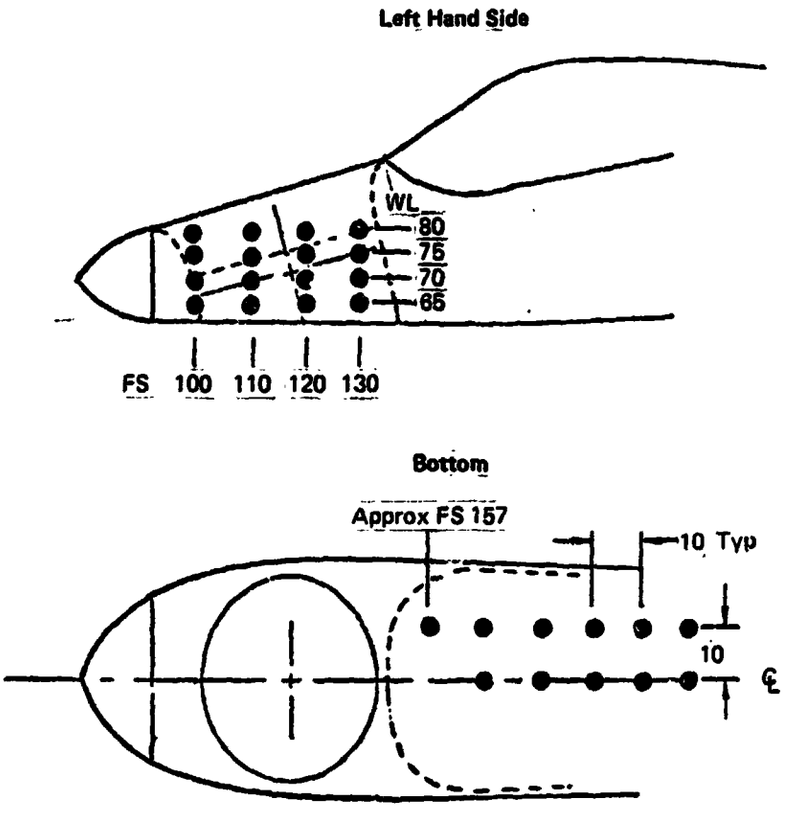

Note: All dimensions are model scale in inches.

GP 6-0622-268

A total of 108 static pressure ports, 247 total pressure probes, and 79 total temperature probes were installed in the propulsion system of the model. A table summarizing the propulsion system instrumentation and the specific purpose for each installation is presented in Figure 3-3. A description of the quantity, type, and location of the instrumentation for each propulsion system component is presented below.

Fan Inlets

The left lift/cruise and nose lift fan inlets were each instrumented with inlet surface static pressure ports, located at various positions on the internal and external surfaces. The left lift/cruise nacelle included a total of 22 static pressure ports located on the upper and side inlet lip, the lower internal duct surface, and on the external upper nacelle surface. In addition, six static pressure ports were also installed on the upper wing surface ahead of the inlet. The locations of these and the inlet ports are shown in Figure 3-4. The locations of the nose lift fan inlet static pressure ports are shown in Figure 3-5. A total of 10 static pressure ports were installed on the nose and side inlet lips.

Engine Inlets

The left lift/cruise and nose fan engine inlets were also instrumented with static pressure ports on the surfaces of the inlets. A total of 10 inlet lip static pressure ports were installed on the internal surface of the left lift/cruise engine inlet side and lower lips. The locations are shown in Figure 3-6. Five inboard lip static pressure ports were installed on the left nose fan engine inlet, as shown in Figure 3-7. This left inlet also included an eight-probe total temperature rake to measure reingestion temperature levels at the inlet throat station. The locations of the thermocouples are also presented in Figure 3-7.

Fan Face

The left lift/cruise fan face and nose lift fan face were both instrumented with identical inlet performance rakes. An 8 leg, 48 total pressure probe rake to measure inlet performance, along with a 4 leg, 8 total temperature probe rake to measure reingestion temperatures, was installed at the fan face, just upstream of the X376B forward support frame on each lift unit. Both the pressure and temperature rakes were equal-area-weighted rakes. Four wall static pressure ports were also located at the rake station of each inlet. The instrumentation locations for the fan face rakes are presented in Figure 3-8.

FIGURE 3-3
SYSTEM INSTRUMENTATION RATIONALE

INSTRUMENTATION UNIT	MEASUREMENTS	PARAMETERS CALCULATED	PRIMARY PURPOSE
FAN EXIT	Total Pressure Total Temperature Static Pressure	Fan Pressure Ratio Airflow Fan Exit Velocity(Ideal)	Jet Velocity Ratio (V_o/V_j) Gross Thrust (F_G) Ram Drag (F_R) Inlet Velocity Ratio (V_o/V_{TH})
TIP TURBINE EXIT		Exit Pressure Ratio Gas Flow Exit Velocity(Ideal)	Jet Velocity Ratio (V_o/V_j) Gross Thrust (F_G) Ram Drag (F_R) Inlet Velocity Ratio (V_o/V_{TH})
GAS GENERATOR EXHAUST		EGT Exit Pressure	Engine Horsepower Output
FAN AND GAS GENERATOR INLETS		Total Pressure Recovery Total Pressure Distortion Static Pressure Coefficients Average Inlet Temperature	Inlet Performance (P_T/Dist.) Inlet Lip Pressure Distributions Temperature Reingestion
NOZZLE EXITS	Total Pressure Static Pressure	Total Pressure Recovery Total Pressure Distortion Base Drag	Nozzle Exit Distortion Base Drag Increments

GP76-0822-200

FIGURE 3-4
LIFT/CRUISE FAN INLET INSTRUMENTATION
Left Side Only

Static Pressure Locations

Port No.	Axial Distance, X (in.)			
	Wing	Cowl	Upper Lip	Side Lip
1	0.00	0.00	0.00	0.00
2	2.95	3.58	0.67	0.38
3	5.27	7.17	1.98	1.55
4	9.68	14.33	4.86	4.10
5	18.95	28.67	8.93	8.70
6	28.30	43.00		
7	32.32			
8	36.94			
9	41.55			
10	46.17			
11	50.79			
12	55.40			

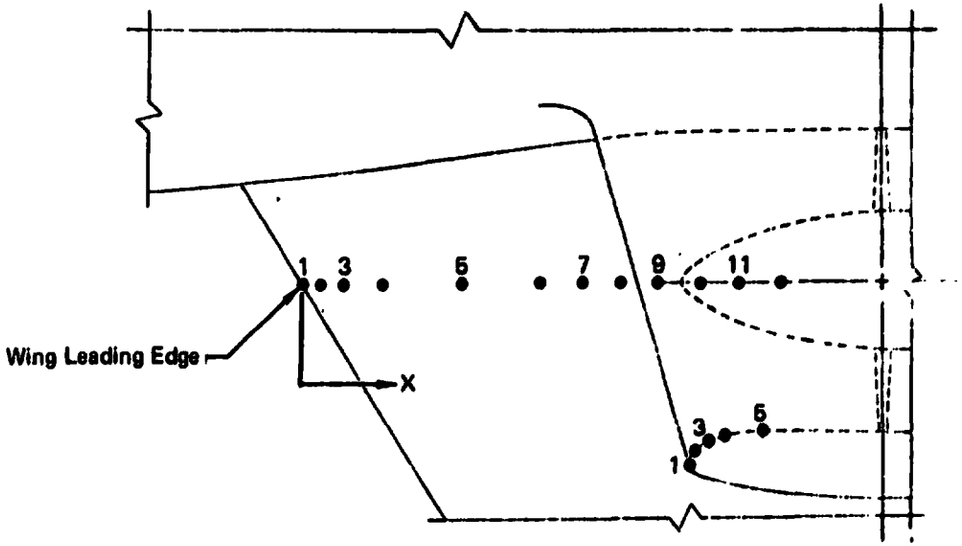

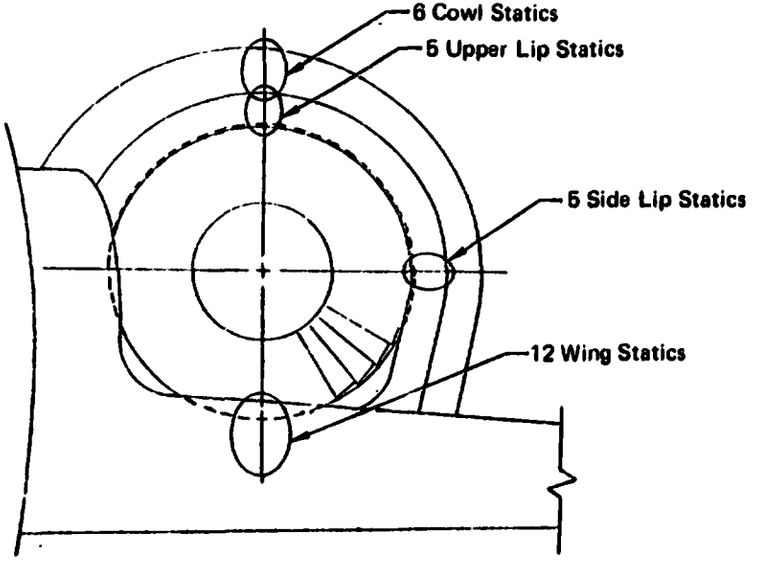

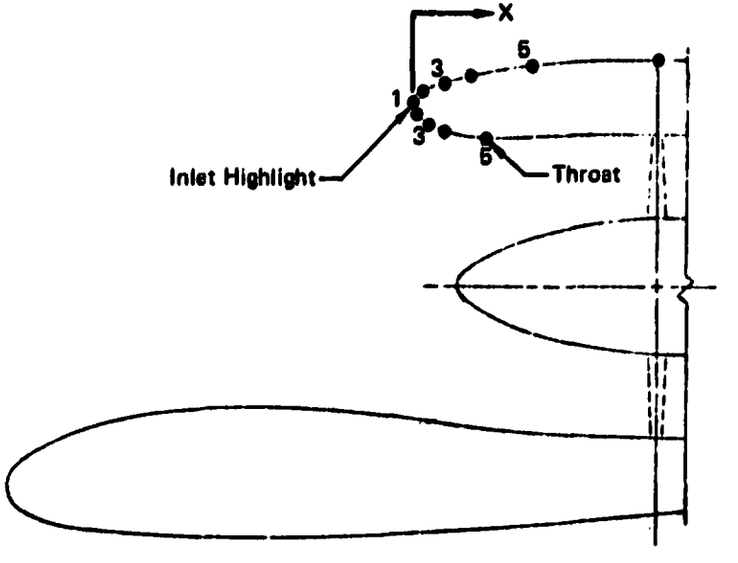

GP76-0822-4

FIGURE 3-5
NOSE FAN INLET INSTRUMENTATION

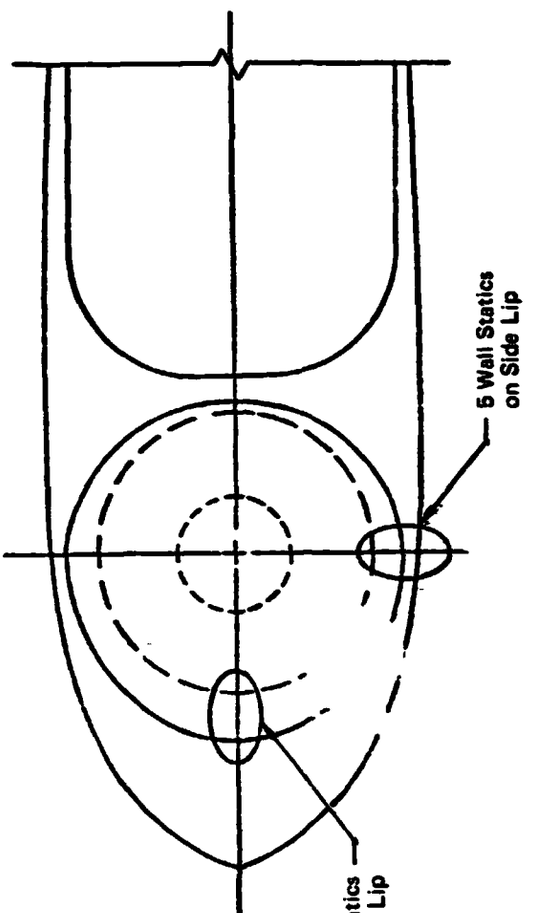

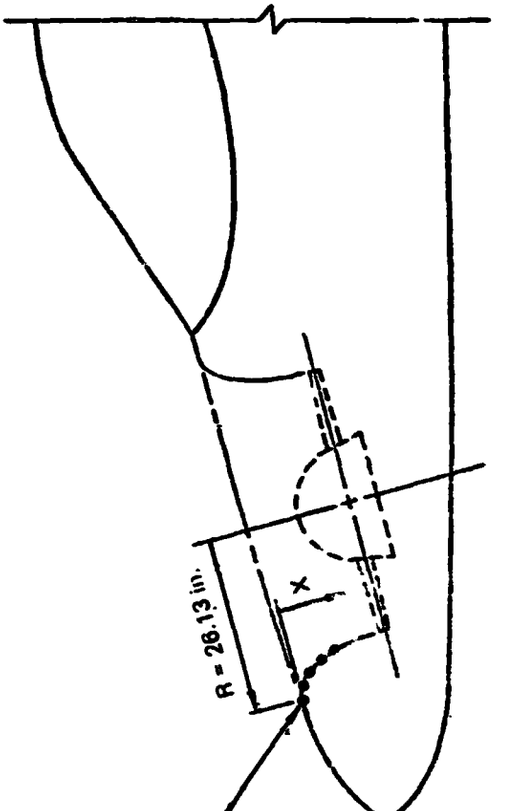

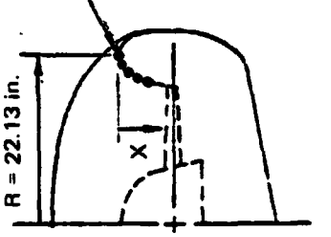

Static Pressure Locations

Port No.	X (in.) Fwd	X (in.) Side
1	0.00	0.00
2	0.08	0.11
3	0.30	0.34
4	1.06	1.77
5	3.01	2.93

GP76-0823-6

FIGURE 3-6
LIFT/CRUISE ENGINE INLET INSTRUMENTATION
Left Side Only

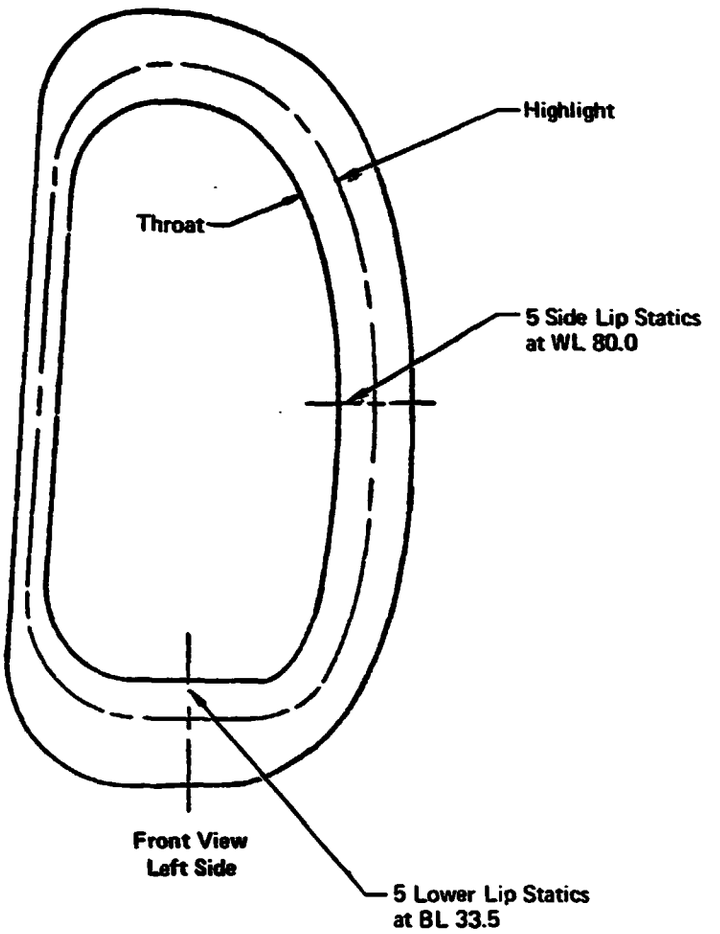

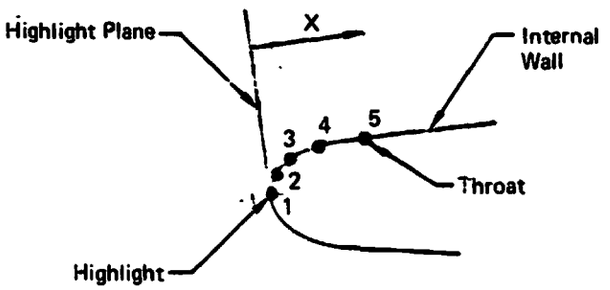

Static Pressure Locations

Port No.	X (in.)
1	0.00
2	0.05
3	0.35
4	0.98
5	2.05

GP76-0622-6

FIGURE 3-7
FORWARD ENGINE INLET INSTRUMENTATION
Left Side Only

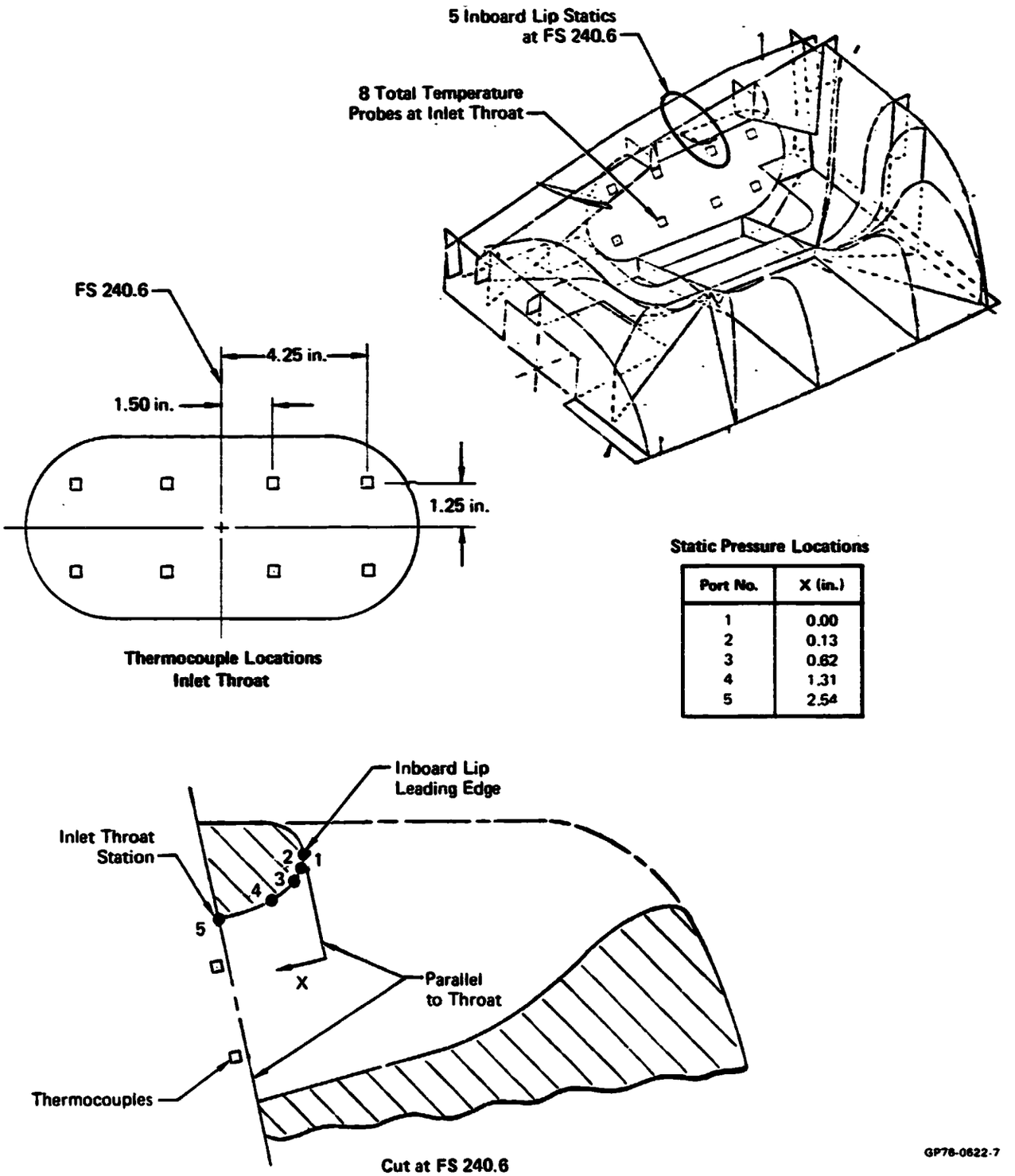

FIGURE 3-8
FAN FACE INSTRUMENTATION

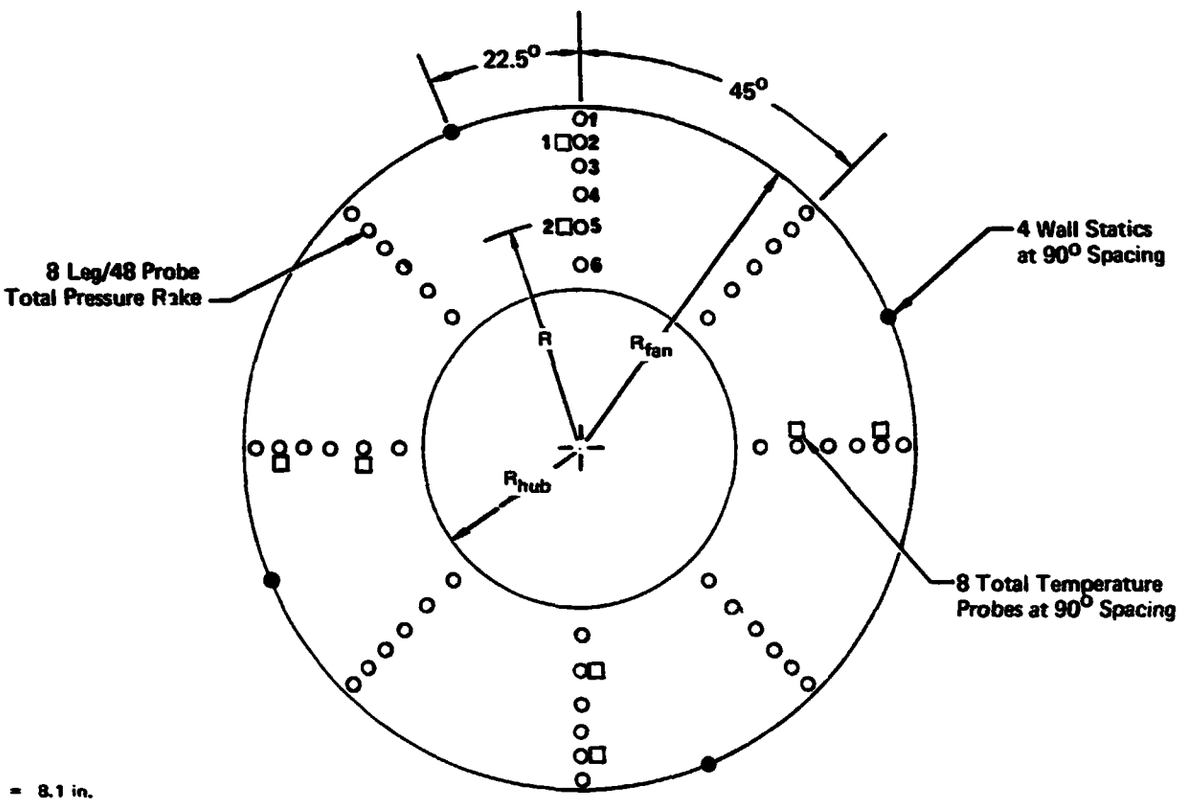

Thermocouple Locations

T/C No.	Radius (in.)
1	16.11
2	11.43

Pressure Tube Locations

Probe No.	Radius (in.)
1	17.39
2	16.11
3	14.72
4	13.17
5	11.43
6	9.36

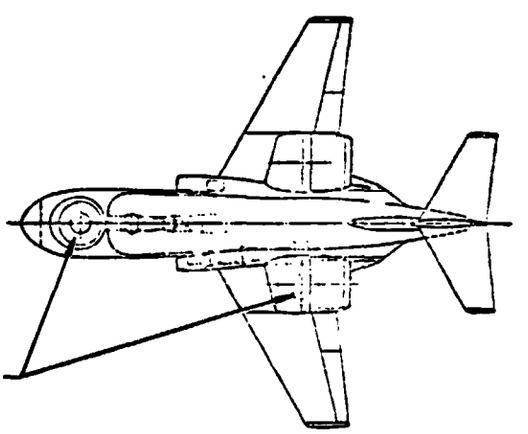

GP76-0622-3

All total pressure and total temperature rake probes installed in the model were made of 1/8" O.D. x .032" wall thickness stainless teel tubing. The pressure probe inlets were chamfered at 15°. All thermocouples installed in the model were made of 30 gauge iron/constantan wire. A teflon liner was utilized within the steel tubing for insulation.

Engine Face

The left lift/cruise engine face and the nose fan engine face were both instrumented with inlet performance rakes. A 4 leg, 16 total pressure probe rake to measure inlet performance, along with a 4 leg, 8 total temperature probe rake to measure reingestion temperature levels, was installed just upstream of the engine face on each unit. Two wall static ports were also located at the rake station of each engine. The instrumentation locations for these engine face rakes are presented in Figure 3-9.

Fan and Tip Turbine Exit

All three turbotip fan units on the model were instrumented in like manner at the fan and tip turbine stator exits. The fan exit instrumentation consisted of a 6 leg 30 probe total pressure rake, a 3 leg 9 probe total temperature rake, and 12 exit static pressure ports, 6 each on the hub and outer wall. The tip turbine exit instrumentation consisted of 4 equal-area-weighted total pressure probes, 4 total temperature probes, and 5 outer wall static pressure ports. The purpose of the fan and tip turbine exit instrumentation was to measure the basic performance of the turbotip fans including the airflow, thrusts, and jet velocities. The detailed location of the fan and tip turbine exit instrumentation is presented in Figure 3-10. A cross-sectional drawing of the turbotip fan illustrating the positioning of both the inlet and fan exit rakes is presented in Figure 3-11. Details of the total pressure and temperature probes are also shown.

Engine Exit

The left lift/cruise and nose fan engine exhaust ducts were each instrumented with three wall static pressure ports, located approximately one duct diameter downstream of the engine exit. The pressure port locations are shown in Figure 3-12. In addition to these static pressure measurements, the eight-probe engine EGT harness was utilized on all three engines to measure the engine exhaust gas total temperatures.

FIGURE 3-9
ENGINE FACE INSTRUMENTATION

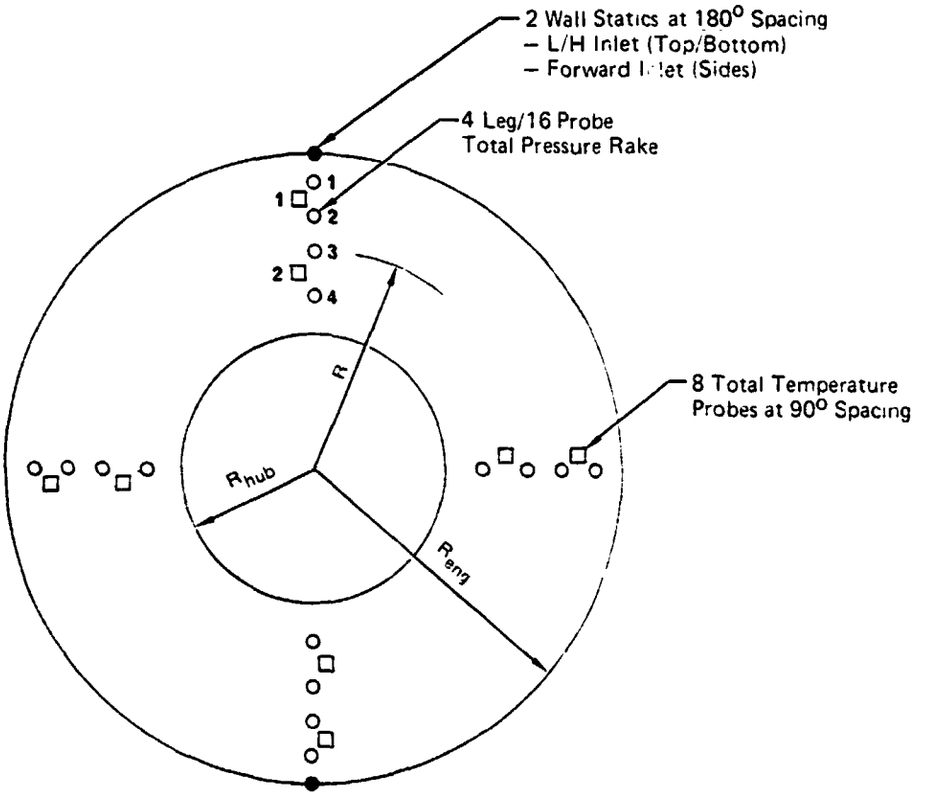

Thermocouple Locations

T/C No.	Radius (in.)	
	L/C	Fwd
1	4.80	4.62
2	3.37	3.35

R_{hub} = 2.54 in.
R_{eng} = 5.35 in.

Pressure Tube Locations

Probe No.	Radius (in.)	
	L/C	Fwd
1	5.20	4.99
2	4.40	4.32
3	3.69	3.62
4	3.14	3.04

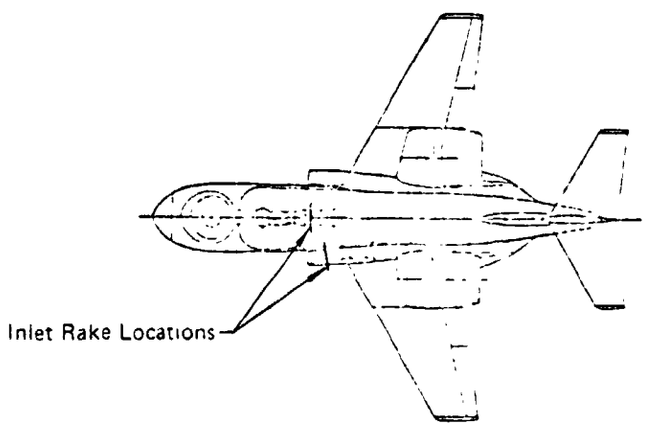

GP76 0622 10

FIGURE 3-10
FAN AND TIP TURBINE EXIT INSTRUMENTATION

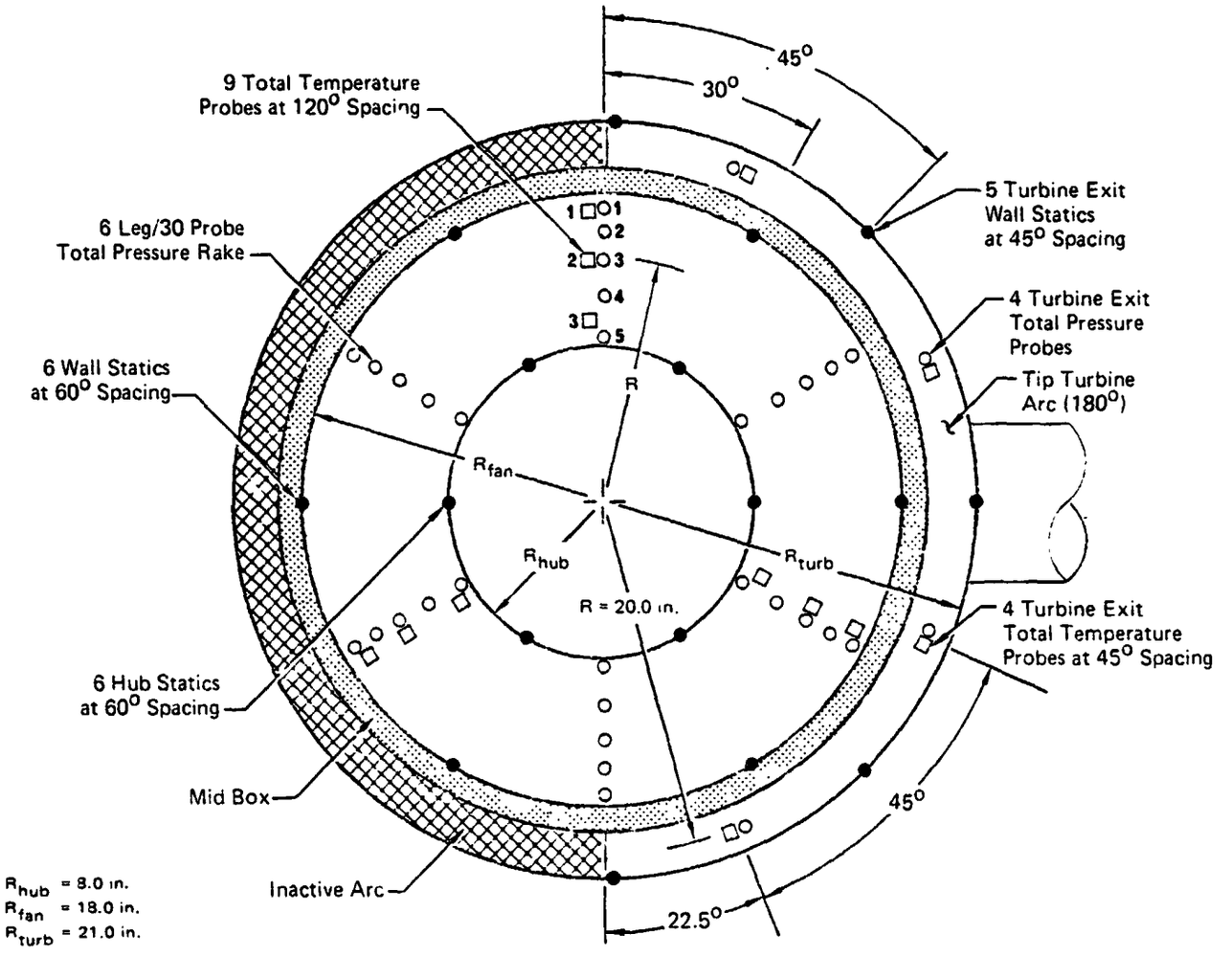

Thermocouple Locations

T/C No.	Radius (in.)	
	L/C	Fwd
1	16.00	16.43
2	13.02	13.43
3	10.70	11.15

Pressure Tube Locations

Tube No.	Radius (in.)	
	L/C	Fwd
1	17.17	17.64
2	14.78	15 24
3	12.76	13.36
4	11.07	11 61
5	9 56	10.10

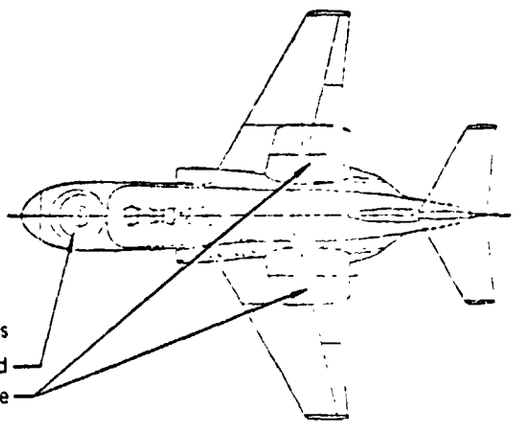

GP76 0622 2

FIGURE 3-11
FAN INLET AND EXIT INSTRUMENTATION INSTALLATION
Left Lift/Cruise and Nose Fan Units

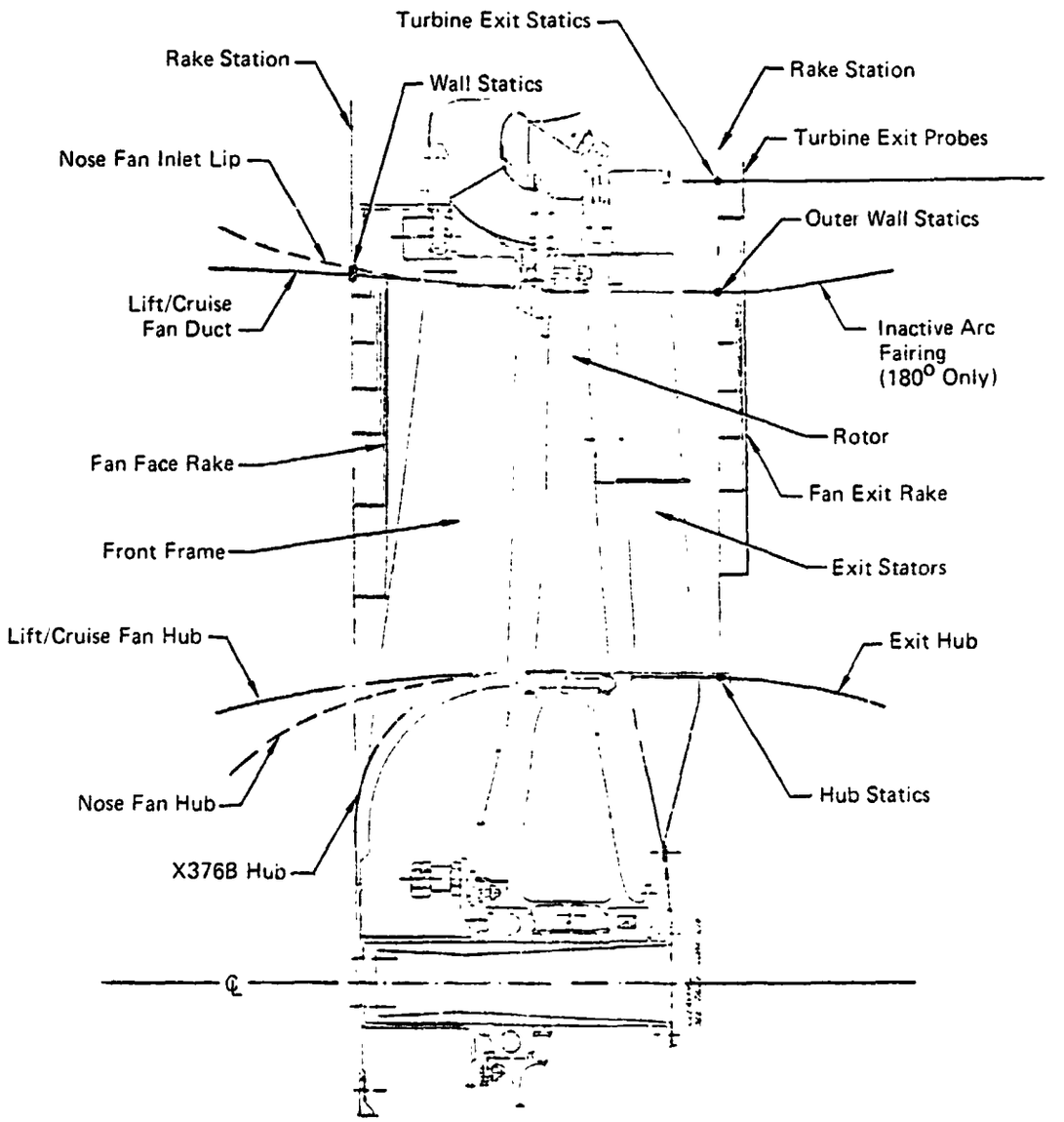

GP76 0622 266

FIGURE 3-12
ENGINE EXIT INSTRUMENTATION

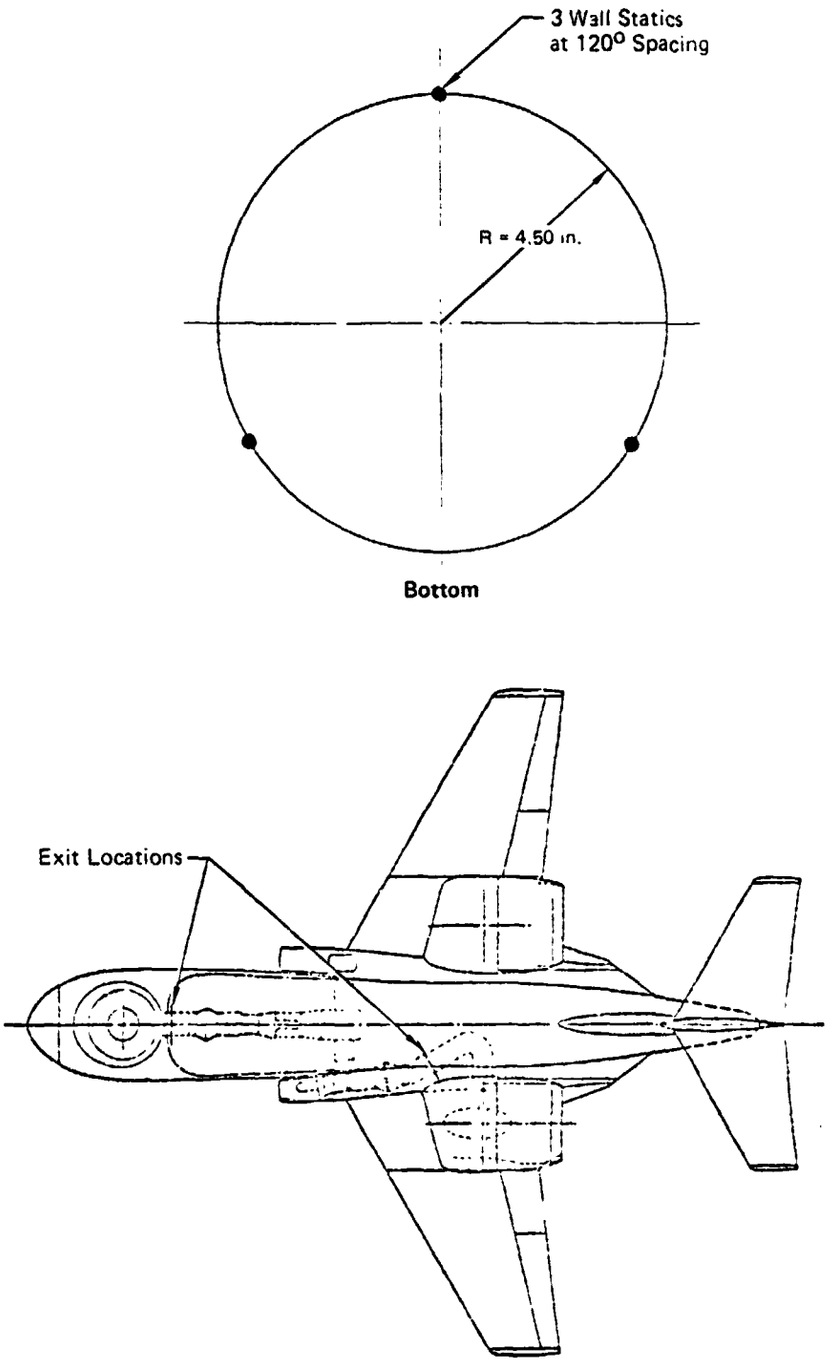

Nozzle Exits

The left lift/cruise and nose fan lift units were each instrumented at the nozzle exit for the purpose of assessing the nozzle exit flow profiles. The left lift/cruise nozzle exit included 10 total pressure probes attached to the leading edge of the two fixed yaw vane struts, and 4 external nozzle exit base pressure static ports. The nose fan nozzle exit included 7 total pressure probes attached to the leading edge of the louver centerline drive strut, and canted 15° to align with the fan exit. The details of the nozzle exit instrumentation are presented for both units in Figure 3-13.

FIGURE 3-13
NOZZLE EXIT INSTRUMENTATION

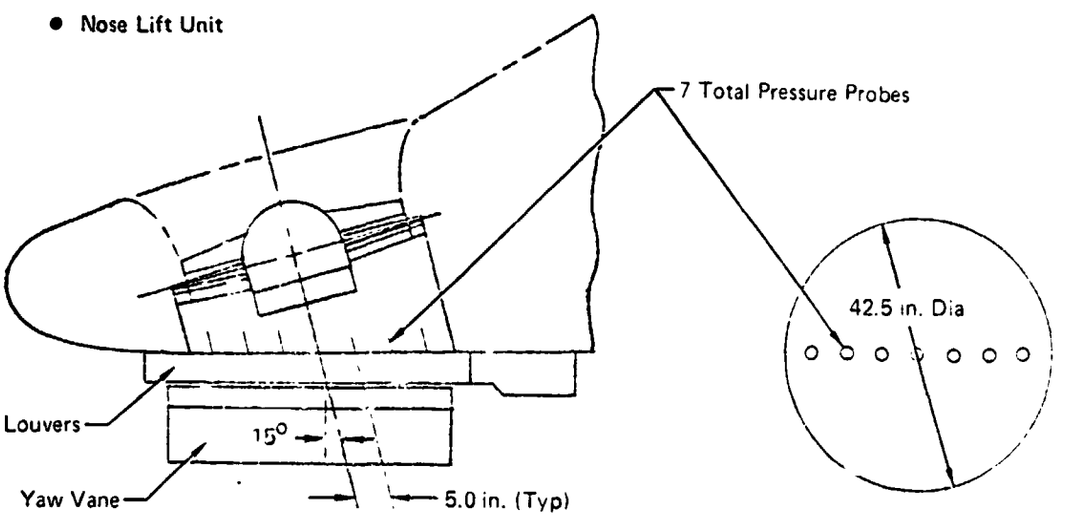

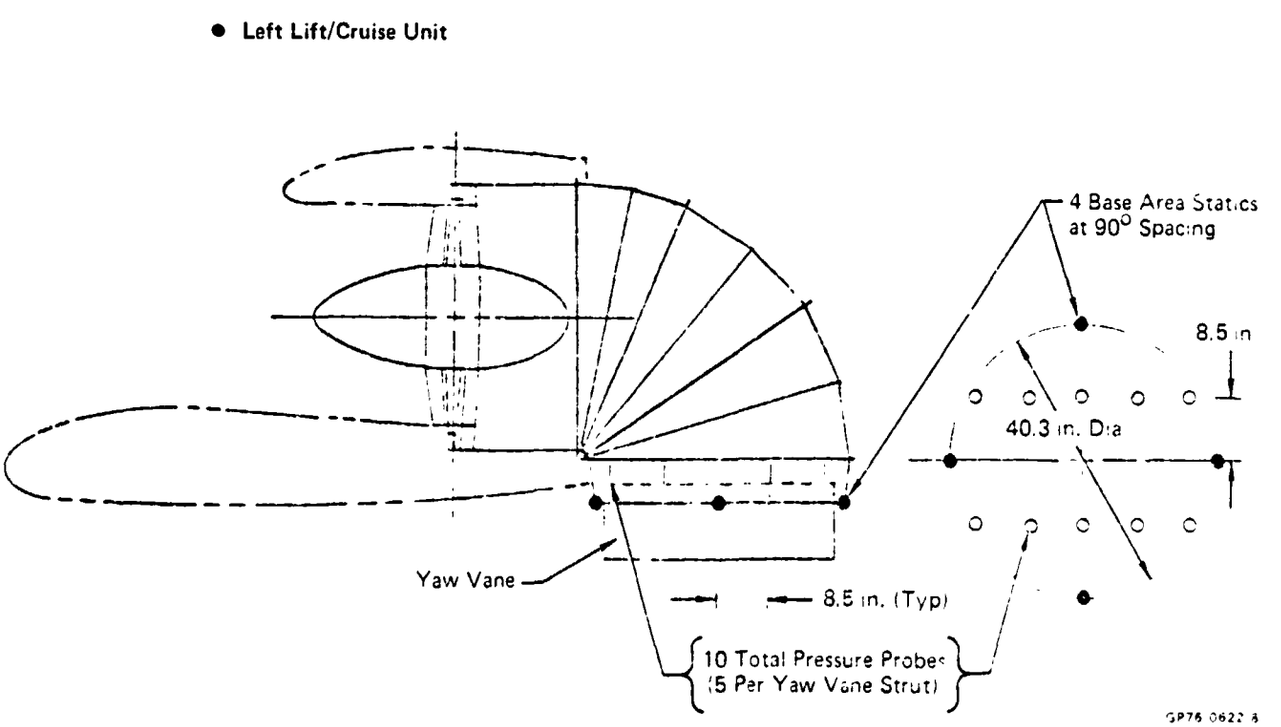

4. WIND TUNNEL TEST FACILITY

The model was tested in the NASA/Ames Research Center 40' x 80' wind tunnel. The tunnel is a low speed closed circuit continuous flow tunnel with a speed range from 0 to 180 knots which operates at a near constant tunnel total pressure of one atmosphere and provides Reynolds numbers up to 2 x 10^6 per foot. The test section is 40 feet high, 80 feet wide at the tunnel centerline, and 80 feet long. The ceiling of the tunnel test section opens to provide for model installation. The wind tunnel model balance is a six-component scale type balance, located directly below the test section. The wind tunnel control room is located adjacent to the test section. A cross section drawing of the tunnel test section and adjacent areas is shown in Figure 4-1. Further details of the 40' x 80' wind tunnel are contained in the user's guide of Reference (2).

4.1 TEST ARRANGEMENT

The model was supported on the tunnel balance with three support struts, two attached to the main wing spar and one attached to the aft fuselage. All model leads were attached to the two main support struts which were fixed in height. The tail strut was remotely varied in height to change angle of attack. The model was positioned at the centerline of the tunnel, 20 feet above the tunnel floor. Photos of the model installed in the test section are presented in Figures 4-2 through 4-6.

The model was equipped with several monitoring and control systems. Leads from these systems were attached to the main support struts and routed down through the balance room and up to the main tunnel control room. The model subsystems with external leads included the following:

- Fuel system
- Engine and fan control and monitoring system
- Fire warning and CO_2 extinguishing system
- Remote controlled model variable systems
- Model pressure and temperature instrumentation system.

A schematic layout of the main tunnel control room is presented in Figure 4-7. The arrangement of the major equipment is shown, including the tunnel control panel, the engine and fan control console, the on-line computer, pressure and temperature recording system, data card punches, computer printout, and TV monitors.

FIGURE 4-1
40 x 80 WIND TUNNEL TEST FACILITY
Test Section Elevation View

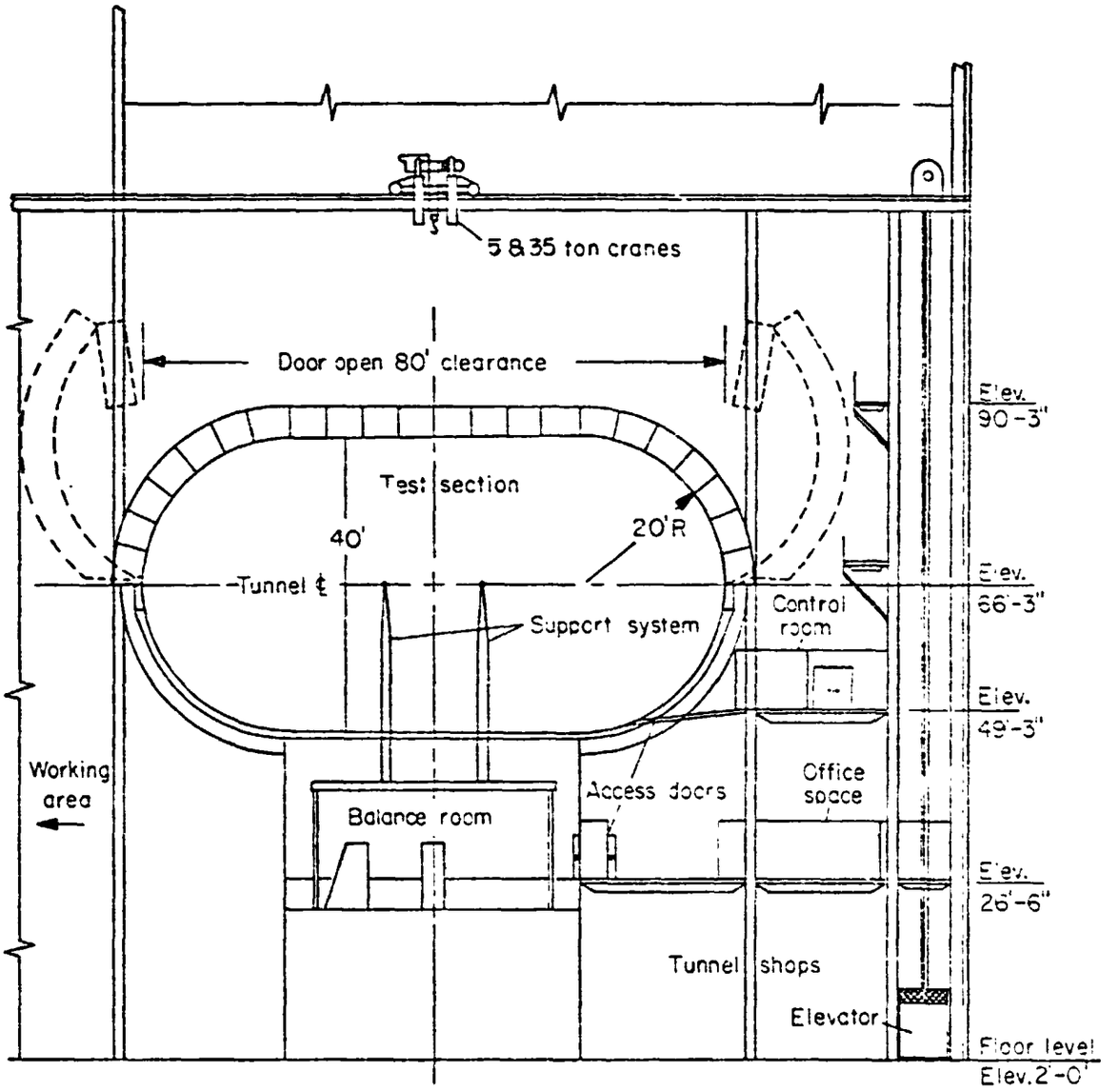

GP76-0622 252

FIGURE 4-2
LARGE SCALE POWERED MODEL INSTALLED IN 40 FT x 80 FT WIND TUNNEL
Front Quarter View of Powered Lift Mode Configuration

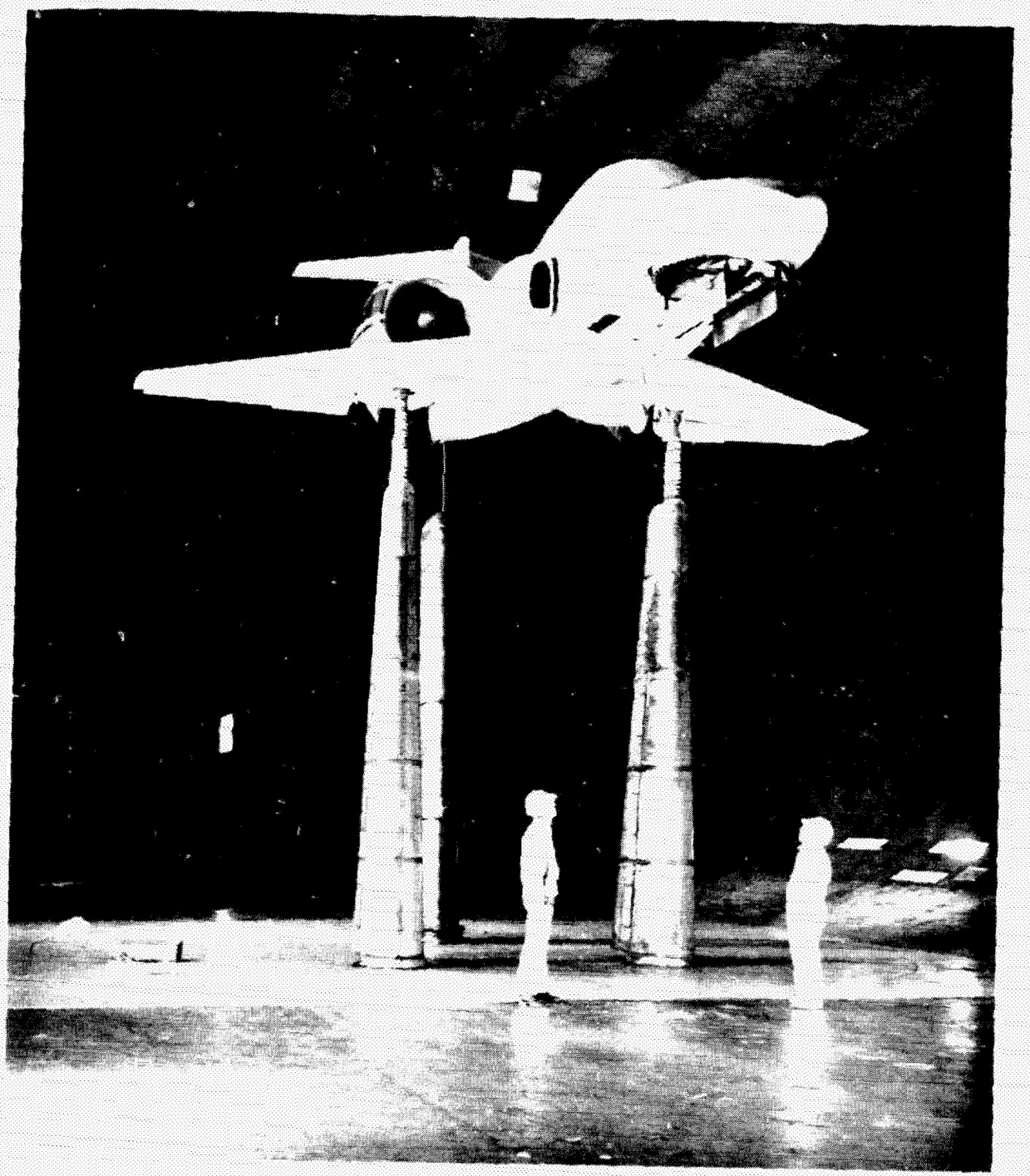

FIGURE 4-3
LARGE SCALE POWERED MODEL INSTALLED IN 40 FT x 80 FT WIND TUNNEL
Rear Quarter View of Powered Lift Mode Configuration

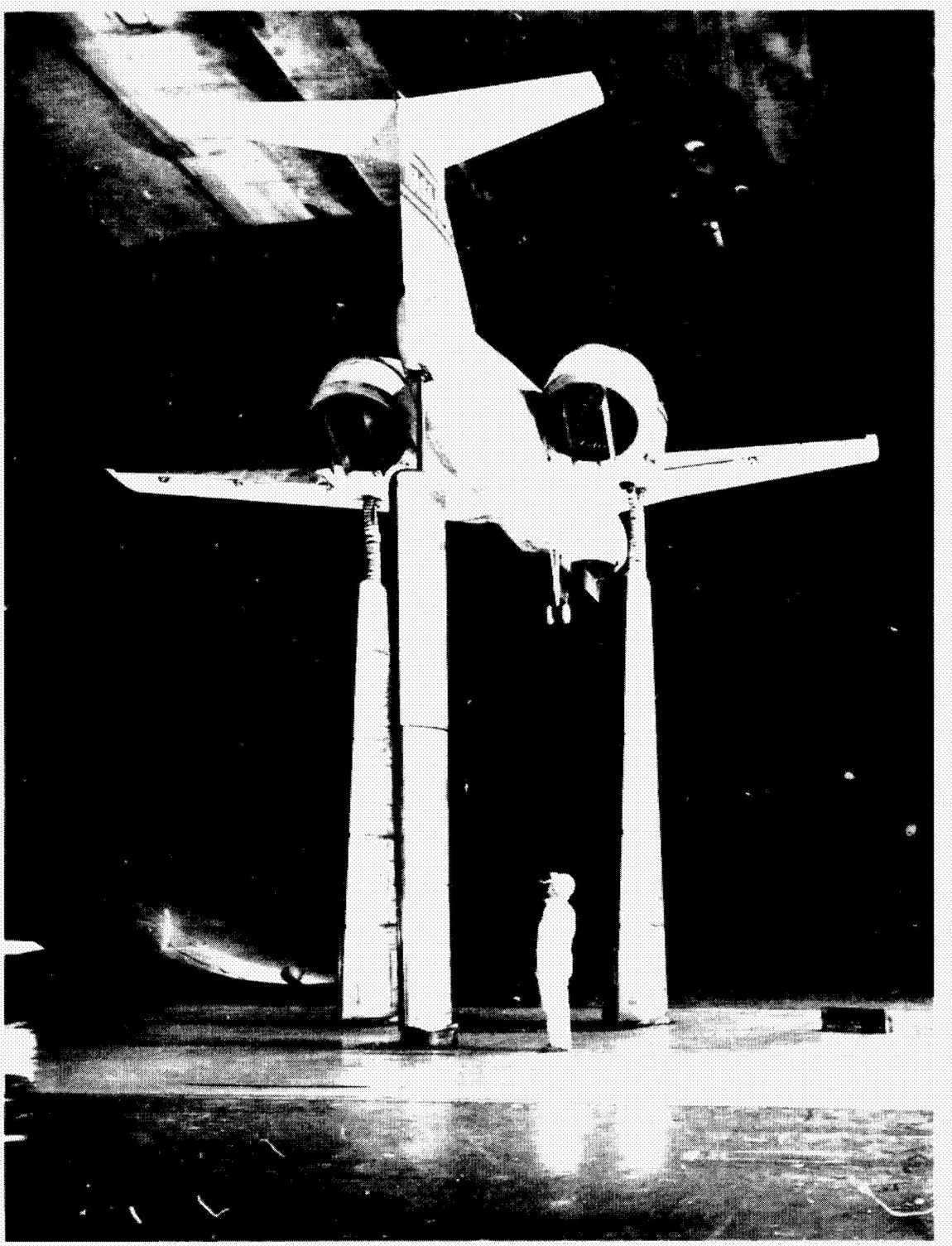

FIGURE 4-4
LARGE SCALE POWERED MODEL INSTALLED IN 40 FT x 80 FT WIND TUNNEL
Front Quarter View of Aerodynamic Lift Mode Configuration

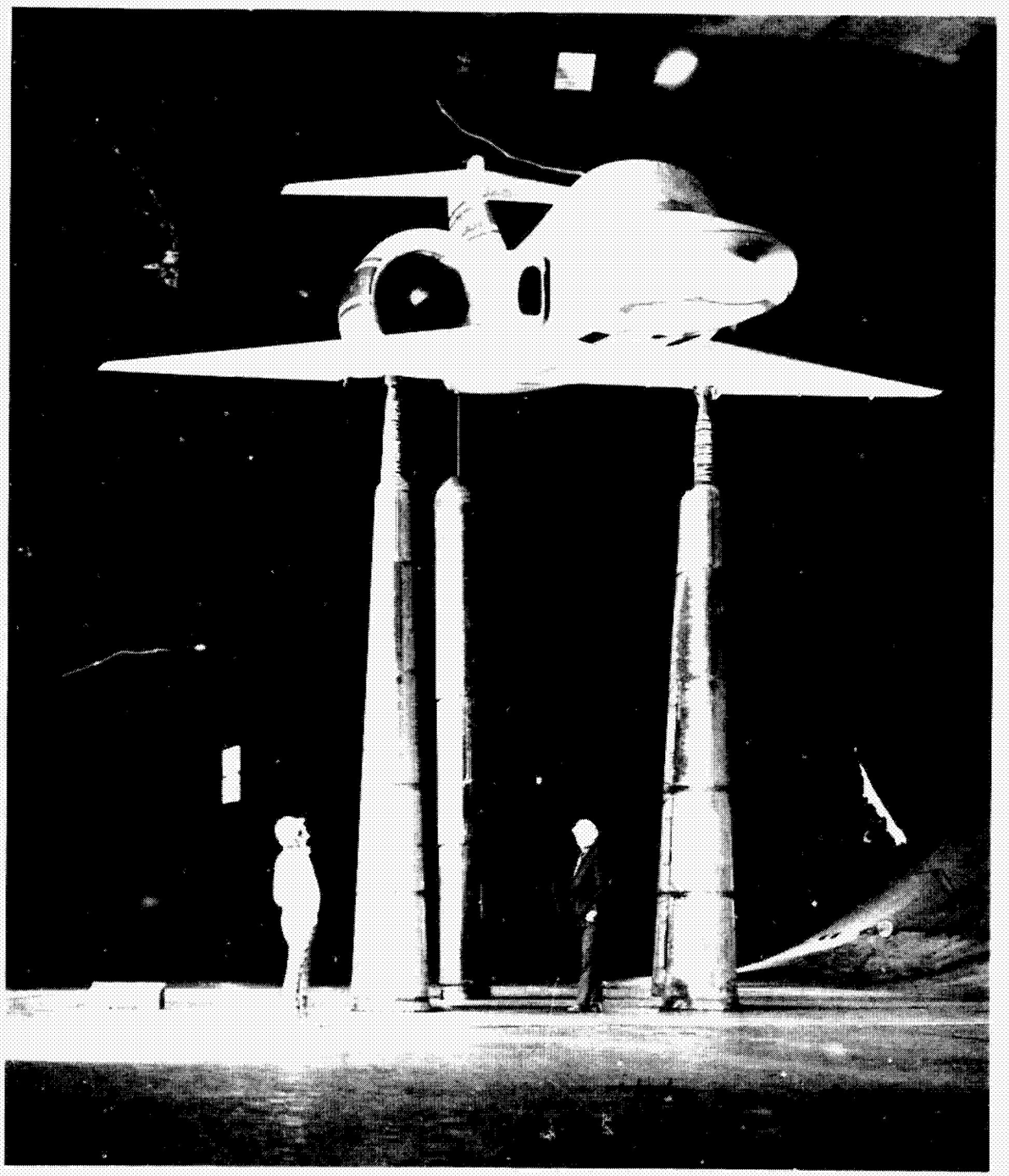

FIGURE 4-5
LARGE SCALE POWERED MODEL INSTALLED IN 40 FT x 80 FT WIND TUNNEL
Top Front Quarter View of Powered Lift Mode Configuration

FIGURE 4-6
LARGE SCALE POWERED MODEL INSTALLED IN 40 FT x 80 FT WIND TUNNEL
Top Front Quarter View of Aerodynamic Lift Mode Configuration

FIGURE 4-7
40 x 80 CONTROL ROOM LAYOUT
Data Systems Arrangement

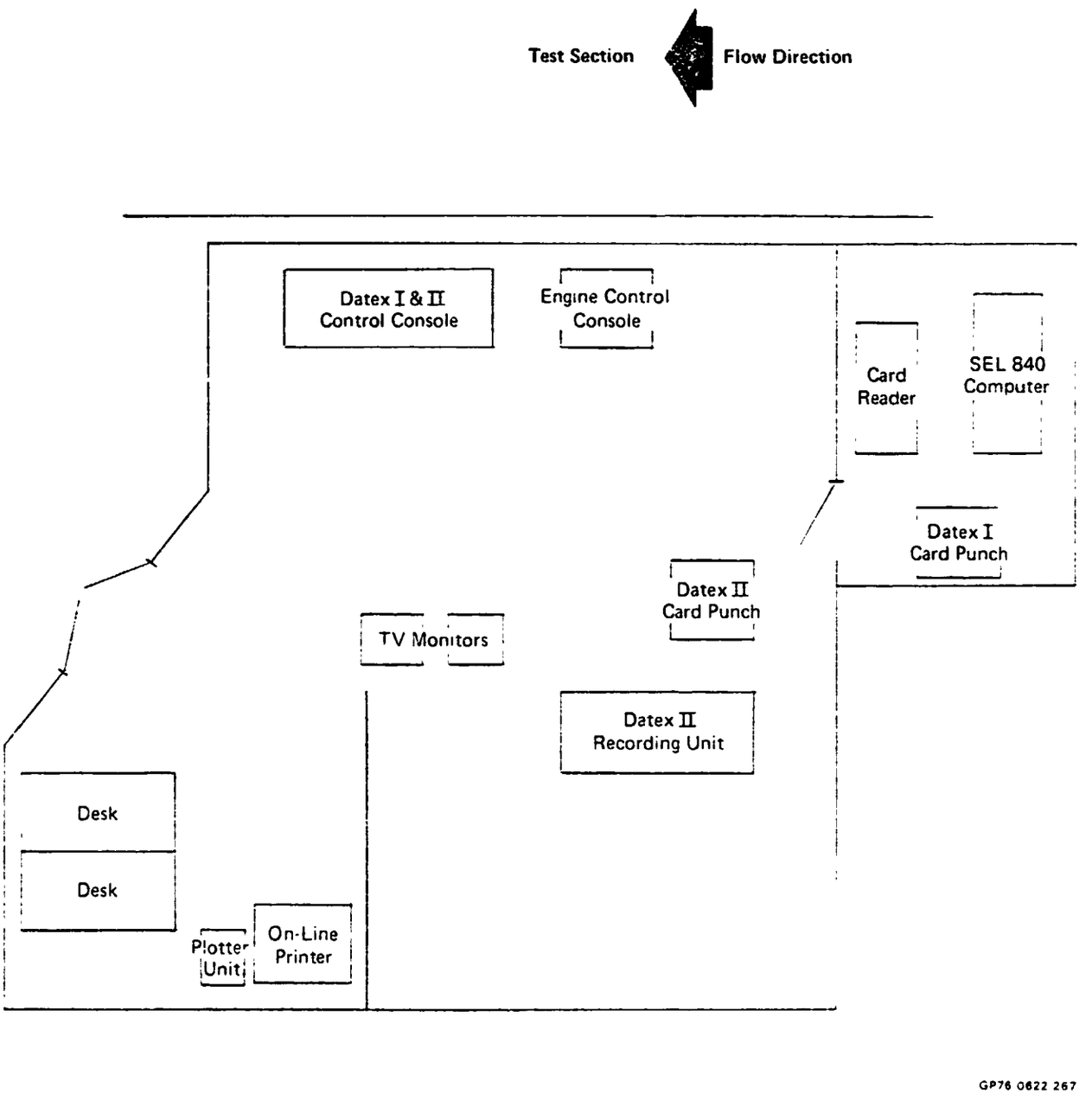

4.2 DATA ACQUISITION SYSTEM

Two separate Datex Corporation data acquisition systems are utilized in the 40' x 80' tunnel for recording the balance force and moment data and the model pressure and temperature data.

The Datex I system records the balance force data, tunnel test conditions, and the fan speeds. The individual balance scale readings are measured utilizing optical scanners and the three fan speeds are measured using rpm counters. These raw data are punched out on an IBM Card Punch located in the on-line computer room adjacent to the tunnel control room. Five readings are taken at each test point for both the balance scale data and fan speed data. Approximately 10 seconds are required to record a given test point on the Datex I system. The Datex I raw data cards are then processed on the SEL-840 on-line computer, and the results printed out on the tunnel control room printer.

The Datex II system was used to record the pressure and temperature data. All model pressures were measured using two Statham Corp. differential pressure transducers mounted in 48 port, "D" sized scanivalve modules. The scanivalve units were installed in the left and right wing sections of the model. The left unit contained five ganged modules and the right unit contained six ganged modules. A total of 460 model pressures were measured by the scanivalve systems.

All model temperature measurements were made using iron/constantan thermocouples. The leads of each thermocouple were routed from the model through the reference junction box located in the balance room to a 48 pickup temperature scanner mounted in the Datex II recording console. The Datex II recording system recorded all pressure and temperature signals on an IBM Card Punch unit. A scanning rate of 0.3 second per measurand was used for both the pressure and temperature data acquisition, resulting in a recording time per test point of approximately 40 seconds. The Datex I and Datex II data were recorded separately for each test point, the Datex I being recorded first. The Datex II raw data cards were processed on the SEL-840 on-line computer.

5. OUTSIDE STATIC TEST FACILITY

The large scale powered model ground effects test program was conducted at the NASA-Ames Research Center Outside Static Test Facility, designated as test site number N-249. The outdoor facility is located at a remote site approximately 1.6 km (1 mile) from the 40' x 80' wind tunnel.

The facility is equipped with adjustable height model support struts and provides a smooth ground plane below the test model. The strut arrangement is similar to that of the 40' x 80' wind tunnel. Height adjustment is achieved with interchangeable main strut sections of various lengths. The tail strut is a remotely driven telescoping unit that provides angle of pitch variation. A below-ground structure supports the three model struts and tail strut drive unit. The facility includes an enclosed trailer that serves as the control room and houses the data acquisition systems. Auxiliary equipment located at the test site includes the engine starter unit, 400 cycle A/C power supply, fuel tanker, and an air compressor. A plan view sketch of the static test facility layout is shown in Figure 5-1.

5.1 TEST ARRANGEMENT

Model Support

The model was supported with three struts arranged in the same location as previously used for the 40' x 80' tunnel test setup. All model and instrumentation leads were attached to the two main support struts and insulated with asbestos cloth wrapping for protection. Strut fairings were also installed at the two lowest heights tested to further protect the model leads from the flow field environment. The model was tested at three heights above the ground plane - 21.0, 8.3, and 3.3 feet. Schematic illustrations of the three ground height arrangements indicating the major components are shown in Figure 5-2. Photos of the test model setups are presented in Figures 5-3, 5-4, and 5-5.

Load Cells

Three load cells, one mounted on each of the support struts, were used to measure the forces on the model. Each load cell was a 3-component strain gauge balance, with a 6000 lb normal force, 4000 lb axial force, and 3000 lb side force capability. The load cells were installed directly below the test model between the support struts and model mounting pads. Metal shrouds were installed around each load cell, and cooling air was supplied to maintain near constant load cell temperatures. The load cell and cooling shrouds can be seen in the photo of Figure 5-3.

FIGURE 5-1
OUTSIDE STATIC TEST FACILITY PLAN VIEW

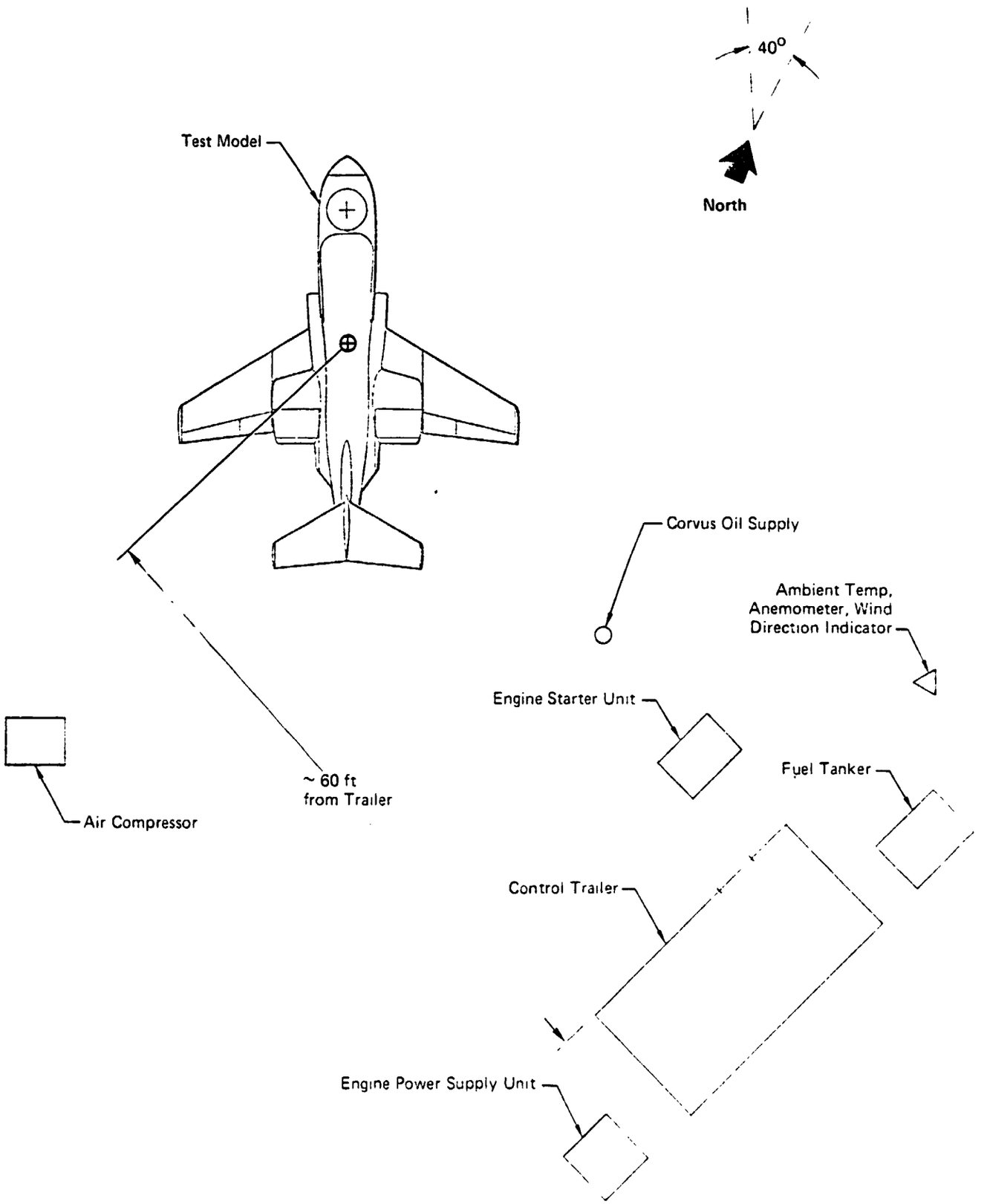

GP76 0622 470

FIGURE 5-2
MODEL GROUND HEIGHT VARIATIONS
Outside Static Test Program

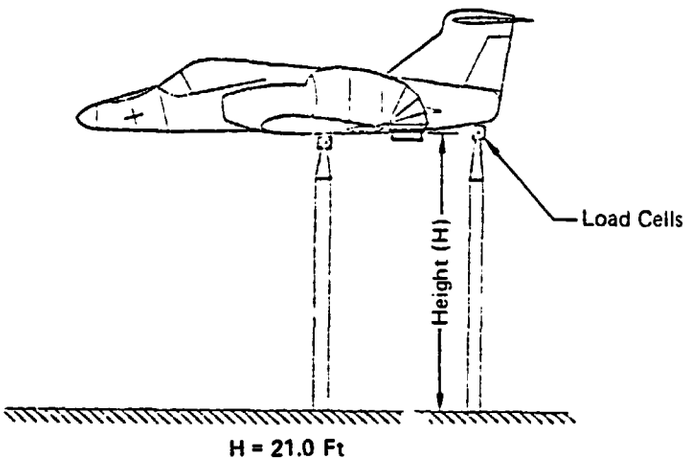

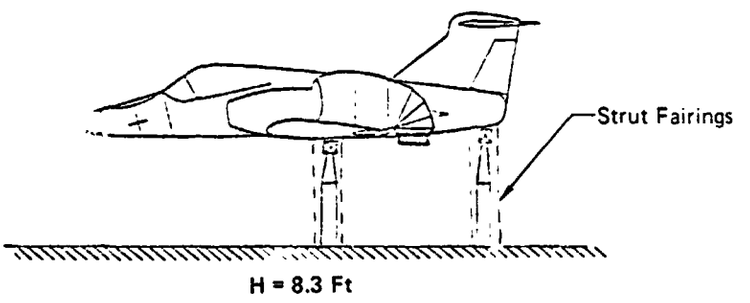

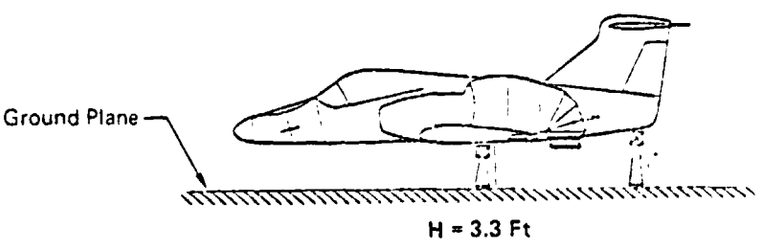

GP76 0622 278

FIGURE 5-3
LARGE SCALE POWERED MODEL INSTALLED IN OUTSIDE STATIC TEST FACI' 'TY
21.0 Ft Ground Height

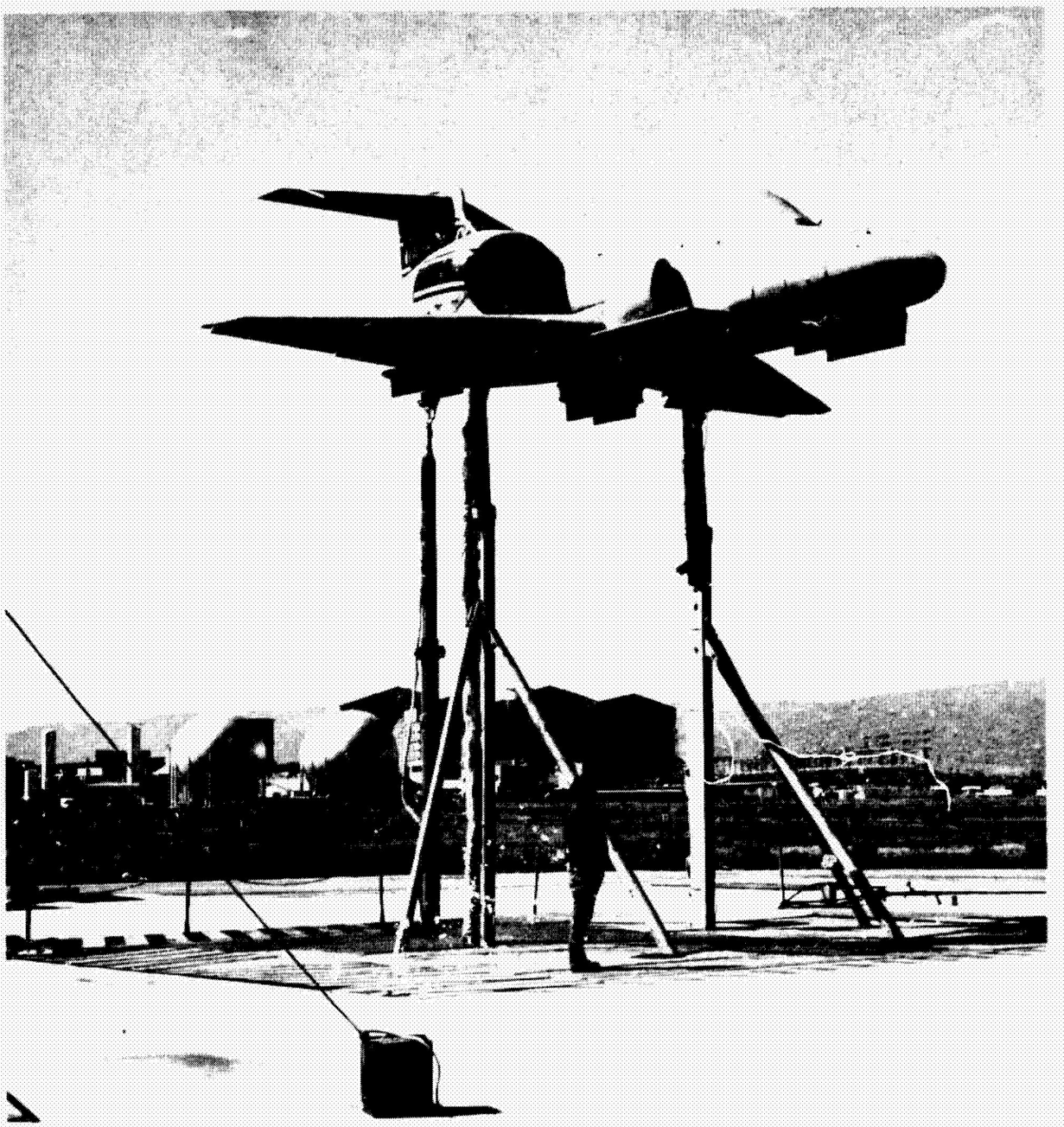

FIGURE 5-4
LARGE SCALE POWERED MODEL INSTALLED IN OUTSIDE STATIC TEST FACILITY
8.3 Ft Ground Height

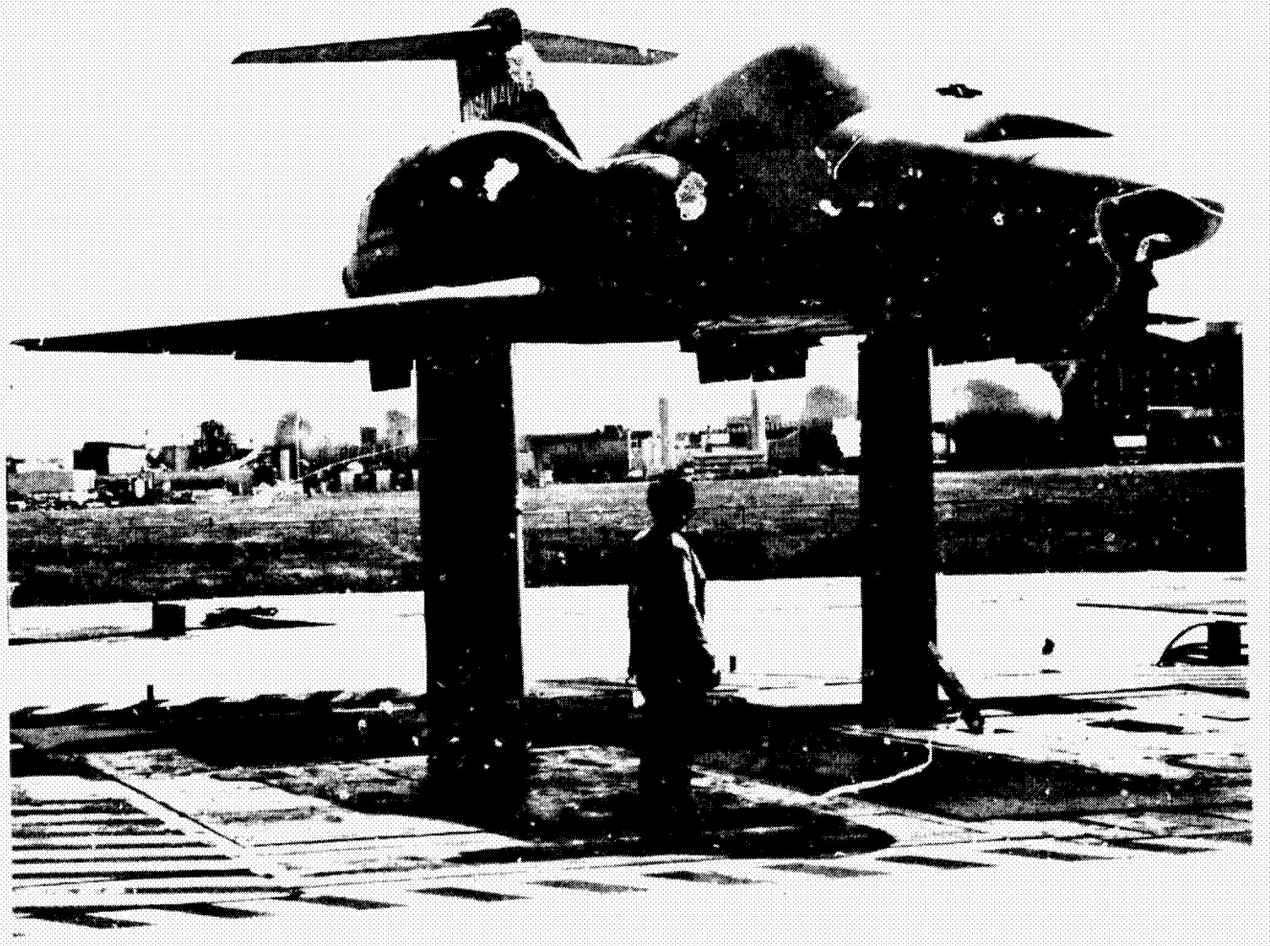

FIGURE 5-5
LARGE SCALE POWERED MODEL INSTALLED IN OUTSIDE STATIC TEST FACILITY
3.3 Ft Ground Height

Model Instrumentation

The model instrumentation utilized during the static ground effects test program was identical to that used during the 40' x 80' wind tunnel test. The quantity, type, and location of all model instrumentation were previously described in Section 3 of this report. The model monitoring and control systems, described in Section 4.2, were also the same.

5.2 DATA ACQUISITION SYSTEM

The measurements made during the static ground effects test program consisted of model pressures, temperatures, fan speeds, and balance forces. Both digital and analog data acquisition systems were utilized to record the data. The parameters measured and the recording systems utilized are discussed below. A detailed schematic flow diagram of the complete data acquisition system utilized during the static test program is presented in Figure 5-6.

Digital Data Acquisition

All model pressures, temperatures, fan speeds, and load cell component forces were measured and recorded utilizing a Vidar Corporation digital data acquisition system. The model pressures were measured in the same manner as during the in-tunnel tests utilizing differential pressure transducers installed in two separate scanivalve systems. Temperature measurements were made with iron-constantan thermocouples. Forty-eight of the 79 temperature measurements were connected to a scanning device for single channel multiplex recording, with the other 31 being recorded on individual temperature channels. The fan speeds were measured with rpm counters and recorded 48 times per test point on Vidar using three scanning channels. Each component of the three load cells was also recorded 48 times per test point using a total of nine scanning channels. The Vidar system digital raw data were recorded on a paper tape punch machine located in the on-site trailer. A schematic layout of the data acquisition system arrangements within the trailer unit is presented in Figure 5-7.

Analog Data Acquisition

All inlet temperature measurements and selected fan and tip turbine exit temperatures were analog recorded on magnetic tape. In addition, fan speed and selected pressures from the inlets and fan tip turbine exits were recorded on the tape. These analog measurements were made in order to determine both the time variant inlet reingestion characteristics and the subsequent variation of the propulsion system characteristics during reingestion. These measurements were recorded on two Ampex Corporation F/M tape recorders. Inlet temperatures were

FIGURE 5-6
DATA ACQUISITION SYSTEMS FLOW DIAGRAM
Outside Static Test Program

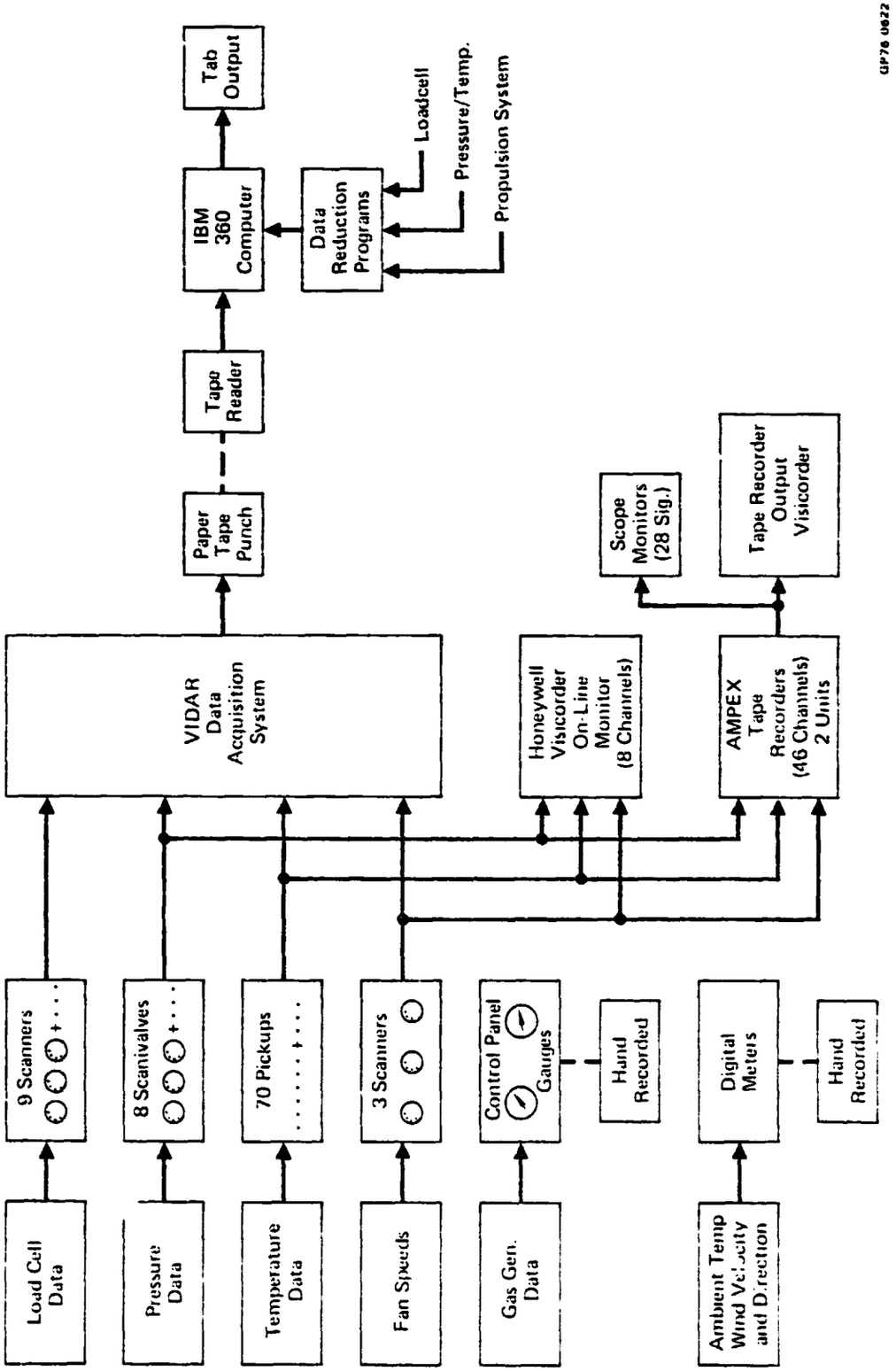

FIGURE 5-7
OUTSIDE STATIC TEST FACILITY CONTROL TRAILER LAYOUT
Data Acquisition Systems Arrangement

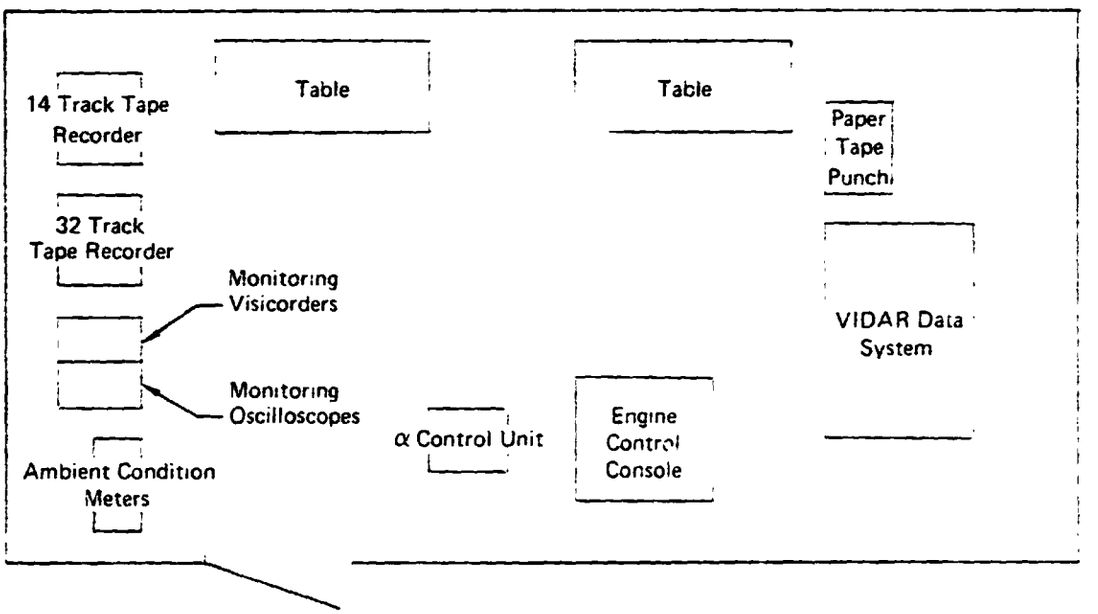

GP76 06.2 268

recorded on a 32-track Model PR2200 Ampex tape recorder, and the pressures and fan exit temperatures were recorded on a 14-track Model 1400 Ampex recorder. Temperature and pressure measurements were recorded simultaneously on both the digital Vidar system and the analog tape recorder systems. Separate high response pressure transducers were used for the analog pressure measurements. These were connected in parallel with the scanivalve transducers. Time code and voice tracks were included on each recorder.

Monitoring Systems

Two Honeywell Type 1858 CRT Visicorder oscillographs were utilized to monitor and display selected analog data. One oscillograph unit was used to monitor directly the on-line variations in selected temperatures, pressures, and fan speed. The other unit was used for displaying playback information recorded on the tape recorders.

Two 7-bank oscilloscope units were used to visually monitor selected time variant signals being recorded on the two tape recorder units. Each bank had the capability to display two signals, providing a total signal display capability of 28 channels.

Ambient atmospheric conditions were measured some distance away from the model and displayed on digital readout panels located in the trailer control room. Ambient temperature, wind velocity, wind direction, and barometric pressure were visually monitored and hand recorded.

The gas generator operating conditions were visually monitored and recorded by hand including the engine speed, exhaust gas temperature, oil pressure and temperature, fuel pressure, and engine vibration. The turbotip fan bearing temperatures and fan vibration levels, together with fan rpm (as a backup), were monitored and hand recorded. The above instrumentation was all included on the engine and fan control console in the control room. The same control unit was used for propulsion system operation in both the 40' x 80' tunnel and outside static test facilities.

6. WIND TUNNEL TEST PROGRAM

The test program conducted in the wind tunnel is described in the following sections.

6.1 TEST CONDITIONS

Powered lift configuration testing was conducted at several values of tunnel dynamic pressure at constant fan speed to obtain the desired variation of jet velocity ratio. Aerodynamic lift configuration testing was conducted at a constant value of dynamic pressure over a range of fan speeds to obtain a variation in inlet mass flow ratio. Test dynamic pressure values, Reynolds number per unit length and nominal jet exit velocity ratios and mass flow ratios are summarized below.

Preliminary Testing

Dynamic Pressure (PSF)	Dynamic Pressure (N/m^2)	Reynolds Number per Unit Length at Standard Atmospheric Conditions: Per Foot	Reynolds Number per Unit Length at Standard Atmospheric Conditions: Per Meter	Nominal Jet Exit Velocity Ratio ($N_F/\sqrt{\theta T_o}$ = 3600 RPM)
1.35	65	0.22×10^6	0.72×10^6	0.12
5.5	260	0.43×10^6	1.41×10^6	0.25
12.3	590	0.65×10^6	2.13×10^6	0.4
21.9	1050	0.87×10^6	2.85×10^6	0.5
34.2	1640	1.08×10^6	3.54×10^6	0.6
49.2	2360	1.30×10^6	4.27×10^6	0.7

Powered Lift Configuration Testing

Dynamic Pressure (PSF)	Dynamic Pressure (N/m^2)	Reynolds Number per Unit Length at Standard Atmospheric Conditions: Per Foot	Reynolds Number per Unit Length at Standard Atmospheric Conditions: Per Meter	Nominal Jet Exit Velocity Ratio ($N_F/\sqrt{\theta T_o}$ = 3600 RPM)
1.35	65	0.22×10^6	0.72×10^6	0.12
3.3	160	0.34×10^6	1.12×10^6	0.20
7.0	335	0.49×10^6	1.61×10^6	0.29
12.3	590	0.65×10^6	2.13×10^6	0.39
19.2	920	0.81×10^6	2.66×10^6	0.48

Aerodynamic Lift Configuration Testing

Dynamic Pressure (PSF)	Dynamic Pressure (N/m^2)	Reynolds Number per Unit Length at Standard Atmospheric Conditions: Per Foot	Reynolds Number per Unit Length at Standard Atmospheric Conditions: Per Meter	Mass Flow Ratio, A_o/A_{HL} @ $N_F/\sqrt{\theta T_o}$
34.2	1640	1.08×10^6	3.54×10^6	0.66 @ 1600 RPM 0.82 @ 2150 RPM 1.00 @ 2700 RPM

Model Variables

Model variables included twelve configuration variables, fan speeds, angle of attack and sideslip.

Preliminary Testing - Initial testing (Runs 1 through 28) was conducted to identify basic model characteristics (flap effectiveness, symmetrical aileron effectiveness and lift variation with angle of attack), the induced lift characteristics of the lift cruise unit alone, the incremental effects of the nose lift unit and the flow field characteristics at the horizontal tail location. A summary of variables tested is shown below. All testing was conducted with the flow survey rake on and the horizontal tail off.

Variable	Range
α_u	-4° to 32°
β	0°
δ_{LC}	0° to 90°
δ_{NL}	0° to 90°
δ_f	0° to 30°
δ_a	0° to 15°
δ_H	Off, Flow Survey Rake On
δ_R	0°
q	0 to 2360 (0 to 49.2) N/m^2 (PSF)
N_F/θ	1600 to 3600 rpm
Nose Gear	Off
Nose Lift Unit Inlet Covers	Open and Covered

Powered Lift Configuration Testing - Powered lift configuration force and moment data were obtained with the horizontal tail on and off for selected combinations of lift cruise unit geometric deflection (δ_{LC}) and nose lift unit geometric deflection (δ_{NL}) for jet velocity ratios (V_o/V_J) representative of the resultant vector angle (θ_J). The effect of sideslip angle was investigated at angles of attack of 0° for δ_{LC}/δ_{NL} of 90°/90°, 56°/43° and 23°/43° and 8° for δ_{LC}/δ_{NL} of 56°/43°. Horizontal tail effectiveness was determined for all configurations tested. Effects of yaw vane deflections were tested at δ_{LC}/δ_{NL} = 90°/90°; effects of aileron deflection and nose gear extension were tested at δ_{LC}/δ_{NL} = 56°/43°; and the effects of rudder deflection were tested at δ_{LC}/δ_{NL} = 38°/43°. A summary of powered lift configuration testing is shown below. Flaps and ailerons were set at 15° and 10°, respectively, for all these tests.

δ_{LC} (DEG)	δ_{NL} (DEG)	Nominal V_O/V_J Range	Comments
90	90	0.12 to 0.29	Hor. Tail off; β variation at $\alpha = 0°$; yaw vane effectiveness
71	55	0.12 to 0.29	Very limited testing
56	43	0.20 to 0.39	Hor. tail off; β variation at $\alpha = 0°$, 8°; aileron control power; nose gear effect; thrust modulation ports open
38	43	0.29 to 0.48	Limited testing; rudder Effectiveness
23	43	0.29 to 0.48	Hor. tail off, β variation at $\alpha = 0°$

Aerodynamic Lift Configuration - Aerodynamic lift configuration data were obtained at a tunnel dynamic pressure of 1640 N/m^2 (34.2 PSF). Corrected fan speeds were varied from 1600 RPM to 2700 RPM to obtain desired mass flow ratio variation. Testing conducted included horizontal tail control power, aileron control power and rudder control power in addition to variations in angle of attack and sideslip.

6.2 TEST PROCEDURES

Static Calibration

The propulsion system was calibrated at zero tunnel airspeed with the overhead tunnel doors open. Each lift/cruise unit geometric deflection was tested separately. Static force and moment data were obtained at corrected fan speeds of 2000, 2900, 3600 and 4100 RPM. In addition, static calibrations were repeated for $\delta_{LC} = 0°$ at corrected fan speeds of 1600, 2150 and 2700 RPM. The nose lift unit was calibrated for nose lift unit geometric deflection from 30° to 104° at approximately 10° increments at corrected fan speeds of 2000, 2900 and 3600 RPM.

Preliminary Testing

In order to provide insight into the sources of power induced force and moment increments identified during testing of the powered lift configuration, the initial testing examined the individual effects of the lift/cruise unit and nose lift units. The lift/cruise units were tested over a large jet velocity ratio range with the nose lift unit inlet covered and $\delta_{NL} = 0°$ to obtain the effect of the lift/cruise units alone. The nose lift unit was tested at a corrected fan speed of 3600 RPM for $\delta_{NL} = 35°$ to 90° with the lift/cruise unit at $\delta_{LC} = 0°$ and corrected fan speed of 3600 RPM and with the lift/cruise units windmilling (power off). Also, the nose lift unit was tested at $\delta_{NL} = 50°$ with the lift/cruise unit at $\delta_{LC} = 56°$. For these tests the horizontal tail was off and the flow survey rake was installed.

Powered Lift Configuration

The major test parameters for the powered lift configuration were jet velocity ratio and resultant thrust vector angle. Testing was restricted to the jet velocity ratios which are likely to be experienced in flight at a resultant thrust vector angle. In order to provide realistic results the combinations of lift/cruise unit and nose lift unit geometric deflection were selected to provide an approximate pitching moment balance at applicable jet velocity ratios. The table below summarizes the combinations selected:

δ_{LC}	δ_{NL}
90	90
71	55
56	43
38	43
23	43

The objectives of the powered lift configuration testing were to determine induced lift and drag characteristics, and to evaluate longitudinal and lateral-directional

stability and control characteristics.

Aerodynamic Lift Configuration

The primary test parameter for the aerodynamic lift configuration was the mass flow ratio (A_O/A_{HL}) for the lift/cruise unit fan inlets. Data were obtained at three values of mass flow ratio.

The objectives of the aerodynamic lift configuration testing were to establish the base line with which to compare the lift and drag characteristics of the powered lift characteristics, and to evaluate overall longitudinal and lateral-directional stability and control characteristics.

6.3 DATA REDUCTION

Force and moment data were obtained using the standard data procedures of the 40' x 80' wind tunnel. The measured data (balance data corrected for appropriate weight tares) were not corrected for wall interference effects, exposed tips of the model support struts, or strut interference effects. Therefore, the measured data includes all aerodynamic, propulsion, and interference forces acting on the model.

A major objective of the test was to determine the aerodynamic characteristics of the configuration at various tunnel and propulsion system operating conditions. In order to identify these aerodynamic characteristics, the measured forces (moments) were separated into a propulsion system component and an aerodynamic component. The direct propulsion system component is the vector sum of the gross thrust and inlet ram drag with propulsion units operating. The total aerodynamic component is the difference between the measured data and the direct propulsion system component. The aerodynamic component is divided into two components - an aerodynamic component at a reference condition and a propulsion system induced aerodynamic component.

Method of Determining Gross Thrust and Mass Flow Rates

The primary propulsion system performance parameters that were calculated during the 40' x 80' test program included the gross thrust (F_G), ram drag (F_{RAM}), jet velocity ratio (V_o/V_j), and inlet mass flow ratio (A_O/A_{HL}) for all three propulsion units. Two basic quantities were determined from measurements taken on the fan and tip turbine exit rakes, namely the mass flow rates ($\dot{w}$) and ideal exit velocities (V_I) for each component of each lift unit. The fan exit and turbine exit mass flows and ideal velocities were calculated using a mass-weighting technique for each individual rake probe. The equations for calculating the propulsion performance parameters are as follows:

$$\text{Gross Thrust } (F_G) = F_I \times C_F = [(\dot{w} \times V_I)_{TURB} + (\dot{w} \times V_I)_{FAN}]C_F$$

$$\text{Ram Drag } (F_{RAM}) = (\dot{w}_{TURB} + \dot{w}_{FAN})\, V_O$$

$$\text{Jet Velocity } (V_j) = F_G/(\dot{w}_{TURB} + \dot{w}_{FAN})$$

$$\text{Inlet Mass Flow } (\dot{w}_i) = \dot{w}_{TURB} + \dot{w}_{FAN}$$

The mass flow rate ($\dot{w}$) of each flow stream was calculated from the continuity equation using the static pressures, total pressures, and total temperatures to compute the flow properties. The ideal exit velocity (V_I), which is the isentropic or maximum velocity that can be obtained expanding the exit flow through a zero loss nozzle, was also calculated from the static pressure, total pressure, and total temperatures measurements used to compute flow properties. The thrust calibration coefficient (C_F) in the above equations was determined for each vector position for each unit

from the static calibrations. This parameter was shown to be essentially constant with fan speed and was assumed to be non-varying with forward speed for the analyses performed in this test program. The thrust calibration coefficient equals the ratio of the balance-measured static and gross thrust (F_S) to the rake-measured static ideal thrust (F_I). The resultant thrust vector angles determined from the static calibrations were also shown to be essentially constant with fan speed.

Method of Removing Direct Propulsion System Component

The propulsion system direct effects were modeled by three terms, i.e., thrust vector angle, gross thrust and mass flow rate. The equations and constants that were used are presented in Figure 6-1. In order to use the in-tunnel static calibration obtained with the propulsion unit installed in the model as the basic propulsion unit performance, the following assumptions were required.

- The induced loads on the model when operating one propulsion unit at a time are negligible.
- The fan-rake-measured mass flow rate is measured at an acceptable level of accuracy.
- The resultant thrust angle is a function of geometric deflection angle and is unaffected by tunnel freestream velocity.

Aerodynamic Reference Configuration

The reference configuration has a significant effect on determining the magnitude of the induced characteristics. The reference configuration selected for this test is the aerodynamic lift configuration (δ_{LC} = 0°, nose fan inlet covered) at unit mass flow ratio (A_O/A_{HL} = 1.0) with all aerodynamic controls deflected the same as for the powered lift configuration. It should be noted that this definition of reference configuration implies that the incremental induced lift and drag include the effects of the external wetted surface of the lift/cruise nozzles, and the nose lift fan inlets and exits as well as the induced effects of the captured stream tubes on the aerodynamic forces and on the other propulsion units.

All powered lift configuration data were obtained with flaps deflected 15° and ailerons deflected 10°. Due to test limitations, the aerodynamic lift configuration was tested with these flap and aileron deflections only during the preliminary testing. Consequently, clean configuration (flap and aileron at 0° deflection) data was used to establish the incremental effects of horizontal tail, landing gear, and flow survey rake. A discrepancy occurred in the drag data with the addition of the horizontal tail at low angles of attack in that drag was reduced instead of increased

as expected (see Section 8.6). In establishing the drag of the reference configuration, the following test results and assumptions were used:

Item	Incremental Drag Coefficient at $C_L = 0.25$ (Based on Wing Area)
Nose Gear	0.0100
Flow Survey Rake	0.0070
Horizontal Tail ($\delta_H = 0°$)	0.0000
Flap ($\delta_F = 15°$) and Aileron ($\delta_a = 10°/10°$)	0.0165

Below is the summary tabulation of the aerodynamic coefficients of the reference configuration at selected conditions:

- Nose Gear On, $\delta_H = 0°$, $\delta_F = 15°$, $\delta_a = 10°/10°$

Angle of Attack (deg)	C_L	C_D
0	0.325	0.0705
8	0.869	0.1033
16	1.36	0.246

- Nose Gear On, Horizontal Tail Off, $\delta_F = 15°$, $\delta_a = 10°/10°$

Angle of Attack (deg)	C_L	C_D
0	0.355	0.0710
8	0.843	0.1009
16	1.28	0.232

- Nose Gear Off, Flow Survey Rake On, $\delta_F = 15°$, $\delta_a = 10°$

Angle of Attack (deg)	C_L	C_D
0	0.355	0.0680
8	0.843	0.0979
16	1.28	0.229

FIGURE 6-1
EQUATIONS FOR MODELING DIRECT PROPULSION SYSTEM COMPONENTS

Force Data

Direct Thrust (No Yaw Vane Deflection)

$L = F_G \sin(\theta + \alpha)$

$D = F_G \cos(\theta + \alpha)$

$Y = 0$

Effect of Inlet Mass Flow Rate

$L = 0$

$D = V_o \dot{W} \cos(\beta)/g$

$Y = -V_o \dot{W} \sin(\beta)/g$

Moment Data

$$m = D\left\{[WL - (WL)_{RC}]\ [\cos(\alpha)] - [FS - (FS)_{RC}]\ [\sin \right.$$
$$- L\left\{[FS - (FS)_{RC}]\ [\cos(\alpha)] + [WL - (WL)_{RC}]\ [\sin(\alpha,\right.,$$

$$\ell = Y\left\{[WL - (WL)_{RC}]\ [\cos(\alpha)] - [FS - (FS)_{RC}]\ [\sin(\alpha)]\right\}$$
$$- L\,[BL - (BL)_{RC}]$$

$$n = -Y\left\{[FS - (FS)_{RC}]\ [\cos(\alpha)] + [WL - (WL)_{RC}\ \sin(\alpha)]\right.,$$
$$+ D\,[BL - (BL)_{RC}]$$

GP76-0622 279

CONSTANTS FOR MODELING DIRECT PROPULSION SYSTEM COMPONENTS

	FS	WL	BL
Model Reference Center	276.29	80.22	0.00
Nose Fan Inlet	114.40	90.80	0.00
Gas Generator Inlet for Nose Fan	238.10	104.50	0.00 (Avg Both Sides)
Left Lift Cruise Fan Inlet	282.00	89.60	−51 24
Gas Generator Inlet for Left Lift Cruise Fan	203.90	80.00	−33.00
Right Lift Cruise Fan Inlet	282.00	89 60	51 24
Gas Generator Inlet for Right Lift Cruise Fan	203.90	80.00	33.00
Nose Fan Thrust Center	117.05	54.90	0.00
Lift Cruise Fan Thrust Center			
Left $\delta_{LC} = 0^o$	354.50	89.60	−51 24
Right $\delta_{LC} = 0^o$	354.50	89 60	51 24

Note: All dimensions are model scale in inches GP76 0622 280

7. OUTSIDE STATIC TEST PROGRAM

A description of the outside static test program, including the test conditions, test procedures, and data reduction employed, is presented in the sections that follow.

7.1 TEST CONDITIONS

The purpose of the outside static test program was to evaluate the ground effects on the three fan V/STOL aircraft concept. Specific objectives of the test program were to measure the effects of ground height on total installed lift and on inlet reingestion. The model was tested at three ground heights of 21.0, 8.3, and 3.3 feet, corresponding to H/D's of 6.45, 2.55, and 1.02, respectively. Landing gear height for this configuration corresponds to an H/D of approximately 1.02 the height being measured from the L/C nozzle exits as shown in Figure 5-2.

Initial testing was conducted at the 21.0 foot reference height, followed by tests at the lowest height of 3.3 feet, and then finishing up at the intermediate height of 8.3 feet. The effects of fan speed variations, thrust vector angle, exhaust jet splaying, and inlet shielding were also evaluated. The specific test conditions and model variable evaluated in the ground effects test program are summarized in the below table:

- Model Height, H (ft) — 21.0, 8.3, 3.3
- Fan Speeds, $N_F/\sqrt{\theta_{TO}}$ (RPM) — 2000, 2900, 3600, 4100
- Nose Unit Geom. Deflection Angle, δ_{NL} (deg) — 80, 95, 102
- Nozzle Yaw Vane Deflection Angle, δ_Y (deg) — 0, $\pm$12
- Gas Generator Inlet Shield Sizes — Large, Small
- Inlet Shield Angle, δ_S (deg) — 0, 45, 90

All remaining model test variables were held at constant values as given below:

- Lift/Cruise Geometric Deflection Angle, δ_{LC} — 90°
- Aileron Deflection Angle, δ_A — 10°
- Flap Deflection Angle, δ_F — 15°
- Rudder Deflection, δ_R — 0°
- Horizontal Stabilator Deflection δ_H — 0°

In addition to the ground effects testing, calibration runs were made on the lift/cruise and nose lift units for comparison with the data obtained in the 40' x 80' wind tunnel tests. Also, a fan performance map was generated for the T58-8B/X376B propulsion system for reference purposes. It was generated varying the following parameters using the L/H lift/cruise unit:

- Percent Corrected Fan Speed, % $N_F/\sqrt{\theta_{T_o}}$ (RPM) 40 to 100
- Nozzle Exit Area, A_N (in^2) 930, 1075, 1385
- Nozzle Deflection Angle, δ_{LC} (deg) 0

The model instrumentation utilized was identical to that of the 40' x 80' wind tunnel tests. The primary quantities measured during the static test were the same as those considered primary in the tunnel tests and included the following:

- Balance-measured Forces and Moments
- Rake-measured Fan Performance including:
  - Ideal Thrusts, $F_{I_{FAN}}$ and $F_{I_{TURB}}$.
  - Airflow Rates, $\dot{w}_{FAN}$ and $\dot{w}_{TURB}$.
  - Nozzle Total Pressure Ratio, NPR
  - Jet Velocity, V_J
  - Jet Total Temperature, T_j
- Rake-measured Inlet Performance including:
  - Inlet Recovery and Distortion, P_{T_2}/P_{T_o} and $(P_{T_{max}} - P_{T_{low}})/P_{T_2}$
  - Inlet Total Temperature Level, T_i

In addition to the above measurements, flow visualization runs were also performed at selected test conditions. The test procedures utilized in conducting the static test program are discussed in the section that follows.

7.2 TEST PROCEDURES

The tests conducted during this program included the following:

- o Individual Unit Calibration Runs
- o T58/X376B Fan Performance Map Generation
- o Three Unit Operation Ground Effects Testing
- o Individual Unit Operation Ground Effects Testing
- o Flow Visualization Tests

The specific tests at the 21-foot height included the following:

- o Reference Height Ground Effect Tests, all units in operation
- o Calibration Runs on each unit individually
- o Fan Map Performance Run, left unit only

At the two lower heights tested, individual unit performance runs were conducted on each unit separately, the three-unit operation ground effects performance runs, were accomplished and flow visualization runs made. At each ground height, all model test variables listed in Section 7.1 were varied in a systematic manner to provide parametric data. The test sequence and approach employed for each specific test conducted are described below.

Fan Performance Map

A T58/X376B fan map was generated at the start of the test program utilizing the left lift/cruise unit. The test was conducted at a height of 21.0 feet with a vector angle of 0°. Three specific nozzle areas were installed on the model in the cruise mode and fan speeds were varied from 1900 to 4100 rpm (40% to 100%) in 10% increments. Force and moment and steady state pressure and temperature data were recorded.

Calibration Runs

The individual unit calibration runs were performed at a height of 21.0 feet (H/D = 6.45) following the fan mapping test. The lift/cruise units were vectored 90° and fan speeds were varied from 2000 to 4100 rpm on each. The nose lift unit was tested at manually positioned vector angles of 40, 60, 80, 95 and 102 degrees while varying the fan speed for each vector angle from 2000 to 4100 rpm. Splay angles of 0° and 12° were also tested for each unit utilizing the yaw vanes. Force and moment balance data along with digital steady state pressure and temperature data were recorded.

Three Unit Ground Effects Testing

The ground effects test sequence with all three units in operation was conducted at all three ground heights. Force and moment data along with inlet reingestion data were recorded for each test point simultaneously, utilizing the digital Vidar and analog tape recorder systems. The test sequence went as follows:

- o Beginning zero's were taken, ambient conditions recorded, the tape recorders and monitoring Visicorders were turned on, and the three engines were started and brought to idle. The two L/C units were brought up to their desired speeds simultaneously, and then the forward unit was brought up to speed.
- o When steady state conditions were reached, the Vidar data system was actuated. Ambient conditions were recorded by hand three times throughout the test point at 30 second intervals. Approximately 90 seconds were required for acquisition of the Vidar data. A time sequence log was recorded by hand for the tape recorder units to serve as backup to the automatic time code generator.
- o The tape recorders and monitoring Visicorder were left on during a complete run, including the excursions between each test point and during the engine shutdown sequence. A given run lasted anywhere from 5 minutes to 45 minutes, depending on the number of test points.
- o At the end of a run, the engines were brought to idle conditions and the tape recorders and monitoring Visicorder turned off. After allowing time for engine cooling, they were shut off and end zeros were taken and ambient conditions recorded.

The only model test variable that was remotely controlled was fan speed. A given run therefore included only rpm variations. The louver angles, yaw vane splay angles, and shield angles were set manually between each run.

Individual Unit Ground Effects Testing

The ground effects tests on the individual units were conducted in similar fashion as described above. Each unit was run individually over an rpm range from 2000 to 4100 rpm, while varying the louver and/or splay angles. In addition to the individual unit runs, combination runs were performed on the two lift/cruise units. The purpose of these tests was to evaluate the differences between the individual and combined effects of unit operation on the force and moment data. Inlet reingestion data were also measured during these individual tests.

Flow Visualization Tests

The test model was equipped with Corvus oil injection nozzles located downstream of the engine in the hot gas interconnect ducting on all three units. At selected intervals during the test program, flow visualization runs were perfo·.ed. The Corvus oil generated dense smoke in the hot stream of each u.it, and both normal speed (24 frames/sec) and high speed (250-500 frames/sec.) color movies were taken. Still color photos were also taken during selected runs. The engines were throttled to fan speeds of 2000 rpm on all three units, and then the Corvus oil line valve was opened to supply oil to all three units simultaneously. Run duration was approximately 10 seconds each. Both the normal and high speed cameras were activated simultaneously prior to oil injection, and were run through the duration of the transient to steady state development of the visualized flow field. Camera angles from the front and side of the model were used, but not simultaneously. Both the Vidar and analog data systems were operated just before the flow visualizacion tests.

7.3 DATA REDUCTION

Four separate data reduction packages were generated during the outside static test program. These data reduction packages included the following sets of reduced data:

- o Load Cell and Fan Speed Data
- o Pressure and Temperature Data
- o Propulsion System Performance Data
- o Analog Temperature and Pressure Data

A description of each data package is presented in the following sections.

Load Cell and Fan Speed Data Package

For each test point, the load cell forces and fan speeds were recorded times on the Vidar system at a rate of 0.8 second per measurement. The arithmetic average of the 48 recordings was determined for each component force and fan speed and printed out on a summary page that included the following reduced data calculations:

- o Normal, Axial, and Side Forces
- o Left, Right, and Nose Fan Speeds
- o Pitching, Yawing, and Rolling Moments
- o Resultant Flow Vector Angles

These data were processed on an IBM 360 computer at NASA/Ames utilizing the Vidar recorded punched paper raw data tapes.

Pressure and Temperature Data Package

For each test point, all model pressures and temperatures were each recorded one time on the Vidar digital system using a scan rate of 0.8 second per port. The pressure and temperature data package consisted of a listing of all quantities measured including the following:

- o All Model Pressures in Ratio Form (P/P_{AMB})
- o All Temperatures in °F
- o Left, Right, and Nose Fan Speeds (48 readings)

Other than the ratioing of the pressure measurements, and the conversion of the temperature and fan speeds to their respective units, no further data reduction was done. This data package was also processed on the IBM 360 computer using the Vidar recorded punched paper raw data tapes.

Propulsion System Performance Data Package

The propulsion system performance data package used in the outside static test program was identical to that utilized in the 40' x 80' tunnel test program. The

performance program utilized the Vidar digital output from the pressure and temperature data package described in the previous section, and calculated all steady state propulsion system performance parameters required for analysis. The primary performance parameters that were calculated and printed out for each lift unit included the following:

- o Fan and Tip Turbine Performance Data
  - Total Corrected Airflows
  - Nozzle Total Pressure Ratio
  - Ideal Gross Thrust
  - Corrected Fan Speeds
  - Ideal Fan Horsepowers
  - Nozzle Jet Velocities
  - Nozzle Exhaust Jet Temperatures
- o Inlet Performance Data
  - Total Pressure Recovery and Distortion
  - Average Inlet Total Temperatures and Distortion

Several additional quantities were also calculated and printed for each component of each propulsion system unit, mainly the basic flow properties calculated for determining the above parameters. The propulsion system data package was also processed on the NASA/Ames IBM 360 computer.

Analog Pressure and Temperature Data

The time variant pressure and temperature data recorded on the two tape recorders was reduced simply by playing back the tapes for specific runs and recording the analog output on oscillograph paper. All inlet temperatures and selected fan and turbine exit pressure and temperatures were recorded. The reduction of selected data from specific runs was accomplished at certain intervals throughout the test program to insure proper operation of the data acquisition process.

8. WIND TUNNEL TEST RESULTS

The results of the 40' x 80' Wind Tunnel Test program are presented in this section. The basic aerodynamic characteristics of the model, along with the propulsion system performance characteristics, are presented for both the powered lift and aerodynamic life configurations. The model was primarily tested at constant corrected fan speeds, while varying tunnel speed to achieve variations in jet velocity ratio. No airframe static pressure data are presented in this report because of problems encountered in the reduction process.

8.1 PROPULSION SYSTEM STATIC CALIBRATIONS

The results of the propulsion system static calibrations are presented in Figures 8.1-1 through 8.1-18, for the left and right lift/cruise and nose lift units. The balance-measured static gross thrusts, the rake-measured ideal gross thrusts, and the resultant thrust vector angles for each unit are presented, along with the resultant thrust calibration coefficients that were determined and utilized throughout the forward speed tunnel tests. The static calibrations on the individual units were performed in the 40' x 80' tunnel, with the units installed in the model.

The balance-measured static gross thrusts for the left, right, and nose lift units are presented in Figures 8.1-1 through 8.1-4, respectively. The resultant static thrust is plotted versus the square of the fan speed (to linearize the variation) for each vector angle where a fan speed range was tested.

The rake-measured ideal gross thrusts for the three units are presented in Figures 8.1-5 through 8.1-8. These data are presented in the same manner as the force data, for the same identical test points and vector angles. The rake determined ideal gross thrusts for both the fan and tip turbine exit flows were calculated using an individual probe mass-weighting technique utilizing the fan and turbine pressure and temperature measurements made at the stator exits of each.

The thrust calibration coefficient, defined here as the ratio of the actual balance-measured static thrust to the rake-measured ideal thrust (F_S/F_I), was determined for each geometric vector angle for all three propulsion units. A representative plot of balance thrust and ideal thrust versus fan speed squared is presented in Figure 8.1-9 for the left lift/cruise unit at a nozzle deflection angle of 90°. The thrust calibration coefficient (C_F) was determined by ratioing the slopes of the two linearly faired curves, as illustrated in the figure. The nozzle thrust coefficient determined in this manner remains constant with corrected

fan speed. Comparison of the measured data points with their linearized fairings for all units at each vector angle over the fan speed range of interest showed a tolerance band of +2% on the thrust calibration coefficients.

The thrust calibration coefficients for the left and right lift/cruise units are presented in Figure 8.1-10. As shown in the figure, both units have similar performance characteristics with vector angle, with the right unit exhibiting approximately 1% greater nozzle thrust calibration coefficients across the vectored range. The nose lift unit thrust calibration results are shown in Figure 8.1-11. The nozzle vectoring performance is a maximum at the 70° vector angle, as expected. This is due to the installation of the nose fan at a forward tilt angle of 15° with respect to a waterline.

The resultant thrust vector angles plotted against corrected fan speed for the left, right, and nose fan units are presented in Figures 8.1-12, 8.1-13, and 8.1-14, respectively. As shown in these figures, the resultant thrust vector angles for each lift unit vary only slightly with fan speed, and were therefore assumed to be constant. These resultant thrust vector angles were calculated using the normal, axial, and side force components of the balance data.

The resultant thrust vector angles used in the analysis of the data in this report are summarized and presented in Figures 8.1-15 and 8.1-16, for the lift/cruise units and nose fan units, respectively. As stated above, the flow vector angles were assumed to be constant versus fan speed for each unit. The right and left lift/cruise vector angles were almost identical, and therefore the same values were used for both units. The nose unit values used in the data analysis are shown in Figure 8.1-16.

The static pitching moment variation for both the lift/cruise and nose lift units as a function of their respective nozzle deflection angles is presented in Figures 8.1-17 and 8.1-18.

FIGURE 8.1-1
LEFT LIFT/CRUISE UNIT STATIC THRUST
Propulsion System Calibration Data
$V_o = 0$

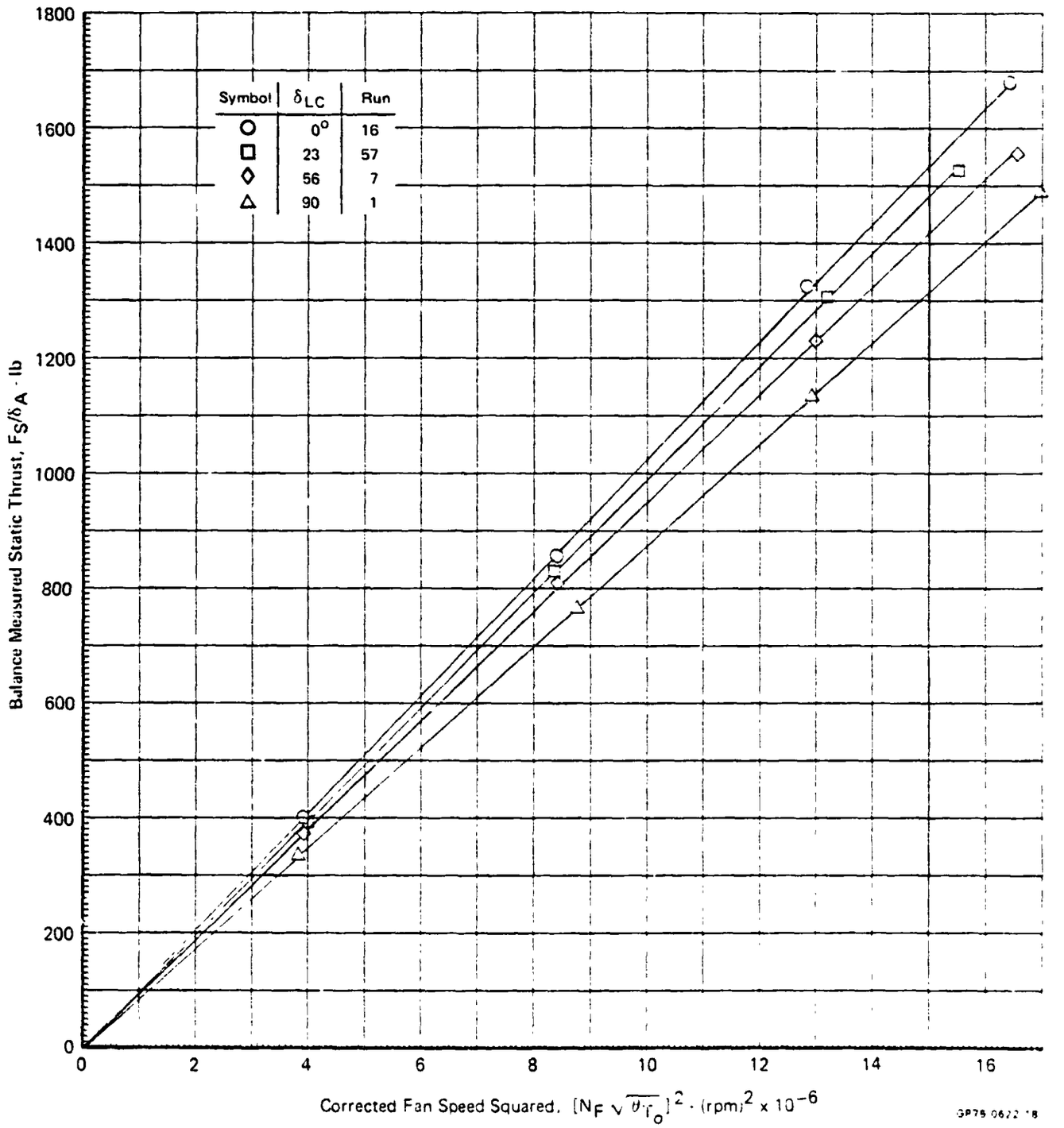

FIGURE 8.1-2
RIGHT LIFT/CRUISE UNIT STATIC THRUST
Propulsion System Calibration Data
$V_o = 0$

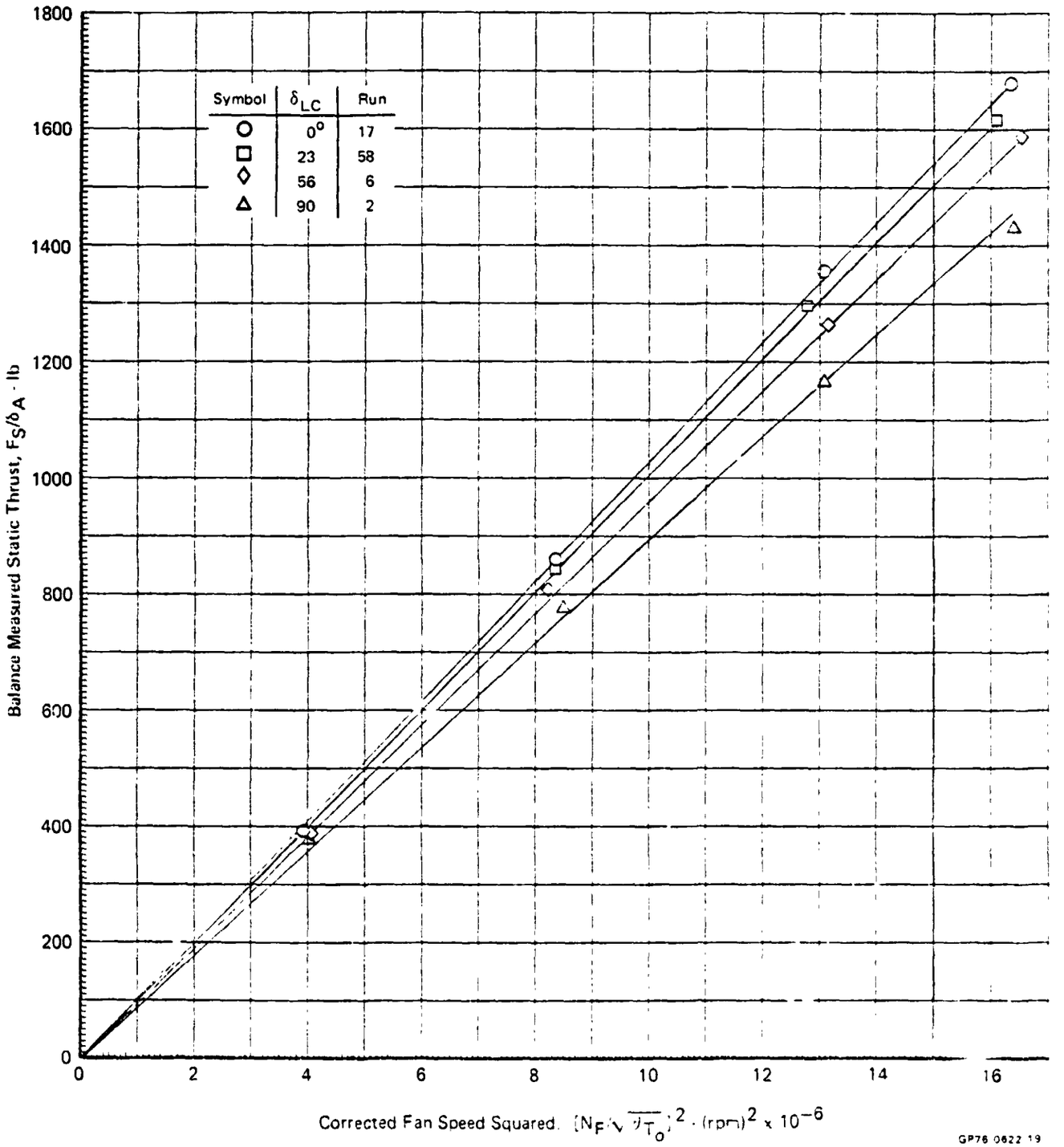

FIGURE 8.1-3
NOSE LIFT UNIT STATIC THRUST
Propulsion System Calibration Data
$V_o = 0$

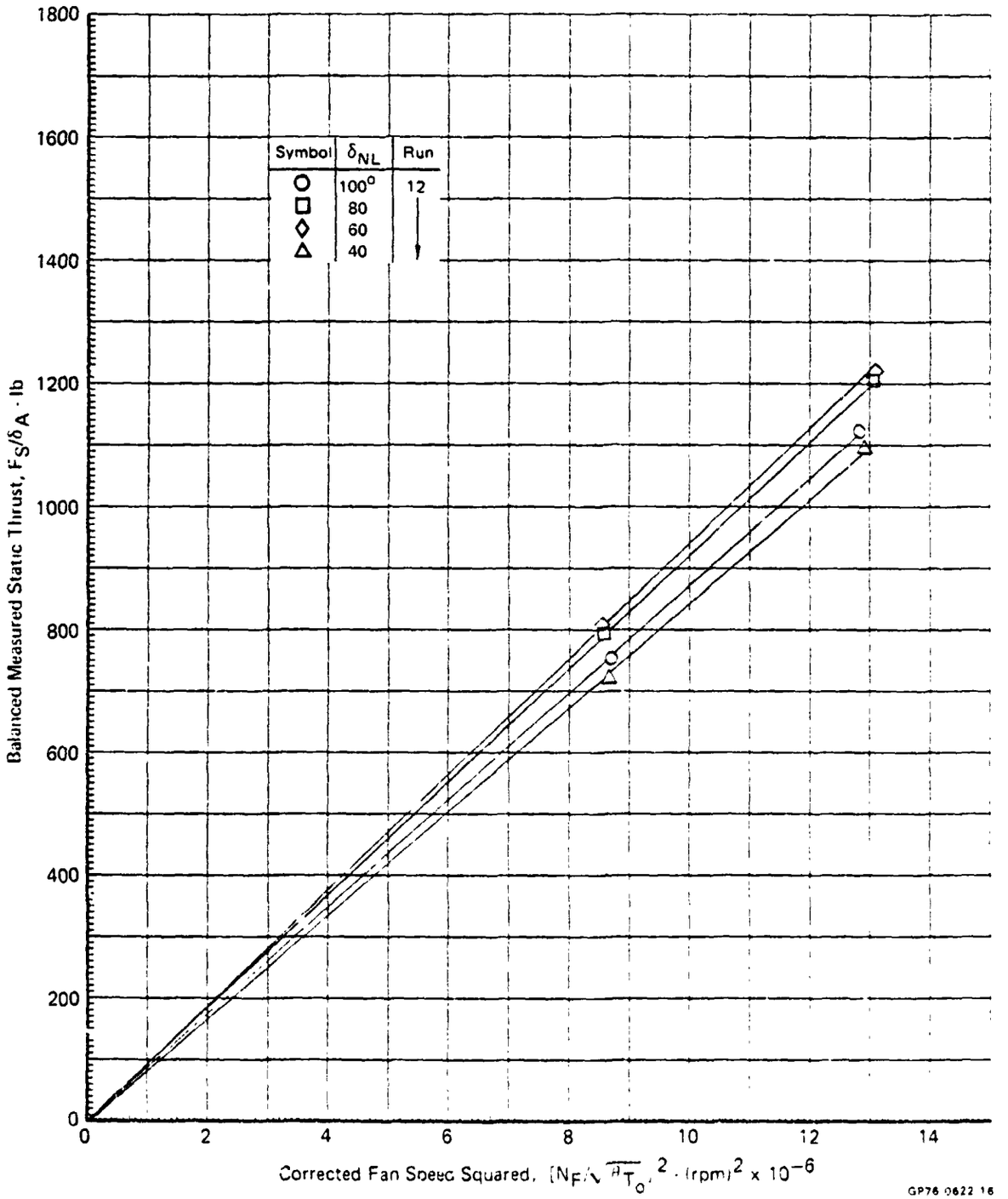

FIGURE 8.1-4
NOSE LIFT UNIT STATIC THRUST
Propulsion System Calibration Data
$V_o = 0$

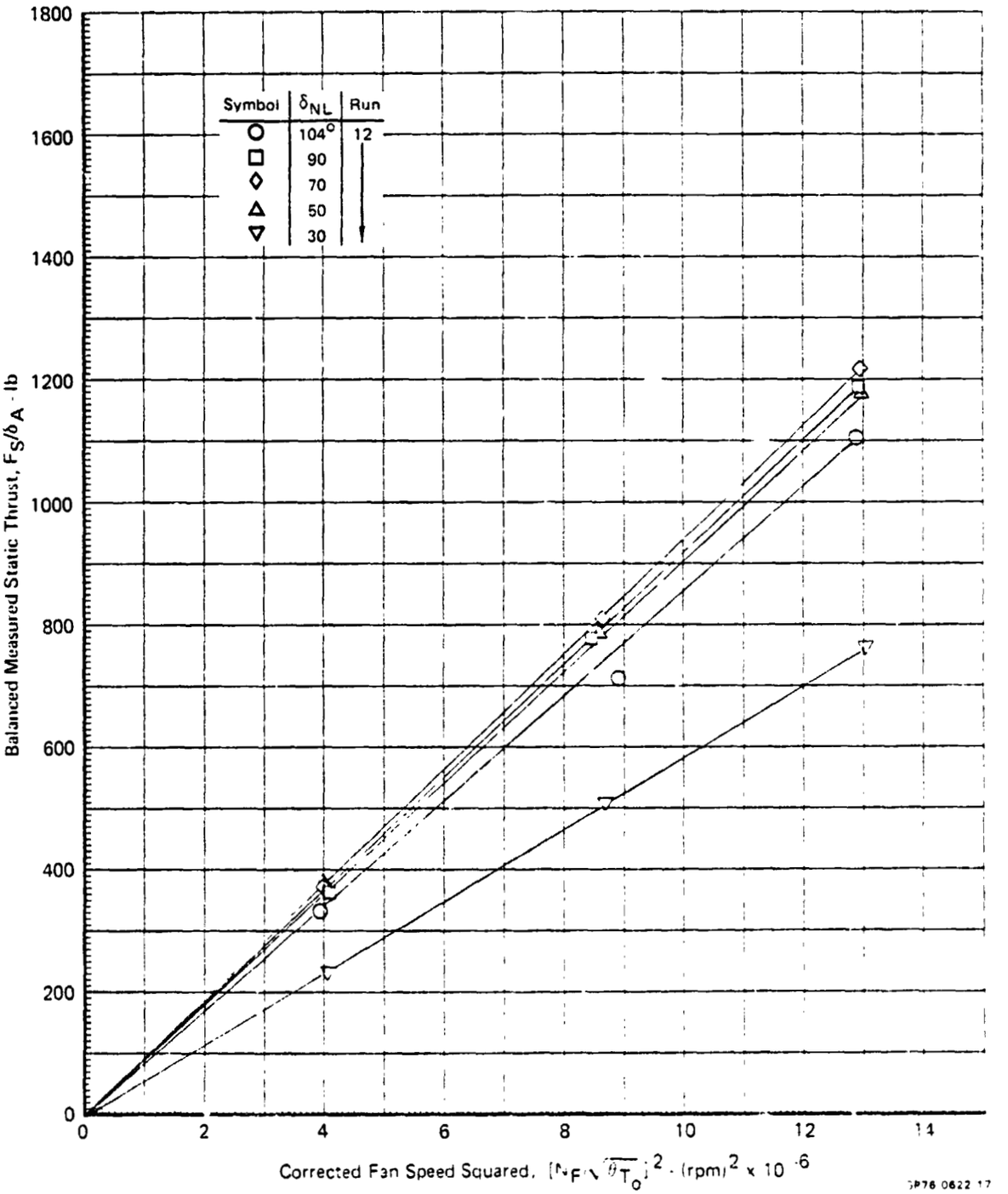

FIGURE 8.1-5
LEFT LIFT/CRUISE UNIT IDEAL THRUST
Propulsion System Calibration Data
$V_o = 0$

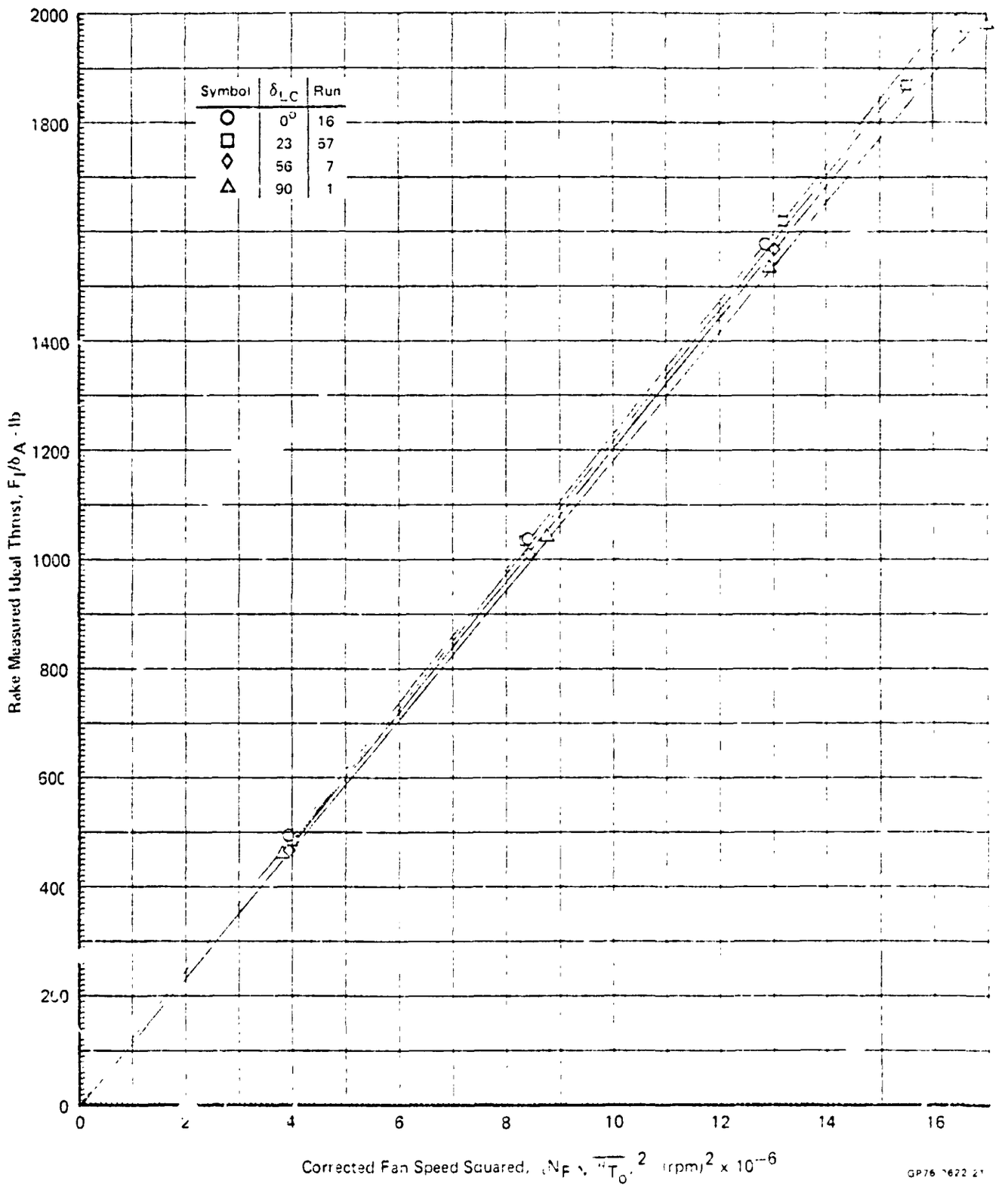

FIGURE 8.1-6
RIGHT LIFT/CRUISE UNIT IDEAL THRUST
Propulsion System Calibration Data
$V_o = 0$

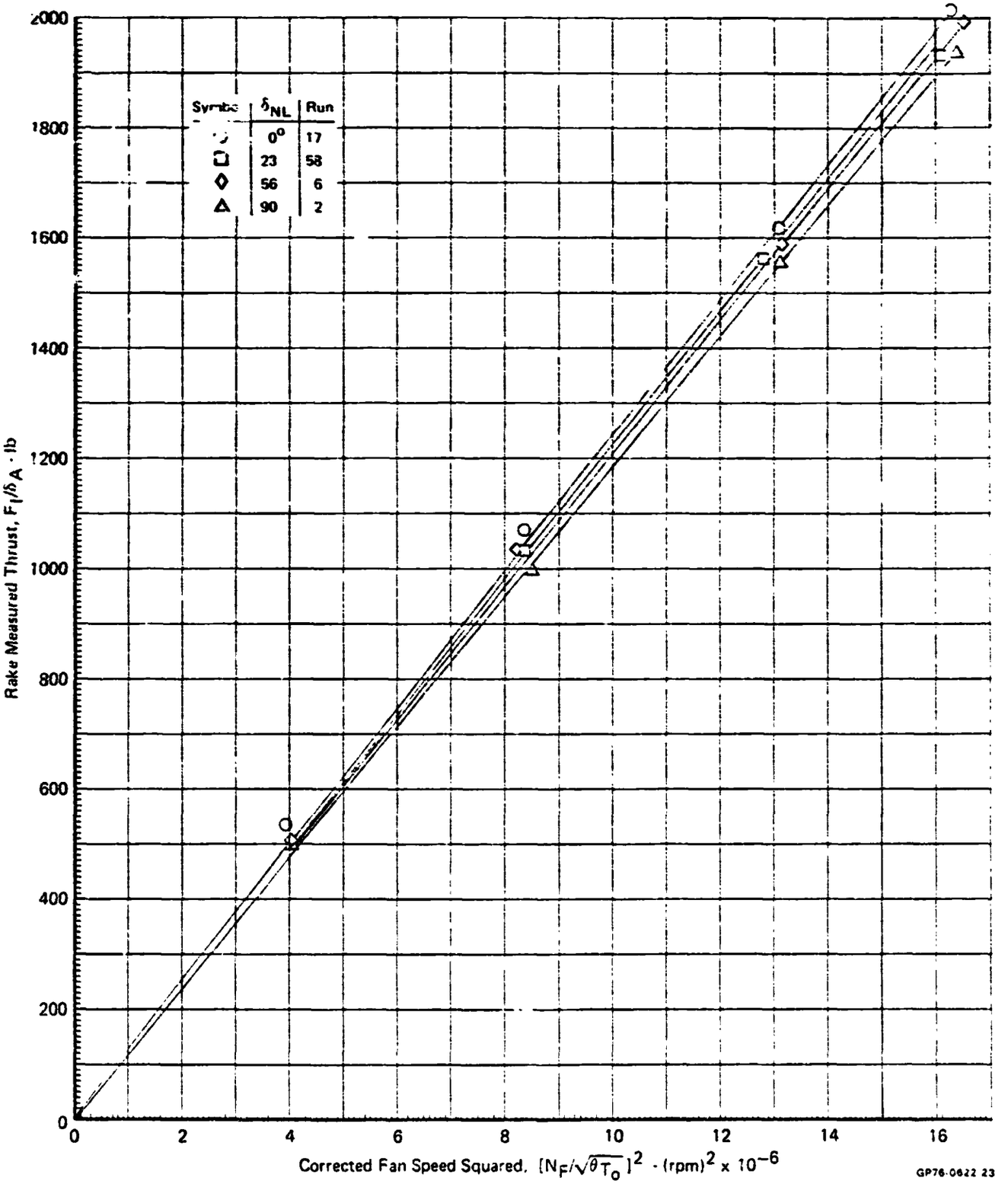

FIGURE 8.1-7
NOSE LIFT UNIT IDEAL THRUST
Propulsion System Calibration Data
$V_o = 0$

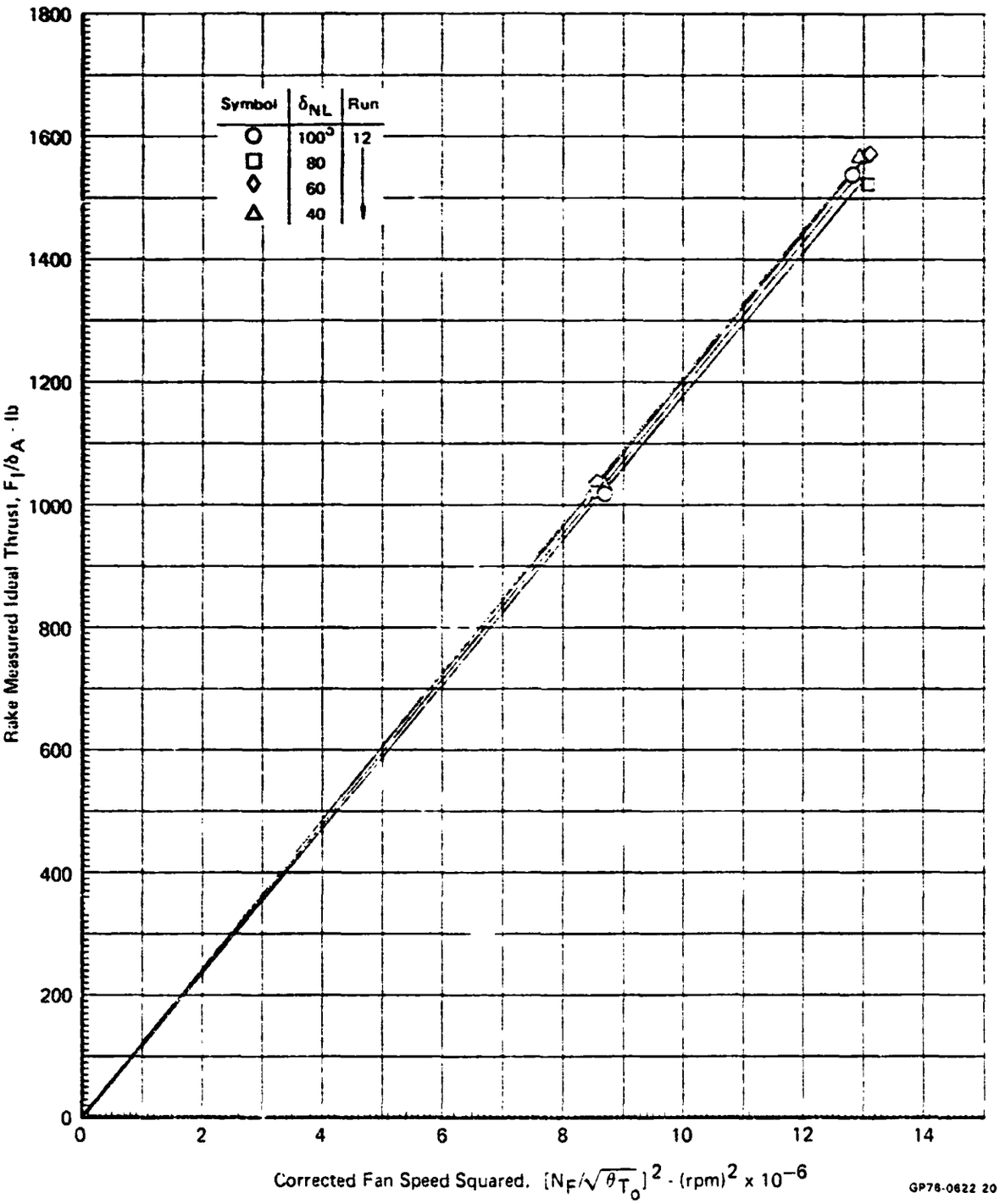

FIGURE 8.1-8
NOSE LIFT UNIT IDEAL THRUST
Propulsion System Calibration Data
$V_o = 0$

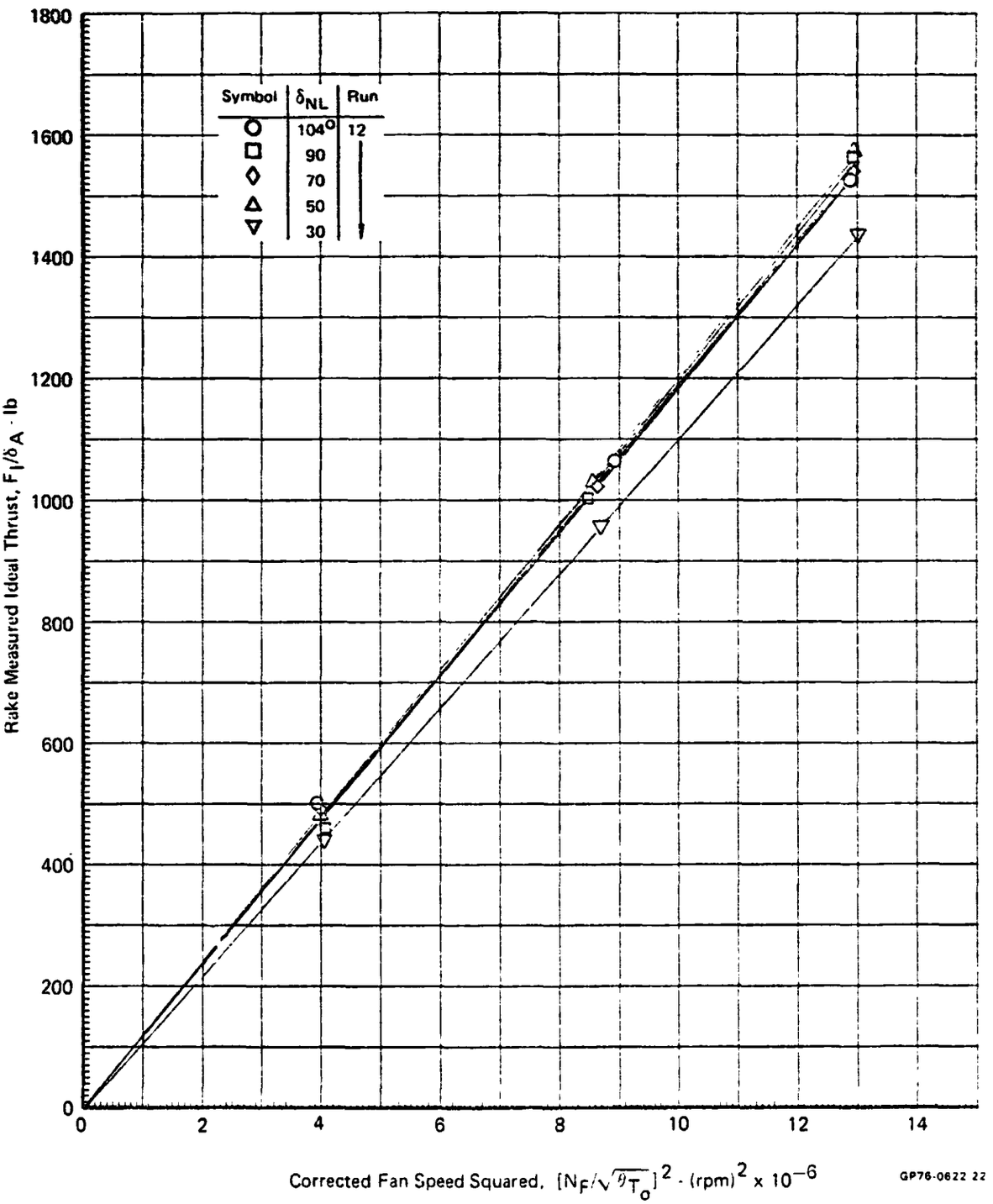

FIGURE 8.1-9
THRUST CALIBRATION COEFFICIENT DETERMINATION
Left Lift/Cruise Unit
$\delta_{LC} = 90^{o}$

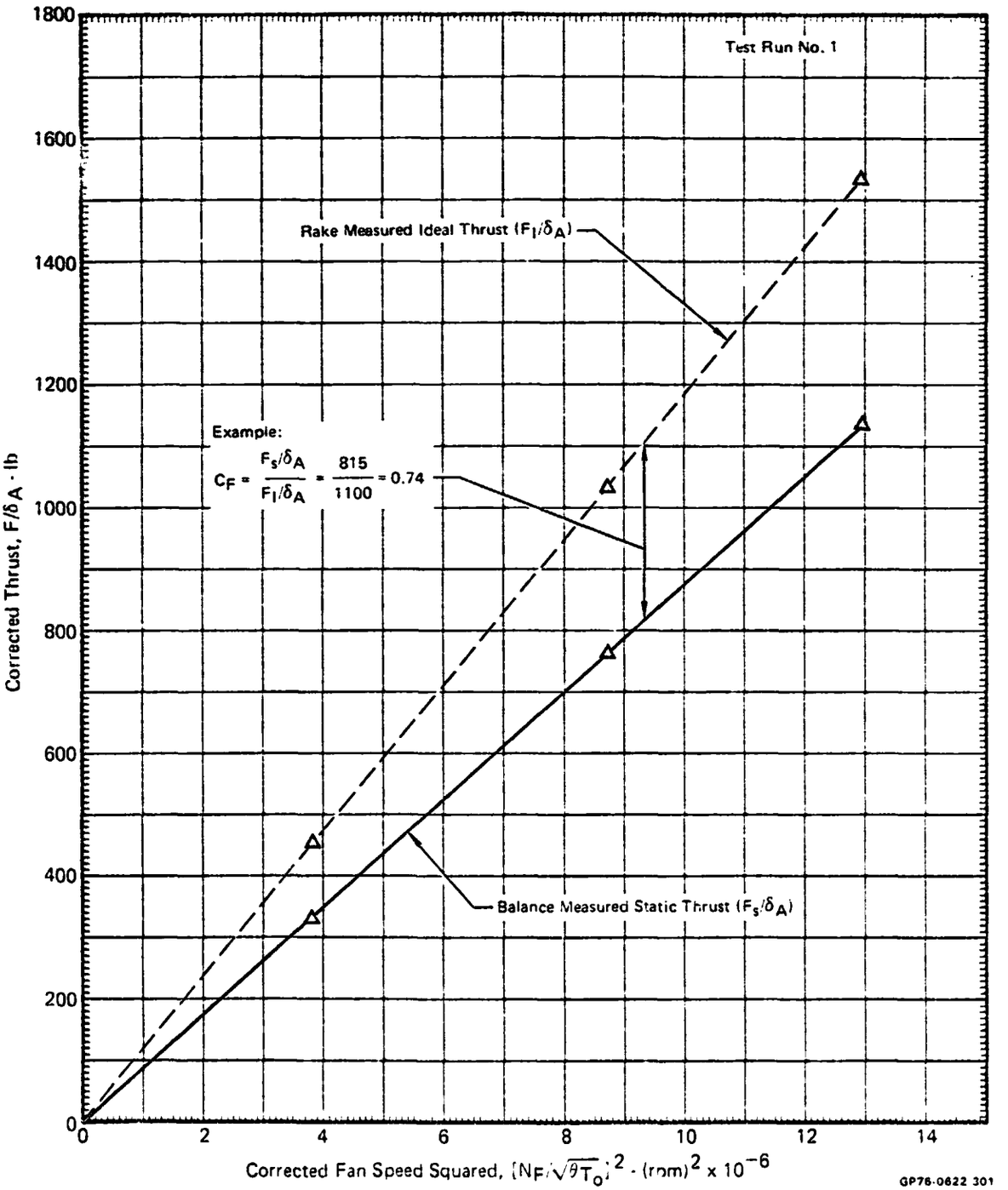

FIGURE 8.1-10

LIFT/CRUISE UNIT THRUST COEFFICIENTS

Propulsion System Calibration Results

$V_o = 0$

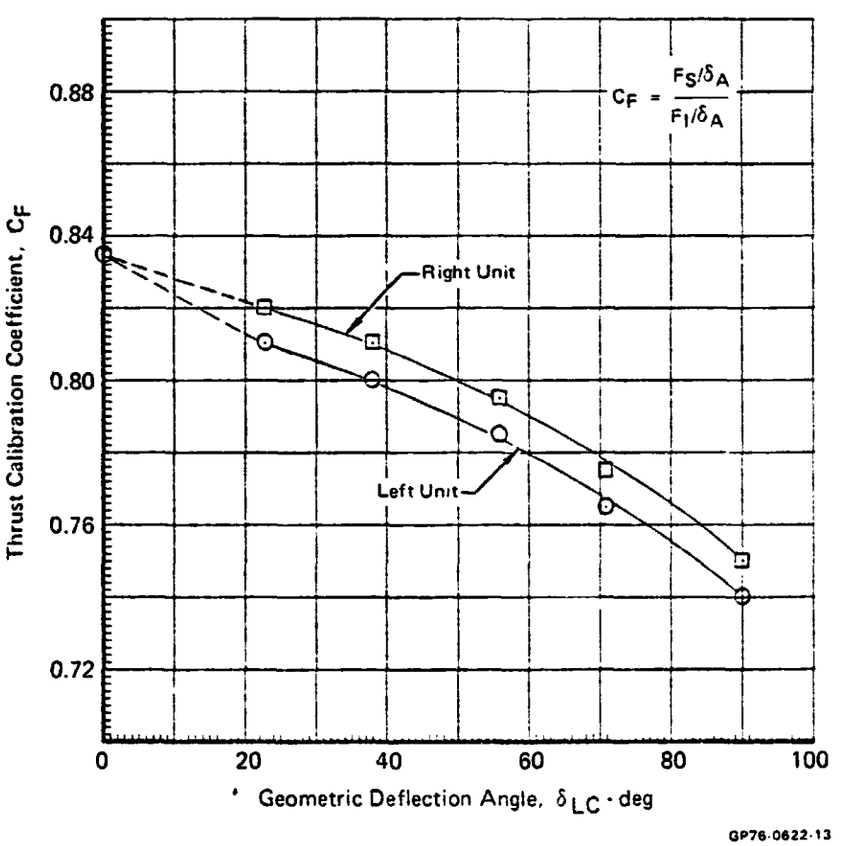

FIGURE 8.1-11

NOSE LIFT UNIT THRUST COEFFICIENTS
Propulsion System Calibration Results
$V_o = 0$

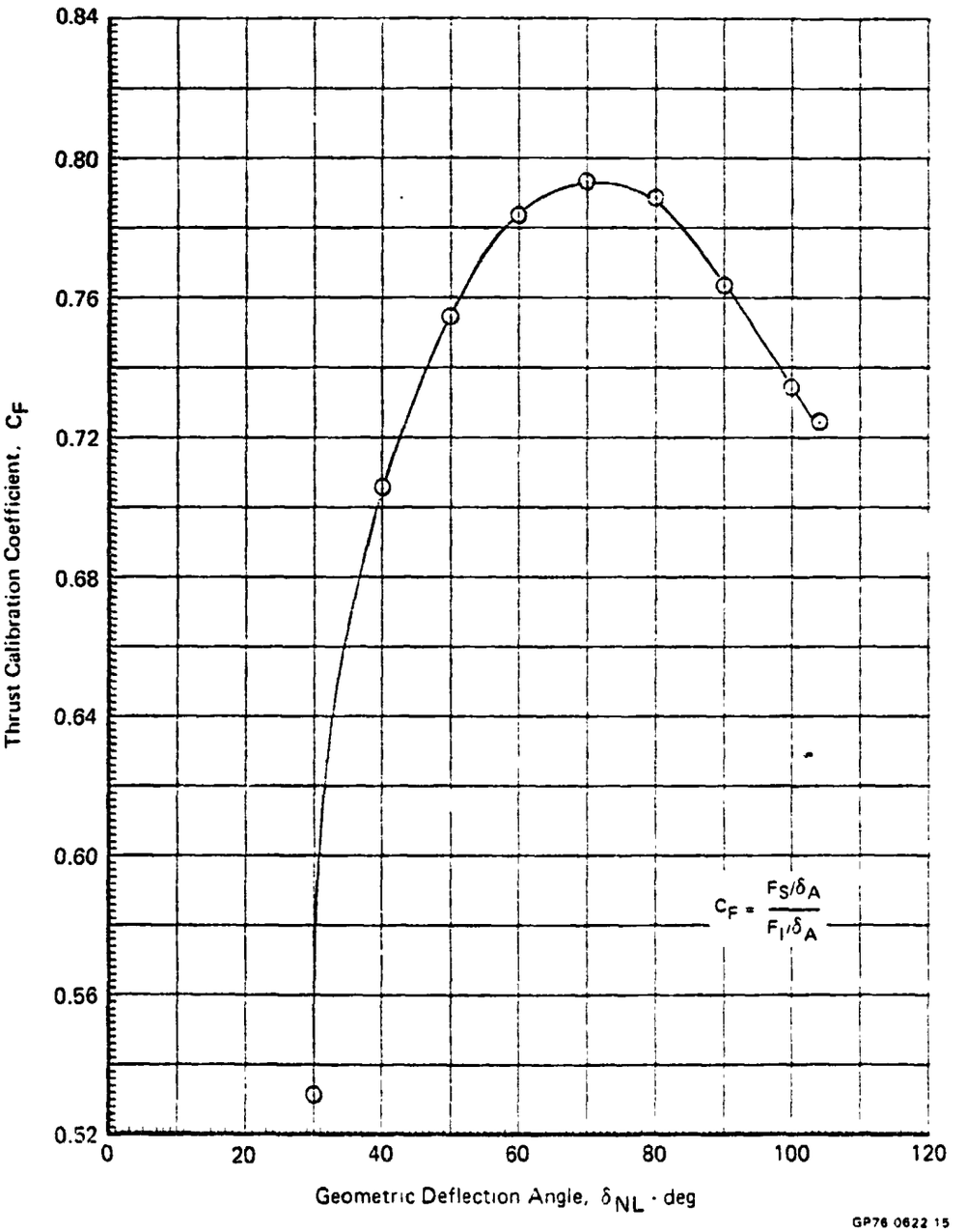

FIGURE 8.1-12
LEFT LIFT/CRUISE UNIT THRUST VECTOR ANGLES
Propulsion System Calibration Data
$V_o = 0$

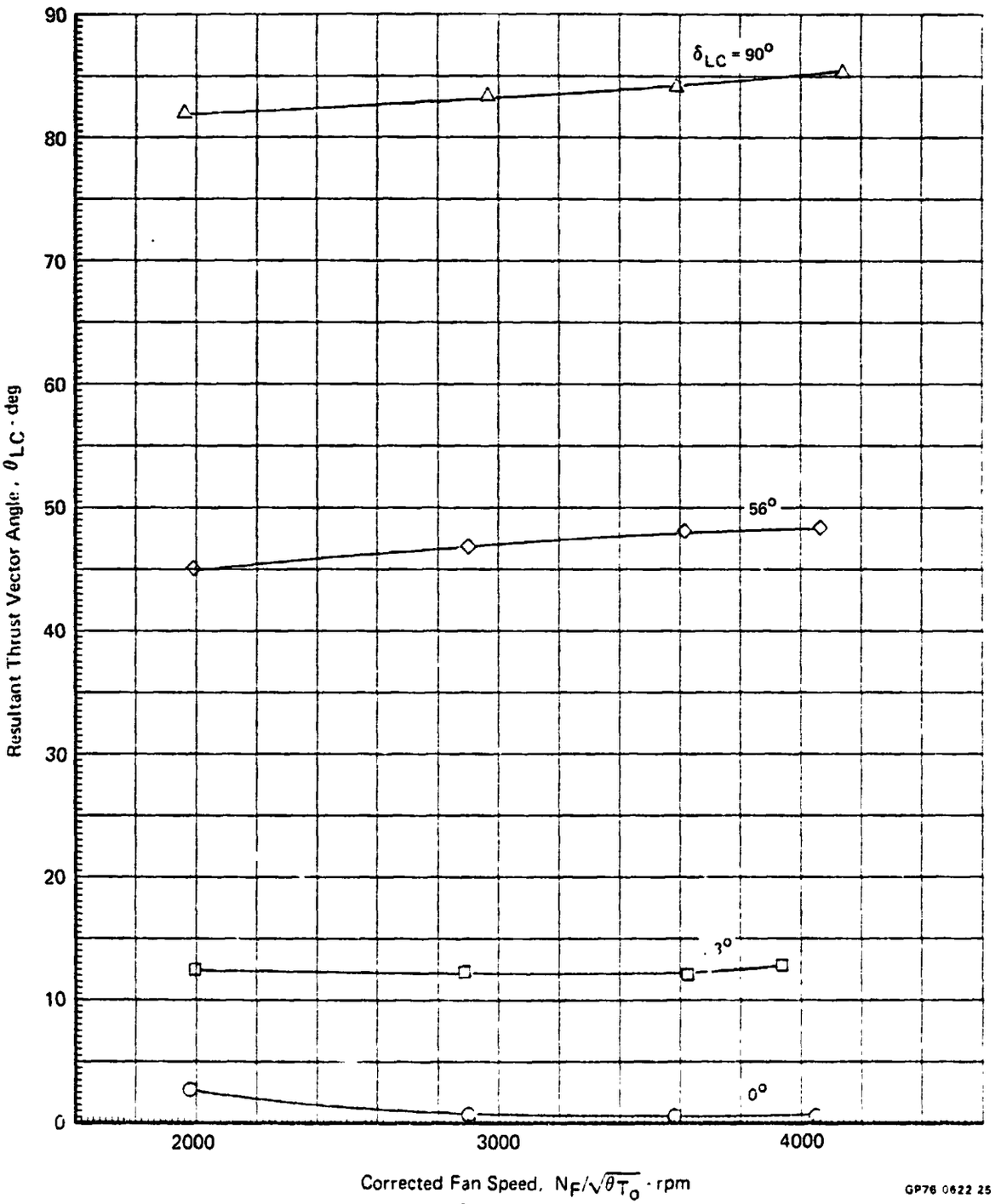

FIGURE 8.1-13
RIGHT LIFT/CRUISE UNIT THRUST VECTOR ANGLES
Propulsion System Calibration Data
$V_o = 0$

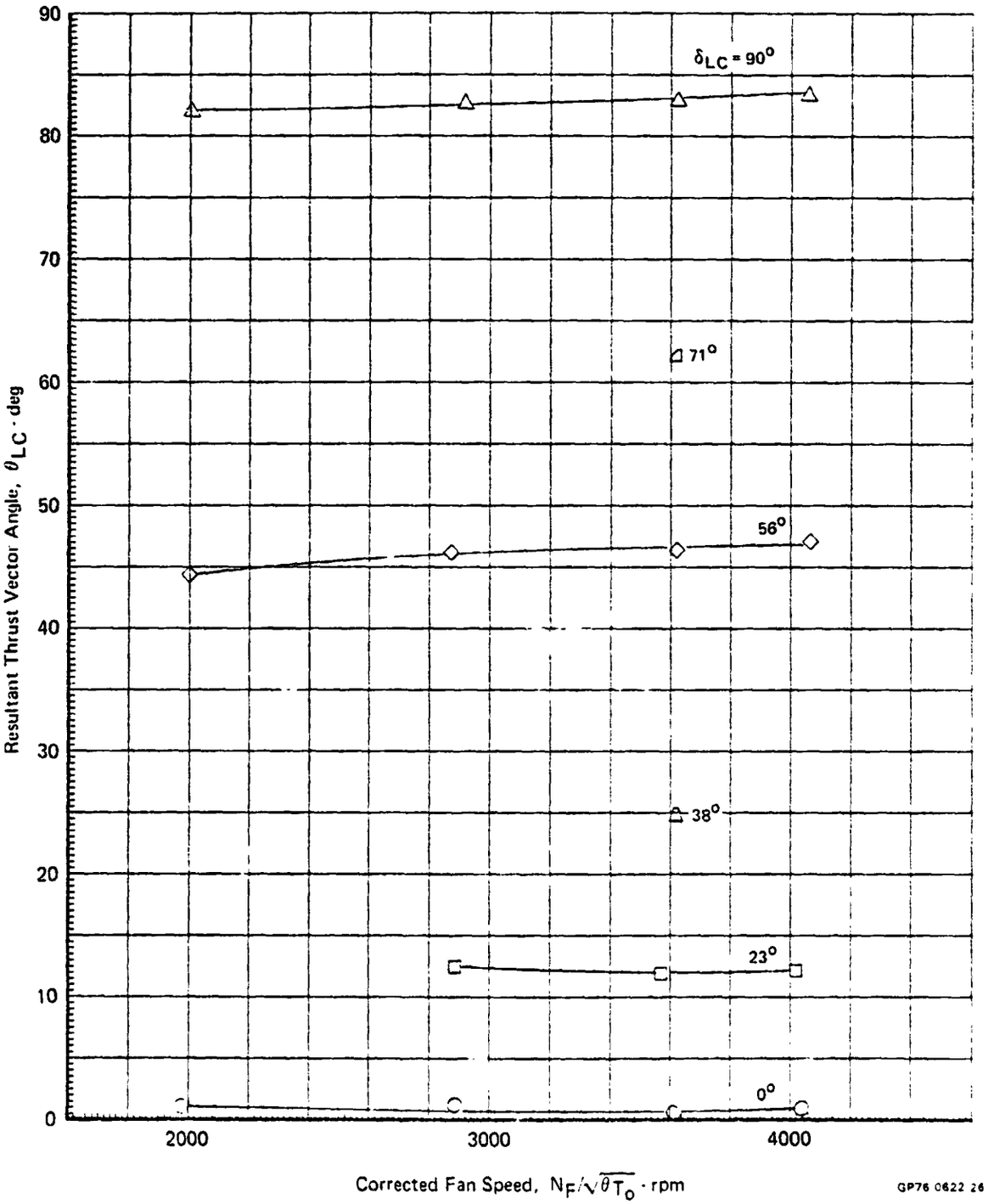

FIGURE 8.1-14
NOSE LIFT UNIT THRUST VECTOR ANGLES
Propulsion System Calibration Data
$V_o = 0$

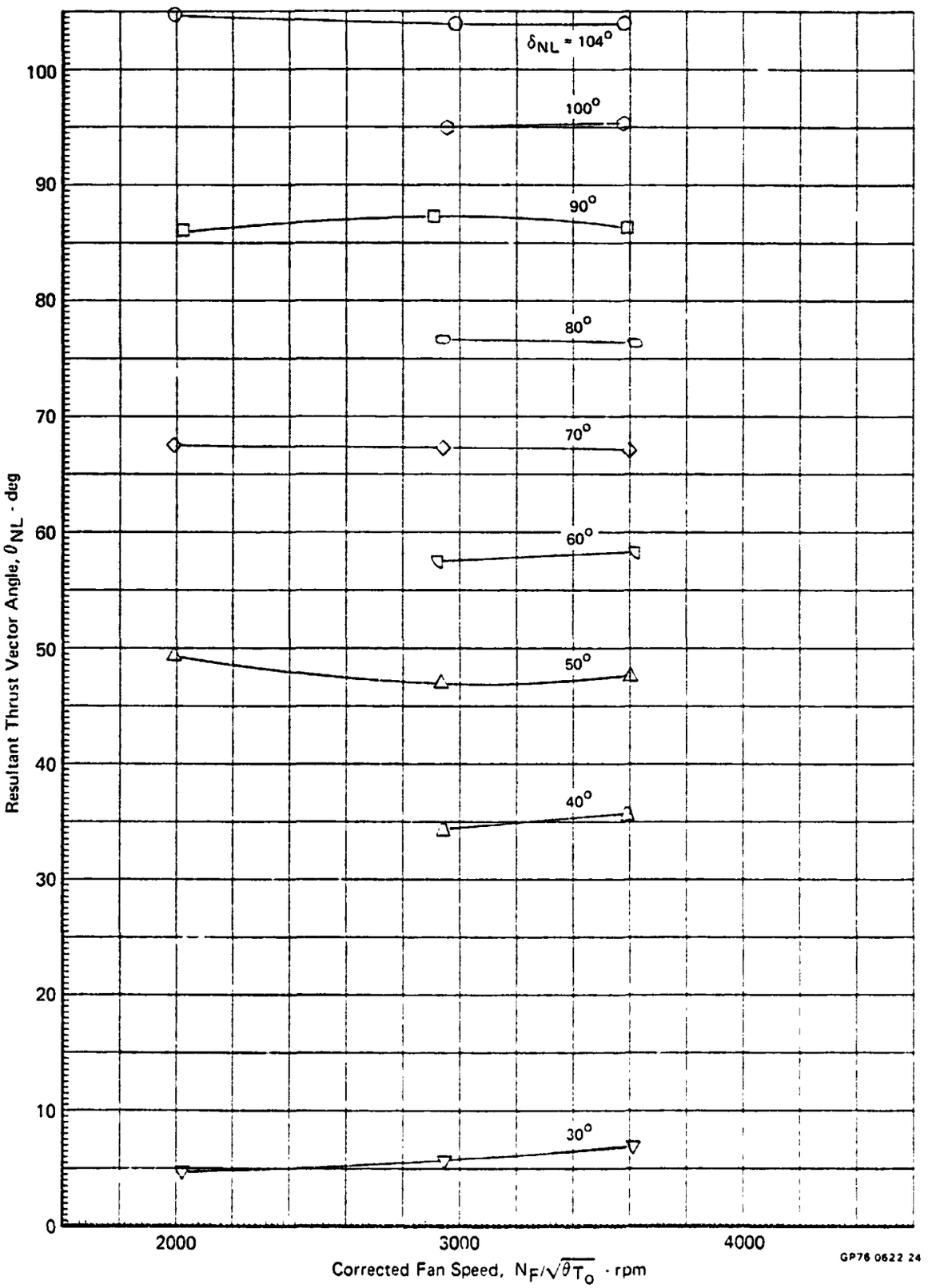

FIGURE 8.1-15

LIFT/CRUISE UNIT THRUST VECTOR ANGLES

Propulsion System Calibration Results

$V_o = 0$

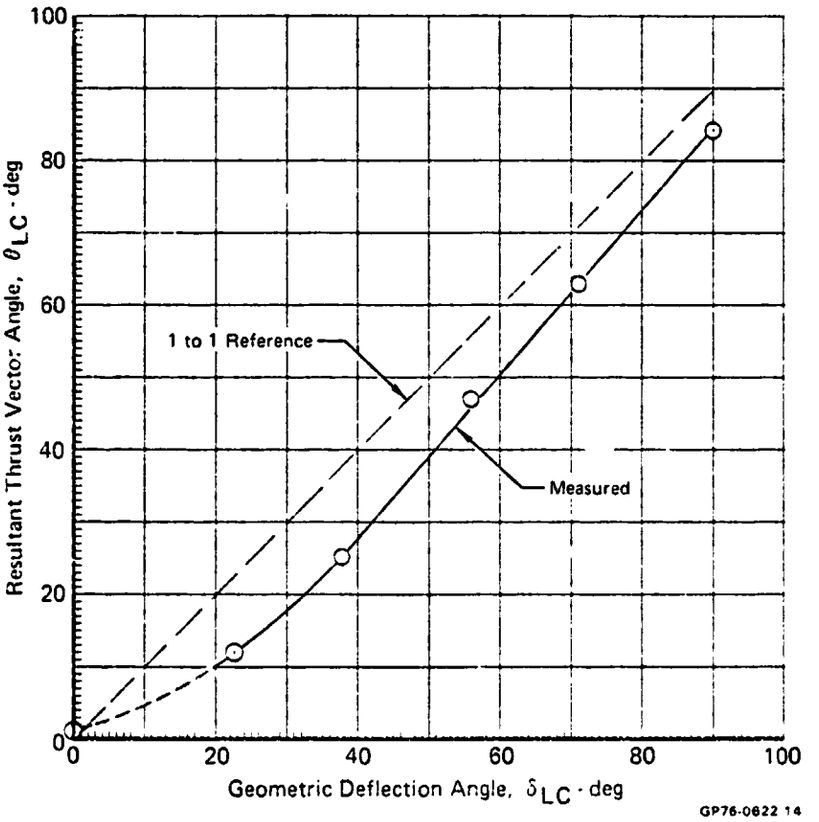

FIGURE 8.1-16
NOSE LIFT UNIT THRUST VECTOR ANGLES
Propulsion System Calibration Results
$V_o = 0$

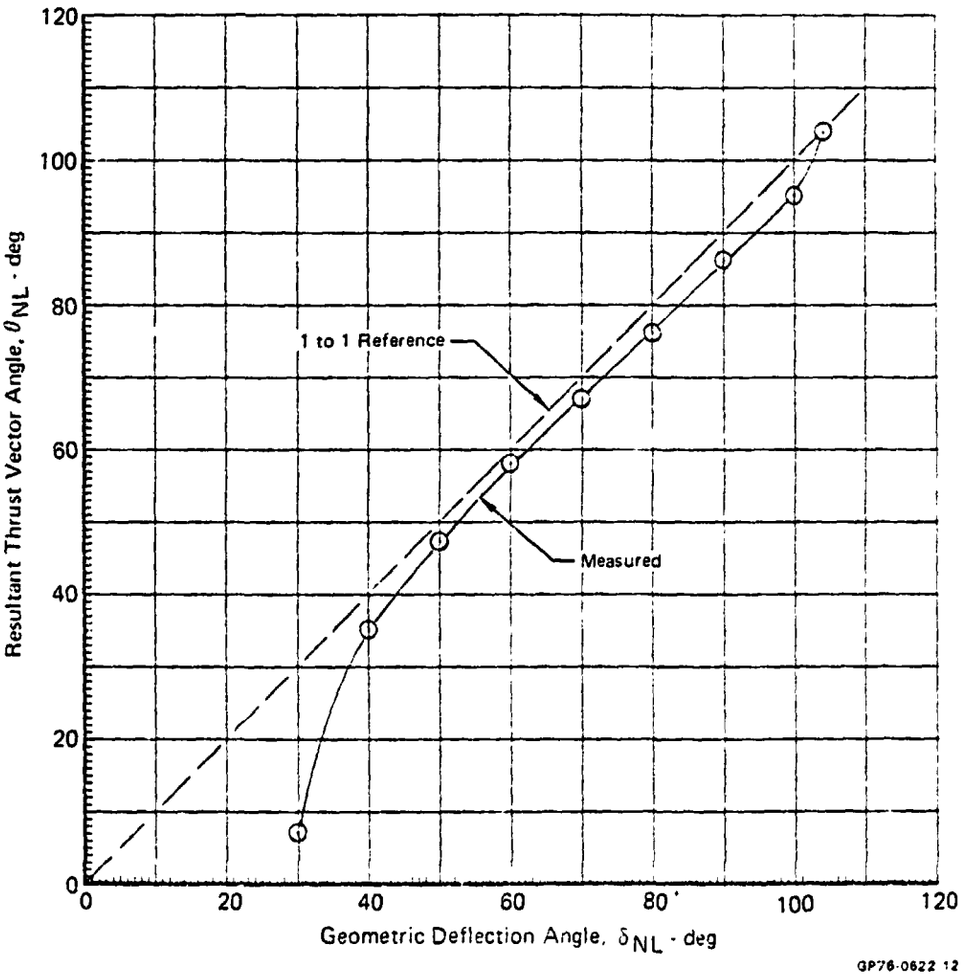

FIGURE 8.1-17
STATIC PITCHING MOMENT VARIATION WITH LIFT/CRUISE UNIT GEOMETRIC DEFLECTION ANGLE
$N_F/\sqrt{\theta_{T_o}}$ = 3600 RPM

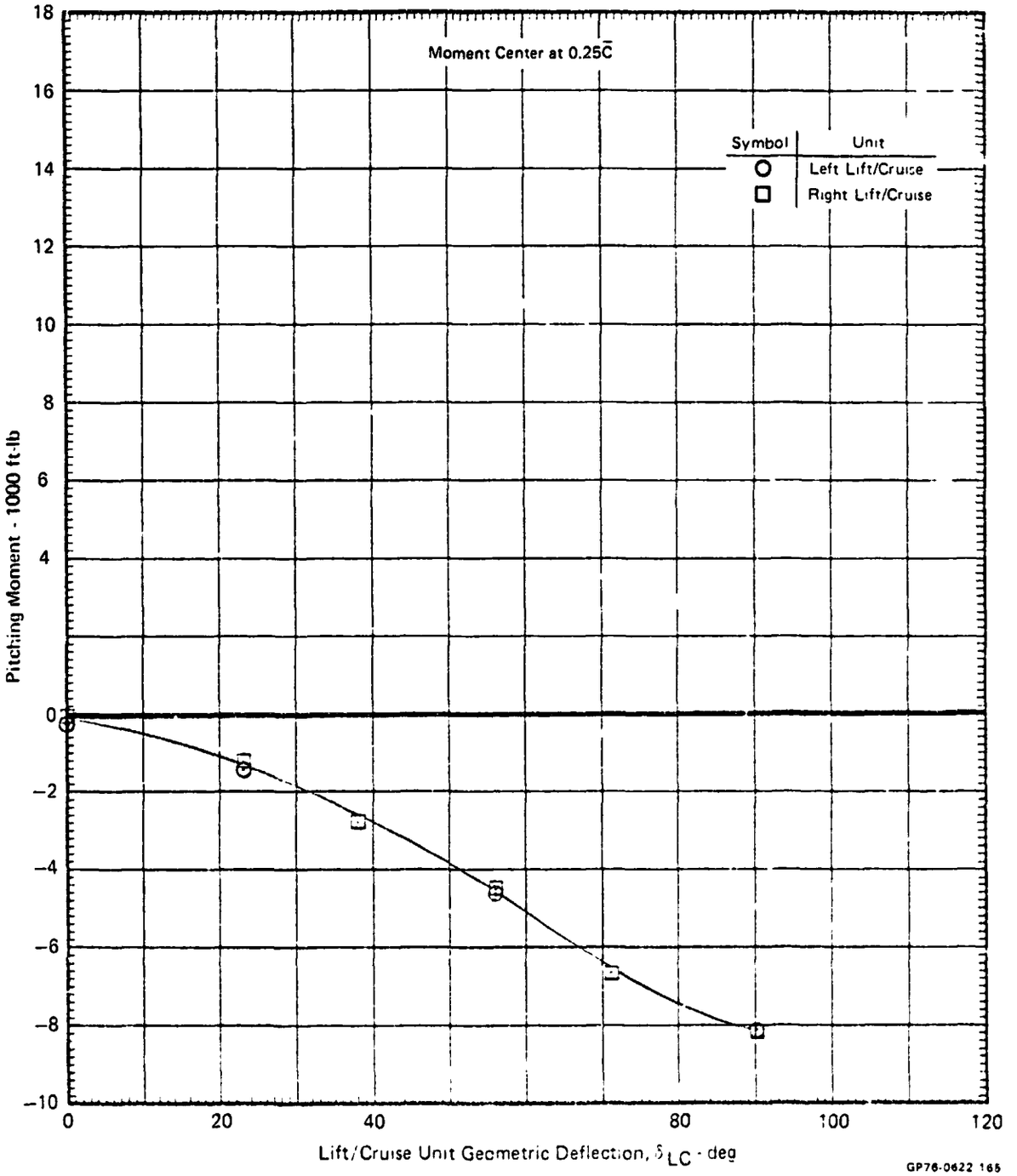

FIGURE 8.1-18
STATIC PITCHING MOMENT VARIATION WITH NOSE LIFT UNIT GEOMETRIC DEFLECTION ANGLE

$N_F/\sqrt{\theta T_o}$ = 3600 RPM

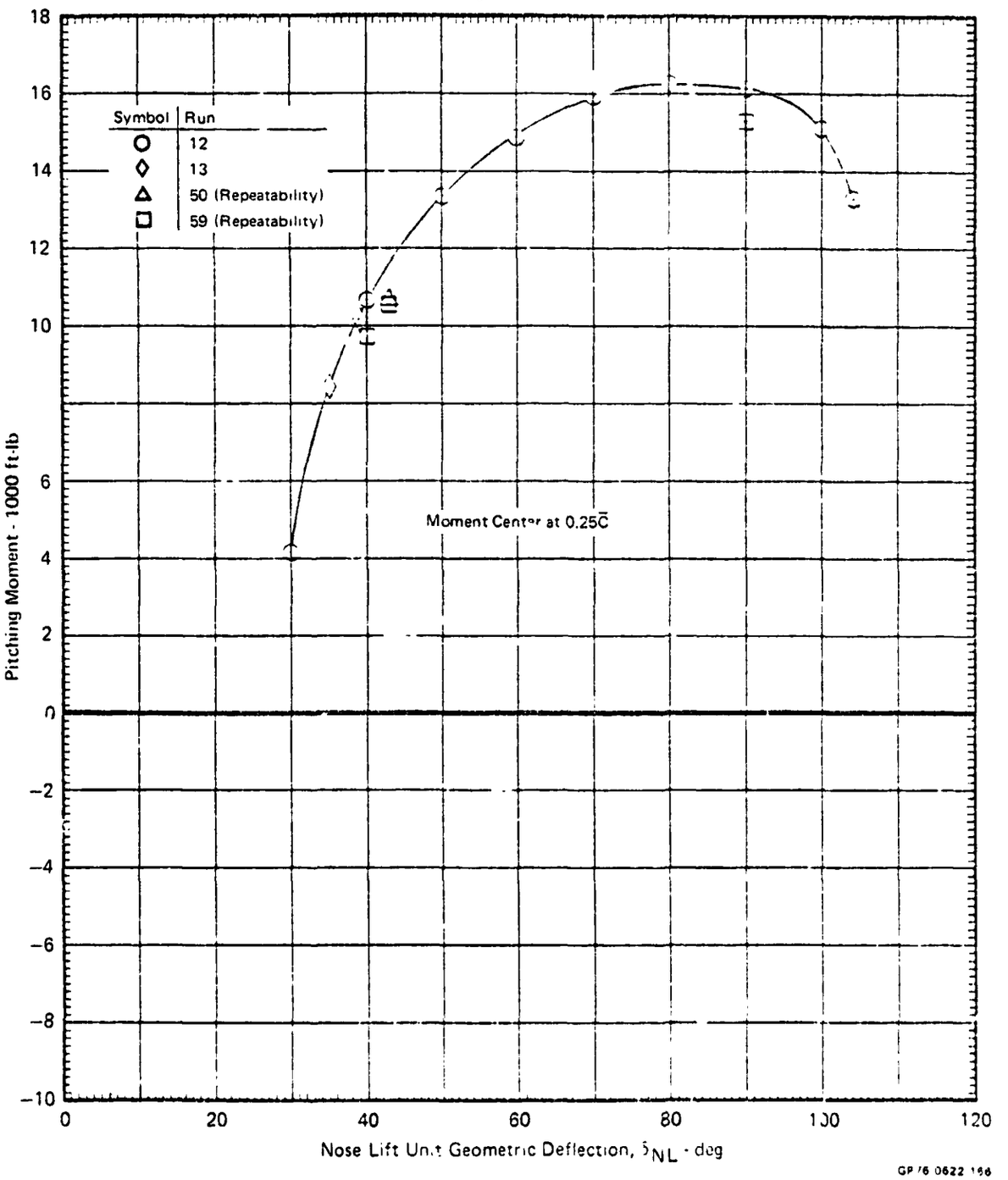

8.2 PROPULSION SYSTEM PERFORMANCE

The primary performance parameters measured on all three lift units for all test points consisted of the gross thrust, ram drag, jet velocity, and mass flow ratio. The typical variation of these parameters with forward speed is shown in Figures 8.2-1 and 8.2-2 for the left lift/cruise and nose lift units, respectively. The data are presented for a constant corrected fan speed at an angle of attack of zero for a fixed nozzle deflection angle.

The effects of angle of attack on the variation of the propulsion system performance parameters are presented in Figures 8.2-3 through 8.2-5. The powered lift mode angle of attack range tested varied from -4° to +20°. Performance data variation for this α range is presented in Figures 8.2-3 and 8.2-4 for the lift/cruise and nose fan units, respectively, at two different tunnel velocities. As is shown in the figures, the primary performance parameters were constant over the range of powered lift angle of attack tested. Cruise mode testing was conducted over a larger angle of attack range up to and including 32.5°. Figure 8.2-5 shows the variation in performance at the higher angle of attack for the left lift/cruise unit, operating at a constant tunnel velocity at the three fan speeds tested in this mode. As shown in the figure, all parameters were maintained at constant values up to an α of 16°. The data at the higher angles of attack begins to deteriorate rapidly due to the flow separation in the inboard wing panel ahead of the lift/cruise inlet.

The effects of forward speed on the lift/cruise and nose lift unit gross thrust and jet velocity ratios at alternate thrust vector angles are shown in Figures 8.2-6 and 8.2-7. As shown in both figures, the forward speed tended to improve the thrust ratio variation of the larger deflection angle configurations (those with the lowest static thrusts) at a higher rate. Comparisons of the lift/cruise and nose unit thrust variation with forward speed are shown in Figure 8.2-8 for nozzle deflections of 90°. Only a slight difference in nose unit thrust variation was experienced with this propulsion system.

A summary of the inlet mass flow ratio data as a function of tunnel and fan speeds is presented in Figures 8.2-9, 8.2-10, and 8.2-11 for the left and right lift/cruise and nose lift units, respectively. A summary correlation of the jet velocity ratio data is also presented in like manner for the three propulsion units in Figures 8.2-12 8.2-13 and 8.2-14.

FIGURE 8.2-1
LIFT/CRUISE UNIT TYPICAL PERFORMANCE CHARACTERISTICS
Left Lift/Cruise Unit

$\alpha = 0^0$ $N_F/\sqrt{\theta T_0} = 3600$ RPM $\delta_{LC} = 56^0$

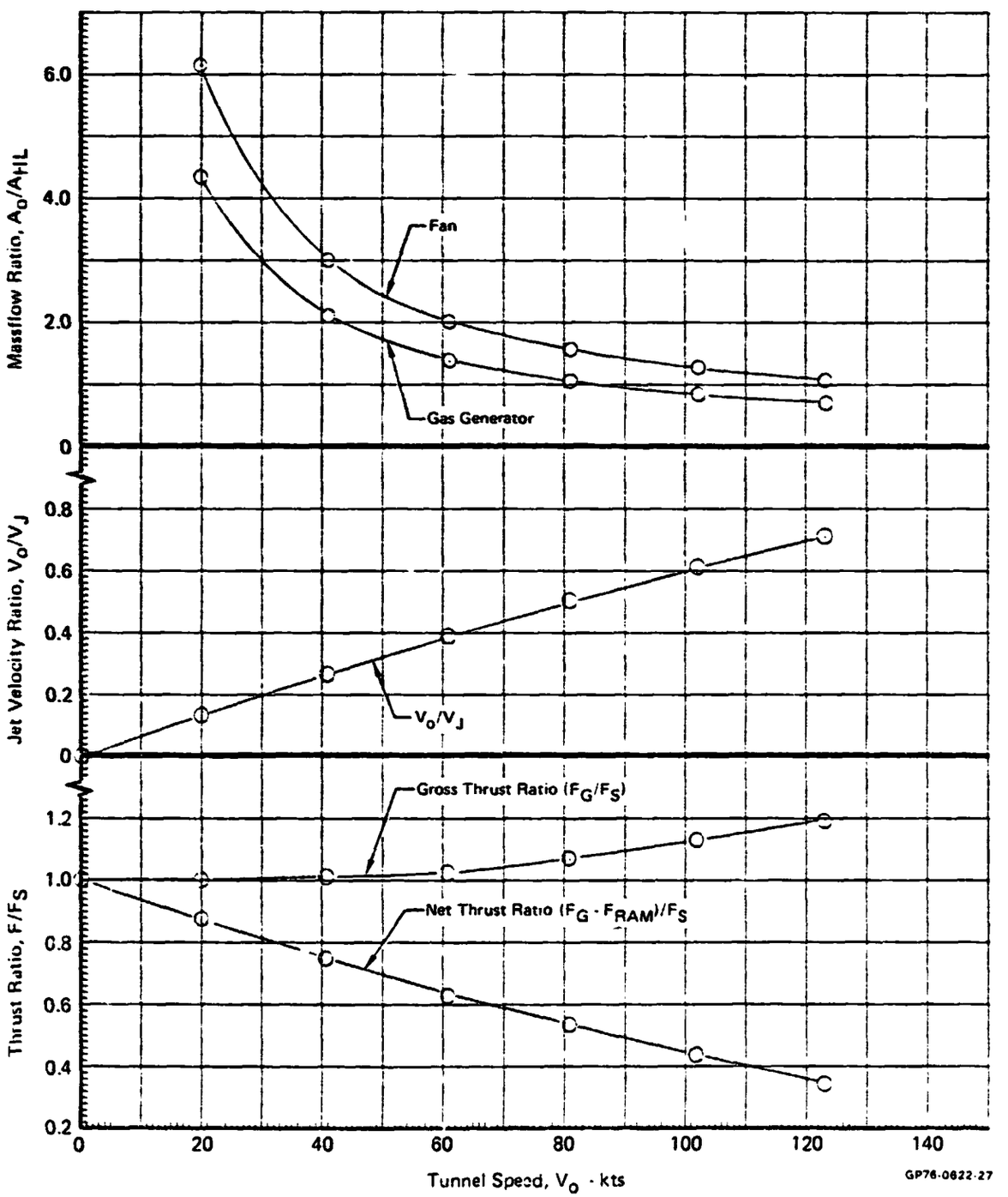

FIGURE 8.2-2
NOSE LIFT UNIT TYPICAL PERFORMANCE CHARACTERISTICS

$\alpha = 0^o$ $N_F/\sqrt{\theta_{T_o}} = 3600$ RPM $\delta_{NL} = 43^o$

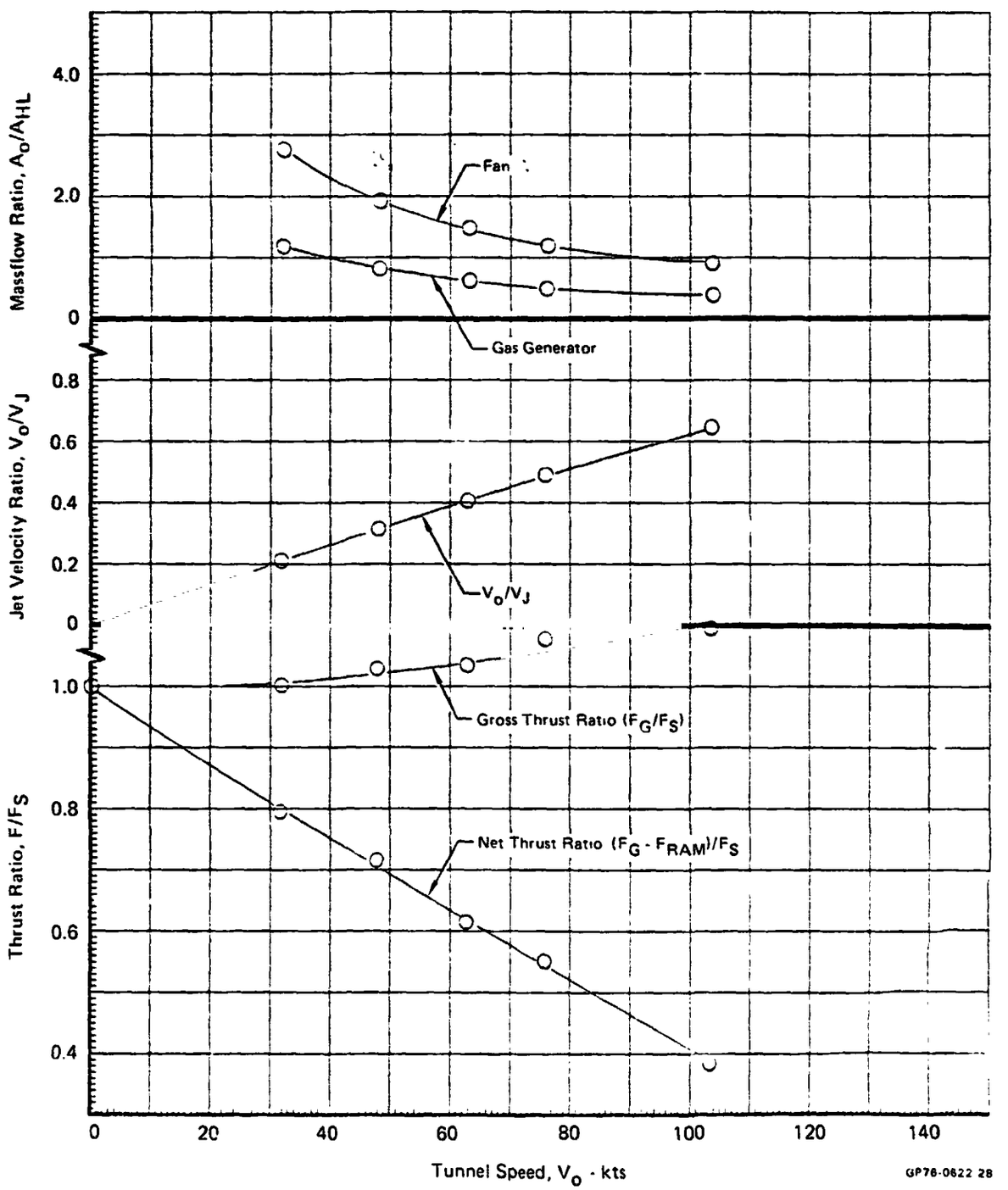

FIGURE 8.2-3
ANGLE OF ATTACK EFFECT ON LIFT/CRUISE UNIT PERFORMANCE
Left Lift/Cruise Unit

$N_F/\sqrt{\theta T_0}$ = 3600 RPM $\delta_{LC} = 56^o$

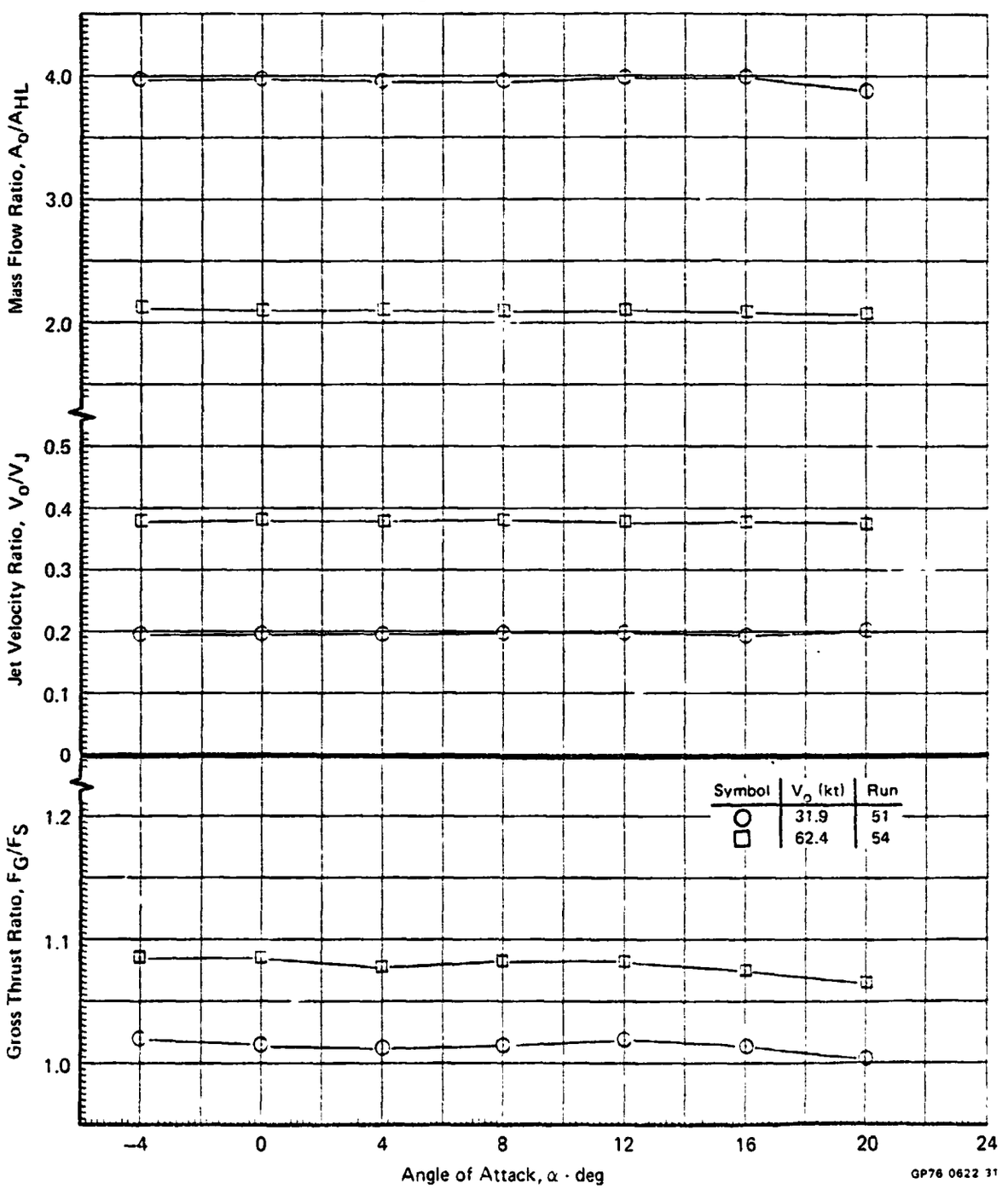

FIGURE 8.2-4
ANGLE OF ATTACK EFFECT ON NOSE LIFT UNIT PERFORMANCE

$N_F/\sqrt{\theta T_o}$ = 3600 RPM δ_{NL} = 43°

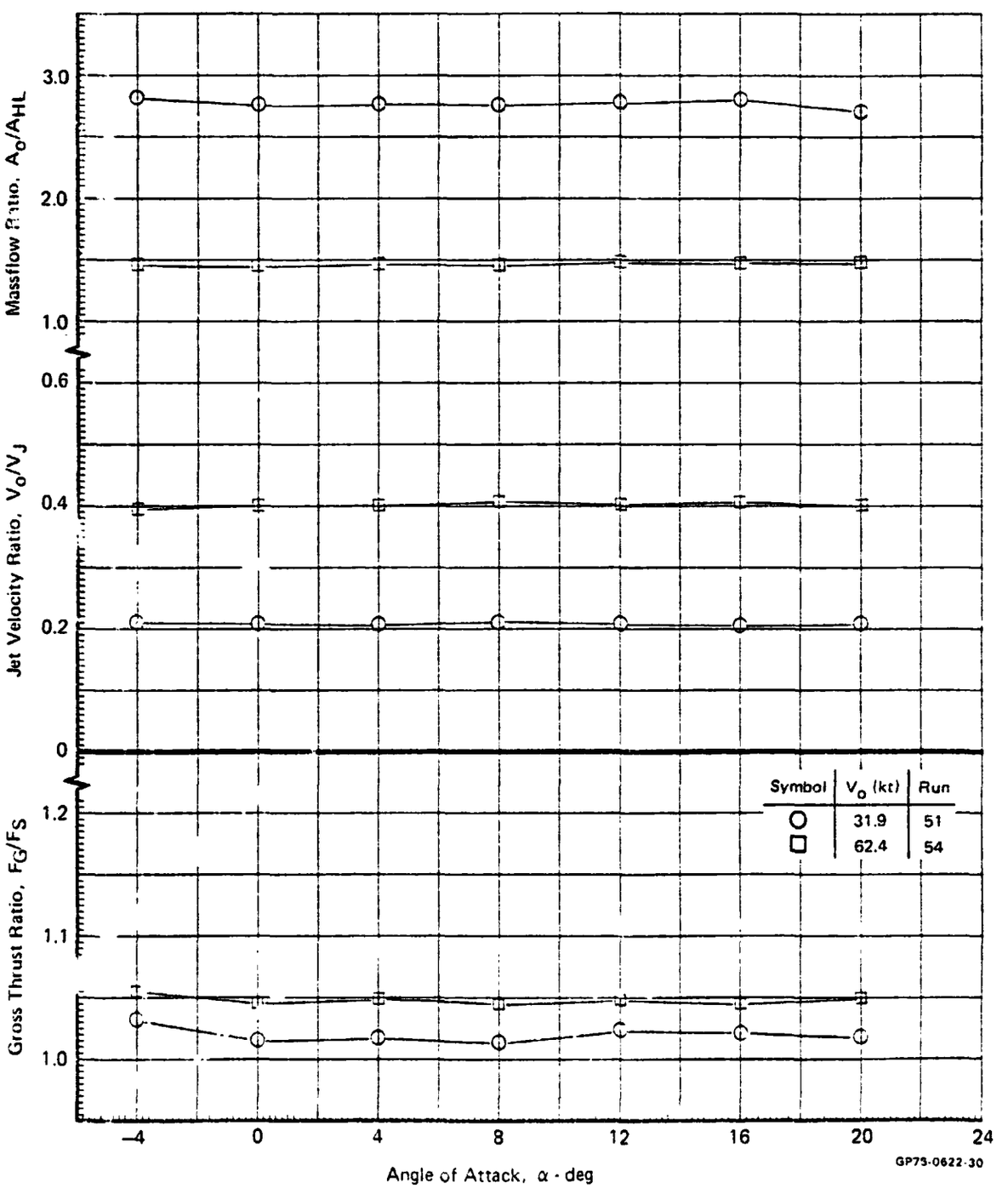

FIGURE 8.2-5
EFFECT OF HIGH ANGLES OF ATTACK ON PROPULSION SYSTEM PERFORMANCE
Left Lift Cruise Unit
$\beta = 0^{o}$ $V_o = 103$ Kts

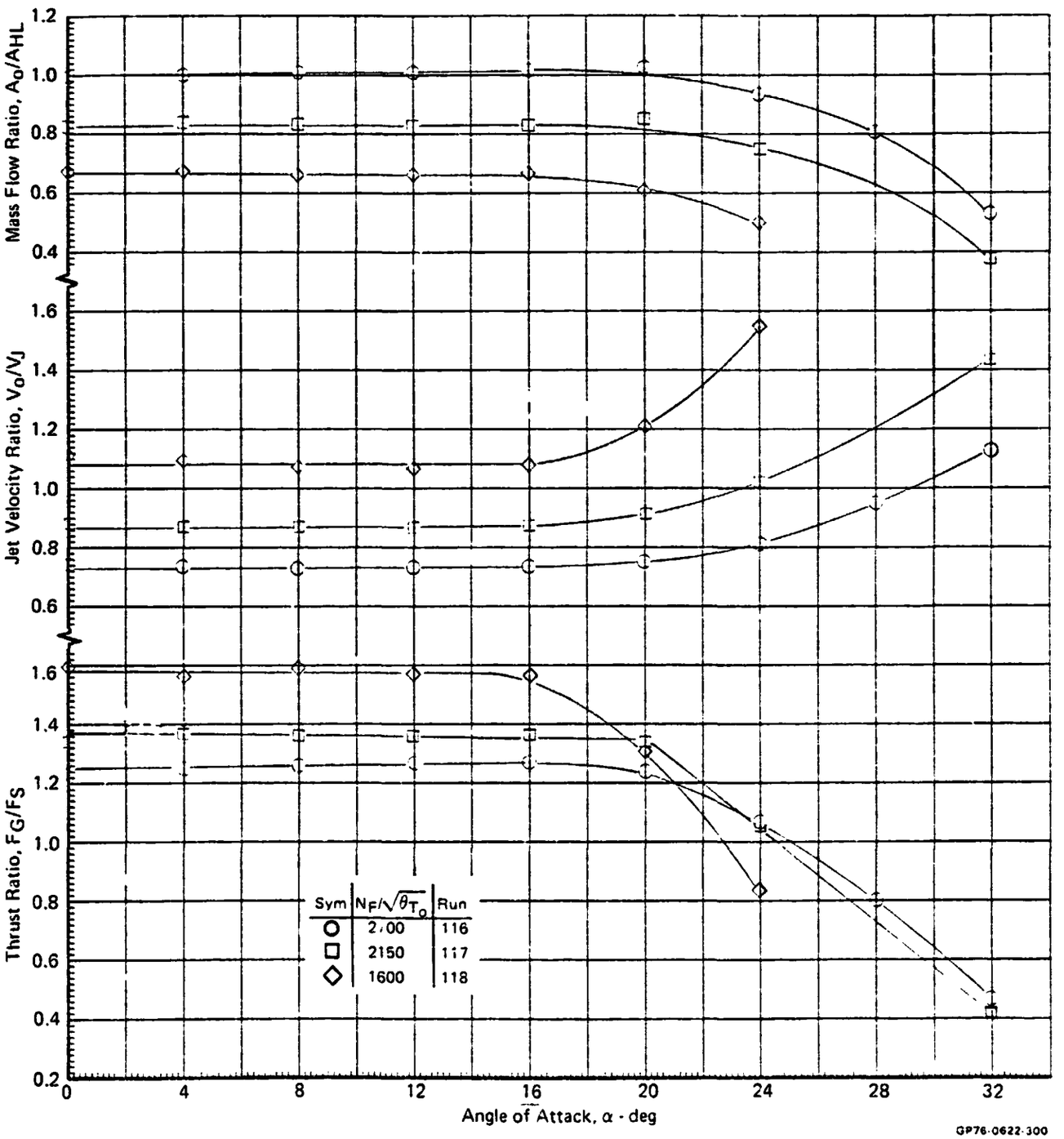

FIGURE 8.2-6
FORWARD SPEED EFFECT ON LIFT/CRUISE UNIT PERFORMANCE
Left Lift/Cruise Unit
$\alpha = 0^o$ $N_F/\sqrt{\theta_{T_o}}$ = 3600 RPM

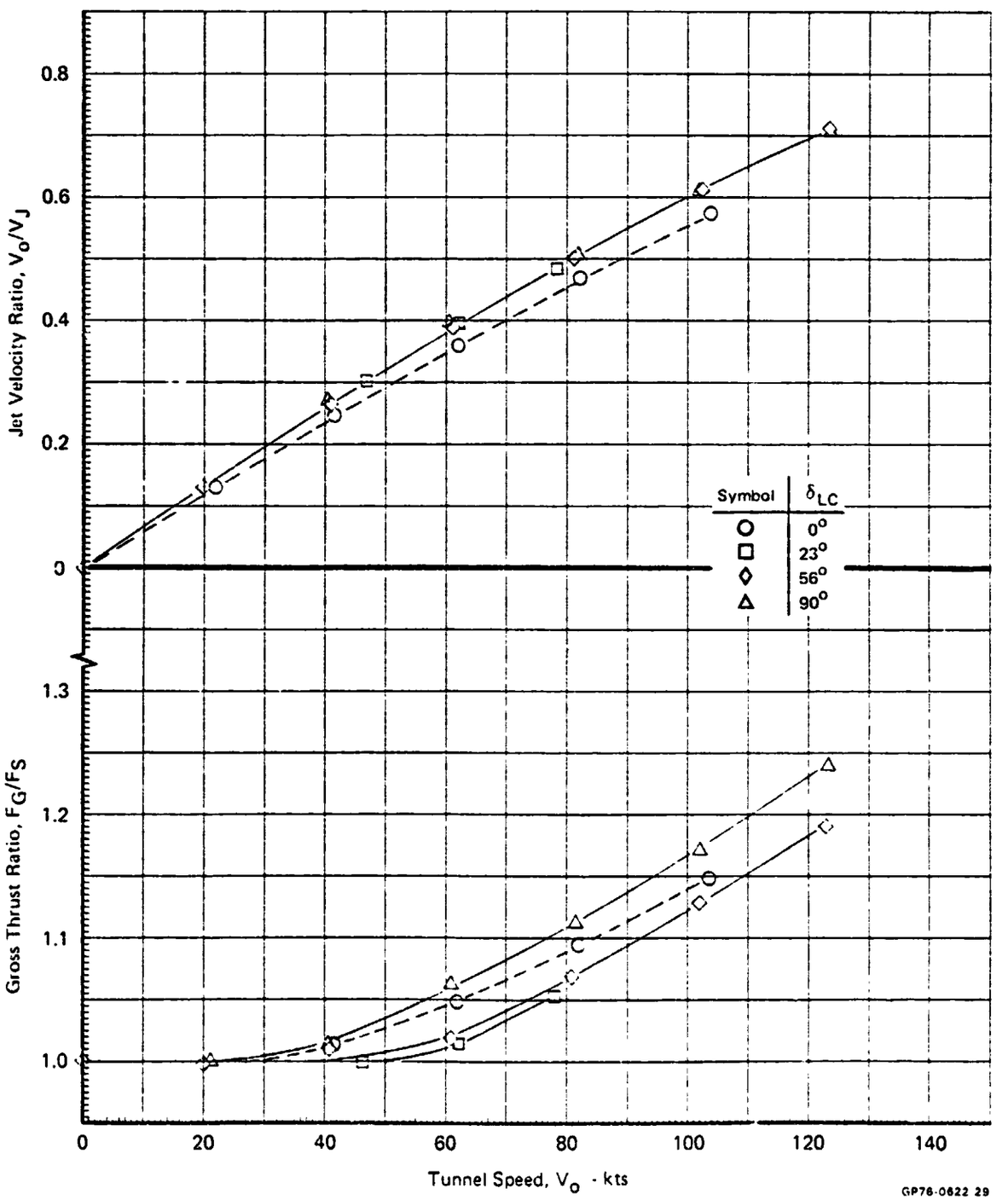

FIGURE 8.2-7
FORWARD SPEED EFFECTS ON VARIOUS NOSE UNIT VECTOR ANGLES
$\alpha = 0^o$ $N_F/\sqrt{\theta T_o} = 3600$ RPM

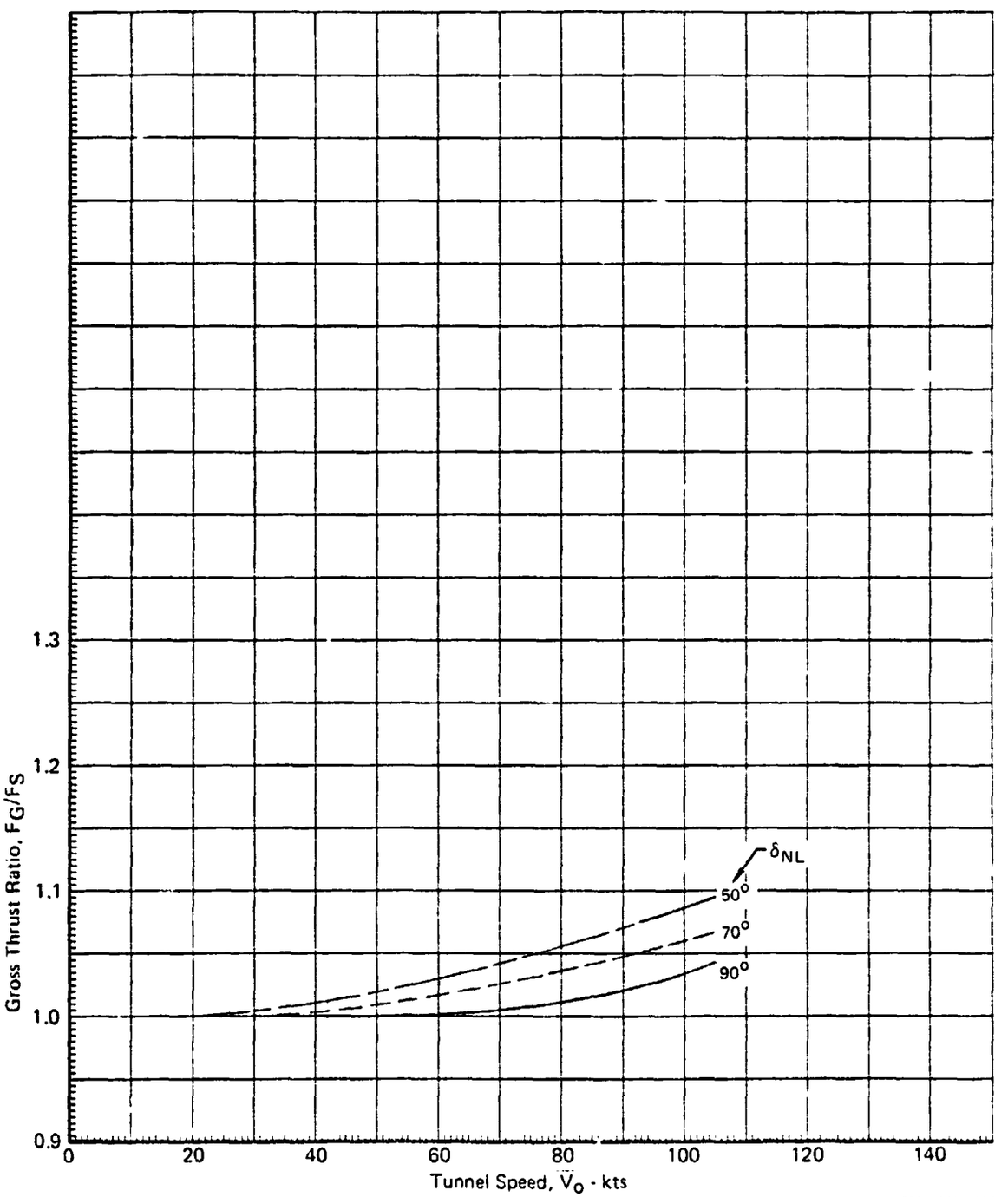

FIGURE 8.2-8
COMPARISON OF FORWARD SPEED EFFECTS ON THE LIFT/CRUISE vs NOSE LIFT UNITS
$\alpha = 0^{o}$ $N_F/\sqrt{\theta T_o} = 3600$ RPM

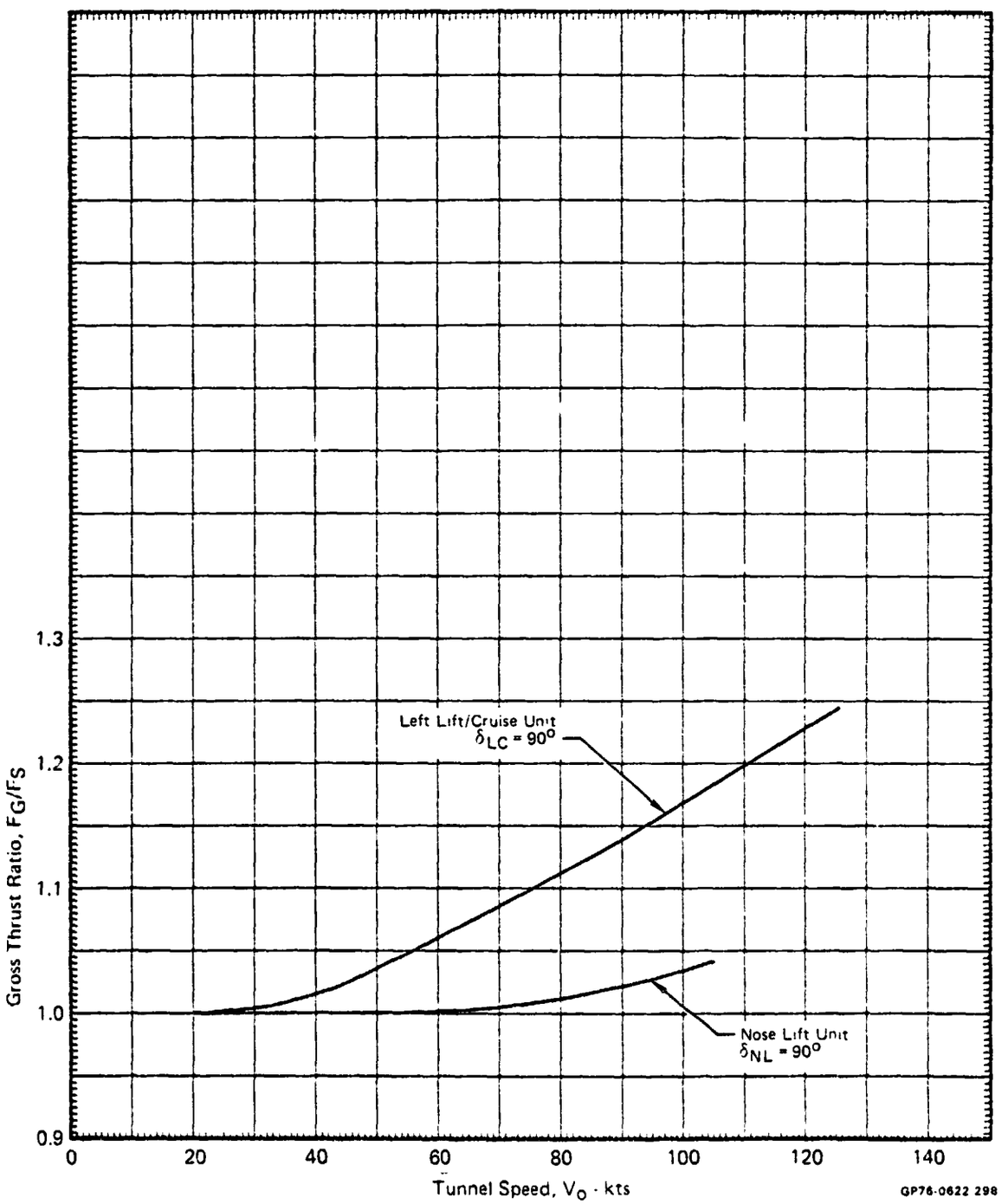

FIGURE 8.2-9
MASS FLOW VARIATIONS WITH FORWARD SPEED
Left Lift/Cruise Unit
$\alpha = 0^{o}$ $N_F/\sqrt{\theta T_o} = 3600$ RPM

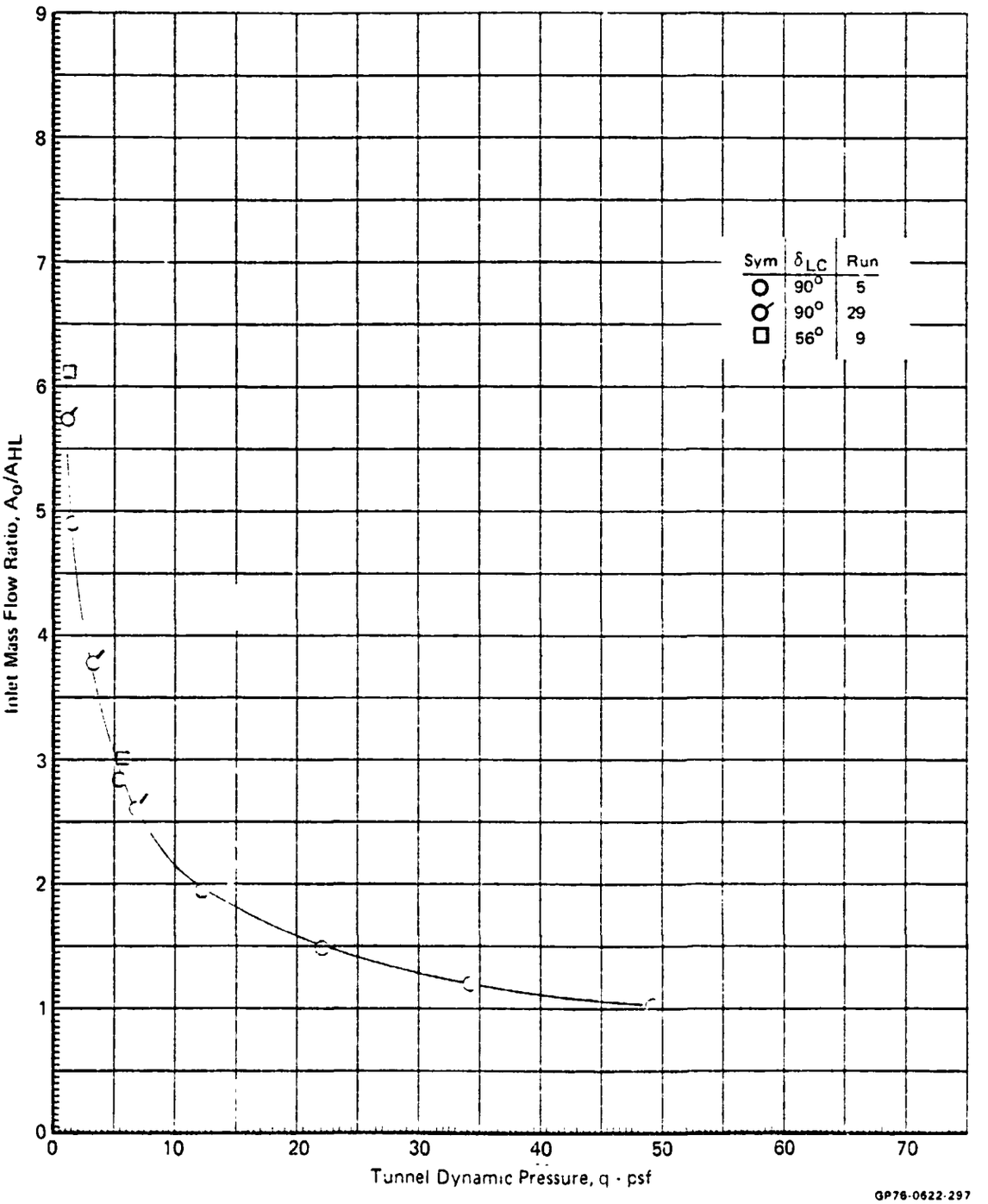

GP76-0622-297

FIGURE 8.2-10
MASS FLOW VARIATIONS WITH FORWARD SPEED
Right Lift/Cruise Unit
$\alpha = 0^{o}$ $N_F/\sqrt{\theta T_o} = 3600$ RPM

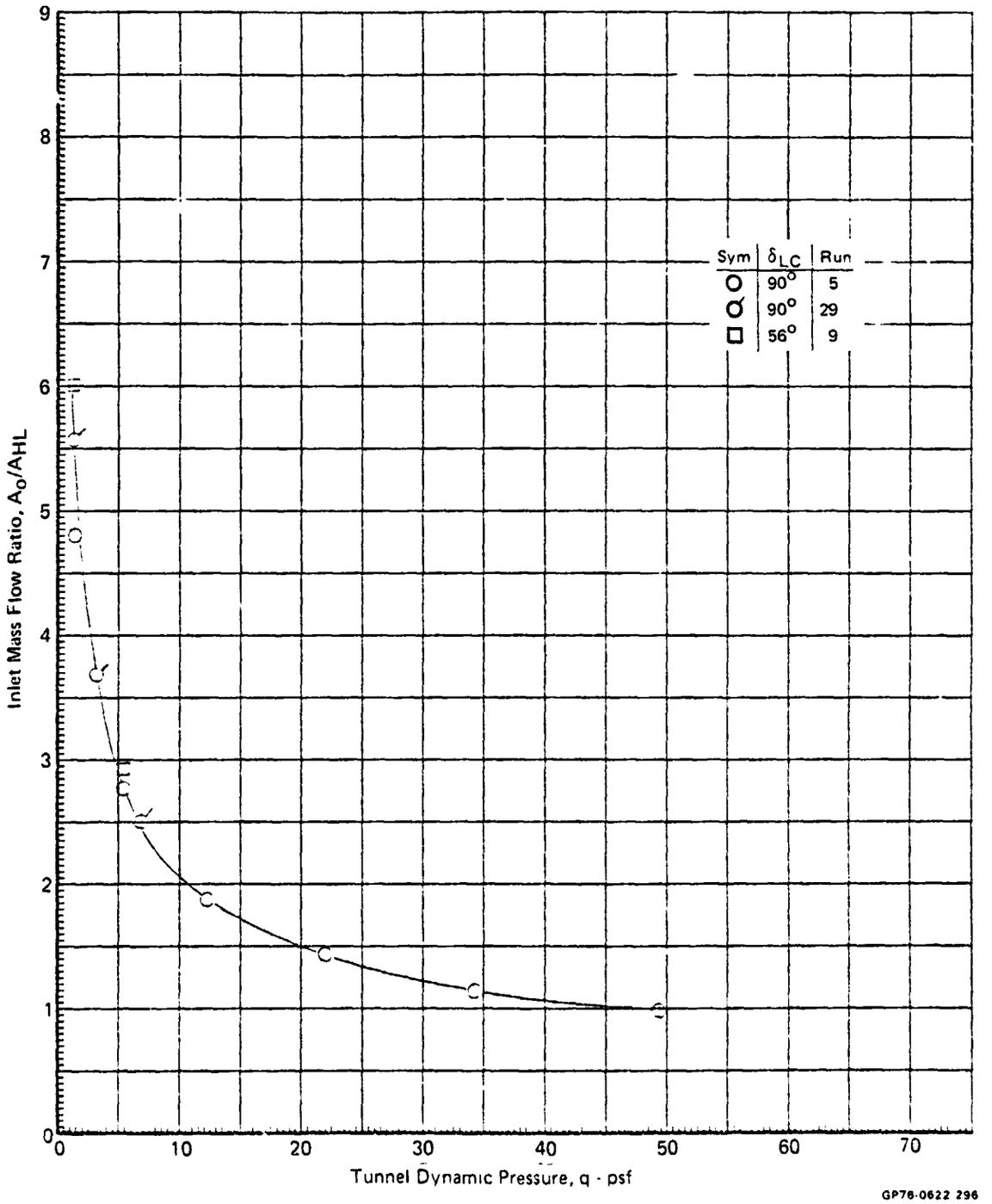

FIGURE 8.2-11
MASS FLOW VARIATIONS WITH FORWARD SPEED
Nose Lift Unit
$\alpha = 0^{o}$ $N_F/\sqrt{\theta T_o} = 3600$ RPM

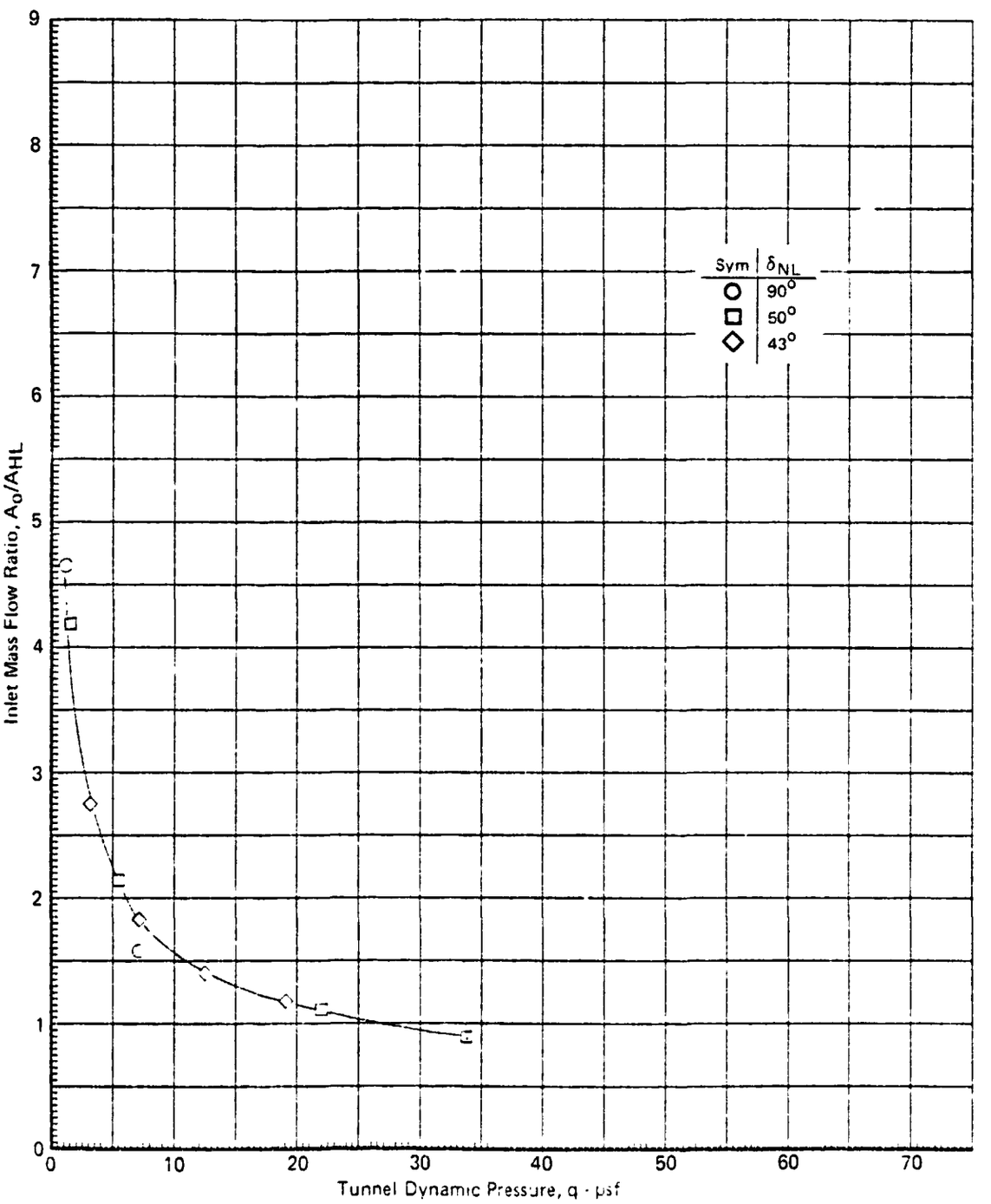

FIGURE 8.2-12
EFFECT OF FORWARD SPEED ON JET VELOCITY RATIO
Left Lift/Cruise Unit
$N_F/\sqrt{\theta T_o}$ = 3600 RPM

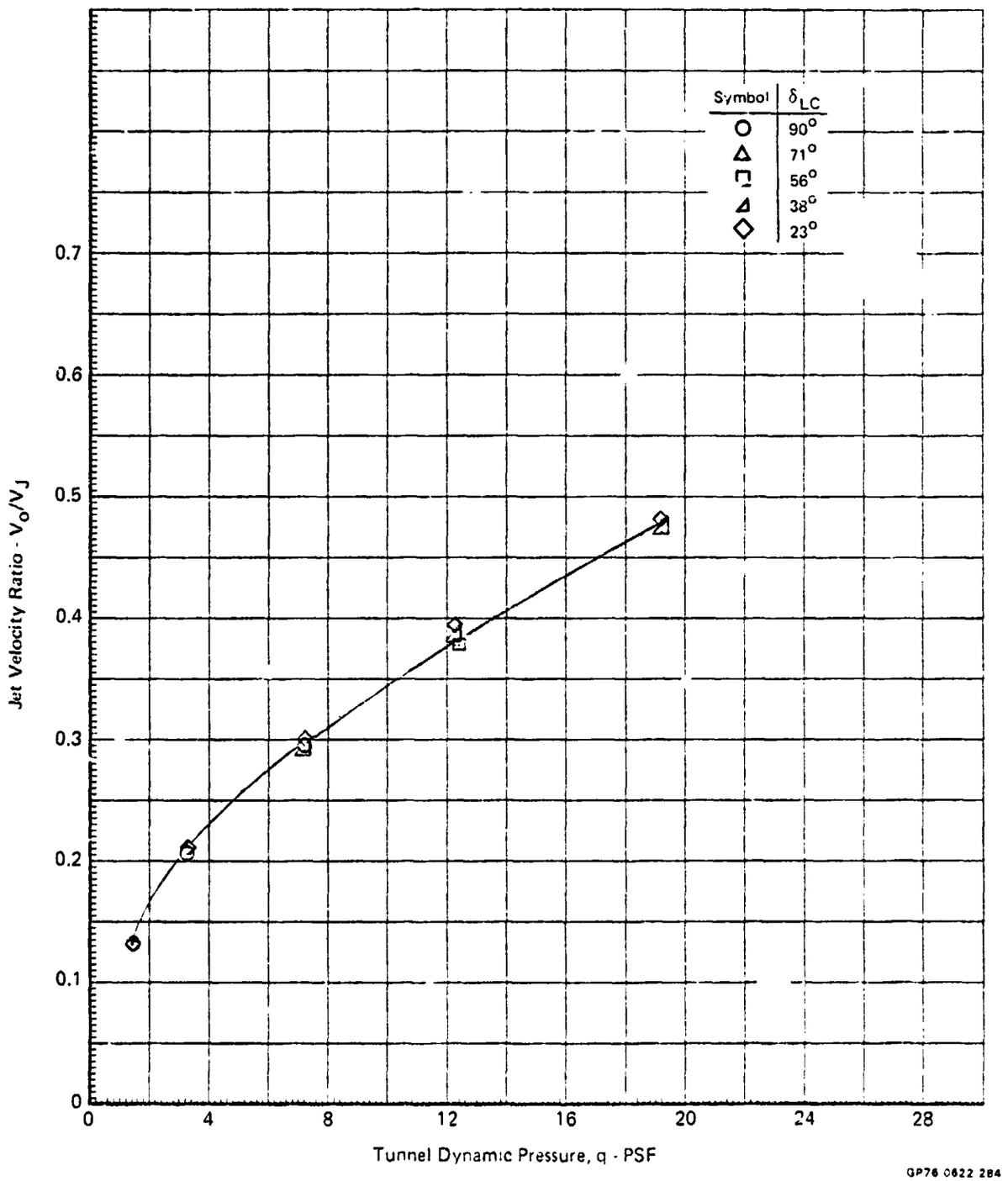

FIGURE 8.2-13
EFFECT OF FORWARD SPEED ON JET VELOCITY RATIO
Right Lift/Cruise Unit
$N_F/\sqrt{\theta T_3}$ = 3600 PPM

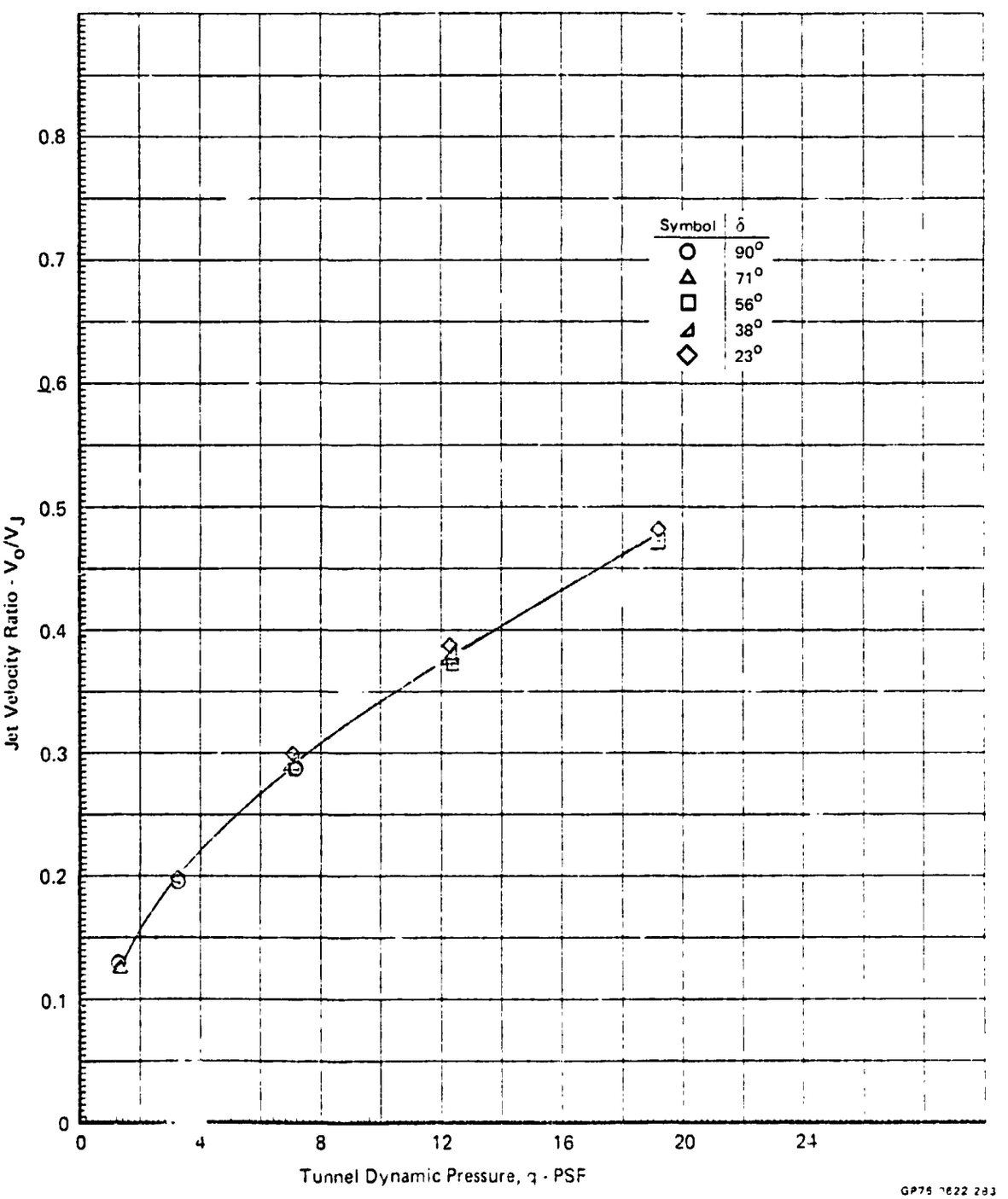

GP75 0622 283

FIGURE 8.2-14
EFFECT OF FORWARD SPEED ON JET VELOCITY RATIO
Nose Lift for Unit
$N_F/\sqrt{\theta T_o}$ = 3600 RPM

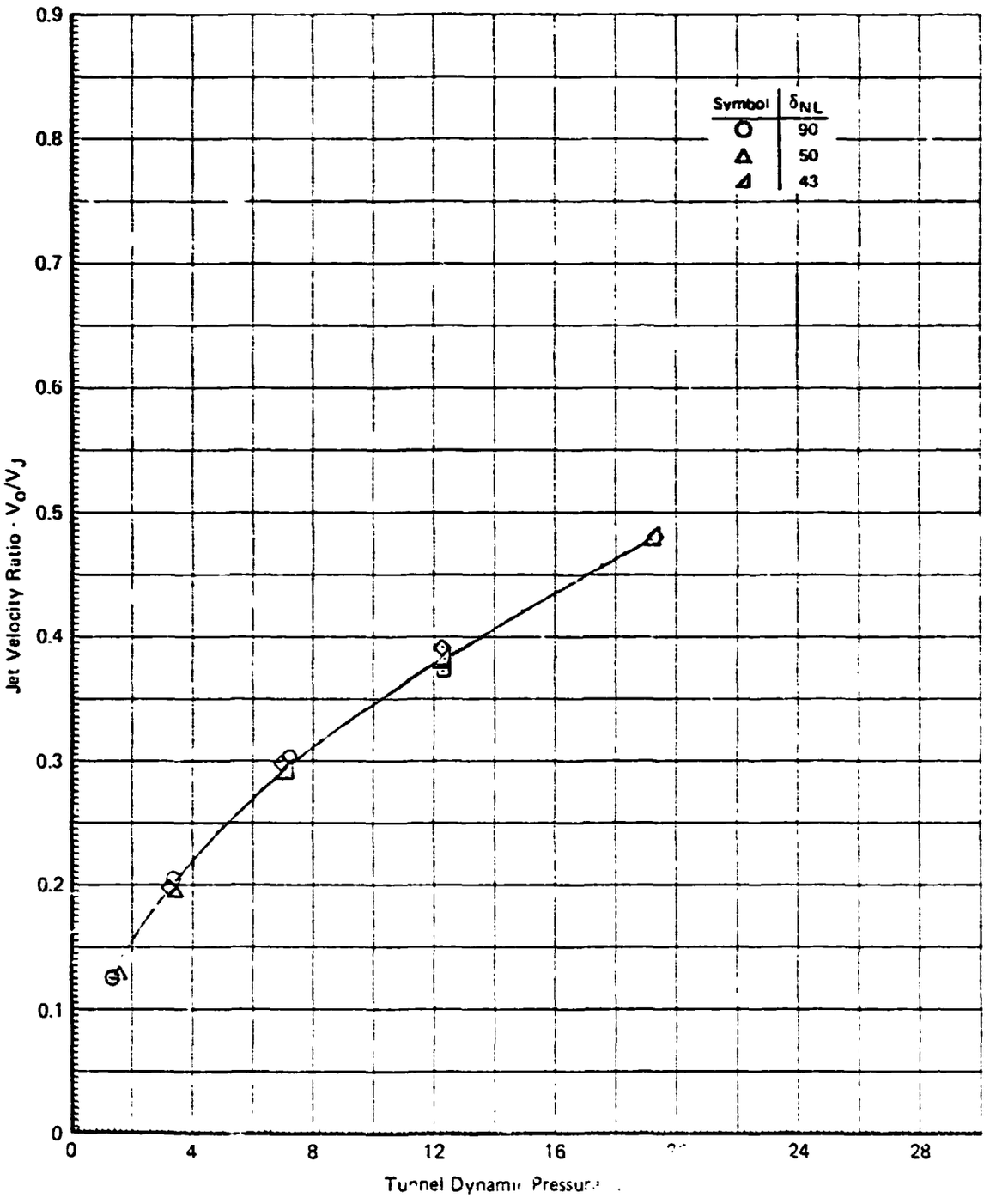

GP76-0622 285

8.3 POWERED LIFT CONFIGURATION - INDUCED LIFT AND DRAG CHARACTERISTICS

A primary objective of the large scale powered model test program was to evaluate the power induced lift and drag characteristics of the powered lift configuration with the horizontal tail on and off. Data with the horizontal tail on were obtained for five combinations of nose lift and lift/cruise unit vector angles: δ_{LC}/δ_{NL} = 23°/43°, 38°/43°, 56°/43°, 71°/55°, and 90°/90°. Data with the horizontal tail off were obtained for δ_{LC}/δ_{NL} = 23°/43°, 56°/43°, and 90°/90°. Additional data were obtained for selected combinations of nose lift and lift/cruise unit operation to evaluate the effect of nose unit operation on induced characteristics. The results of these tests are discussed in the following paragraphs.

Induced Lift and Drag - Horizontal Tail On

Figures 8.3-1 through 8.3-30 present the measured lift and drag data and the calculated propulsion and aerodynamic contributions for the five powered lift configurations with horizontal tail on at 0°. It will be noted that the aerodynamic contribution is the difference between two large values. Thus any error in the measured forces or calculated propulsion system force will result in significant error in the aerodynamic contribution.

The reference levels of lift and drag are noted on each figure. The difference between the reference lift or drag and the total aerodynamic lift or drag is the aerodynamic component induced by the propulsion system. The induced lift and drag characteristics for each configuration with horizontal tail on are summarized in Figures 8.3-31 through 8.3-35. The induced characteristics at 0° angle of attack for the five configurations are summarized in Figure 8.3-36. These data illustrate that, in general, positive induced lift and negative induced drag are indicated for all five configurations. However, it should be noted that both increments depend strongly on the accuracy to which total forces are measured and direct thrust effects are calculated.

Induced Lift and Drag - Horizontal Tail Off

Figures 8.3-37 through 8.3-54 present measured and calculated data for the three powered lift configurations with horizontal tail off. The comments for the tail on configurations are also applicable to these data. The induced lift and drag characteristics for each configuration are summarized in Figures 8.3-55 through 8.3-57. The induced characteristics at 0° angle of attack for the three configurations are summarized in Figure 8.3-58. Comparison of these data with

tail on data, Figure 8.3-36, demonstrates that removing the horizontal tail increases the induced lift, i.e., that induced lift values are more positive. This increase in lift due to removing the tail can be attributed to a propulsion induced downwash field enveloping the horizontal tail. During powered lift operation, this lift decrement could be minimized by changing the tail incidence.

Power Induced Effects - Nose Unit Contribution

During the preliminary testing, selected combinations of lift/cruise unit and nose lift unit deflection angles were tested to evaluate the effect of the nose lift unit on induced lift and drag characteristics. Test data were obtained for lift/cruise deflection angles of 0°, 56°, and 90° with the nose lift unit inlet and exit covered and for nose lift unit deflection angles of 50°, 70°, 90° with the lift/cruise unit at 0°.

Figures 8.3-59 through 8.3-64 present the measured lift and drag data and the calculated propulsion and aerodynamic contributions for the nose lift unit closed configurations. The induced lift and drag characteristics obtained from these data are summarized in Figures 8.3-65 and 8.3-66. These two lift/cruise unit induced characteristics are substantially larger than three fan characteristics obtained with comparable lift/cruise unit nozzle settings. This result is illustrated in Figures 8.3-67 through 8.3-70 which compare the total aerodynamic lift and drag of two fan and three fan configurations. The adverse effect of nose lift unit operation on aerodynamic lift is readily apparent.

Figures 3.3-71 through 8.3-76 present the measured lift and drag data and the calculated propulsion and aerodynamic contributions obtained for nose lift unit deflections of 50°, 70°, and 90°, with the lift/cruise unit at 0°. The aerodynamic lift and drag data obtained from these results are summarized in Figures 8.3-77 and 8.3-78. The adverse effect of nose unit operation on induced lift is evident.

The effect of nose lift unit operation on induced lift characteristics is summarized in Figure 8.3-79 which shows the nose unit induced lift, $\Delta L/FG_{NL}$, versus jet velocity ratio. In this figure the jet velocity of the nose unit is used in computing the ratio, V/V_J. When $\delta_{LC} = 0$, the lift decrement due to forward fan operation is reduced relative to that obtained when $\delta_{LC} = 56°$ or 90° since the induced lift for $\delta_{LC} = 0$ is much smaller.

FIGURE 8.3-1
LIFT vs DYNAMIC PRESSURE

$\delta_H = 0^o$ $\alpha = 0^o$ $\delta_{LC} = 23^o$ $\delta_{NL} = 43^o$ $\theta_J = 20.1^o$

Graphical Summary of Measured and Calculated Force Data

$\delta_f = 15^o$ $\delta_a = 10^o/10^o$ Nose Gear On

$N_F/\sqrt{\theta_{T_o}} = 3600$ RPM

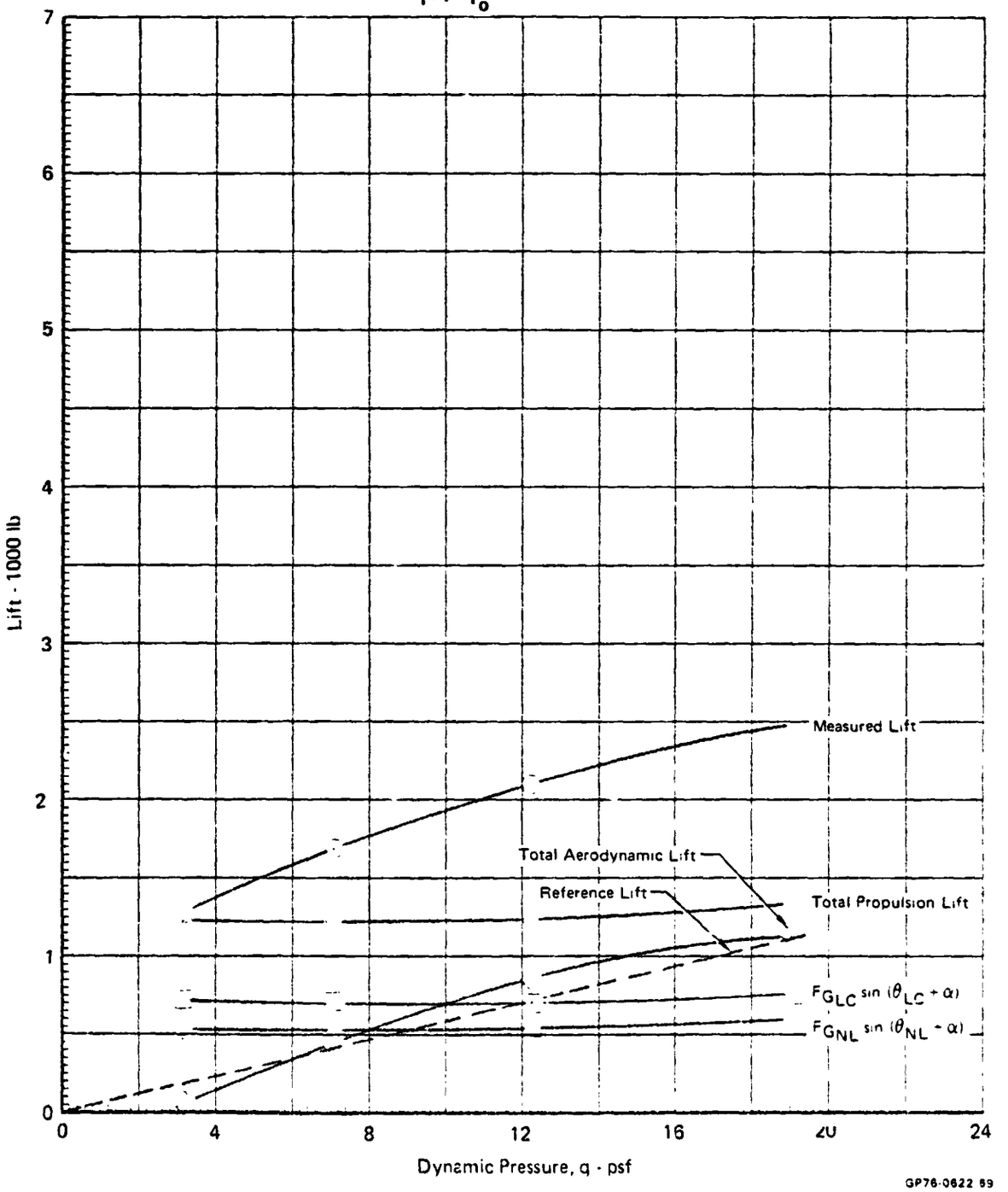

FIGURE 8.3-2

DRAG vs DYNAMIC PRESSURE

$\delta_H = 0^o$ $\alpha = 0^o$ $\delta_{LC} = 23^o$ $\delta_{NL} = 43^o$ $\theta_J = 20.1^o$

Graphical Summary of Measured and Calculated Force Data

$\delta_f = 15^o$ $\delta_a = 10^o/10^o$ Nose Gear On

$N_F/\sqrt{\theta_{T_o}} = 3600$ RPM

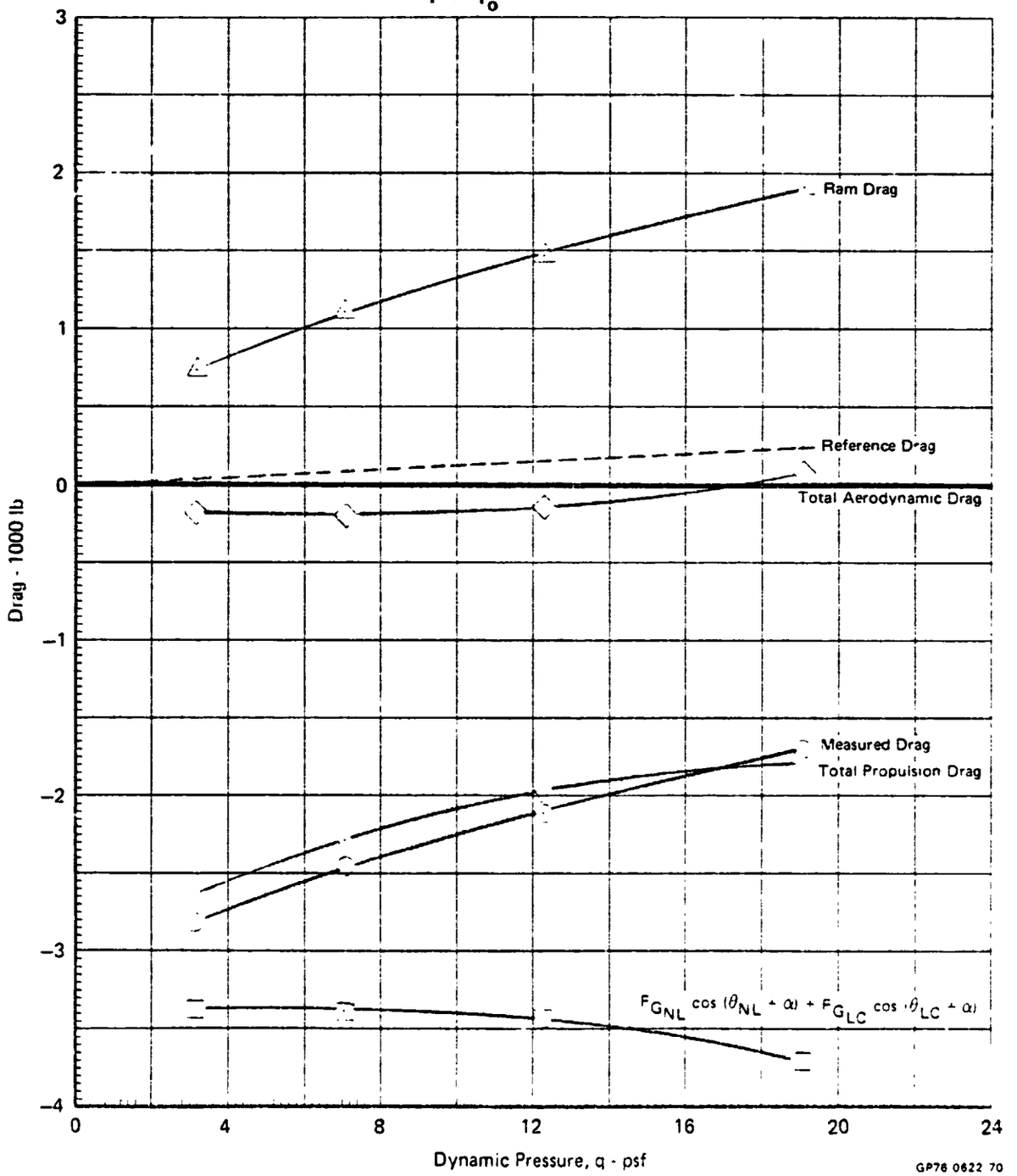

FIGURE 8.3-3

LIFT vs DYNAMIC PRESSURE

$\delta_H = 0^o$ $\alpha = 8^o$ $\delta_{LC} = 23^o$ $\delta_{NL} = 43^o$ $\theta_J = 20.1^o$

Graphical Summary of Measured and Calculated Force Data

$\delta_f = 15^o$ $\delta_a = 10^o/10^o$ Nose Gear On

$N_F/\sqrt{\theta_{T_o}} = 3600$ RPM

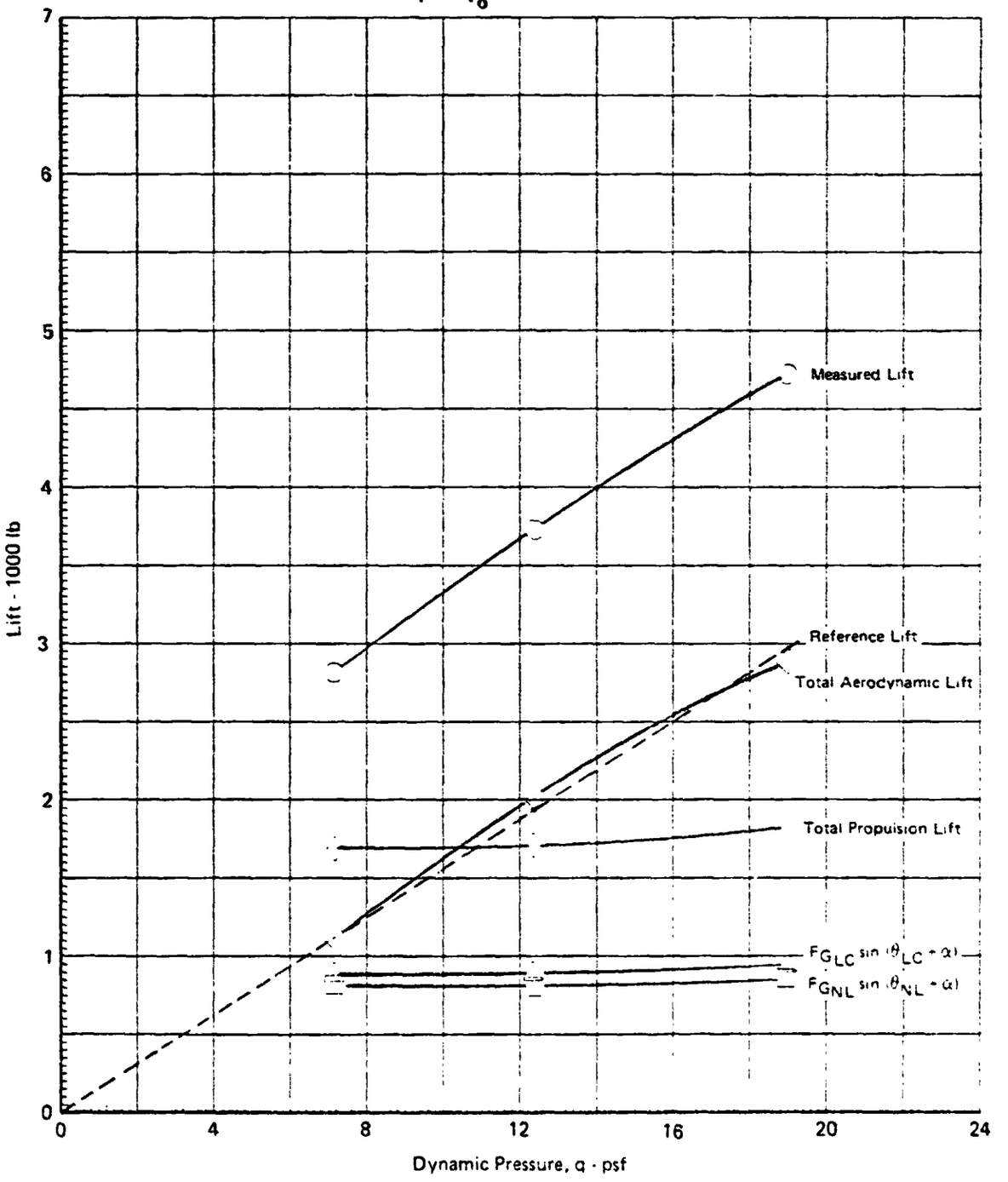

GP76-0622-71

FIGURE 8.3-4
DRAG vs DYNAMIC PRESSURE

$\delta_H = 0^o$ $\alpha = 8^o$ $\delta_{LC} = 23^o$ $\delta_{NL} = 43^o$ $\theta_J = 20.1^o$

Graphical Summary of Measured and Calculated Force Data

$\delta_f = 15^o$ $\delta_a = 10^o/10^o$ Nose Gear On

$N_F/\sqrt{\theta T_o} = 3600$ RPM

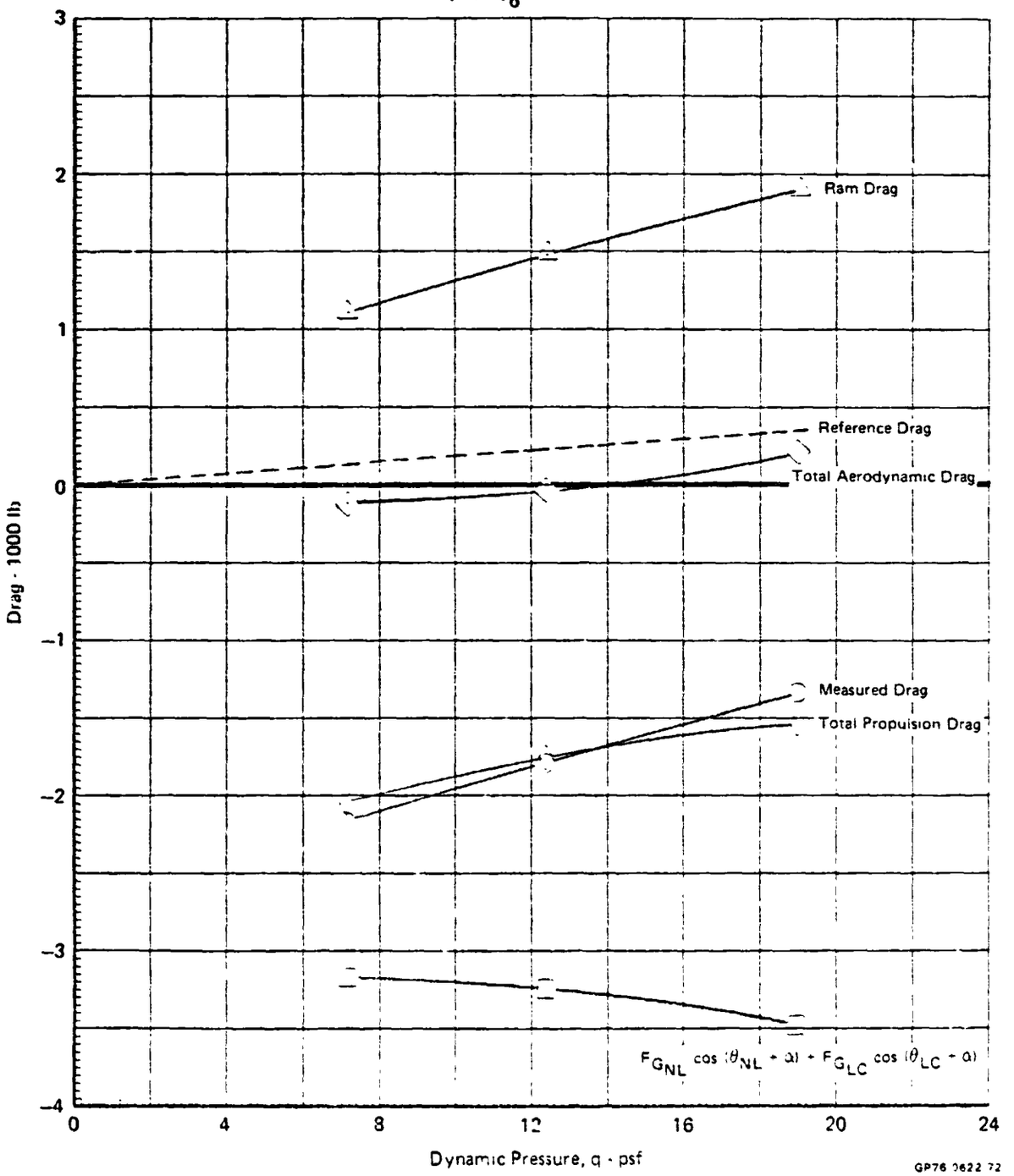

FIGURE 8.3-5

LIFT vs DYNAMIC PRESSURE

$\delta_H = 0^o$ $\alpha = 16^o$ $\delta_{LC} = 23^o$ $\delta_{NL} = 43^o$ $\theta_J = 20.1^o$

Graphical Summary of Measured and Calculated Force Data

$\delta_f = 15^o$ $\delta_a = 10^o/10^o$ Nose Gear On

$N_F/\sqrt{\theta_{T_o}} = 3600$ RPM

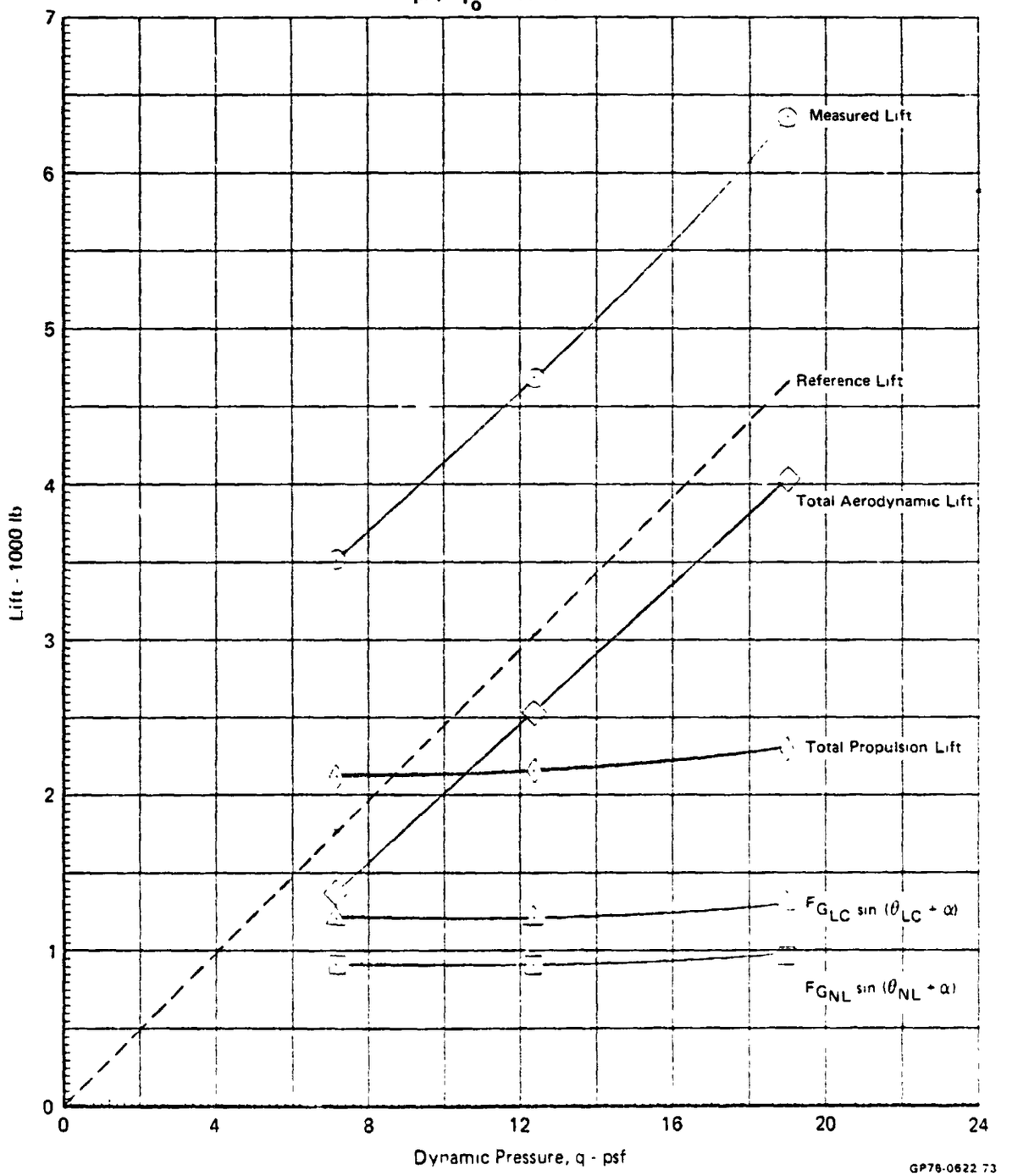

GP76-0622 73

FIGURE 8.3-6

DRAG vs DYNAMIC PRESSURE

$\delta_H = 0^o$ $\alpha = 16^o$ $\delta_{LC} = 23^o$ $\delta_{NL} = 43^o$ $\theta_J = 20.1^o$

Graphical Summary of Measured and Calculated Force Data

$\delta_f = 15^o$ $\delta_a = 10^o/10^o$ Nose Gear On

$N_F/\sqrt{\theta T_o} = 3600$ RPM

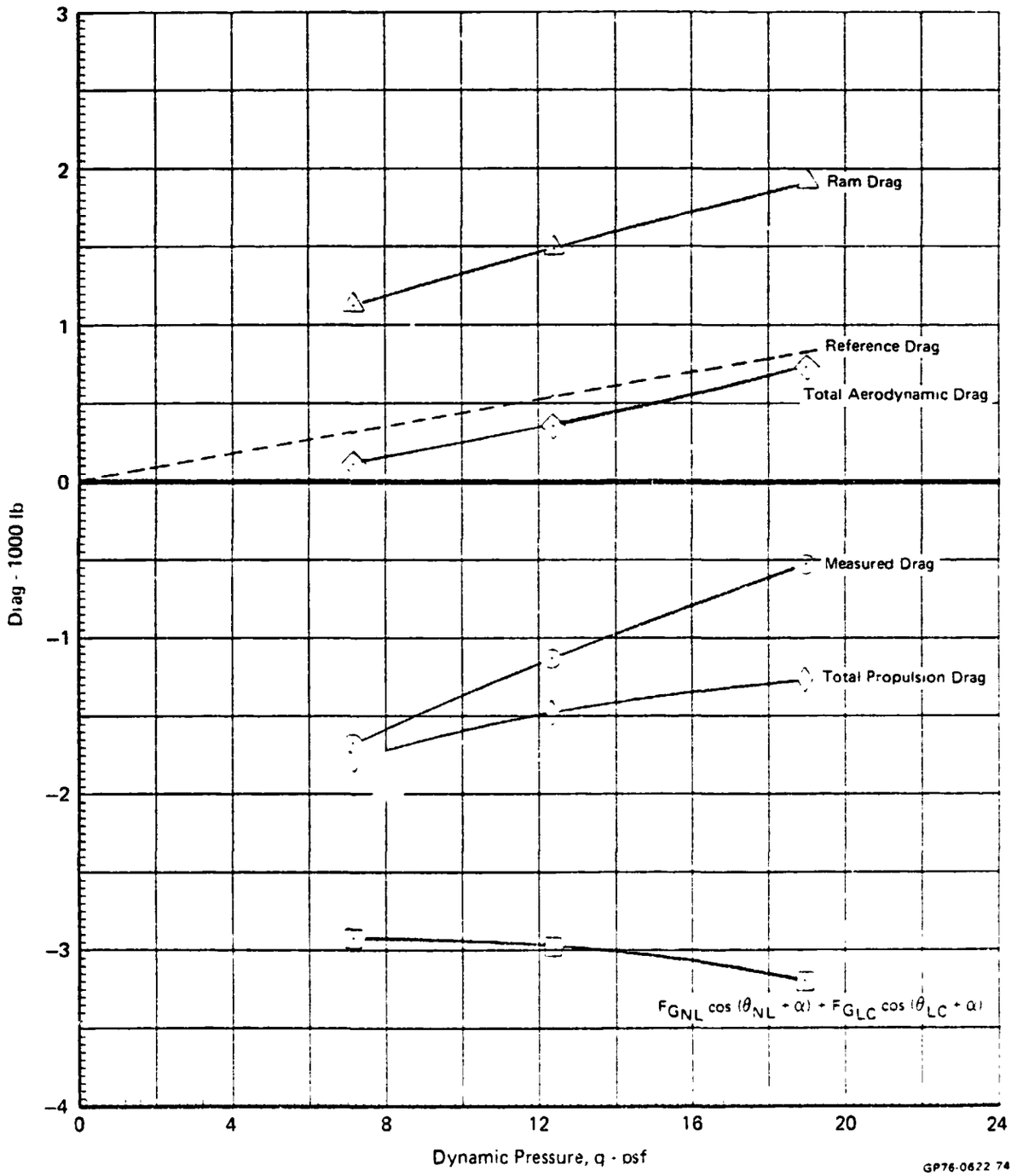

GP76-0622 74

FIGURE 8.3-7
LIFT vs DYNAMIC PRESSURE
$\delta_H = 0^o$ $\alpha = 0^o$ $\delta_{LC} = 38^o$ $\delta_{NL} = 43^o$ $\theta_J = 29.2^o$
Graphical Summary of Measured and Calculated Force Data
$\delta_f = 15^o$ $\delta_a = 10^o/10^o$ Nose Gear On
$N_F/\sqrt{\theta_{T_o}} = 3600$ RPM

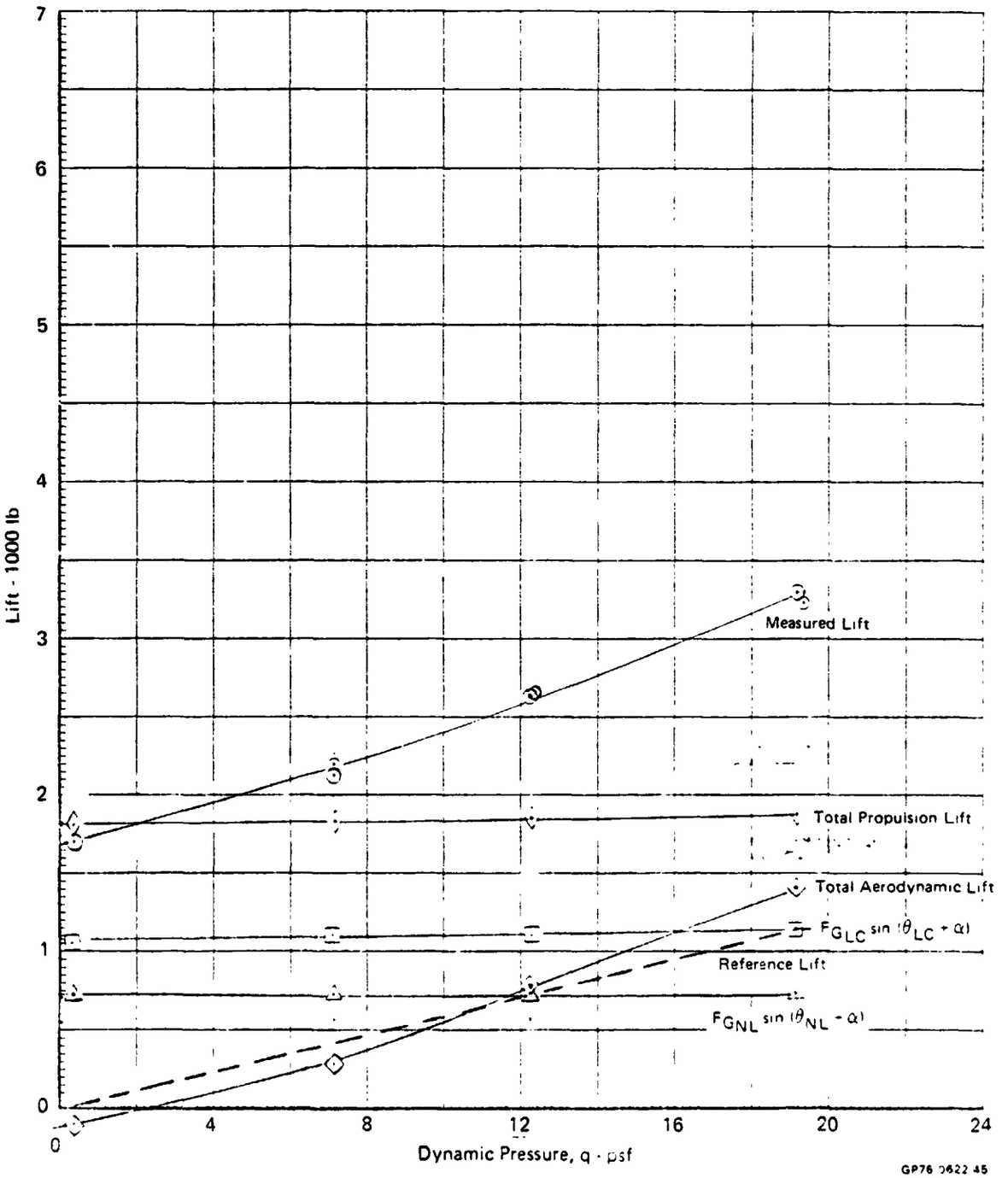

FIGURE 8.3-8

DRAG vs DYNAMIC PRESSURE

$\delta_H = 0^o$ $\alpha = 0^o$ $\delta_{LC} = 38^o$ $\delta_{NL} = 43^o$ $\theta_J = 29.2^o$

Graphical Summary of Measured and Calculated Force Data

$\delta_T = 15^o$ $\delta_a = 10^o/10^o$ Nose Gear On

$N_F/\sqrt{\theta_{T_o}} = 3600$ RPM

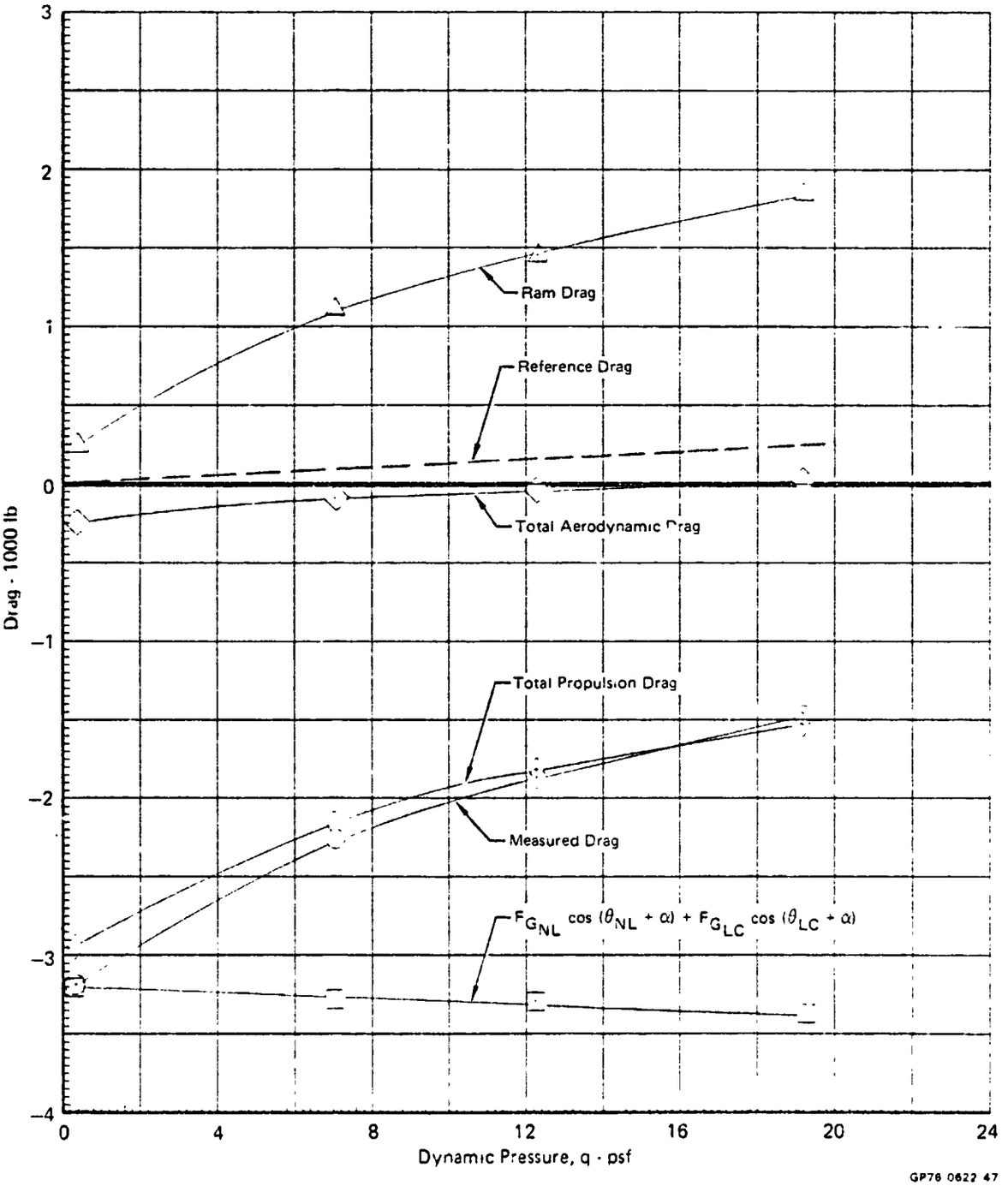

GP76 0622 47

FIGURE 8.3-9
LIFT vs DYNAMIC PRESSURE
$\delta_H = 0^o$ $\alpha = 8^o$ $\delta_{LC} = 38^o$ $\delta_{NL} = 43^o$ $\theta_J = 29.2^o$
Graphical Summary of Measured and Calculated Force Data
$\delta_f = 15^o$ $\delta_a = 10^o/10^o$ Nose Gear On
$N_F/\sqrt{\theta_{T_o}} = 3600$ RPM

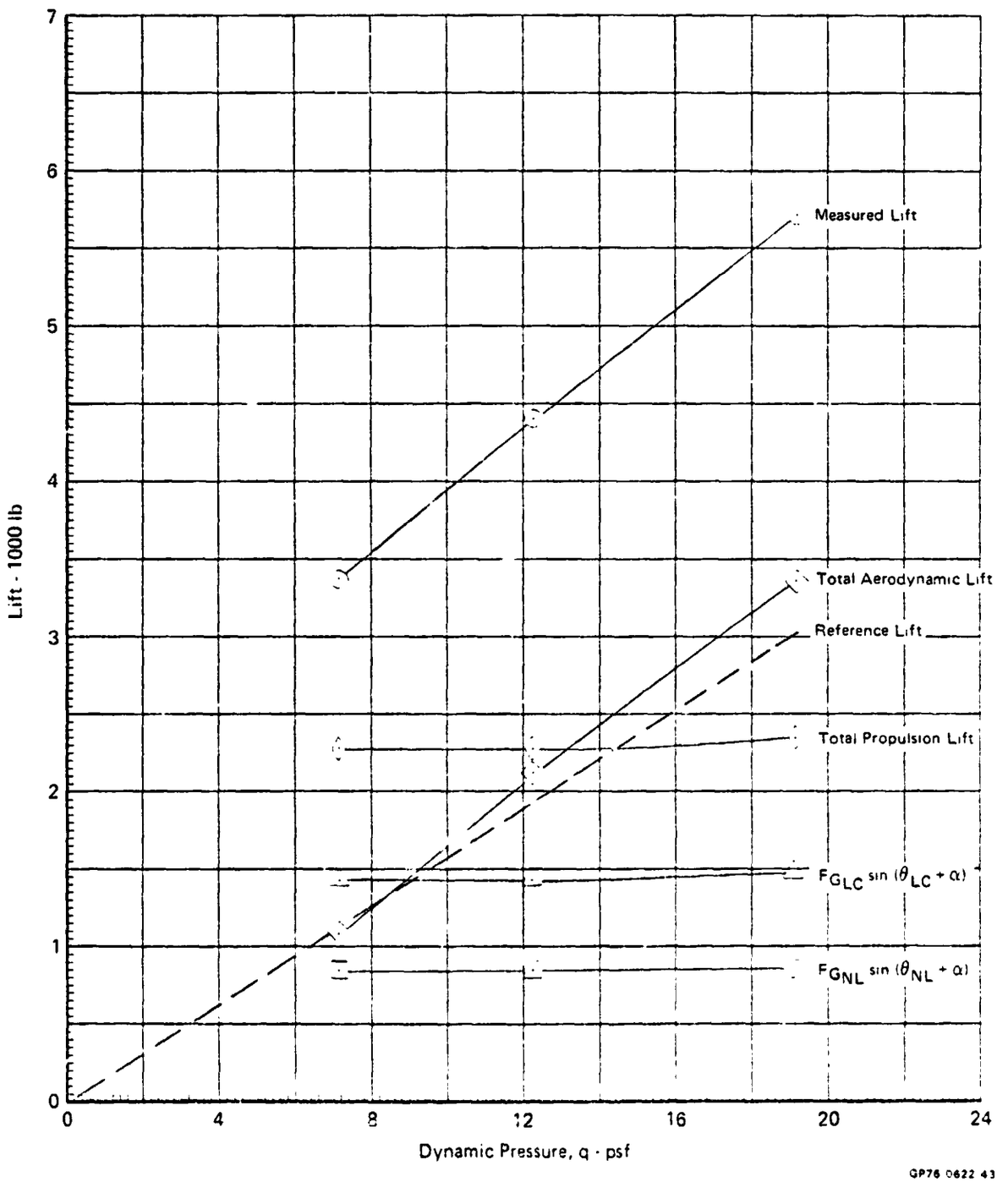

FIGURE 8.3-10
DRAG vs DYNAMIC PRESSURE
$\delta_H = 0^o$ $\alpha = 8^o$ $\delta_{LC} = 38^o$ $\delta_{NL} = 43^o$ $\theta_J = 29.2^o$
Graphical Summary of Measured and Calculated Force Data
$\delta_f = 15^o$ $\delta_a = 10^o/10^o$ Nose Gear On
$N_F/\sqrt{\theta T_o} = 3600$ RPM

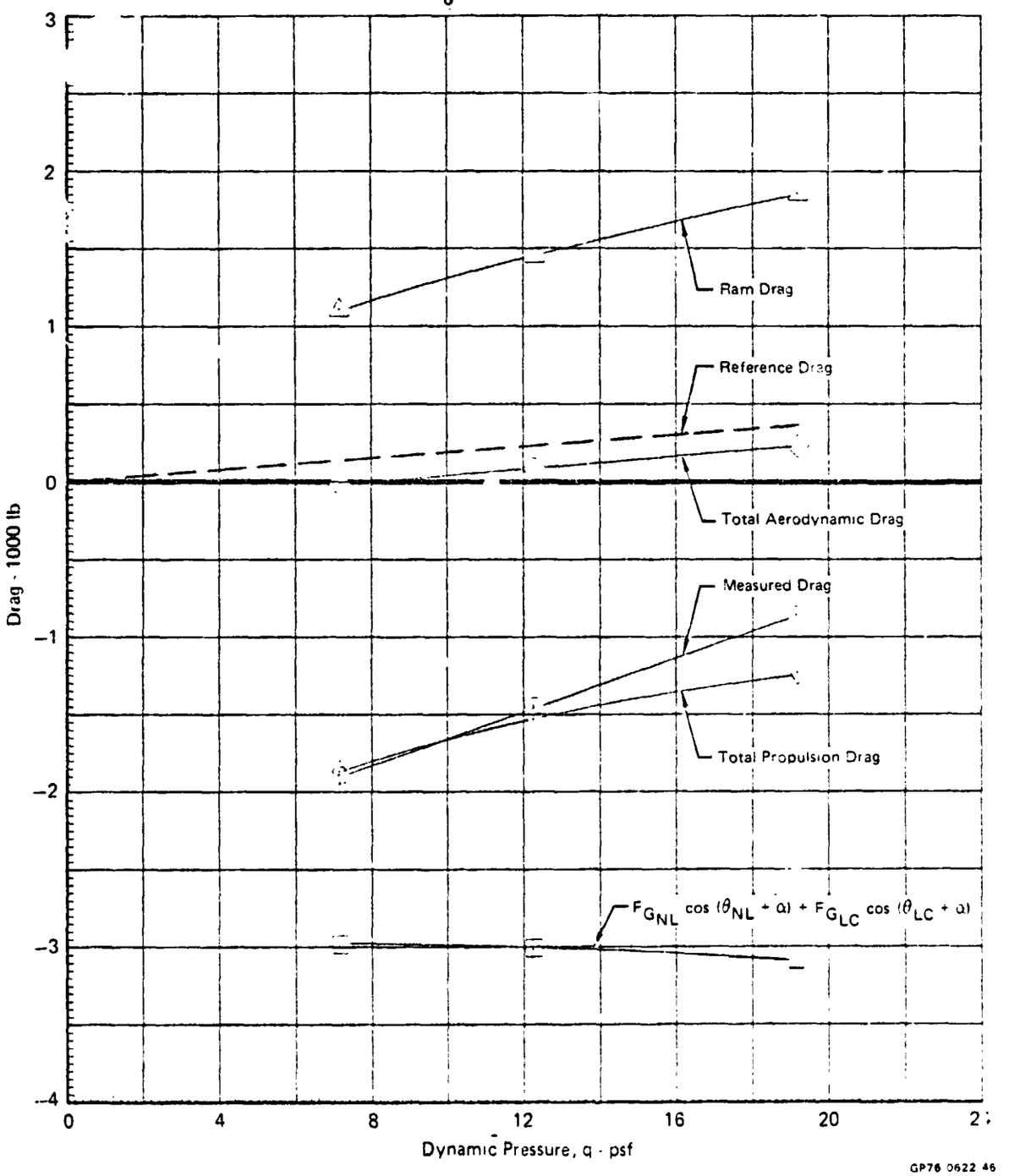

GP76 0622 46

FIGURE 8.3-11
LIFT vs DYNAMIC PRESSURE
$\delta_H = 0^o$ $\alpha = 16^o$ $\delta_{LC} = 38^o$ $\delta_{NL} = 43^o$ $\theta_J = 29.2^o$
Graphical Summary of Measured and Calculated Force Data
$\delta_f = 15^o$ $\delta_a = 10^o/10^o$ Nose Gear On

$N_F/\sqrt{\theta T_o}$ = 3600 RPM

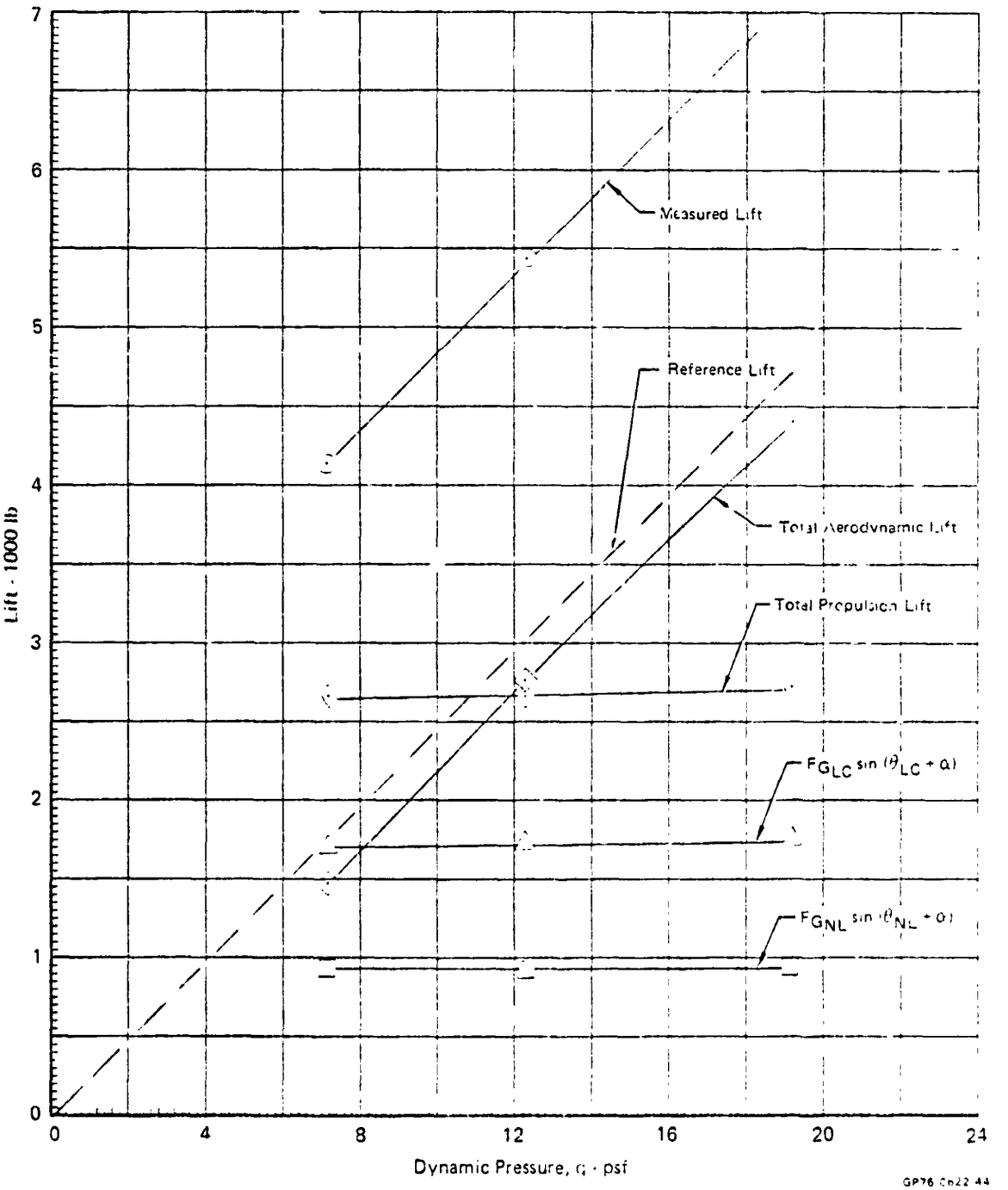

GP76 0622 44

FIGURE 8.3-12

DRAG vs DYNAMIC PRESSURE

$\delta_H = 0^o$ $\alpha = 16^o$ $\delta_{LC} = 38^o$ $\delta_{NL} = 43^o$ $\theta_J = 29.2^o$

Graphical Summary of Measured and Calculated Force Data

$\delta_f = 15^o$ $\delta_a = 10^o/10^o$ Nose Gear On

$N_F/\sqrt{\theta_{T_o}} = 3600$ RPM

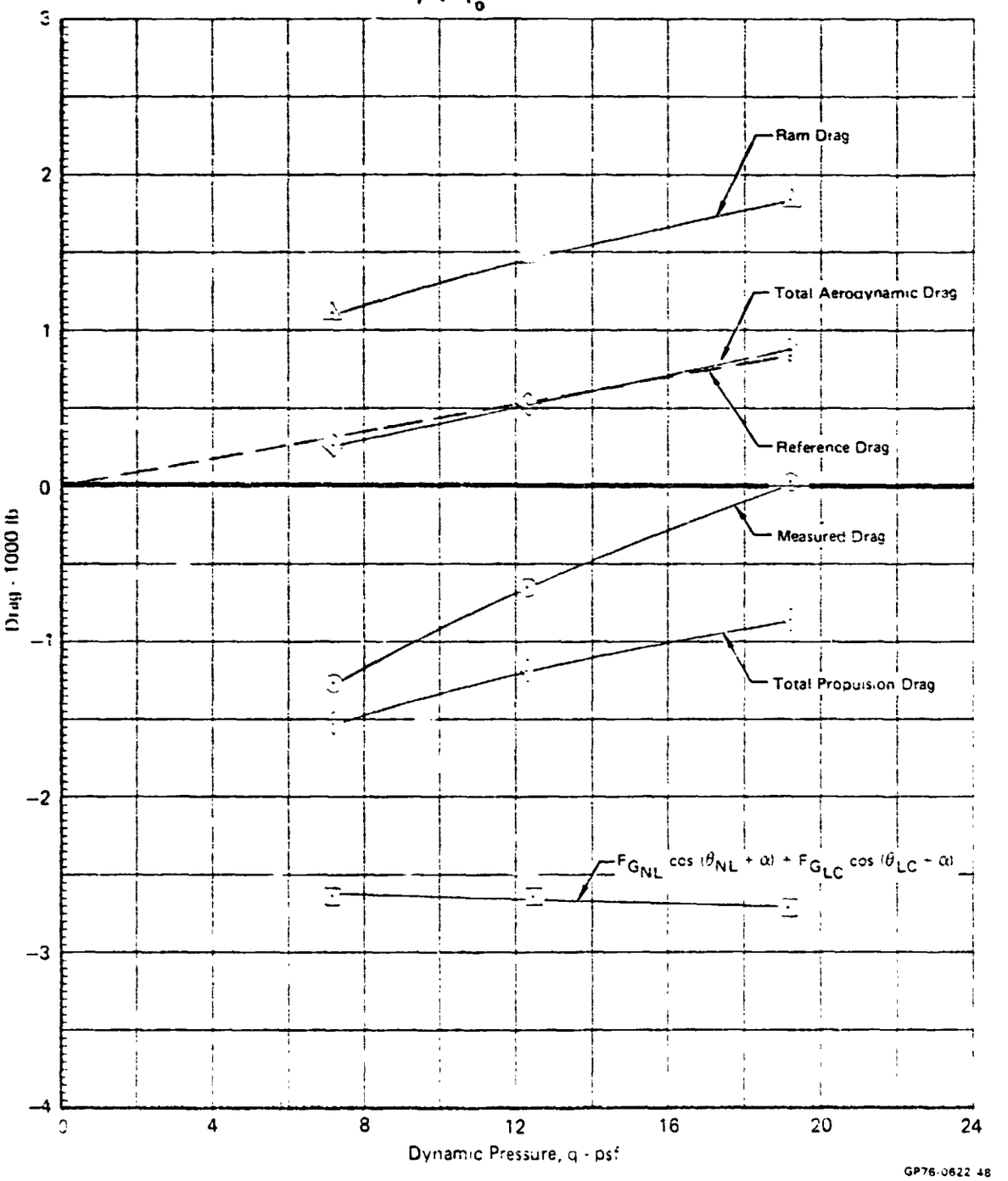

GP76-0622 48

FIGURE 8.3-13
LIFT vs DYNAMIC PRESSURE
$\delta_H = 0^o$ $\alpha = 0^o$ $\delta_{LC} = 56^o$ $\delta_{NL} = 43^o$ $\theta_J = 44.5^o$
Graphical Summary of Measured and Calcuated Force Data
$\delta_f = 15^o$ $\delta_a = 10^o/10^o$ Nose Gear On
$N_F/\sqrt{\theta_{T_o}} = 3600$ RPM

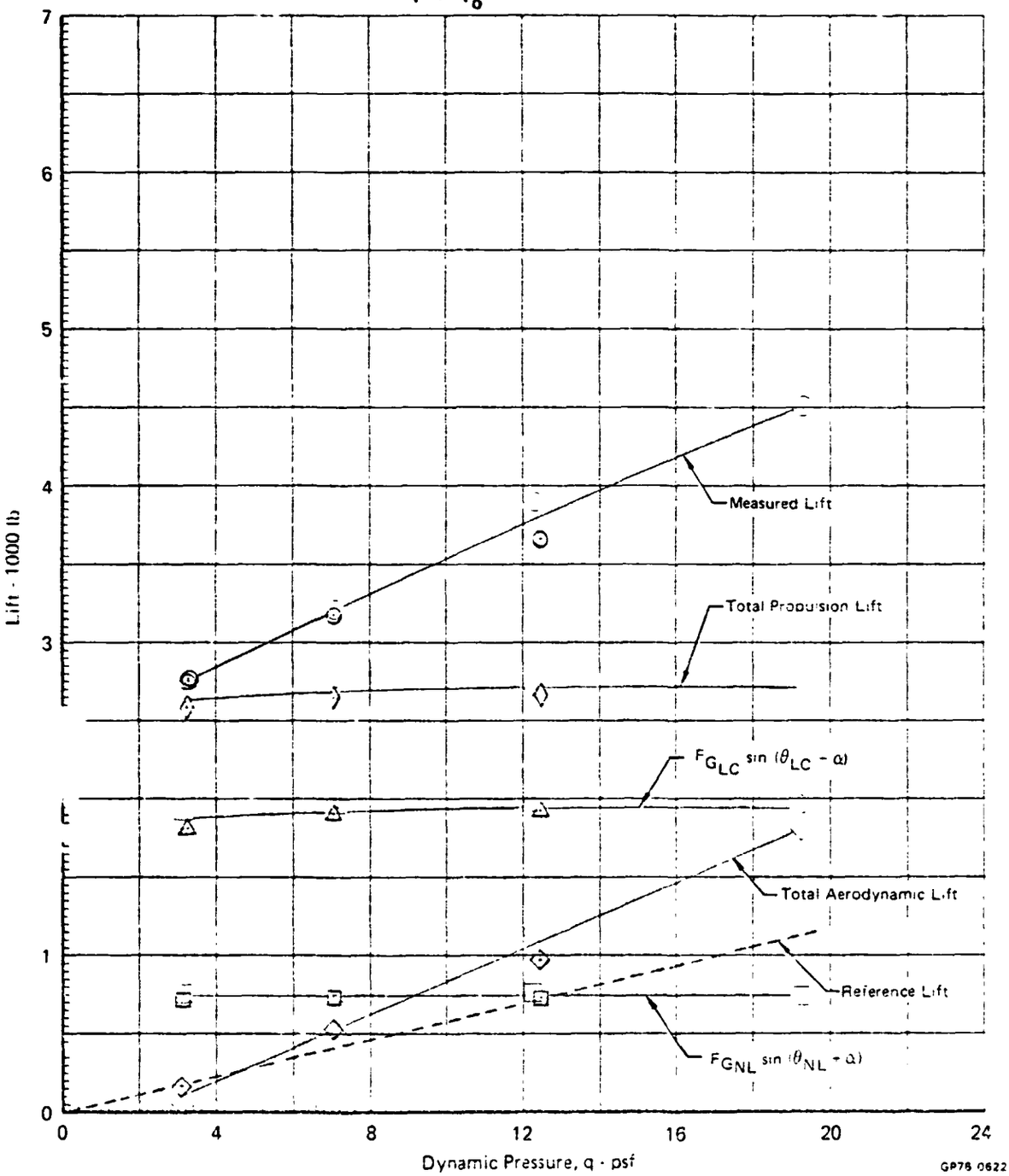

FIGURE 8.3-14
DRAG vs DYNAMIC PRESSURE
$\delta_H = 0^o$ $\alpha = 0^o$ $\delta_{LC} = 56^o$ $\delta_{NL} = 43^o$ $\theta_J = 44.5^o$
Graphical Summary of Measured and Calculated Force Data
$\delta_f = 15^o$ $\delta_a = 10^o/10^o$ Nose Gear On

$N_F/\sqrt{\theta_{T_o}} = 3600$ RPM

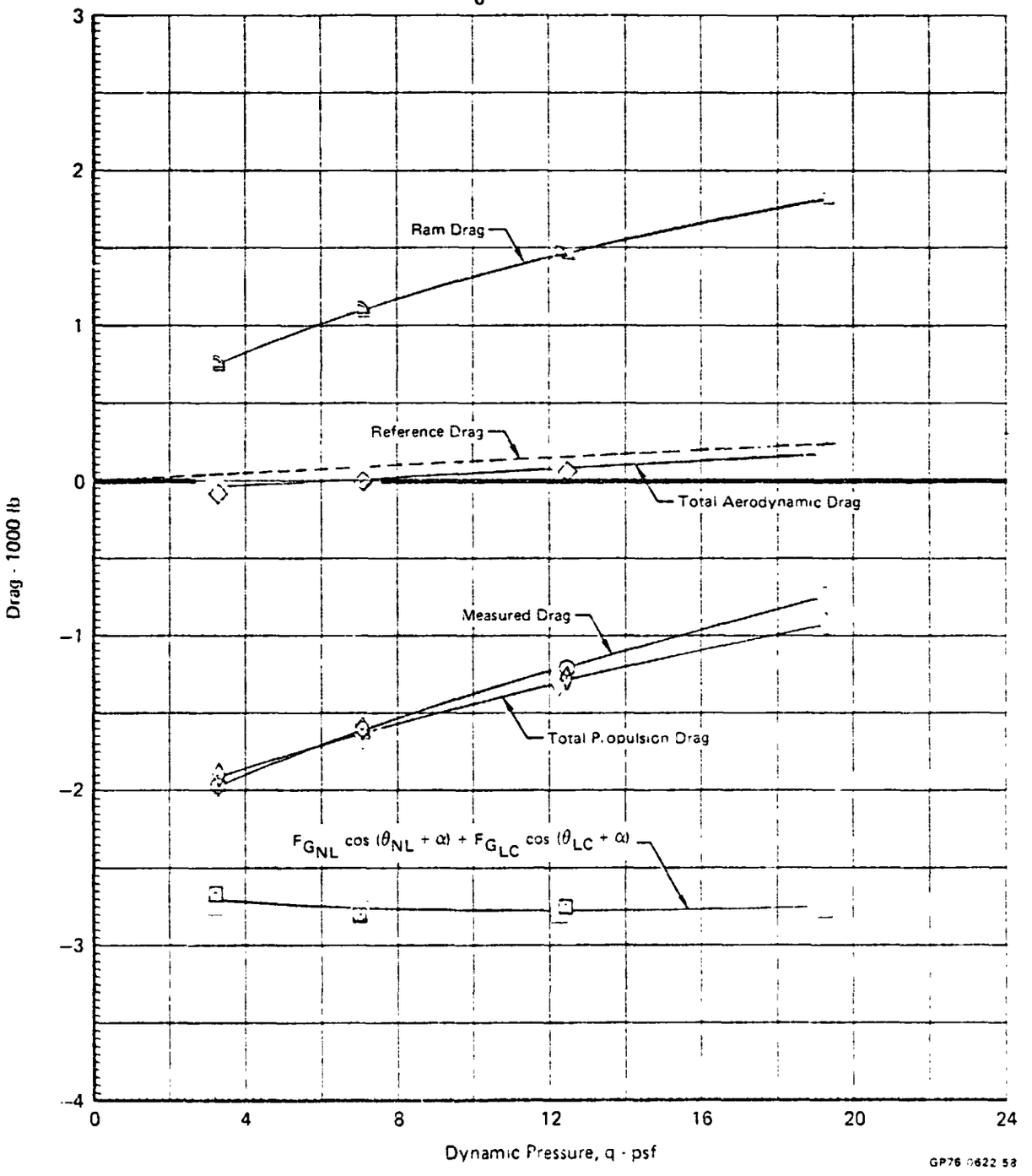

FIGURE 8.3-15

LIFT vs DYNAMIC PRESSURE

$\delta_H = 0^o$ $\alpha = 8^o$ $\delta_{LC} = 56^o$ $\delta_{NL} = 43^o$ $\theta_J = 44.5^c$

Graphical Summary of Measured and Calculated Force Data

$\delta_f = 15^o$ $\delta_a = 10^o/10^o$ Nose Gear On

$N_F/\sqrt{\theta_{T_o}} = 3600$ RPM

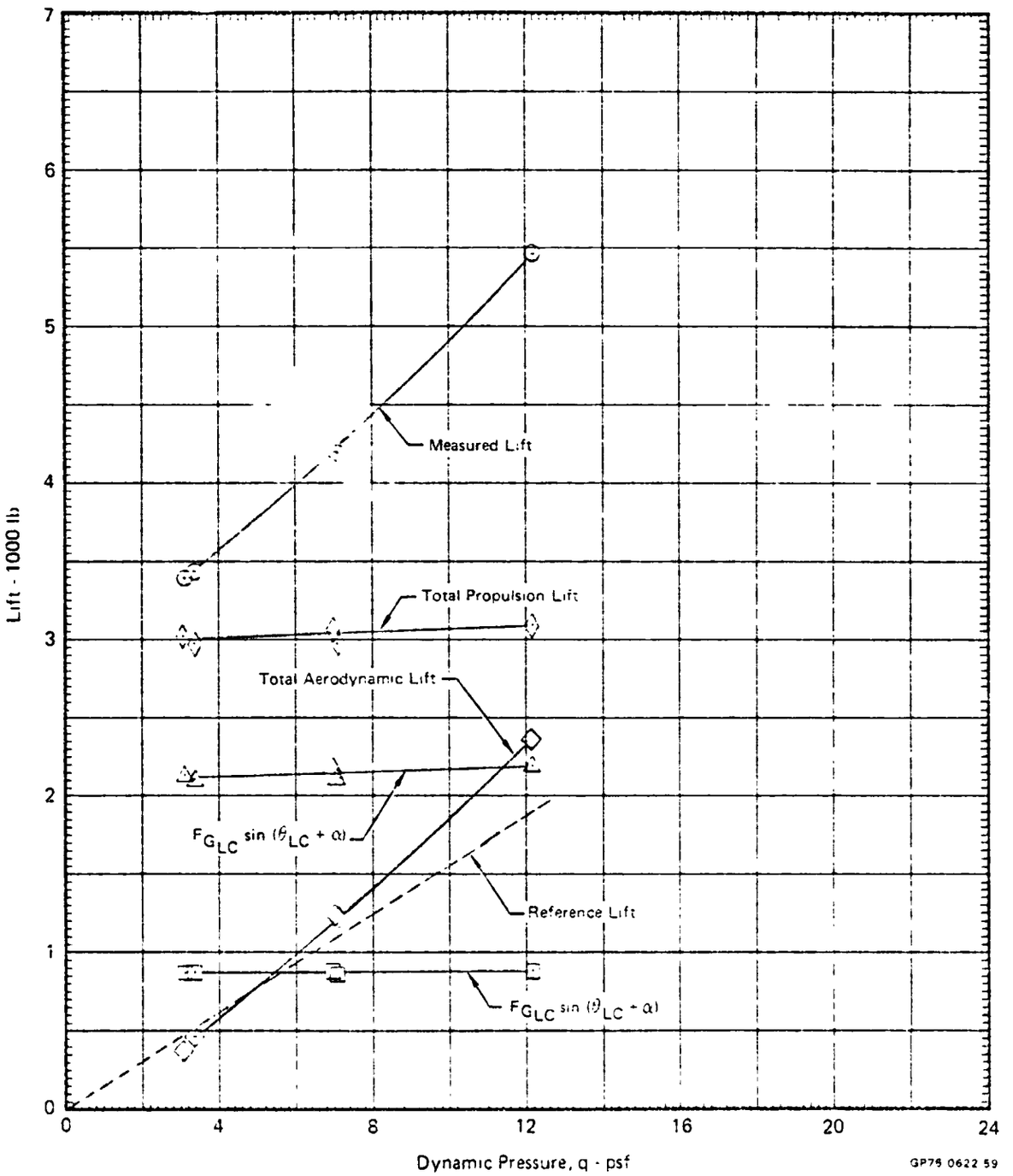

FIGURE 8.3-16

DRAG vs DYNAMIC PRESSURE

$\delta_H = 0^o$ $\alpha = 8^o$ $\delta_{LC} = 56^o$ $\delta_{NL} = 43^o$ $\theta_J = 44.5^o$

Graphical Summary of Measured and Calculated Force Data

$\delta_f = 15^o$ $\delta_a = 10^o/10^o$ Nose Gear On

$N_F/\sqrt{\theta_{T_o}} = 3600$ RPM

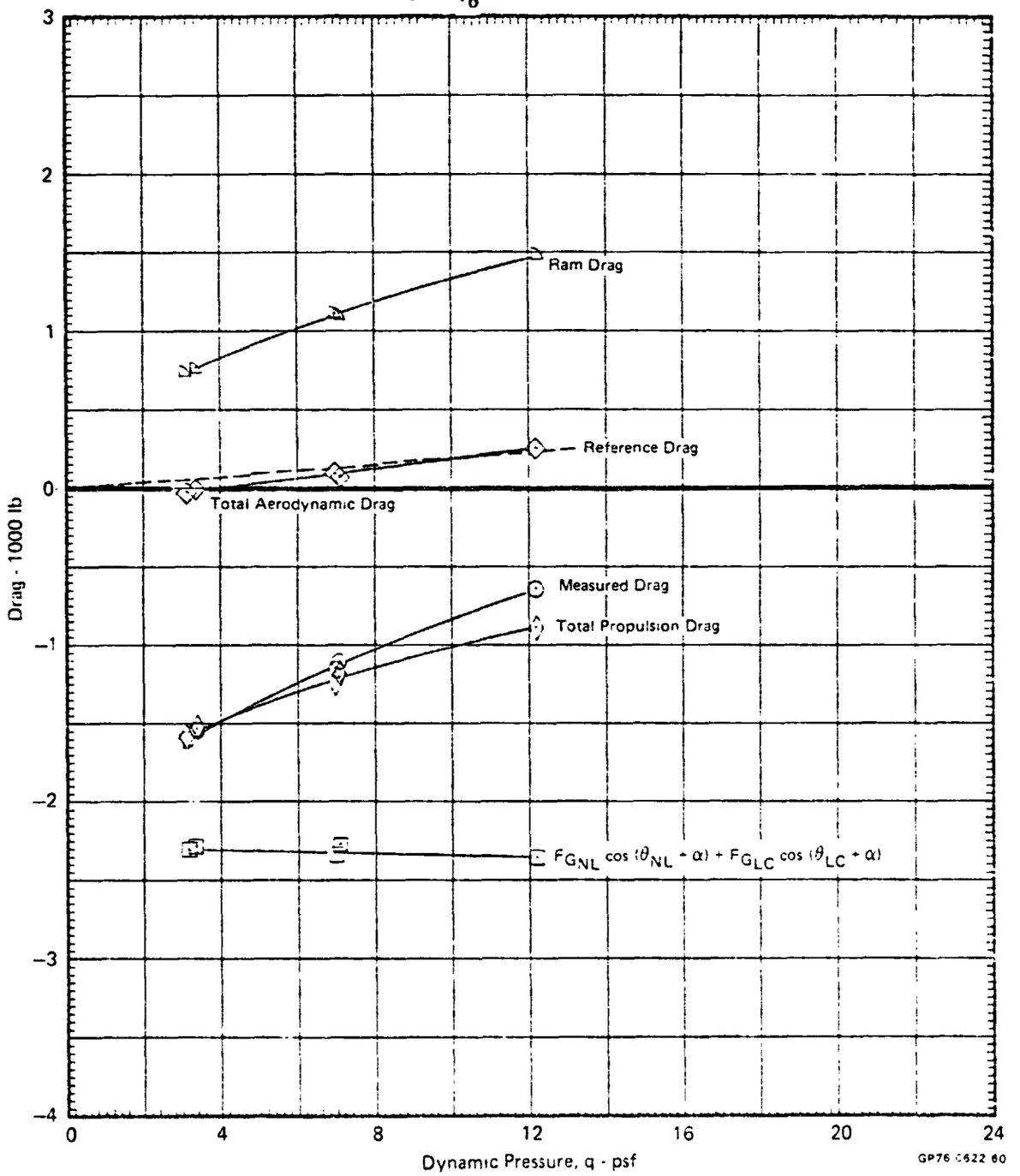

FIGURE 8.3-17
LIFT vs DYNAMIC PRESSURE
$\delta_H = 0^o$ $\alpha = 16^o$ $\delta_{LC} = 56^o$ $\delta_{NL} = 43^o$ $\theta_J = 44.5^o$
Graphical Summary of Measured and Calculated Force Data
$\delta_f = 15^o$ $\delta_a = 10^o/10^o$ **Nose Gear On**
$N_F/\sqrt{\theta T_o} = 3600$ RPM

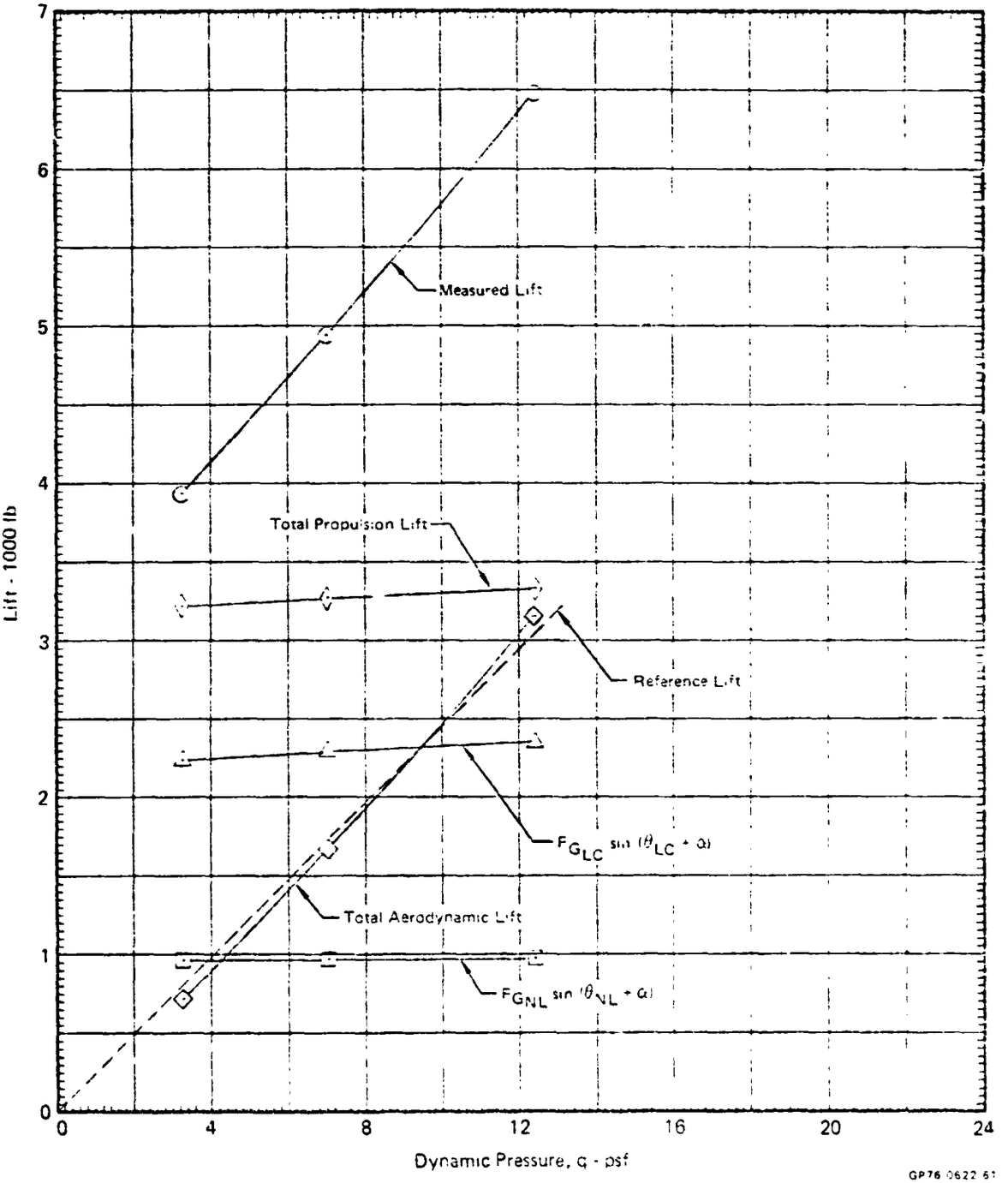

FIGURE 8.3-18

DRAG vs DYNAMIC PRESSURE

$\delta_H = 0^o$ $\alpha = 16^o$ $\delta_{LC} = 56^o$ $\delta_{NL} = 43^o$ $\theta_J = 44.5^o$

Graphical Summary of Measured and Calculated Force Data

$\delta_f = 15^o$ $\delta_a = 10^o/10^o$ Nose Gear On

$N_F/\sqrt{T_o} = 3600$ RPM

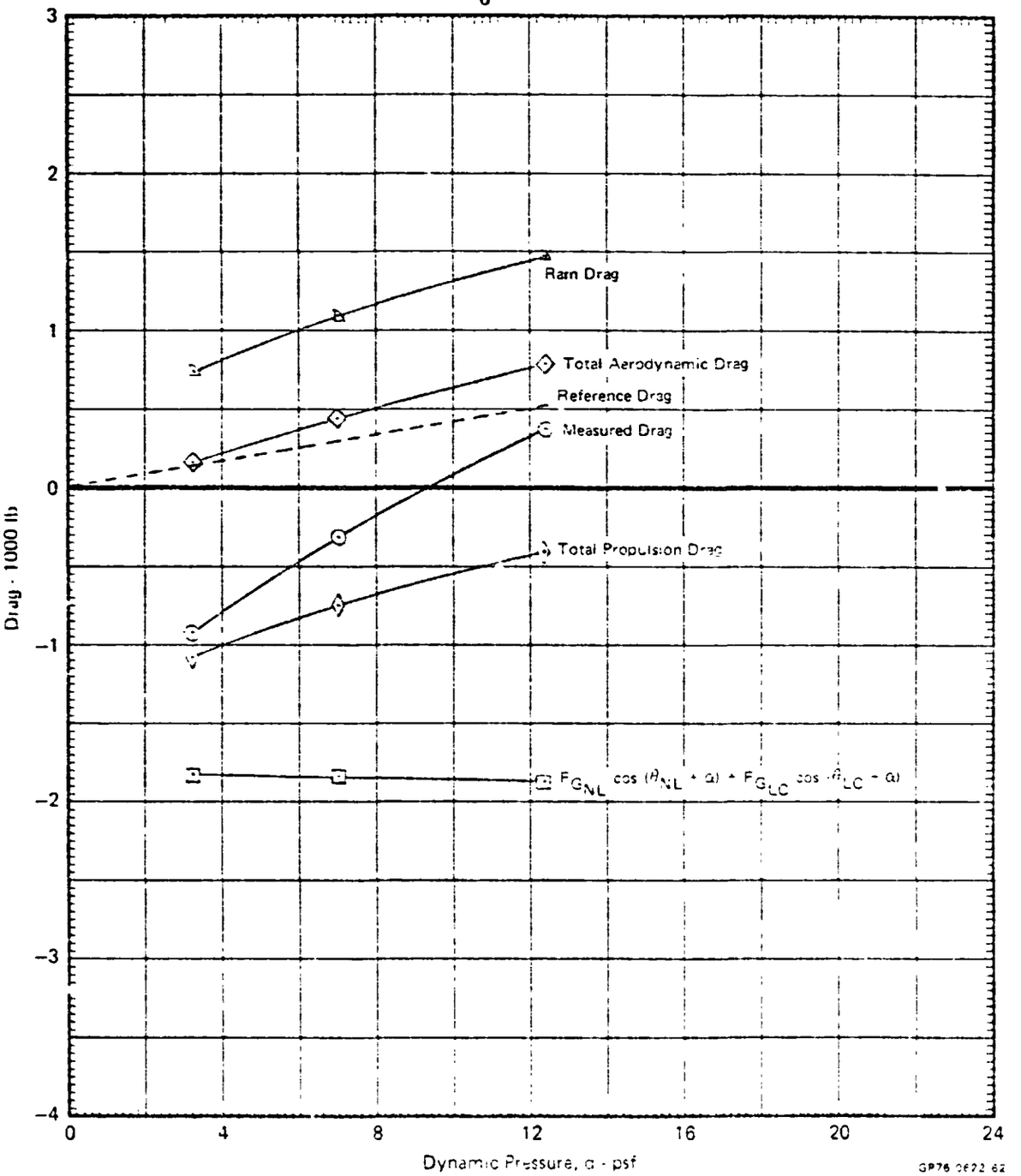

FIGURE 8.3-19
LIFT vs DYNAMIC PRESSURE
$\delta_H = 0^o$ $\alpha = 0^o$ $\delta_{LC} = 71^o$ $\delta_{NL} = 55^o$ $\theta_J = 59.8^o$
Graphical Summary of Measured and Calculated Force Data
$\delta_f = 15^o$ $\delta_a = 10^o/10^o$ Nose Gear On
$N_F/\sqrt{\theta T_o} = 3600$ RPM

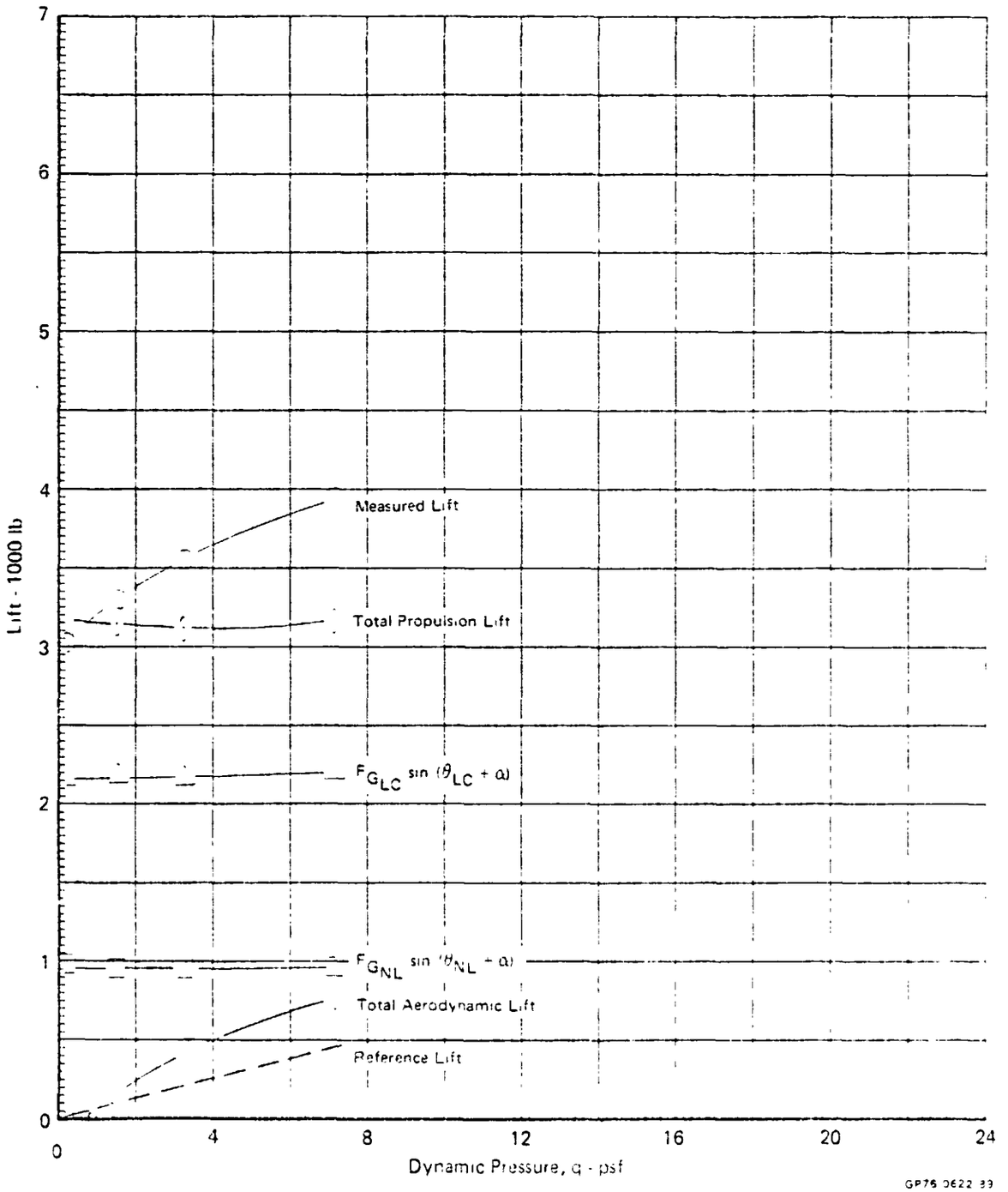

FIGURE 8.3-20
DRAG vs DYNAMIC PRESSURE
$\delta_H = 0^o$ $\alpha = 0^o$ $\delta_{LC} = 71^o$ $\delta_{NL} = 55^o$ $\theta_J = 59.8^o$
Graphical Summary of Measured and Calculated Force Data
$\delta_f = 15^o$ $\delta_a = 10^o/10^o$ Nose Gear On

$N_F/\sqrt{\theta T_o}$ = 3600 RPM

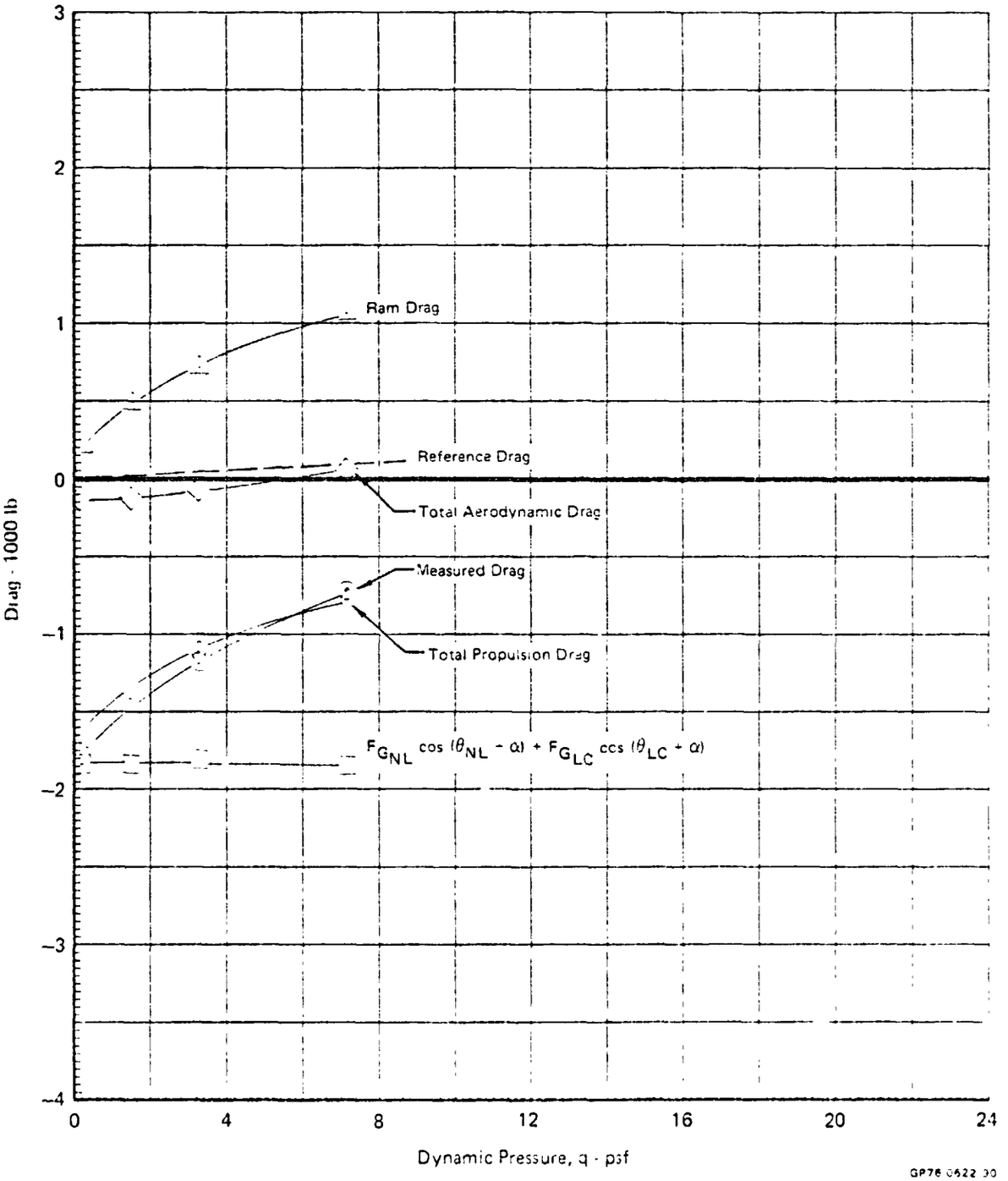

GP76 0622 30

FIGURE 8.3-21

LIFT vs DYNAMIC PRESSURE

$\delta_H = 0^o$ $\alpha = 8^o$ $\delta_{LC} = 71^o$ $\delta_{NL} = 55^o$ $\theta_J = 59.8^o$

Graphical Summary of Measured and Calculated Force Data

$\delta_f = 15^o$ $\delta_a = 10^o/10^o$ Nose Gear On

$N_F/\sqrt{\theta_{T_o}} = 3600$ RPM

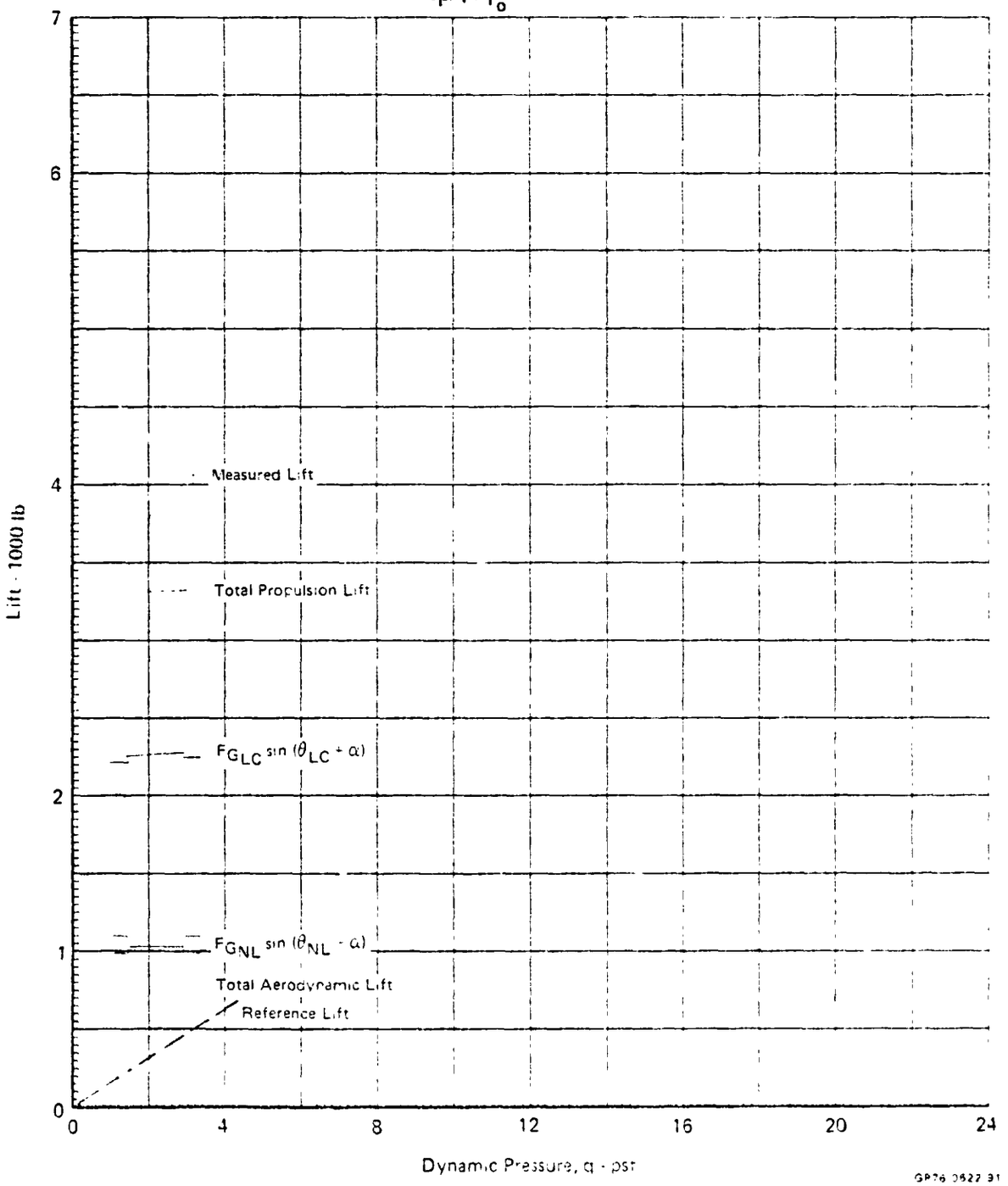

FIGURE 8.3-22

DRAG vs DYNAMIC PRESSURE

$\delta_H = 0^o$ $\alpha = 8^o$ $\delta_{LC} = 71^o$ $\delta_{NL} = 55^o$ $\theta_J = 59.8^o$

Graphical Summary of Measured and Calculated Force Data

$\delta_f = 15^o$ $\delta_a = 10^o/10^o$ Nose Gear On

$N_F/\sqrt{\theta T_o} = 3600$ RPM

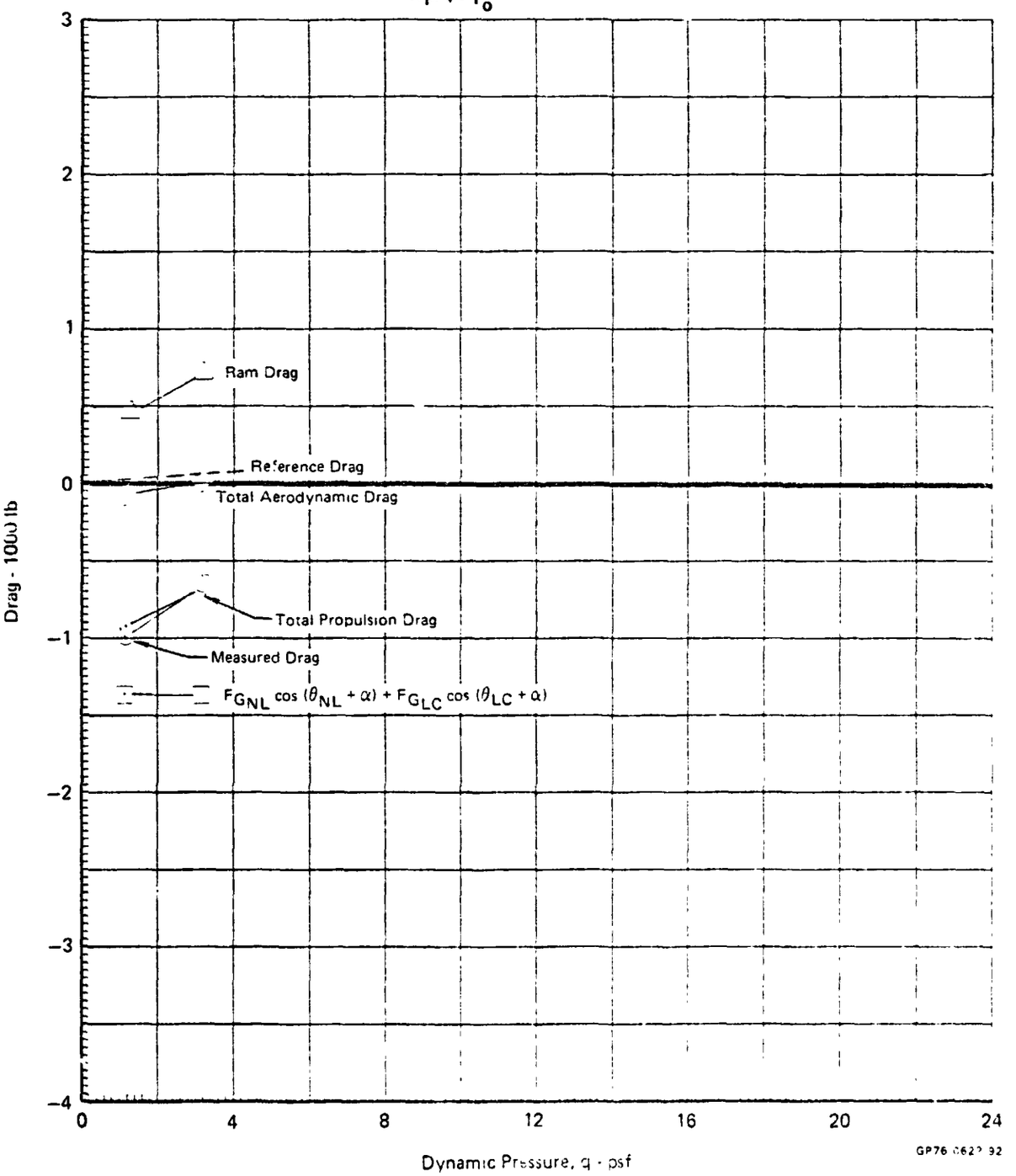

FIGURE 8.3-23

LIFT vs DYNAMIC PRESSURE

$\delta_H = 0^o$ $\alpha = 16^o$ $\delta_{LC} = 71^o$ $\delta_{NL} = 55^o$ $\theta_J = 59.8^o$

Graphical Summary of Measured and Calculated Force Data

$\delta_f = 15^o$ $\delta_a = 10^o/10^o$ Nose Gear On

$N_F/\sqrt{\theta T_o} = 3600$ RPM

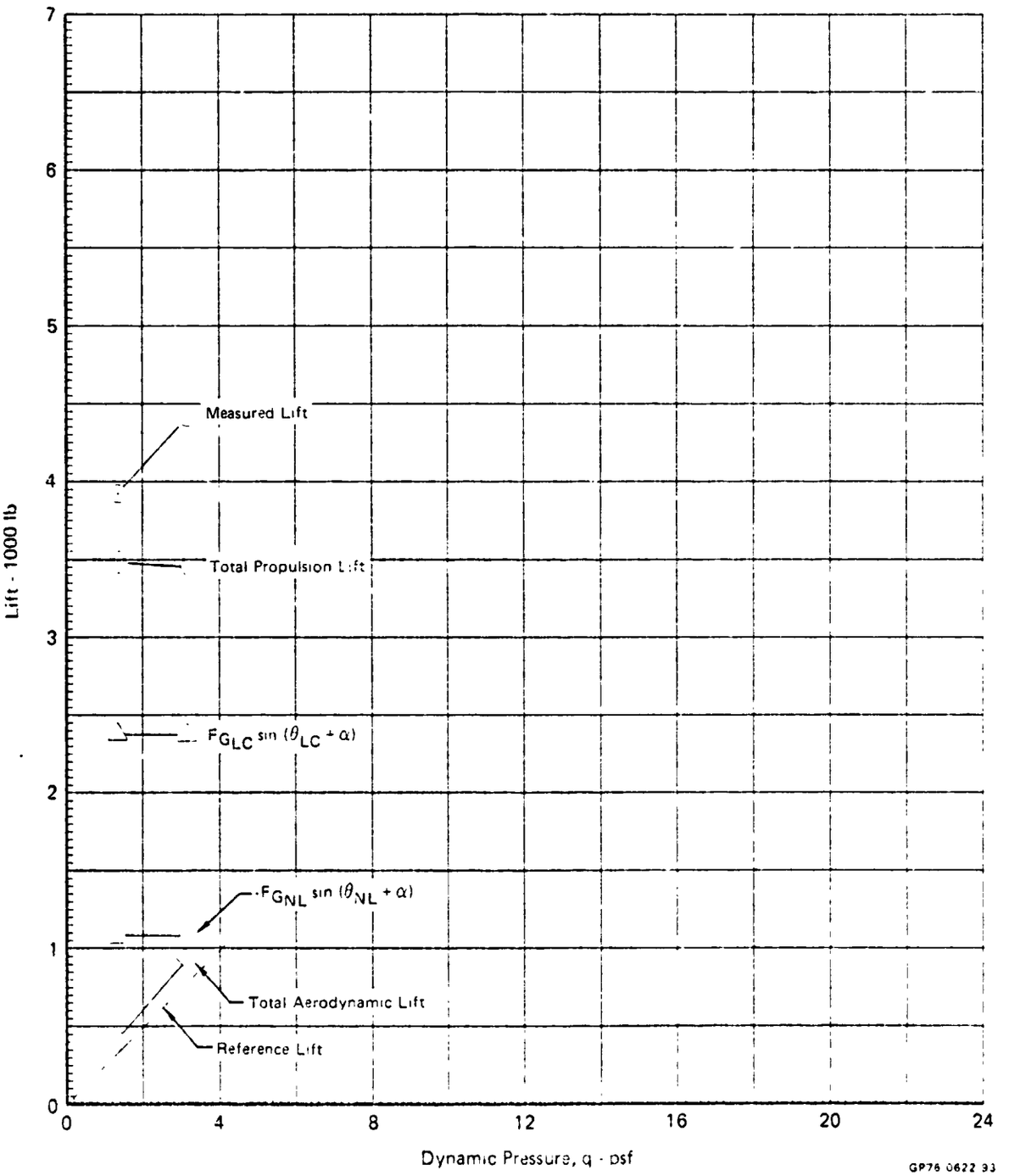

FIGURE 8.3-24

DRAG vs DYNAMIC PRESSURE

$\delta_H = 0^o$ $\alpha = 16^o$ $\delta_{LC} = 71^o$ $\delta_{NL} = 55^o$ $\theta_J = 59.8^o$

Graphical Summary of Measured and Calculated Force Data

$\delta_f = 15^o$ $\delta_a = 10^o/10^o$ Nose Gear On

$N_F/\sqrt{\theta_{T_o}} = 3600$ RPM

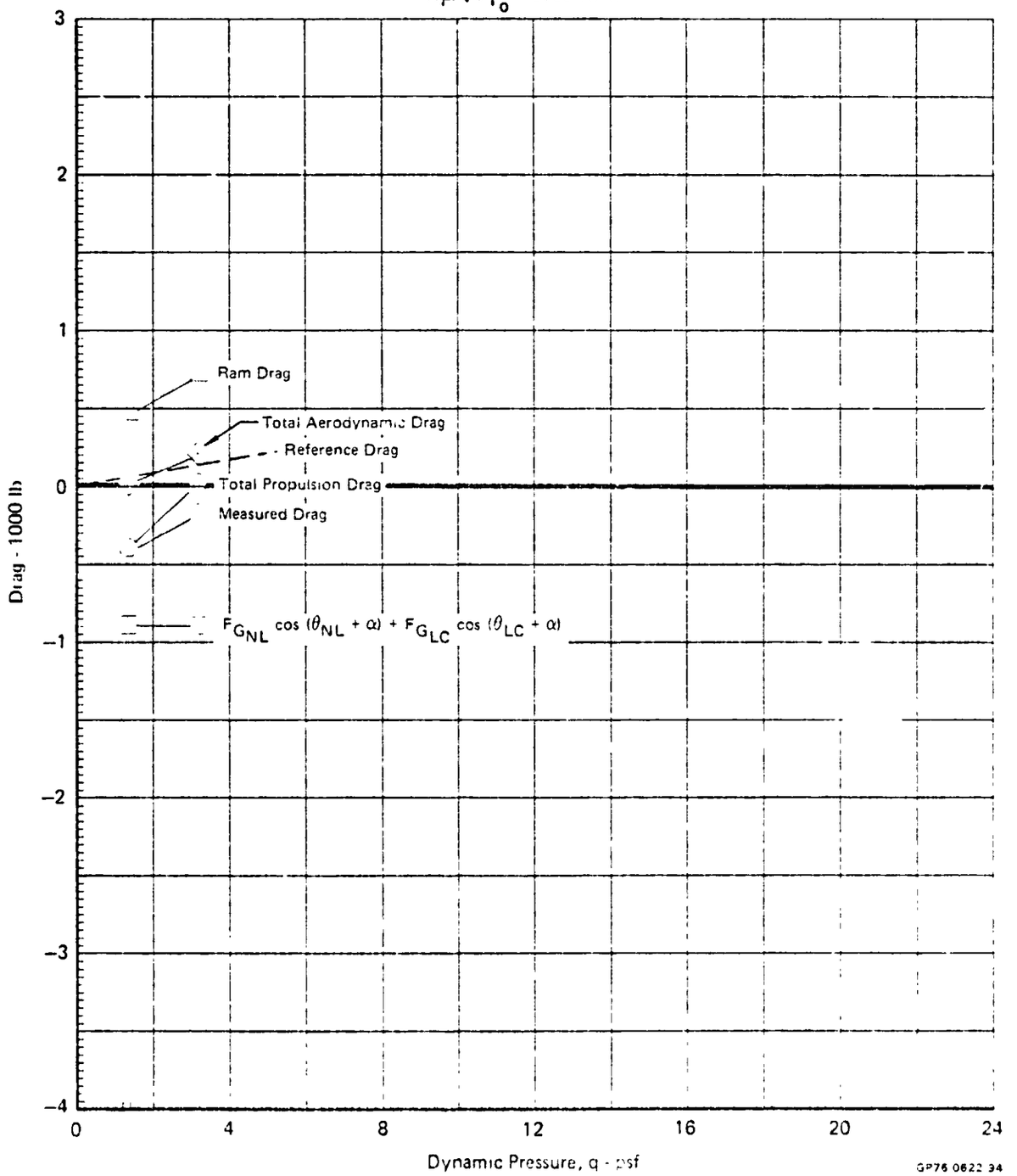

FIGURE 8.3-25

LIFT vs DYNAMIC PRESSURE

$\delta_H = 0^o$ $\alpha = 0^o$ $\delta_{LC} = 90^o$ $\delta_{NL} = 90^o$ $\theta_J = 84.7^o$

Graphical Summary of Measured and Calculated Force Data

$\delta_f = 15^o$ $\delta_a = 10^o/10^o$ Nose Gear On

$N_F/\sqrt{\theta_{T_o}} = 3600$ RPM

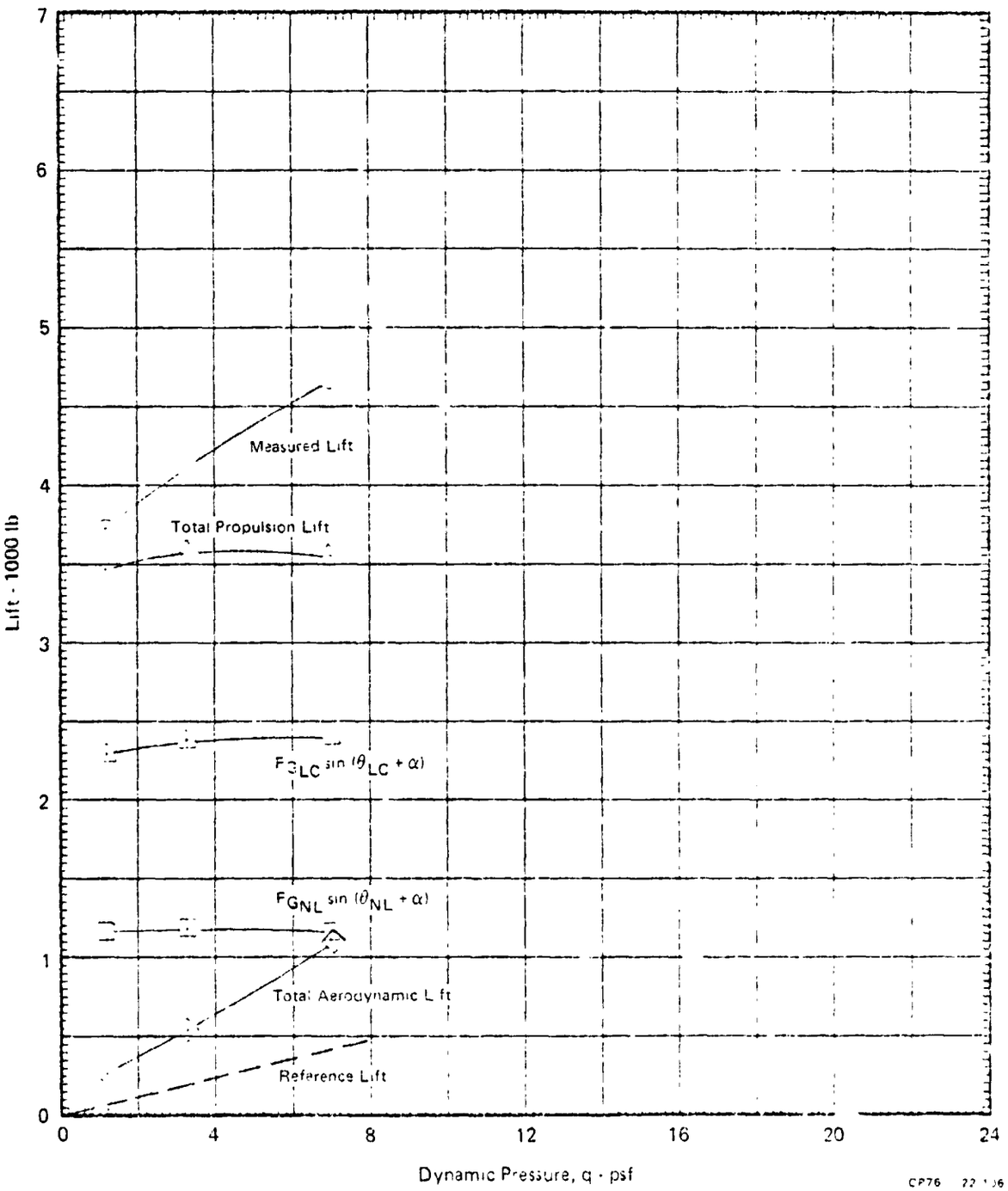

CP76 22 106

FIGURE 8.3-26
DRAG vs DYNAMIC PRESSURE
$\delta_H = 0^o$ $\alpha = 0^o$ $\delta_{LC} = 90^o$ $\delta_{NL} = 90^o$ $\theta_J = 84.7^o$
Graphical Summary of Measured and Calculated Force Data
$\delta_f = 15^o$ $\delta_a = 10^o/10^o$ Nose Gear On
$N_F/\sqrt{T_o} = 3600$ RPM

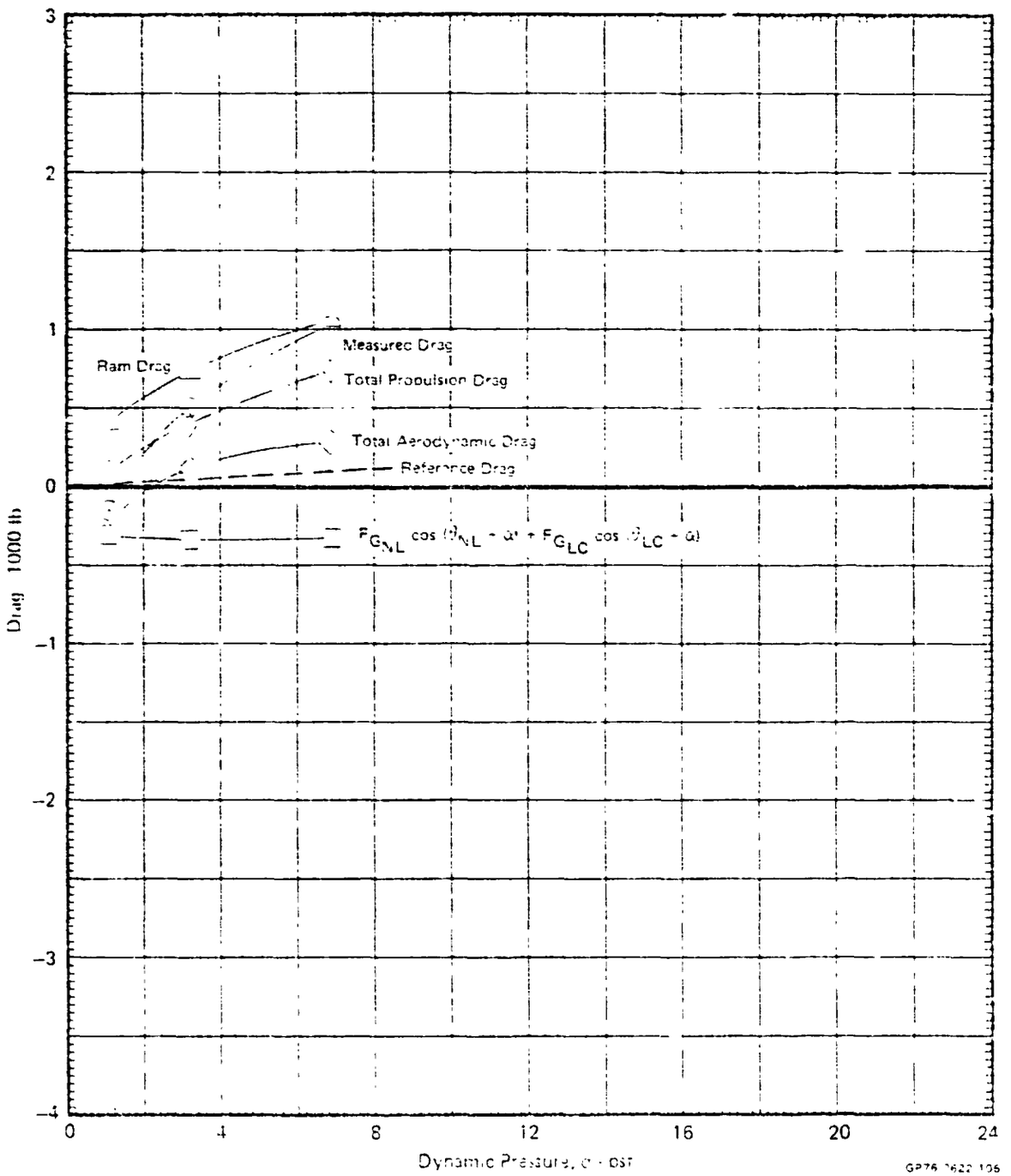

FIGURE 8.3-27
LIFT vs DYNAMIC PRESSURE
$\delta_H = 0^o$ $\alpha = 8^o$ $\delta_{LC} = 90^o$ $\delta_{NL} = 90^o$ $\theta_J = 84.7^o$
Graphical Summary of Measured and Calculated Force Data
$\delta_f = 15^o$ $\delta_a = 10^o/10^o$ Nose Gear On
$N_F/\sqrt{T_o} = 3600$ RPM

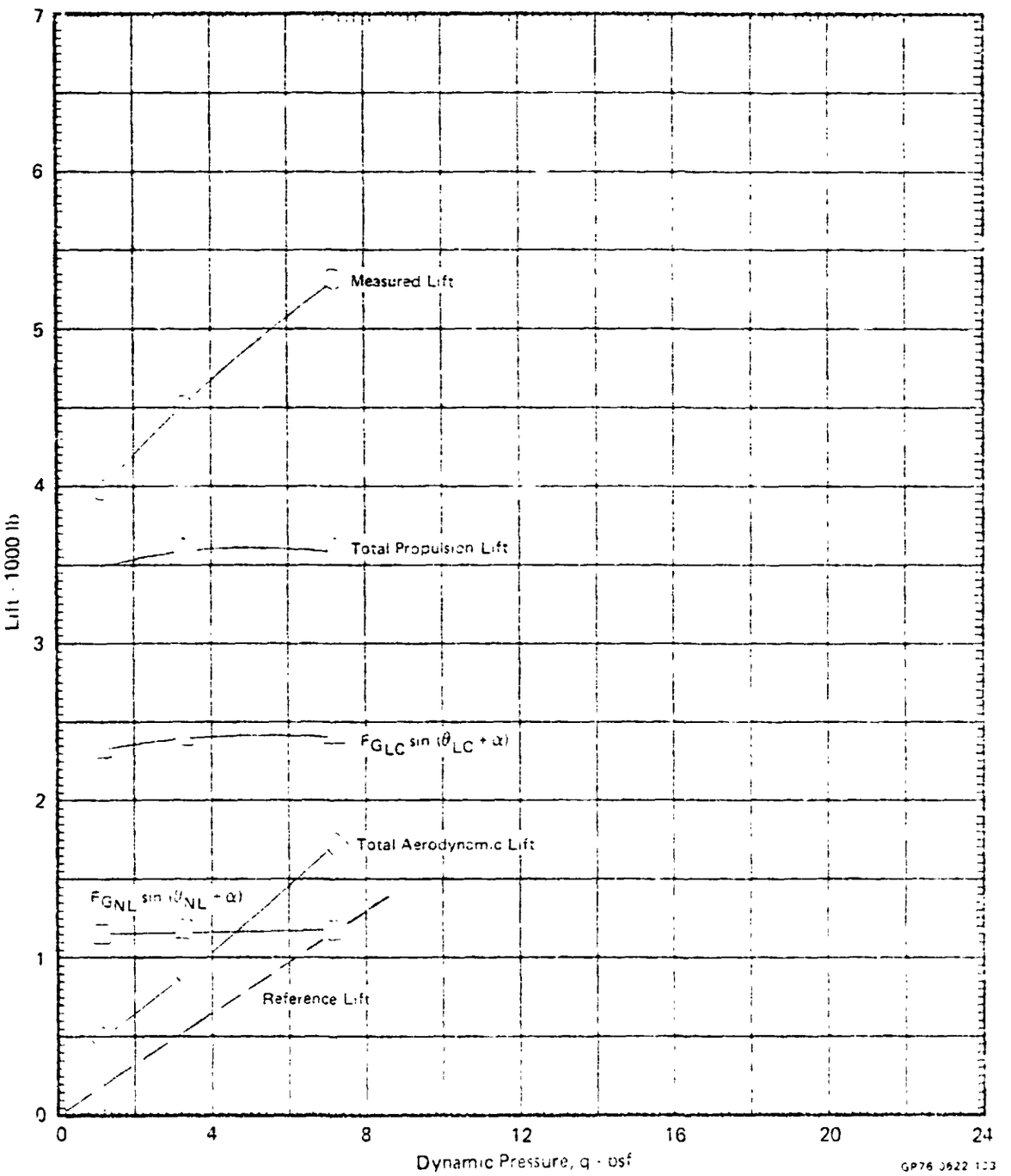

FIGURE 8.3-28
DRAG vs DYNAMIC PRESSURE
$\delta_H = 0^o$ $\alpha = 8^o$ $\delta_{LC} = 90^o$ $\delta_{NL} = 90^o$ $\theta_J = 84.7^o$
Graphical Summary of Measured and Calculated Force Data
$\delta_f = 15^o$ $\delta_a = 10^o/10^o$ Nose Gear On
$N_F/\sqrt{\theta_{T_o}} = 3600$ RPM

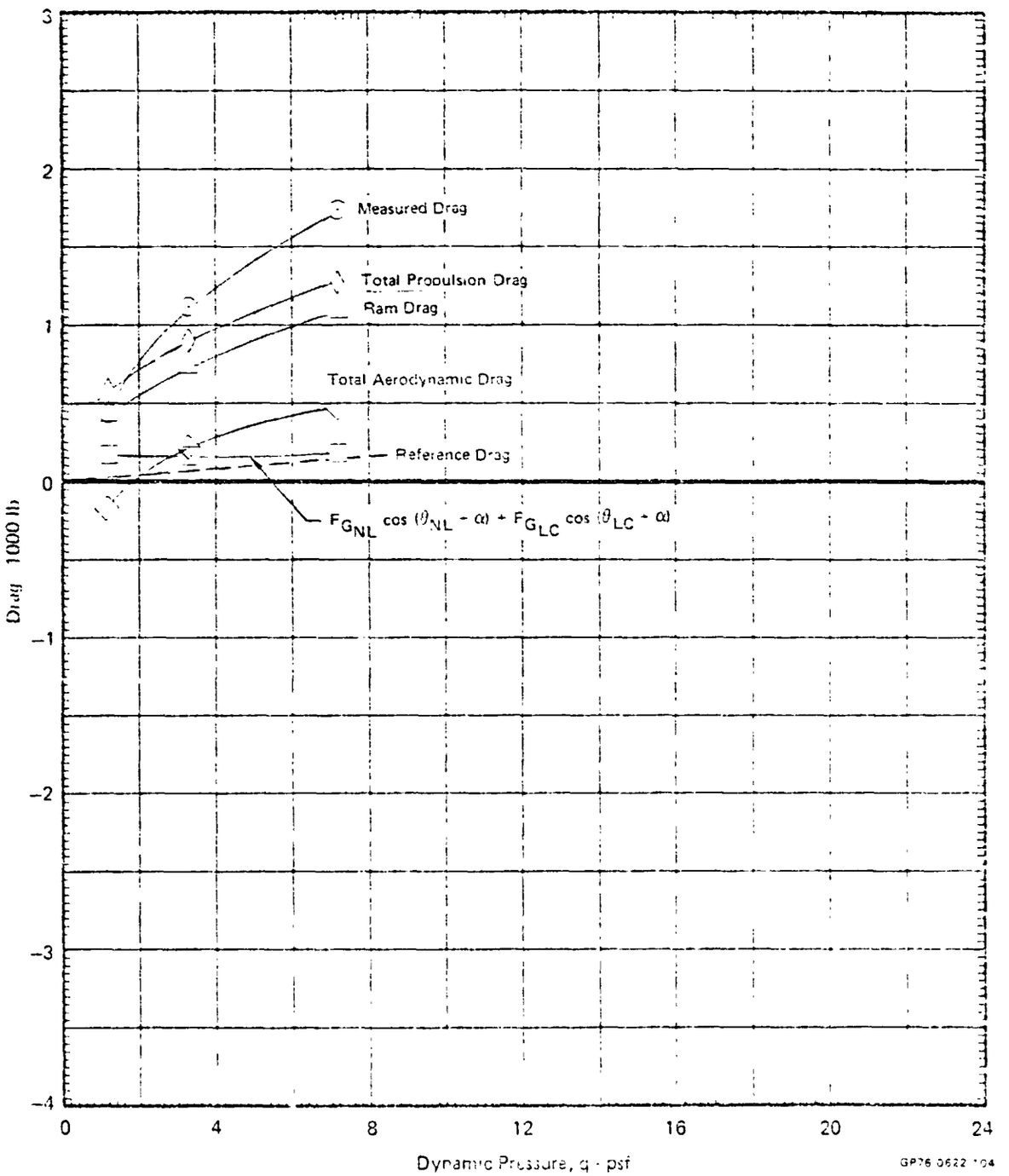

FIGURE 8.3-29
LIFT vs DYNAMIC PRESSURE
$\delta_H = 0^o$ $\alpha = 16^o$ $\delta_{LC} = 90^o$ $\delta_{NL} = 90^o$ $\theta_J = 84.7^o$
Graphical Summary of Measured and Calculated Force Data
$\delta_f = 15^o$ $\delta_a = 10^o/10^o$ Nose Gear On
$N_F/\sqrt{\theta T_o} = 3600$ RPM

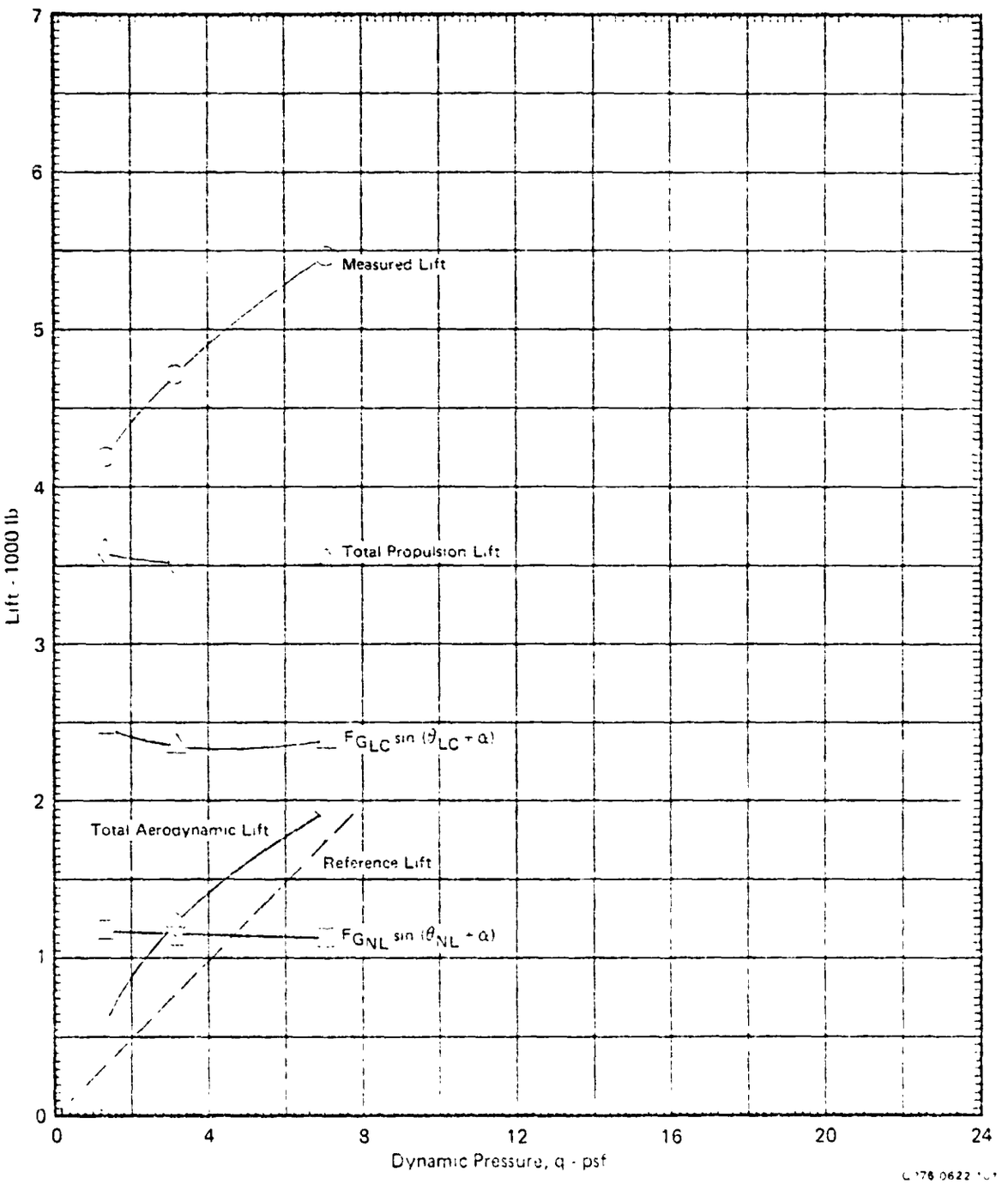

FIGURE 8.3-30

DRAG vs DYNAMIC PRESSURE

$\delta_H = 0^o$ $\alpha = 16^o$ $\delta_{LC} = 90^o$ $\delta_{NL} = 90^o$ $\theta_J = 84.7^o$

Graphical Summary of Measured and Calculated Force Data

$\delta_f = 15^o$ $\delta_a = 10^o/10^o$ Nose Gear On

$N_F/\sqrt{\theta_{T_o}} = 3600$ RPM

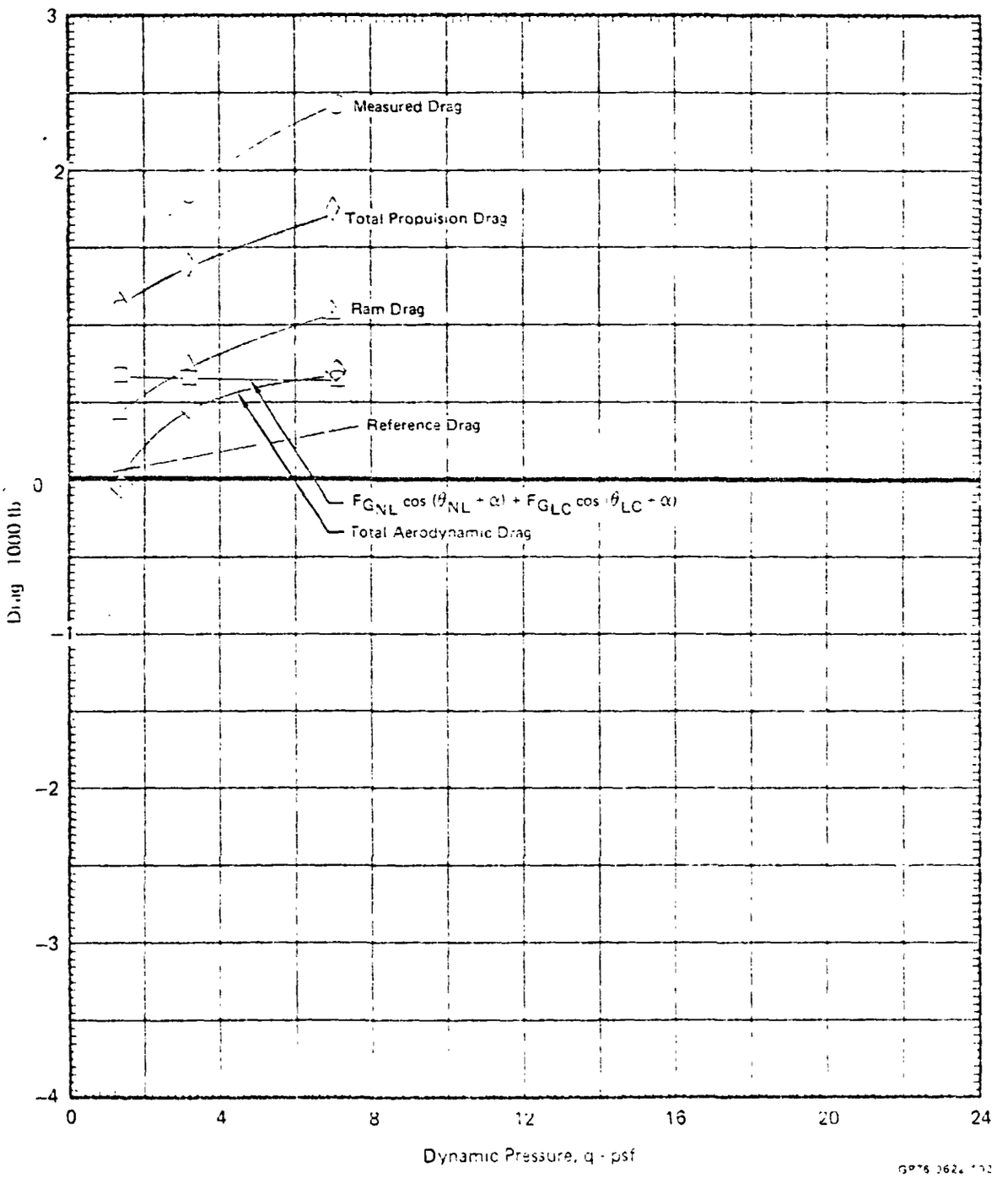

FIGURE 8.3-31

INDUCED LIFT AND DRAG PARAMETERS vs JET VELOCITY RATIO

$\delta_H = 0^o$ $\delta_{LC} = 23^o$ $\delta_{NL} = 43^o$ $\phi_J = 20.1^o$

$\delta_f = 15^o$ $\delta_a = 10^o/10^o$ Nose Gear On

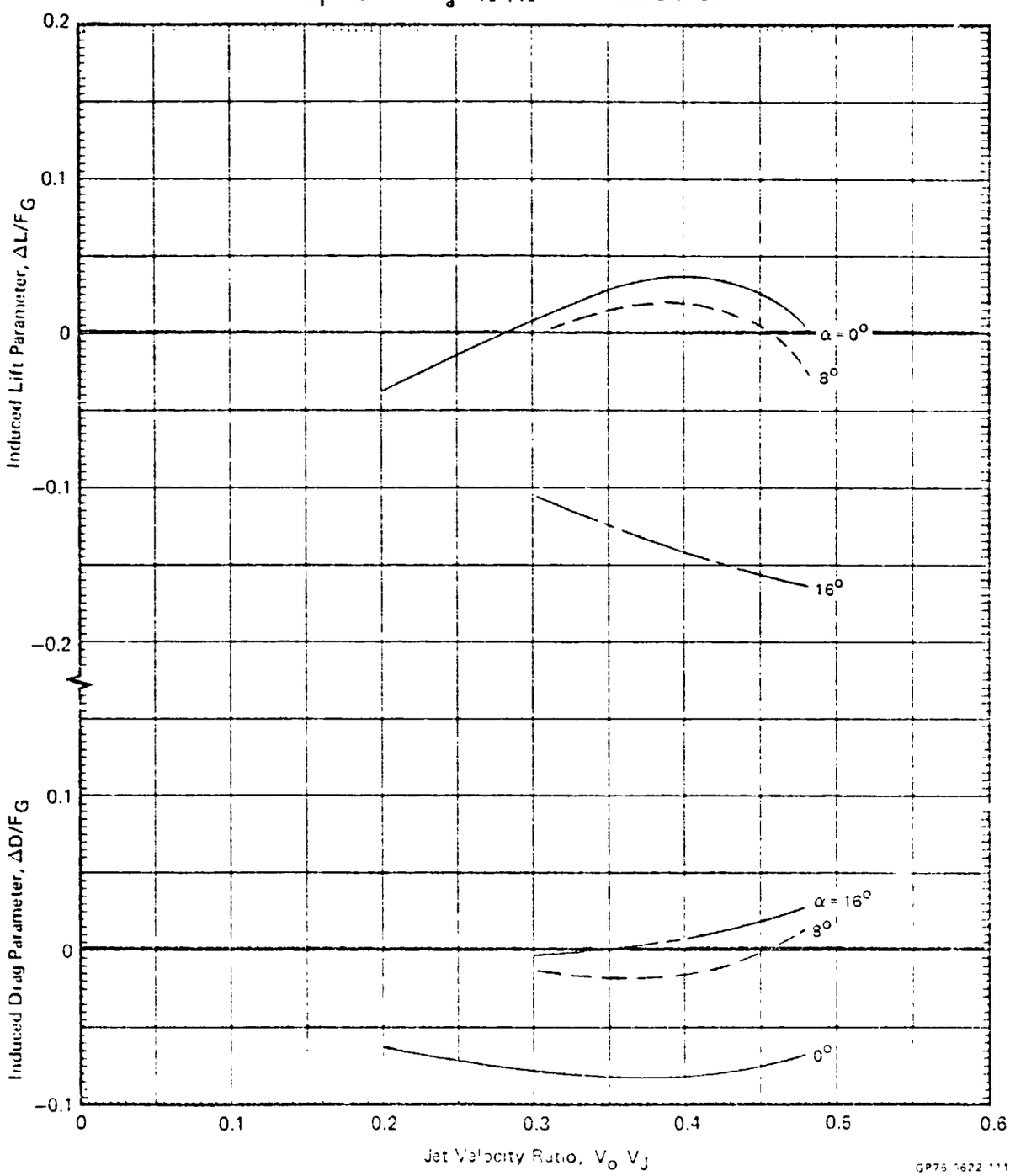

FIGURE 3.3-32

INDUCED LIFT AND DRAG PARAMETERS vs JET VELOCITY RATIO

$\delta_H = 0^o$ $\delta_{LC} = 38^o$ $\delta_{NL} = 43^o$ $\vartheta_J = 29.2^o$

$\delta_f = 15^o$ $\delta_a = 10^o/10^o$ Nose Gear On

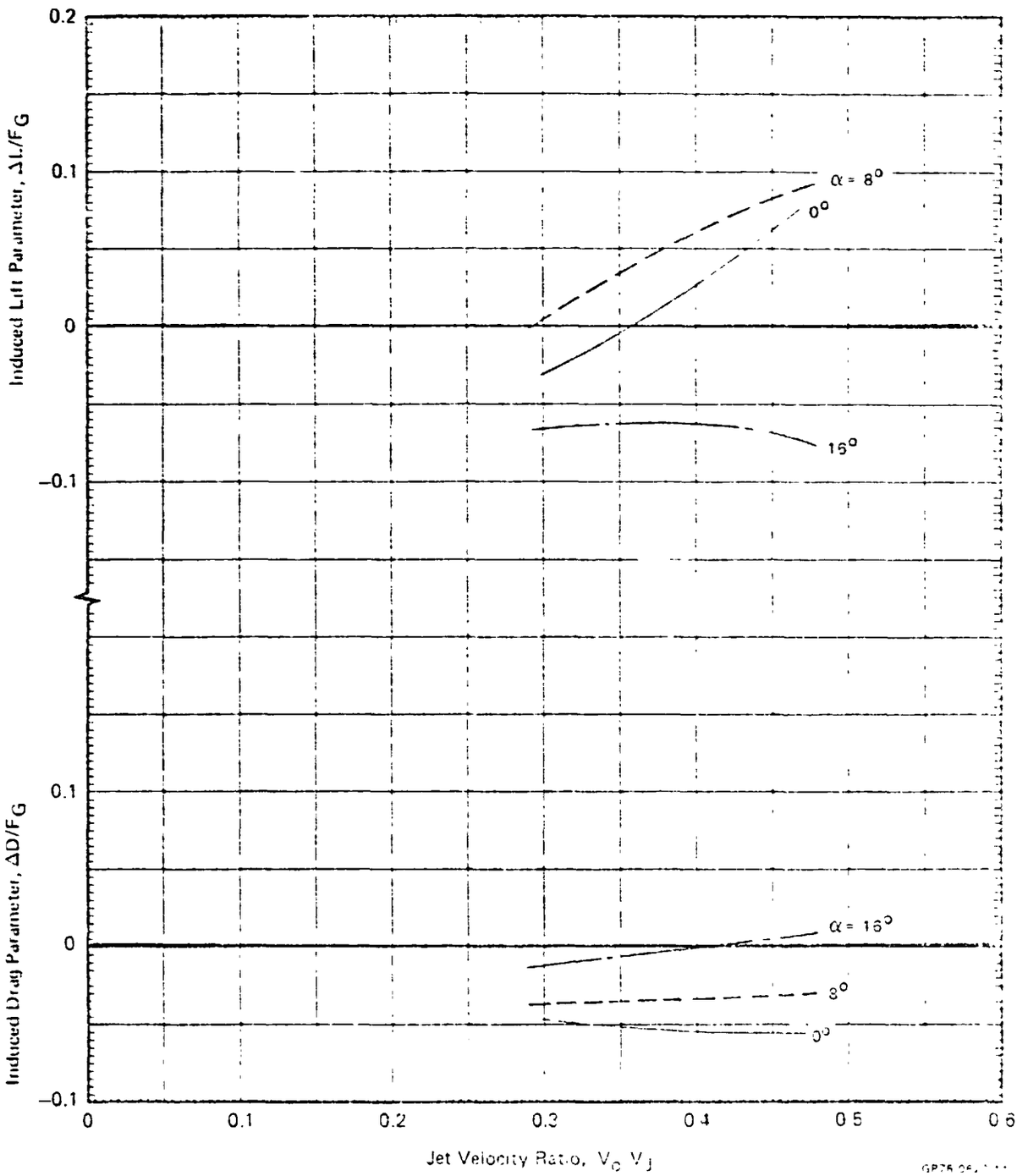

FIGURE 8.3-33

INDUCED LIFT AND DRAG PARAMETERS vs JET VELOCITY RATIO

$\delta_H = 0^o$ $\delta_{LC} = 56^o$ $\delta_{NL} = 43^o$ $\vartheta_J = 44.5^o$

$\delta_f = 15^o$ $\delta_a = 10^o/10^o$ Nose Gear On

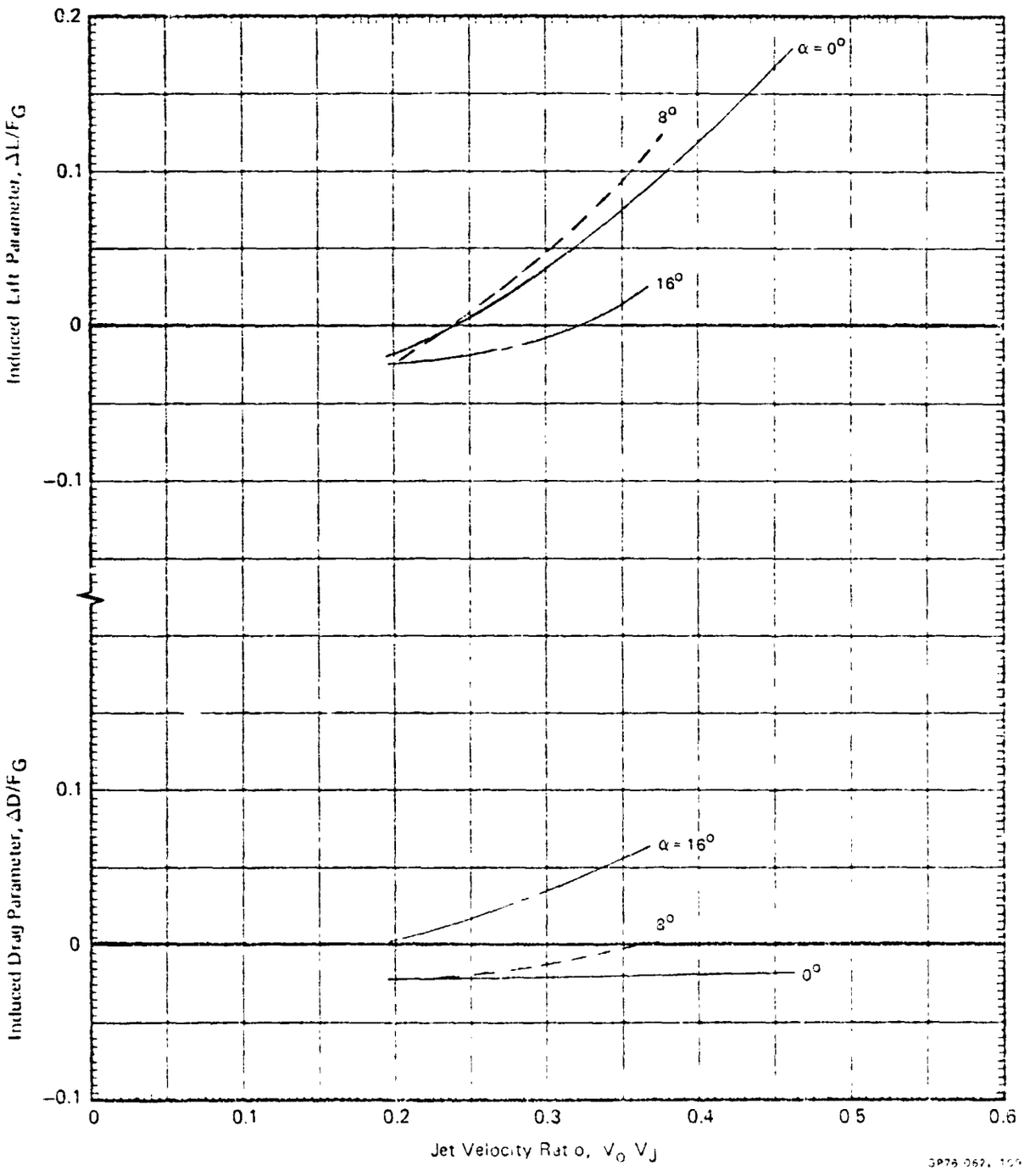

FIGURE 8.3-34
INDUCED LIFT AND DRAG PARAMETERS vs JET VELOCITY RATIO
$\delta_H = 0^o$ $\delta_{LC} = 71^o$ $\delta_{NL} = 55^o$ $\delta_J = 59.8^o$
$\delta_f = 15^o$ $\delta_a = 10^o/10^o$ Nose Gear On

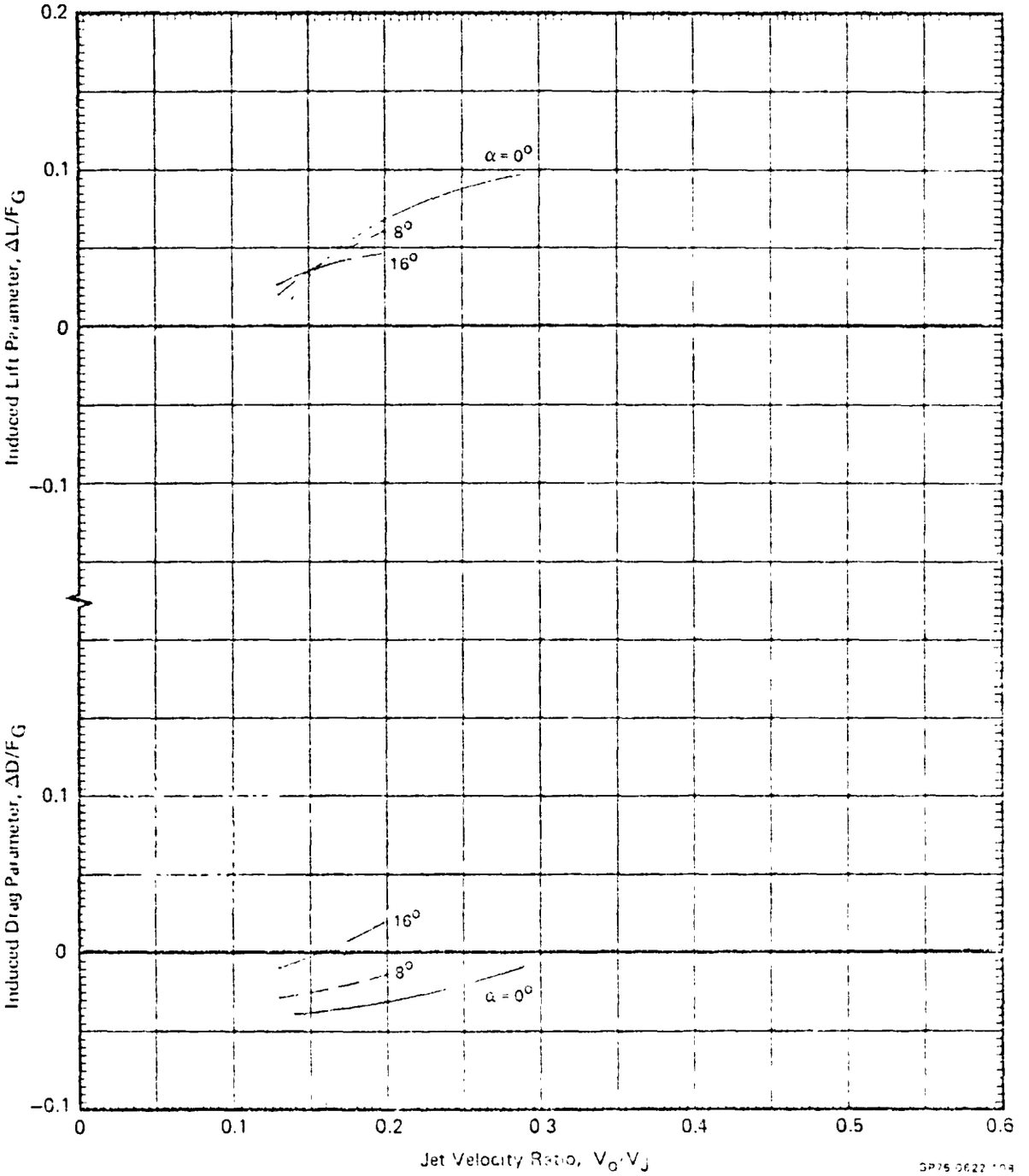

FIGURE 8.3-35
INDUCED LIFT AND DRAG PARAMETERS vs JET VELOCITY RATIO
$\delta_H = 0^o$ $\delta_{LC} = 90^o$ $\delta_{NL} = 90^o$ $\vartheta_J = 84.7^o$
$\delta_f = 15^o$ $\delta_a = 10^o/10^o$ Nose Gear On

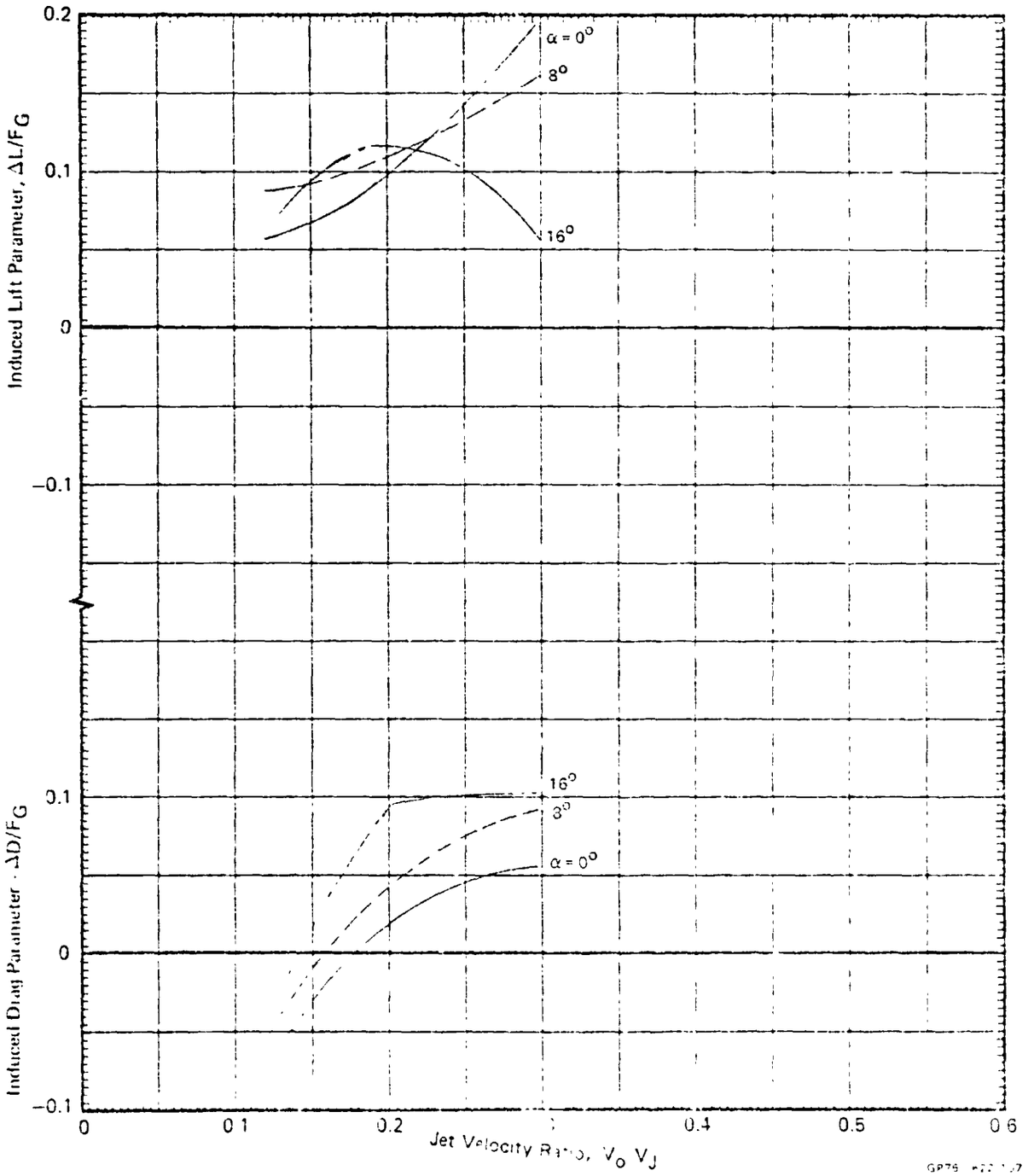

FIGURE 8.3-36
SUMMARY OF PROPULSION INDUCED EFFECTS AT 0° ANGLE OF ATTACK
THREE FAN OPERATION, HORIZONTAL TAIL ON
$\delta_H = 0°$ $\delta_f = 15°$ $\delta_a = 10°/10°$ Nose Gear On

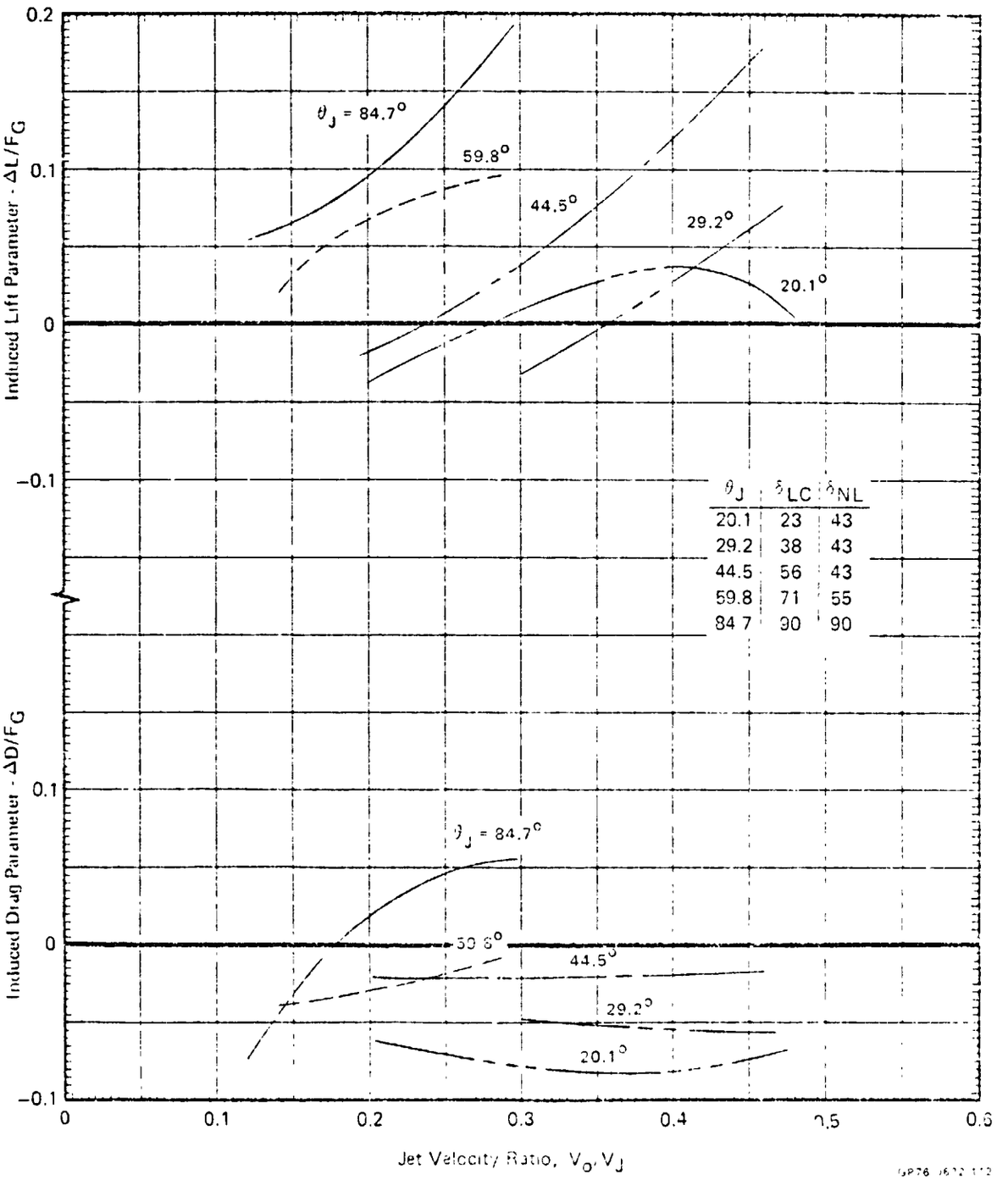

FIGURE 8.3-37

LIFT vs DYNAMIC PRESSURE, HORIZONTAL TAIL OFF

$\alpha = 0^o$ $\delta_{LC} = 23^o$ $\delta_{NL} = 43^o$ $\theta_J = 20.1^o$

Graphical Summary of Measured and Calculated Force Data

$\delta_f = 15^o$ $\delta_a = 10^o/10^o$ Nose Gear On

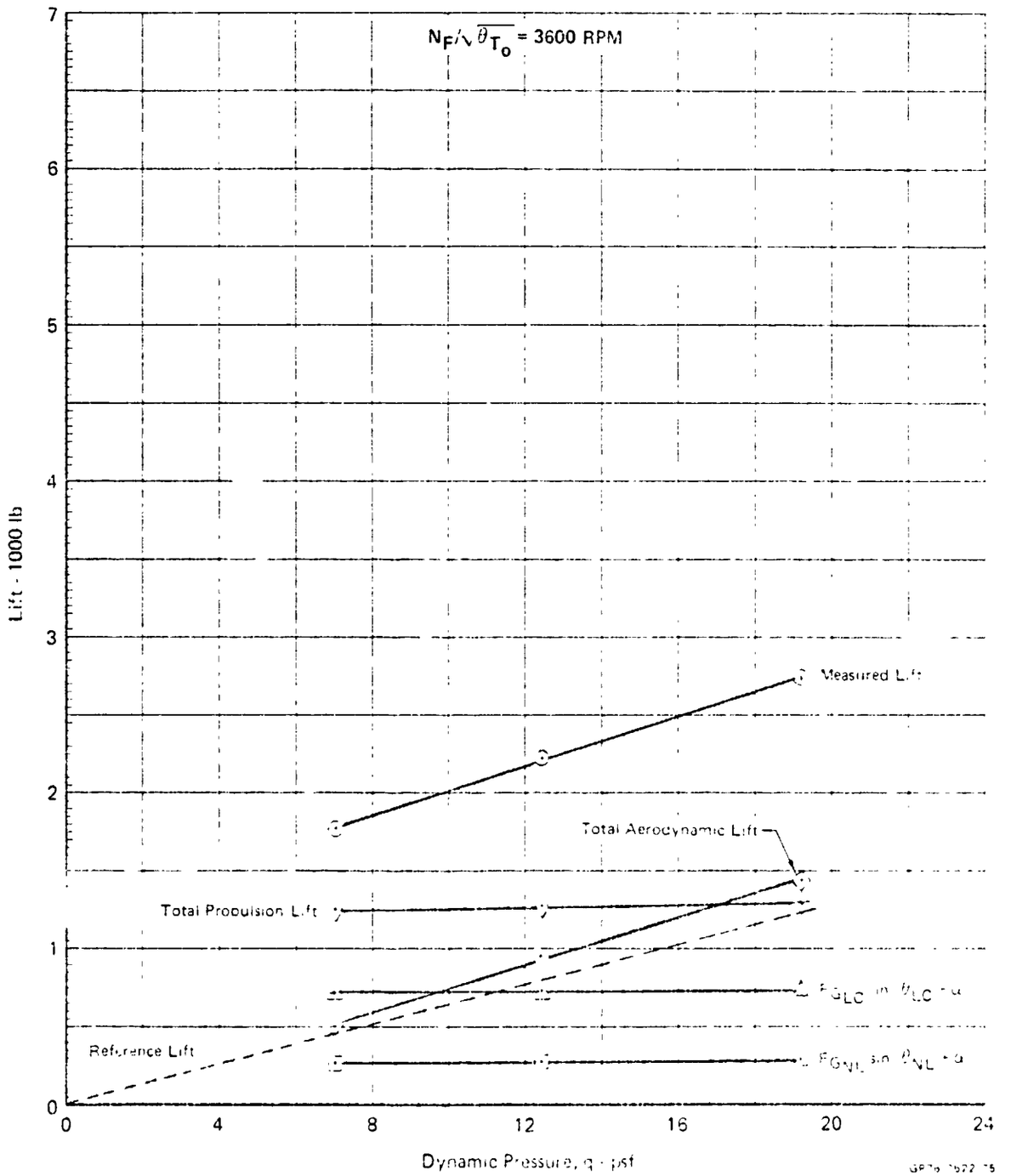

FIGURE 8.3-38
DRAG vs DYNAMIC PRESSURE, HORIZONTAL TAIL OFF
$\alpha = 0^o$ $\delta_{LC} = 23^o$ $\delta_{NL} = 43^o$ $\theta_J = 20.1^o$
Graphical Summary of Measured and Calculated Force Data
$\delta_f = 15^o$ $\delta_a = 10^o/10^o$ Nose Gear On
$N_F/\sqrt{\theta_{T_o}} = 3600$ RPM

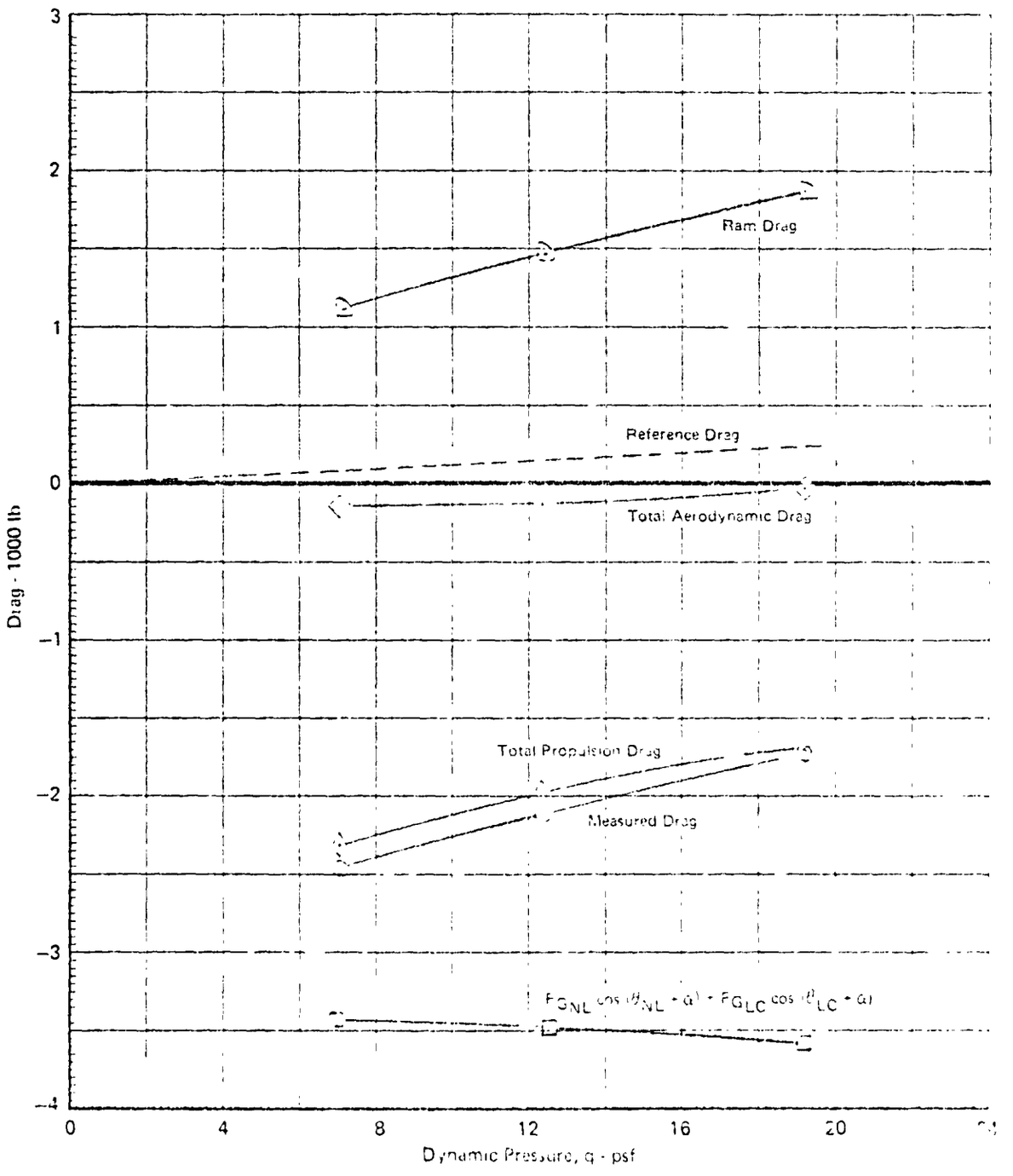

FIGURE 8.3-39
LIFT vs DYNAMIC PRESSURE, HORIZONTAL TA
$\alpha = 8^o$ $\delta_{LC} = 23^o$ $\delta_{NL} = 43^o$ $\theta_J = 20.$
Graphical Summary of Measured and Calculated Force Data
$\delta_f = 15^o$ $\delta_a = 10^o/10^o$ Nose Gear On
$N_F/\sqrt{\theta T_o} = 3600$ RPM

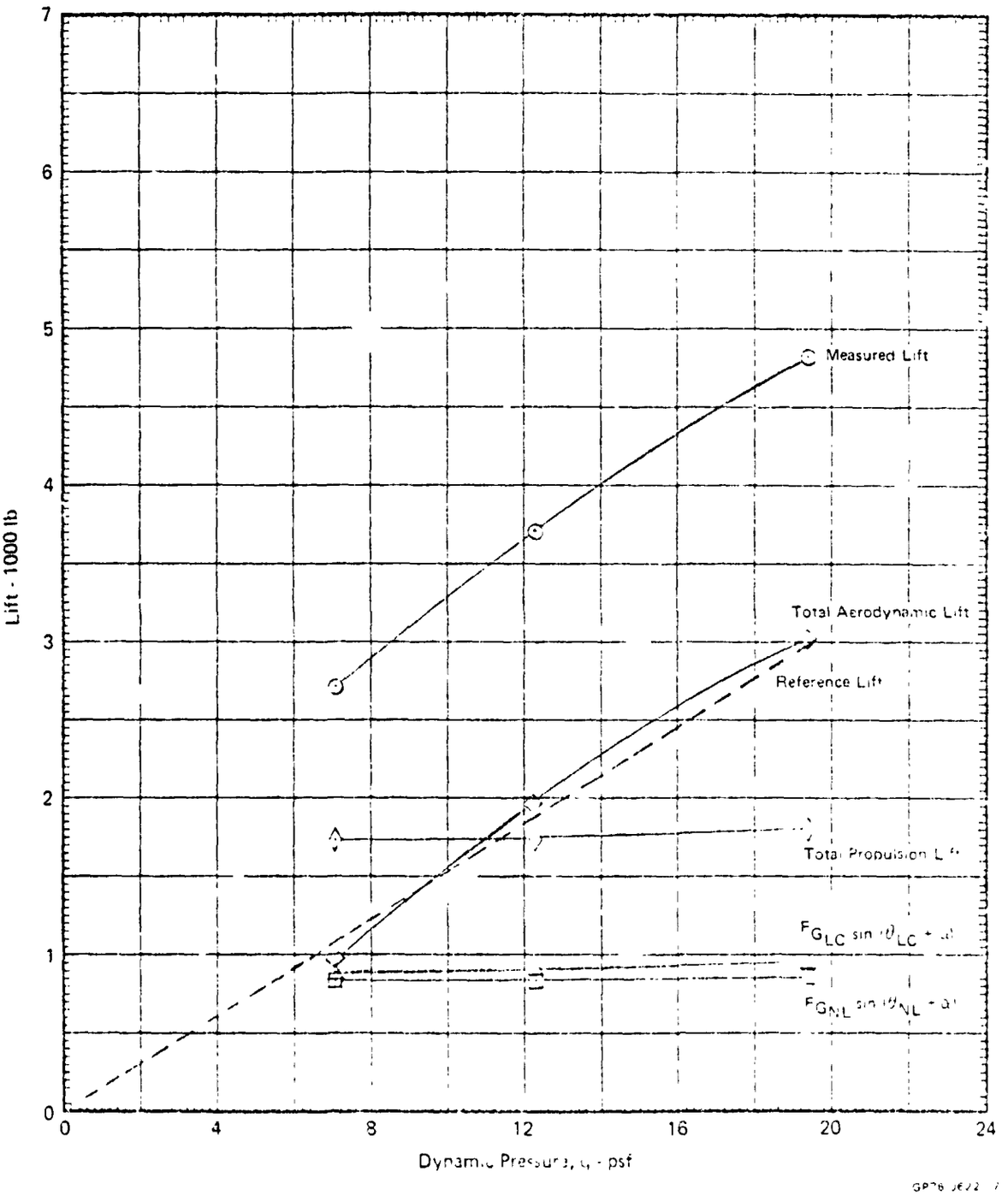

FIGURE 8.3-40
DRAG vs DYNAMIC PRESSURE, HORIZONTAL TAIL OFF
$\alpha = 8^o$ $\delta_{LC} = 23^o$ $\delta_{NL} = 43^o$ $\theta_J = 20.1^o$
Graphical Summary of Measured and Calculated Force Data
$\delta_f = 15^o$ $\delta_a = 10^o, 10^o$ Nose Gear On
$N_F/\sqrt{\vartheta_{T_o}} = 3600$ RPM

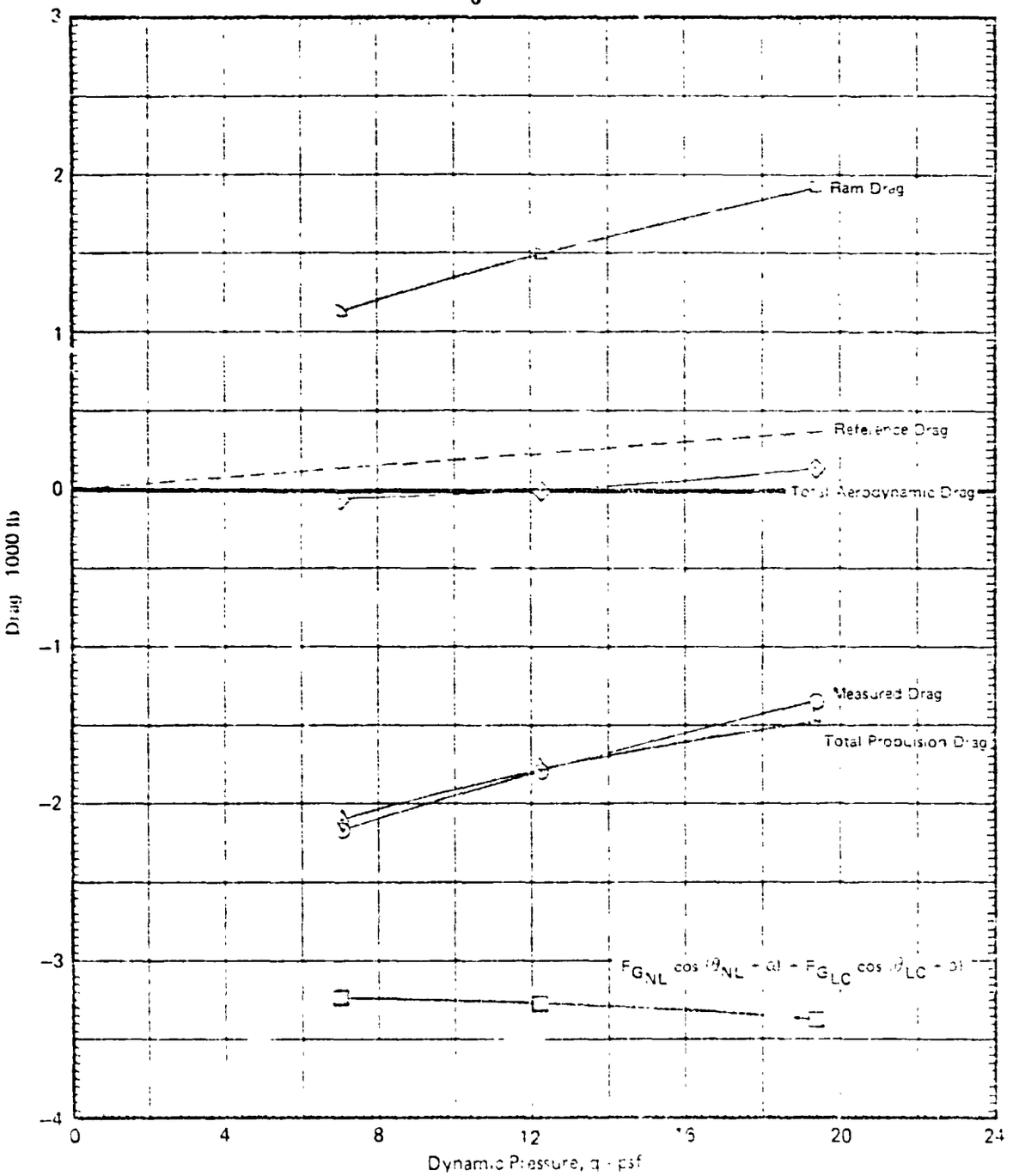

GP76 0622 78

FIGURE 8.3-41
LIFT vs DYNAMIC PRESSURE, HORIZONTAL TAIL OFF
$\alpha = 16^{o}$ $\delta_{LC} = 23^{o}$ $\delta_{NL} = 43^{o}$ $\vartheta_J = 20.1^{o}$
Graphical Summary of Measured and Calculated Force Data
$\delta_f = 15^{o}$ $\delta_a = 10^{o}/10^{o}$ Nose Gear On
$N_F/\sqrt{\vartheta T_o} = 3600$ RPM

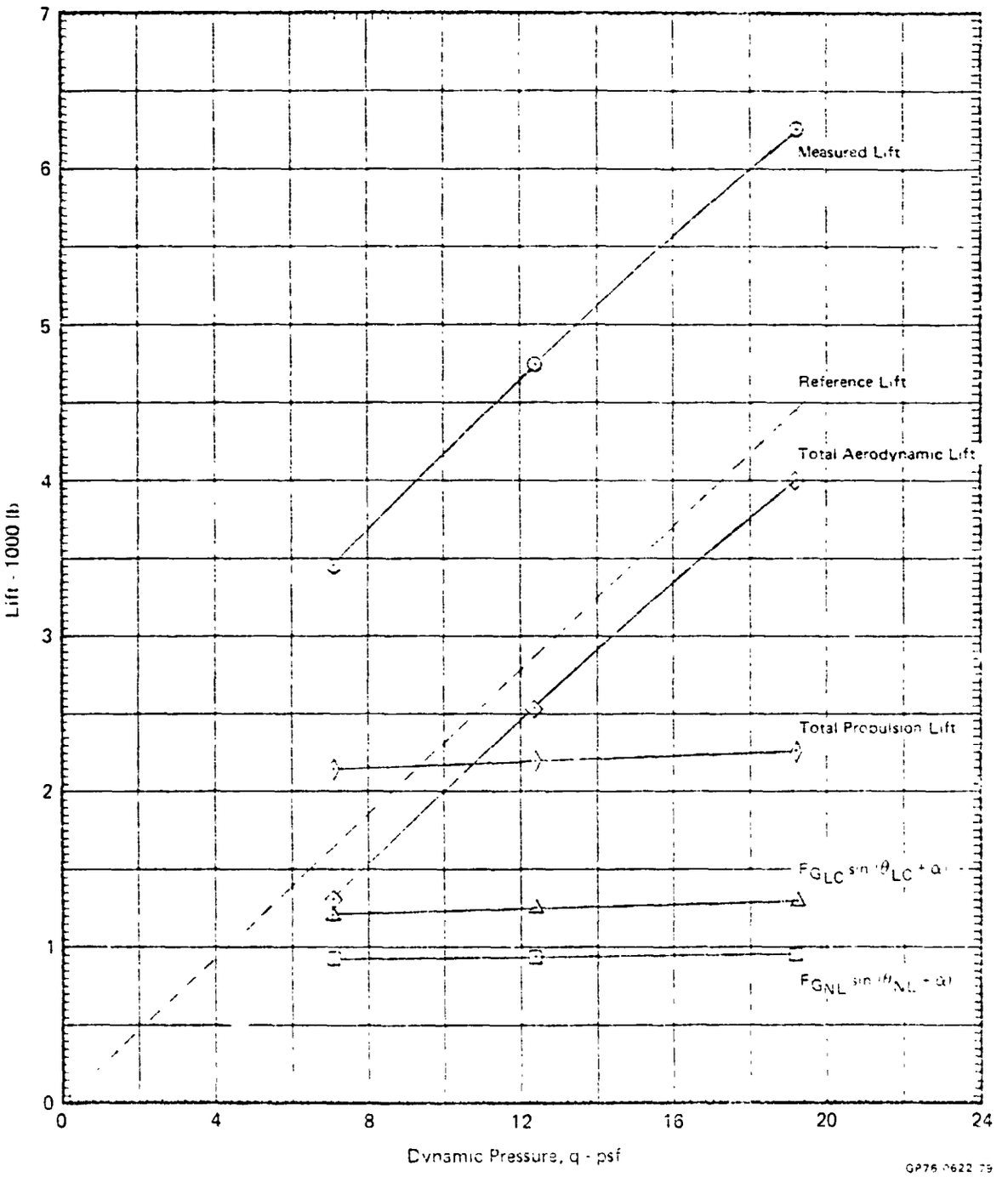

GP76-0622-79

FIGURE 8.3-42
DRAG vs DYNAMIC PRESSURE, HORIZONTAL TAIL OFF
$\alpha = 16^o$ $\delta_{LC} = 23^o$ $\delta_{NL} = 43^o$ $\theta_J = 20.1^o$
Graphical Summary of Measured and Calculated Force Data
$\delta_f = 15^o$ $\delta_a = 10^o/10^o$ Nose Gear On
$N_F/\sqrt{\theta_{T_o}} = 3600$ RPM

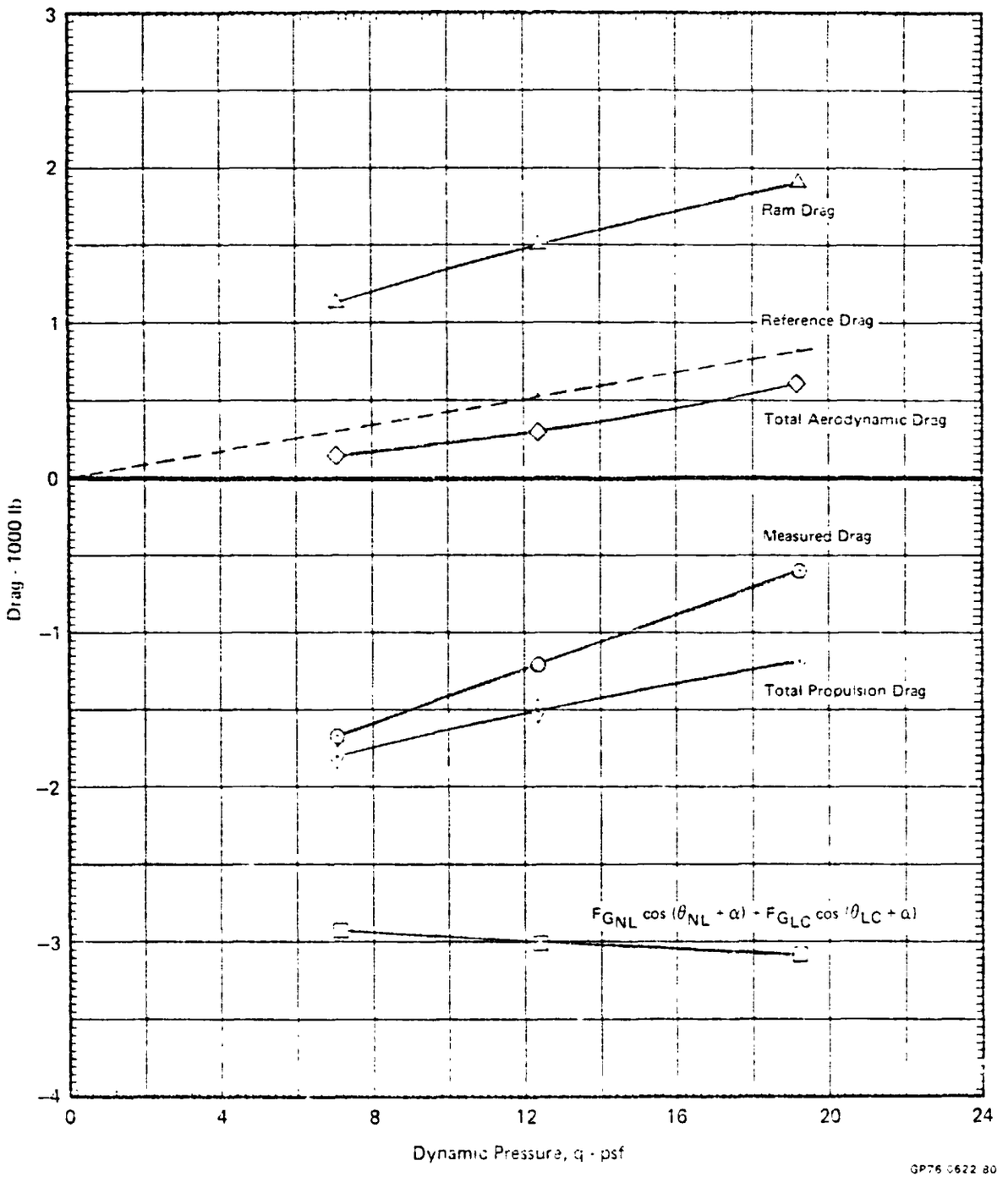

GP76 0622 80

FIGURE 8.3-43
LIFT vs DYNAMIC PRESSURE, HORIZONTAL TAIL OFF
$\alpha = 0^{o}$ $\delta_{LC} = 56^{o}$ $\delta_{NL} = 43^{o}$ $\theta_J = 44.5^{o}$
Graphical Summary of Measured and Calculated Force Data
$\delta_f = 15^{o}$ $\delta_a = 10^{o}/10^{o}$ Nose Gear On
$N_F/\sqrt{\theta_{T_0}} = 3600$ RPM

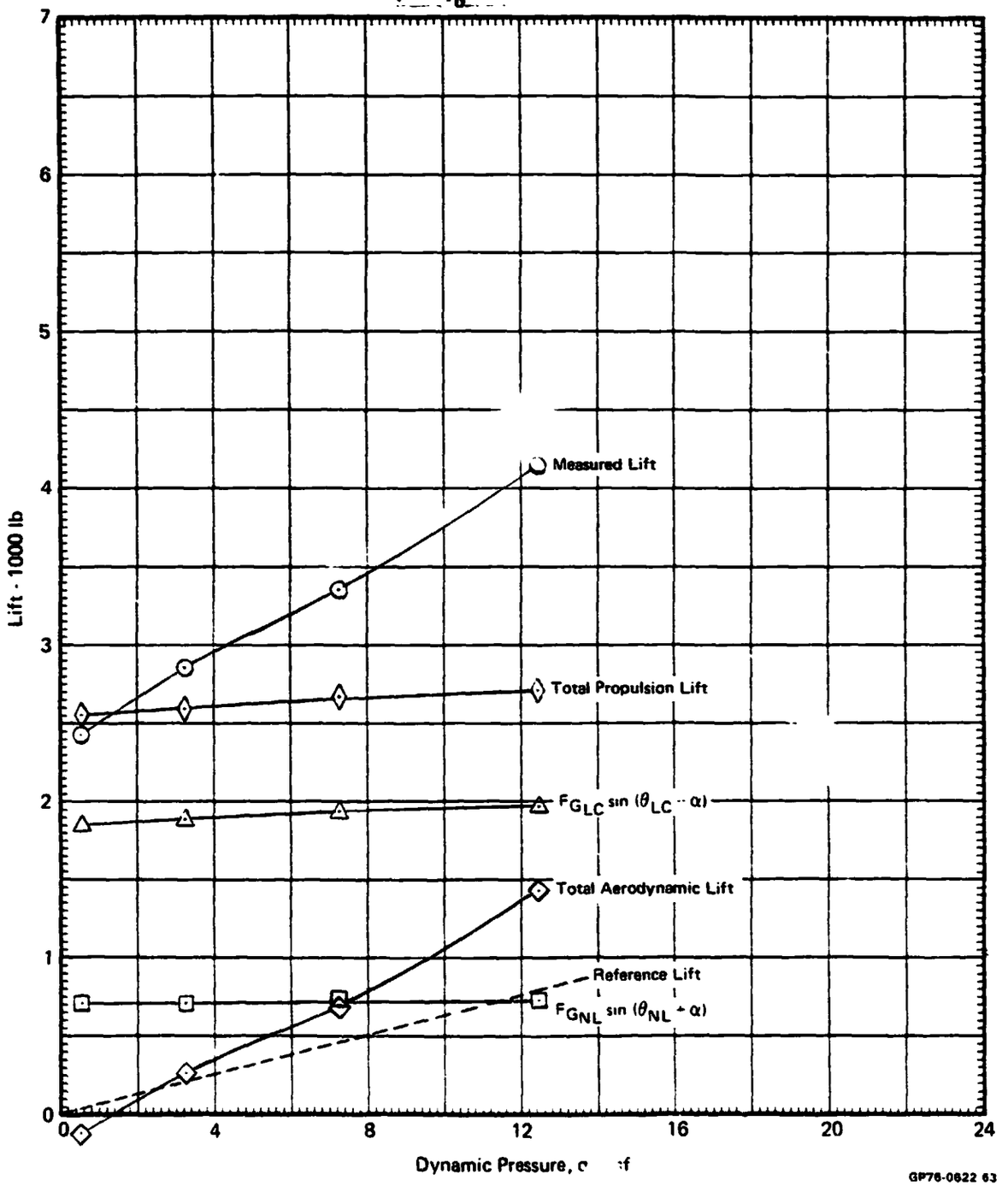

FIGURE 8.3-44
DRAG vs DYNAMIC PRESSURE, HORIZONTAL TAIL OFF
$\alpha = 0^o$ $\delta_{LC} = 56^o$ $\delta_{NL} = 43^o$ $\theta_J = 44.5^o$
Graphical Summary of Measured and Calculated Force Data
$\delta_f = 15^o$ $\delta_a = 10^o/10^o$ Nose Gear On

$N_F/\sqrt{\theta_{T_o}} = 3600$ RPM

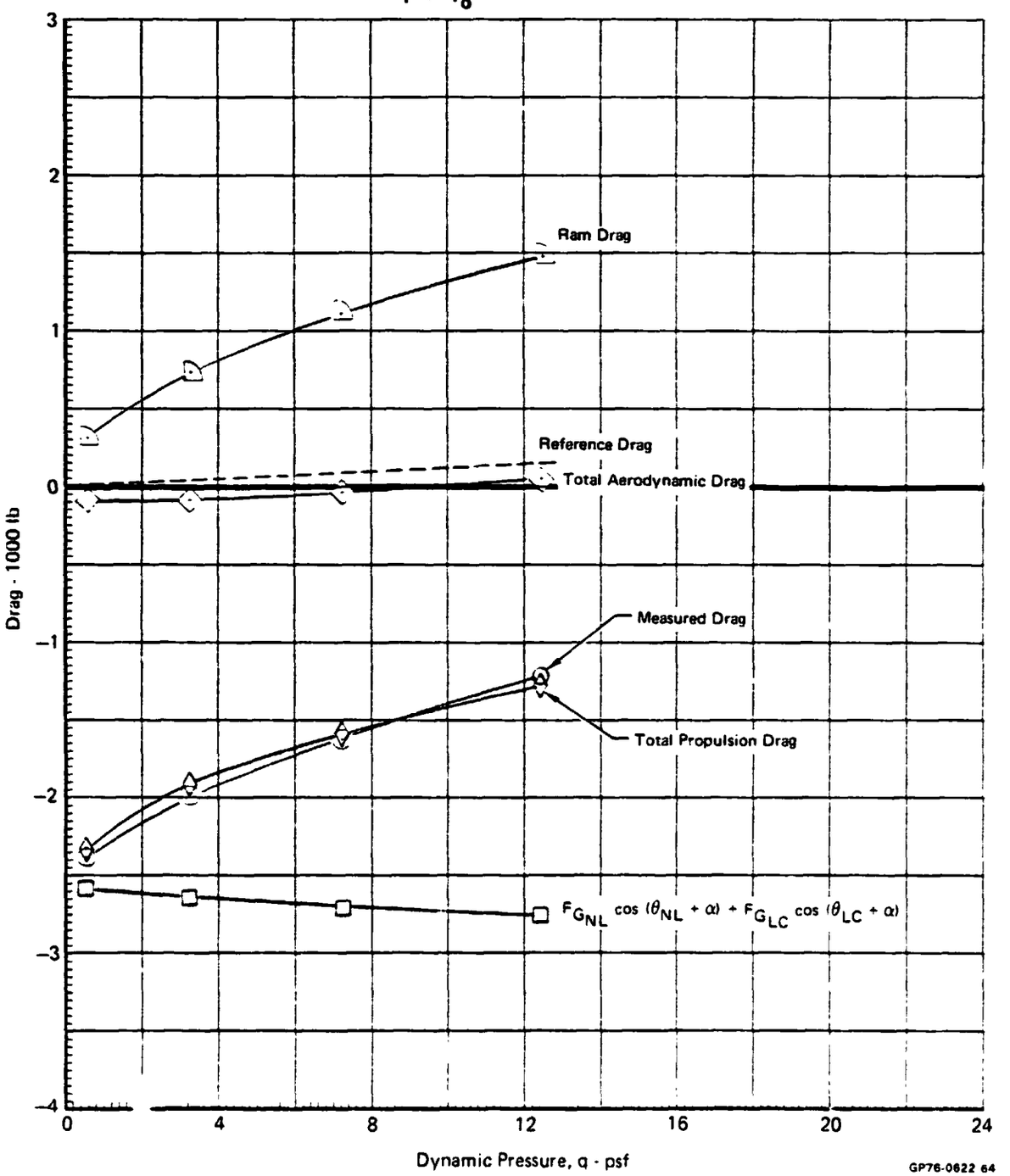

FIGURE 8.3-45
LIFT vs DYNAMIC PRESSURE, HORIZONTAL TAIL OFF
$\alpha = 8^o$ $\delta_{LC} = 56^o$ $\delta_{NL} = 43^o$ $\theta_J = 44.5^o$
Graphical Summary of Measured and Calculated Force Data
$\delta_f = 15^o$ $\delta_a = 10^o/10^o$ Nose Gear On
$N_F/\sqrt{\theta_{T_o}} = 3600$ RPM

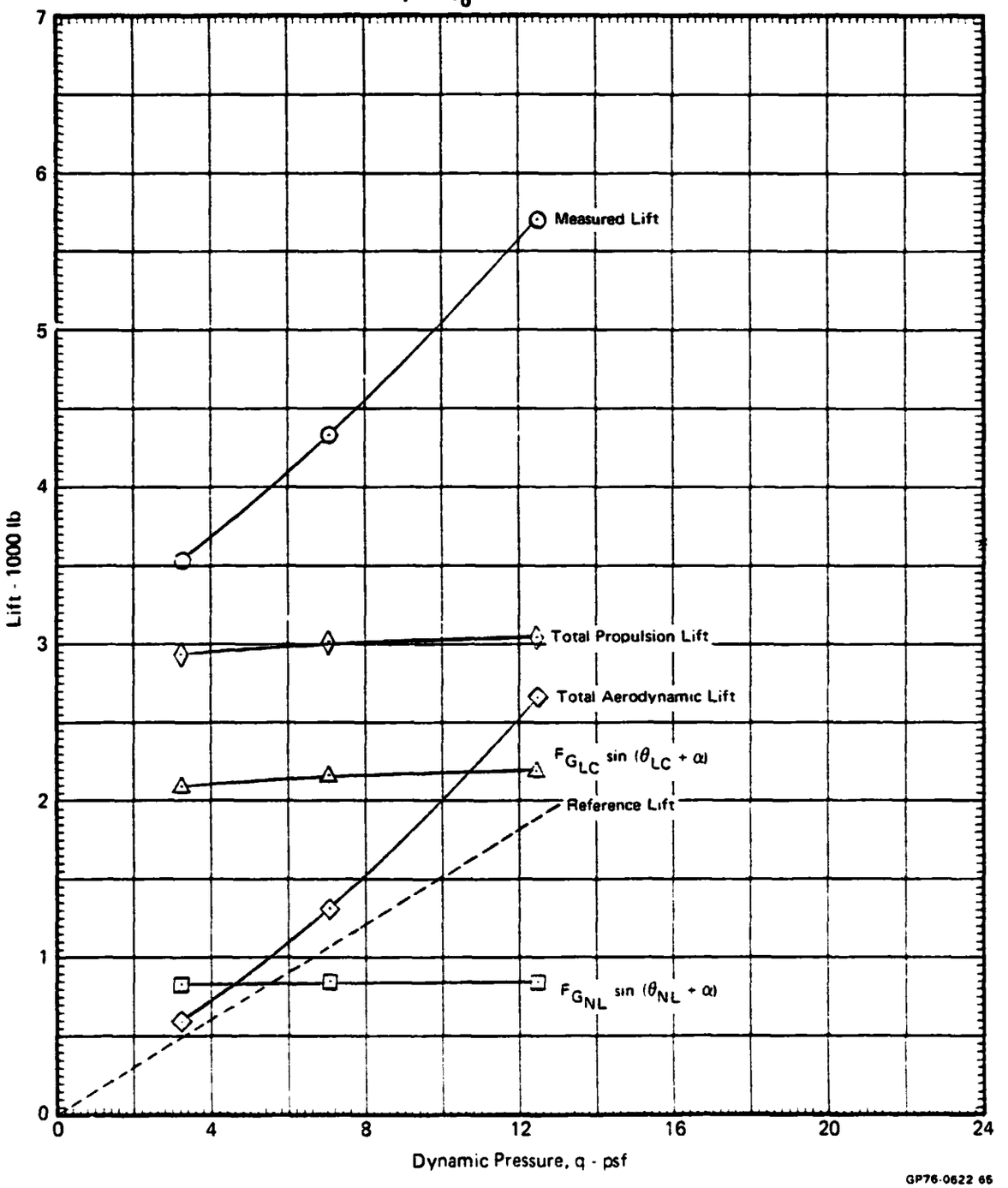

FIGURE 8.3-46

DRAG vs DYNAMIC PRESSURE, HORIZONTAL TAIL OFF

$\alpha = 8^{o}$ $\delta_{LC} = 56^{o}$ $\delta_{NL} = 43^{o}$ $\theta_J = 44.5^{o}$

Graphical Summary of Measured and Calculated Force Data

$\delta_f = 15^{o}$ $\delta_a = 10^{o}/10^{o}$ Nose Gear On

$N_F/\sqrt{\theta_{T_o}} = 3600$ RPM

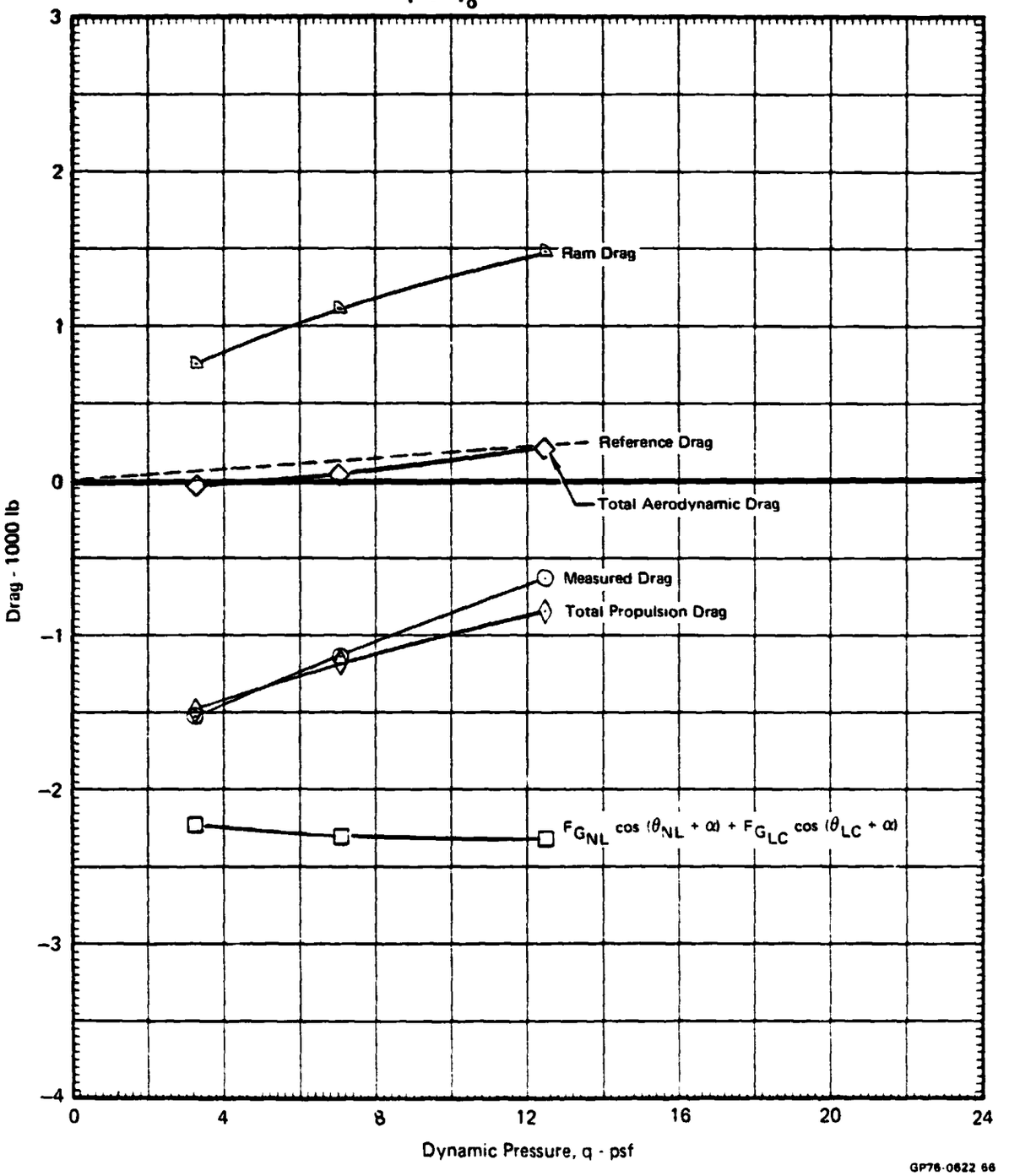

FIGURE 8.3-47
LIFT vs DYNAMIC PRESSURE, HORIZONTAL TAIL OFF
$\alpha = 16^{o}$ $\delta_{LC} = 56^{o}$ $\delta_{NL} = 43^{o}$ $\theta_J = 44.5^{o}$
Graphical Summary of Measured and Calculated Force Data
$\delta_f = 15^{o}$ $\delta_a = 10^{o}/10^{o}$ Nose Gear On
$N_F/\sqrt{\theta_{T_o}} = 3600$ RPM

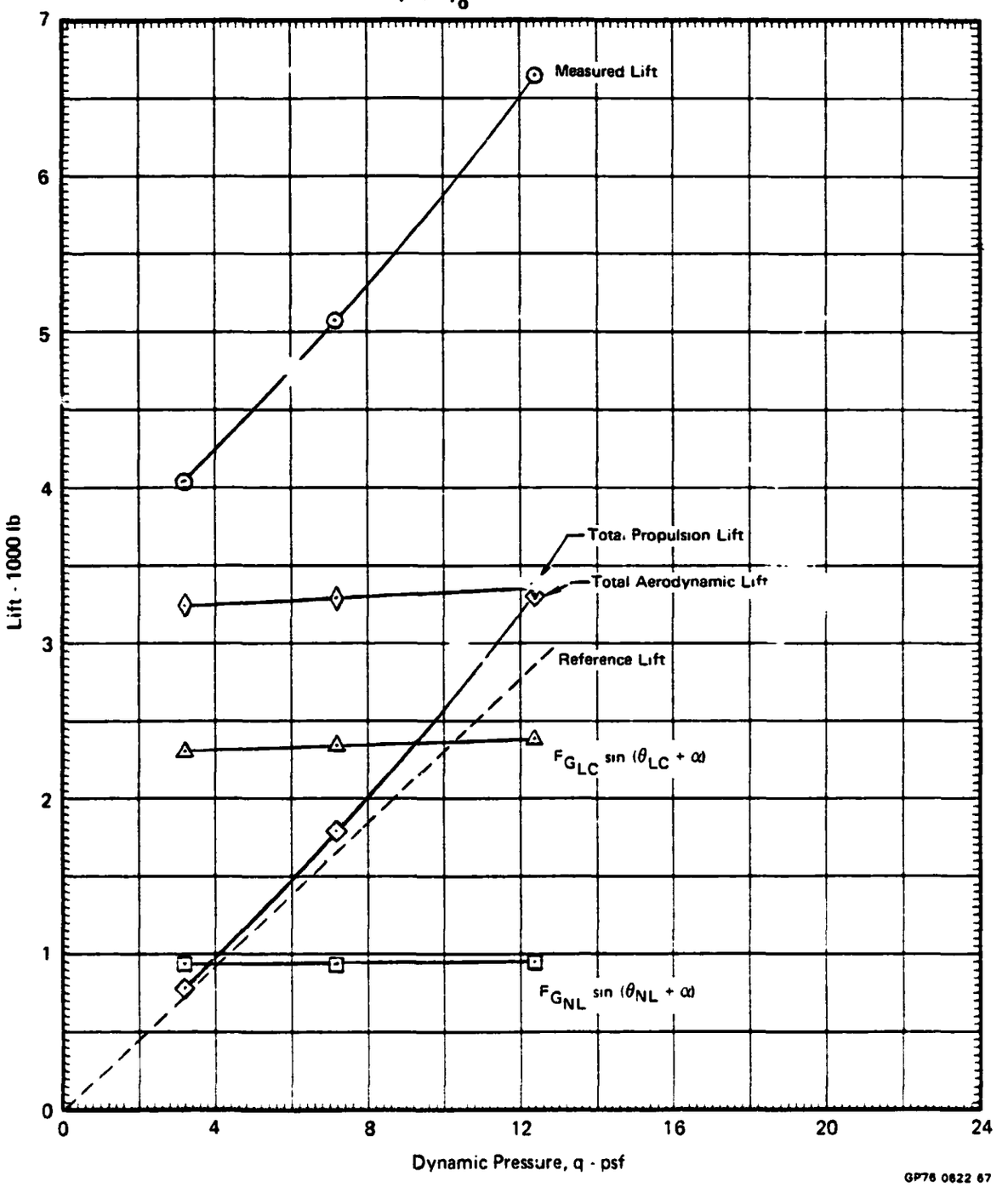

GP76 0622 67

FIGURE 8.3-48
DRAG vs DYNAMIC PRESSURE, HORIZONTAL TAIL OFF
$\alpha = 16^{o}$ $\delta_{LC} = 56^{o}$ $\delta_{NL} = 43^{o}$ $\theta_J = 44.5^{o}$
Graphical Summary of Measured and Calculated Force Data
$\delta_f = 15^{o}$ $\delta_a = 10^{o}/10^{o}$ Nose Gear On
$N_F/\sqrt{\theta_{T_o}} = 3600$ RPM

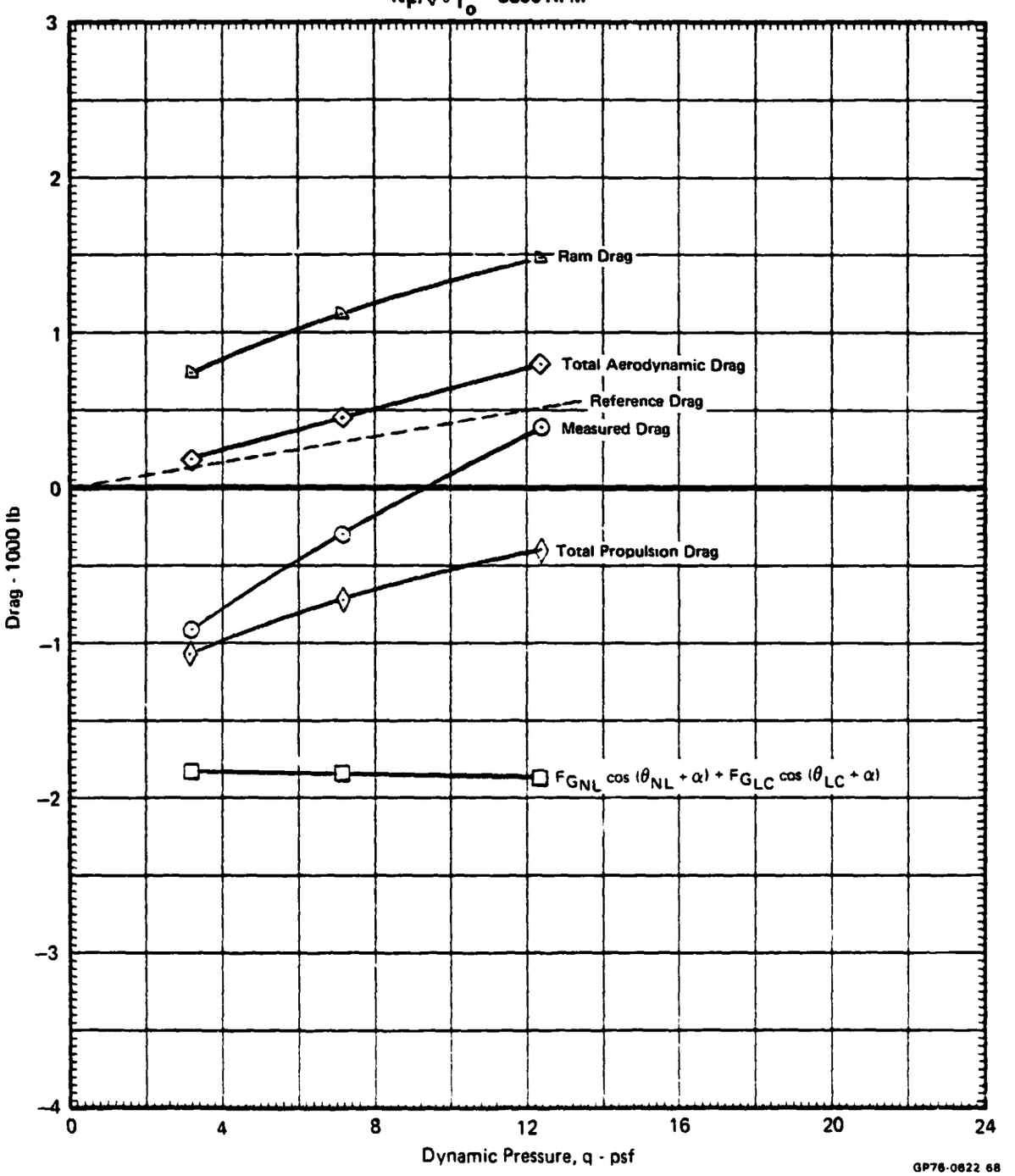

FIGURE 8.3-49

LIFT vs DYNAMIC PRESSURE, HORIZONTAL TAIL OFF

$\alpha = 0^o$ $\delta_{LC} = 90^o$ $\delta_{NL} = 90^o$ $\theta_J = 84.7^o$

Graphical Summary of Measured and Calculated Force Data

$\delta_f = 15^o$ $\delta_a = 10^o/10^o$ Nose Gear On

$N_F/\sqrt{\theta_{T_o}} = 3600$ RPM

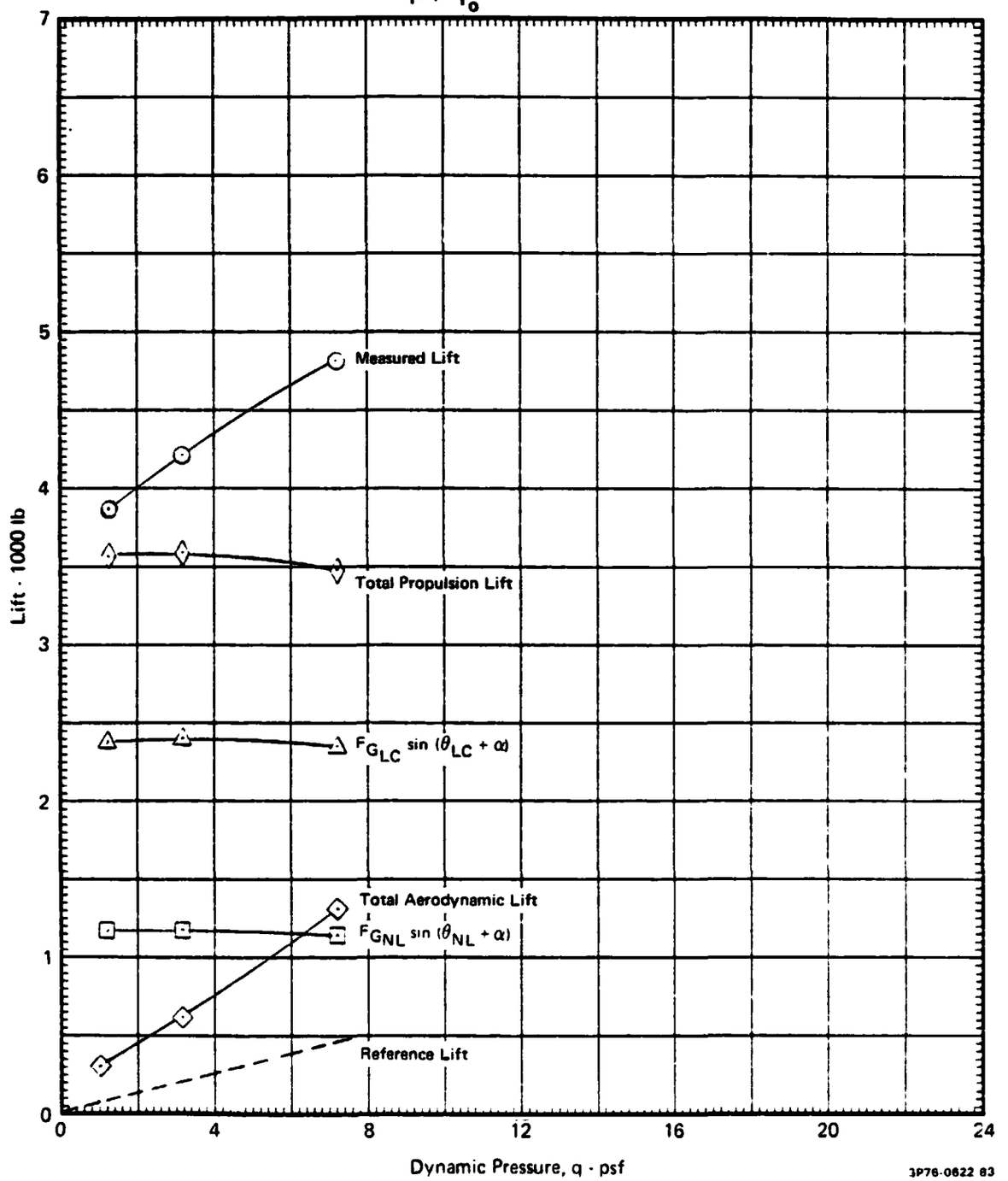

FIGURE 8.3-50

DRAG vs DYNAMIC PRESSURE, HORIZONTAL TAIL OFF
$\alpha = 0^o$ $\delta_{LC} = 90^o$ $\delta_{NL} = 90^o$ $\theta_J = 84.7^o$
Graphical Summary of Measured and Calculated Force Data
$\delta_f = 15^o$ $\delta_a = 10^o/10^o$ Nose Gear On
$N_F/\sqrt{\theta T_o} = 3600$ RPM

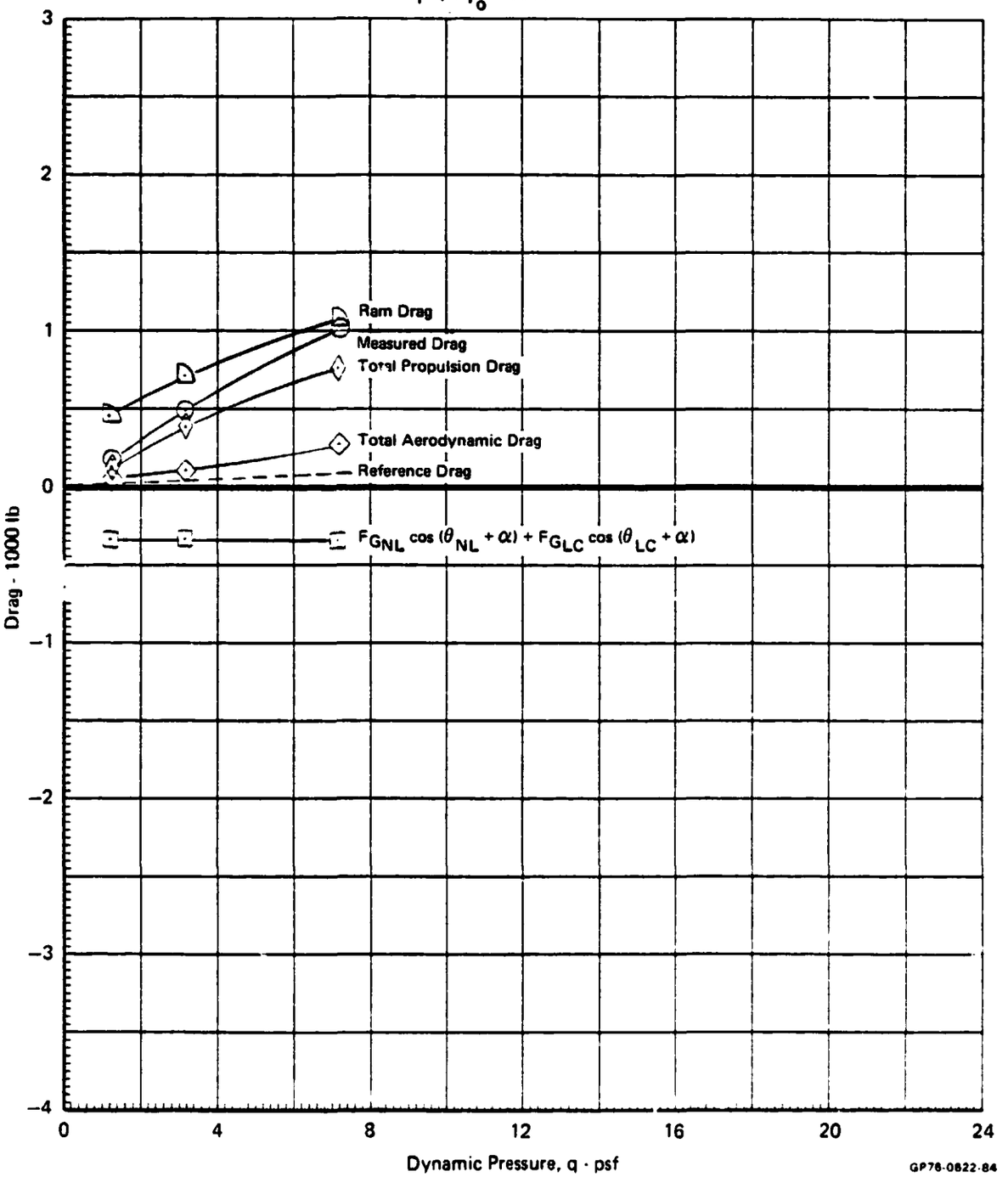

FIGURE 8.3-51

LIFT vs DYNAMIC PRESSURE, HORIZONTAL TAIL OFF

$\alpha = 8^0$ $\delta_{LC} = 90^0$ $\delta_{NL} = 90^0$ $\theta_J = 84.7^0$

Graphical Summary of Measured and Calculated Force Data

$\delta_f = 15^0$ $\delta_a = 10^0/10^0$ Nose Gear On

$N_F/\sqrt{\theta T_o} = 3600$ RPM

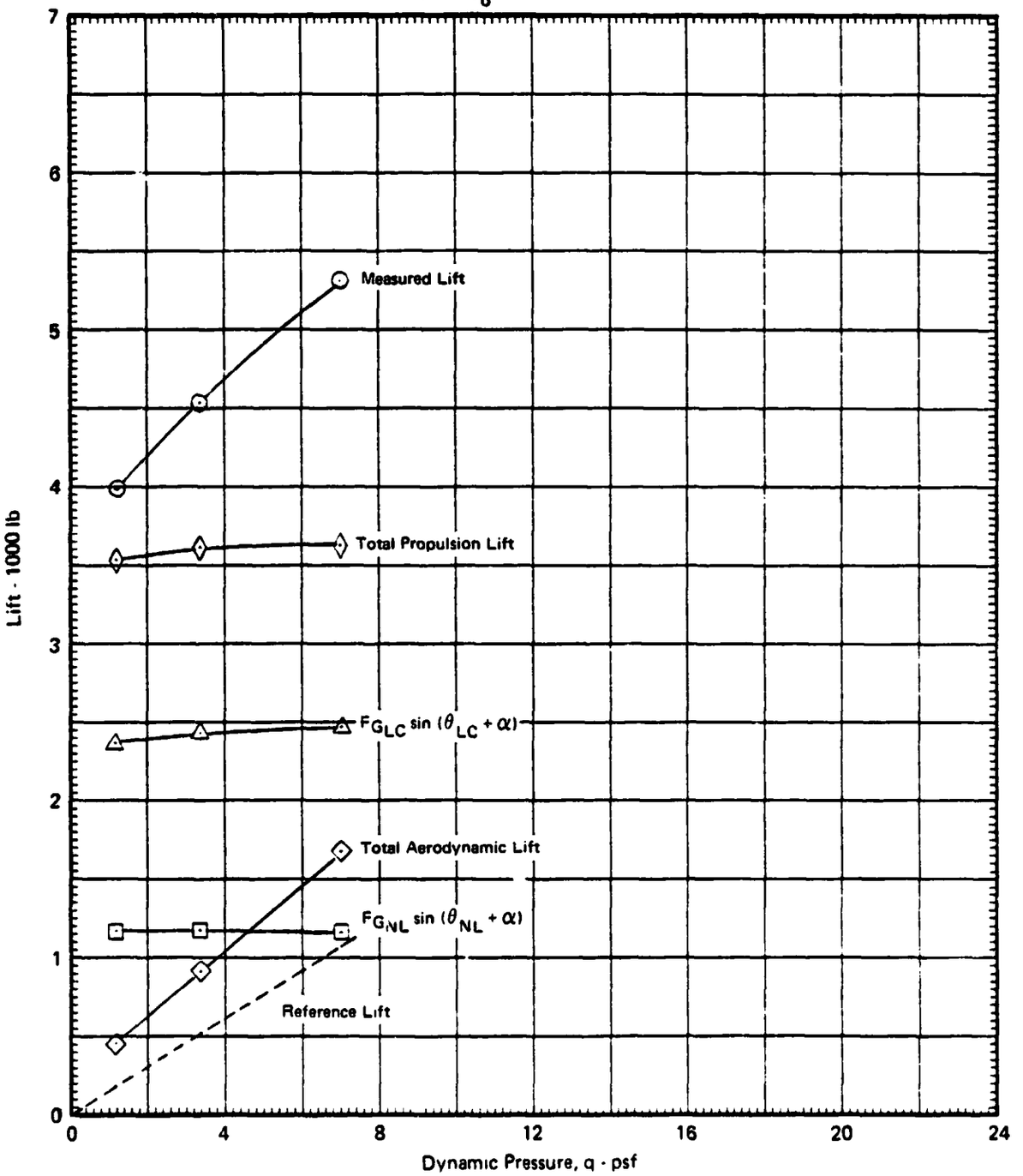

GP76-0622 85

FIGURE 8.3-52

DRAG vs DYNAMIC PRESSURE, HORIZONTAL TAIL OFF

$\alpha = 8^o$ $\delta_{LC} = 90^o$ $\delta_{NL} = 90^o$ $\theta_J = 84.7^o$

Graphical Summary of Measured and Calculated Force Data

$\delta_f = 15^o$ $\delta_s = 10^o/10^o$ Nose Gear On

$N_F/\sqrt{\theta_{T_o}} = 3600$ RPM

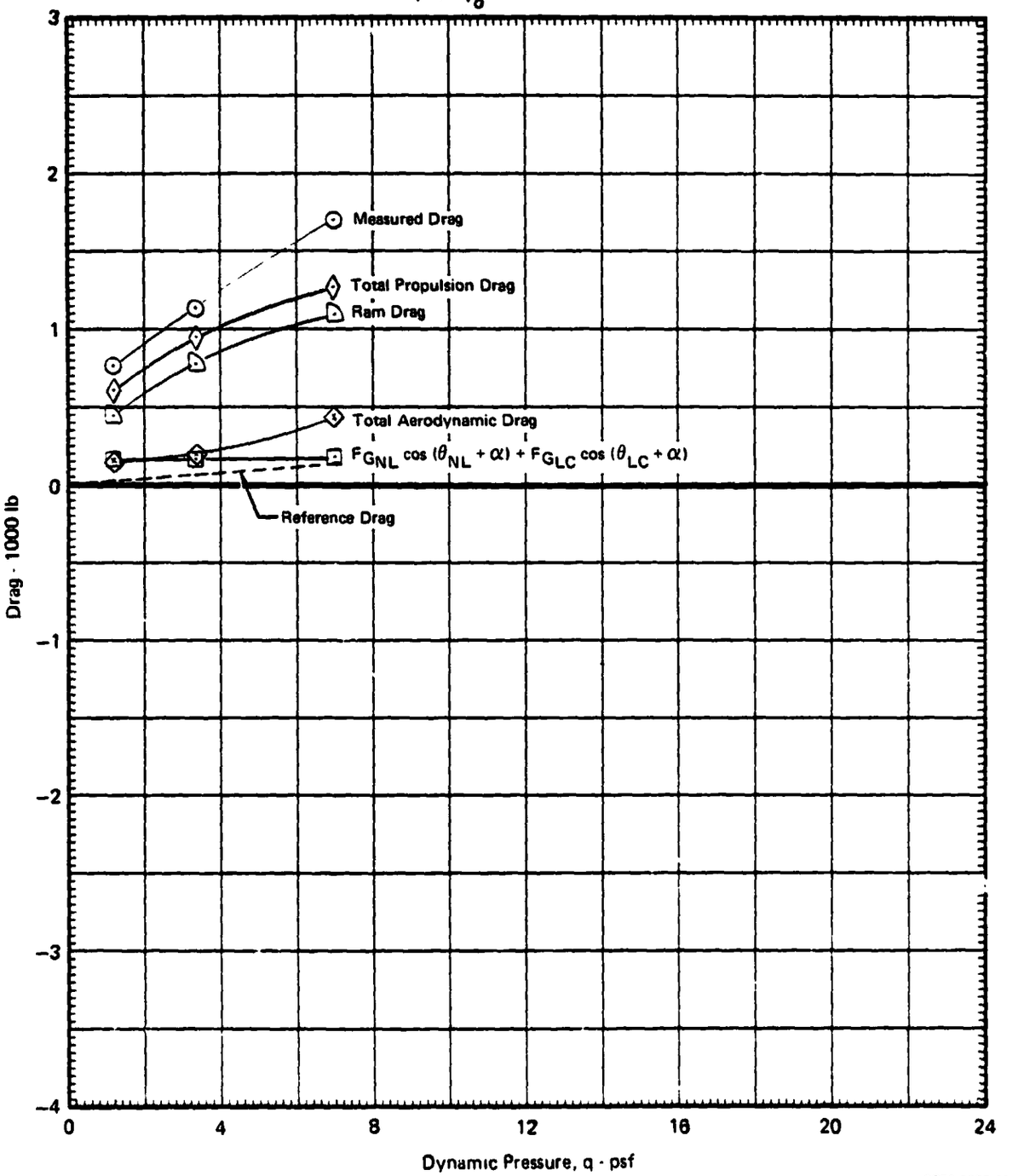

GP76-0522 86

FIGURE 8.3-53
LIFT vs DYNAMIC PRESSURE, HORIZONTAL TAIL OFF
$\alpha = 16^{o}$ $\delta_{LC} = 90^{o}$ $\delta_{NL} = 90^{o}$ $\theta_J = 84.7^{o}$
Graphical Summary of Measured and Calculated Force Data
$\delta_f = 15^{o}$ $\delta_a = 10^{o}/10^{o}$ Nose Gear On
$N_F/\sqrt{\theta_{T_o}} = 3600$ RPM

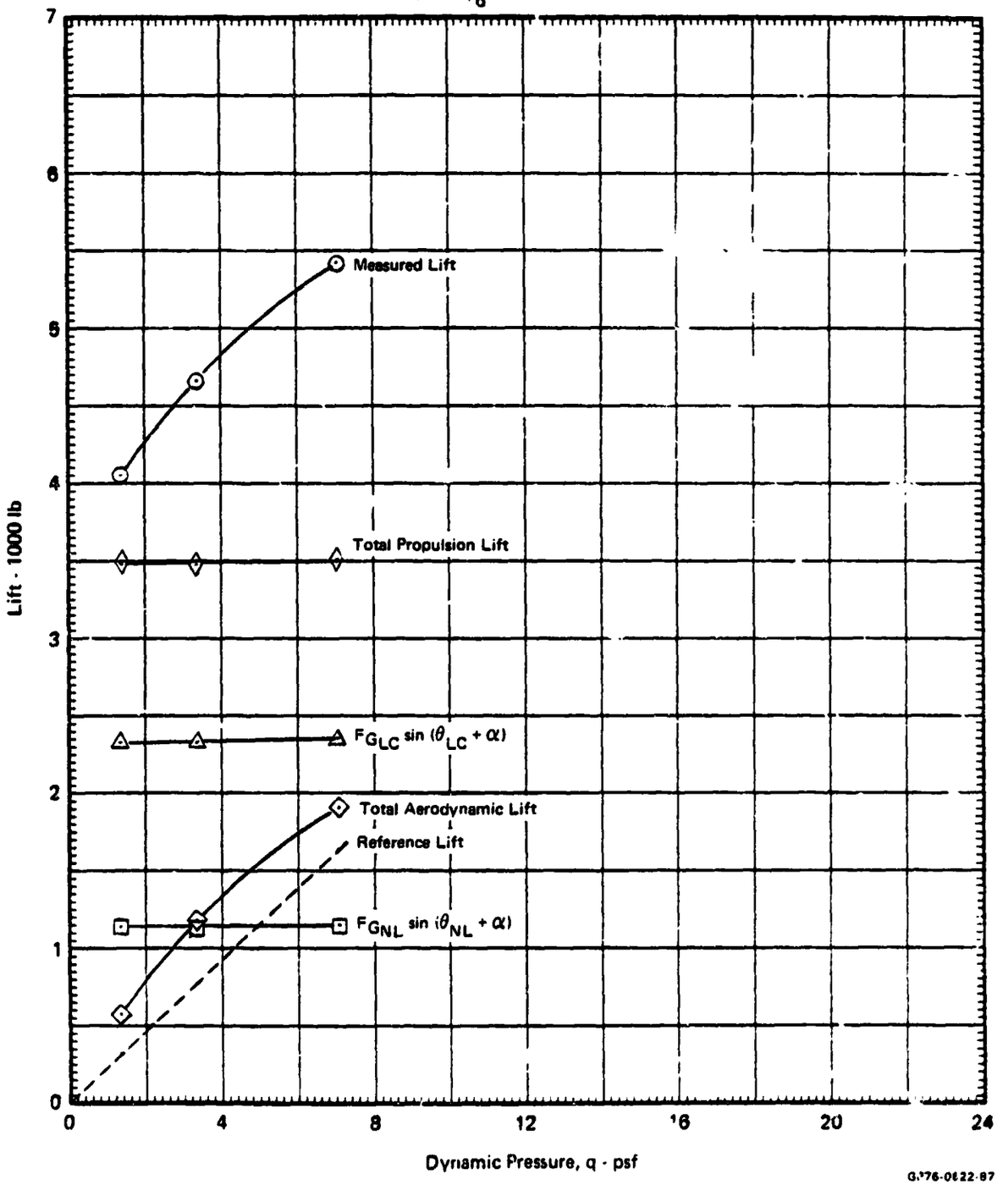

FIGURE 8.3-54
DRAG vs DYNAMIC PRESSURE, HORIZONTAL TAIL OFF
$\alpha = 16^{o}$ $\delta_{LC} = 90^{o}$ $\delta_{NL} = 90^{o}$ $\theta_J = 84.7^{o}$
Graphical Summary of Measured and Calculated Force Data
$\delta_f = 15^{o}$ $\delta_a = 10^{o}/10^{o}$ Nose Gear On
$N_F/\sqrt{\theta T_o} = 3600$ RPM

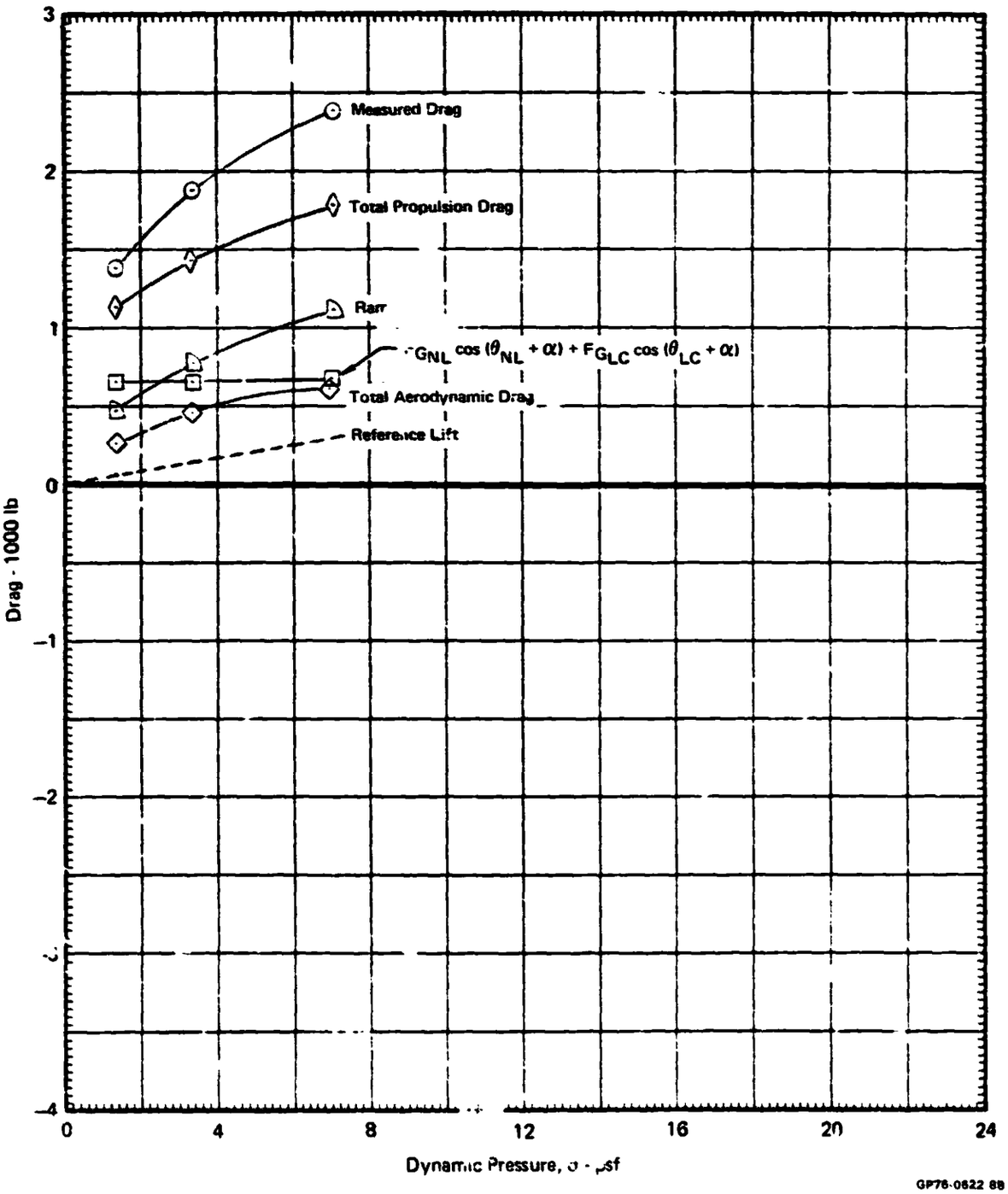

GP76-0822 88

FIGURE 8.3-55

INDUCED LIFT AND DRAG PARAMETERS vs JET VELOCITY RATIO

HORIZONTAL TAIL OFF $\delta_{LC} = 23^o$ $\delta_{NL} = 43^o$ $\theta_J = 20.1^o$

$\delta_f = 15^o$ $\delta_a = 10^o/10^o$ Nose Gear On

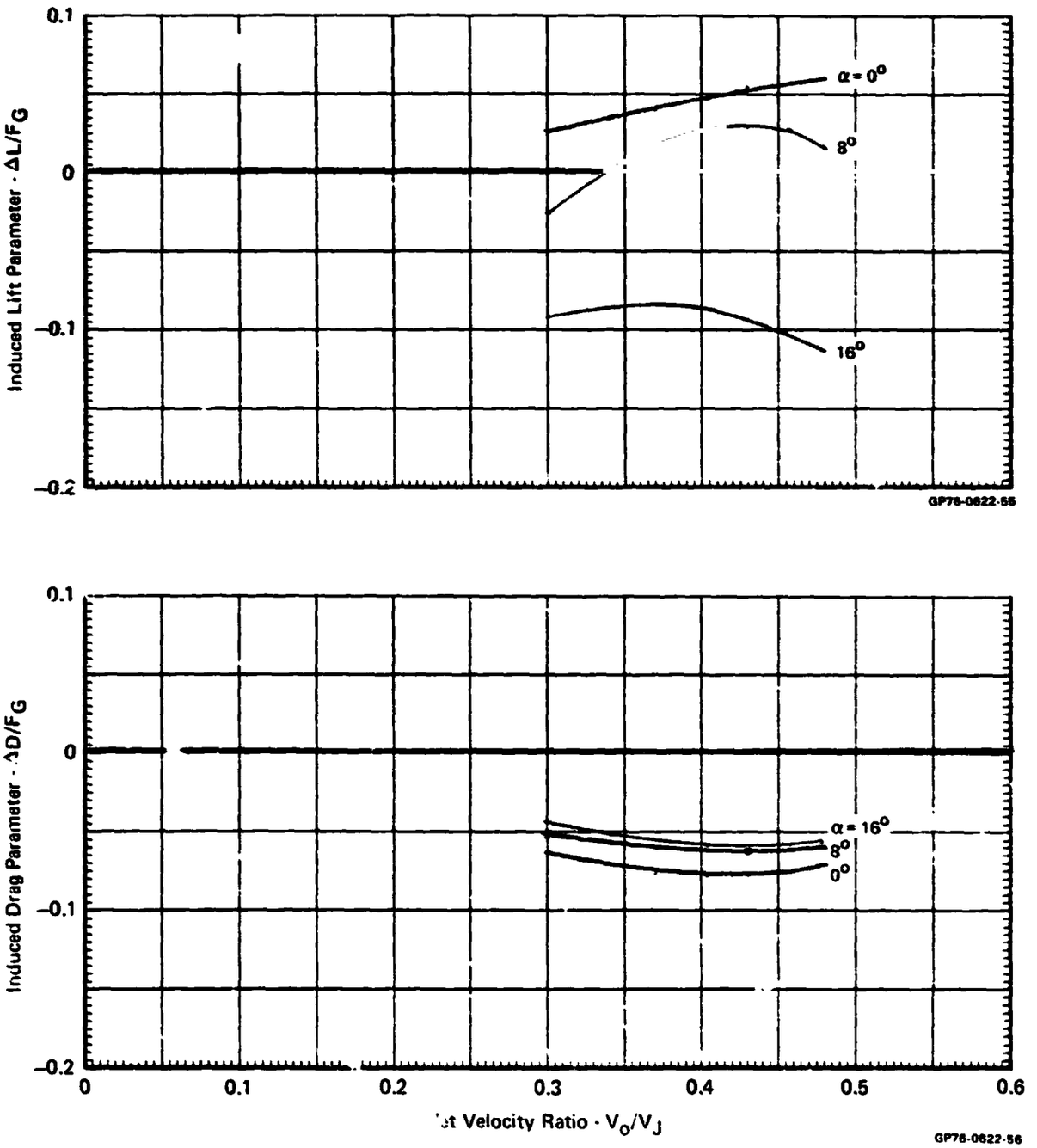

FIGURE 8.3-56
INDUCED LIFT AND DRAG PARAMETERS vs JET VELOCITY RATIO
HORIZONTAL TAIL OFF $\delta_{LC} = 56^{o}$ $\delta_{NL} = 43^{o}$ $\theta_J = 44.5^{o}$
$\delta_f = 15^{o}$ $\delta_a = 10^{o}/10^{o}$ Nose Gear On

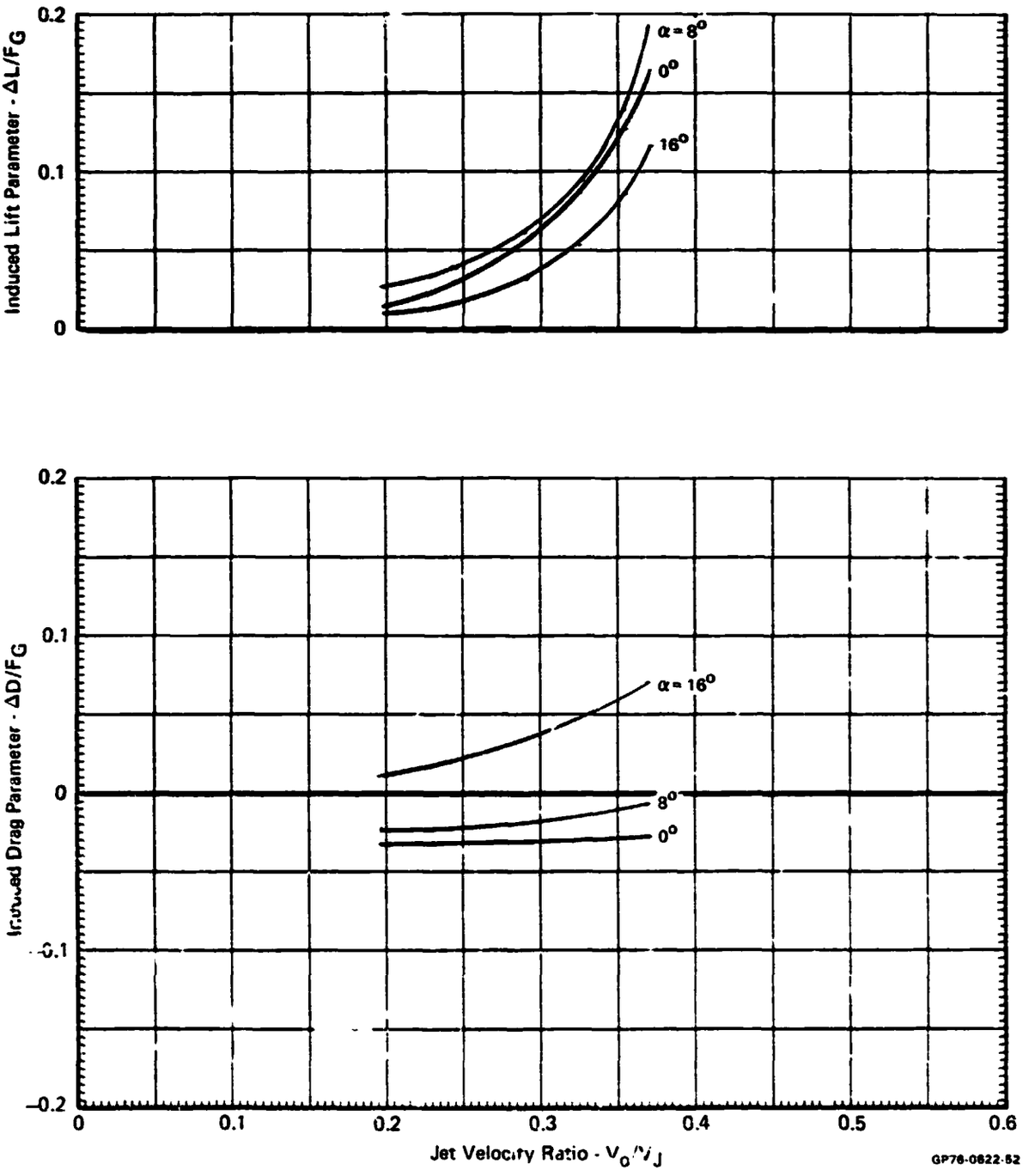

FIGURE 8.3-57

INDUCED LIFT AND DRAG PARAMETERS vs JET VELOCITY RATIO

HORIZONTAL TAIL OFF $\delta_{LC} = 90^{o}$ $\delta_{NL} = 90^{o}$ $\theta_J = 84.7^{o}$

$\delta_f = 15^{o}$ $\delta_a = 10^{o}/10^{o}$ Nose Gear On

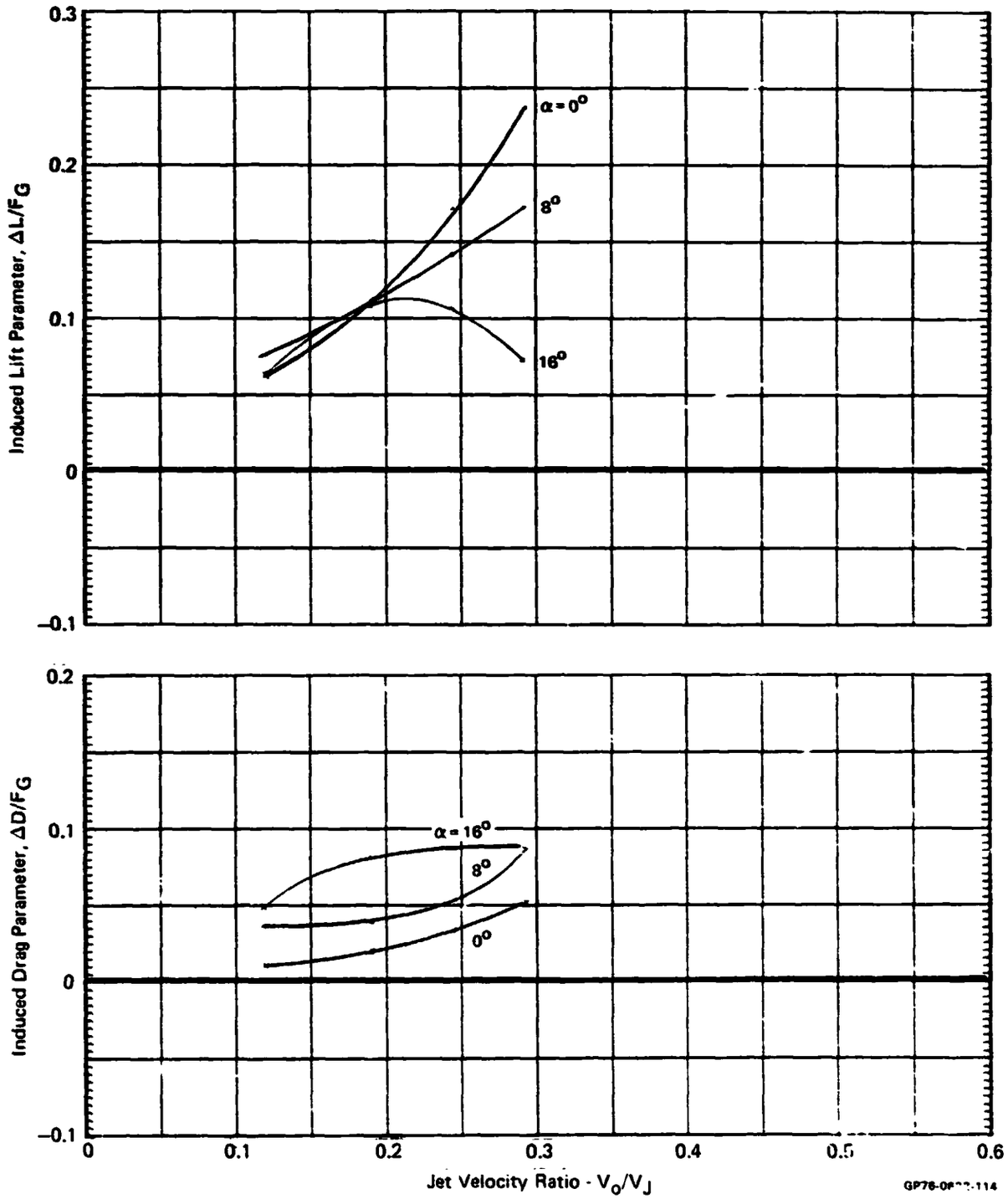

FIGURE 8.3-58

SUMMARY OF PROPULSION INDUCED EFFECTS AT 0° ANGLE OF ATTACK
THREE FAN OPERATION, HORIZONTAL TAIL OFF

$\delta_f = 15^0$ $\delta_a = 10^0/10^0$ Nose Gear On

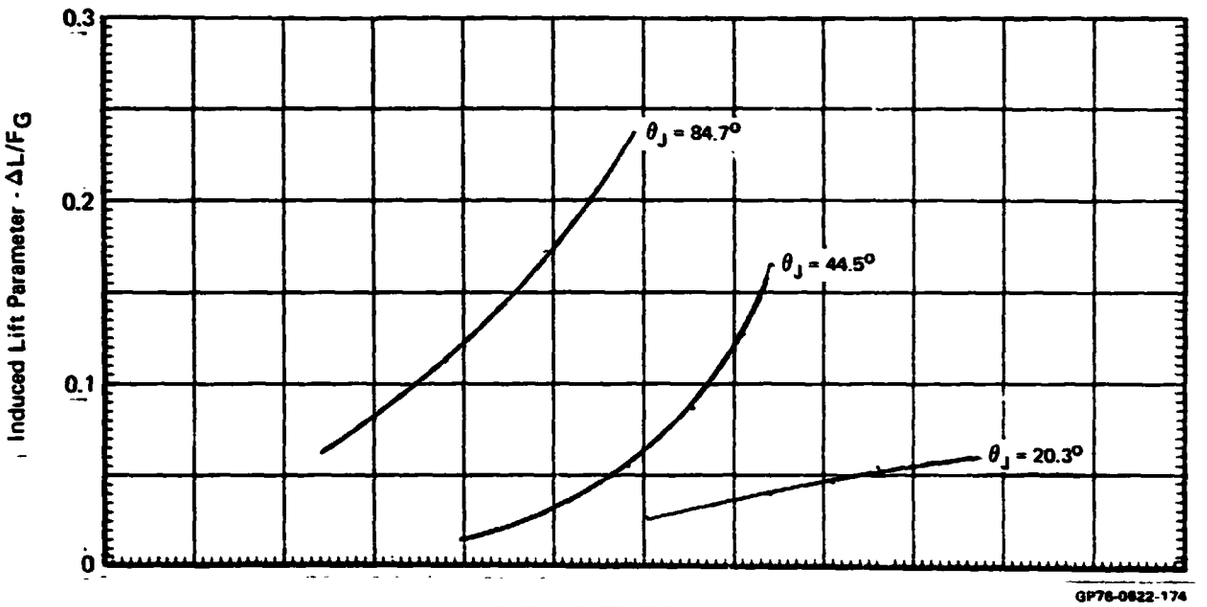

θ_J	δ_{LC}	δ_{NL}
20.3°	23°	43°
44.5°	56°	43°
84.7°	90°	90°

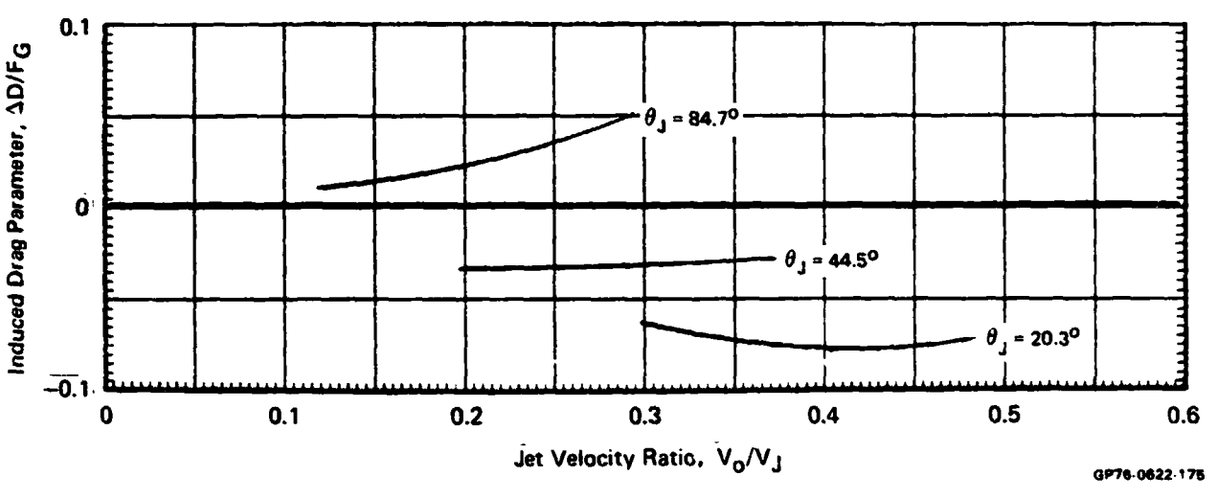

FIGURE 8.3-59

LIFT vs DYNAMIC PRESSURE, FLOW SURVEY RAKE ON

$\alpha = 0^o$ $\delta_{LC} = 0^o$ $\delta_{NL} = 0^o$ Inlets Covered $\theta_J = 1^o$

Graphical Summary of Measured and Calculated Force Data

$\delta_f = 15^o$ $\delta_a = 10^o/10^o$ Nose Gear Off

$N_F/\sqrt{\theta_{T_o}} = 3600$ RPM

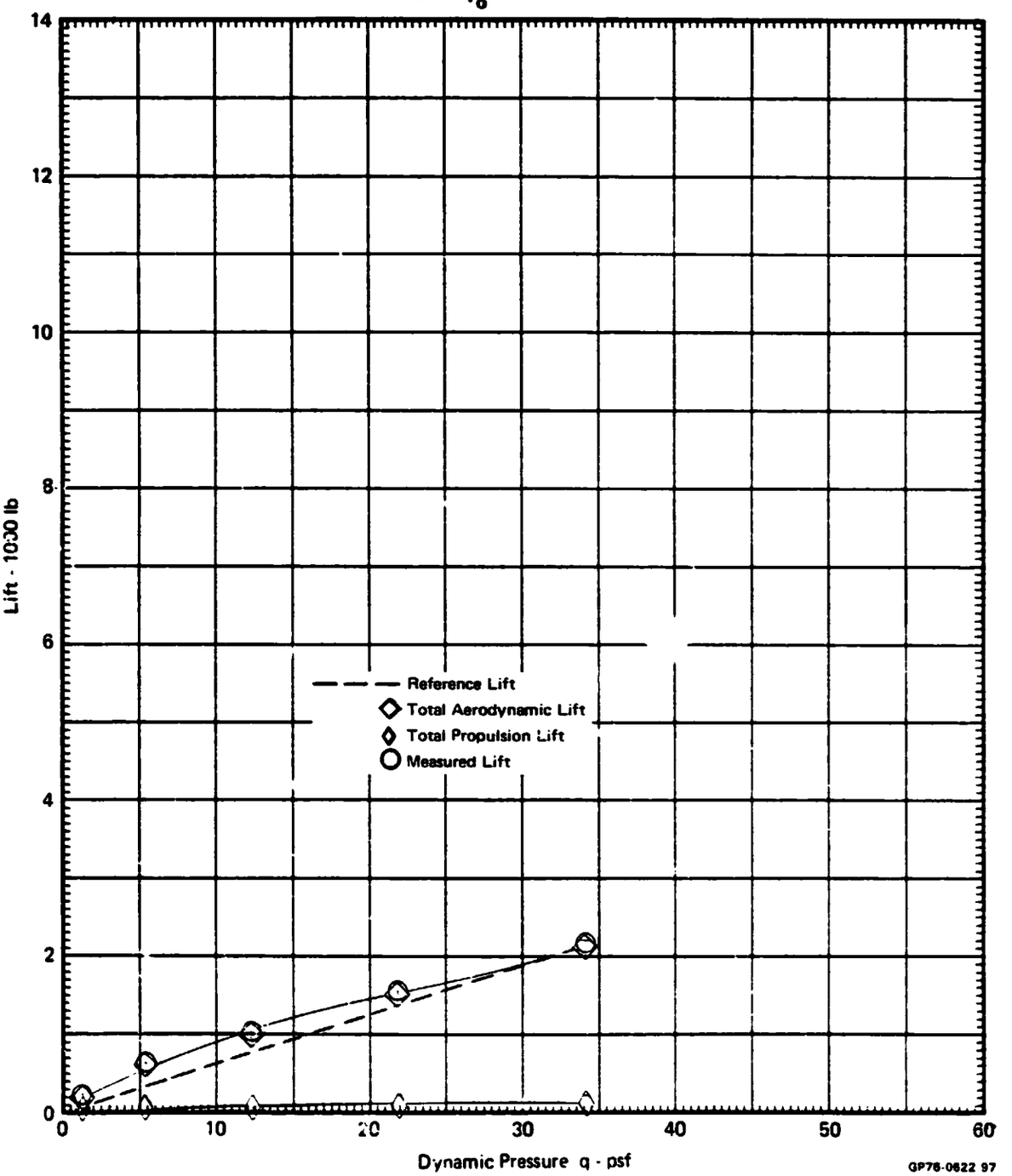

FIGURE 8.3-60
DRAG vs DYNAMIC PRESSURE, FLOW SURVEY RAKE ON
$\alpha = 0^o$ $\delta_{LC} = 0^o$ $\delta_{NL} = 0^o$ Inlets Covered $\theta_J = 1^o$
Graphical Summary of Measured and Calculated Force Data
$\delta_f = 15^o$ $\delta_a = 10^o/10^o$ Nose Gear Off
$N_F/\sqrt{\theta_{T_o}} = 3600$ RPM

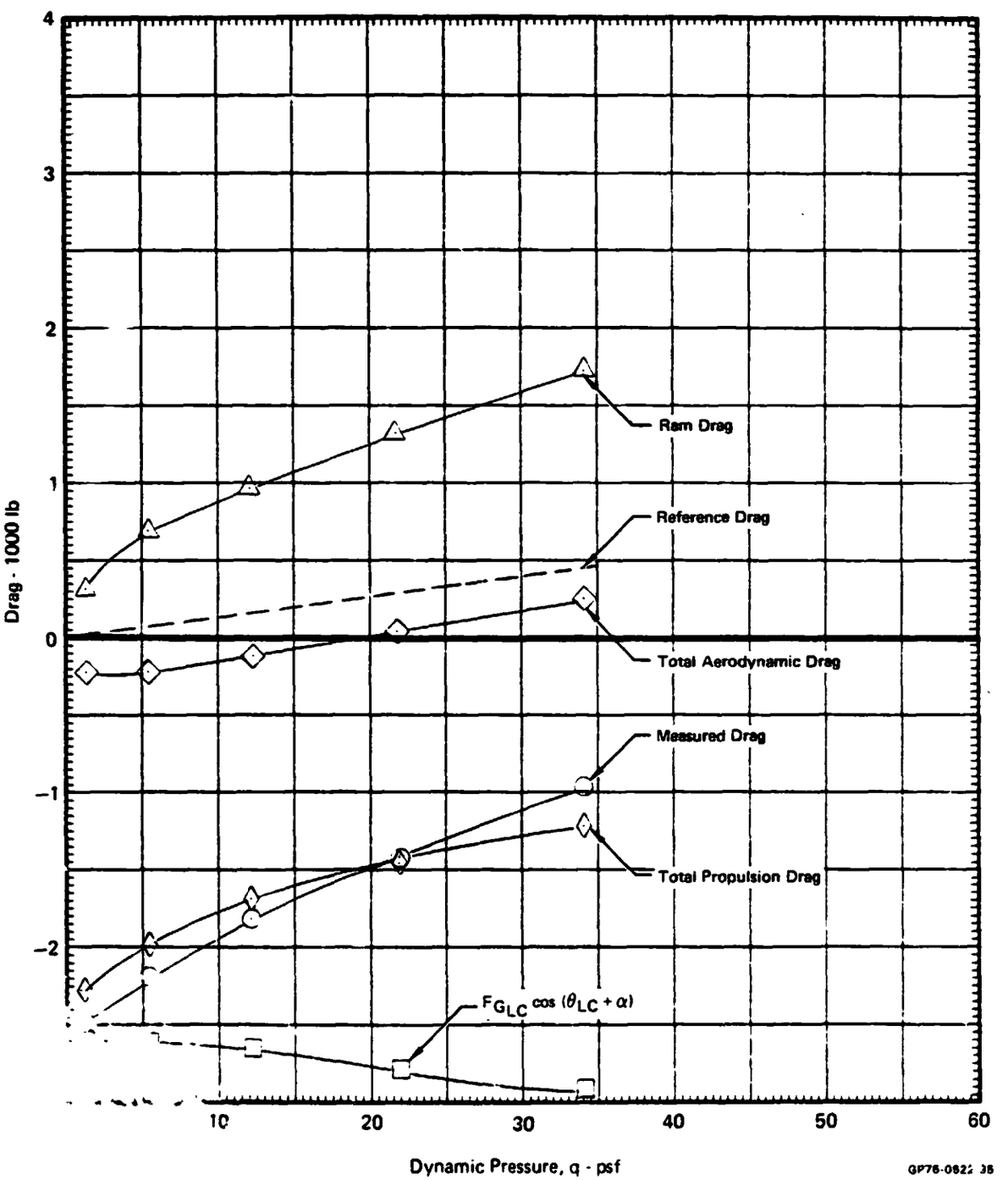

FIGURE 8.3-61
LIFT vs DYNAMIC PRESSURE, FLOW SURVEY RAKE ON
$\alpha = 0^o$ $\delta_{LC} = 56^o$ $\delta_{NL} = 0^o$ Inlets Covered $\theta_J = 47^o$
Graphical Summary of Measured and Calculated Force Data
$\delta_f = 15^o$ $\delta_a = 10^o/10^o$ Nose Gear Off
$N_F/\sqrt{\theta_{T_o}} = 3600$ RPM

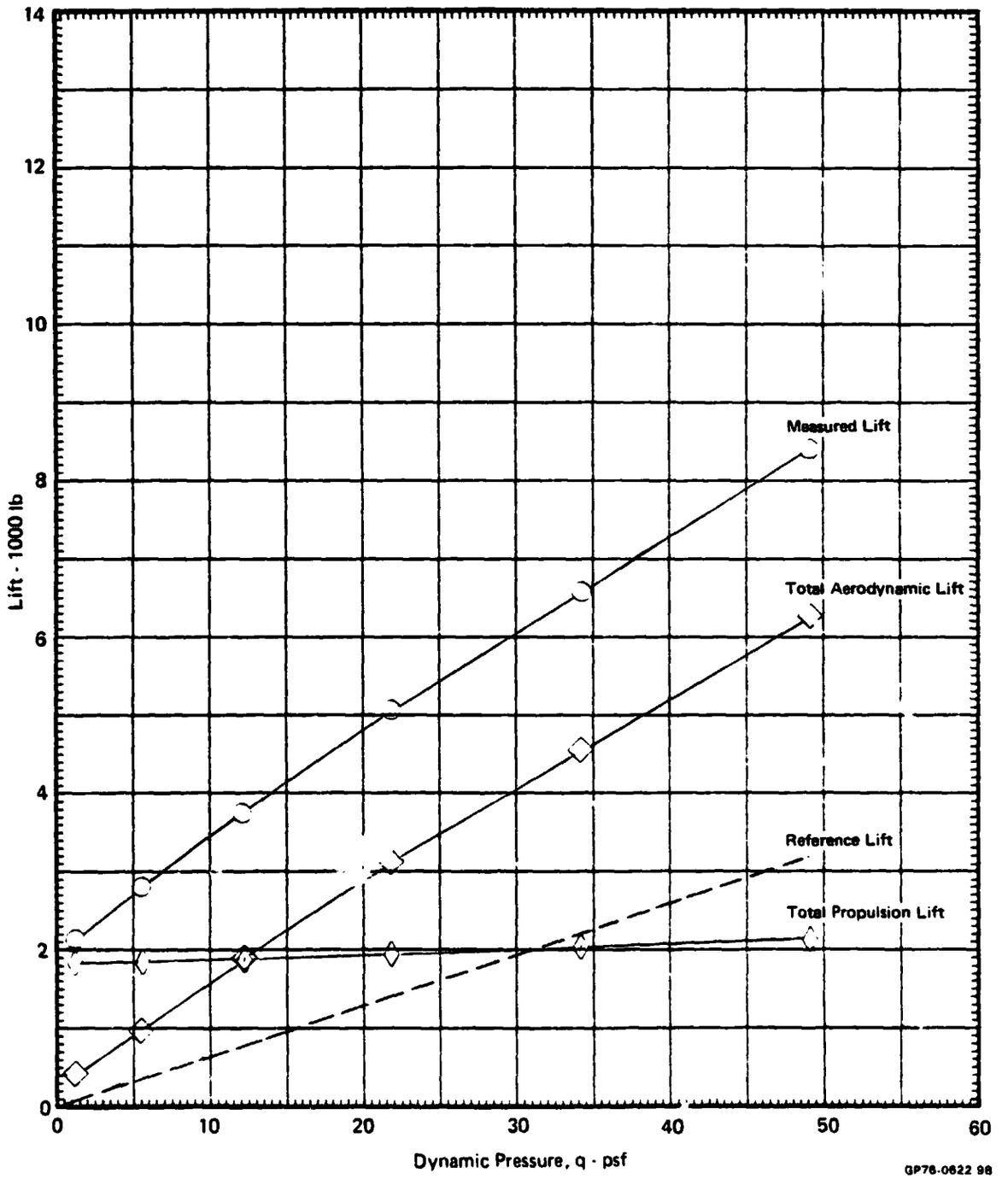

FIGURE 8.3-62

DRAG vs DYNAMIC PRESSURE , FLOW SURVEY RAKE ON

$\alpha = 0^{o}$ $\delta_{LC} = 56^{o}$ $\delta_{NL} = 0^{o}$ Inlets Covered $\theta_J = 47^{o}$

Graphical Summary of Measured and Calculated Force Data

$\delta_f = 15^{o}$ $\delta_a = 10^{o}/10^{o}$ Nose Gear Off

$N_F/\sqrt{\theta T_o} = 3600$ RPM

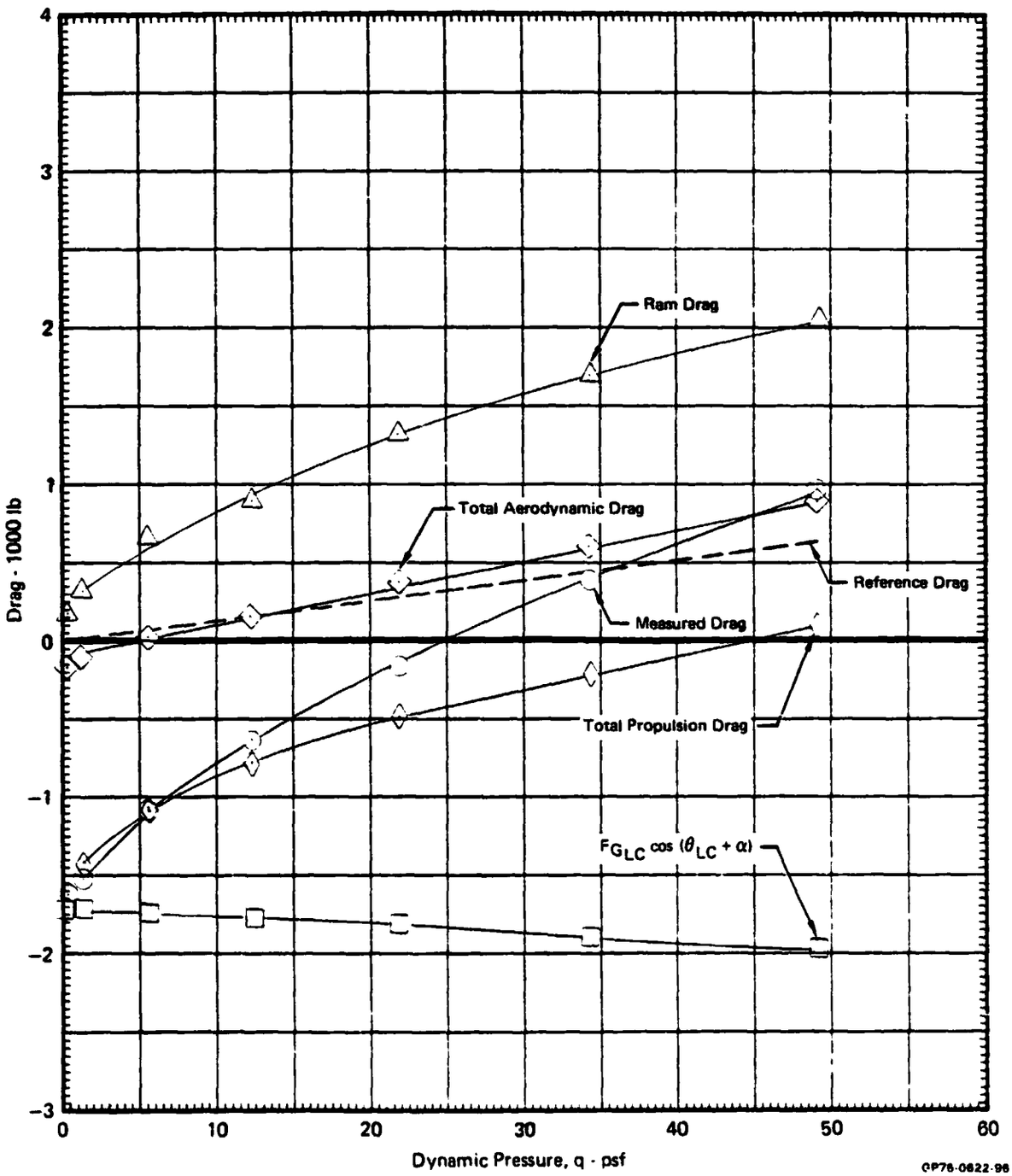

FIGURE 8.3-63

LIFT vs DYNAMIC PRESSURE, FLOW SURVEY RAKE ON

$\alpha = 0^o$ $\delta_{LC} = 90^o$ $\delta_{NL} = 0^o$ Inlets Covered $\theta_J = 84^o$

Graphical Summary of Measured and Calculated Force Data

$\delta_f = 15^o$ $\delta_a = 10^o/10^o$ Nose Gear Off

$N_F/\sqrt{\theta T_o} = 3600$ RPM

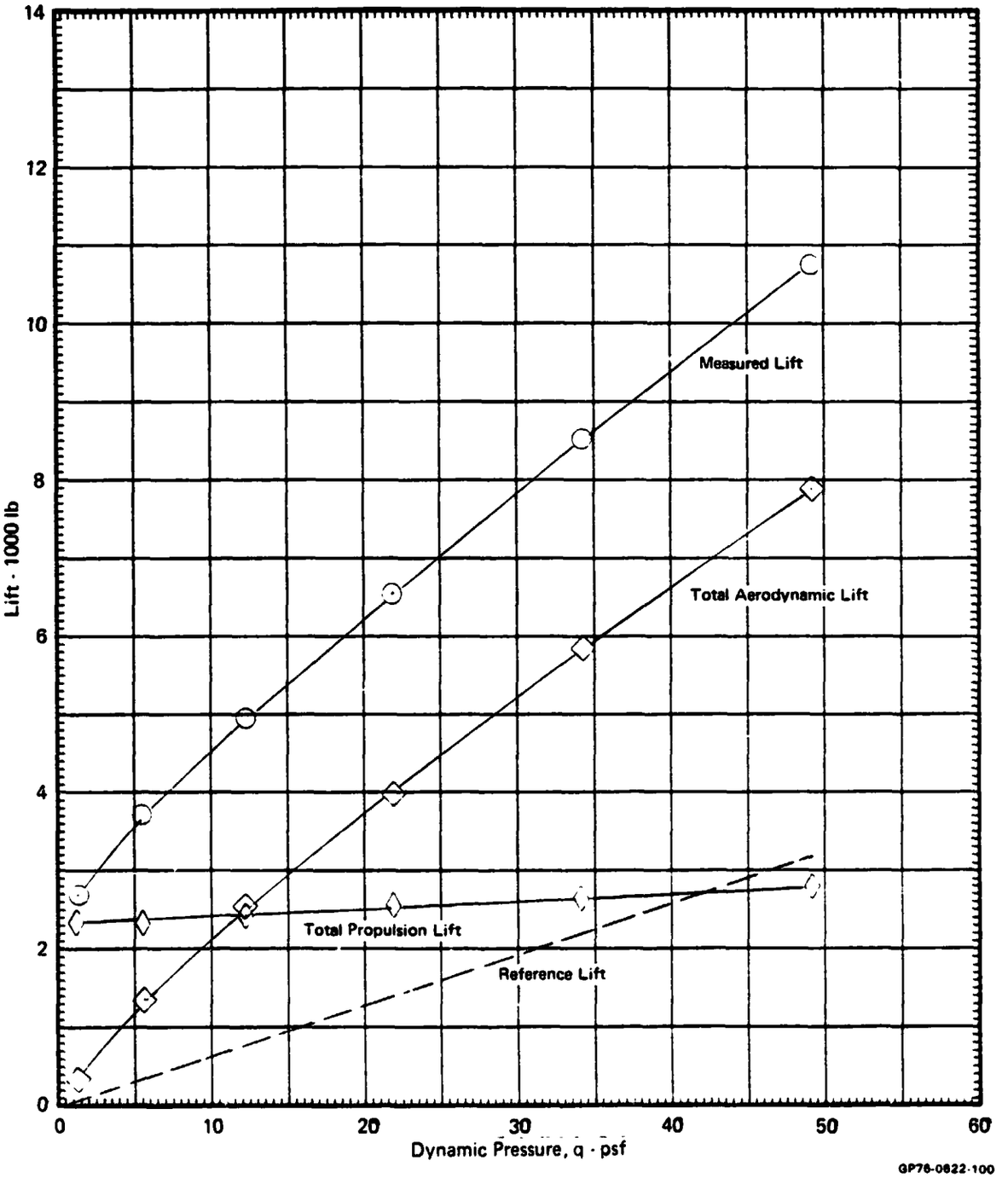

FIGURE 8.3-64

DRAG vs DYNAMIC PRESSURE, FLOW SURVEY RAKE ON

$\alpha = 0^0$ $\delta_{LC} = 90^0$ $\delta_{NL} = 0^0$ Inlets Covered $\theta_J = 84^0$

Graphical Summary of Measured and Calculated Force Data

$\delta_f = 15^0$ $\delta_a = 10^0/10^0$ Nose Gear Off

$N_F/\sqrt{\theta T_o} = 3600$ RPM

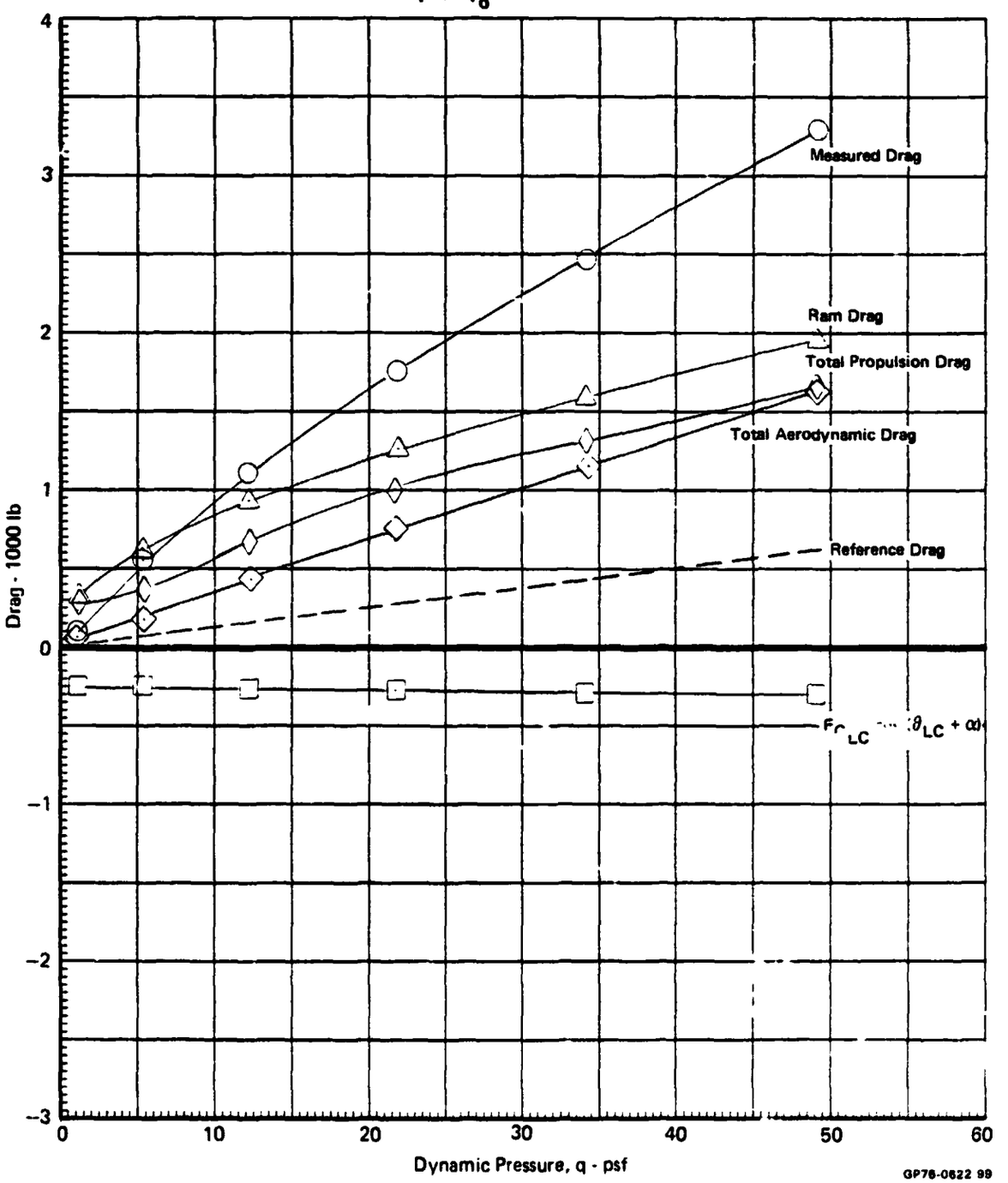

FIGURE 8.3-65

SUMMARY OF PROPULSION INDUCED EFFECTS AT 0° ANGLE OF ATTACK
TWO FAN OPERATION, FLOW SURVEY RAKE ON

$\delta_f = 15^o$ $\delta_a = 10^o/10^o$ Nose Gear On

Nose Unit Inlets Covered $\delta_{NL} = 0^o$

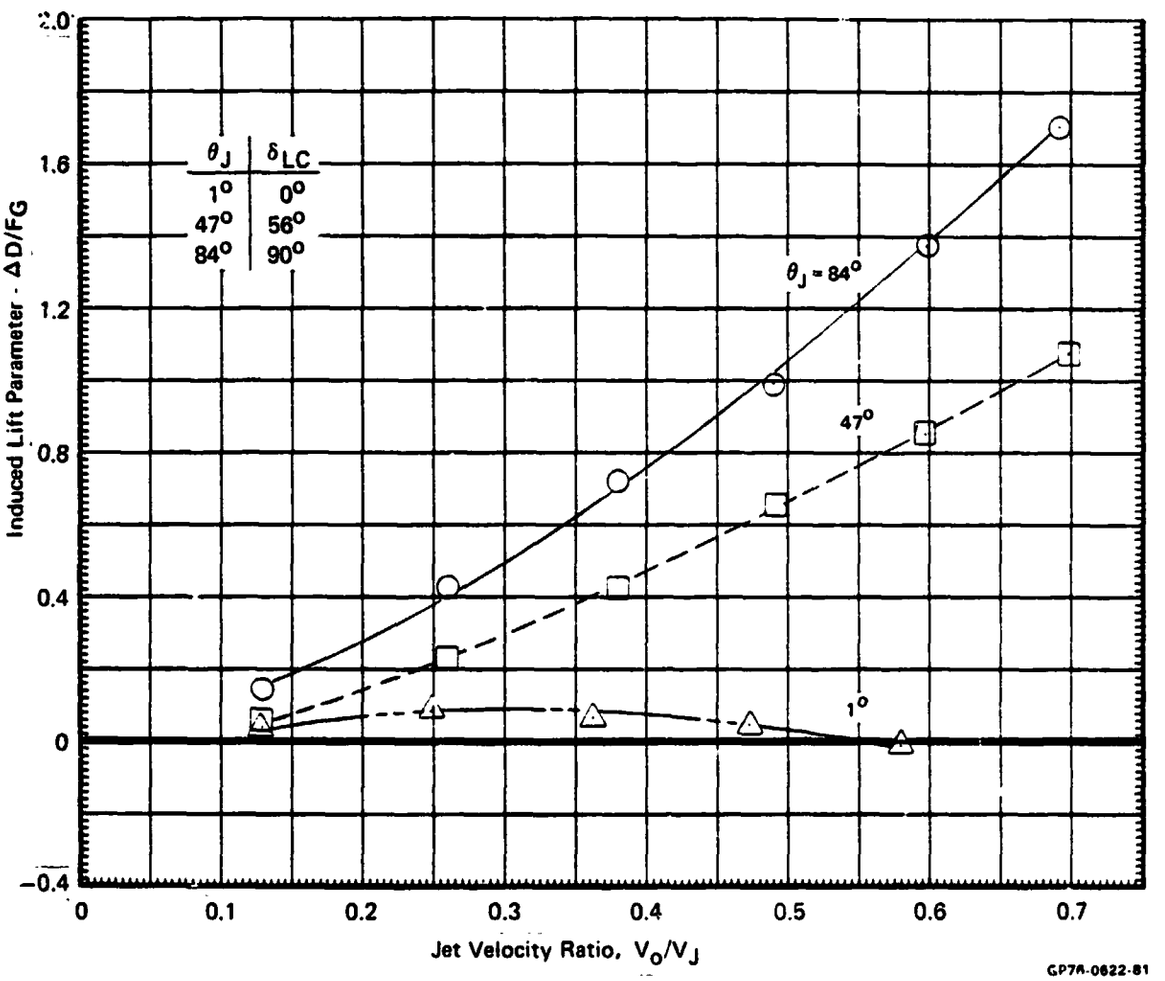

FIGURE 8.3-66
SUMMARY OF PROPULSION INDUCED EFFECTS AT 0° ANGLE OF ATTACK
TWO FAN OPERATION, FLOW SURVEY RAKE ON
$\delta_f = 15^0$ $\delta_a = 10^0/10^0$ Nose Gear Off
Nose Unit Inlets Covered $\delta_{NL} = 0^0$

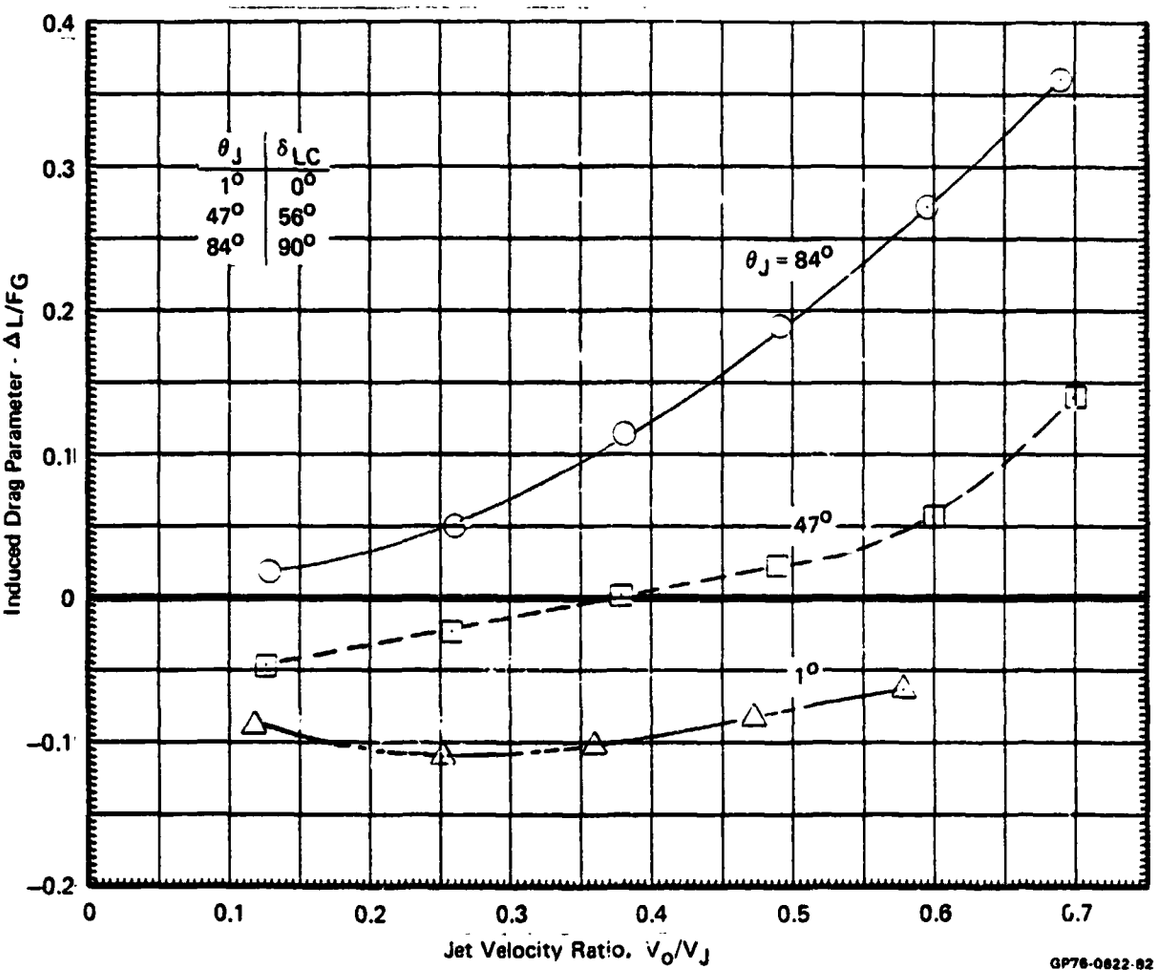

FIGURE 8.3-67
EFFECT OF NOSE LIFT UNIT ON TOTAL AERODYNAMIC LIFT
$\delta_{LC} = 56^{o}$ $\alpha = 0^{o}$
$\delta_f = 15^{o}$ $\delta_a = 10^{o}/10^{o}$ **Horizontal Tail Off**

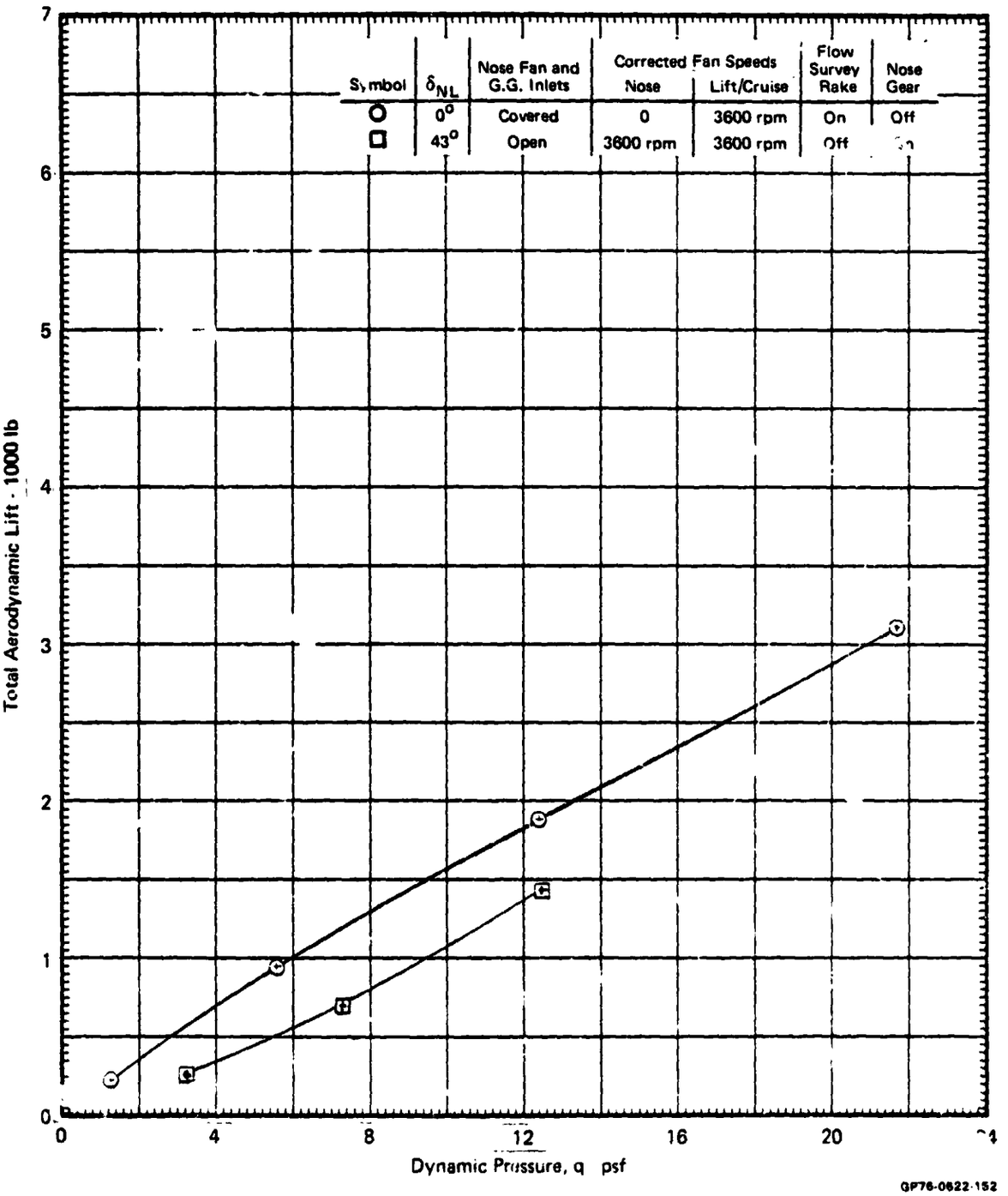

FIGURE 8.3-68
EFFECT OF NOSE LIFT UNIT ON TOTAL AERODYNAMIC DRAG

$\delta_{LC} = 56^0$, $\alpha = 0^0$

$\delta_f = 15^0$ $\delta_a = 10^0/10^0$ Horizontal Tail Off

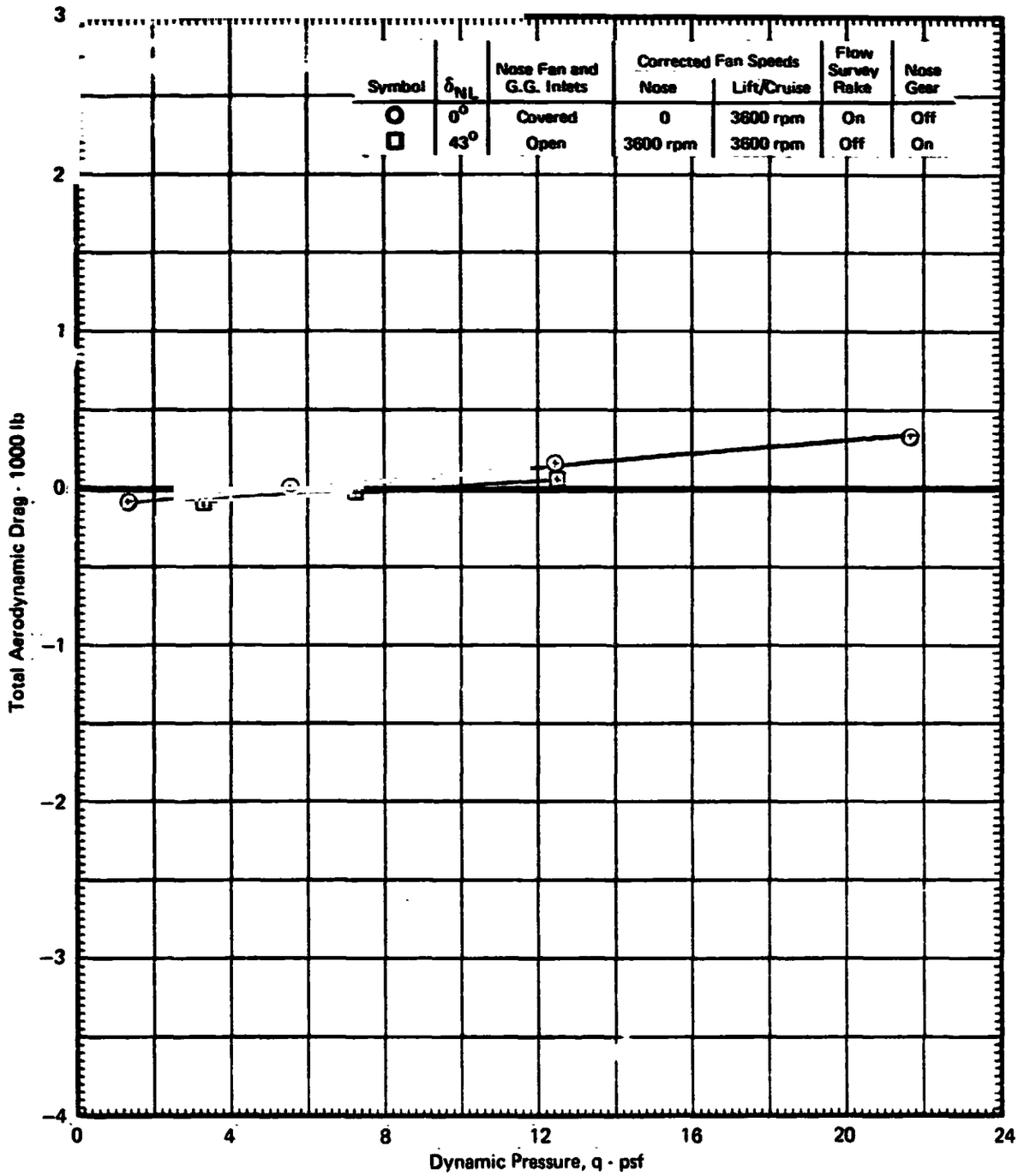

FIGURE 8.3-6º
EFFECT OF NOSE LIFT UNIT ON TOTAL AERODYNAMIC LIFT

$\delta_{LC} = 90^{o}$ $\alpha = 0^{o}$

$\delta_f = 15^{o}$ $\delta_a = 10^{o}/10^{o}$ Horizontal Tail Off

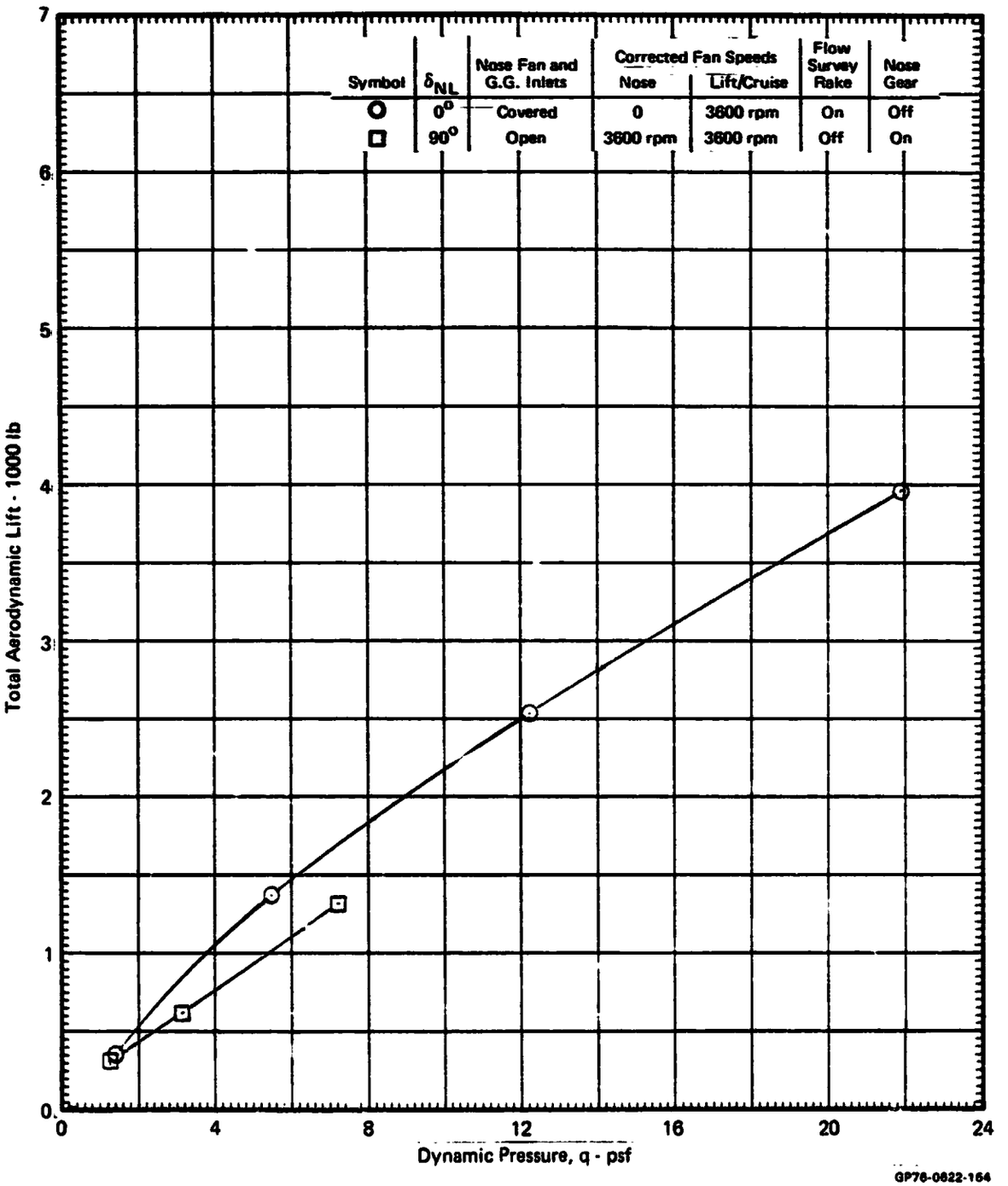

FIGURE 8.3-70
EFFECT OF NOSE LIFT UNIT ON TOTAL AERODYNAMIC DRAG

$\delta_{LC} = 90^{o}$ $\alpha = 0^{o}$

$\delta_f = 15^{o}$ $\delta_a = 10^{o}/10^{o}$ Horizontal Tail Off

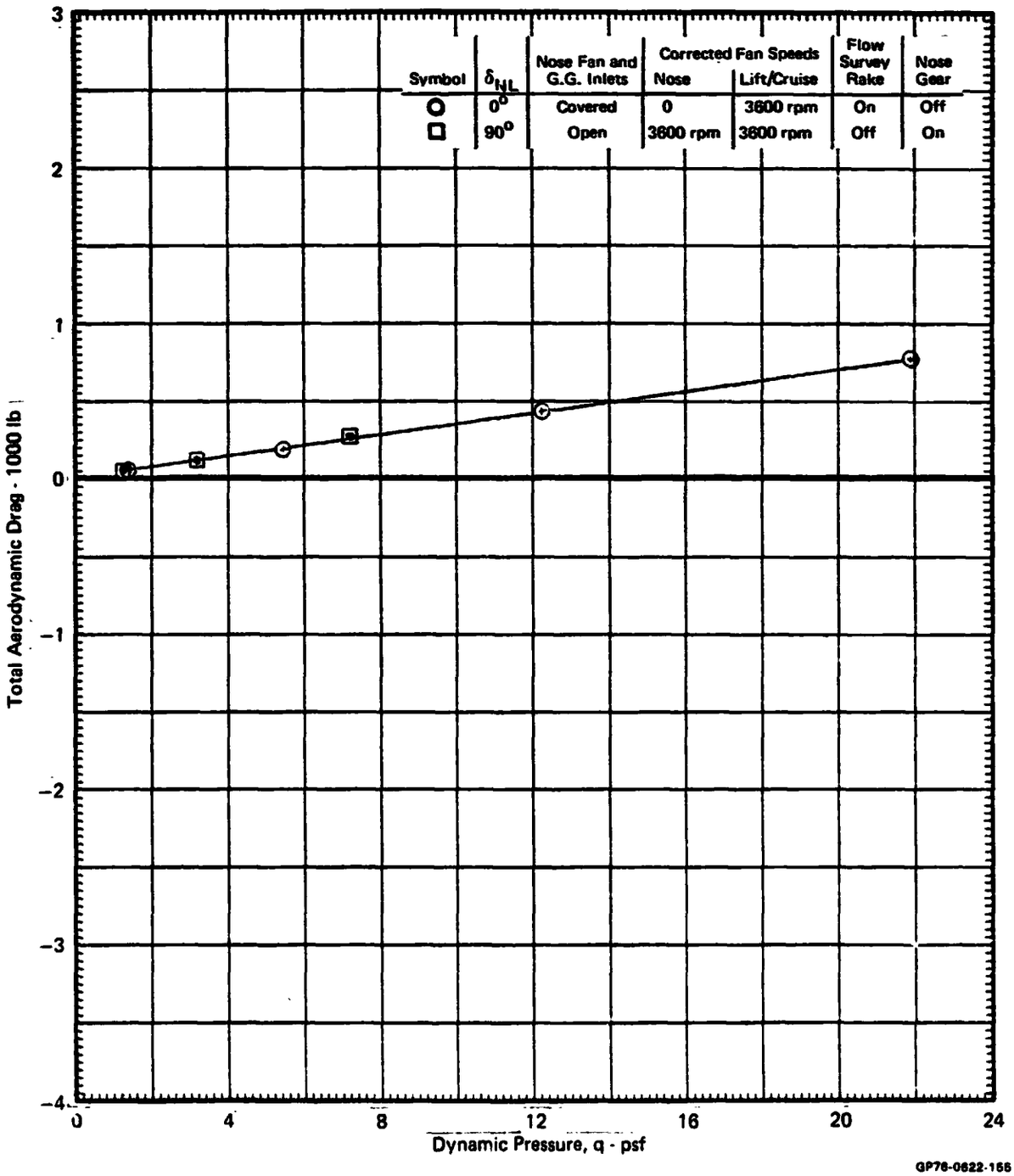

GP78-0622-166

FIGURE 8.3-71

LIFT vs DYNAMIC PRESSURE, FLOW SURVEY RAKE ON

$\alpha = 0^0$ $\delta_{LC} = 0^0$ $\delta_{NL} = 50^0$ $\theta_J = 14.8^0$

Graphical Summary of Measured and Calculated Force Data

$\delta_f = 15^0$ $\delta_a = 10^0/10^0$ Nose Gear Off

$N_F/\sqrt{\theta_{T_o}} = 3600$ RPM

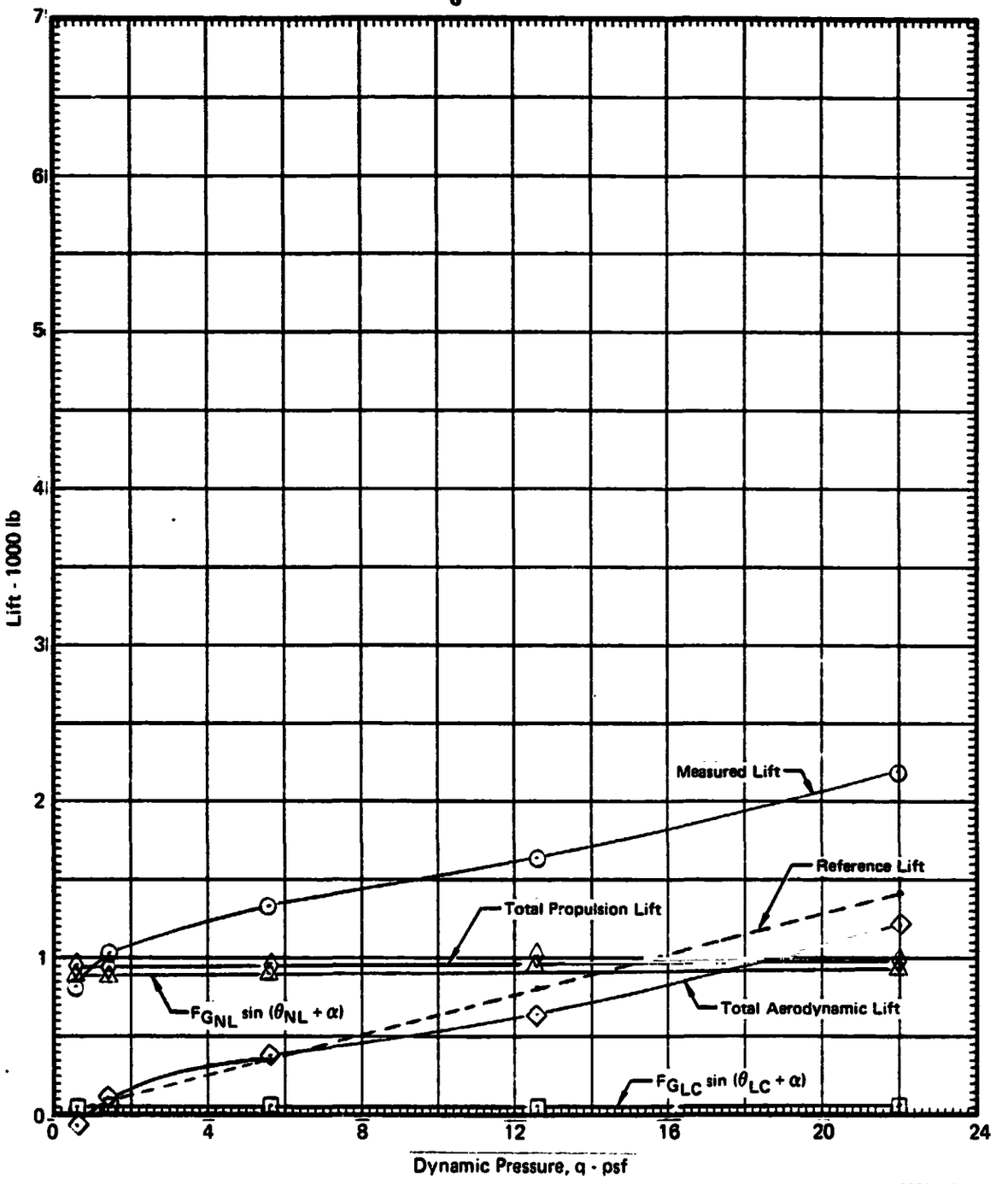

GP76-0622-116

FIGURE 8.3-72
DRAG vs DYNAMIC PRESSURE, FLOW SURVEY RAKE ON
$\alpha = 0^{o}$ $\delta_{LC} = 0^{o}$ $\delta_{NL} = 50^{o}$ $\theta_J = 14.8^{o}$
Graphical Summary of Measured and Calculated Force Data
$\delta_f = 15^{o}$ $\delta_a = 10^{o}/10^{o}$ Nose Gear Off

$N_F/\sqrt{\theta_{T_o}} = 3600$ RPM

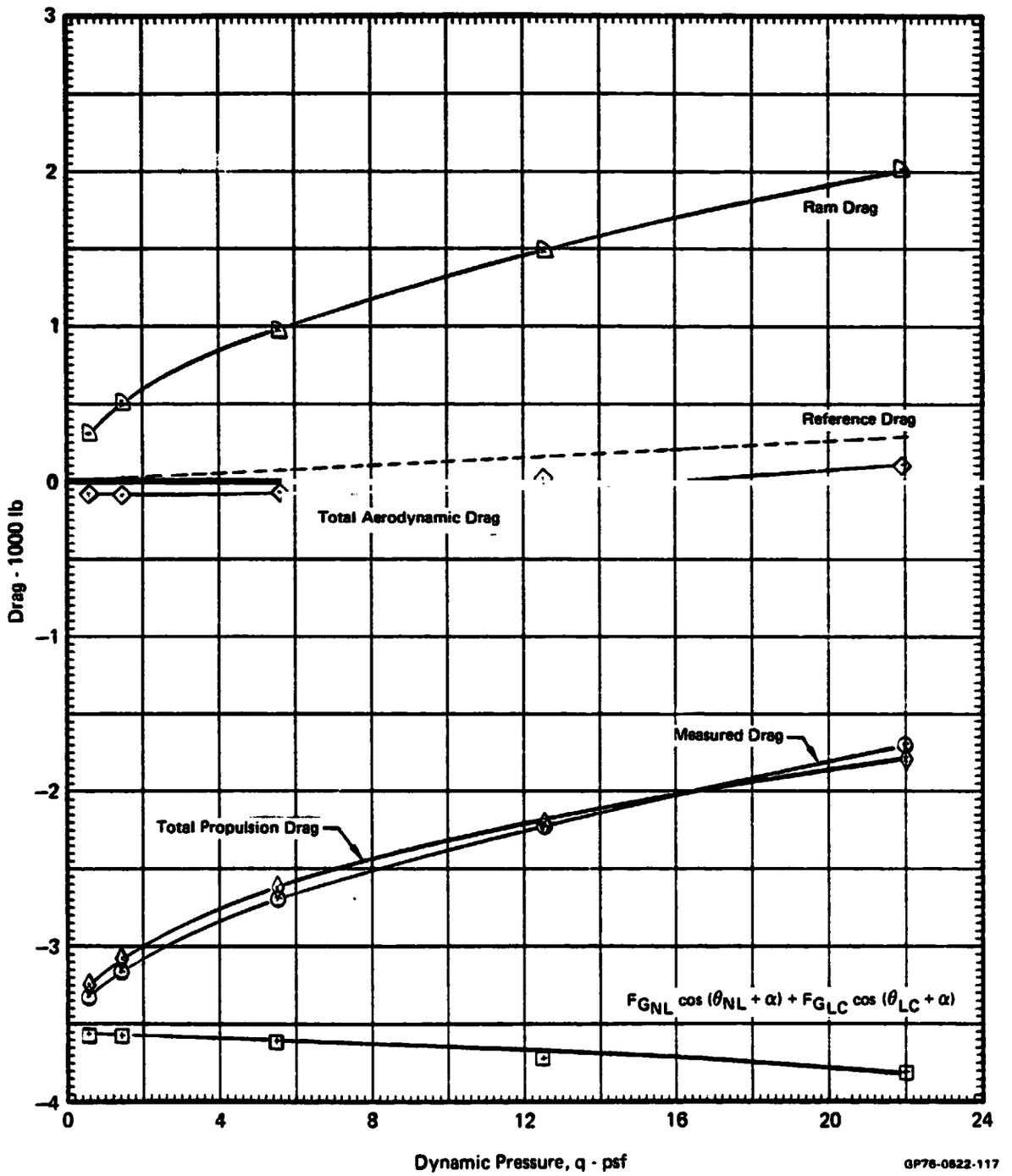

FIGURE 8.3-73
LIFT vs DYNAMIC PRESSURE, FLOW SURVEY RAKE ON
$\alpha = 0^0$ $\delta_{LC} = 0^0$ $\delta_{NL} = 70^0$ $\theta_J = 20.3^0$
$\delta_f = 15^0$ $\delta_a = 10^0/10^0$ Nose Gear Off
Graphical Summary of Measured and Calculated Force Data
$N_F/\sqrt{\theta T_o}$ = 3600 RPM

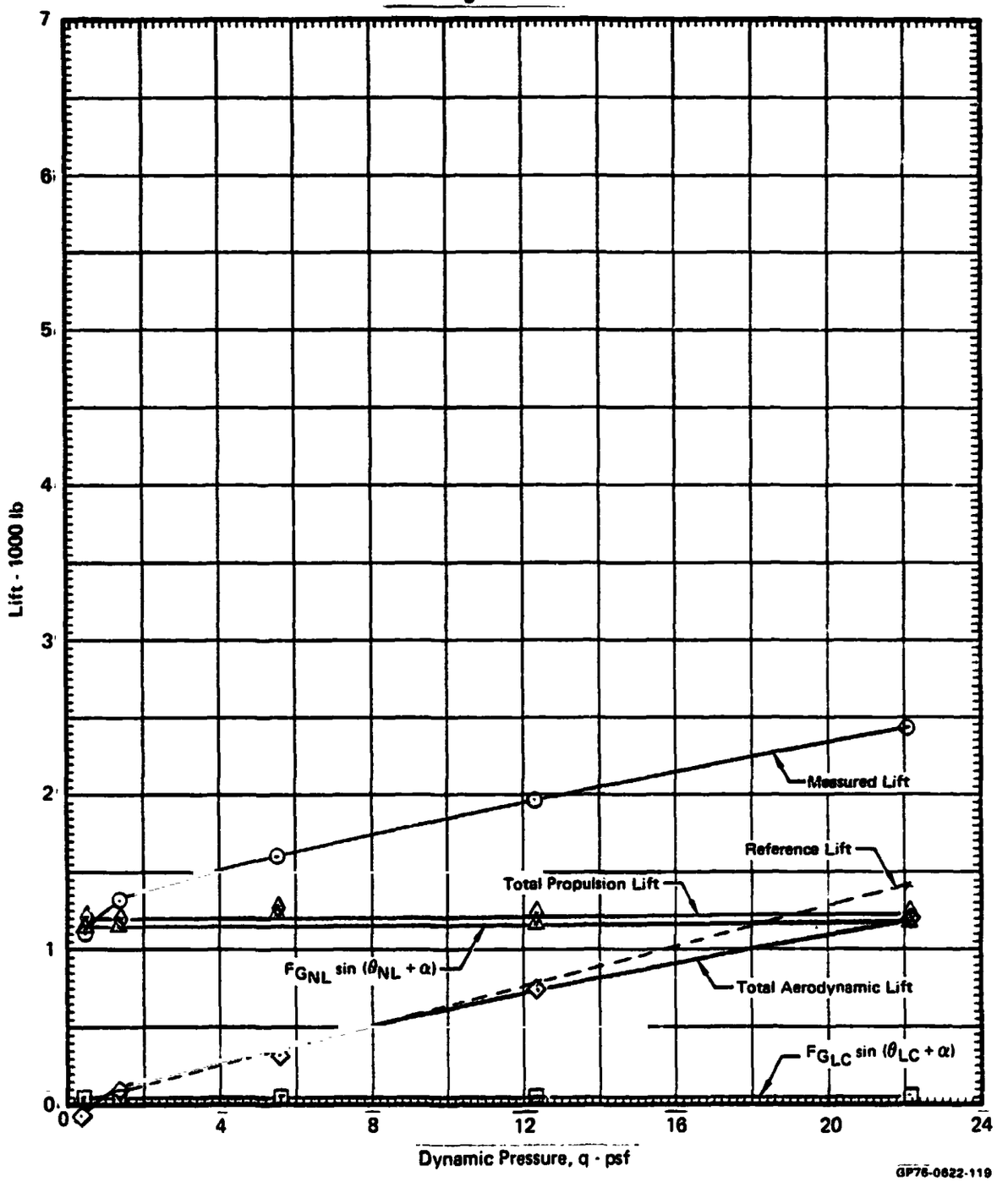

FIGURE 8.3-74

DRAG vs DYNAMIC PRESSURE, FLOW SURVEY RAKE ON

$\alpha = 0^o$ $\delta_{LC} = 0^o$ $\delta_{NL} = 70^o$ $\theta_J = 20.3^o$

Graphical Summary of Measured and Calculated Force Data

$\delta_f = 15^o$ $\delta_a = 10^o/10^o$ Nose Gear Off

$N_F/\sqrt{\theta T_o} = 3600$ RPM

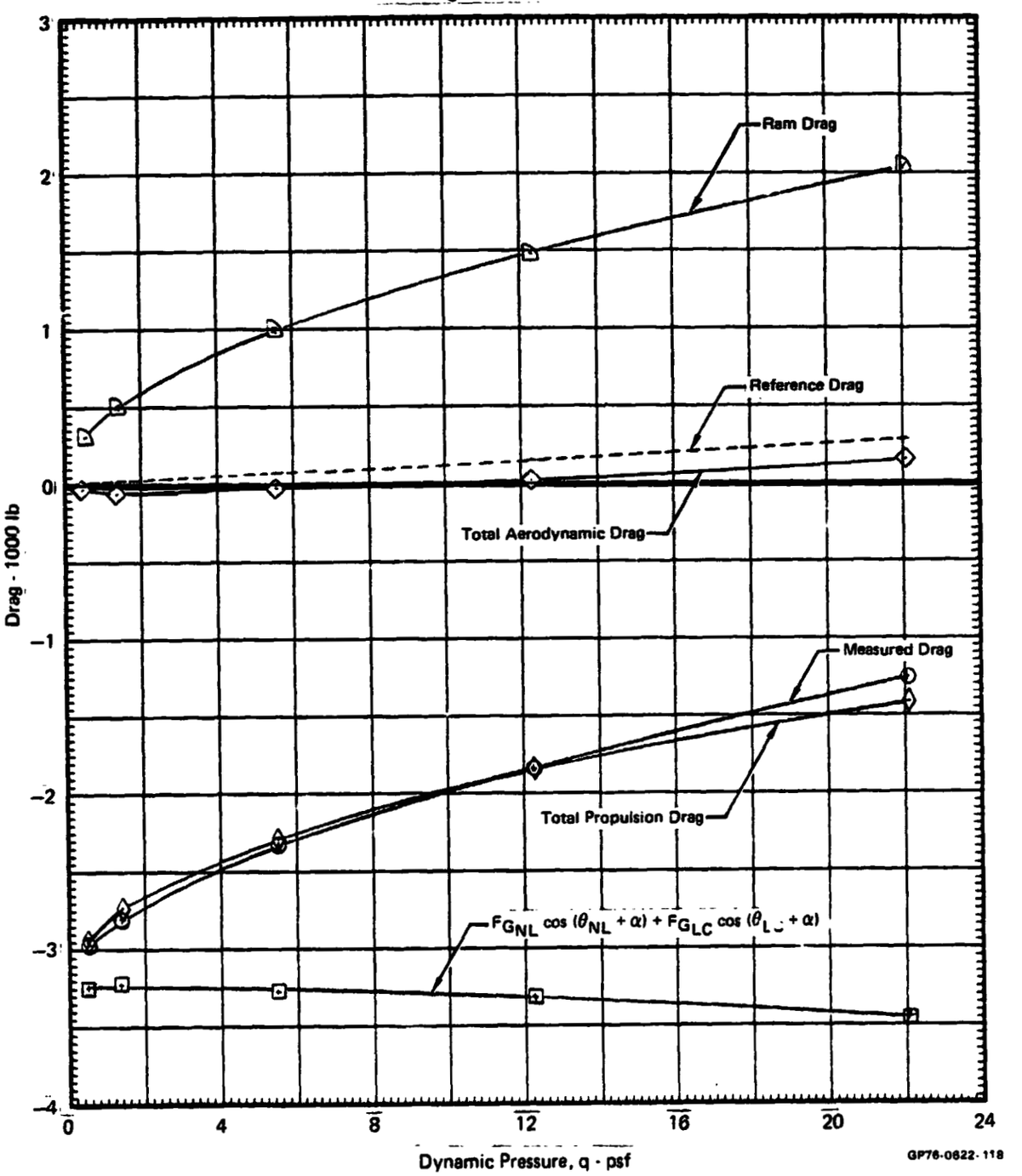

FIGURE 8.3-75
LIFT vs DYNAMIC PRESSURE, FLOW SURVEY RAKE ON
$\alpha = 0^o$ $\delta_{LC} = 0^o$ $\delta_{NL} = 90^o$ $\theta_J = 23.8^o$
Graphical Summay of Measured and Calculated Force Data
$\delta_f = 15^o$ $\delta_a = 10^o/10^o$ Nose Gear Off
$N_f/\sqrt{\theta_{T_o}} = 3600$ RPM

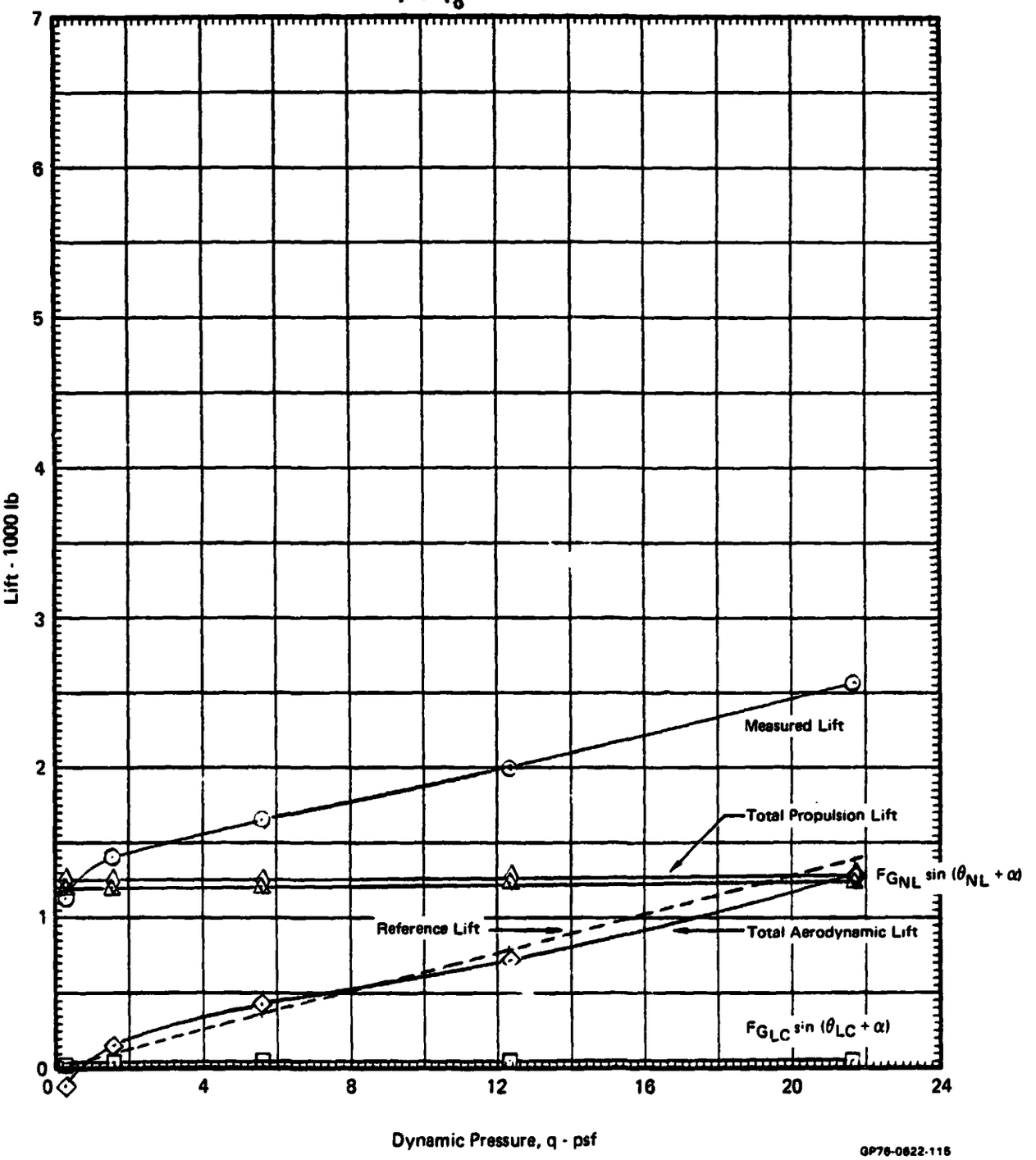

GP76-0822-116

FIGURE 8.3-76
DRAG vs DYNAMIC PRESSURE, FLOW SURVEY RAKE ON
$\alpha = 0^o$ $\delta_{LC} = 0^o$ $\delta_{NL} = 90^o$ $\theta_J = 23.8^o$
Graphical Summary of Measured and Calculated Force Data
$\delta_f = 15^o$ $\delta_a = 10^o/10^o$ Nose Gear Off
$N_F/\sqrt{\theta_{T_o}} = 3600$ RPM

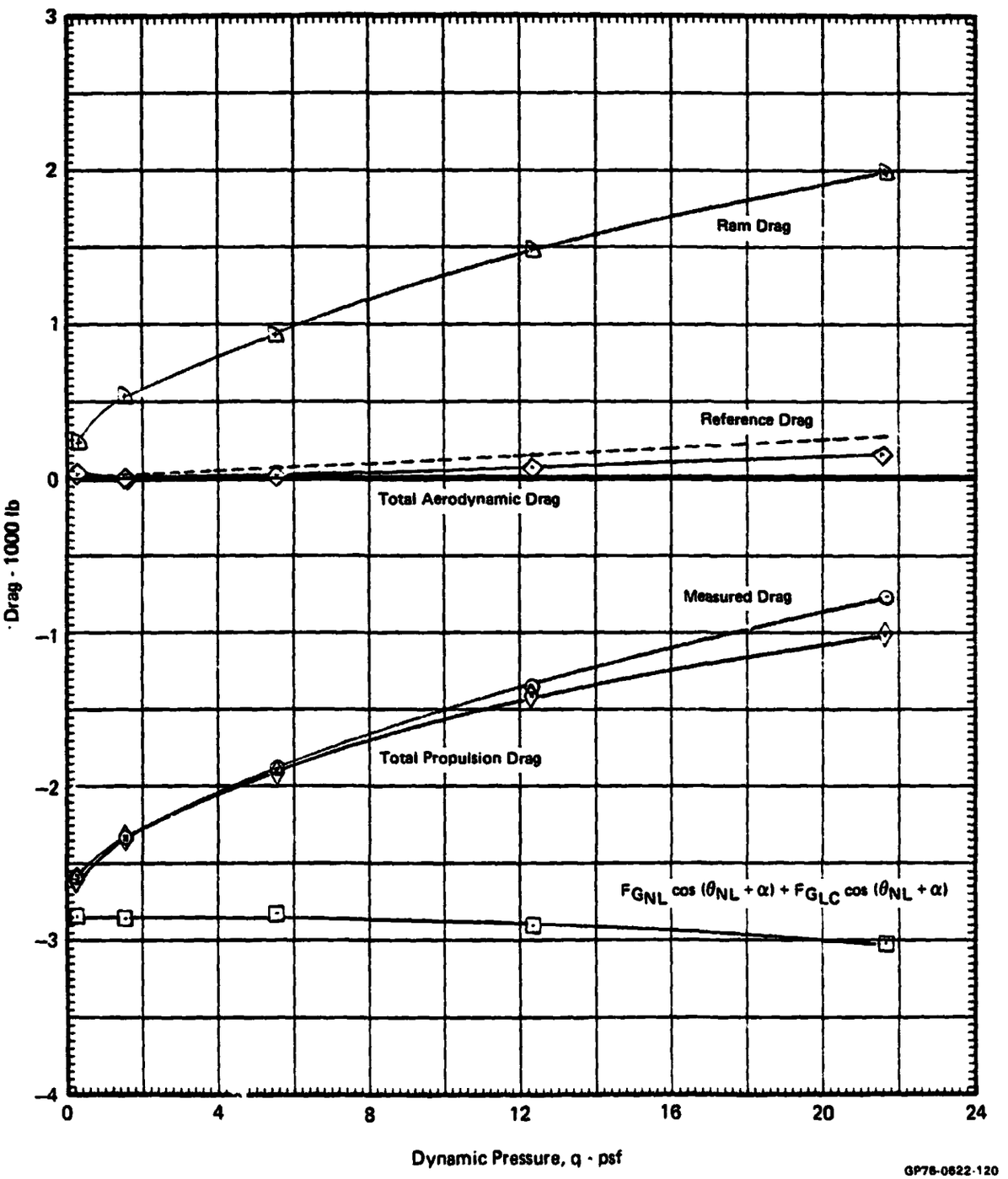

FIGURE 8.3-77
EFFECT OF NOSE LIFT UNIT ON TOTAL AERODYNAMIC LIFT
$\delta_{LC} = 0^0 \quad \alpha = 0^0$

$\delta_f = 15^0 \quad \delta_a = 10^0/10^0$ Horizontal Tail Off

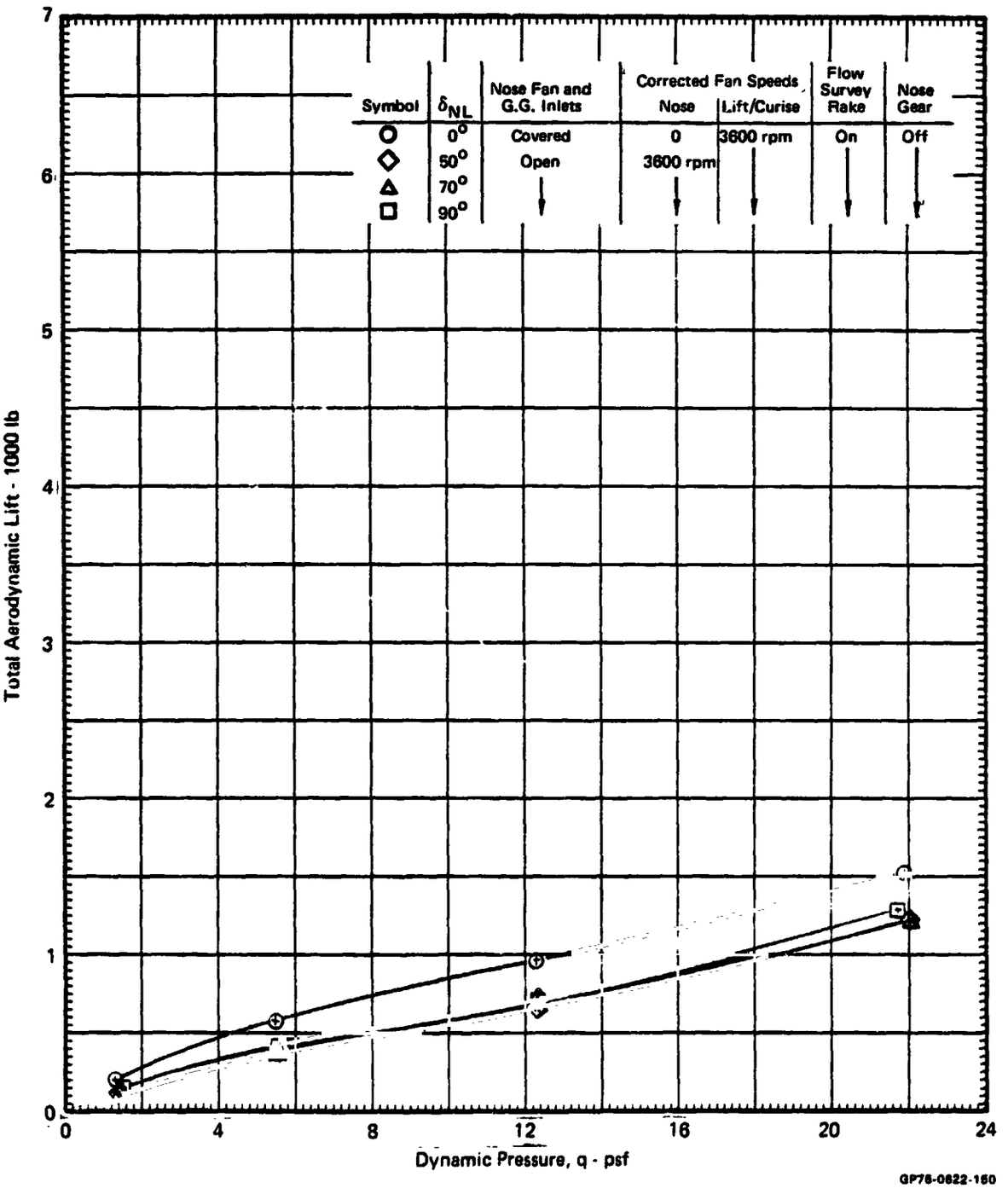

GP76-0622-160

FIGURE 8.3-78
EFFECT OF NOSE LIFT UNIT ON TOTAL AERODYNAMIC DRAG
$\delta_{LC} = 0^o \quad \alpha = 0^o$
$\delta_f = 15^o \quad \delta_a = 10^o/10^o$ Horizontal Tail Off

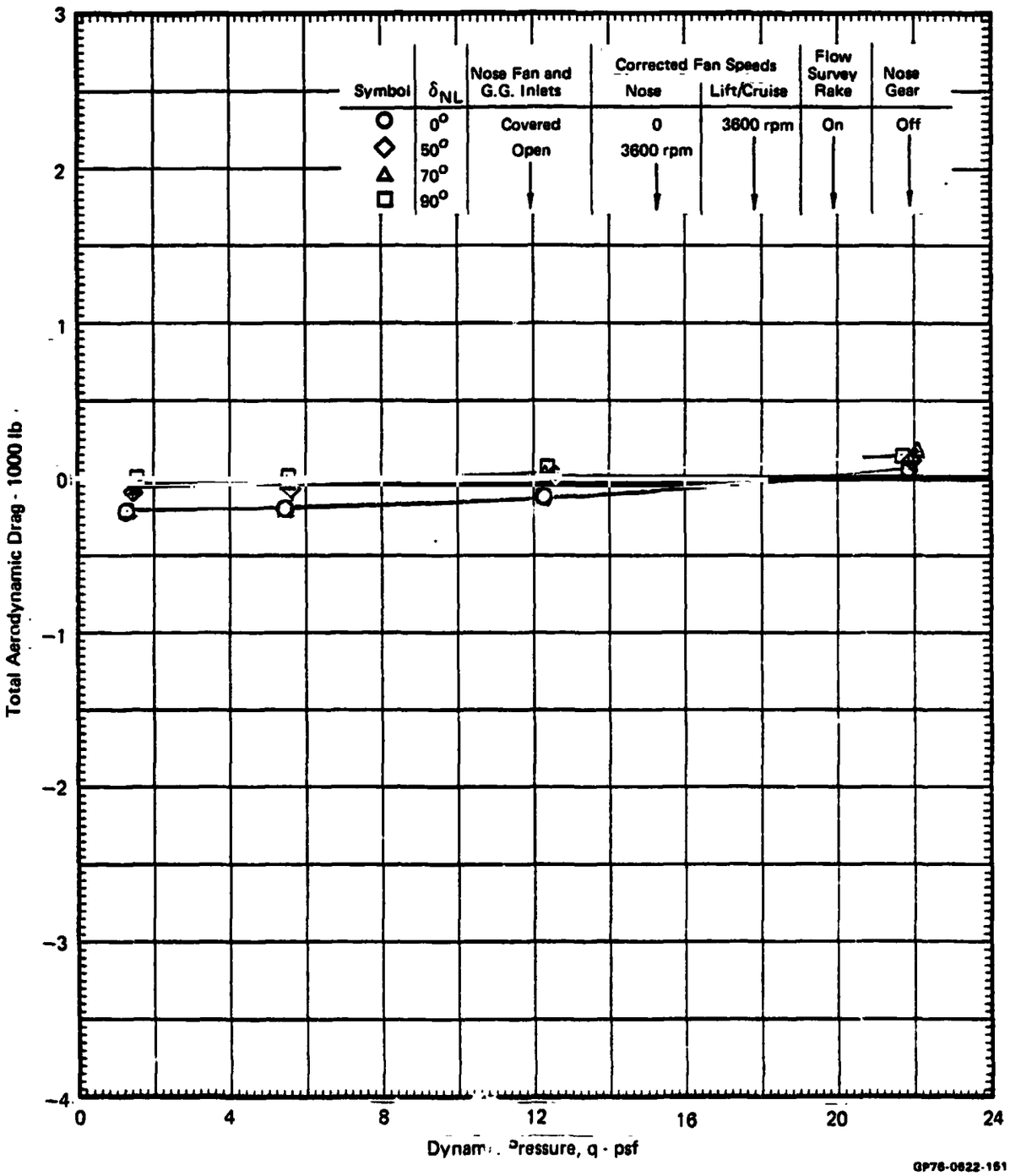

FIGURE 8.3-79
SUMMARY OF PROPULSION INDUCED EFFECTS AT 0° ANGLE OF ATTACK
EFFECT OF NOSE UNIT , HORIZONTAL TAIL OFF
$\delta_f = 15^o \quad \delta_a = 10^o/10^o$

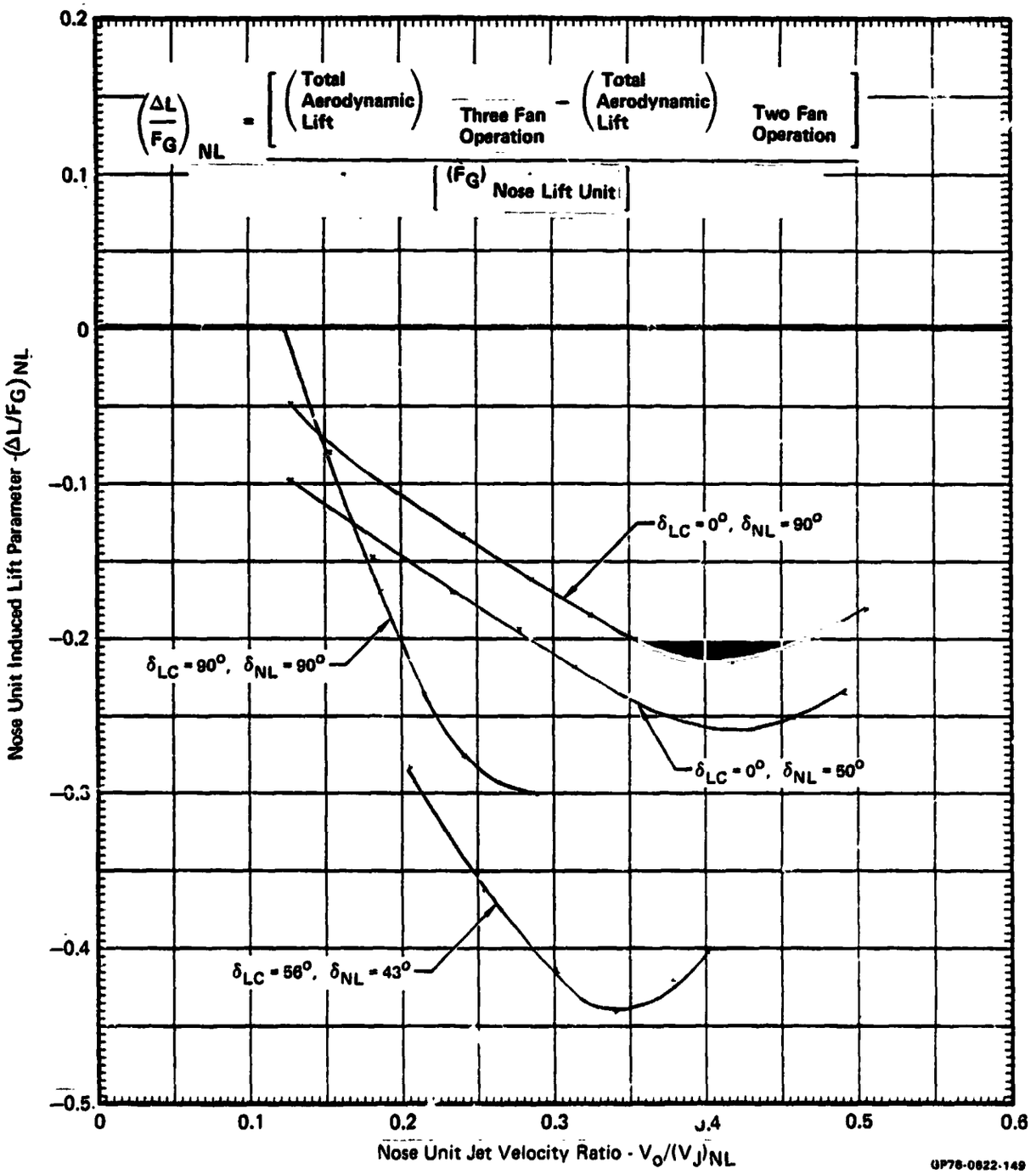

8.4 POWERED LIFT CONFIGURATION - PITCHING MOMENT CHARACTERISTICS

Total aircraft pitching moments for V/STOL aircraft must be balanced for all flight conditions from vertical takeoff through aerodynamic lift flight. The configuration tested was configured to provide moment balance at zero speed with the lift/cruise and nose lift units deflected at 90° (vertical takeoff), at all speeds and appropriate thrust deflections in powered lift flight and in aerodynamic lift flight.

There are two primary pitching moment trimming devices in powered lift flight - the horizontal tail and nose lift unit. Testing was conducted to obtain sufficient data to evaluate the proper distribution of trim moments from these two devices. During the preliminary and powered lift testing, the variation in total pitching moment with nose unit geometric deflection was evaluated. These tests, with the horizontal tail off and the flaps deflected 15° and the ailerons 10°, were conducted over a range of dynamic pressures for lift/cruise unit deflections of 0°, 56°, and 90°. The results of these tests, Figures 8.4-1 through 8.4-3, demonstrate the capability of nose lift unit to balance pitching moments due to the lift/cruise units and aerodynamic characteristics. These results were utilized to select the nose lift geometric deflections for the powered lift configuration testing. It should be noted that the nose lift geometric deflections are not necessarily optimum but are considered representative.

During the powered lift configuration testing, the five powered lift configurations were tested over a range of dynamic pressure with the horizontal tail on and, for three configurations, with the horizontal tail off. The results of these tests, Figures 8.4-4 through 8.4-8, illustrate the capability of the horizontal tail to trim any residual moments due to the lift/cruise and nose lift units.

FIGURE 8.4-1
PITCHING MOMENT vs NOSE LIFT UNIT GEOMETRIC DEFLECTION, FLOW SURVEY RAKE ON

$\delta_{LC} = 0^{o}$ $\alpha = 0^{o}$

Measured Data

$\delta_f = 15^{o}$ $\delta_a = 10^{o}/10^{o}$ NOSE GEAR OFF

$N_E/\sqrt{\theta_{T_o}} = 3800$ RPM

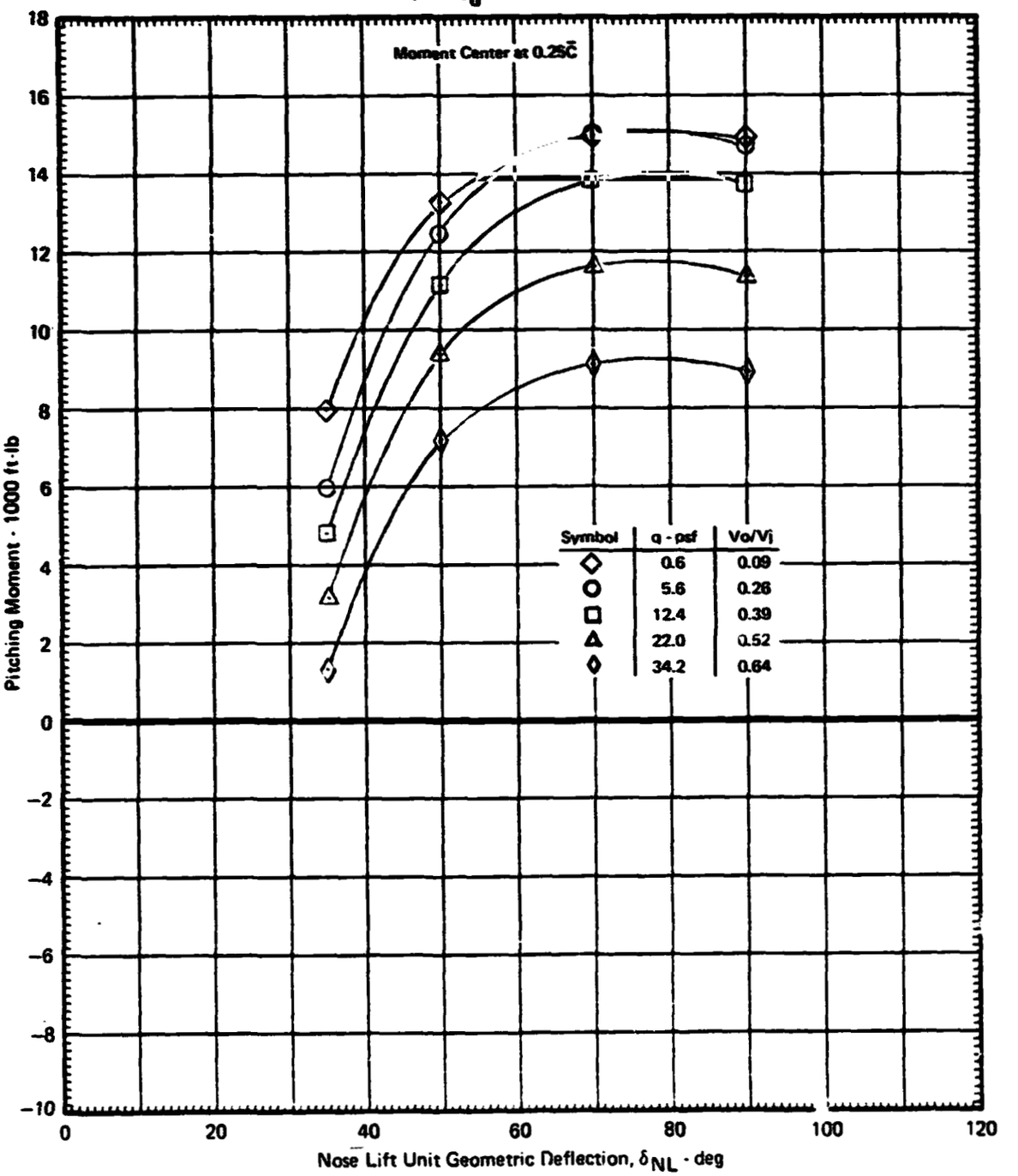

GP78-0622-232

FIGURE 8.4-2
PITCHING MOMENT vs NOSE LIFT UNIT GEOMETRIC DEFLECTION, HORIZONTAL TAIL OFF

$\alpha = 0^{o}$ $\delta_{LC} = 56^{o}$

Measured Data

$\delta_f = 15^{o}$ $\delta_a = 10^{o}/10^{o}$ Nose Gear On

$N_F/\sqrt{\theta_{T_o}} = 3600$ RPM

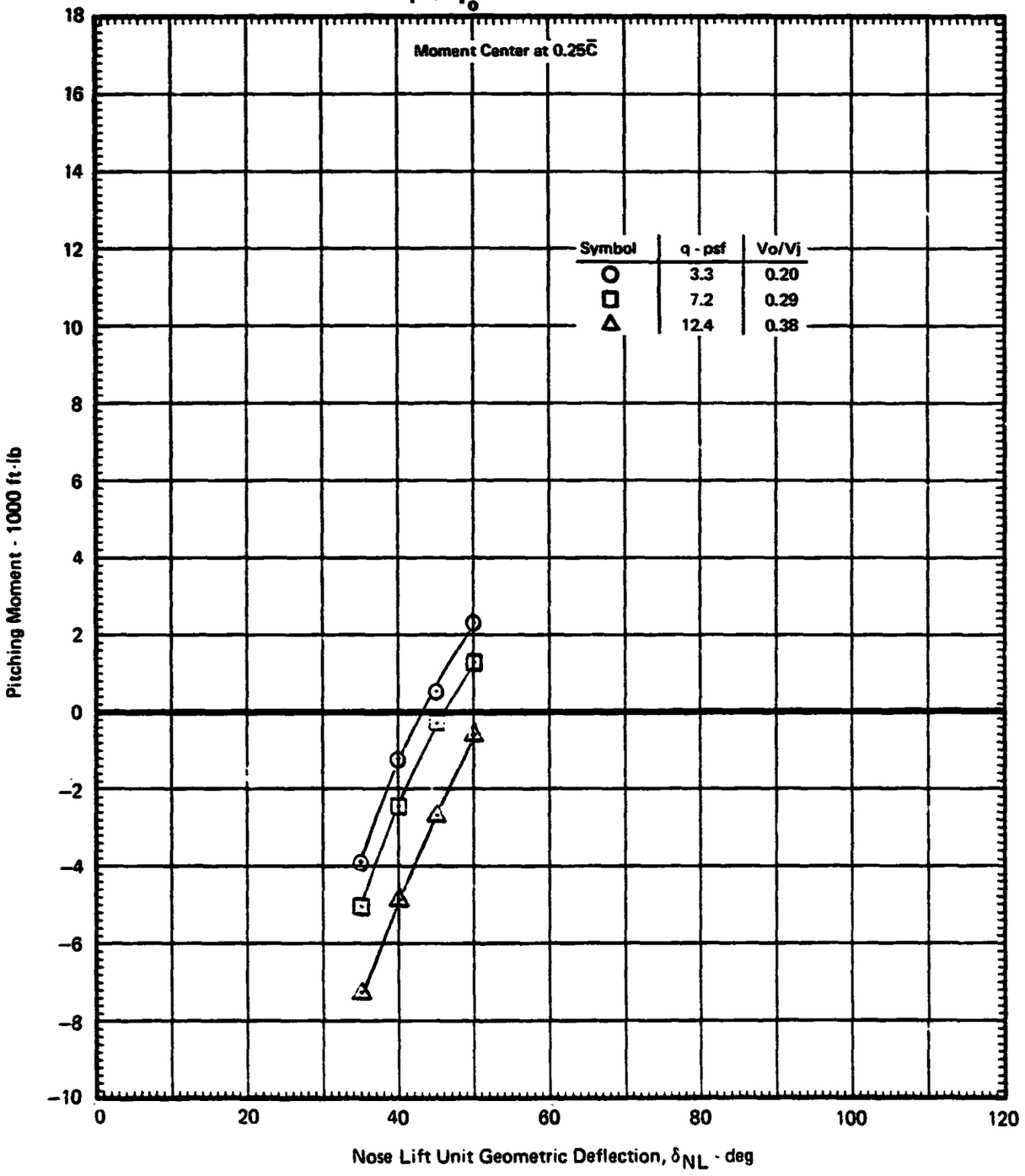

GP76-0622-233

FIGURE 8.4-3
PITCHING MOMENT vs NOSE LIFT UNIT GEOMETRIC DEFLECTION, HORIZONTAL TAIL OFF

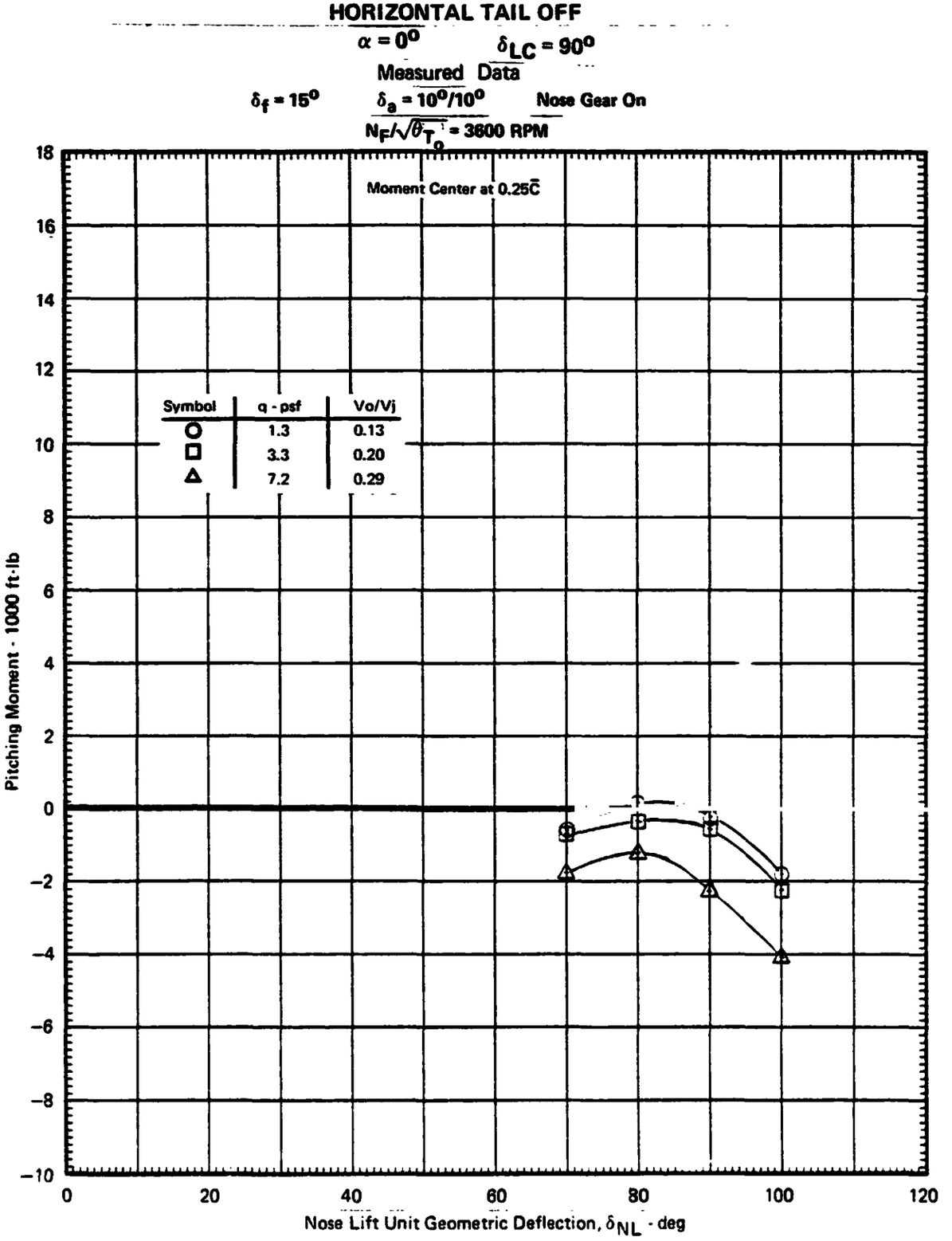

GP76-0822-234

FIGURE 8.4-4

PITCHING MOMENT vs DYNAMIC PRESSURE

$\alpha = 0^o$ $\delta_{LC} = 23^o$ $\delta_{NL} = 43^o$ $\theta_J = 20.1^o$

Measured Data

$\delta_f = 15^o$ $\delta_a = 10^o/10^o$ Nose Gear On

$N_F/\sqrt{\theta_{T_o}} = 3600$ RPM

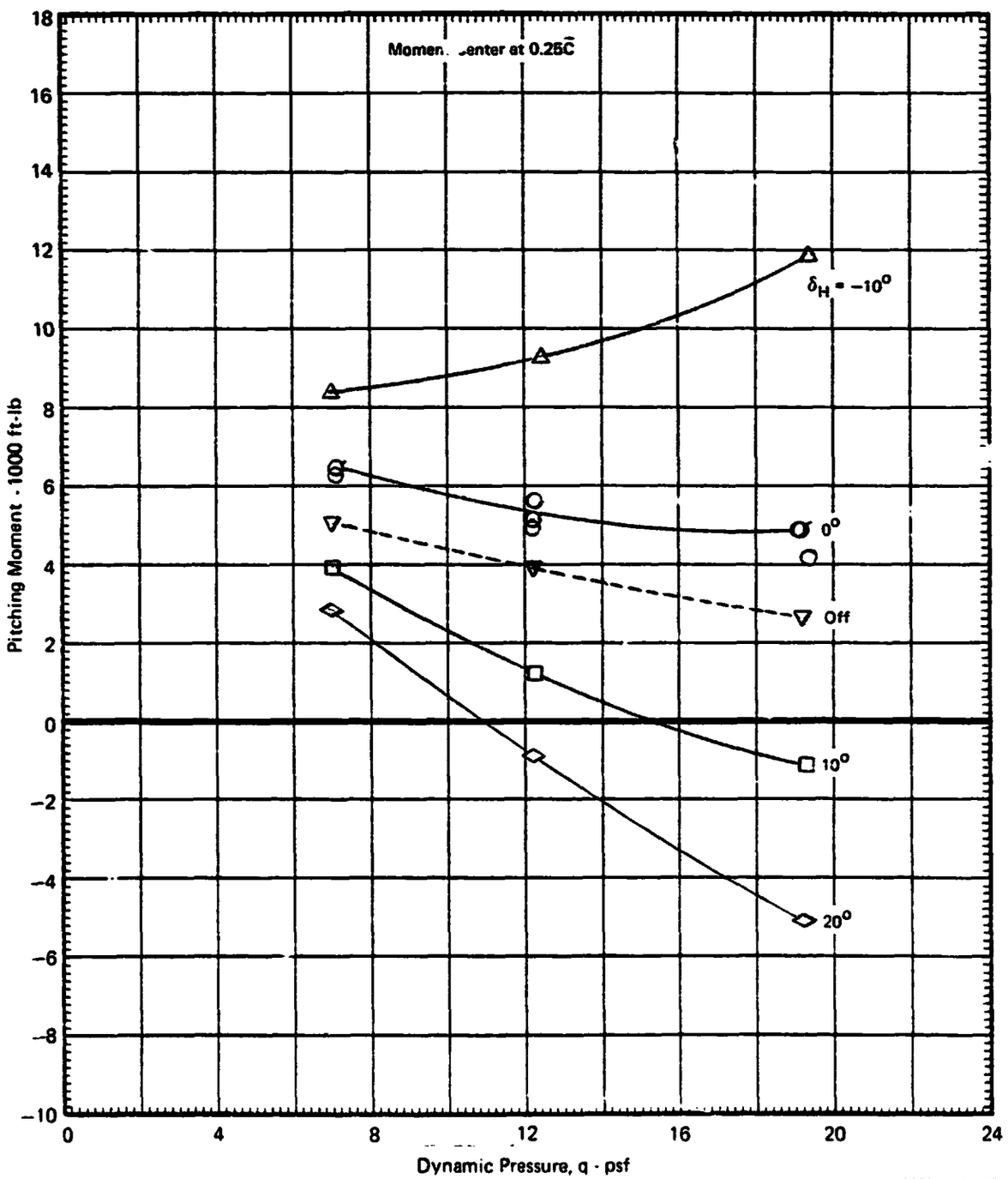

GP78-0822-167

FIGURE 8.4-5

PITCHING MOMENT vs DYNAMIC PRESSURE

$\alpha = 0^o$ $\delta_{LC} = 38^o$ $\delta_{NL} = 43^o$ $\theta_J = 29.2^o$

Measured Data

$\delta_f = 15^o$ $\delta_a = 10^o/10^o$ Nose Gear On

$N_F/\sqrt{\theta_{T_o}} = 3600$ RPM

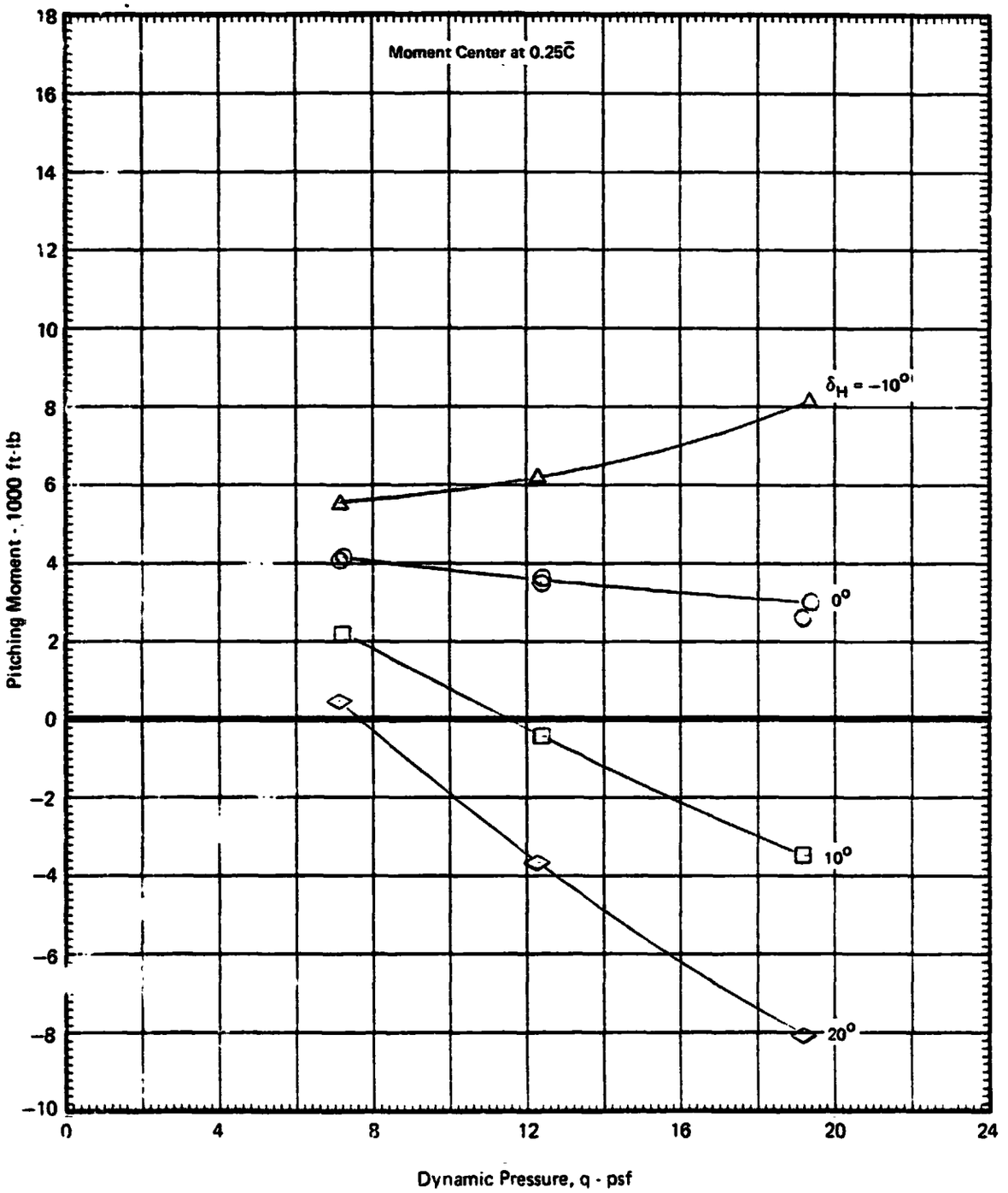

GP76-0622-168

FIGURE 8.4-6
PITCHING MOMENT vs DYNAMIC PRESSURE
$\alpha = 0^0$ $\delta_{LC} = 56^0$ $\delta_{NL} = 43^0$ $\theta_J = 44.5^0$
Measured Data
$\delta_f = 15^0$ $\delta_a = 10^0/10^0$ Nose Gear On
$N_F/\sqrt{\theta_{T_0}} = 3600$ RPM

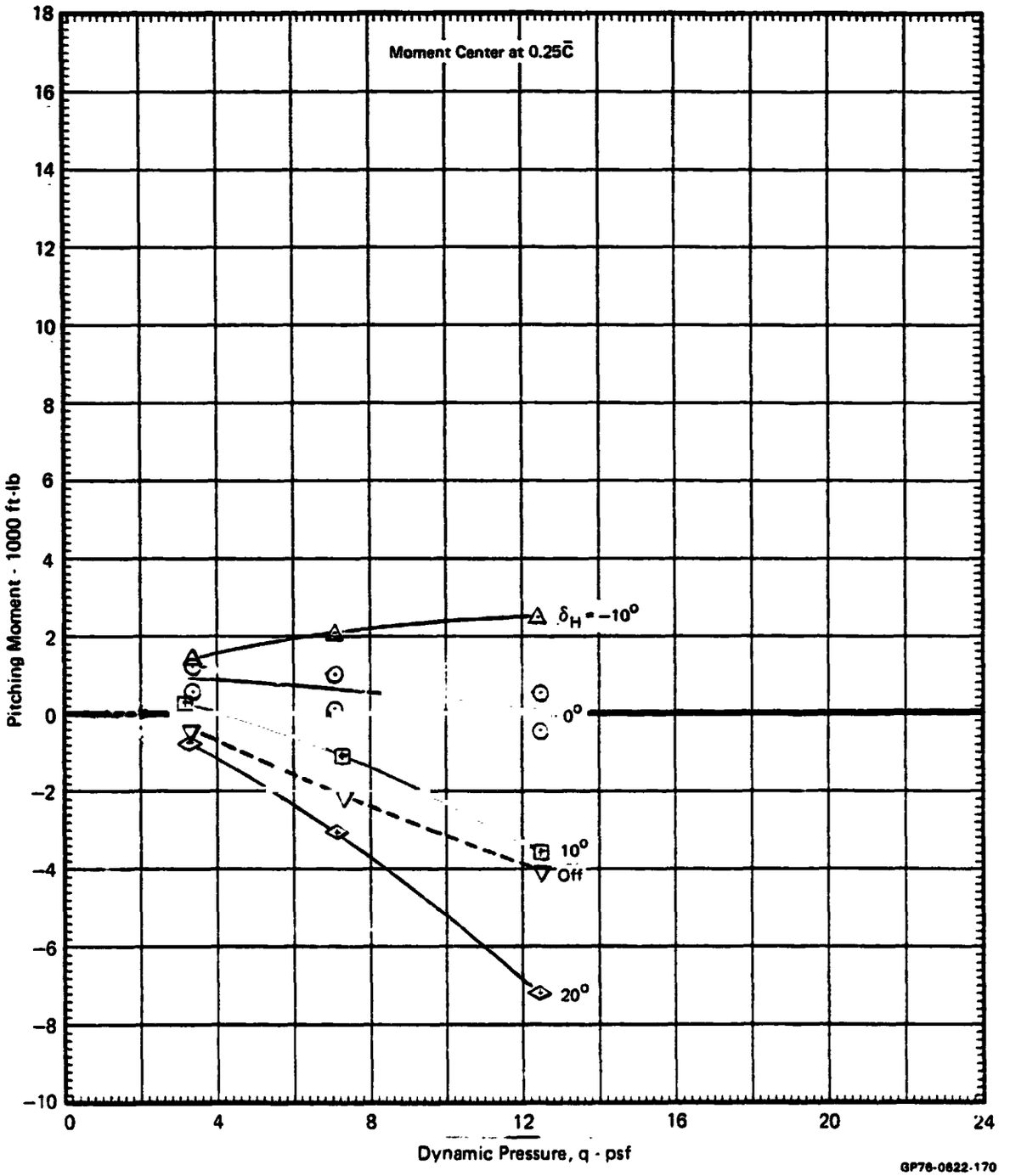

FIGURE 8.4-7
PITCHING MOMENT vs DYNAMIC PRESSURE
$\alpha = 0^o$ $\delta_{LC} = 71^o$ $\delta_{NL} = 55^o$ $\theta_J = 59.8^o$
Measured Data
$\delta_f = 15^o$ $\delta_a = 10^o/10^o$ Nose Gear On
$\overline{N_F/\sqrt{\theta_{T_o}}} = 3600$ RPM

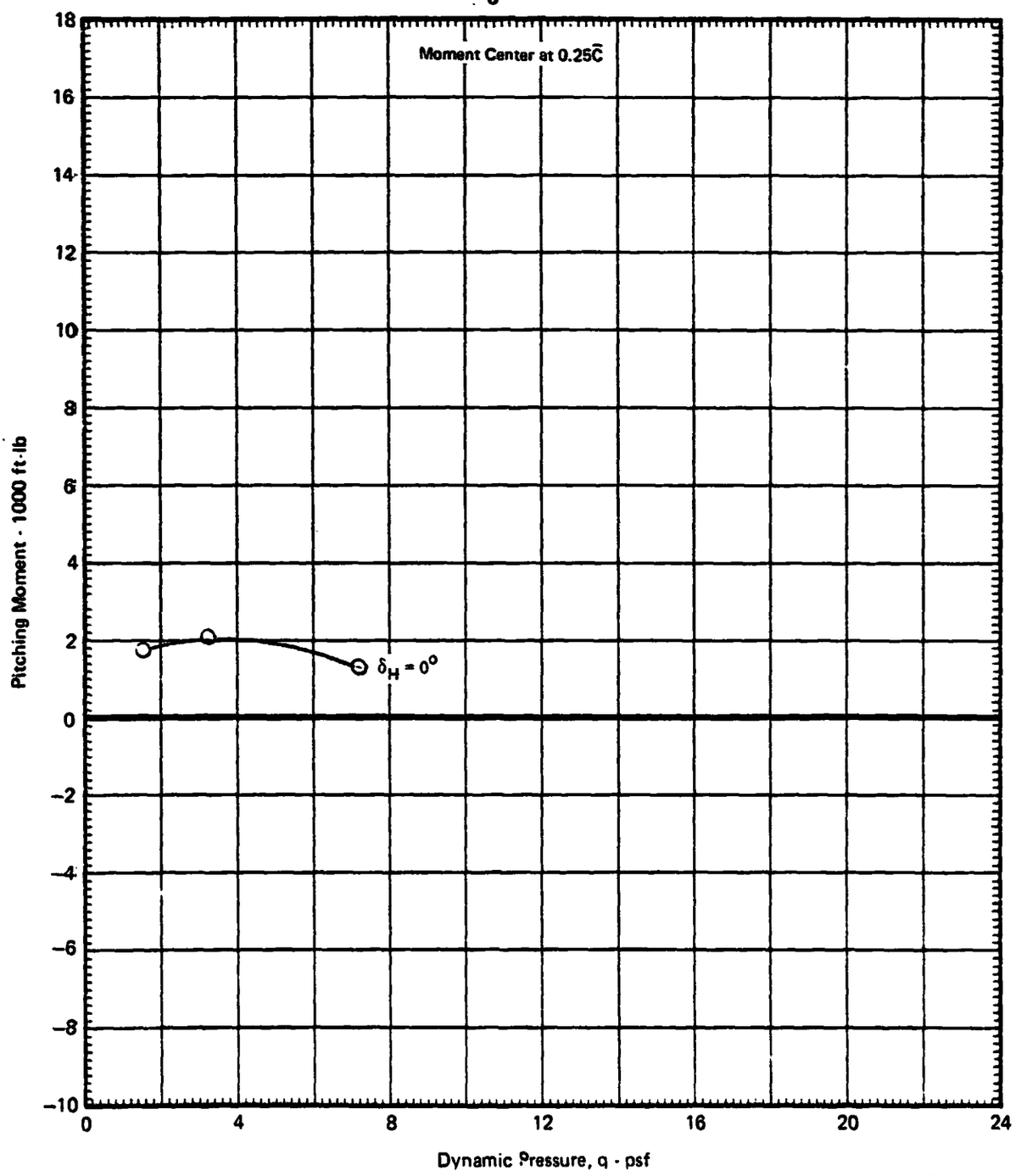

GP76-0622-169

FIGURE 8.4-8
PITCHING MOMENT vs DYNAMIC PRESSURE
$\alpha = 0^o$ $\delta_{LC} = 90^o$ $\delta_{NL} = 90^o$ $\theta_J = 84.7^o$
Measured Data
$\delta_f = 15^o$ $\delta_a = 10^o/10^o$ Nose Gear On
$N_F/\sqrt{\theta_{T_o}} = 3600$ RPM

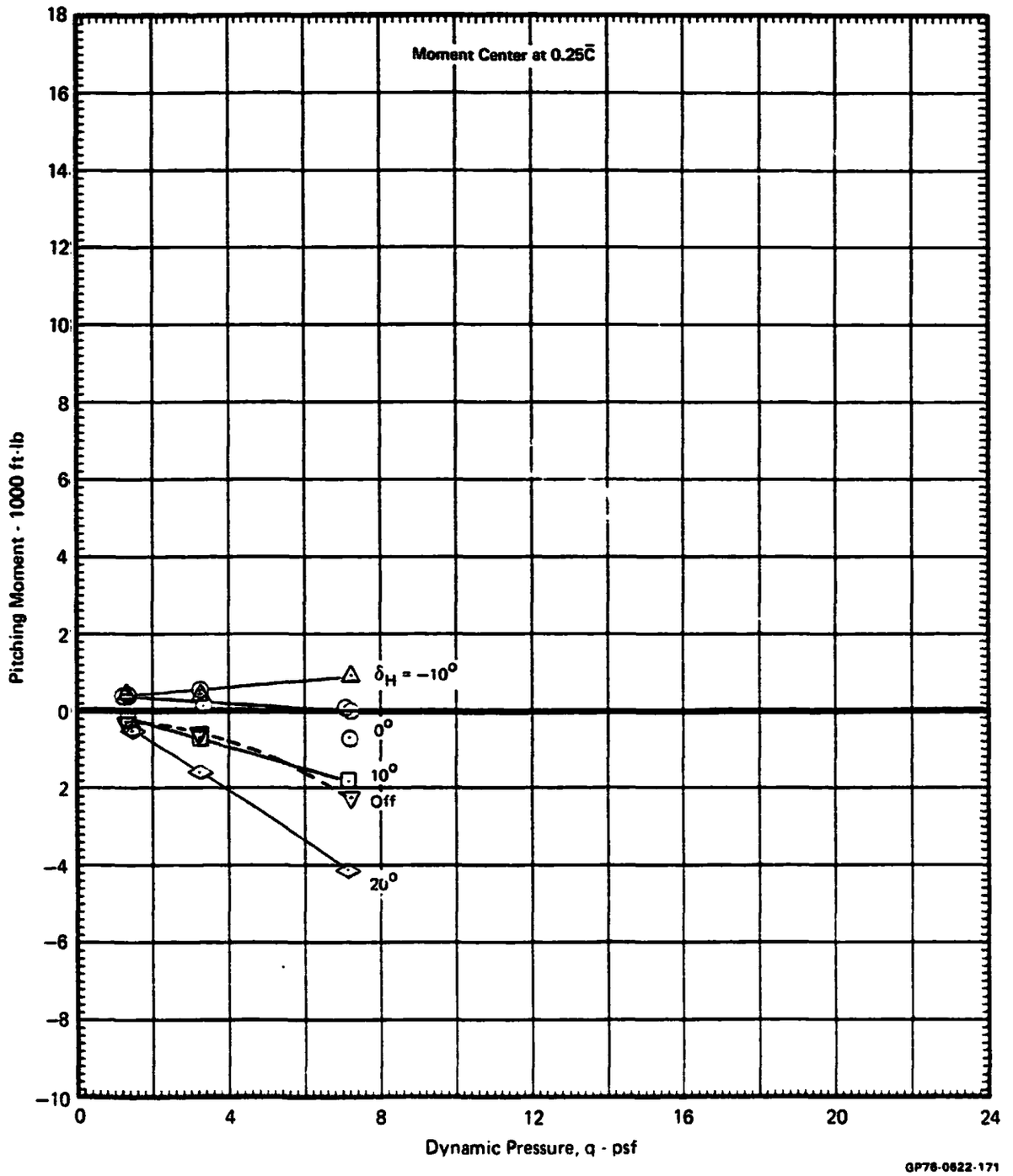

GP76-0622-171

8.5 POWERED LIFT CONFIGURATION - LATERAL-DIRECTIONAL CHARACTERISTICS

Three powered lift configurations were tested at 0° angle of attack with variations in angle of sideslip from -4° to 12° or 20°. The detailed results of these tests are shown in Figures 8.5-1 through 8.5-16 for resultant thrust vector angles of 20.1°, 44.5° and 84.7°. These data show asymmetries at 0° angle of sideslip (for example, Figure 8.5-4) and non-uniform variation with angle of sideslip (Figure 8.5-12). The probable cause of these discrepancies is the difficulty of precisely setting equal lift/cruise unit thrusts and maintaining these equal values for the 10 to 20 minutes required to complete a given angle of sideslip test run. The net resulting rolling and yawing moments at 0° sideslip are the result of adding two large and balancing components from the left and right lift/cruise units.

Figures 8.5-17 and 8.5-18 present the directional stability derivatives for the powered lift configuration in dimensional and coefficient form. These data show the dominant effects of the propulsion system and the resulting directional instability at low jet velocity ratios. The primary source of yawing moment due to the propulsion system at low jet velocity ratios is due to the nose fan inlet mass flow during sideslip. At higher jet velocity ratios, the aerodynamic contribution becomes the dominant term. Figures 8.5-19 through 8.5-20 and 8.5-21 through 8.5-22 present the lateral stability and side force derivatives, respectively. These data show less propulsion system effects than the directional data. The configuration is laterally stable at all but one condition tested. For this condition, shown in Figure 8.5-6, the abrupt stable change in rolling moment between 4 and 8 degrees angle of sideslip demonstrates the difficulty of objectively determining representative slopes at 0° angle of sideslip.

Lateral-Directional Control Effectiveness

Aileron control effectiveness data are presented in Figure 8.5-23 and 8.5-24 for one powered lift configuration with θ_J = 44.5 (δ_{LC} = 56°, δ_{NL} = 43°) at 0° angle of attack. The data show the effect of varying the left aileron from +25° (TED) to -25° (TEU) with the right aileron at +10° (TED). Also shown are data for equal differential aileron deflections of $\pm$25° on Figure 8.5-23 only.

Rudder control effectiveness is shown in Figure 8.5.25 for one powered lift configuration with θ_J = 29.2° (δ_{LC} = 38°, δ_{NL} = 43°, δ_r = 23°) for two dynamic pressure values over a large angle of attack range.

FIGURE 8.5-1
YAWING MOMENT vs ANGLE OF SIDESLIP
$\delta_H = 0^o$ $\alpha = 0^o$ $\delta_{LC} = 23^o$ $\delta_{NL} = 43^o$ $\theta_J = 20.1^o$ q = 12.4 PSF
Graphical Summary of Measured and Calculated Force and Moment Data
$\delta_f = 15^o$ $\delta_a = 10^o/10^o$ Nose Gear On
$N_F/\sqrt{\theta_{T_o}} = 3600$ RPM

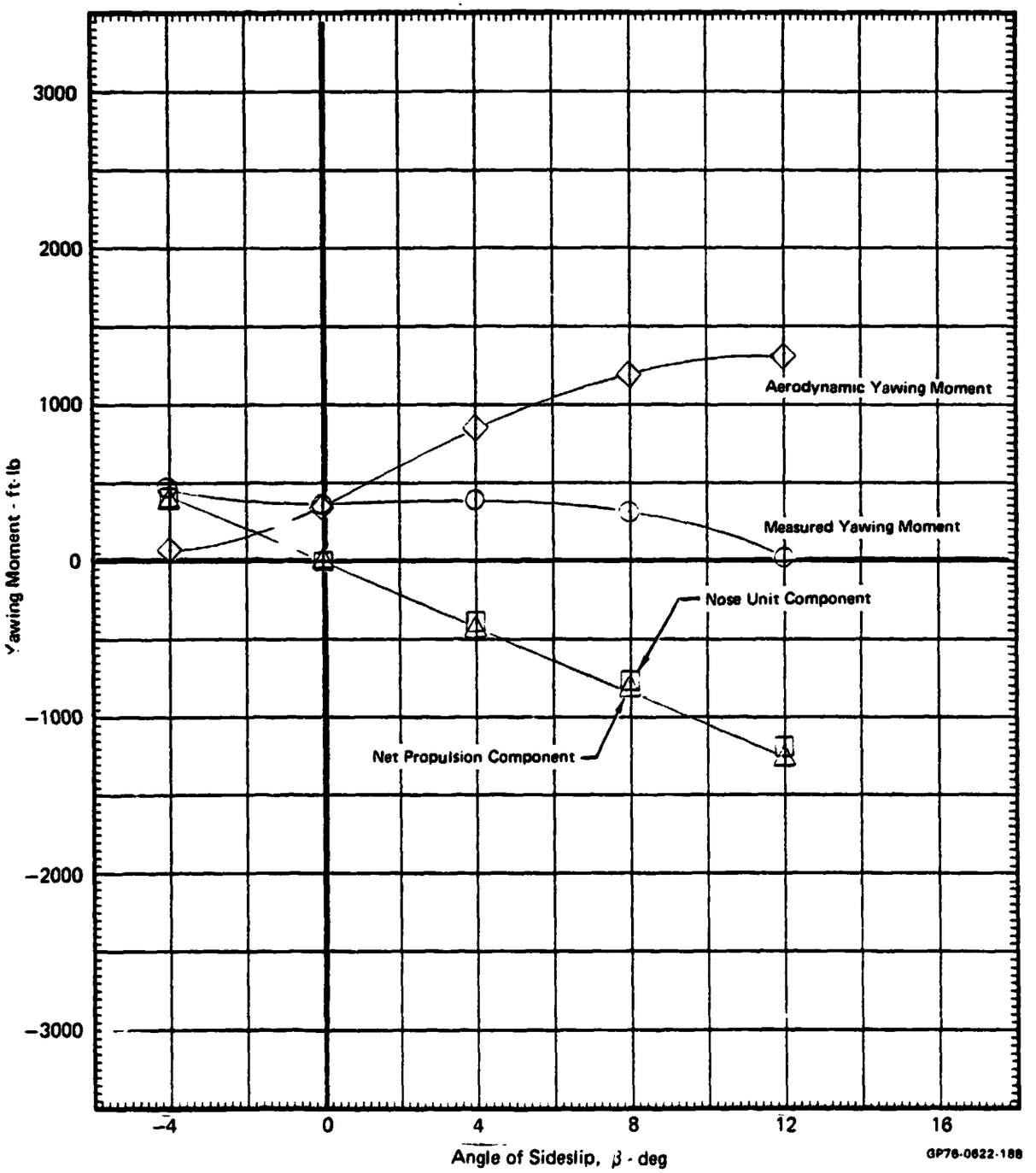

FIGURE 8.5-2
ROLLING MOMENT AND SIDE FORCE vs ANGLE OF SIDESLIP
$\delta_H = 0^o$ $\alpha = 0^o$ $\delta_{LC} = 23^o$ $\delta_{NL} = 43^o$ $\theta_J = 20.1^o$ q = 12.4 PSF
Graphical Summary of Measured and Calculated Force and Moment Data
$\delta_f = 15^o$ $\delta_a = 10^o/10^o$ Nose Gear On
$N_F/\sqrt{\theta_{T_o}} = 3600$ R. M

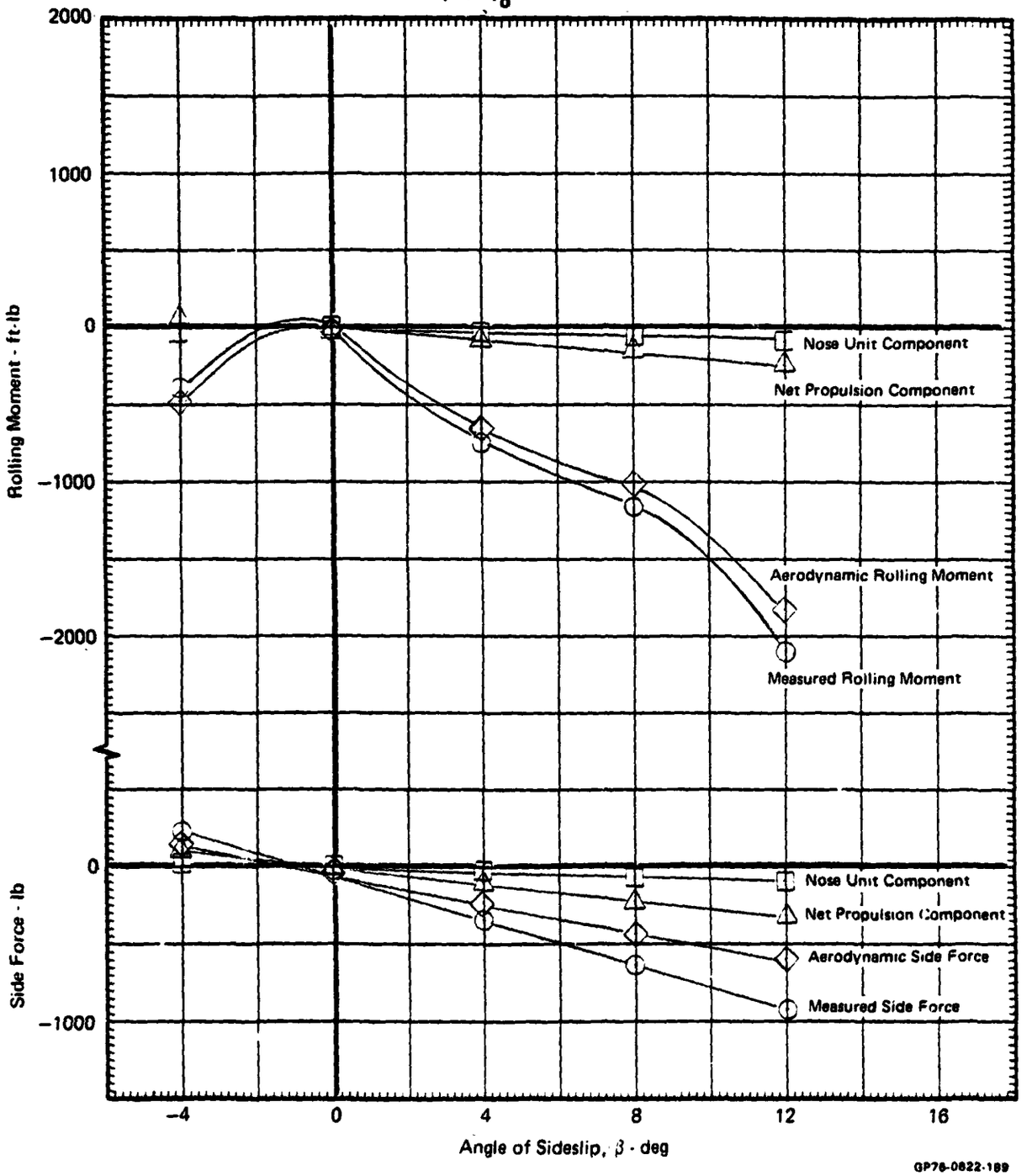

FIGURE 8.5-3
YAWING MOMENT vs ANGLE OF SIDESLIP
$\delta_H = 0^o$ $\alpha = 0^o$ $\delta_{LC} = 23^o$ $\delta_{NL} = 43^o$ $\theta_J = 20.1^o$ $q = 19.4$ PSF
Graphical Summary of Measured and Calculated Force and Moment Data
$\delta_f = 15^o$ $\delta_a = 10^o/10^o$ Nose Gear On
$N_F/\sqrt{\theta_{T_o}} = 3600$ RPM

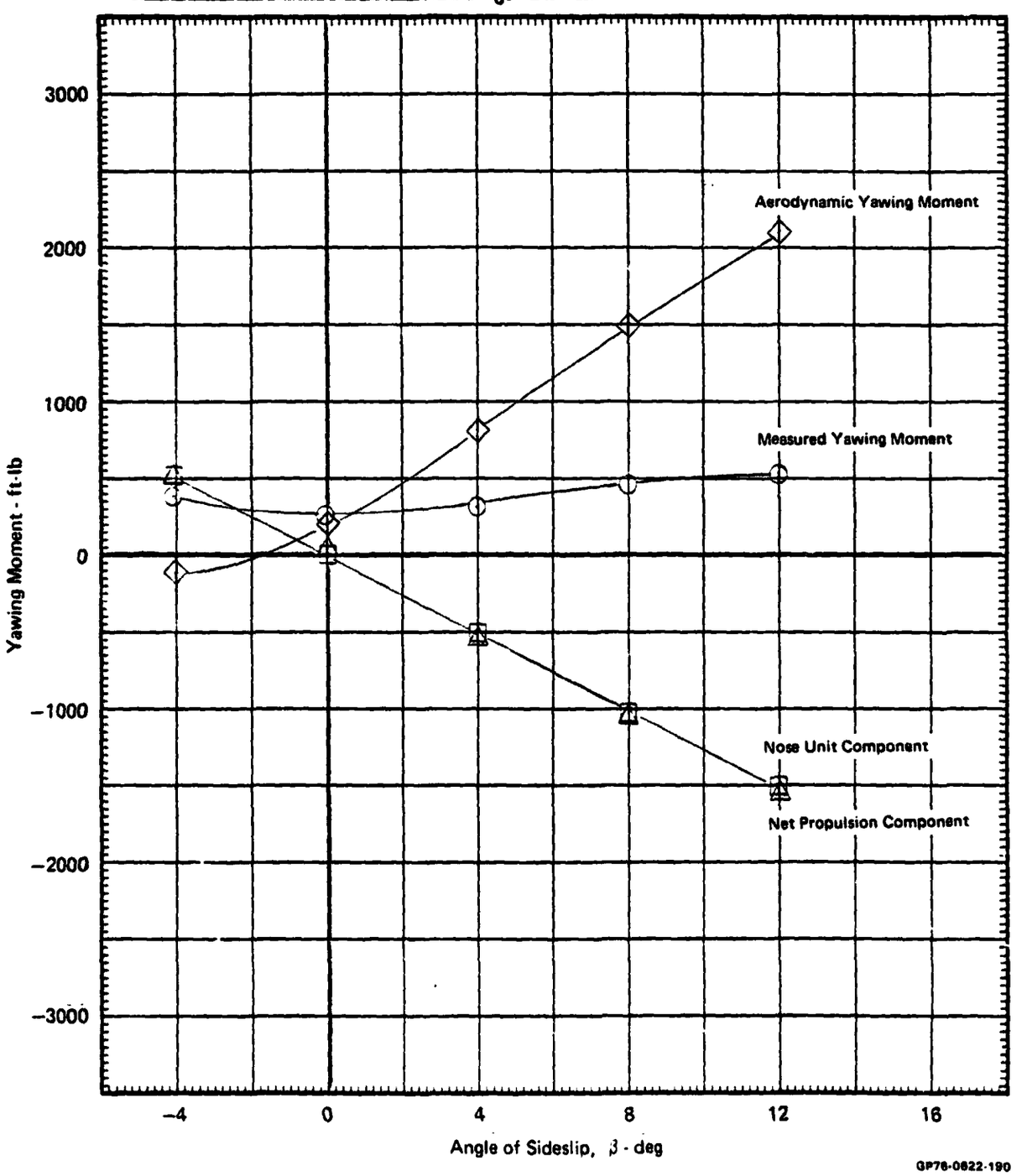

FIGURE 8.5-4
ROLLING MOMENT AND SIDE FORCE vs ANGLE OF SIDESLIP
$\delta_H = 0^o$ $\alpha = 0^o$ $\delta_{LC} = 23^o$ $\delta_{NL} = 43^o$ $\theta_J = 20.1^o$ q = 19.4 PSF
Graphic Summary of Measured and Calculated Force and Moment Data
$\delta_f = 15^o$ $\delta_a = 10^o/10^o$ Nose Gear On
$N_F/\sqrt{\theta_{T_o}} = 3600$ RPM

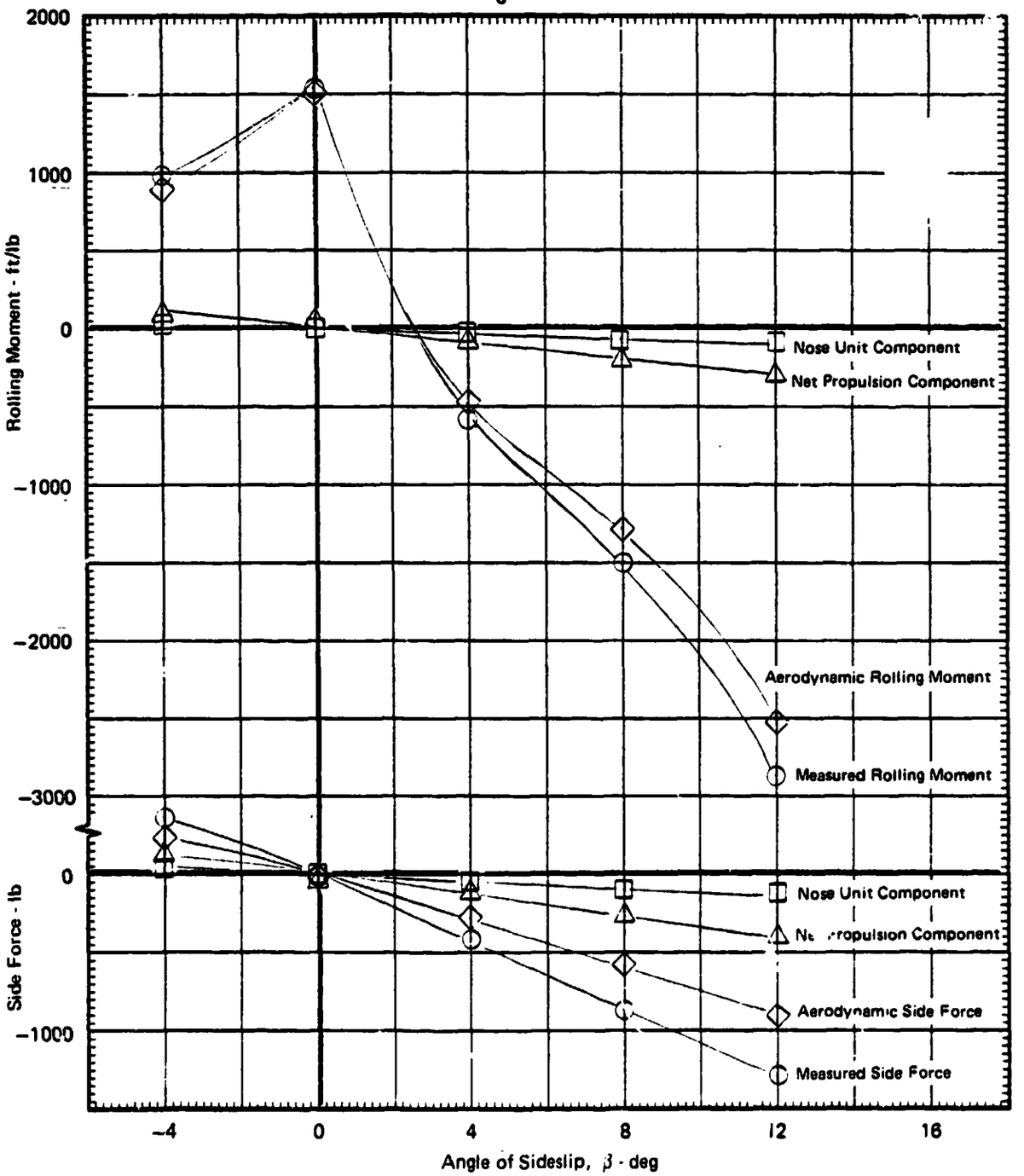

FIGURE 8.5-5

YAWING MOMENT vs ANGLE OF SIDESLIP

$\delta_H = 0^o$ $\alpha = 0^o$ $\delta_{LC} = 56^o$ $\delta_{NL} = 43^o$ $\theta_J = 44.5^o$ $q = 3.2$ PSF

Graphical Summary of Measured and Calculated Force and Moment Data

$\delta_f = 15^o$ $\delta_a = 10^o/10^o$ Nose Gear On

$N_F/\sqrt{\theta_{T_o}} = 3600$ RPM

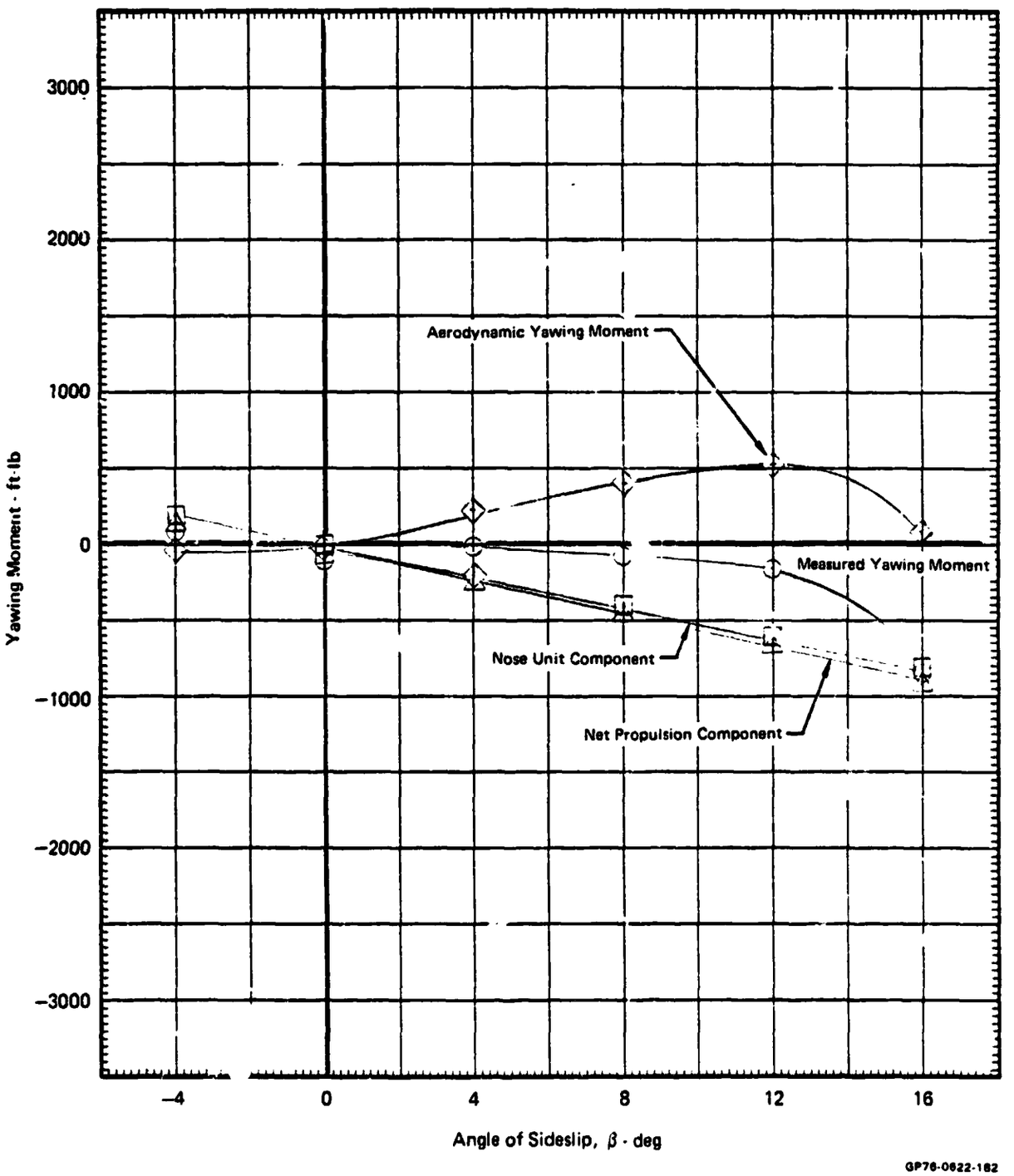

GP76-0622-182

FIGURE 8.5-6

ROLLING MOMENT AND SIDE FORCE vs ANGLE OF SIDESLIP

$\delta_H = 0^o$ $\alpha = 0^o$ $\delta_{LC} = 56^o$ $\delta_{NL} = 43^o$ $\theta_J = 44.5^o$ $q = 3.2$ PSF

Graphical Summary of Measured and Calculated Force and Moment Data

$\delta_f = 15^o$ $\delta_a = 10^o/10^o$ Nose Gear On

$N_F/\sqrt{\theta_{T_o}} = 3600$ RPM

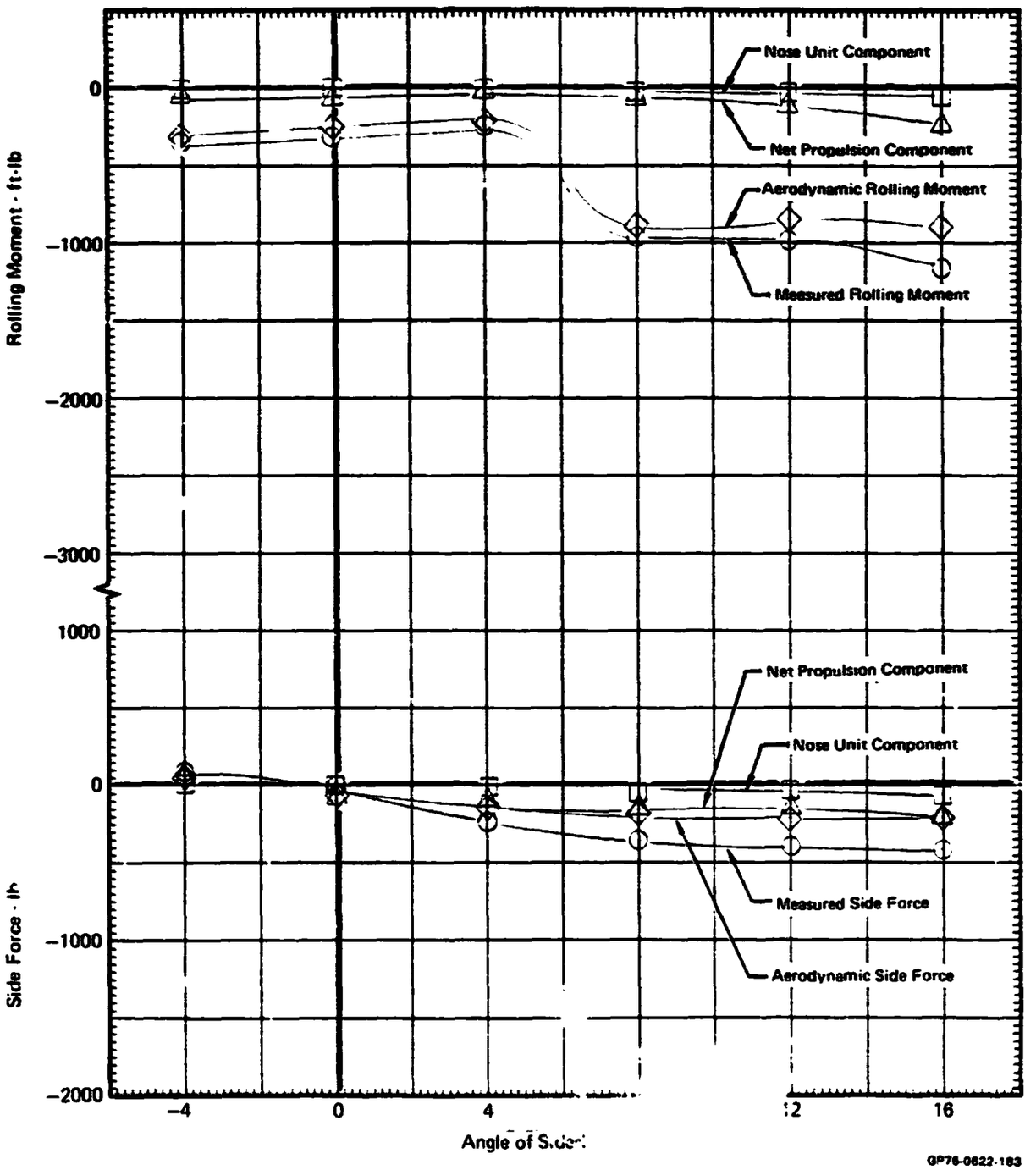

GP76-0622-183

FIGURE 8.5-7

YAWING MOMENT vs ANGLE OF SIDESLIP

$\delta_H = 0^o$ $\alpha = 0^o$ $\delta_{LC} = 56^o$ $\delta_{NL} = 43^o$ $\theta_J = 44.5^o$ $q = 7.1$ PSF

Graphical Summary of Measured and Calculated Force and Moment Data

$\delta_f = 15^o$ $\delta_a = 10^o/10^o$ Nose Gear On

$N_F/\sqrt{\theta_{T_0}} = 3600$ RPM

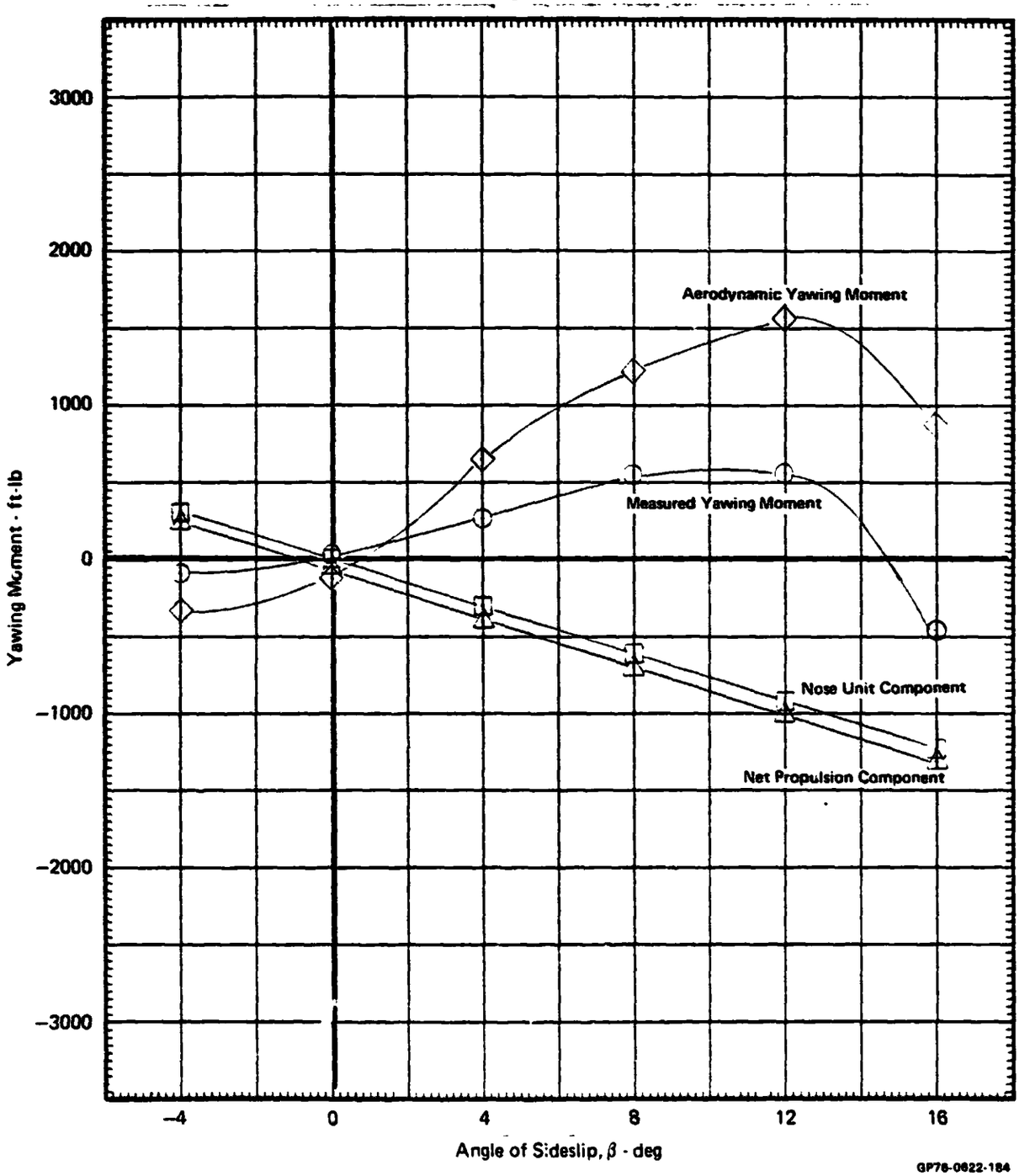

FIGURE 8.5-8

ROLLING MOMENT AND SIDE FORCE vs ANGLE OF SIDESLIP

$\delta_H = 0^o$ $\alpha = 0^o$ $\delta_{LC} = 56^o$ $\delta_{NL} = 43^o$ $\theta_J = 44.5^o$ $q = 7.1$ PSF

Graphical Summary of Measured and Calculated Force and Moment Data

$\delta_f = 15^o$ $\delta_a = 10^o/10^o$ Nose Gear On

$N_F/\sqrt{\theta_{T_o}} = 3600$ RPM

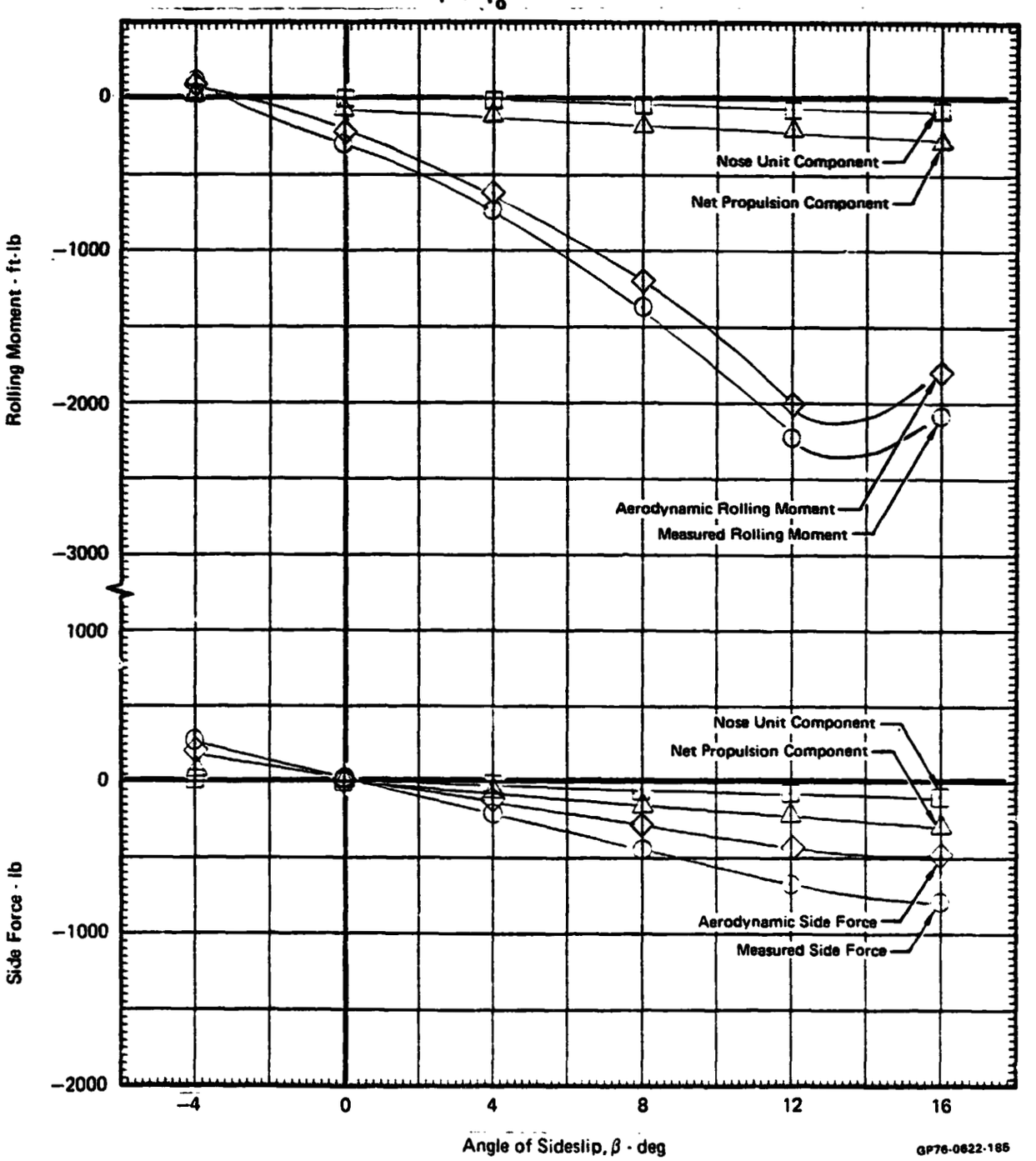

FIGURE 8.5-9

YAWING MOMENT vs ANGLE OF SIDESLIP

$\delta_H = 0^o$ $\alpha = 0^o$ $\delta_{LC} = 56^o$ $\delta_{NL} = 43^o$ $\theta_J = 44.5^o$ $q = 12.2$ PSF

Graphical Summary of Measured and Calculated Force and Moment Data

$\delta_f = 15^o$ $\delta_a = 10^o/10^o$ Nose Gear On

$N_F/\sqrt{\theta_{T_o}} = 3800$ RPM

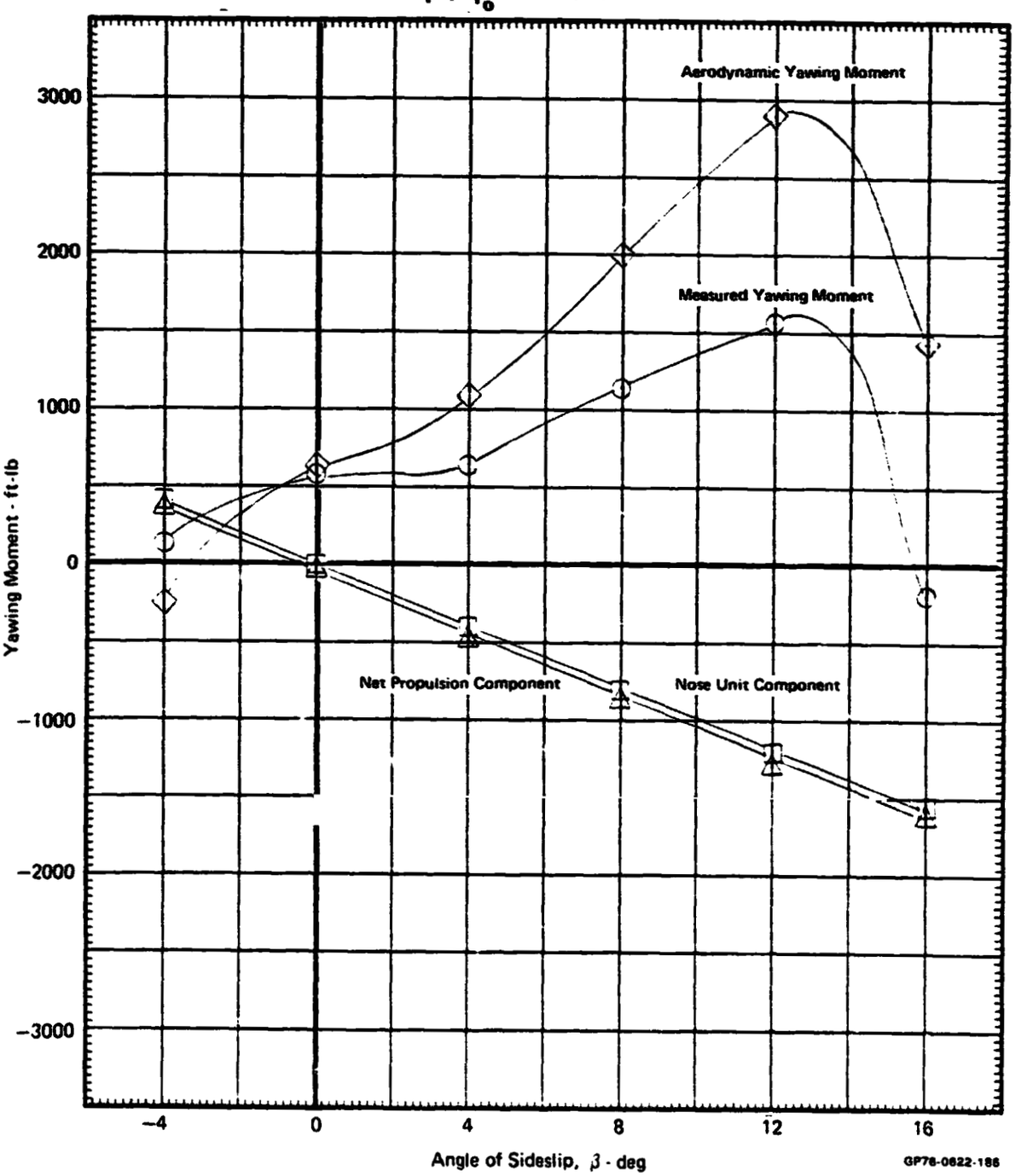

FIGURE 8.5-10

ROLLING MOMENT AND SIDE FORCE vs ANGLE OF SIDESLIP

$\delta_H = 0^o$ $\alpha = 0^o$ $\delta_{LC} = 56^o$ $\delta_{NL} = 43^o$ $\theta_J = 44.5^o$ $q = 12.2$ PSF

Graphical Summary of Measured and Calculated Force and Moment Data

$\delta_f = 15^o$ $\delta_a = 10^o/10^o$ Nose Gear On

$N_F/\sqrt{\theta_{T_o}} = 3600$ RPM

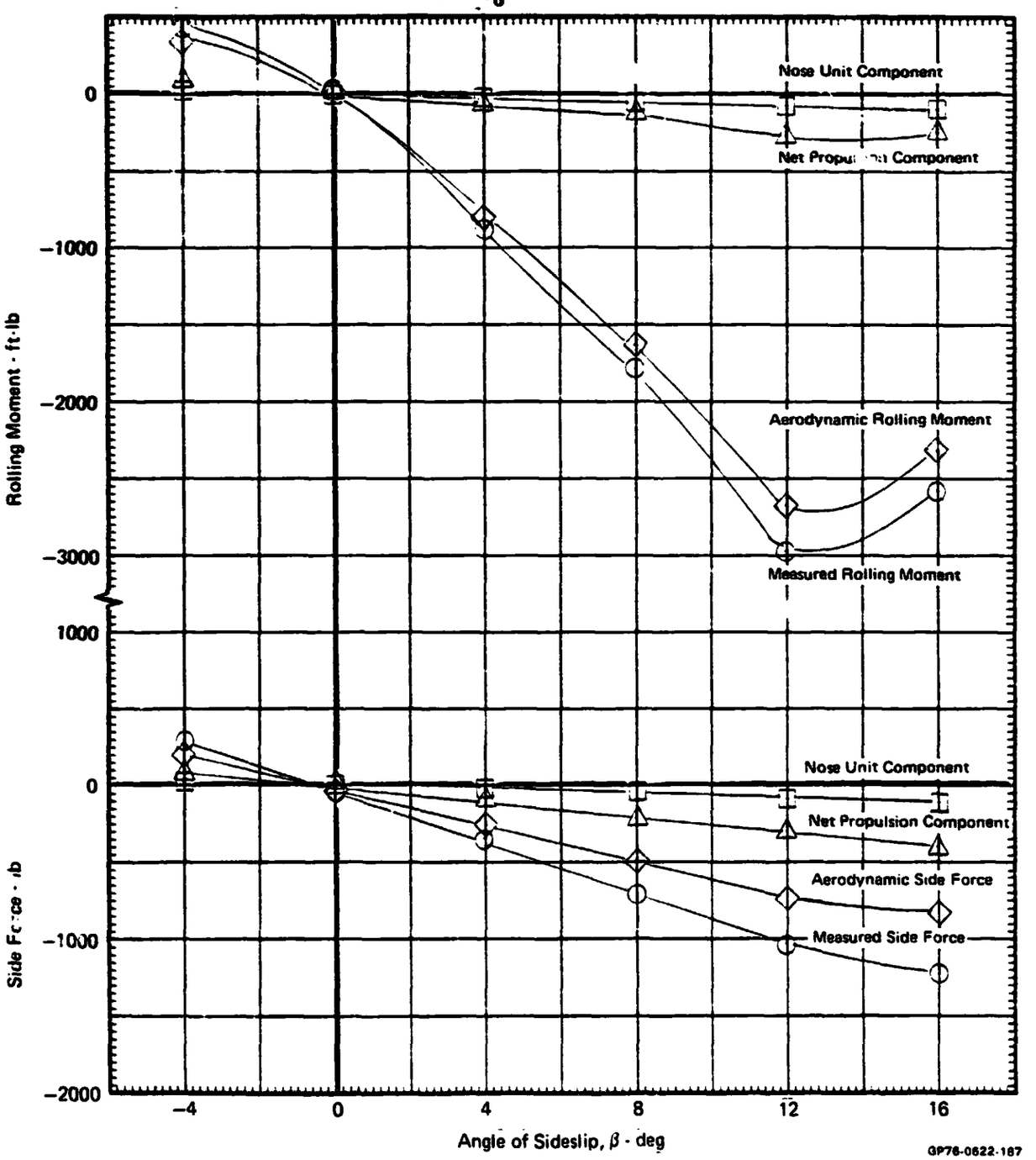

FIGURE 8.5-11
YAWING MOMENT vs ANGLE OF SIDESLIP
$\delta_H = 0^o$ $\alpha = 0^o$ $\delta_{LC} = 90^o$ $\delta_{NL} = 90^o$ $\theta_J = 84.7^o$ q = 1.4 PSF
Graphical Summary of Measured and Calculated Force and Moment Data
$\delta_f = 15^o$ $\delta_a = 10^o/10^o$ Nose Gear On
$N_F/\sqrt{\theta_{T_o}} = 3600$ RPM

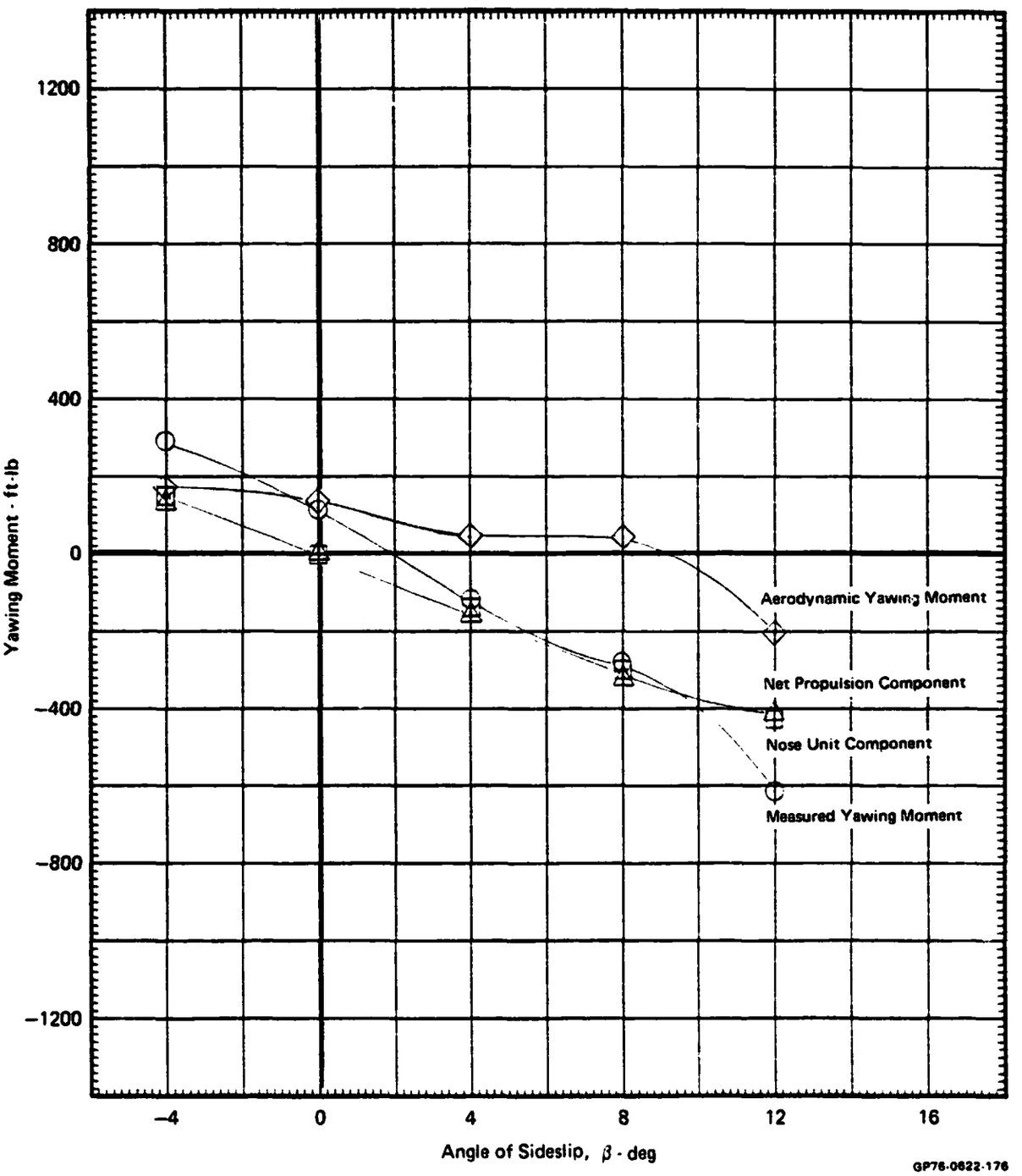

FIGURE 8.5-12

ROLLING MOMENT AND SIDE FORCE vs ANGLE OF SIDESLIP

$\delta_H = 0^o$ $\alpha = 0^o$ $\delta_{LC} = 90^o$ $\delta_{NL} = 90^o$ $\theta_J = 84.7^o$ $q = 1.4$ PSF

Graphical Summary of Measured and Calculated Force and Moment Data

$\delta_f = 15^o$ $\delta_a = 10^o/10^o$ Nose Gear On

$N_F/\sqrt{\theta_{T_o}} = 3600$ RPM

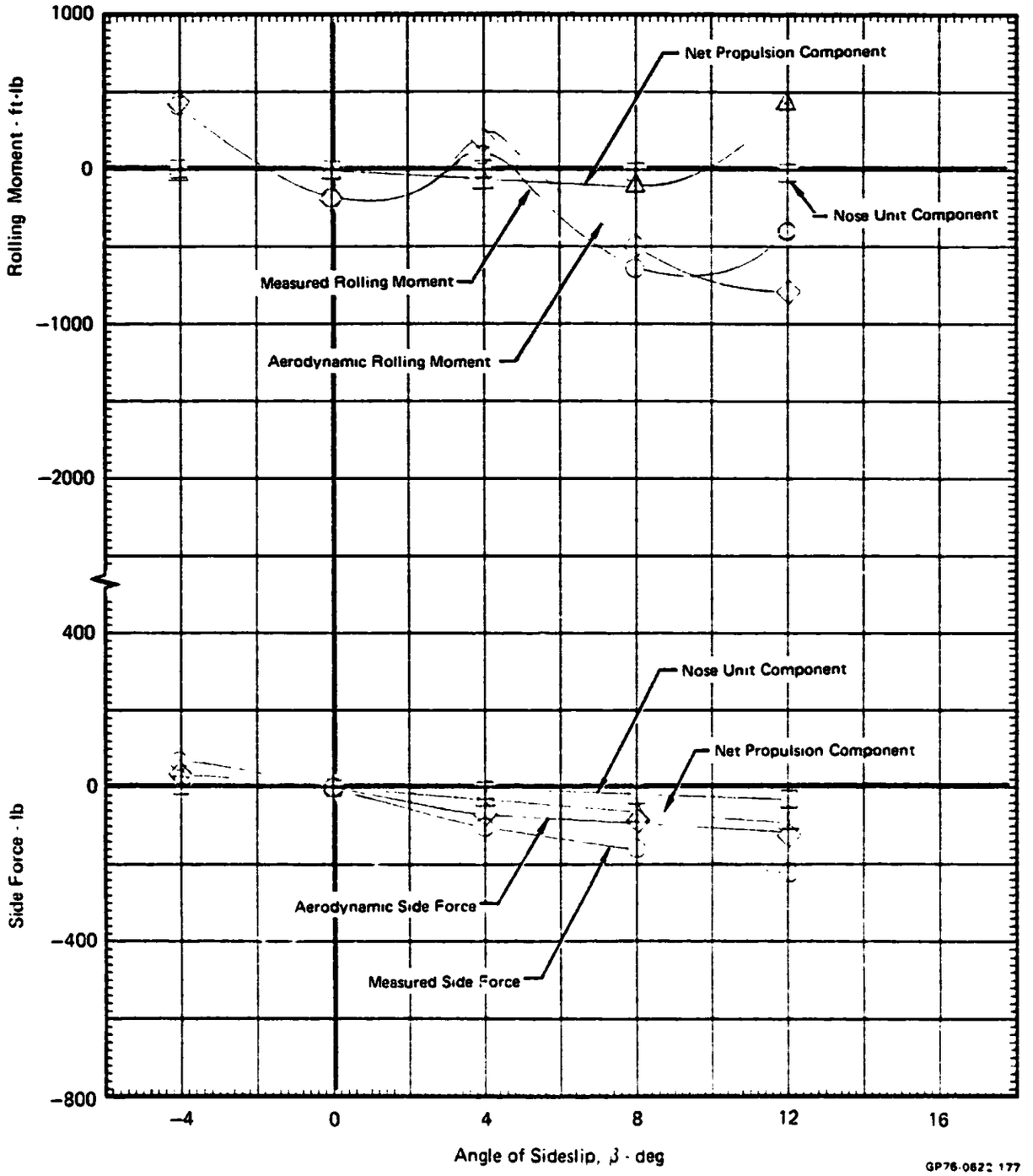

FIGURE 8.5-13
YAWING MOMENT vs ANGLE OF SIDESLIP
$\delta_H = 0^o$ $\alpha = 0^o$ $\delta_{LC} = 90^o$ $\delta_{NL} = 90^o$ $\theta_J = 84.7^o$ $q = 3.3$ PSF
Graphical Summary of Measured and Calculated Force and Moment Data
$\delta_f = 15^o$ $\delta_a = 10^o/10^o$ Nose Gear On
$N_F/\sqrt{\theta_{T_o}} = 3600$ RPM

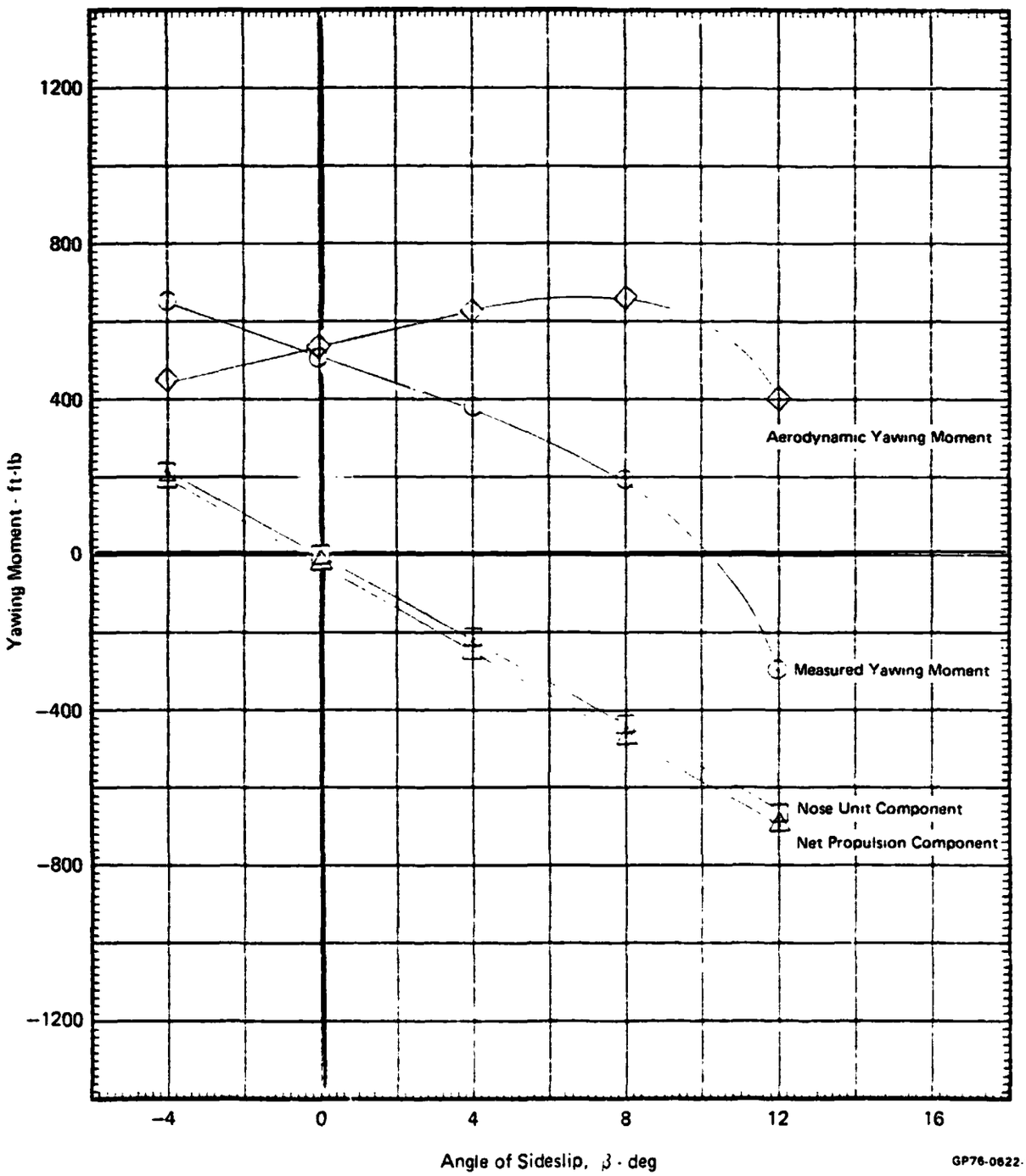

FIGURE 8.5-14

ROLLING MOMENT AND SIDE FORCE vs ANGLE OF SIDESLIP

$\delta_H = 0^o$ $\alpha = 0^o$ $\delta_{LC} = 90^o$ $\delta_{NL} = 90^o$ $\theta_J = 84.7^o$ $q = 3.3$ PSF

Graphical Summary of Measured and Calculated Force and Moment Data

$\delta_f = 15^o$ $\delta_a = 10^o/10^o$ Nose Gear On

$N_F/\sqrt{\theta_{T_o}} = 3600$ RPM

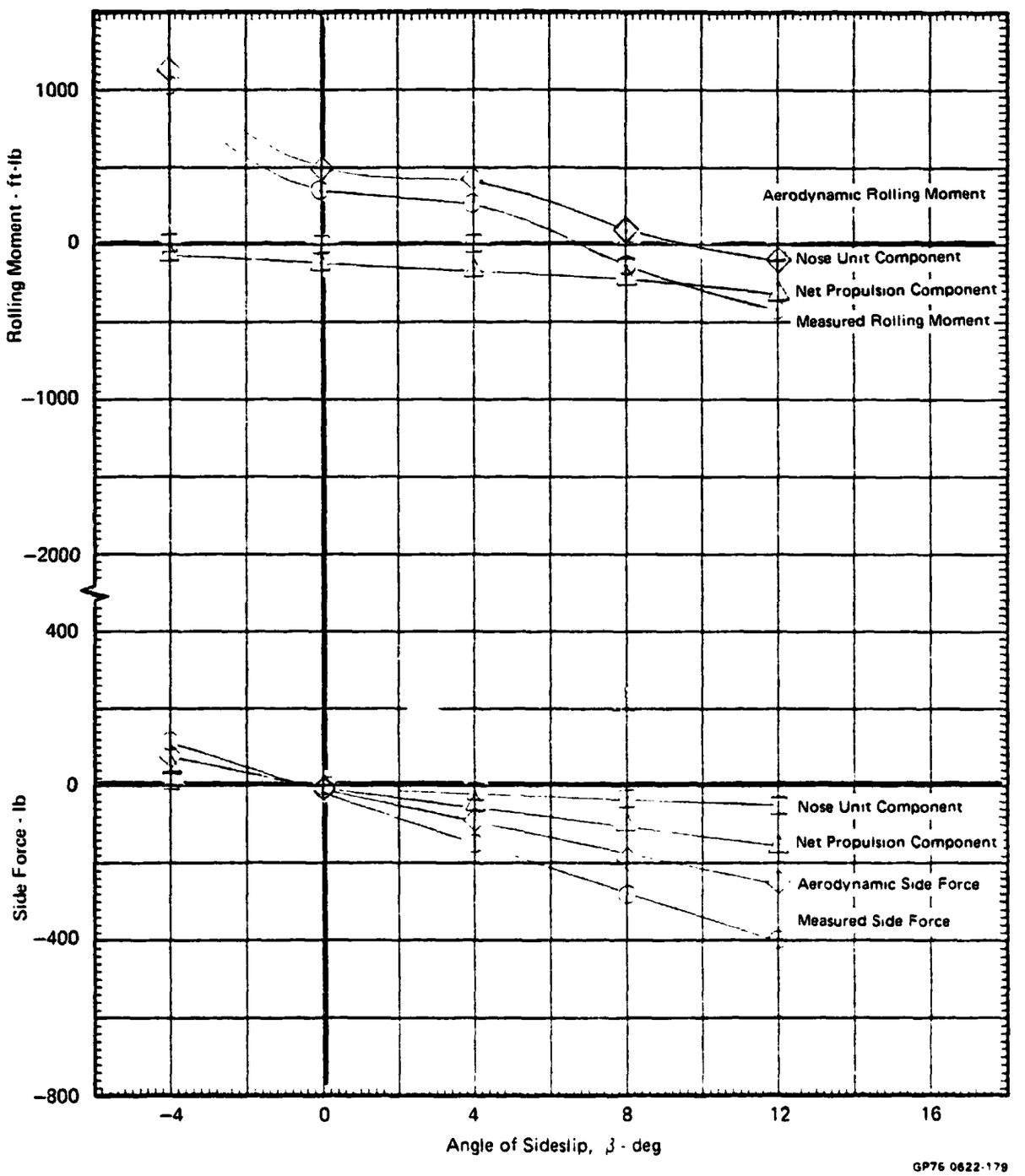

GP76 0622-179

FIGURE 8.5-15

YAWING MOMENT vs ANGLE OF SIDESLIP

$\delta_H = 0^o$ $\alpha = 0^o$ $\delta_{LC} = 90^o$ $\delta_{NL} = 90^o$ $\theta_J = 84.7^o$ $q = 7.2$ PSF

Graphical Summary of Measured and Calculated Force and Moment Data

$\delta_f = 15^o$ $\delta_a = 10^o/10^o$ Nose Gear On

$N_F/\sqrt{\theta_{T_o}} = 3600$ RPM

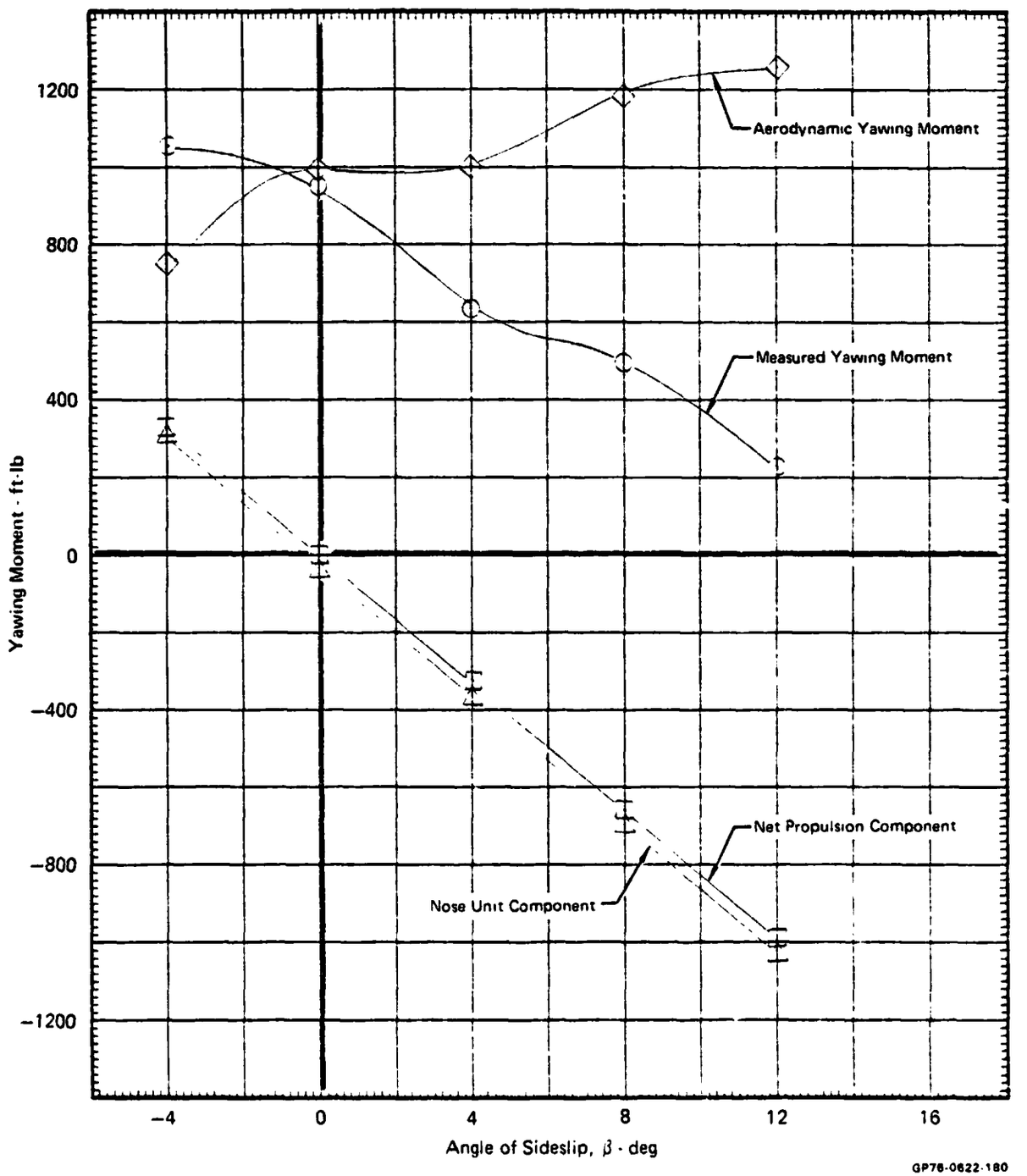

FIGURE 8.5-16
ROLLING MOMENT AND SIDE FORCE vs ANGLE OF SIDESLIP
$\delta_H = 0^o$ $\alpha = 0^o$ $\delta_{LC} = 90^o$ $\delta_{NL} = 90^o$ $\theta_J = 84.7^o$ $q = 7.2$ PSF
Graphical Summary of Measured and Calculated Force and Moment Data
$\delta_f = 15^o$ $\delta_a = 10^o/10^o$ Nose Gear On
$N_F/\sqrt{\theta_{T_o}} = 3600$ RPM

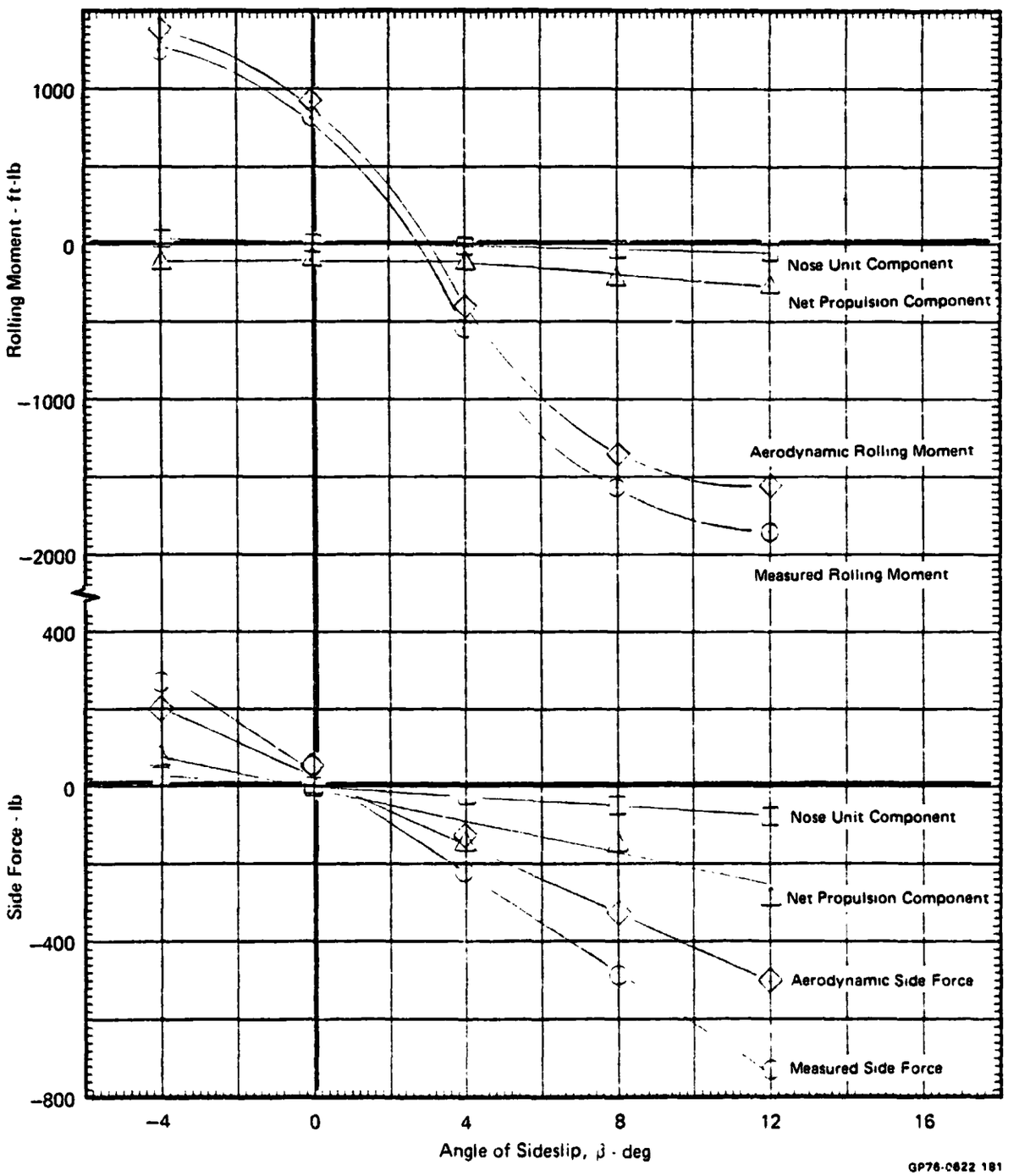

FIGURE 8.5-17
THREE FAN CONFIGURATION DIRECTIONAL CHARACTERISTICS
$\delta_H = 0^o \quad \alpha = 0^o$
Summary of Measured and Calculated Moment Data
$\delta_f = 15^o \quad \delta_a = 10^o/10^o$ Nose Gear On
$N_F/\sqrt{\theta_{T_o}} = 3600$ RPM

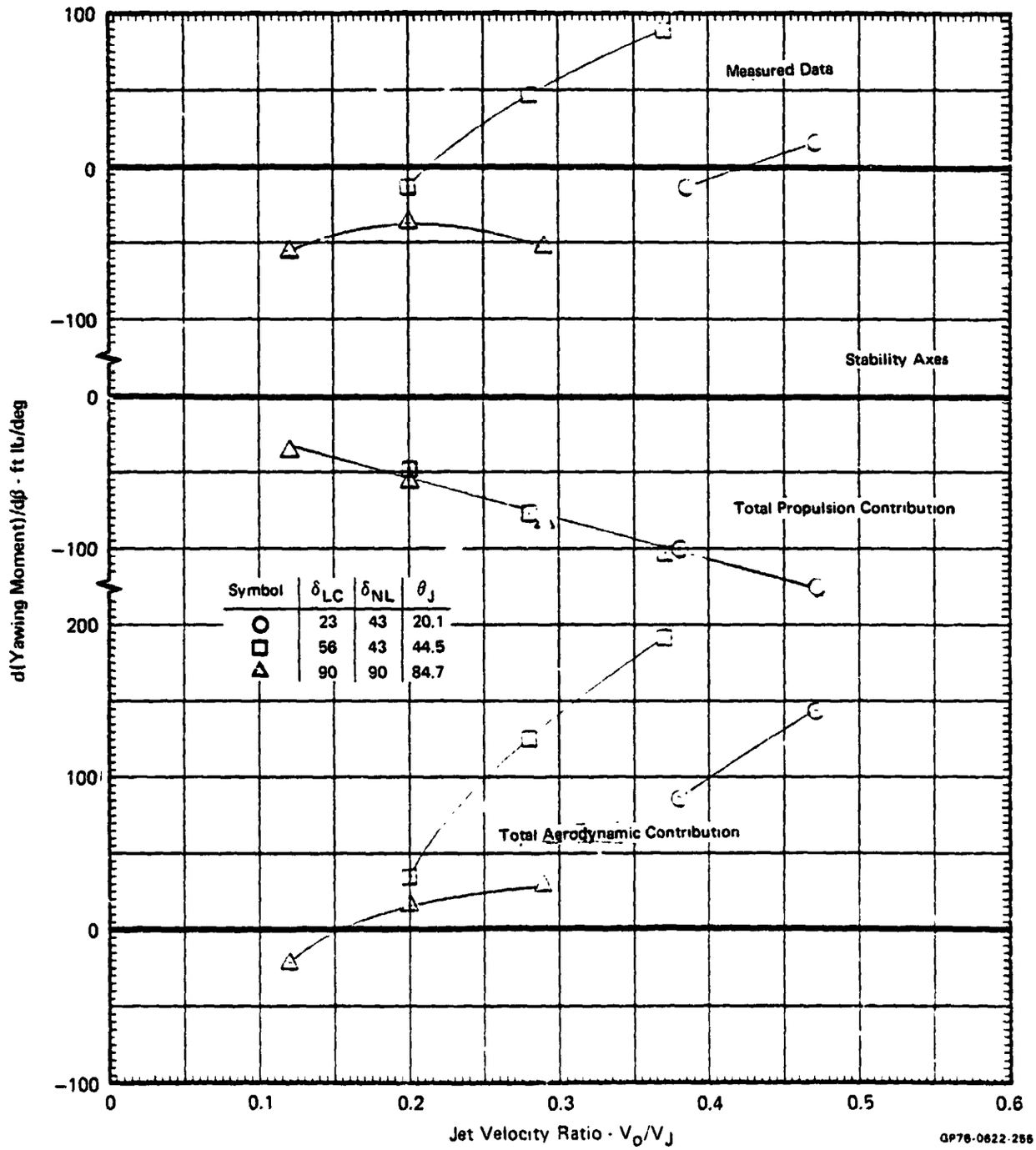

FIGURE 8.5-18
THREE FAN CONFIGURATION DIRECTIONAL CHARACTERISTICS
$\delta_H = 0^o \quad \alpha = 0^o$
Summary of Measured and Calculated Moment Coefficient Data
$\delta_f = 15^o \quad \delta_a = 10^o/10^o$ Nose Gear On

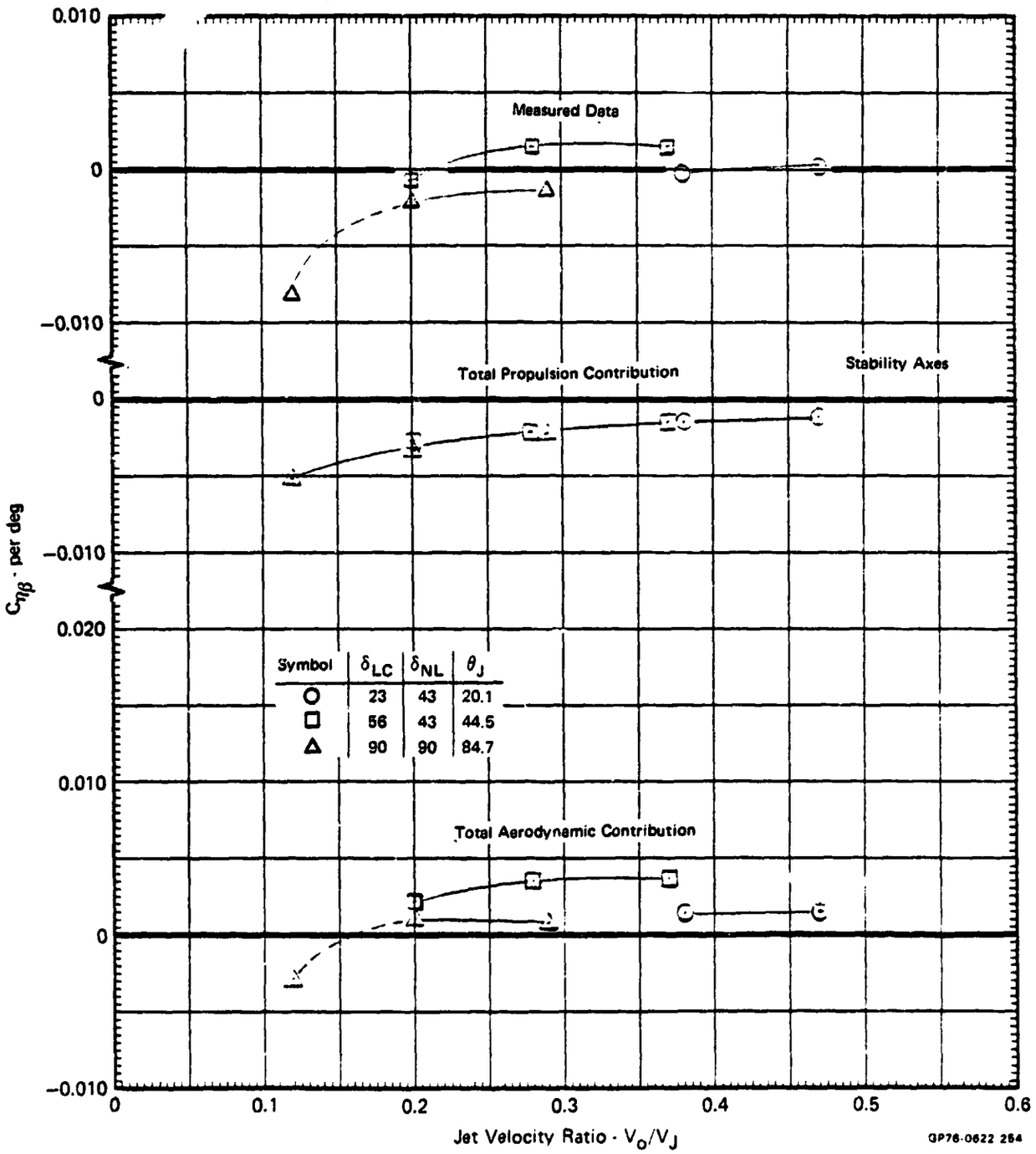

FIGURE 8.5-19
THREE FAN CONFIGURATION LATERAL CHARACTERISTICS
$\delta_H = 0^o$ $\alpha = 0^o$
Summary of Measured and Calculated Moment Data
$\delta_f = 15^o$ $\delta_a = 10^o/10^o$ Nose Gear On

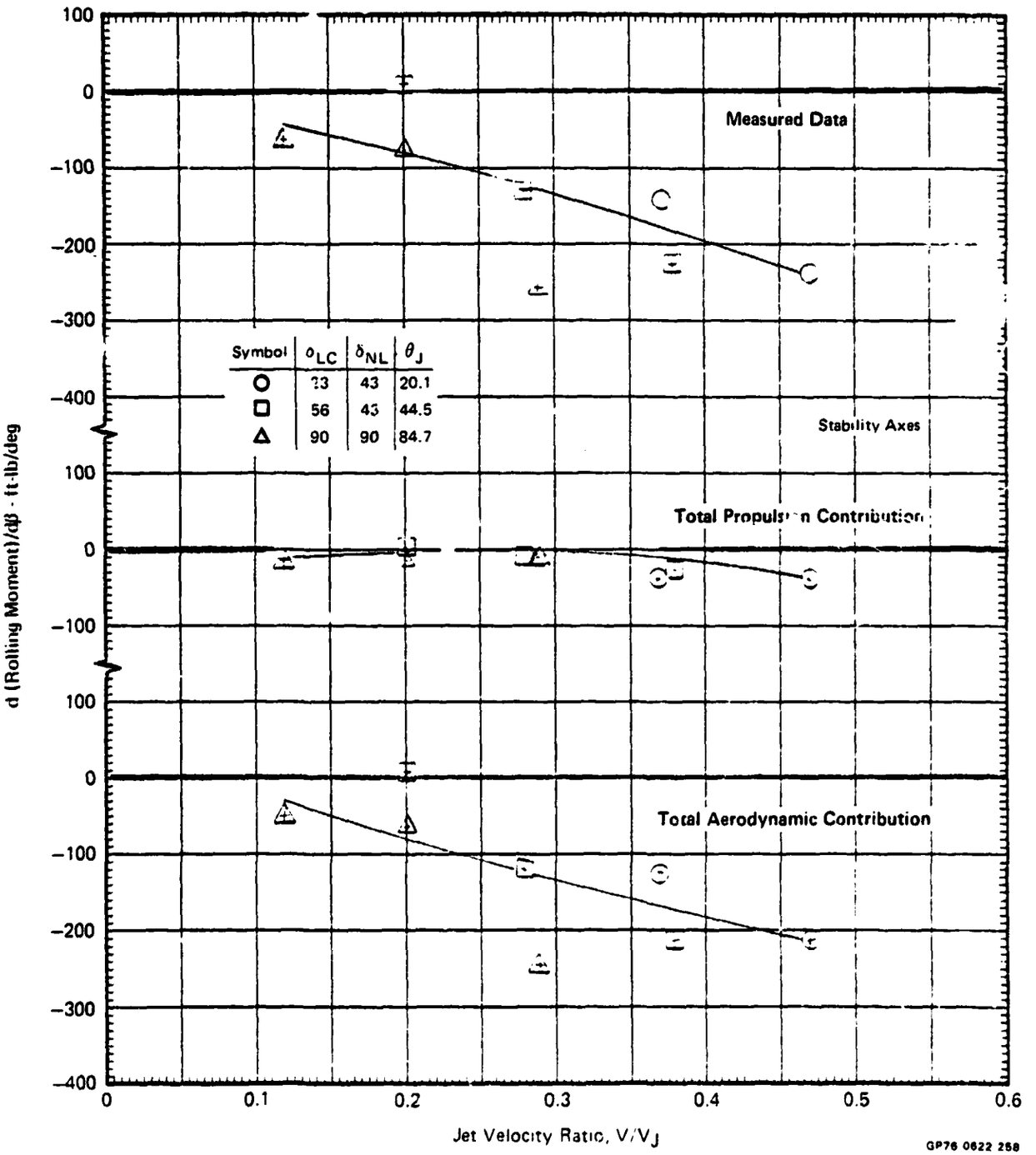

FIGURE 8.5-20
THREE FAN CONFIGURATION LATERAL CHARACTERISTICS
$\delta_H = 0^o \quad \alpha = 0^o$
Summary of Measured and Calculated Moment Coefficient Data
$\delta_f = 15^o \quad \delta_a = 10^o/10^o$ Nose Gear On

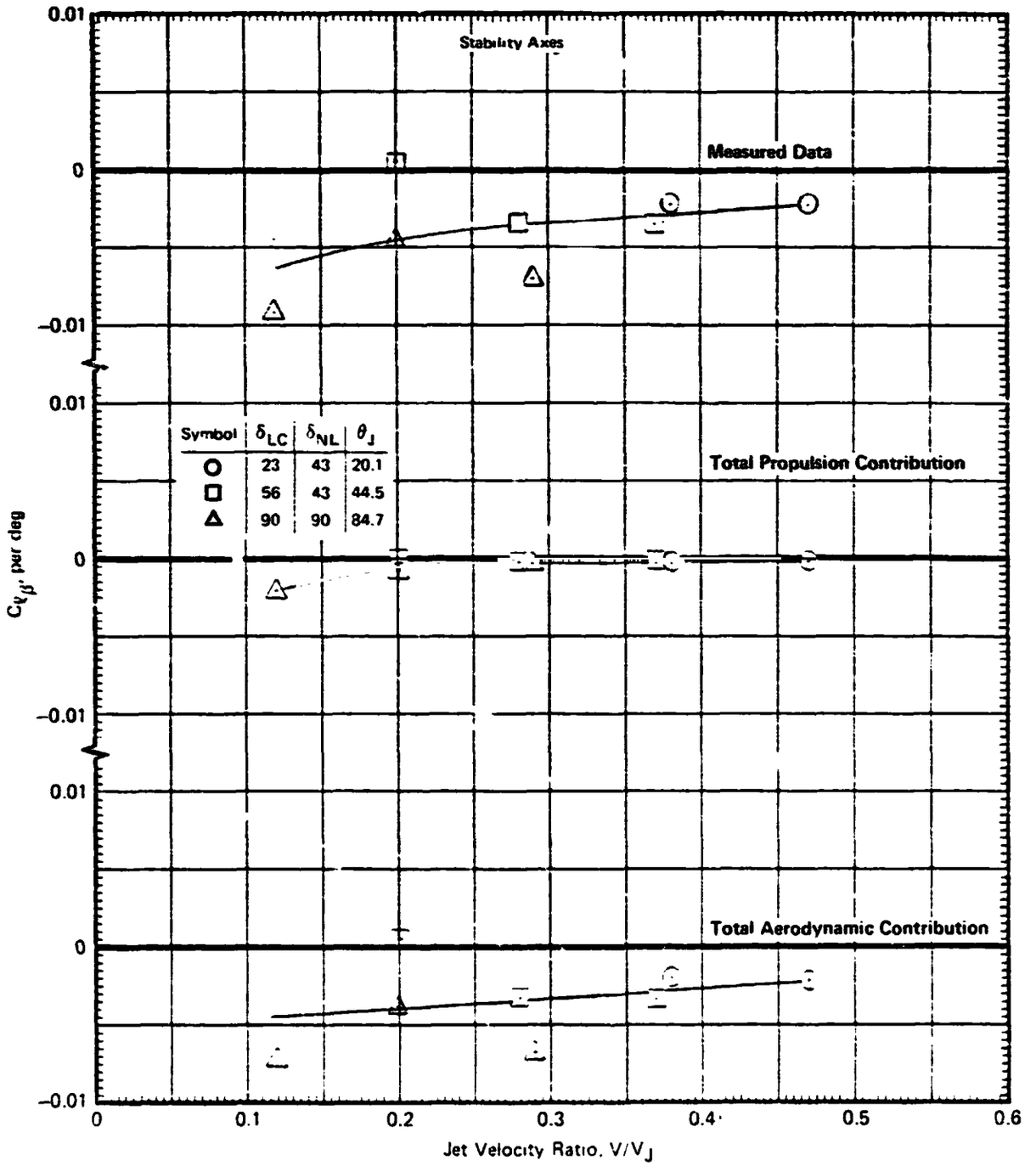

FIGURE 8.5-21

THREE FAN CONFIGURATION SIDE FORCE CHARACTERISTICS

$\delta_H = 0^o$ $\alpha = 0^o$

Summary of Measured and Calculated Moment Data

$\delta_f = 15^o$ $\delta_a = 10^o/10^o$ Nose Gear On

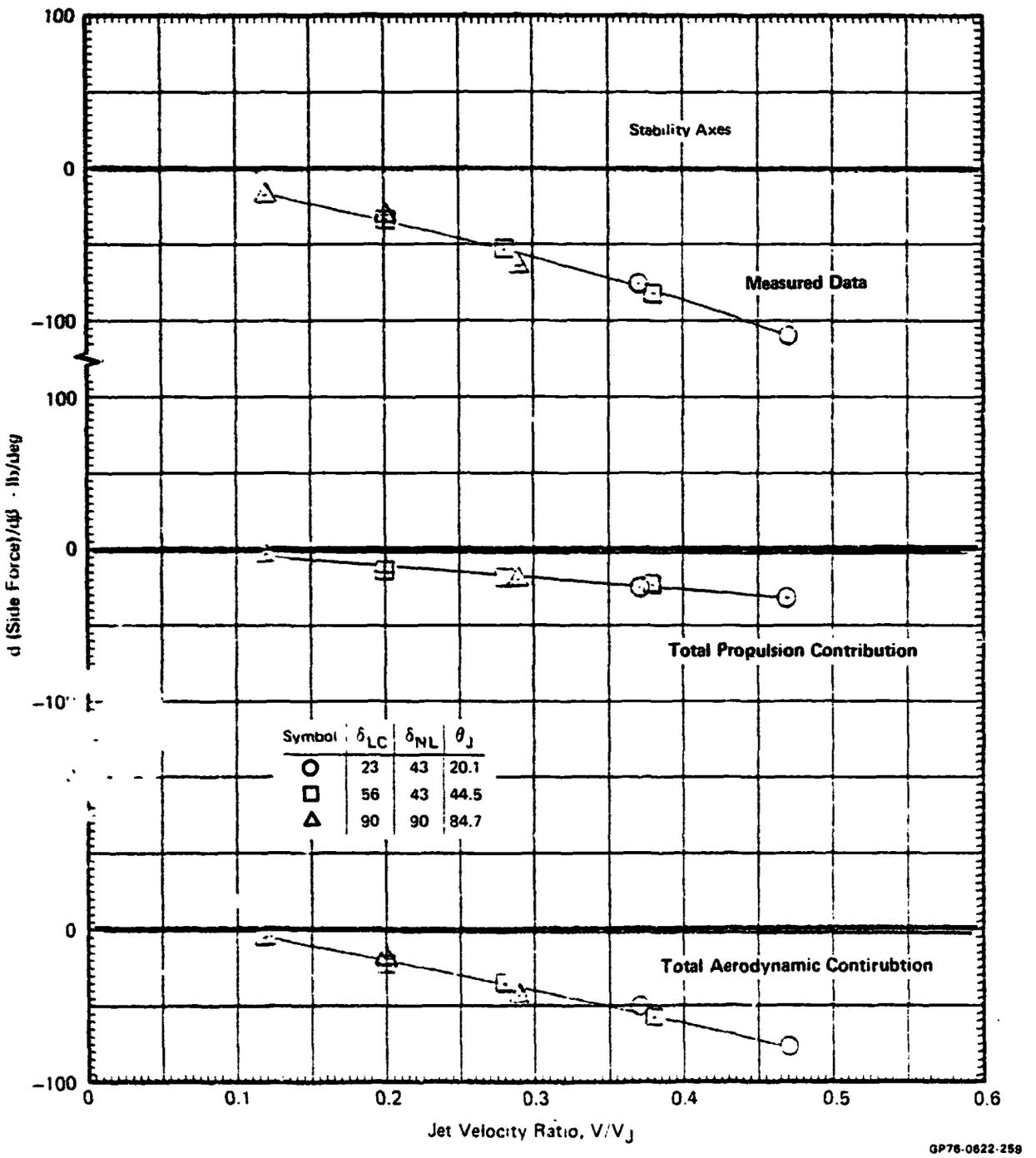

GP76-0622-259

FIGURE 8.5-22
THREE FAN CONFIGURATION SIDE FORCE CHARACTERISTICS
$\delta_H = 0^o \quad \alpha = 0^o$
Summary of Measured and Calculated Force Coefficient Data
$\delta_f = 15^o \quad \delta_a = 10^o/10^o$ Nose Gear On

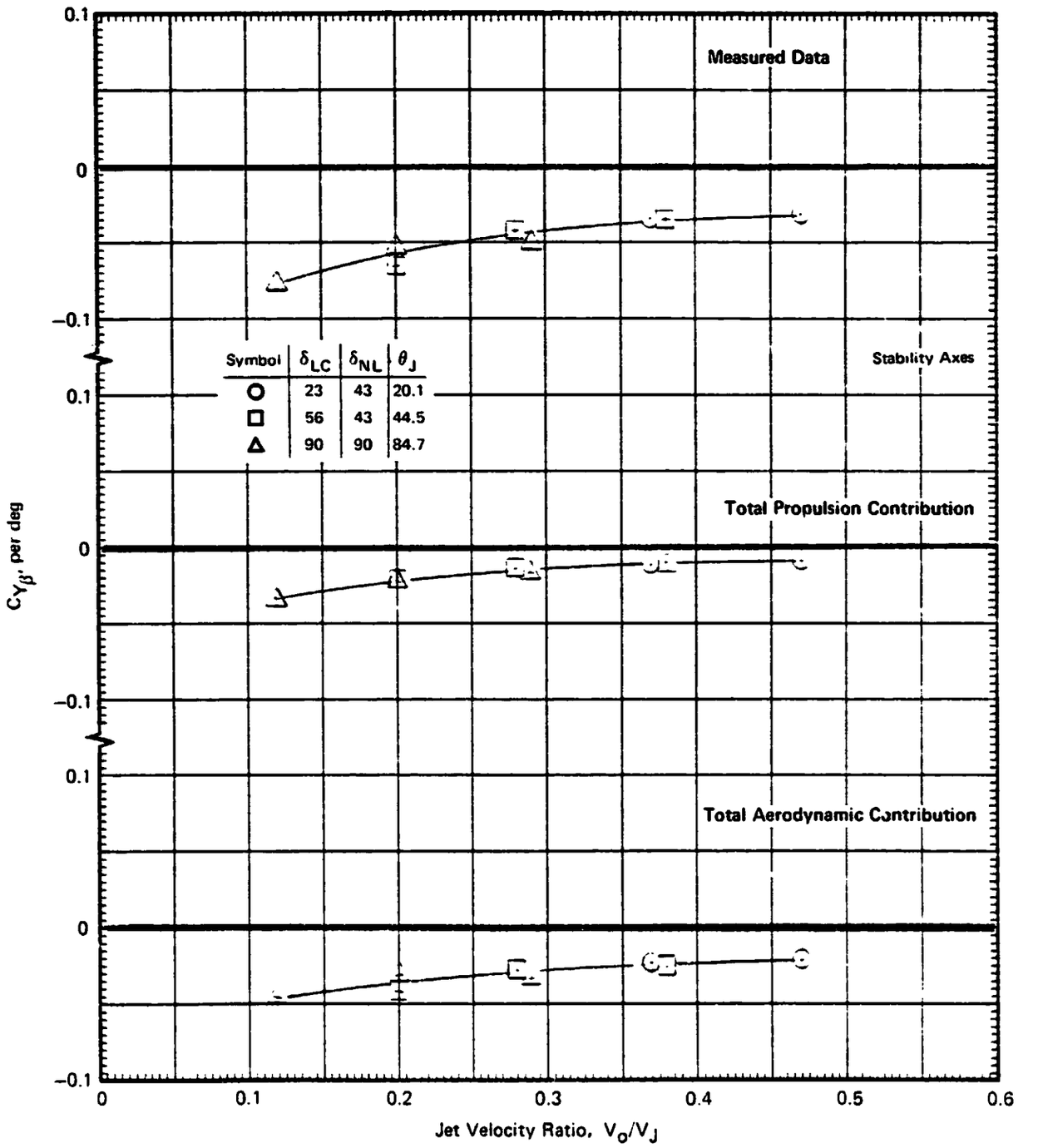

GP76-0622-257

FIGURE 8.5-23
EFFECT OF AILERON DEFLECTION ON LATERAL-DIRECTIONAL CHARACTERISTICS, q = 7.1 PSF

$\delta_H = 0^o$ $\alpha = 0^o$ $\delta_{LC} = 56^o$ $\delta_{NL} = 43^o$ $\theta_J = 44.5^o$

Measured Data

$\delta_f = 15^o$ Nose Gear On

$N_F/\sqrt{\theta T_o} = 3600$ RPM

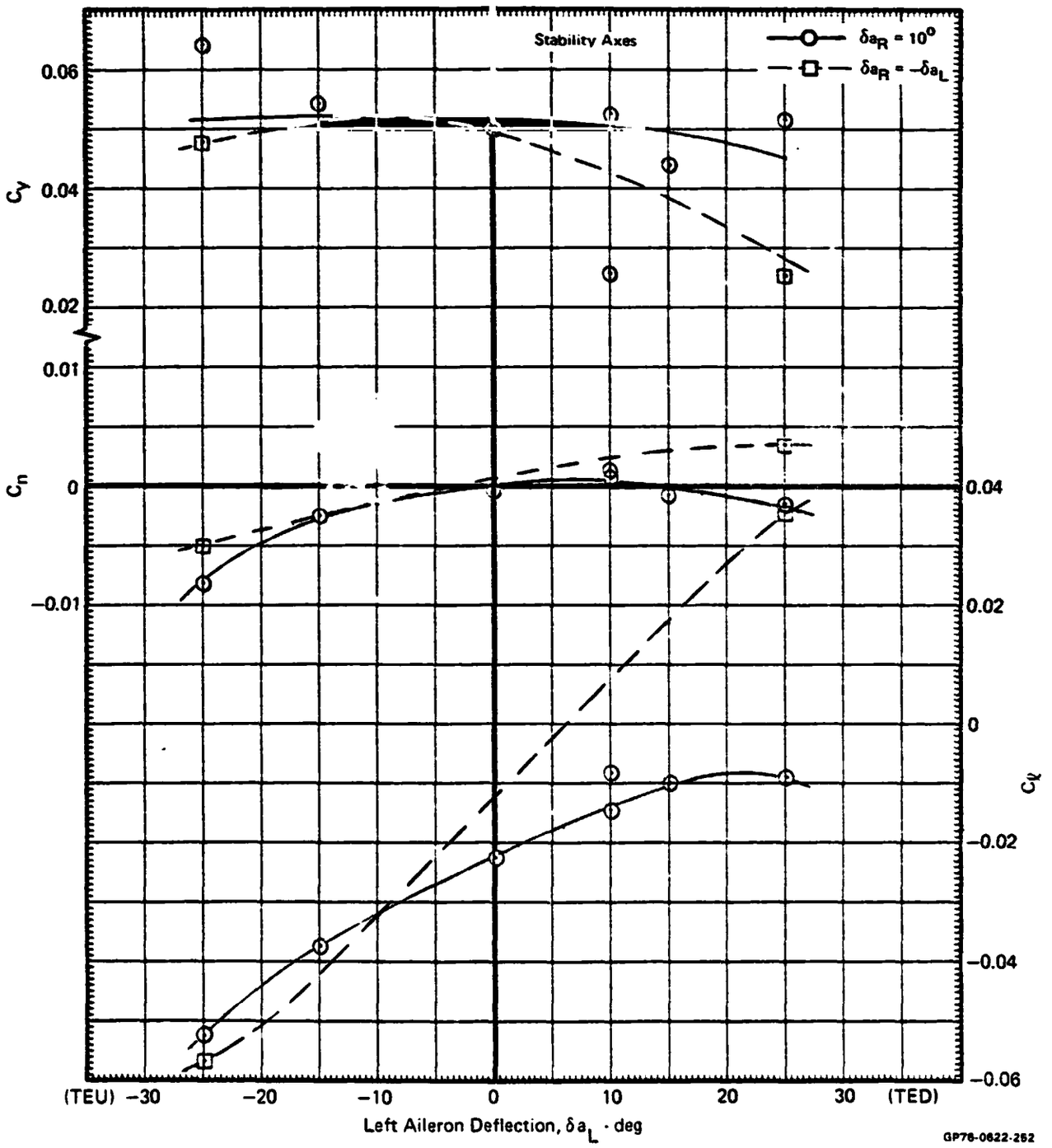

FIGURE 8.5-24

EFFECT OF AILERON DEFLECTION ON LATERAL-DIRECTIONAL CHARACTERISTICS, q = 12.3 PSF

$\delta_H = 0^o$ $\alpha = 0^o$ $\delta_{LC} = 56^o$ $\delta_{NL} = 43^o$ $\theta_J = 44.5^o$

Measured Data

$\delta_f = 15^o$ Nose Gear On

$N_F/\sqrt{\theta_{T_o}} = 3600$ RPM

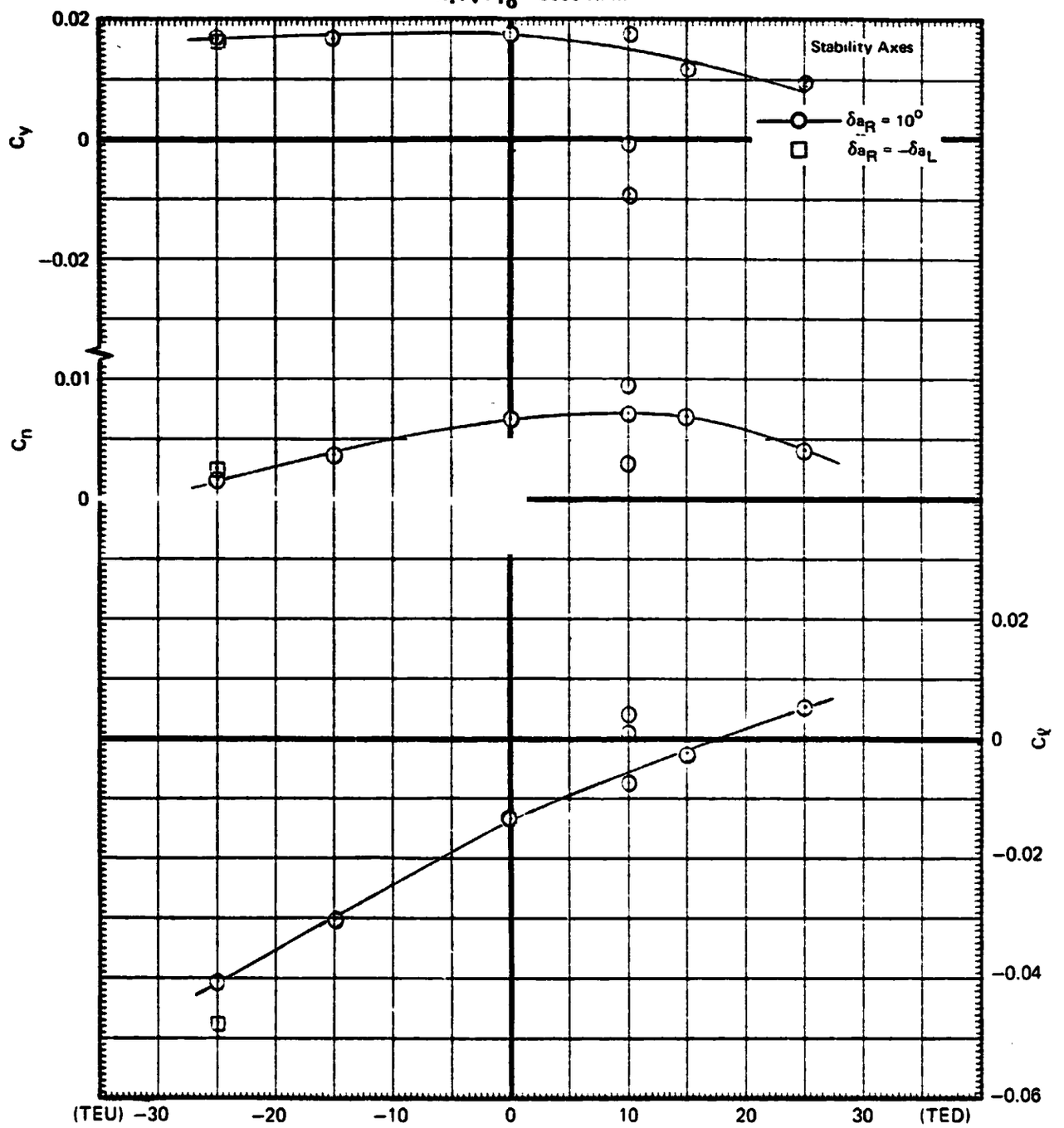

GP76-0622-208

FIGURE 8.5-25
EFFECT OF RUDDER DEFLECTION ON LATERAL-DIRECTIONAL CHARACTERISTICS
$\delta_H = 0^o$ $\delta_{LC} = 38^o$ $\delta_{NL} = 43^o$ $\theta_J = 29.2^o$
Measured Data
$\beta = 0^o$ $\delta_r = 23^o$ $\delta_f = 15^o$ $\delta_a = 10^o/10^o$ Nose Gear On
$N_F/\sqrt{\theta T_0} = 3600$ RPM

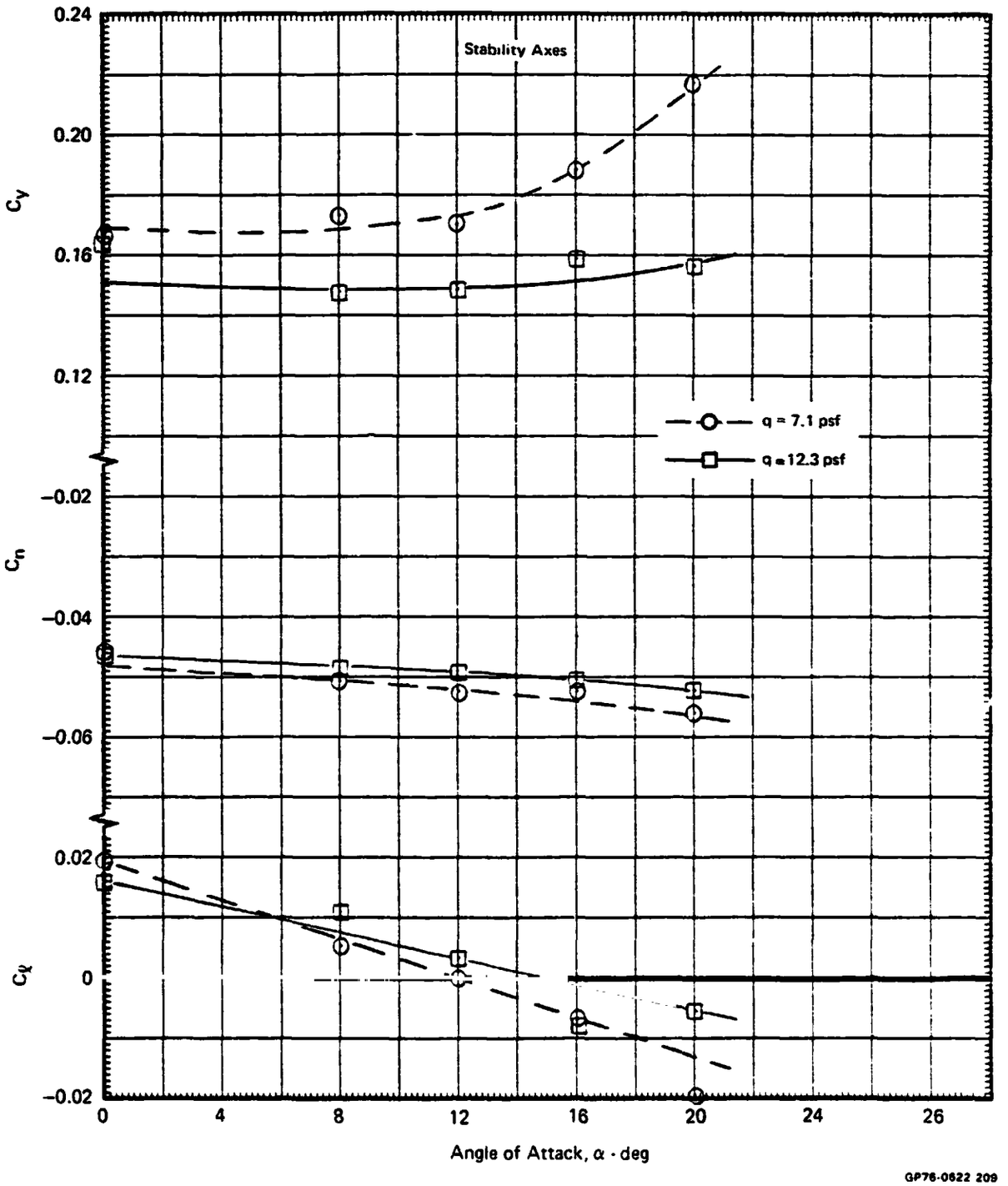

8.6 AERODYNAMIC LIFT CONFIGURATION - LONGITUDINAL CHARACTERISTICS

The aerodynamic lift configuration is defined as any configuration with a lift/cruise unit geometric deflection, δ_{LC}, of 0°, the nose fan shut off, and the nose fan inlet covered. This configuration is used as the reference in determining the level of the power induced effects. In order to establish this level, the aerodynamic lift configuration data must correspond to a standardized inlet mass flow ratio. This condition was selected prior to the test as an inlet mass flow ratio, A_O/A_{HL}, of 1.0. For this test a lift cruise fan speed of 2700 rpm at a tunnel dynamic pressure of 34.2 psf resulted in a unity inlet mass flow ratio. The data presented in this section were used to establish the reference levels presented in Section 8.3. It should be noted that this definition of reference configuration implies that the incremental induced lift and drag include the effects of the external wetted surface of the lift/cruise nozzles, and the nose lift fan inlets and exits as well as the induced effects of the captured stream tubes on the aerodynamic forces and on the other propulsion units.

Basic Data Used to Establish Reference Configuration Characteristics

The basic data used to establish the reference levels for the powered lift configuration are presented in this section in both dimensional and coefficient form. The dimensional form has been included in order to emphasize the magnitude of the propulsion system contribution to the balance measured forces and moments. Data are presented for the three configurations described in the following table.

Configuration	δ_a	δ_f	δ_H	Rake
1	0	0	On	Off
2	0	0	Off	Off
3	10	15	Off	On

Dimensional Data - The dimensional data are presented in Figures 8.6-1 through 8.6-9. The lift contribution of the propulsion system is simply the component of gross thrust vector normal to the relative wind, $F_{G_{LC}} \sin(\theta_{LC} + \alpha)$. The propulsion contribution to the lift results in an increase in both lift curve slope and maximum lift. It is a maximum of 630 lb at an angle of attack of 22°. This maximum is a result of a reduction in calculated fan thrust at angles of attack above wing stall.

The propulsion system drag component includes the gross thrust component parallel to the relative wind and ram drag. The variation of the total ram drag and the gross thrust drag component with angle of attack are presented with the measured drag data. The data illustrate the reduction in ram drag and thrust at angles of attack above wing stall discussed in the previous paragraph.

The propulsion system contribution to the pitching moment consists of the same components as the drag: gross thrust and ram drag. The thrust contributes a considerable nose down pitching moment due to the thrust line being located above the moment reference center. The ram drag, which is the result of airflow into both the gas generator and fan inlets, contributes a nose up pitching moment. The resulting total propulsion system pitching moment is nose down.

Coefficient Data - The coefficient form of the total aerodynamic forces and moments is presented in Figures 8.6-10 through 8.6-15. These data are the coefficient form of the aerodynamic forces and moments remaining after subtracting the propulsion system components. Two irregularities are present in these data:

- o An apparent incorrect 2° and 6° angle of attack setting
- o A higher than anticipated lift coefficient at 0° angle of attack

The former can be explained if, for some reason, the angle of attack settings of 2° and 6° were actually closer to 2.5° and 6.5°. The latter is more difficult to resolve since the current data are self-consistent. The lift coefficient at zero angle of attack, C_{L_o}, is 0.230 for the clean wing configuration with horizontal tail on at 0° deflection. Previous MCAIR small scale (4.1%) wind tunnel testing of a comparable configuration (Reference (3)) indicated a C_{L_o} of 0.100. The difference of 0.130 in the C_{L_o} could be caused by the following:

- o Reynolds number differences and scale effects
- o Model support system interference effects
- o Fabrication accuracy and flexibility differences effects

The MCAIR small scale testing of this configuration had been performed at a Reynolds number of 0.6×10^6 based on wing MAC as compared to the present testing performed at a Reynolds number of 7.5×10^6 based on wing MAC. However, the literature does not suggest that C_{L_o} is affected significantly by Reynolds number. As mentioned in Section 6.3, the data reduction performed for this test did not include any model support system interference effects. To ascertain the magnitude of this interference effect, additional small scale wind tunnel testing was performed by MCAIR. These tests utilized a scale model of the Ames 40' x 80'

model support system and the small scale model of the aircraft configuration. The results of these tests indicated the model support system interference on lift coefficient to be only 0.025. The one remaining possibility, that of fabrication differences and flexibility effects between the tests, cannot be quantitatively evaluated at this time.

In addition to the high C_{L_O}, the clean wing configuration has a $C_{L_{MAX}}$ of 1.280 at the stall angle of attack of 15°. A comparison of lift data from Configurations 2 and 3 (see page 8-152) indicates that deflecting the flaps to 15° and drooping the ailerons to 10° results in ΔC_{L_O} and $\Delta C_{L_{MAX}}$ of 0.100 while maintaining the 15° stall angle of attack. Figure 8.6-11 presents the effect of the horizontal tail on drag. The data indicate that installation of the horizontal tail reduces the aerodynamic drag. This result is probably not valid. The discrepancy may be an indication of the accuracy associated with the separation of the propulsion and aerodynamic contributions to the measured drag.

The tail on pitching moment data indicate the configuration to have static longitudinal stability (prestall) with the neutral point located at 42% MAC. Deflecting the flaps to 15° and drooping the ailerons 10° on the tail off configuration resulted in a nose down pitching moment of $\Delta C_m = -.04$, with a slight loss in static longitudinal stability. No data were obtained for the tail on aerodynamic lift configuration with flaps and ailerons deflected and the horizontal tail installed.

Horizontal Tail Control Effectiveness

The effect of horizontal tail deflection on the longitudinal characteristics is presented in Figures 8.6-16 through 8.6-18. It is shown that the configuration has static longitudinal stability (prestall) and that negative (TEU) stabilator deflections would be utilized for trimming. Data for the positive deflections indicate a stalled horizontal tail.

FIGURE 8.6-1
LIFT vs ANGLE OF ATTACK
$\delta_H = 0^o$ q = 34.2 PSF $\delta_{LC} = 0^o$ δ_{NL} = SEALED $\theta_J = 1^o$
Graphical Summary of Measured and Calculated Force Data
Run 116 $\delta_f = 0^o$ $\delta_a = 0^o/0^o$ Nose Gear Off
$N_F/\sqrt{\theta_{T_o}}$ = 2700 RPM

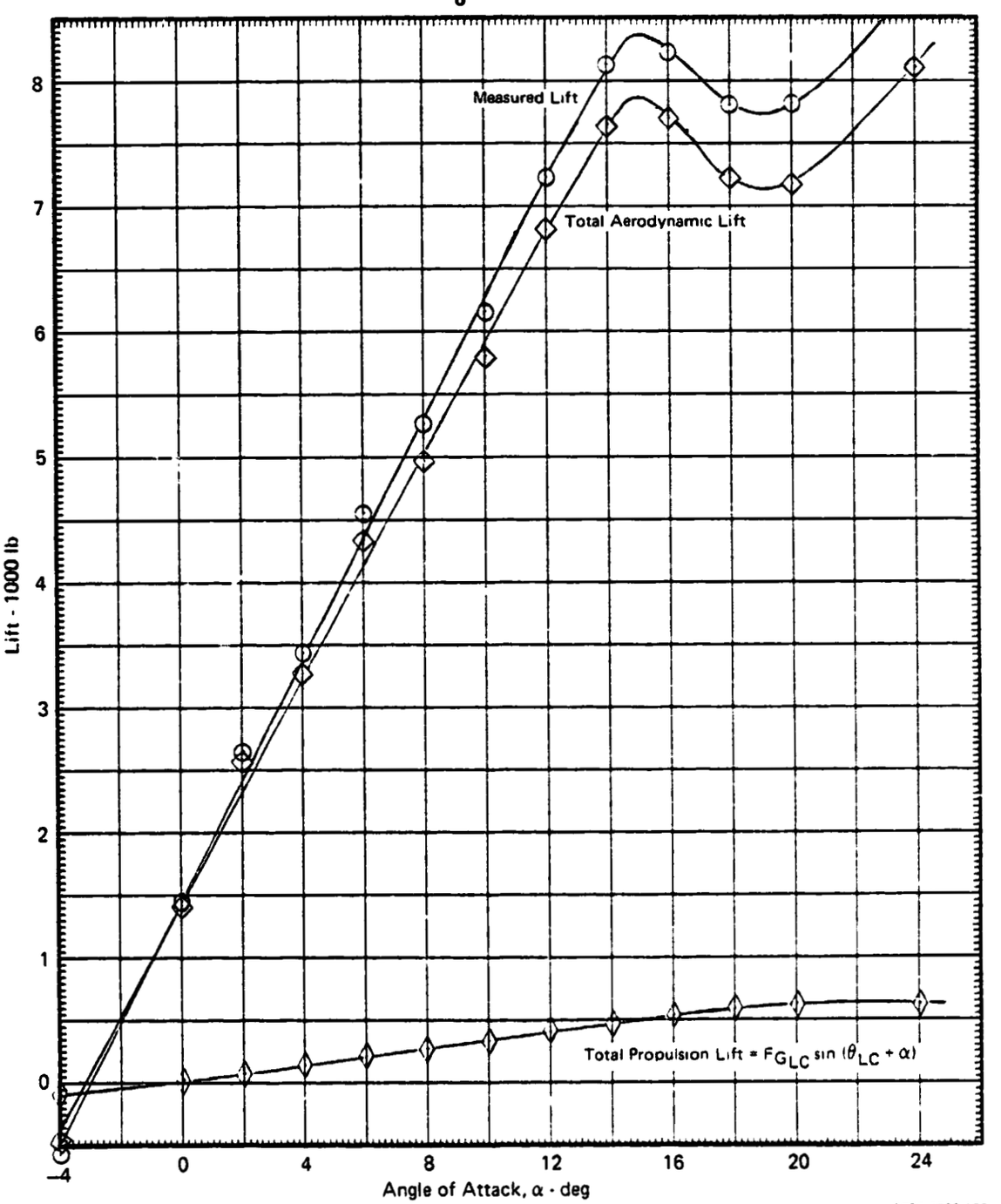

GP76-0622 156

FIGURE 8.6-2
DRAG vs ANGLE OF ATTACK
$\delta_H = 0^o$ q = 34.2 PSF $\delta_{LC} = 0^o$ δ_{NL} = SEALED $\theta_J = 1^o$
Graphical Summary of Measured and Calculated Force Data
Run 116 $\delta_f = 0^o$ $\delta_a = 0^o/0^o$ Nose Gear Off
$N_F/\sqrt{\theta_{T_o}}$ = 2700 RPM

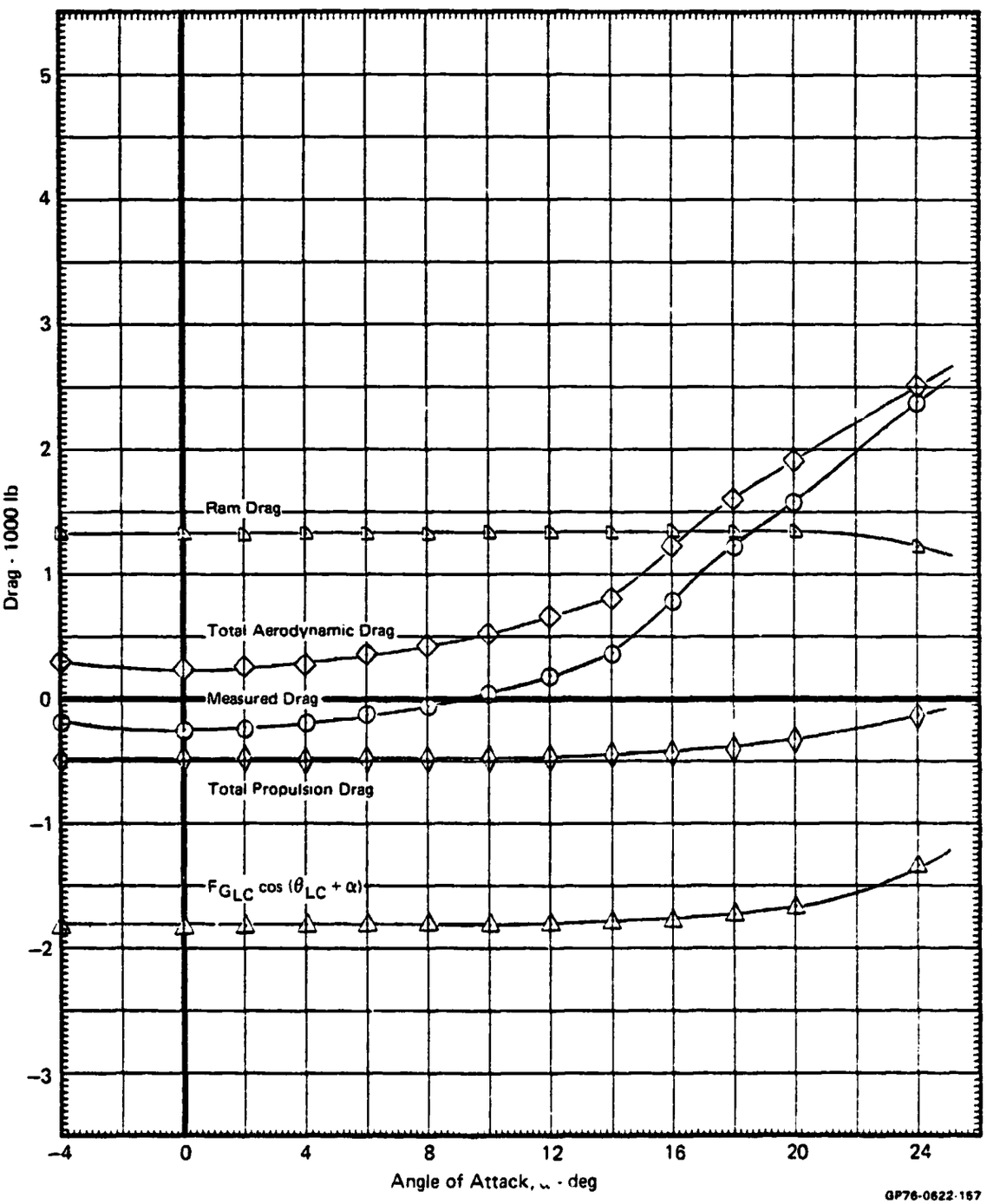

FIGURE 8.6-3
PITCHING MOMENT vs ANGLE OF ATTACK
$\delta_H = 0^o$ q = 34.2 PSF $\delta_{LC} = 0^o$ δ_{NL} = SEALED $\theta_J = 1^o$
Graphical Summary of Measured and Calculated Moment Data
Run 116 $\delta_f = 0^o$ $\delta_a = 0^o/0^o$ Nose Gear Off
$N_F/\sqrt{\theta_{T_o}}$ = 2700 RPM

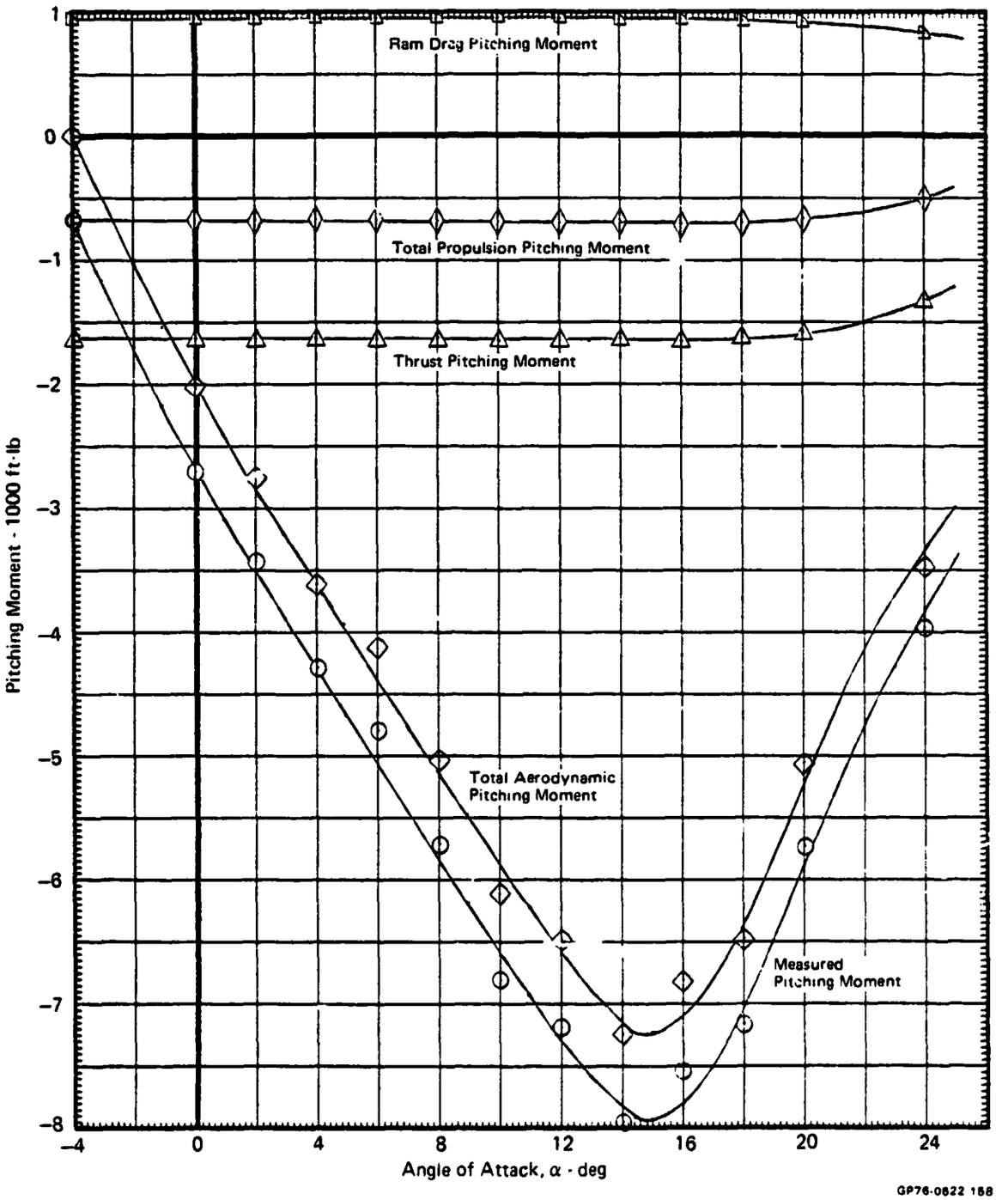

FIGURE 8.6-4
LIFT vs ANGLE OF ATTACK, HORIZONTAL TAIL OFF
$q = 34.2$ PSF $\delta_{LC} = 0^o$ δ_{NL} = SEALED $\theta_J = 1^o$
Graphical Summary of Measured and Calculated Force Data
Run 140 $\delta_f = 0^o$ $\delta_a = 0^o/0^o$ Nose Gear Off
$N_F/\sqrt{\theta_{T_o}} = 2700$ RPM

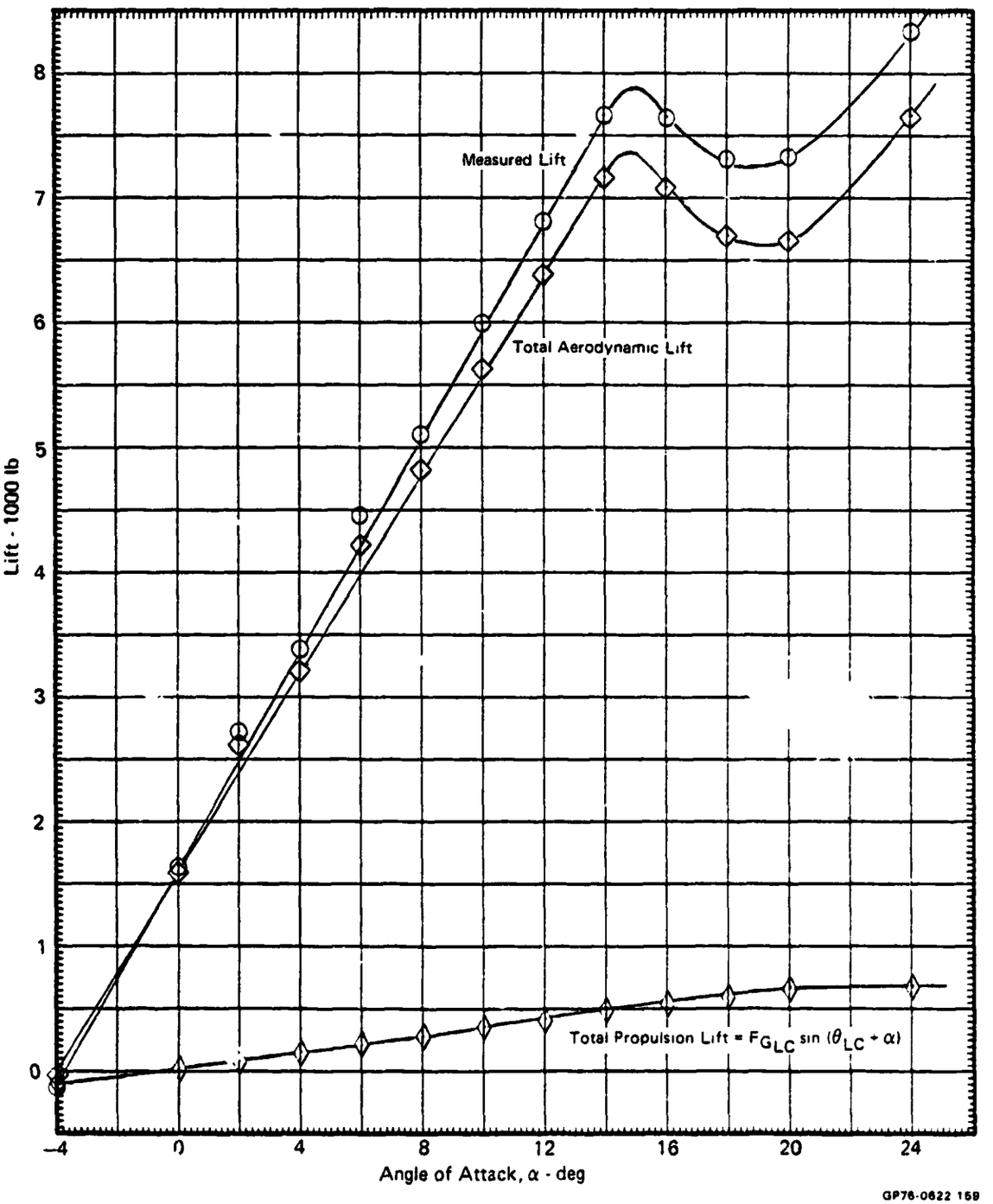

GP76-0622 159

FIGURE 8.6-5
DRAG vs ANGLE OF ATTACK, HORIZONTAL TAIL OFF
q = 34.2 PSF $\delta_{LC} = 0^o$ δ_{NL} = SEALED $\theta_J = 1^o$
Graphical Summary of Measured and Calculated Force Data
Run 140 $\delta_f = 0^o$ $\delta_a = 0^o/0^o$ Nose Gear Off
$N_F/\sqrt{\theta T_o}$ = 2700 RPM

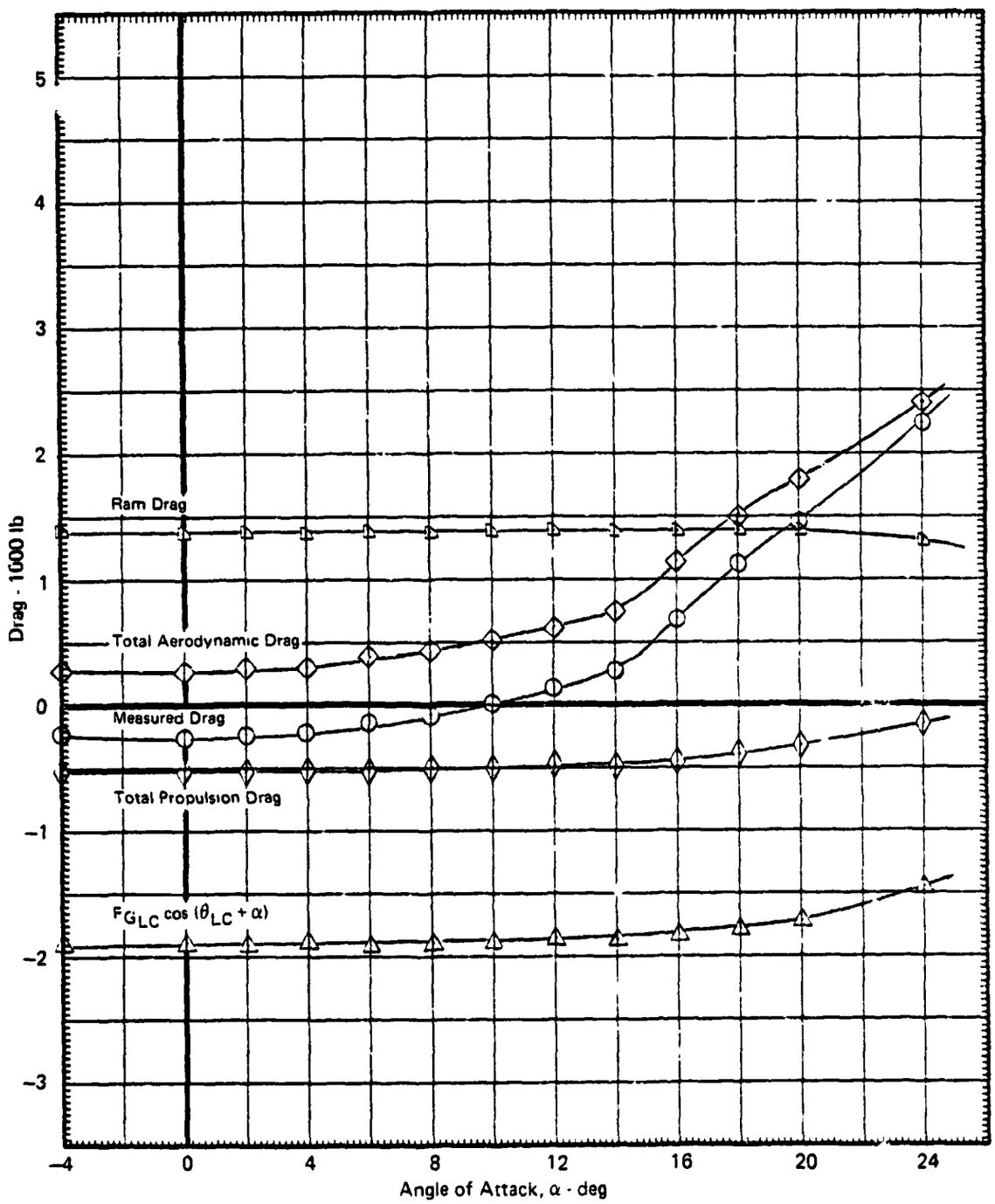

GP76 0622-160

FIGURE 8.6-6
PITCHING MOMENT vs ANGLE OF ATTACK, HORIZONTAL TAIL OFF
$q = 34.2$ PSF $\delta_{LC} = 0^o$ δ_{NL} = SEALED $\theta_J = 1^o$
Graphical Summary of Measured and Calculated Moment Data
Run 140 $\delta_f = 0^o$ $\delta_a = 0^o/0^o$ Nose Gear Off
$N_F/\sqrt{\theta_{T_o}} = 2700$ RPM

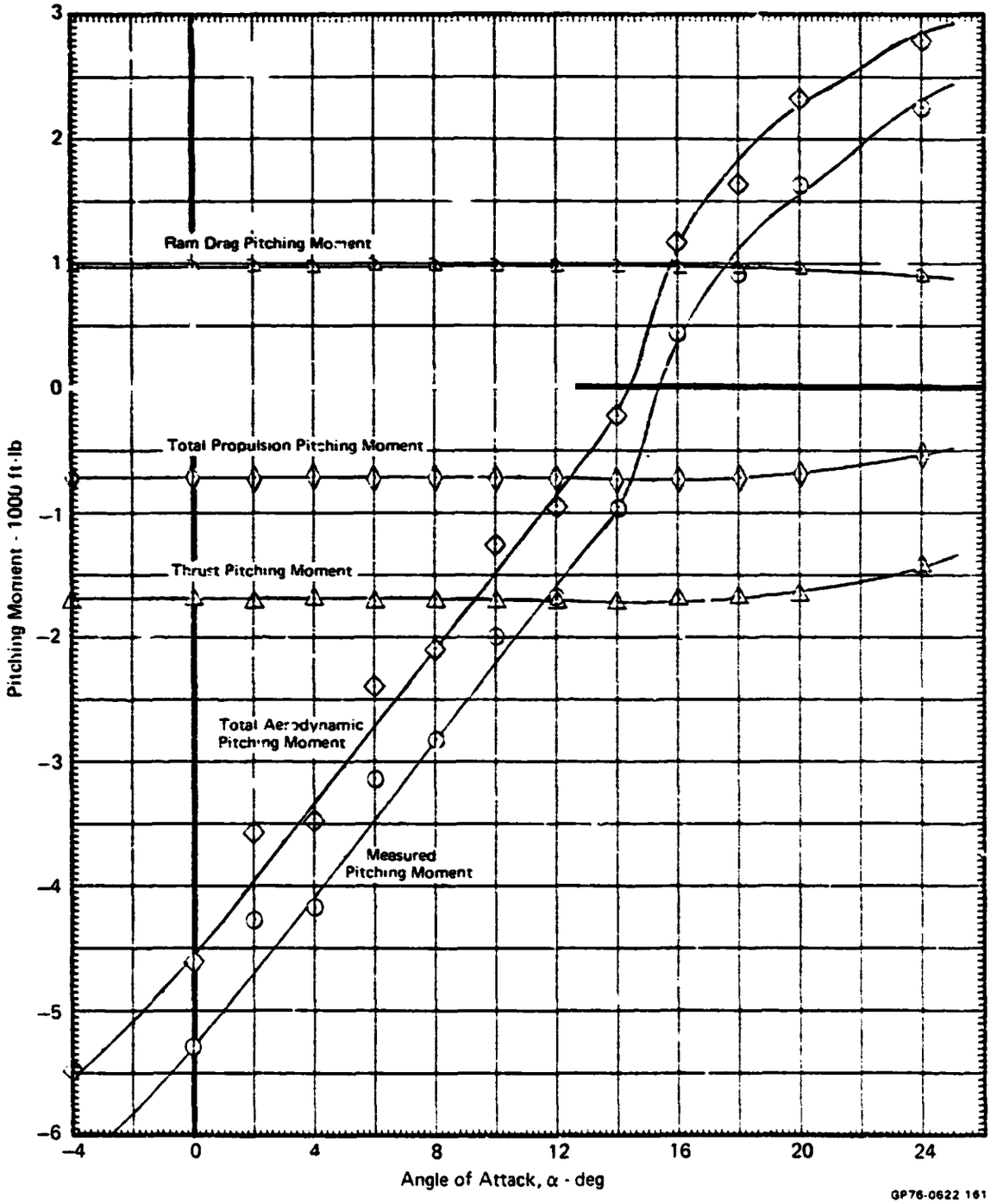

FIGURE 8.6-7
LIFT vs ANGLE OF ATTACK, FLOW SURVEY RAKE ON
q = 34.2 PSF $\delta_{LC} = 0^o$ $\delta_{NL} = 0^o$ Inlets Covered $\theta_J = 1^o$
Graphical Summary of Measured and Calculated Force Data
Run 26 $\delta_f = 15^o$ $\delta_a = 10^o/10^o$ Nose Gear Off
$N_F/\sqrt{\theta_{T_o}}$ = 2700 RPM

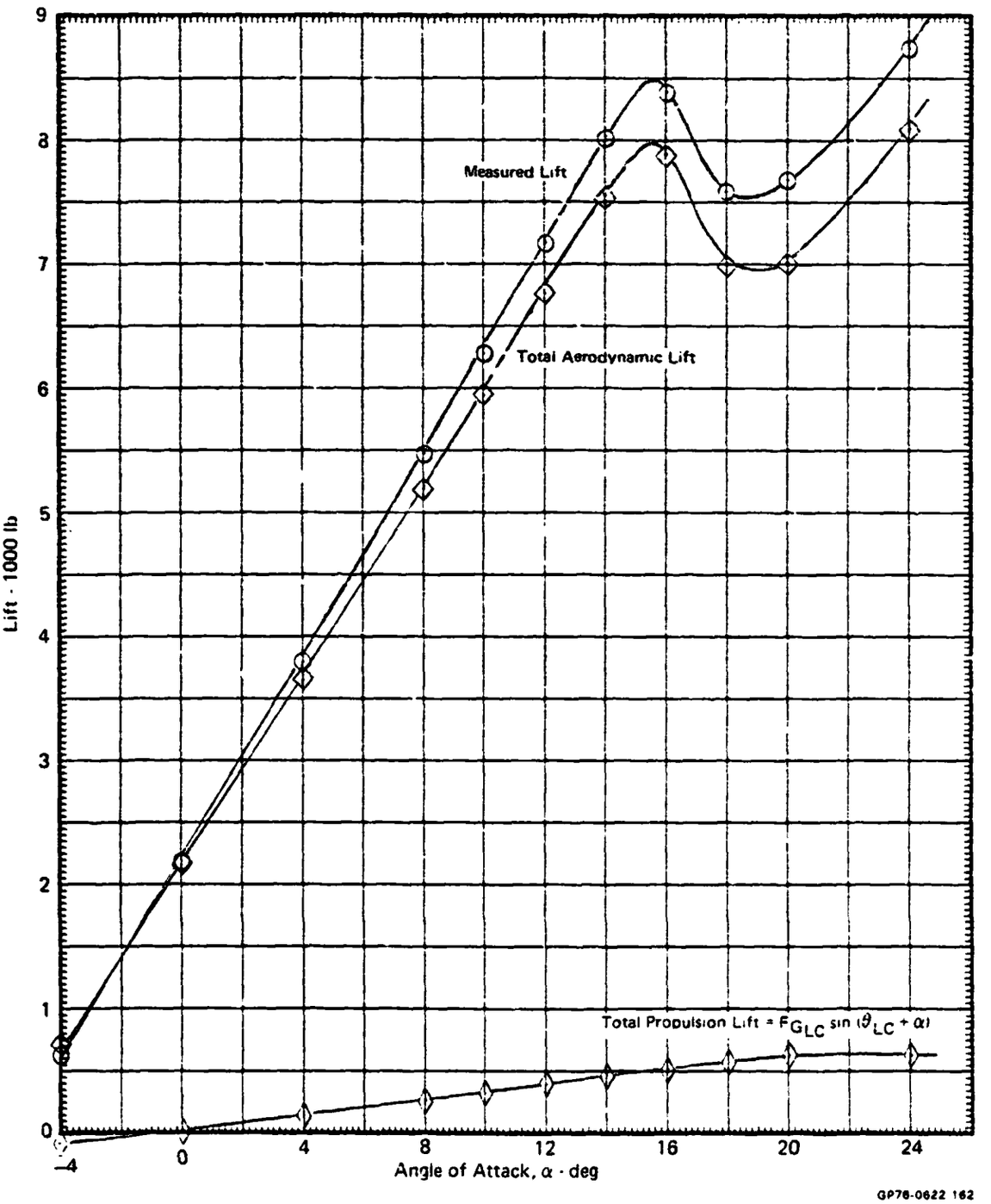

FIGURE 8.6-8

DRAG vs ANGLE OF ATTACK, FLOW SURVEY RAKE ON

q = 34.2 PSF $\delta_{LC} = 0^o$ $\delta_{NL} = 0^o$ Inlets Covered $\theta_J = 1^o$

Graphical Summary of Measured and Calculated Force Data

Run 26 $\delta_f = 15^o$ $\delta_a = 10^o/10^o$ Nose Gear Off

$N_F/\sqrt{\theta T_o}$ = 2700 RPM

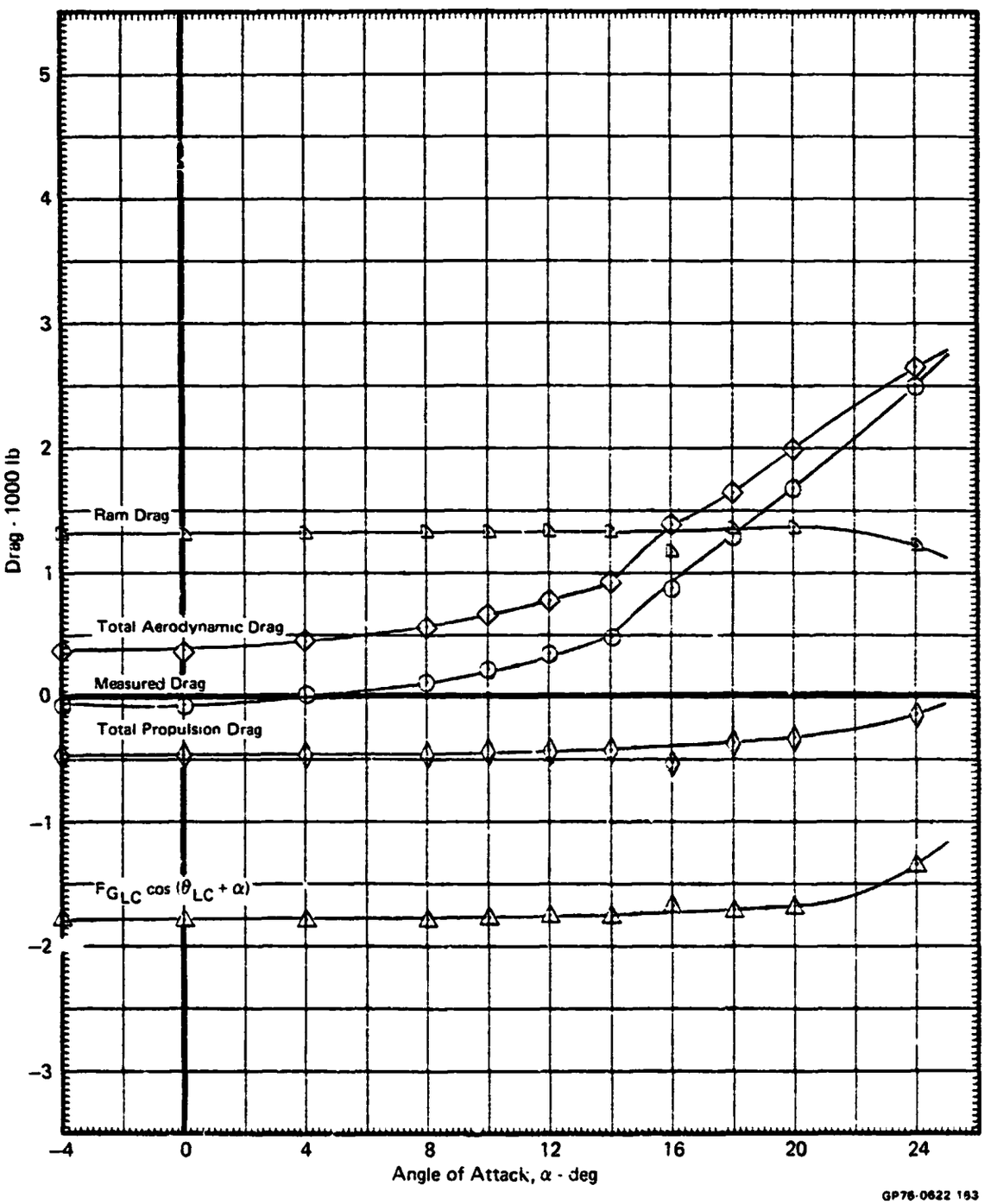

FIGURE 8.6-9

PITCHING MOMENT vs ANGLE OF ATTACK, FLOW SURVEY RAKE ON
q = 34.2 PSF $\delta_{LC} = 0^o$ $\delta_{NL} = 0^o$ Inlets Covered $\theta_J = 1^o$
Graphical Summary of Measured and Calculated Moment Data
Run 26 $\delta_f = 15^o$ $\delta_a = 10^o/10^o$ Nose Gear Off
$N_F/\sqrt{\theta T_o}$ = 2700 RPM

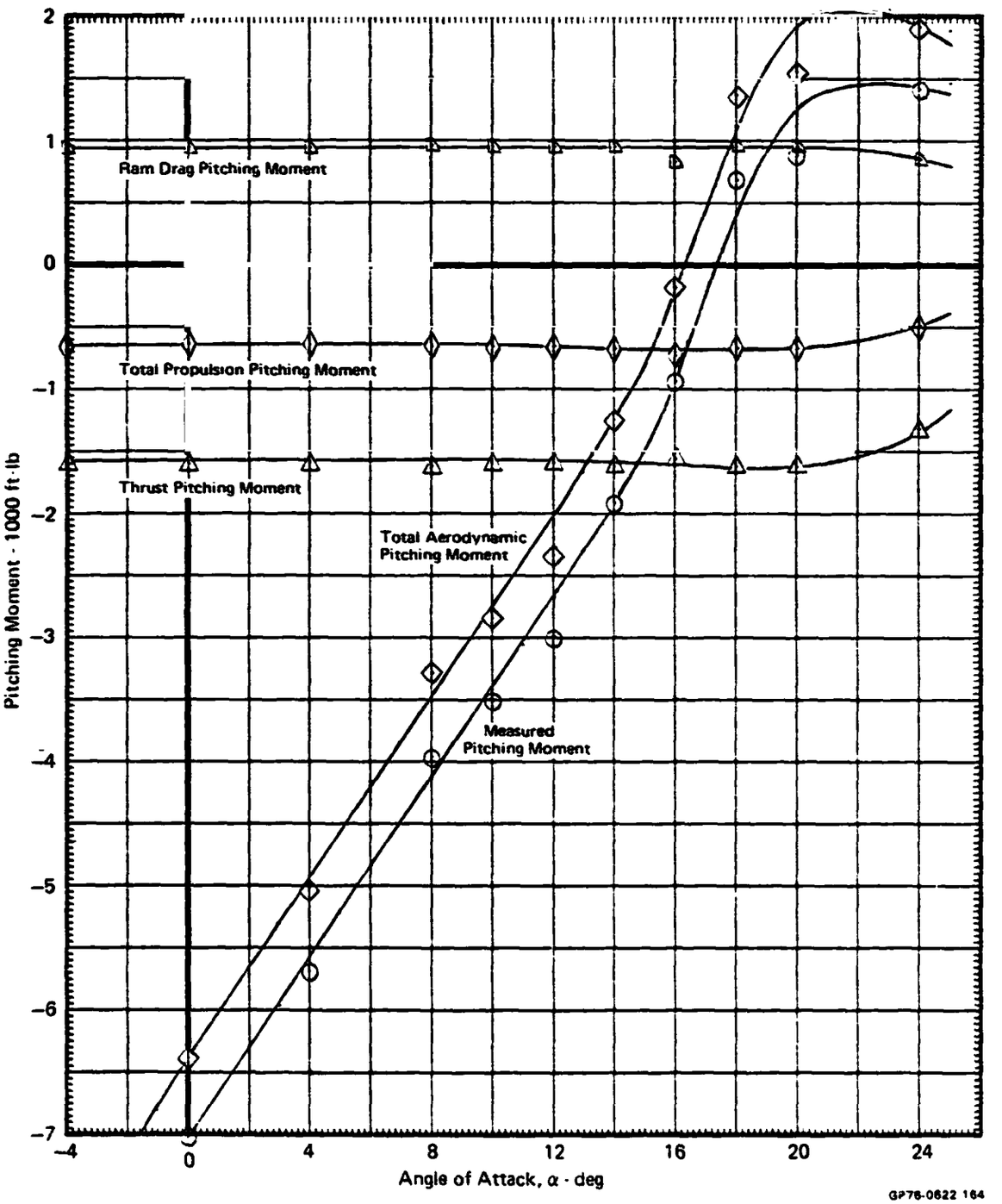

FIGURE 8.6-10

EFFECT OF HORIZONTAL TAIL ON LIFT COEFFICIENT vs ANGLE OF ATTACK

$q = 34.2$ PSF $\quad \delta_{LC} = 0^o \quad \delta_{NL}$ = SEALED $\quad \theta_J = 1^o$

Direct Thrust Effects Removed

$\delta_f = 0^o \quad \delta_a = 0^o/0^o$ Nose Gear Off

$N_F/\sqrt{\theta_{T_o}} = 2700$ RPM

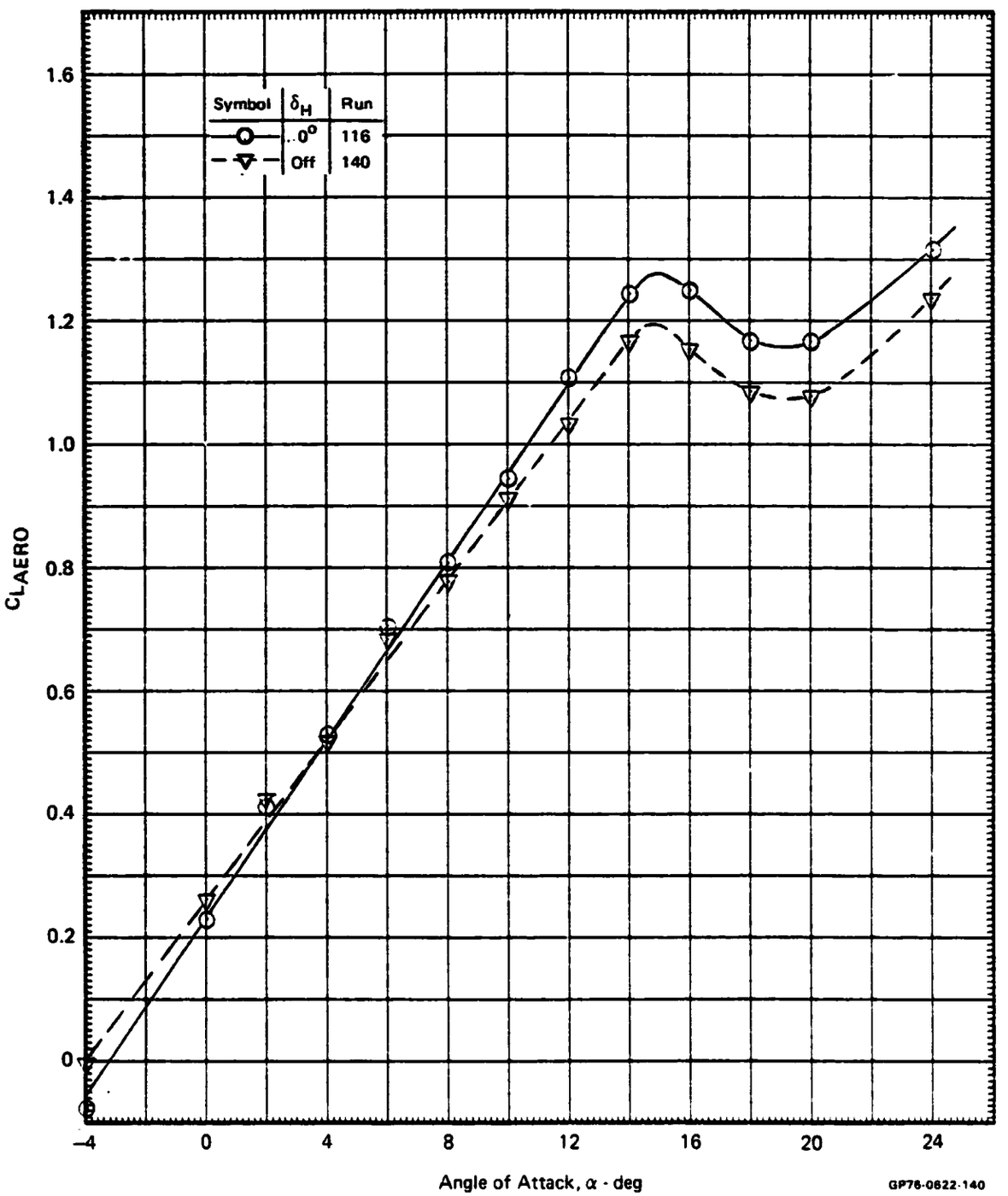

FIGURE 8.6-11
EFFECT OF HORIZONTAL TAIL ON LIFT COEFFICIENT vs DRAG COEFFICIENT
q = 34.2 PSF $\delta_{LC} = 0^0$ δ_{NL} = SEALED $\theta_J = 1^0$
Direct Thrust Effects Removed
$\delta_f = 0^0$ $\delta_s = 0^0/0^0$ Nose Gear Off
$N_F/\sqrt{\theta_{T_0}}$ = 2700 RPM

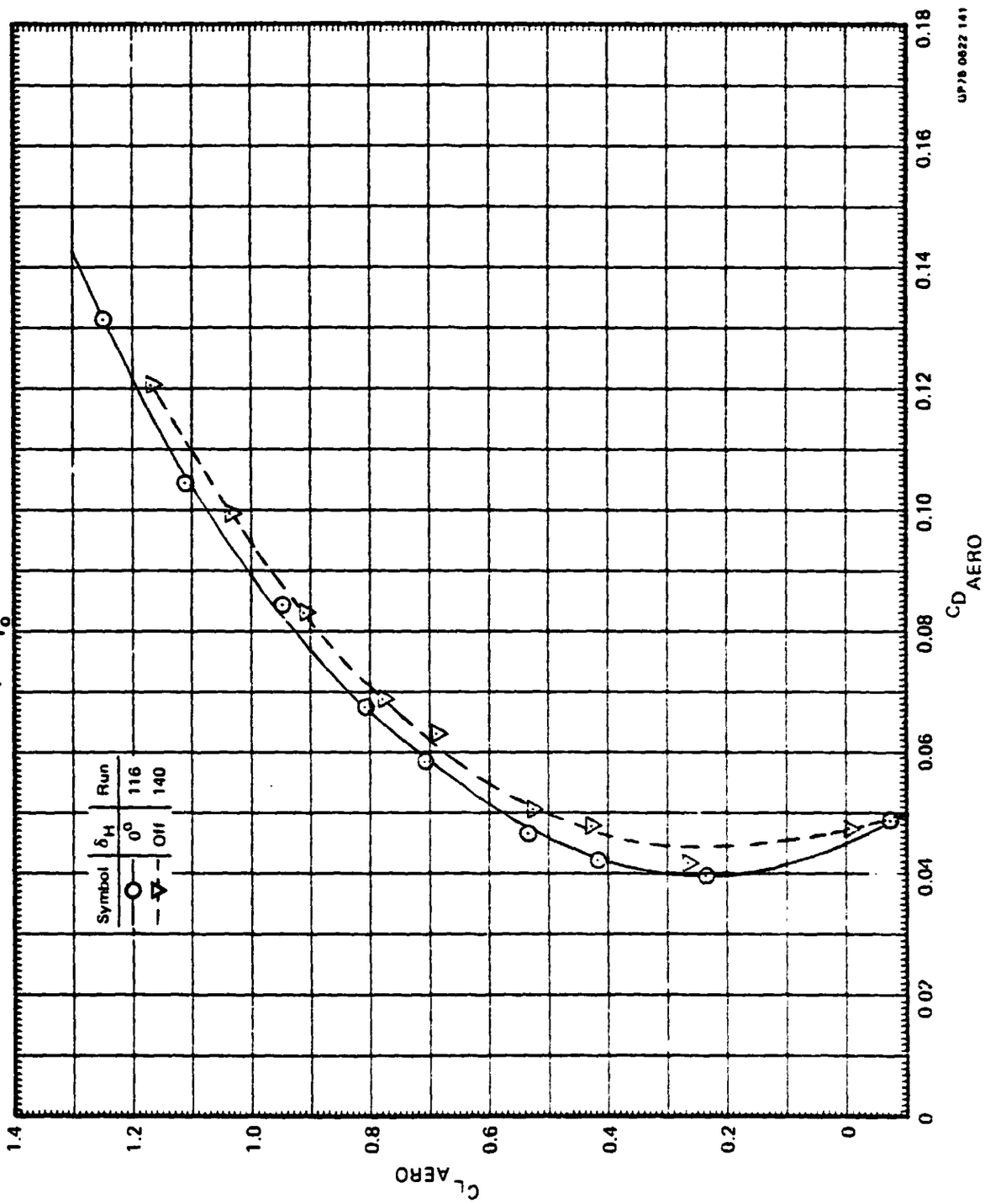

FIGURE 8.6-12
EFFECT OF HORIZONTAL TAIL ON PITCHING MOMENT COEFFICIENT vs ANGLE OF ATTACK

$\delta_H = 0^o$ q = 34.2 PSF $\delta_{LC} = 0^o$ δ_{NL} = SEALED $\theta_J = 1^o$
Direct Thrust Effects Removed
$\delta_f = 0^o$ $\delta_a = 0^o/0^o$ Nose Gear Off
$N_F/\sqrt{\theta T_o}$ = 2700 RPM

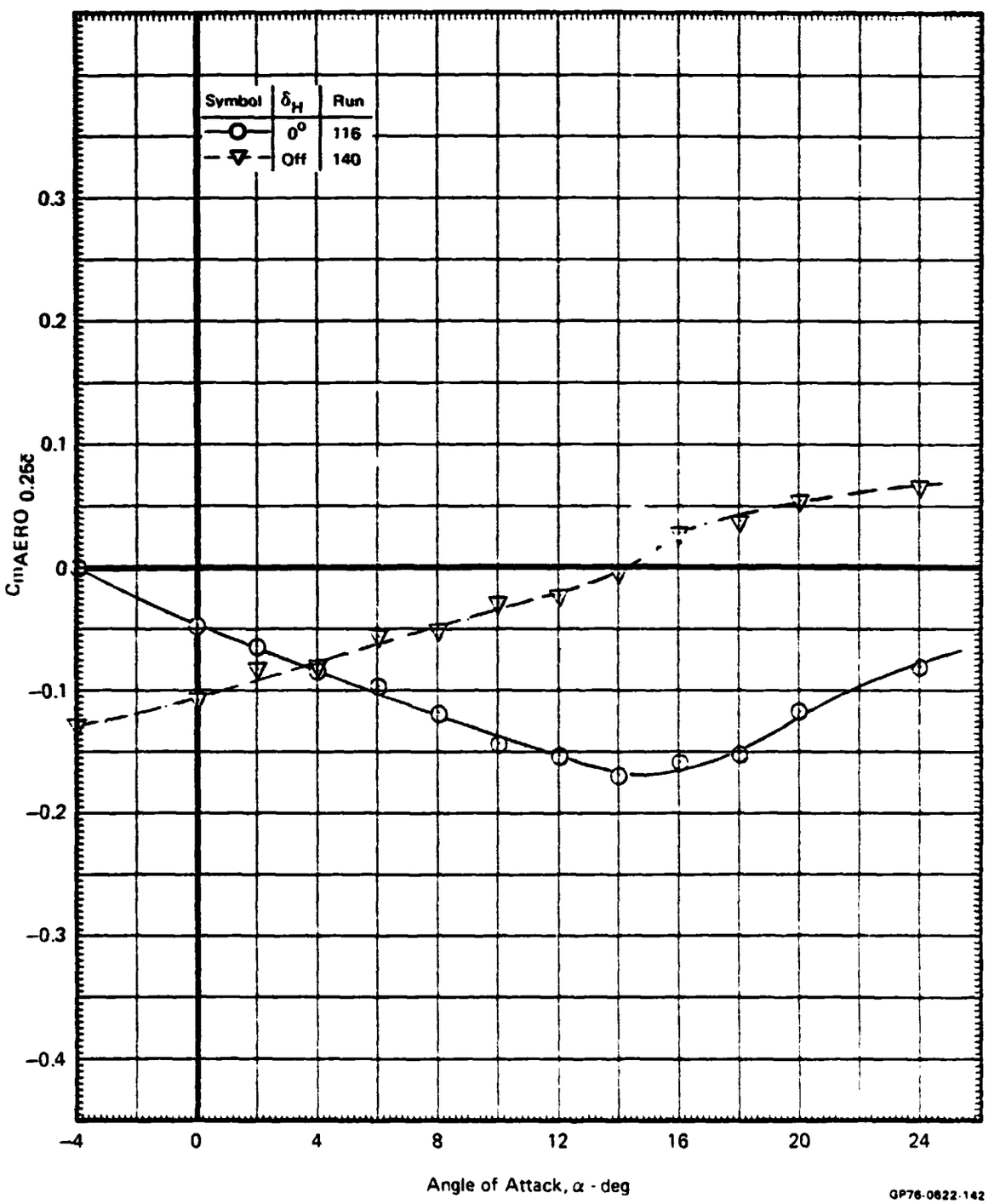

FIGURE 8.6-13
LIFT COEFFICIENT vs ANGLE OF ATTACK, FLOW SURVEY RAKE ON
q = 34.2 PSF $\delta_{LC} = 0^o$ $\delta_{NL} = 0^o$ Inlets Covered $\theta_J = 1^o$
Direct Thrust Effects Removed
Run 26 $\delta_f = 15^o$ $\delta_a = 10^o/10^o$ Nose Gear Off
$N_F/\sqrt{\theta T_o}$ = 2700 RPM

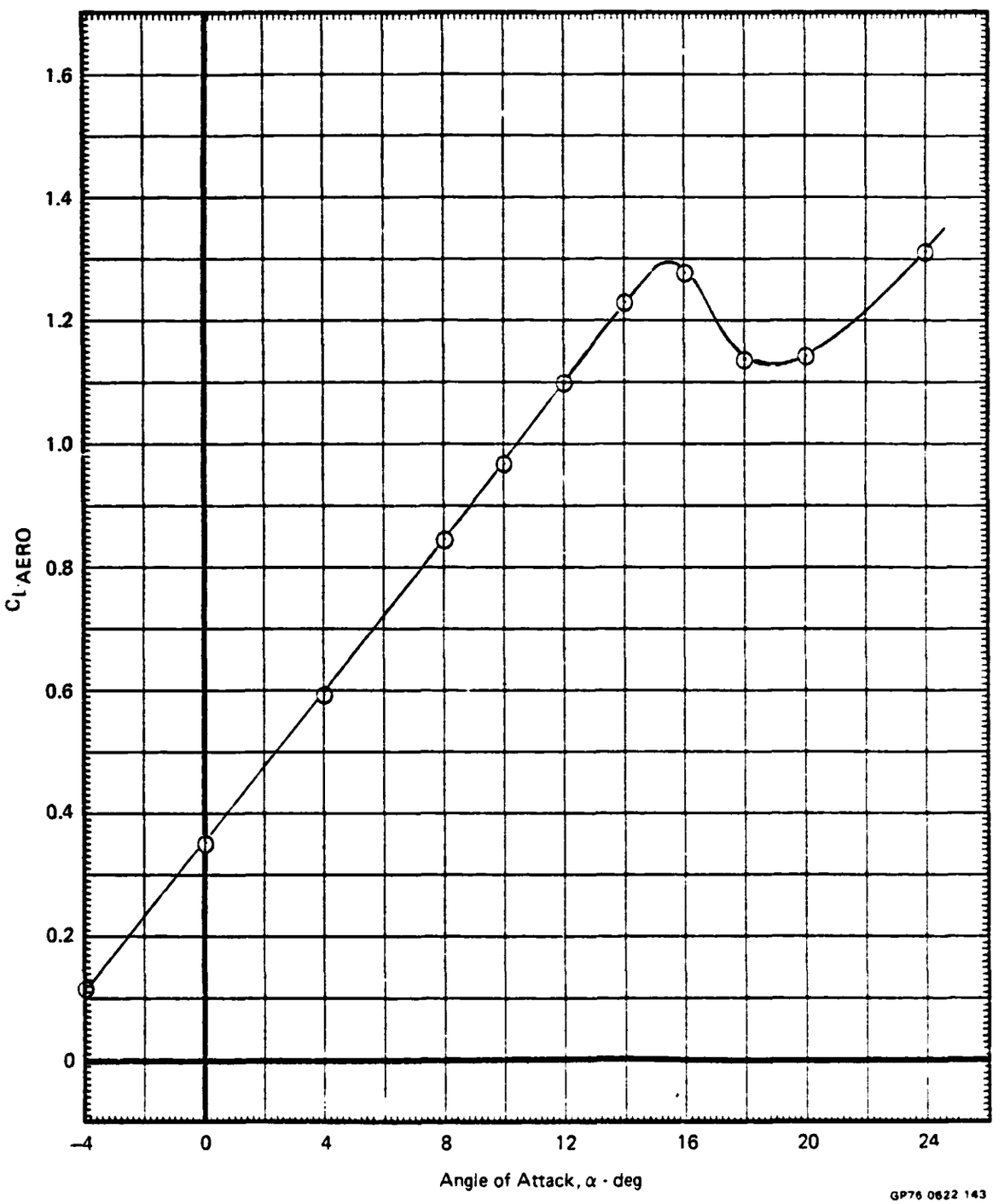

FIGURE 8.6-14
LIFT COEFFICIENT vs DRAG COEFFICIENT, FLOW SURVEY RAKE ON
q = 34.2 PSF $\delta_{LC} = 0^o$ $\delta_{NL} = 0^o$ Inlets Covered $\theta_J = 1^o$
Direct Thrust Effects Removed
Run 26 $\delta_f = 15^o$ $\delta_a = 10^o/10^o$ Nose Gear Off
$N_F/\sqrt{\theta T_o}$ = 2700 RPM

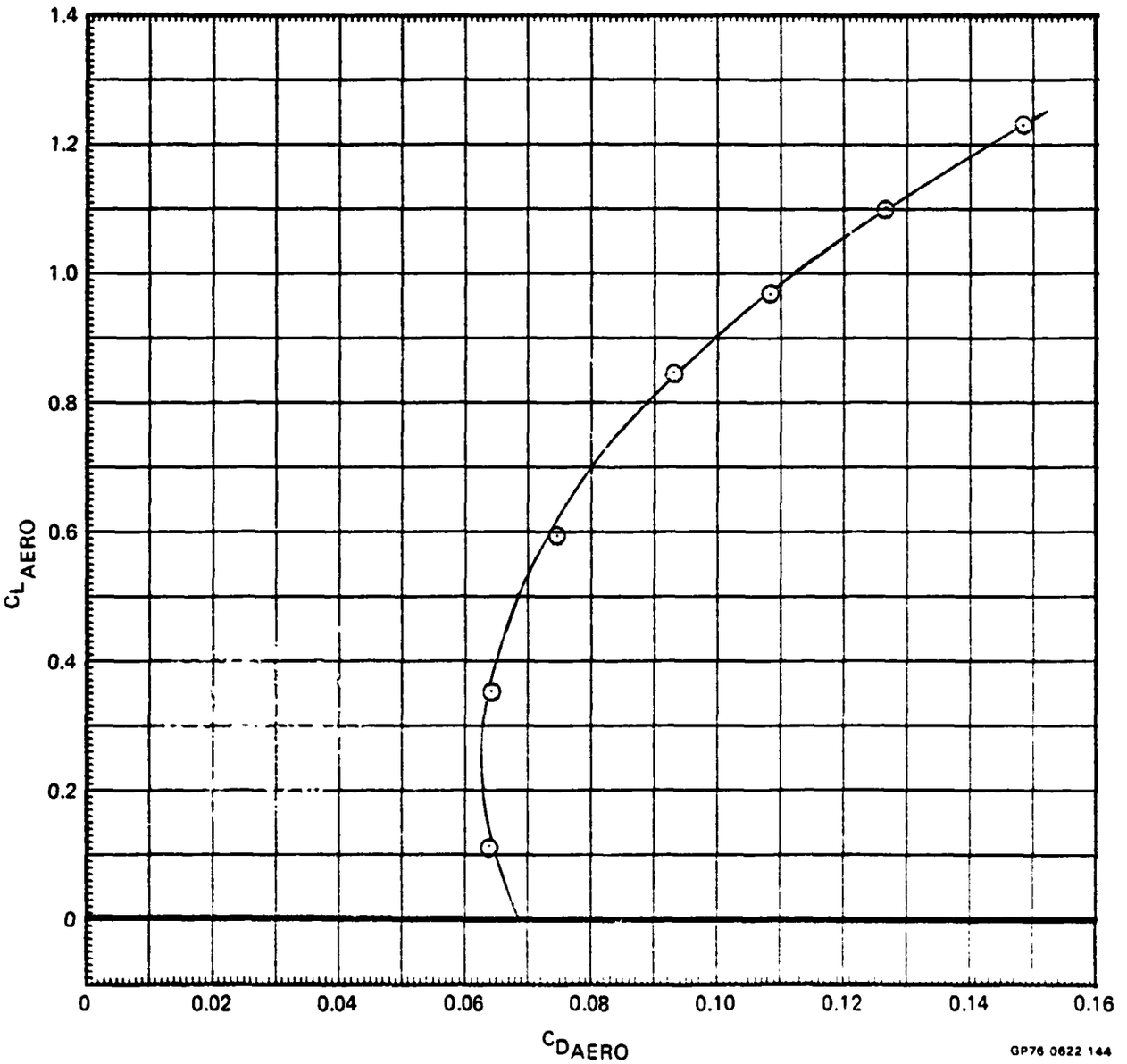

FIGURE 8.6-15
PITCHING MOMENT COEFFICIENT vs ANGLE OF ATTACK, FLOW SURVEY RAKE ON
q = 34.2 PSF $\delta_{LC} = 0^o$ $\delta_{NL} = 0^o$ Inlets Covered $\theta_J = 1^o$
Direct Thrust Effects Removed
Run 26 $\delta_f = 15^o$ $\delta_a = 10^o/10^o$ Nose Gear On
$N_F/\sqrt{\theta T_o} = 2700$ RPM

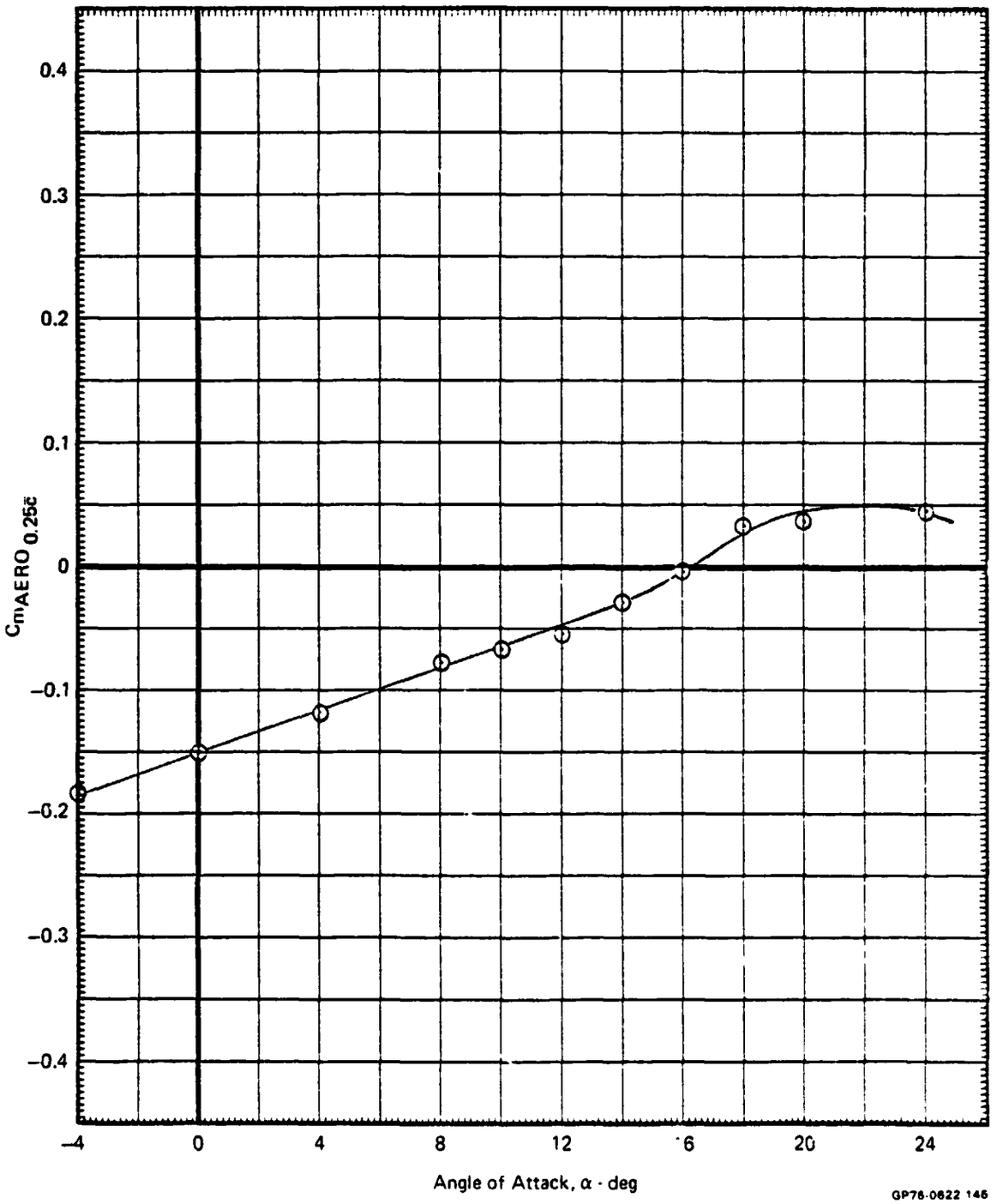

FIGURE 8.6-16
EFFECT OF HORIZONTAL TAIL ON LIFT COEFFICIENT vs ANGLE OF ATTACK
q = 34.2 PSF $\delta_{LC} = 0^o$ δ_{NL} = SEALED $\theta_J = 1^o$
Direct Thrust Effects Removed
$\delta_f = 0^o$ $\delta_a = 0^o/0^o$ Nose Gear Off
$N_F/\sqrt{\theta T_o}$ = 2700 RPM

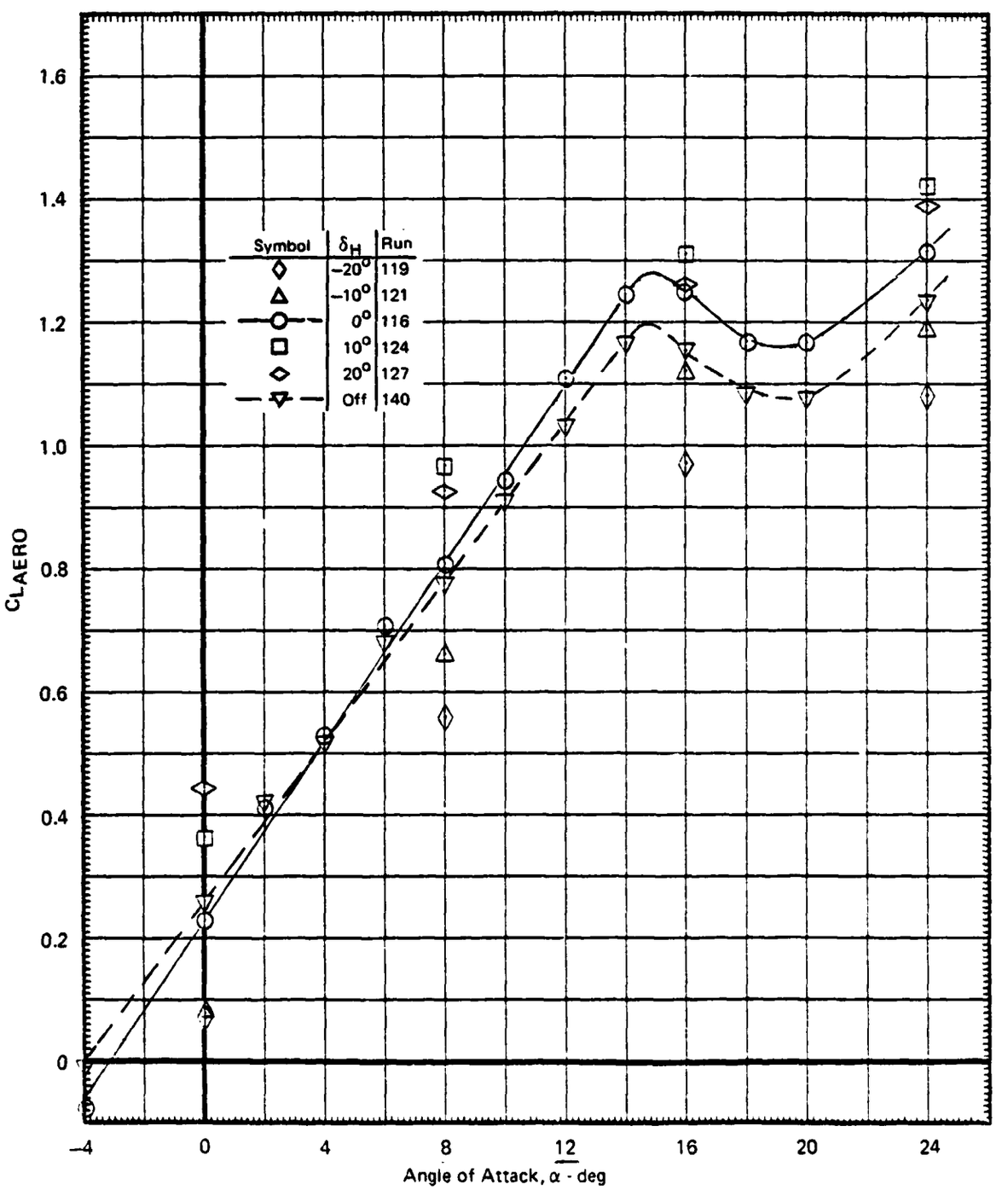

GP76-0622 146

FIGURE 8.6-17
EFFECT OF HORIZONTAL TAIL ON LIFT COEFFICIENT vs DRAG COEFFICIENT
q = 34.2 PSF $\delta_{LC} = 0^o$ δ_{NL} = SEALED $\theta_J = 1^o$
Direct Thrust Effects Removed
$\delta_f = 0^o$ $\delta_a = 0^o/0^o$ Nose Gear Off
$N_F/\sqrt{\theta T_o}$ = 2700 RPM

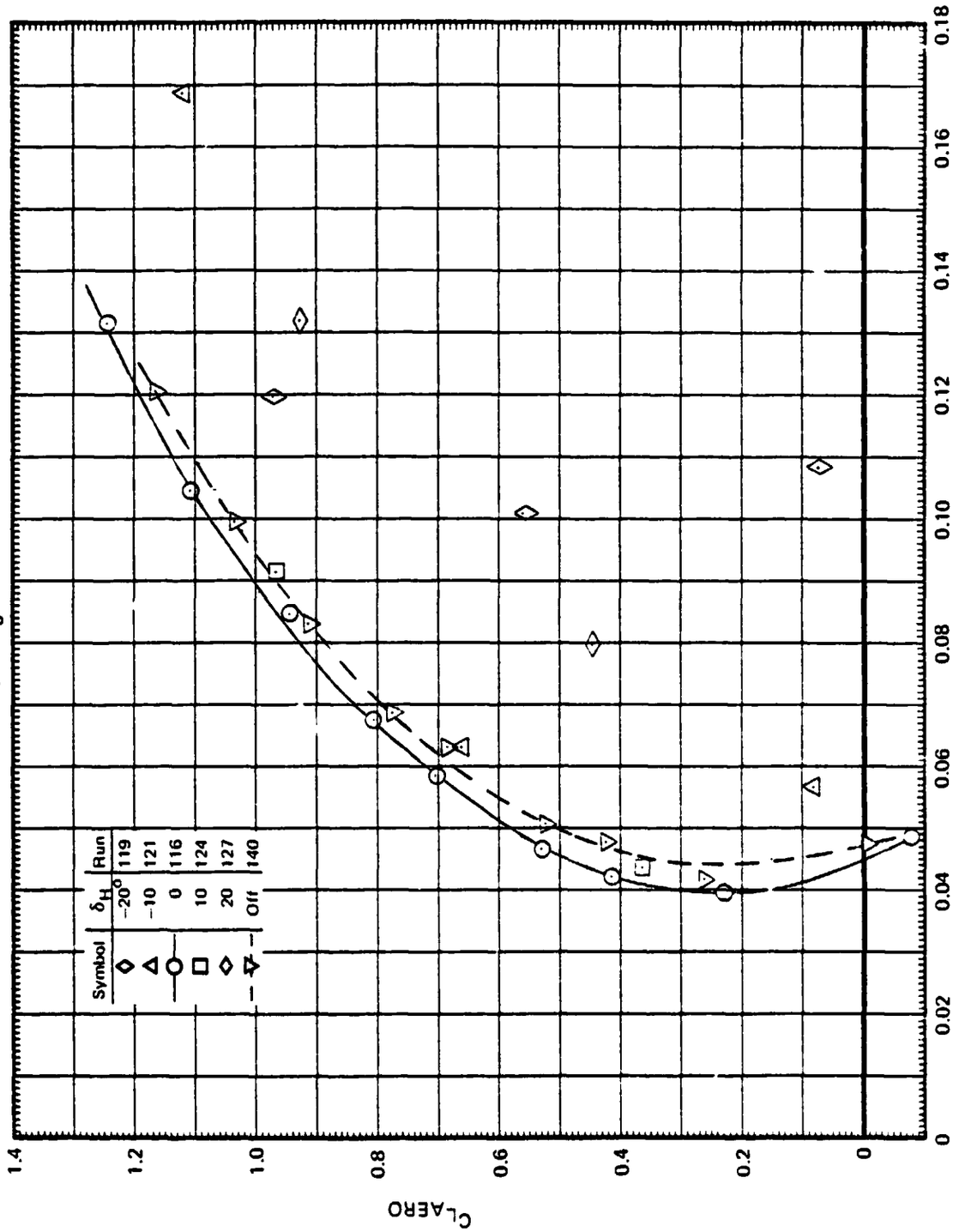

GP76 0622 147

FIGURE 8.6-18
EFFECT OF HORIZONTAL TAIL ON PITCHING MOMENT COEFFICIENT vs ANGLE OF ATTACK
q = 34.2 PSF $\delta_{LC} = 0^o$ δ_{NL} = SEALED $\theta_J = 1^o$
Direct Thrust and Ram Air Drag Effects Removed
$\delta_f = 0^o$ $\delta_a = 0^o/0^o$ Nose Gear Off
$N_F/\sqrt{\theta T_o}$ = 2700 RPM

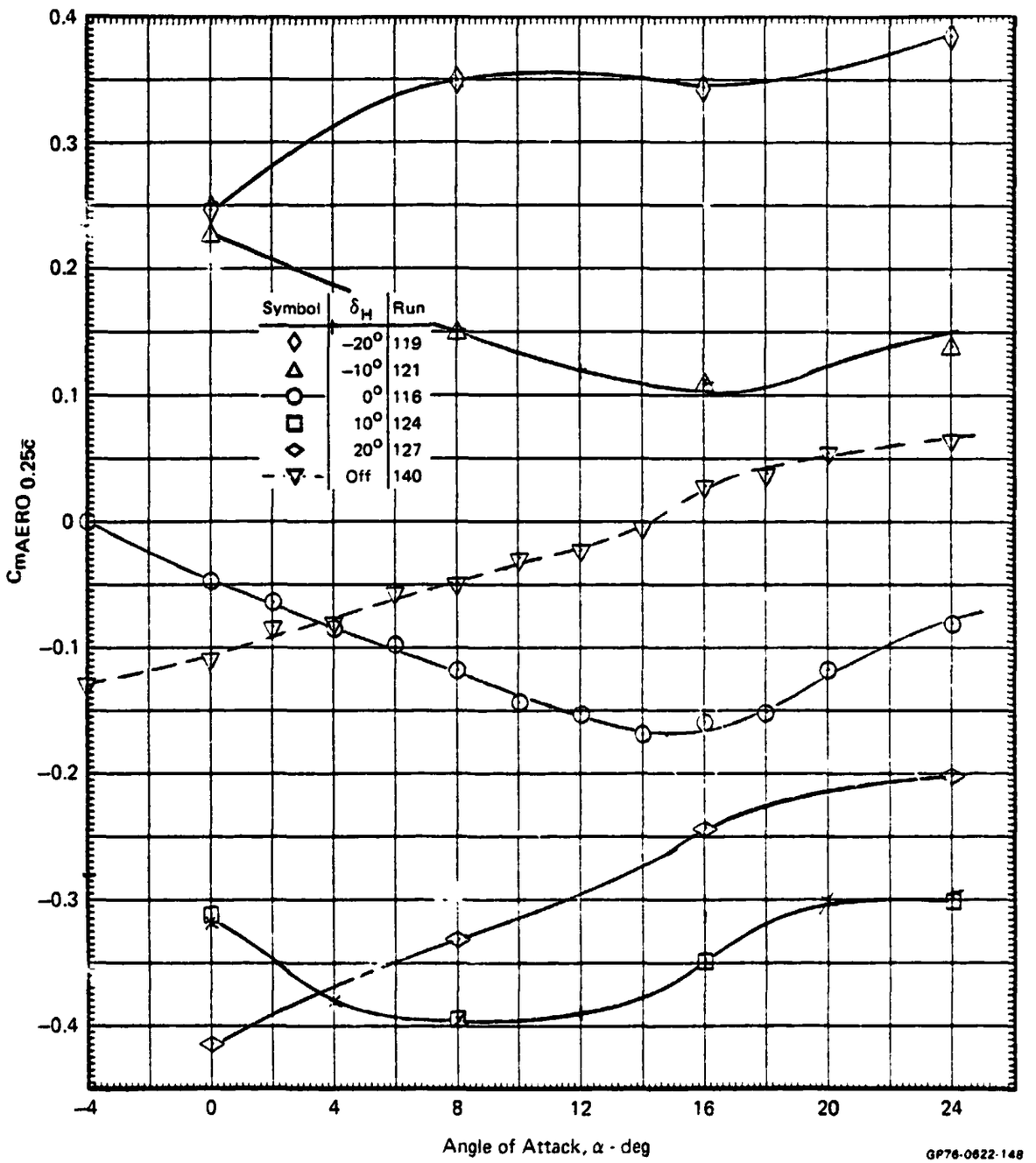

8.7 AERODYNAMIC LIFT CONFIGURATION - LATERAL-DIRECTIONAL CHARACTERISTICS

This section presents the lateral-directional stability and control characteristics of the aerodynamic lift configuration. Stability data are presented for angles of attack of 0°, 8°, and 16°. Lateral and directional control effectiveness data are presented for angles of attack up to 24°. The stability data are presented in both dimensional and coefficient form. The dimensional form has been included in order to emphasize the magnitude of the propulsion system contribution to the balance-measured forces and moments. All data are presented for stability axes.

Dimensional Data

The lateral-directional dimensional data are presented in Figures 8.7-1 through 8.7-9. The direct propulsion system contribution to the measured side force is the result of the ram drag contributions of the gas generators and lift/cruise units. Since the ram drag is essentially constant through an angle of attack of 16°, the propulsion system contribution to the side force remains constant through this angle. The propulsion system contributions to the measured yawing moment and rolling moments are the result of both the differential thrust between the two lift/cruise units and the ram drag contributions from the gas generators and lift/cruise units. The data indicate that the propulsion system contribution was negligible except for the yawing moment at 16° angle of attack.

Coefficient Data

The coefficient form of the aerodynamic force and moment data is presented in Figures 8.7-10 through 8.7-12. These data are the coefficient form of the total aerodynamic force and moments presented in Figures 8.7-1 through 8.7-9.

The characteristics are essentially linear with sideslip angle for angles of attack of 0° and 8°. At 16° angle of attack, the characteristics vary in a nonlinear manner typical of post-stall operation. The configuration does exhibit positive directional stability, C_{n_β}, through 16° angle of attack. The dihedral effect, C_{ℓ_β}, is stable for angles of attack of 8° and 16°, and neutrally stable for 0°.

Lateral-Directional Control Effectiveness

The lateral-directional control effectiveness is presented in Figures 8.7-13 through 8.7-16. Aileron control power is presented for a single aileron deflection from -25° to +25° at 0° angle of attack. Dual aileron deflection, -25°/+25°, data are presented as a function of angle of attack. The variation of rudder effectiveness with angle of attack is presented for a rudder deflection of 23°.

Aileron Effectiveness - The aileron effectiveness for a single aileron deflection from -25° to +25° and dual aileron, -25°/+25°, deflection is presented in Figure 8.7-13 at 0° angle of attack. The single aileron deflection data exhibit the trends associated with wings having a supercritical airfoil section in that the roll effectiveness is higher for the TEU deflections. The data for the dual aileron, -25°/+25° as a function of angle of attack, are presented in Figure 8.7-14. Aileron effectiveness is maintained at a high level below 12° angle of attack. At higher angles the roll effectiveness is reduced but the ailerons remain effective through 28° angle of attack.

Rudder Effectiveness - The variation in rudder effectiveness with angle of attack is presented in Figures 8.7-15 through 8.7-16 for a rudder deflection of 23° TEL. Rudder effectiveness is essentially constant below 24° angle of attack.

FIGURE 8.7-1
SIDE FORCE vs ANGLE OF SIDESLIP, $\alpha = 0^{o}$
$\delta_H = 0^{o}$ q = 34.2 PSF $\delta_{LC} = 0^{o}$ δ_{NL} = SEALED $\theta_J = 1^{o}$
Graphical Summary of Measured and Calculated Force Data
Run 129 $\delta_f = 0^{o}$ $\delta_a = 0^{o}/0^{o}$ Nose Gear Off
$N_F/\sqrt{\theta T_o}$ = 2700 RPM

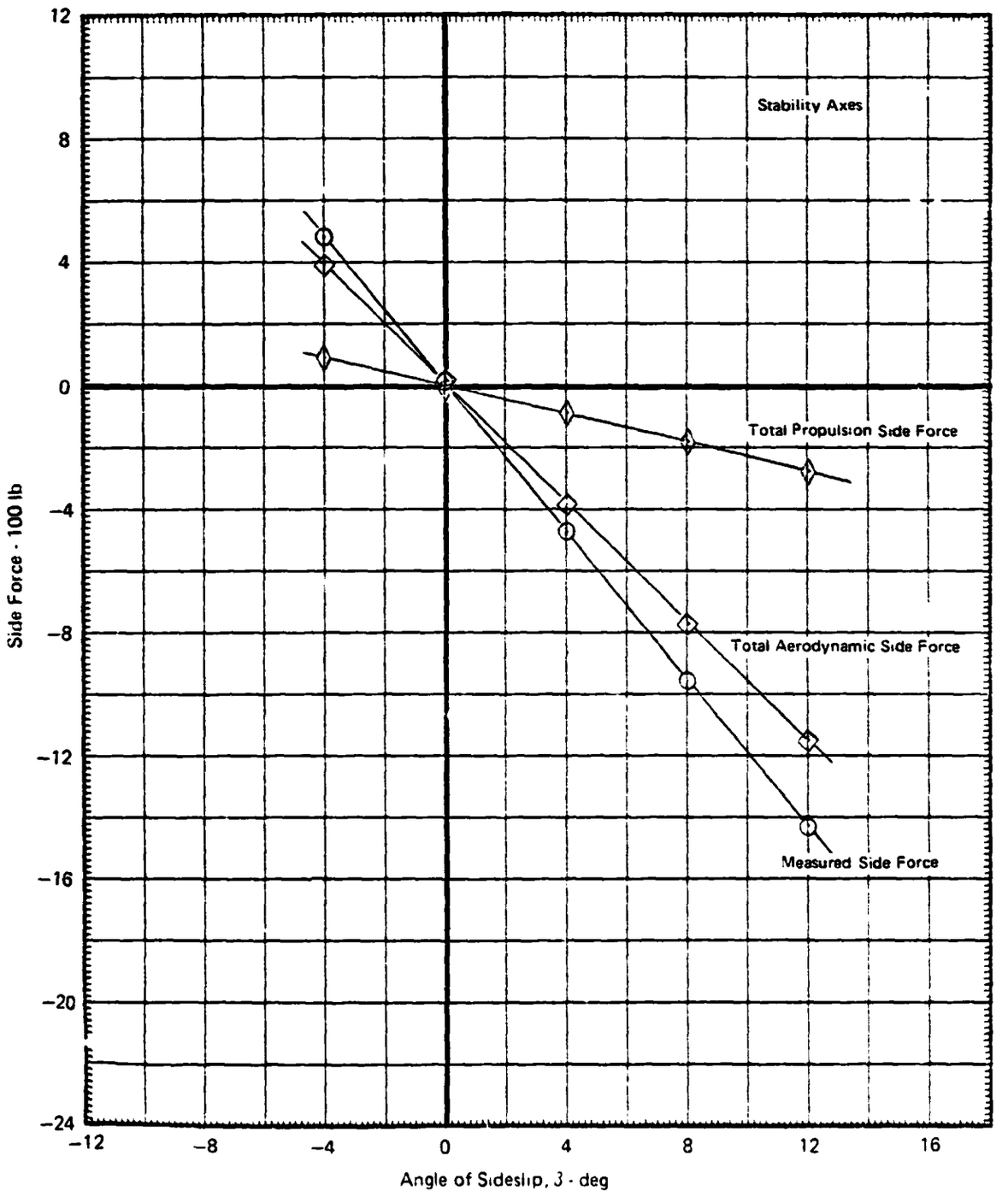

GP76-0622-192

FIGURE 8.7-2
YAWING MOMENT vs ANGLE OF SIDESLIP, $\alpha = 0^o$
$\delta_H = 0^o$ $q = 34.2$ PSF $\delta_{LC} = 0^o$ δ_{NL} = SEALED $\theta_J = 1^o$
Graphical Summary of Measured and Calculated Moment Data
Run 129 $\delta_f = 0^o$ $\delta_a = 0^o/0^o$ Nose Gear Off
$N_F/\sqrt{\theta_{T_o}} = 2700$ RPM

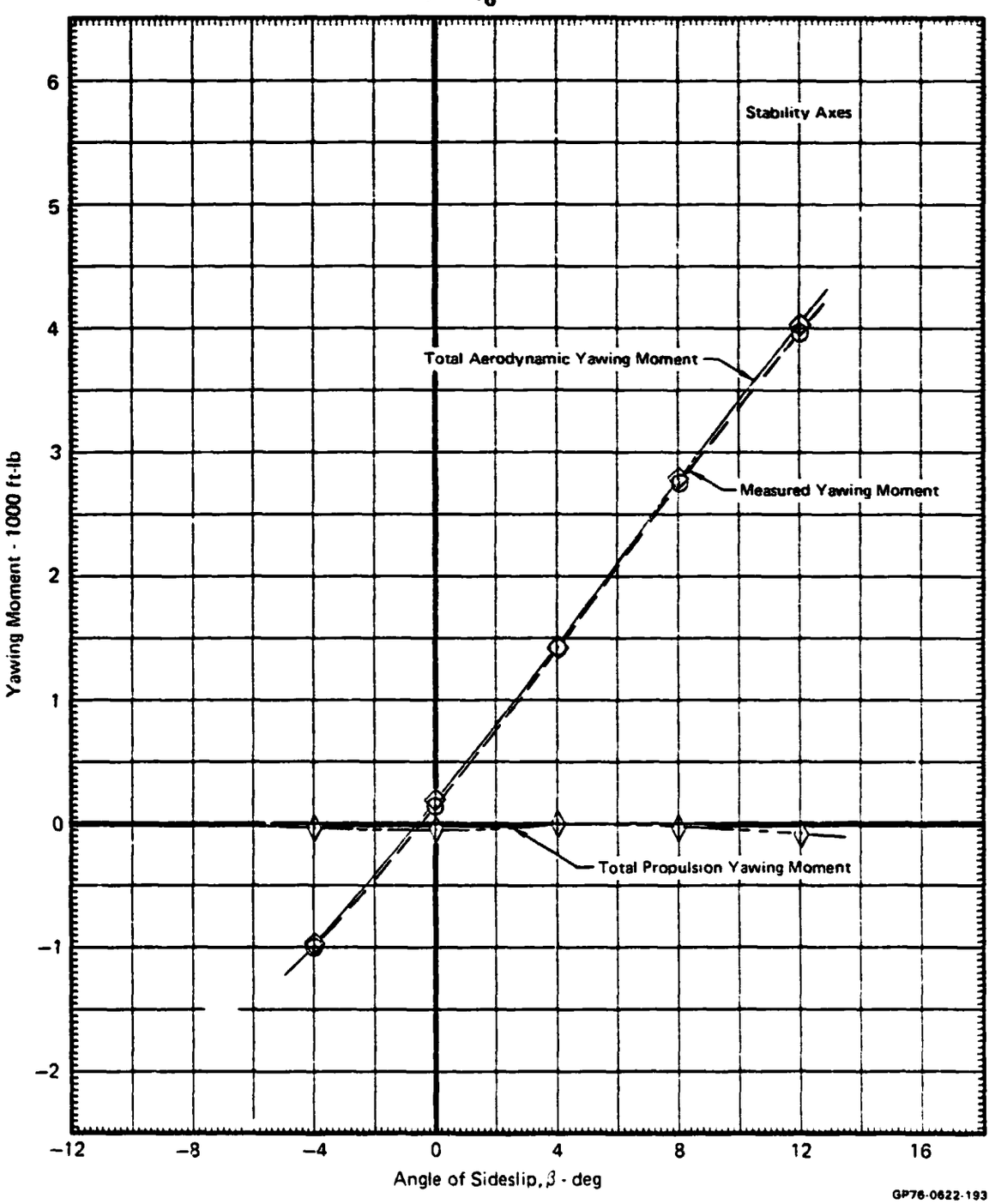

FIGURE 8.7-3
ROLLING MOMENT vs ANGLE OF SIDESLIP, $\alpha = 0^0$
$\delta_H = 0^0$ q = 34.2 PSF $\delta_{LC} = 0^0$ δ_{NL} = SEALED $\bar{\theta}_J = 1^0$
Graphical Summary of Measured and Calculated Moment Data
Run 129 $\delta_f = 0^0$ $\delta_a = 0^0/0^0$ Nose Gear Off
$N_F/\sqrt{\theta T_o}$ = 2700 RPM

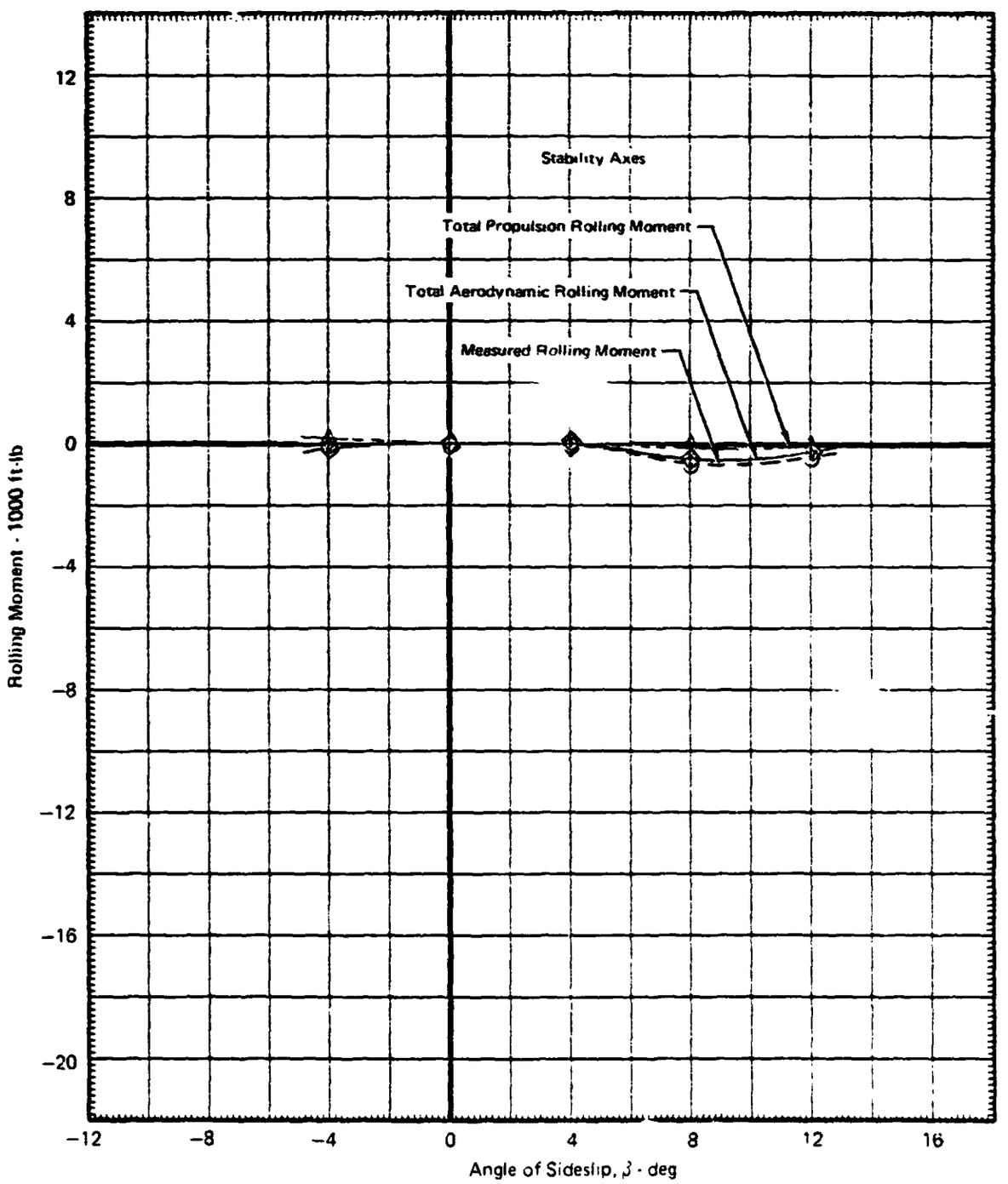

GP78-0622-194

FIGURE 8.7-4
SIDE FORCE vs ANGLE OF SIDESLIP, $\alpha = 8^0$
$\delta_H = 0^0$ q = 34.2 PSF $\delta_{LC} = 0^0$ δ_{NL} = SEALED $\theta_J = 1^0$
Graphical Summary of Measured and Calculated Force Data
Run 130 $\delta_f = 0^0$ $\delta_a = 0^0/0^0$ Nose Gear Off
$N_F/\sqrt{\theta T_o}$ = 2700 RPM

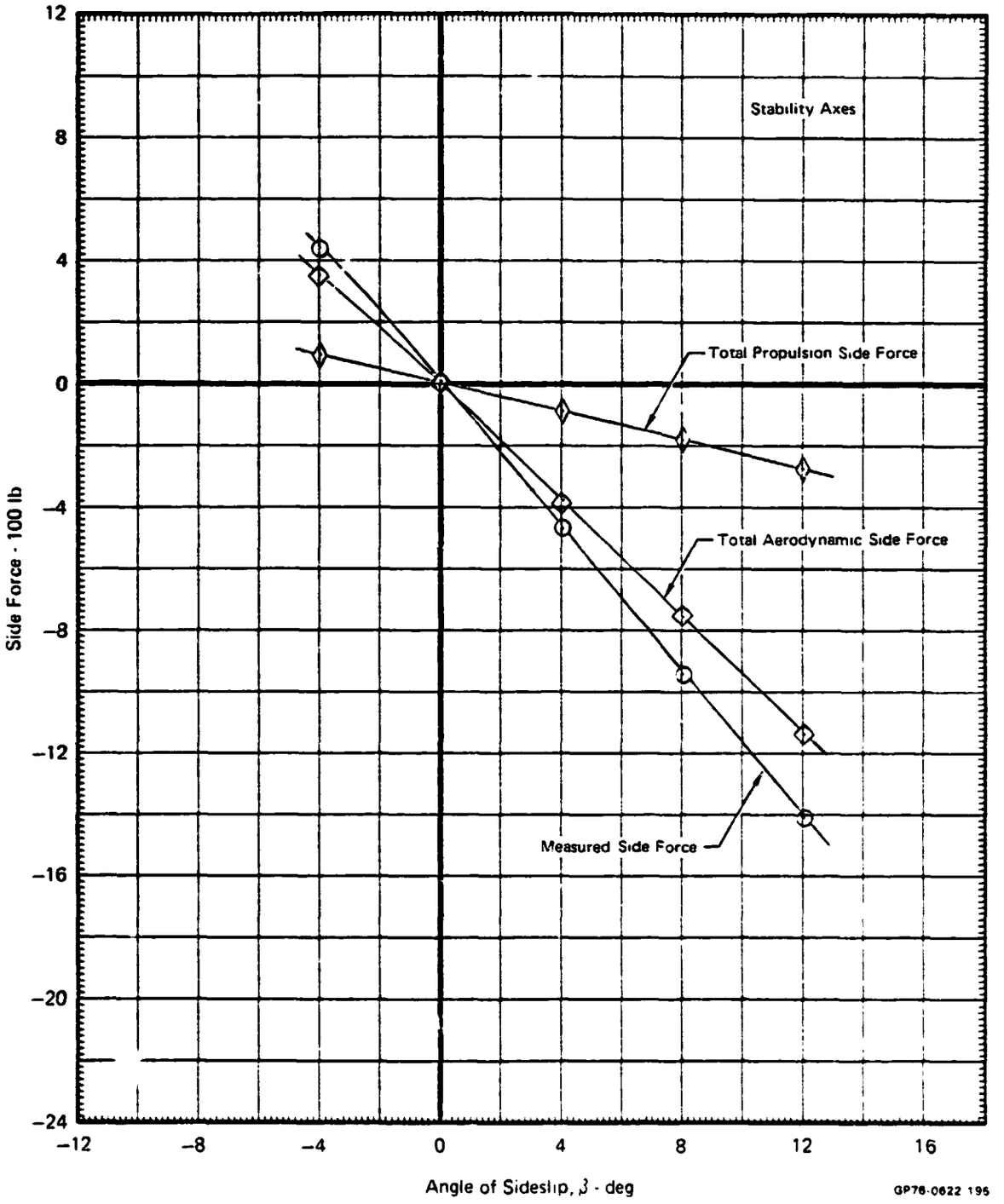

FIGURE 8.7-5
YAWING MOMENT vs ANGLE OF SIDESLIP, $\alpha = 8^{o}$
$\delta_H = 0^{o}$ q = 34.2 PSF $\delta_{LC} = 0^{o}$ δ_{NL} = SEALED $\theta_J = 1^{o}$
Graphical Summary of Measured and Calculated Moment Data
Run 130 $\delta_f = 0^{o}$ $\delta_a = 0^{o}/0^{o}$ Nose Gear Off
$N_F/\sqrt{\theta T_o}$ = 2700 RPM

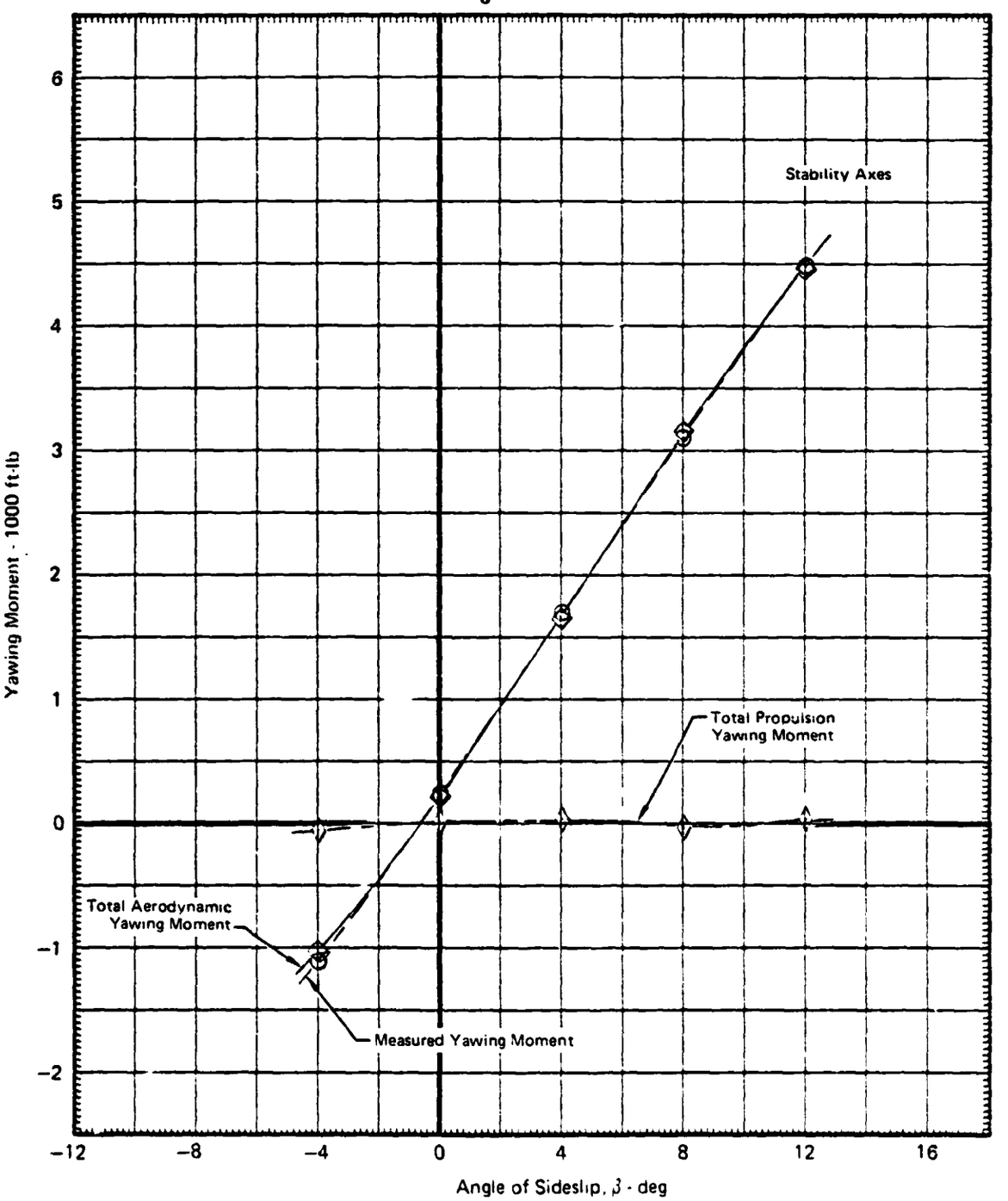

GP76-0822-196

FIGURE 8.7-6

ROLLING MOMENT vs ANGLE OF SIDESLIP, $\alpha = 8^{o}$

$\delta_H = 0^{o}$ q = 34.2 PSF $\delta_{LC} = 0^{o}$ δ_{NL} = SEALED $\theta_J = 1^{o}$

Graphical Summary of Measured and Calculated Moment Data

Run 130 $\delta_f = 0^{o}$ $\delta_a = 0^{o}/0^{o}$ Nose Gear Off

$N_F/\sqrt{\theta T_o}$ = 2700 RPM

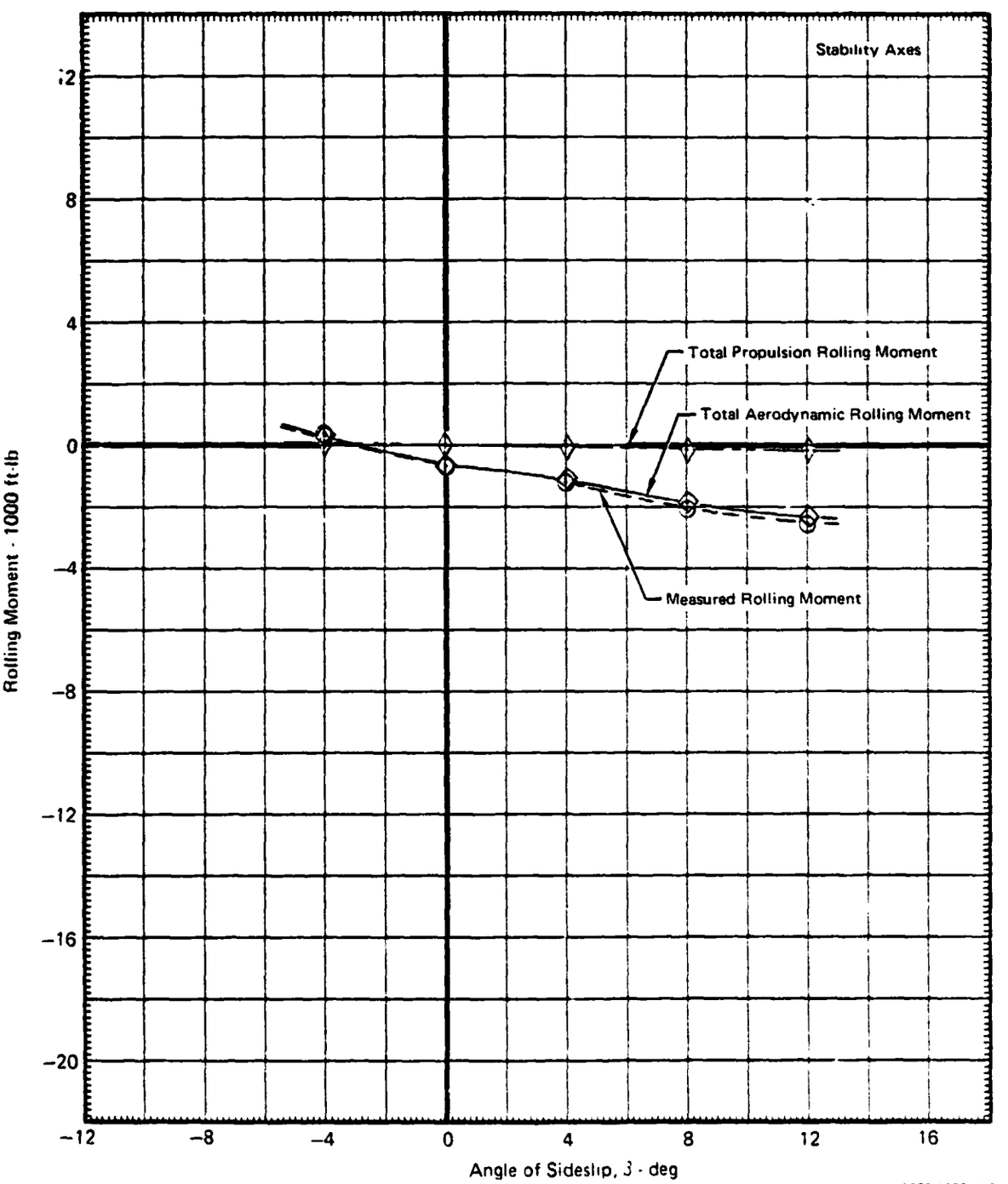

GP76-0622 197

FIGURE 8.7-7
SIDE FORCE vs ANGLE OF SIDESLIP, $\alpha = 16^{o}$
$\delta_H = 0^{o}$ q = 34.2 PSF $\delta_{LC} = 0^{o}$ δ_{NL} = SEALED $\theta_J = 1^{o}$
Graphical Summary of Measured and Calculated Force Data
Run 131 $\delta_f = 0^{o}$ $\delta_a = 0^{o}/0^{o}$ Nose Gear Off
$N_F/\sqrt{\theta_{T_o}}$ = 2700 RPM

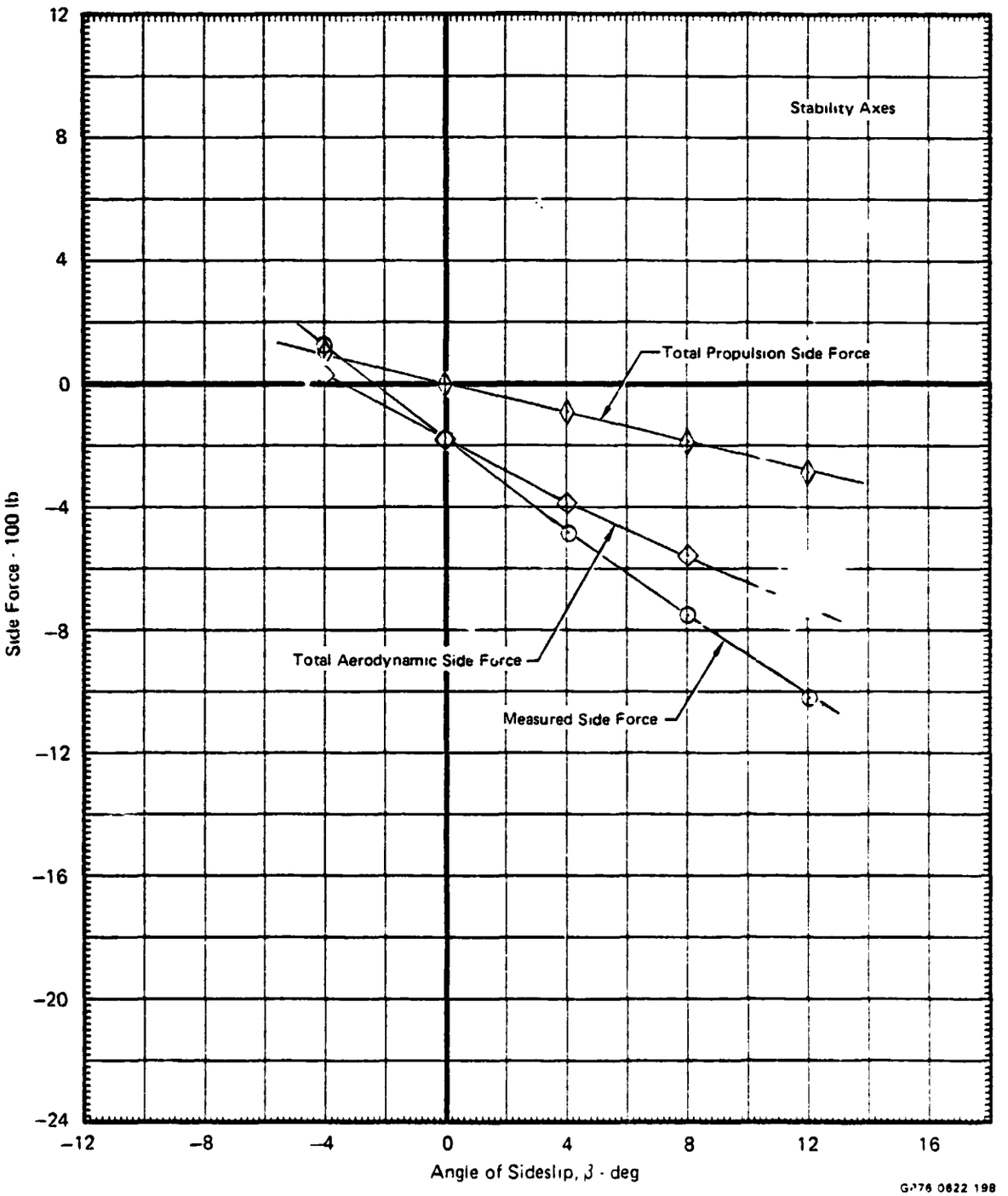

G276 0822 198

FIGURE 8.7-8
YAWING MOMENT vs ANGLE OF SIDESLIP, $\alpha = 16^{o}$
$\delta_H = 0^{o}$ q = 34.2 PSF $\delta_{LC} = 0^{o}$ δ_{NL} = SEALED $\theta_J = 1^{o}$
Graphical Summary of Measured and Calculated Moment Data
Run 131 $\delta_f = 0^{o}$ $\delta_a = 0^{o}/0^{o}$ Nose Gear Off
$N_F/\sqrt{\theta_{T_o}}$ = 2700 RPM

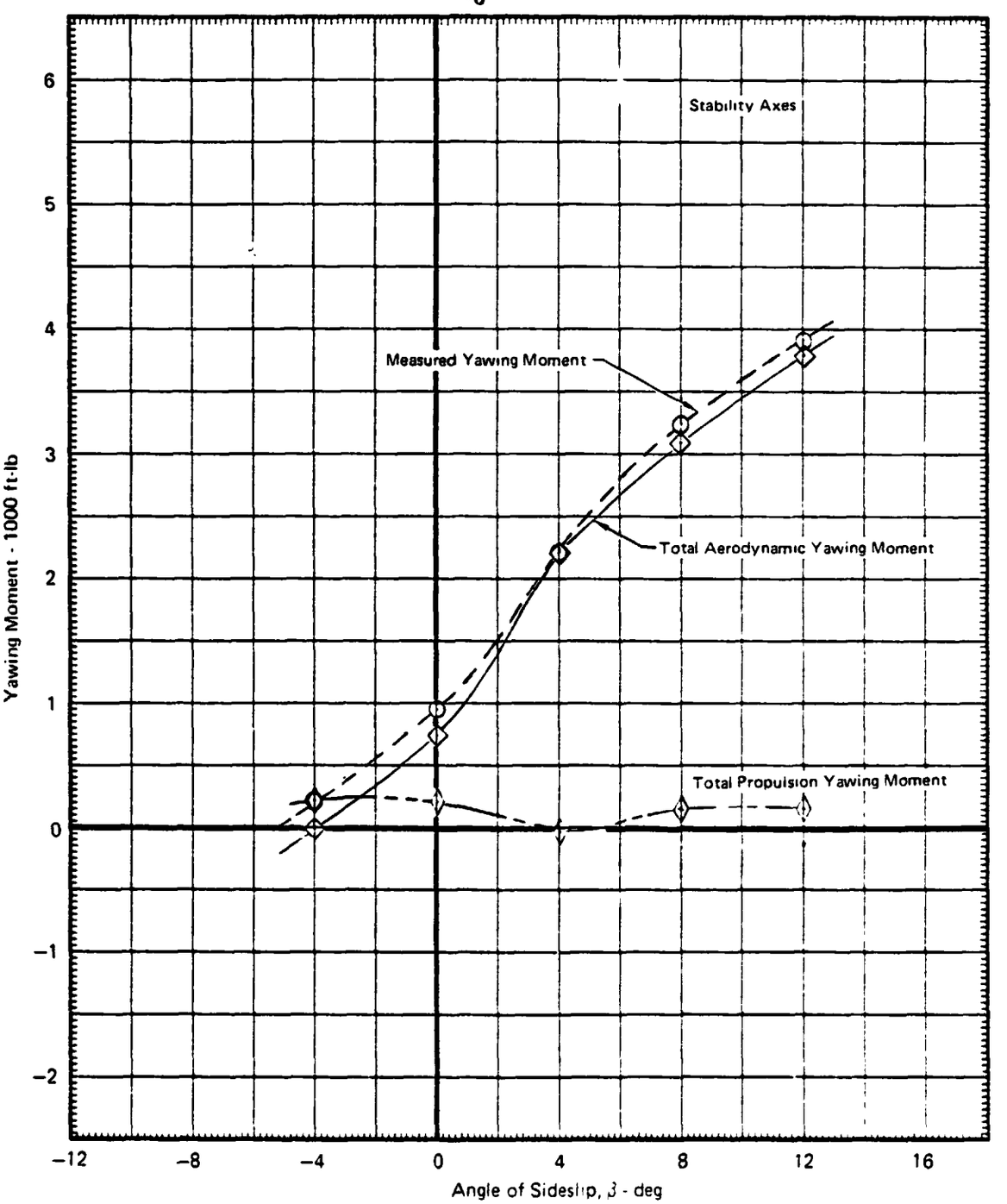

FIGURE 8.7-9
ROLLING MOMENT vs ANGLE OF SIDESLIP, $\alpha = 16^{o}$
$\delta_H = 0^{o}$ q = 34.2 PSF $\delta_{LC} = 0^{o}$ δ_{NL} = SEALED $\theta_J = 1^{o}$
Graphical Summary of Measured and Calculated Moment Data
Run 131 $\delta_f = 0^{o}$ $\delta_a = 0^{o}/0^{o}$ Nose Gear Off
$N_F/\sqrt{\theta_{T_o}}$ = 2700 RPM

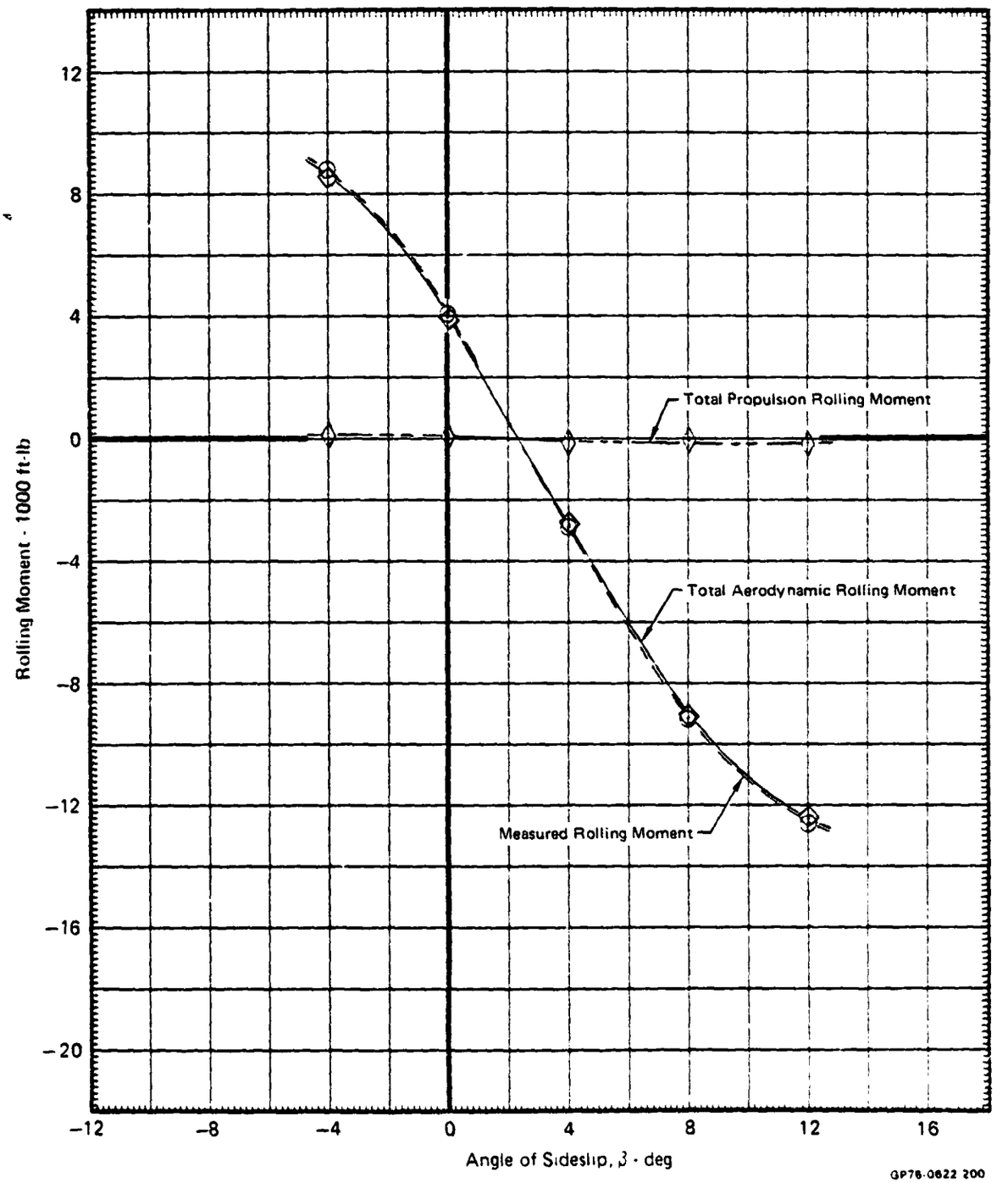

FIGURE 8.7-10
EFFECT OF ANGLE OF ATTACK ON SIDE FORCE COEFFICIENT vs ANGLE OF SIDESLIP

$\delta_H = 0^o$ $q = 34.2$ PSF $\delta_{LC} = 0^o$ δ_{NL} = SEALED $\theta_J = 1^o$
Direct Thrust Effects Removed
$\delta_f = 0^o$ $\delta_a = 0^o/0^o$ Nose Gear Off
$N_F/\sqrt{\theta_{T_o}} = 2700$ RPM

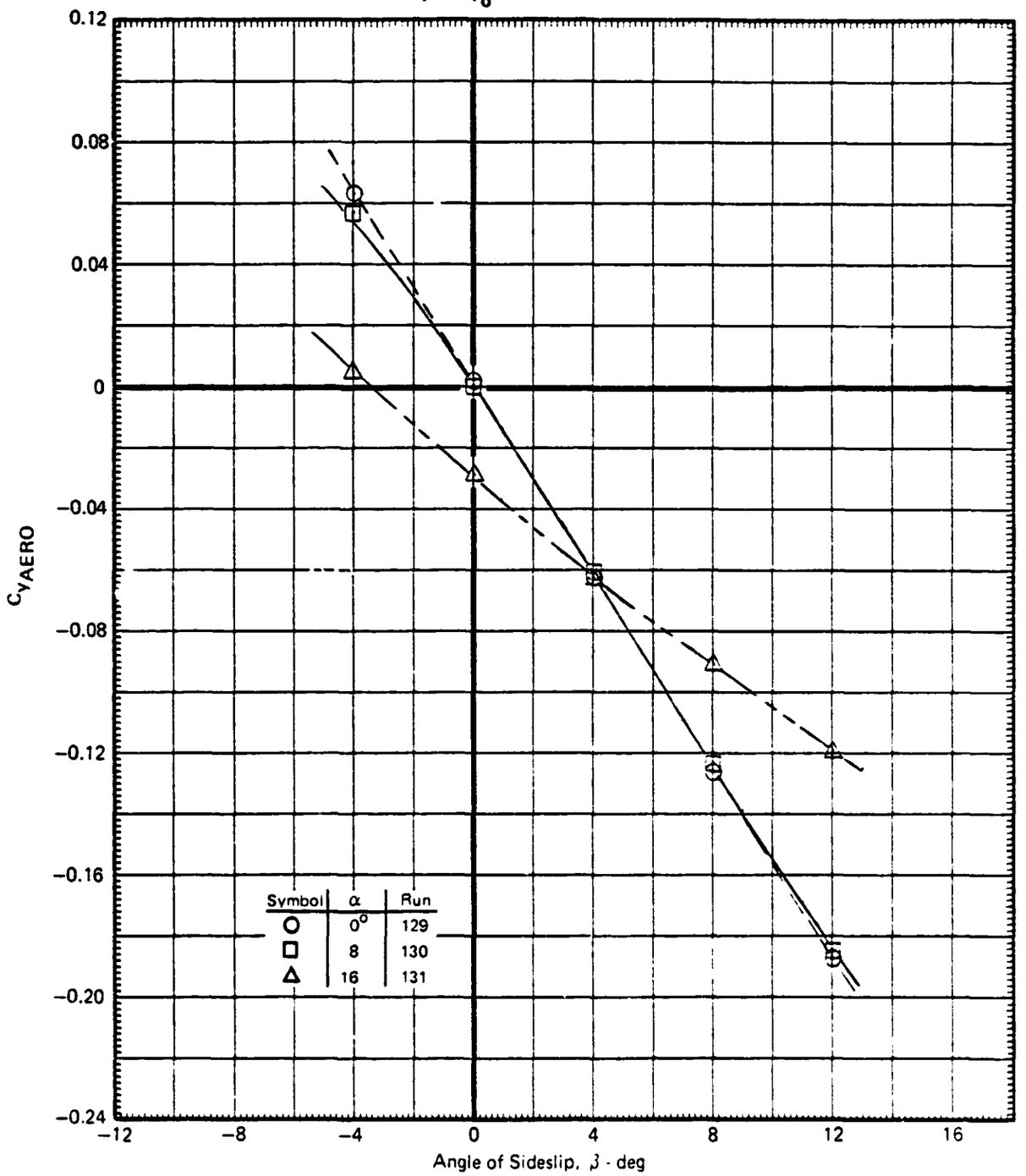

GP78-0822 201

FIGURE 8.7-11
EFFECT OF ANGLE OF ATTACK ON YAWING MOMENT COEFFICIENT vs ANGLE OF SIDESLIP

$\delta_H = 0^o$ $q = 34.2$ PSF $\delta_{LC} = 0^o$ δ_{NL} = SEALED $\theta_J = 1^o$

Direct Thrust Effects Removed

$\delta_f = 0^o$ $\delta_a = 0^o/0^o$ Nose Gear Off

$N_F/\sqrt{\theta T_o} = 2700$ RPM

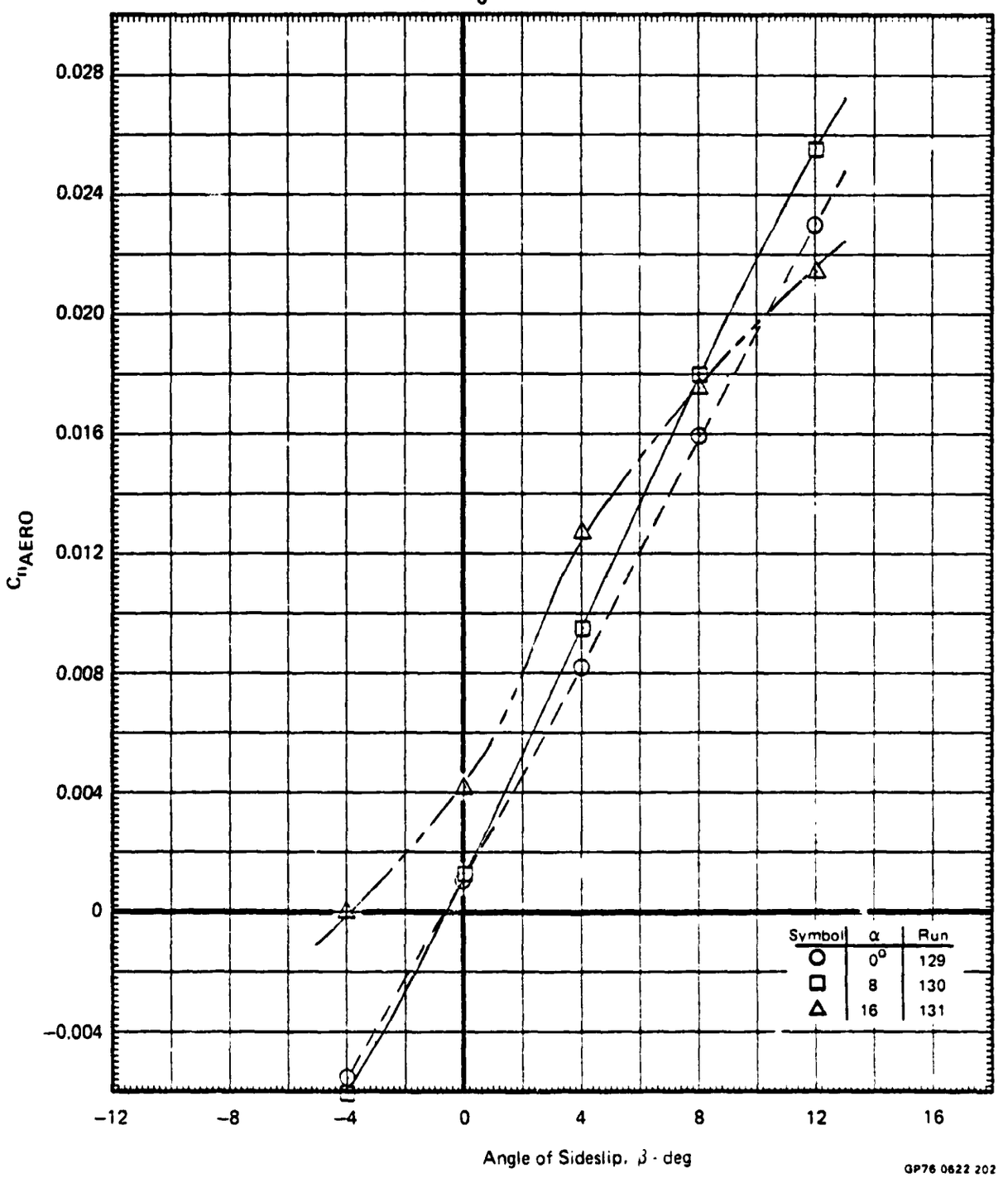

FIGURE 8.7-12
EFFECT OF ANGLE OF ATTACK ON ROLLING MOMENT COEFFICIENT vs ANGLE OF SIDESLIP

$\delta_H = 0^o$ $q = 34.2$ PSF $\delta_{LC} = 0^o$ δ_{NL} = SEALED $\theta_J = 1^o$

Direct Thrust Effects Removed

$\delta_f = 0^o$ $\delta_a = 0^o/0^o$ Nose Gear Off

$N_F/\sqrt{\theta_{T_o}} = 2700$ RPM

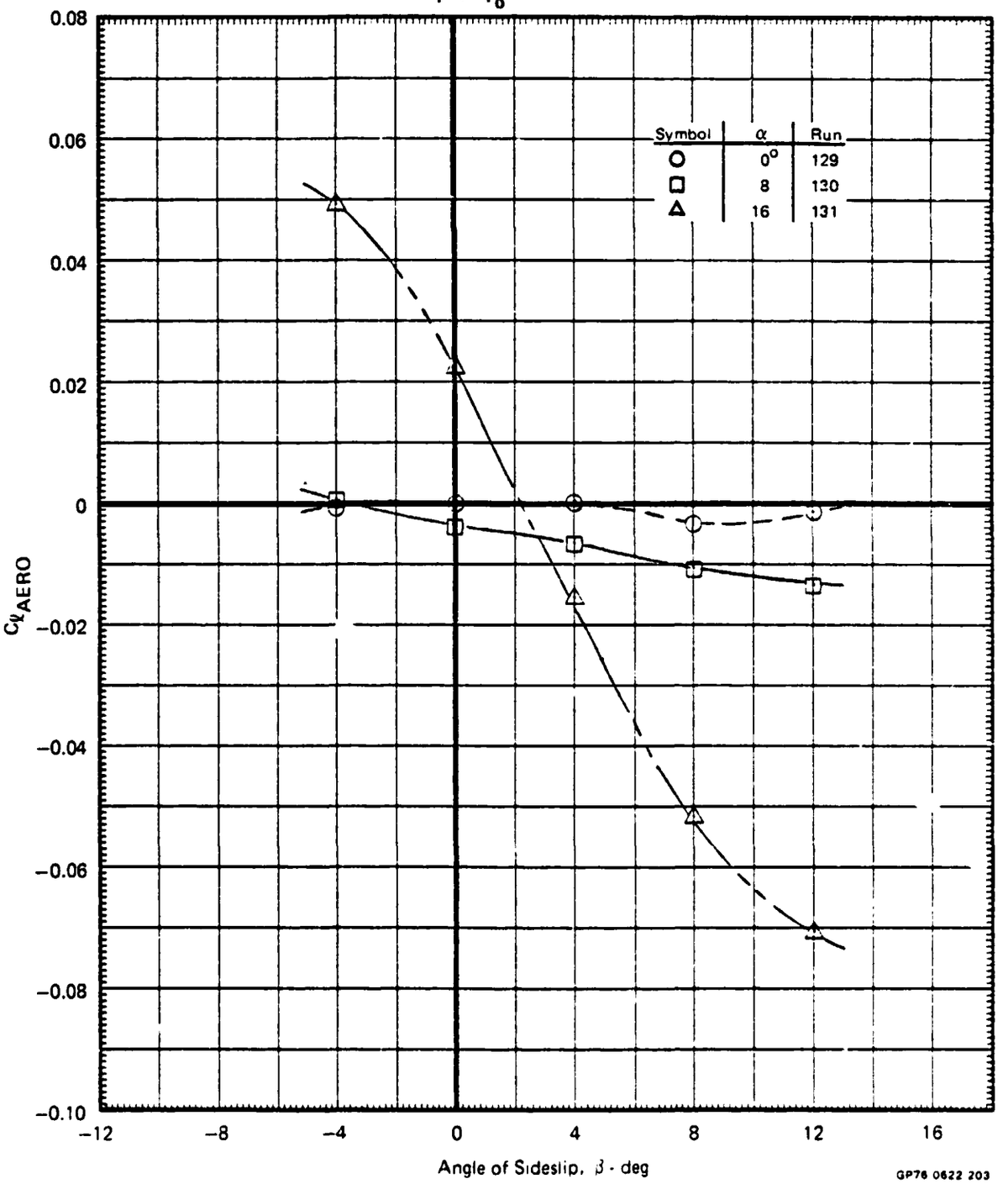

FIGURE 8.7-13
EFFECT OF AILERON DEFLECTION ON LATERAL-DIRECTIONAL CHARACTERISTICS, $\alpha = 0^{o}$

$\delta_H = 0^{o}$ $q = 34.2$ PSF $\delta_{LC} = 0^{o}$ δ_{NL} = SEALED $\theta_J = 1^{o}$

Measured Data

$\delta_f = 0^{o}$ Nose Gear Off

$N_F/\sqrt{\theta_{T_o}} = 2700$ RPM

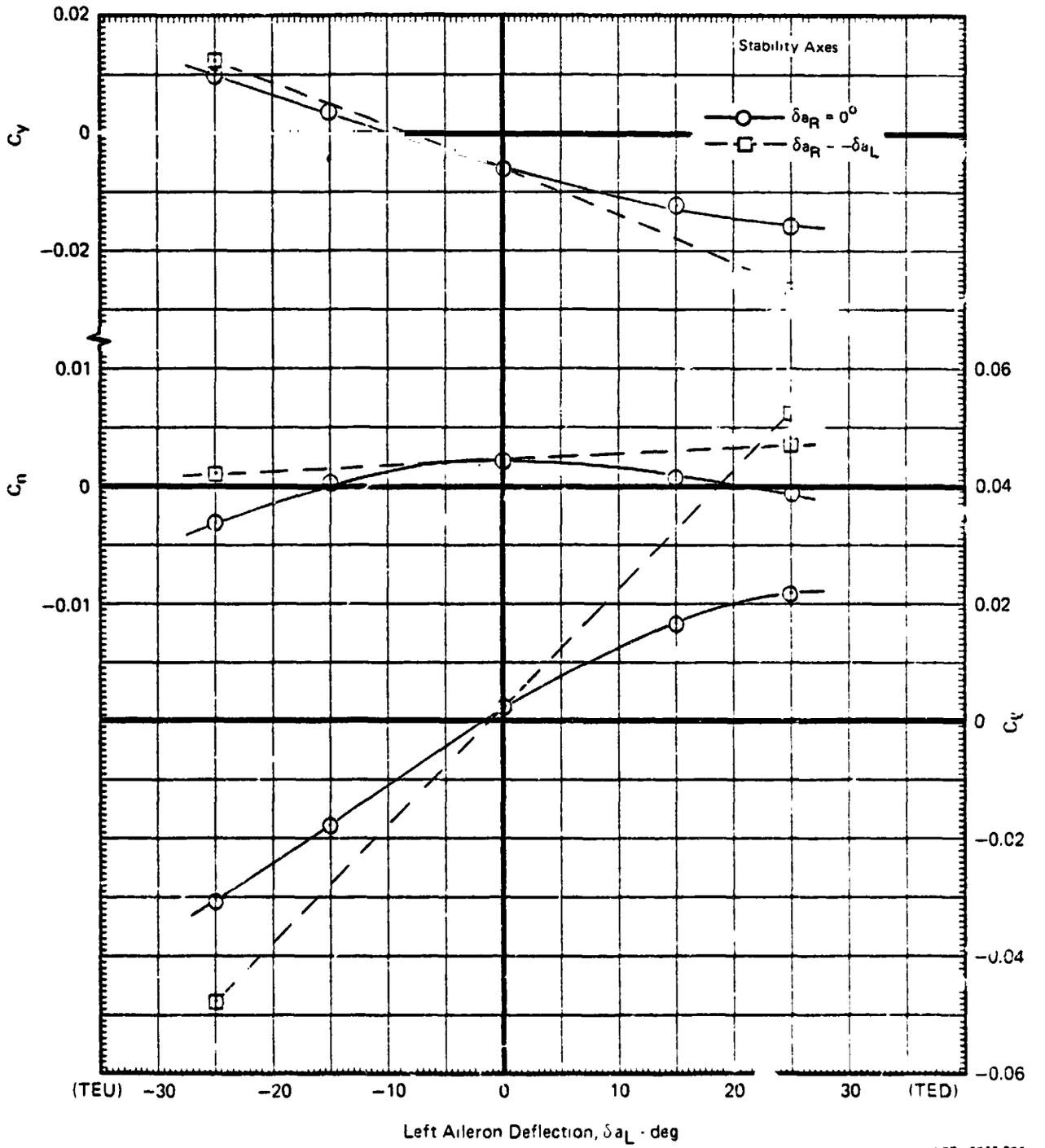

AF7, 0672 206

FIGURE 8.7-14
EFFECT OF AILERON DEFLECTION ON LATERAL-DIRECTIONAL CHARACTERISTICS, $\delta = 0$

$\delta_H = 0^o$ $q = 34.2$ PSF $\delta_{LC} = 0^o$ δ_{NL} = SEALED $\theta_J = 1^o$

Direct Thrust Effects Removed

$\delta_f = 0^o$ $\delta_a = -25^o/+25^o$ Nose Gear Off

$N_F/\sqrt{\theta_{T_o}} = 2700$ RPM

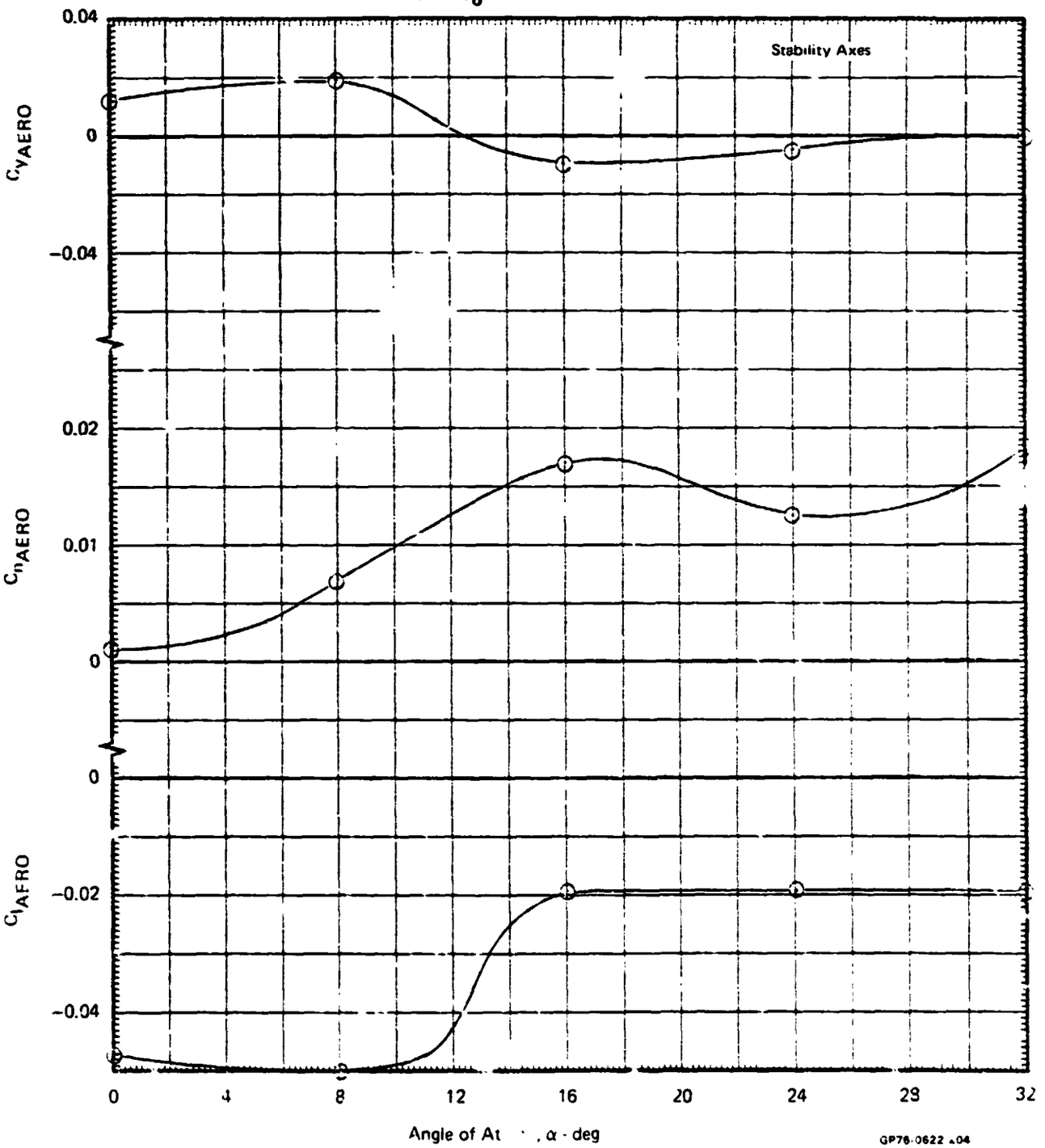

FIGURE 8.7-15
EFFECT OF RUDDER DEFLECTION ON SIDE FORCE
$\delta_H = 0^o$ q = 34.2 PSF $\delta_{LC} = 0^o$ δ_{NL} = SEALED $\theta_J = 1^o$
Direct Thrust Effects Removed
$\delta_f = 0^o$ $\delta_a = 0^o/0^o$ Nose Gear Off
$N_F/\sqrt{\theta T_o}$ = 2700 RPM

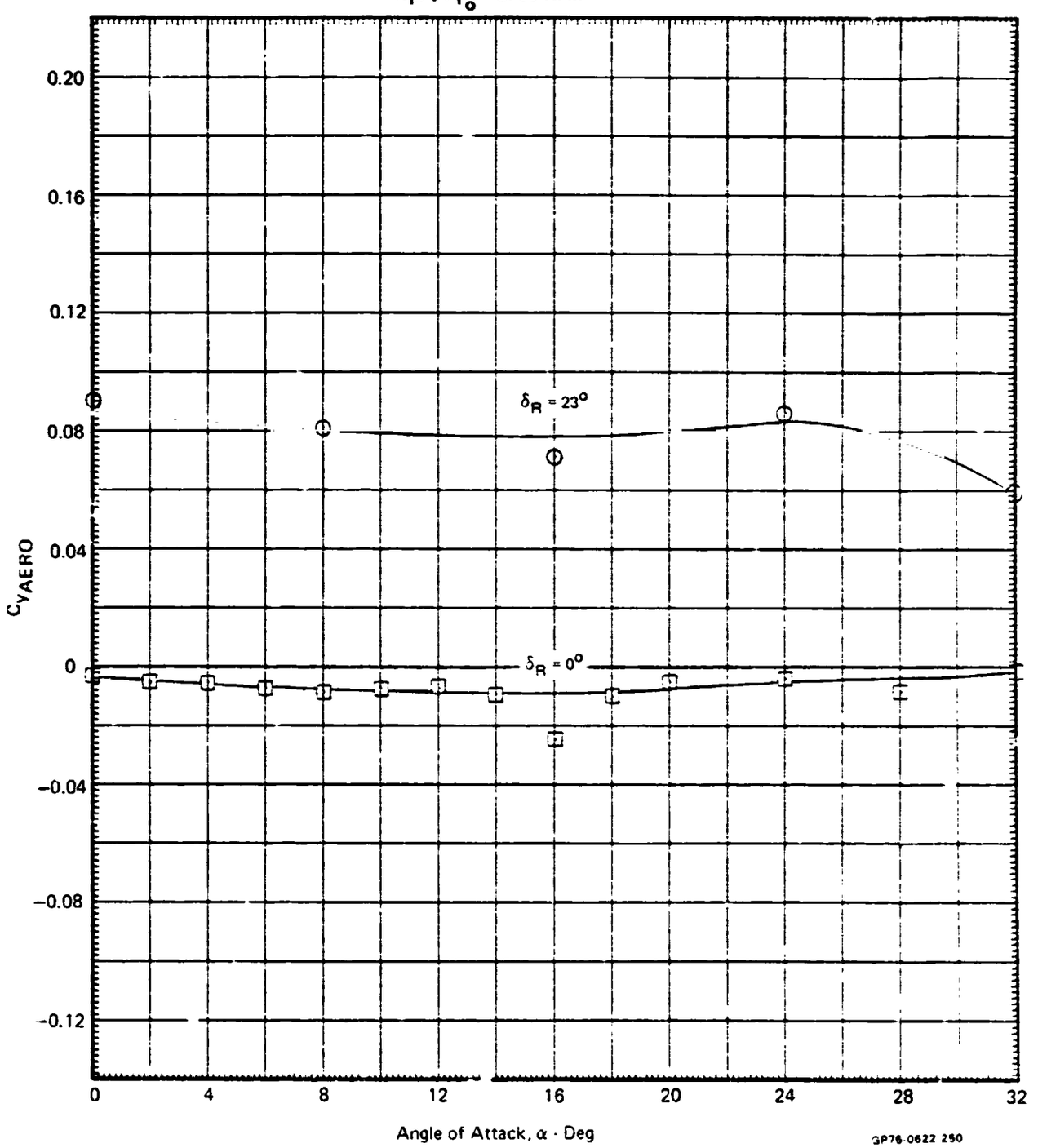

FIGURE 8.7-16
EFFECT OF RUDDER DEFLECTION ON YAWING AND ROLLING MOMENTS
$\delta_H = 0^o$ $q = 34.2$ PSF $\delta_{LC} = 0^o$ δ_{NL} = SEALED $\theta_J = 1^o$
Direct Thrust Effects Removed
$\delta_f = 0^o$ $\delta_a = 0^o/0^o$ Nose Gear Off
$N_F/\sqrt{\theta T_o}$ = 2700 RPM

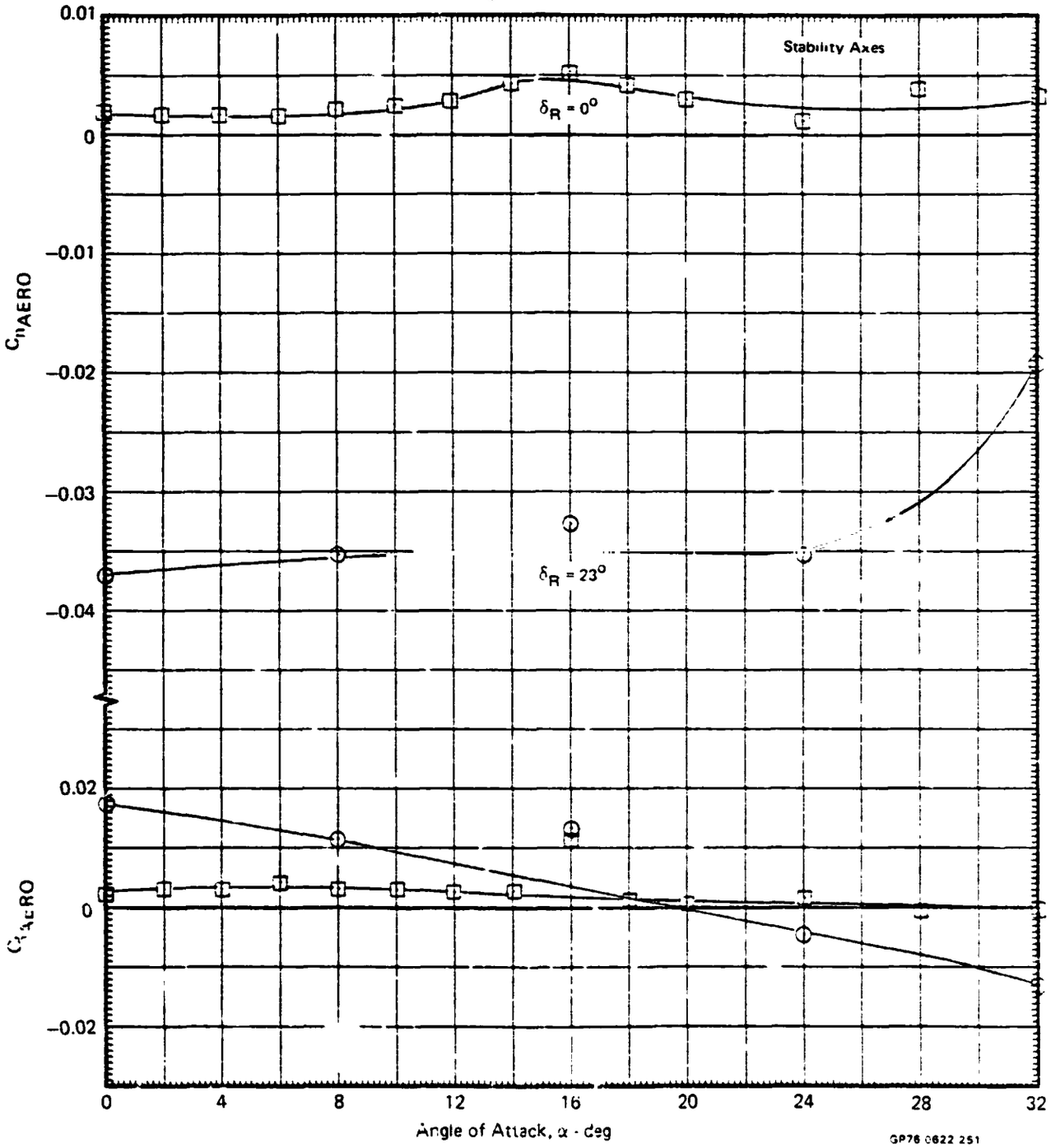

8.8 AIR INDUCTION SYSTEM PERFORMANCE

The air induction system performance characteristics were measured at selected test conditions throughout the wind tunnel test program on the left lift/cruise fan inlet, the nose lift fan inlet, the left lift/cruise gas generator inlet, and the nose fan engine inlet/duct. The inlet performance rake geometries utilized to measure the inlet data were presented and discussed in Section 3. The total pressure recovery and steady state distortion were measured to show the effects of mass flow ratio, angle of attack, angle of sideslip, and forward speed on the performance of each inlet. The results of those inlet performance tests are discussed for each inlet in the sections that follow.

Left Lift/Cruise Fan Inlet

The effects of angle of attack and fan speed on the performance of the over-the-wing mounted lift/cruise fan inlet are presented in Figure 8.8-1. The average total pressure recovery (P_{T_2}/P_{T_o}) and the inlet distortion factor ($P_{T_{high}} - P_{T_{low}}/P_{T_{avg}}$) are presented along with the inlet mass flow ratio (A_o/A_{HL}) as a function of corrected fan speed at the highest tunnel speed (V_o = 103 knots) tested. The mass flow ratio data shown was calculated using the fan exit rake, as previously described. The data presented in the figure were measured with the model in the cruise mode configuration, nose unit off.

At a mass flow ratio of 1.0, the inlet performance is shown to maintain a very high level up to an angle of attack of 20°. Above this up to angles of 32° it continually deteriorates. This falloff in performance at the higher α is due to the unsteadiness and the subsequent separation of the flow on the inboard panel as α is increased. Note that at the lower mass flow ratios, i.e., reduced power levels, the performance deteriorates at lower angles of attack. This is also due to inboard wing panel separation, which is occurring at lower α due to a lesser amount of inlet induced flow over the inboard wing. Throughout the test, the tufts on the wing were observed to indicate flow separation at angles of attack of approximately 8° higher on the inboard wing ahead of the inlet than on the outboard wing, at mass flow ratios greater than 1.0. The lift/cruise inlet rake data shown herein substantiate these observations.

It should be noted here that throughout the test program at lower angles of attack (0°-20°) and higher mass flow ratios (A_o/A_{HL} > 1.0) the inlet recovery ranged between 0.999 and 1.00. The reason for these very high levels of performance is the low specific flow ($\dot{W}_{FAN}/A$) of the low fan pressure ratio X376B turbotip fan and the resulting low inlet throat Mach numbers (0.35 and below). The intent of

the inlet performance data presented herein for all inlet systems is to show trends and the specific effects of angle of attack, sideslip, and mass flow ratio, and not necessarily the absolute levels of performance, for example, of higher pressure ratio fan systems.

The effect of sideslip angle on inlet performance at various angles of attack is shown in Figures 8.8-2 and 8.8-3 for the range of test conditions where inlet data were measured. Sideslip angles of up to +12° (left inlet on leeward side of fuselage) show no effect on lift/cruise inlet performance at angles of attack of 12° and lower. The deterioration in performance at higher angles of attack and sideslip is apparent in the figures. Inlet distortion levels were found to be less than 10% throughout all test conditions during this program.

The effects of forward speed on inlet performance variation are shown in Figure 8.8-4. Only the distortion was found to show any variation, and this occurred only at the higher angles of attack.

A summary of the lift/cruise fan inlet performance is presented in Figure 8.8-5. The data are presented in terms of the nondimensional inlet loss coefficient ($\Delta P_T/q_{TH}$) for correlation purposes. High speed (M_O = 0.5 to 0.9) performance data for this inelt are contained in Reference (3).

Left Lift/Cruise Gas Generator Inlet

The effects of angle of attack and engine speed on the performance of the fuselage side mounted gas generator inlet are shown in Figure 8.8-6. The inlet data are presented in the same manner as the fan inlet data described above. The effects of both angle of attack and sideslip are shown in Figures 8.8-3 and 8.8-7. In general, the inlet exhibited very good performance throughout the test range of variables. Total pressure recovery was found to deteriorate less than 1%, and distortion was measured to be less than 5% throughout the angle of attack and sideslip angles tested.

Nose Lift Fan Inlet

The effects of angle of attack and fan speed on the performance of the nose fan inlet for three tunnel velocities are presented in Figures 8.8-8, 8.8-9, and 8.8-10. The data are shown for α's ranging from -4° to +20° which covered the powered lift test range of this program. As shown in the figures, the effects of angle of attack up to 20° for all forward speeds had very little effect on either the total pressure recovery or distortion of the inlet. The data presented also cover the fan speed ranges tested in the powered lift mode. The operating mass flow of the inlet is presented in terms of the mass flow ratio (A_O/A_{HL}) rather than the more typical inlet velocity ratio (V_O/V_{TH}) for reasons of comparison and

consistency with the lift/cruise inlet performance data previously discussed. A plot of the inlet velocity ratio (V_O/V_{TH}) expressed in terms of the mass flow ratio (A_O/A_{HL}) for the nose fan inlet is shown in Figure 8.8-11.

The effects of sideslip also had very little if no effects on inlet recovery and distortion, as shown in Figure 8.8-12. The data presented also encompass the range of test variables examined in the powered lift mode.

A summary of the nose fan inlet performance is presented in Figure 8.8-13. The recovery data here are presented in terms of the nondimensional inlet loss coefficient ($\Delta P_T/q_{TH}$) versus the inlet velocity ratio for correlation purposes. The data presented in this figure encompass the complete range of tunnel and fan speeds tested on this inlet. For the nominal operating range of the nose fan inlet for a V/STOL aircraft of this type, the performance of this inlet exhibited excellent characteristics, as shown in the figure.

FIGURE 8.8-1
EFFECTS OF ANGLE OF ATTACK AND FAN SPEED ON LIFT/CRUISE FAN INLET PERFORMANCE
L/H Inlet
V_o = 103 Kts

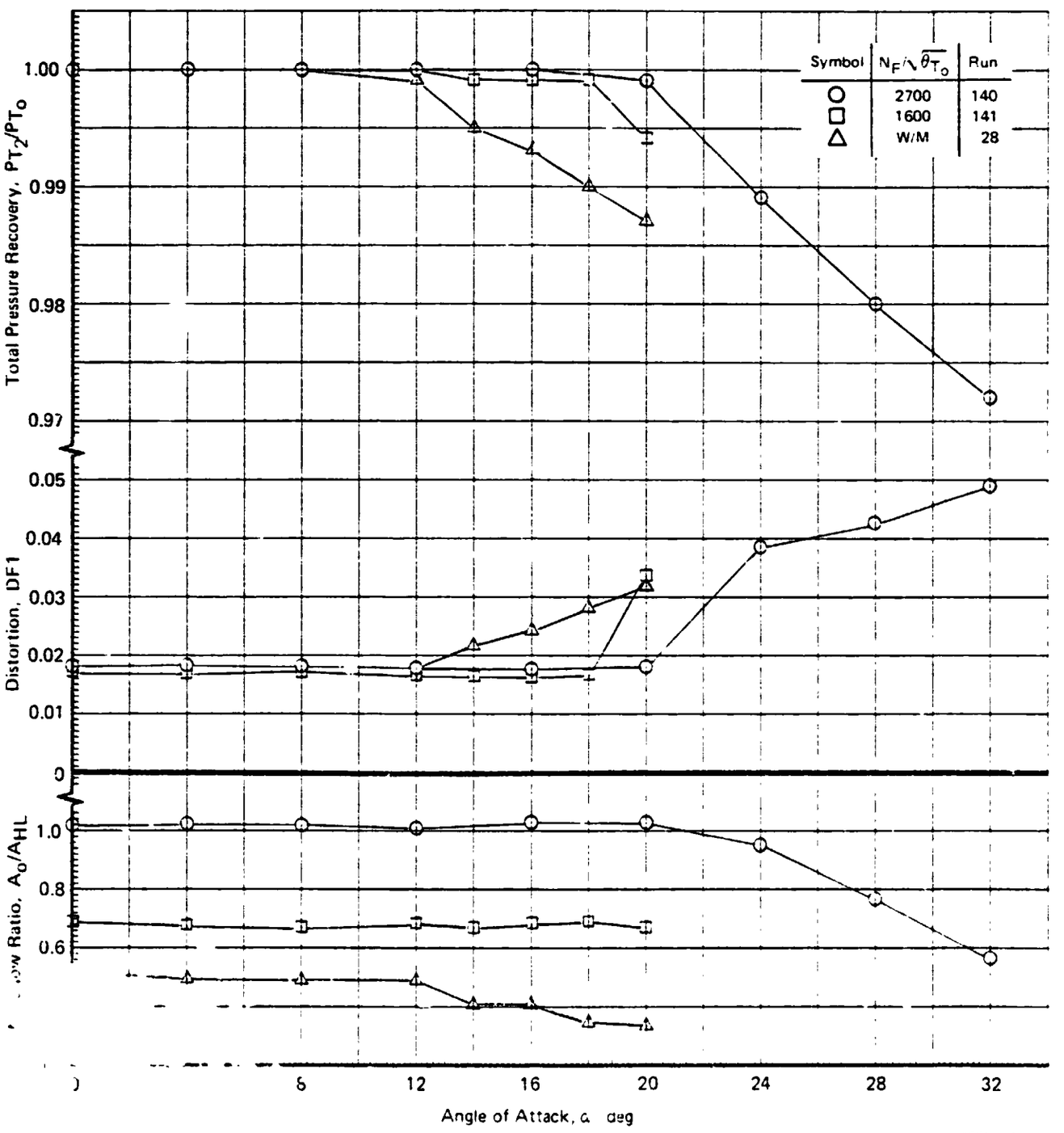

FIGURE 8.8-2
EFFECTS OF ANGLE OF ATTACK AND SIDESLIP ON LIFT/CRUISE FAN INLET PERFORMANCE
L/H Inlet
V_o = 103 Kts $NF/\sqrt{\theta T_o}$ = 2700 RPM

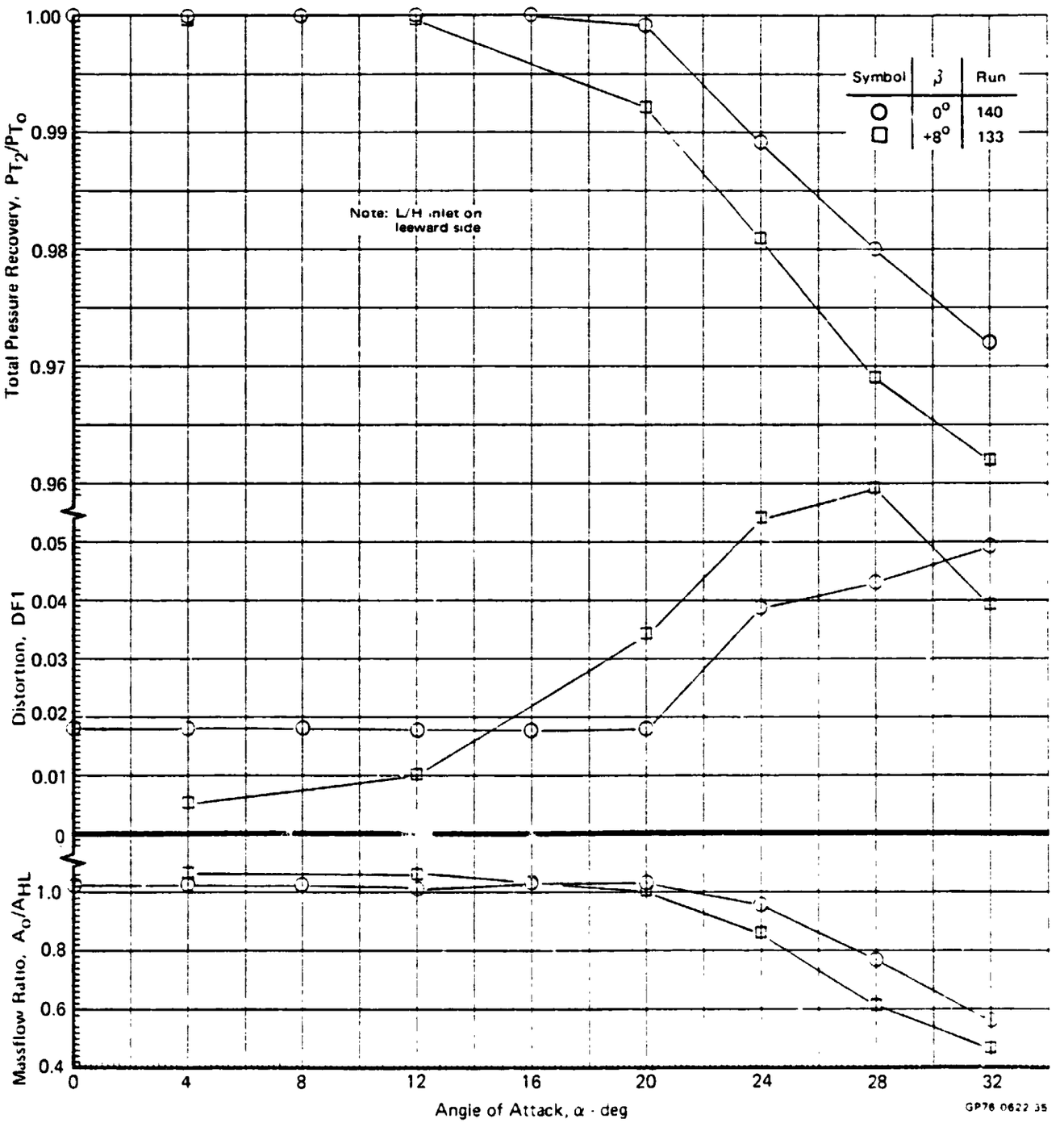

FIGURE 8.8-3
EFFECTS OF SIDESLIP ANGLE AND ANGLE OF ATTACK ON LIFT/CRUISE FAN AND GAS GENERATOR INLET PERFORMANCE
L/H Inlets

V_o = 103 Kts $N_F/\sqrt{\theta_{T_o}}$ = 2700 RPM

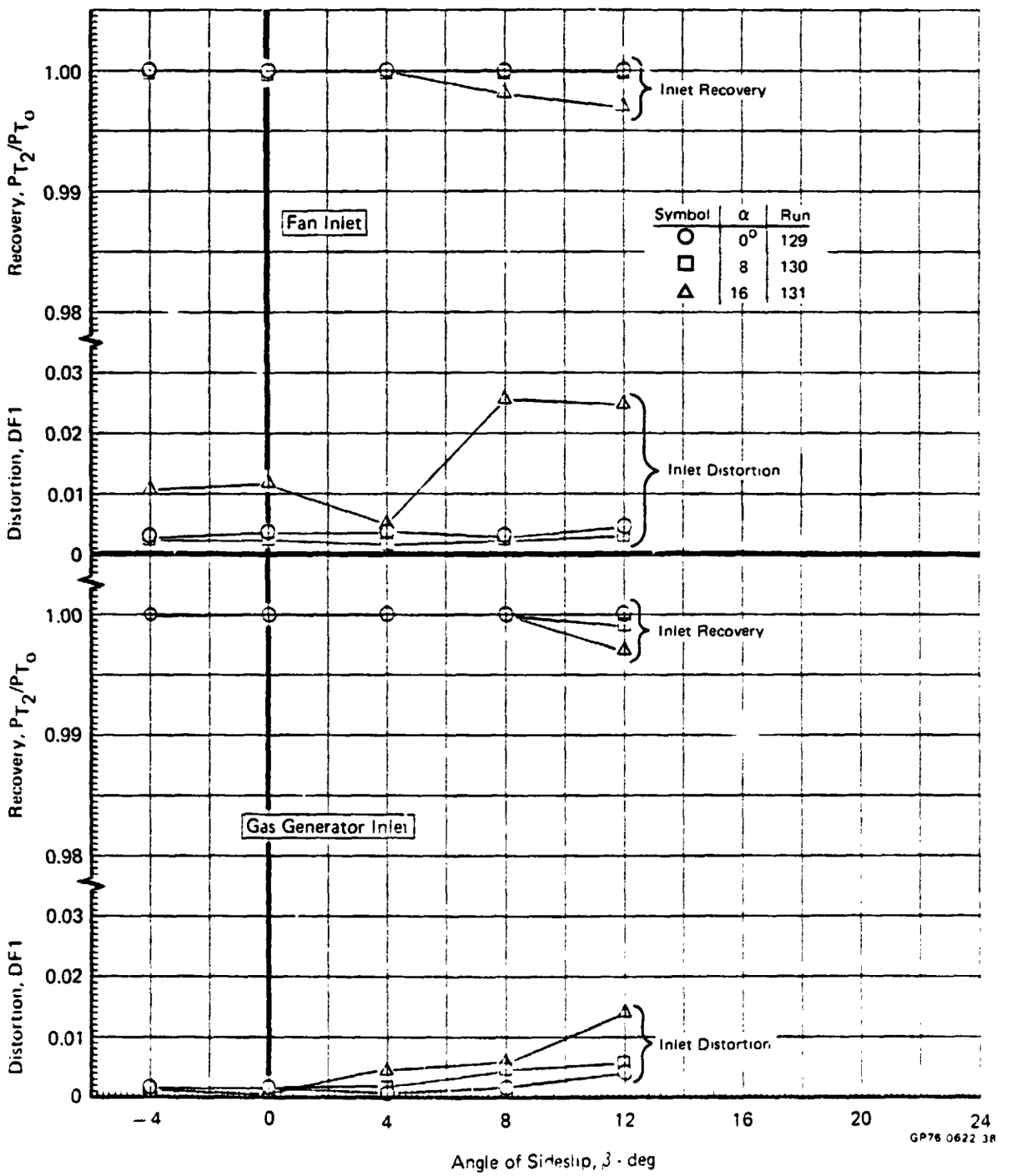

FIGURE 8.8-4

EFFECTS OF FORWARD SPEED AND ANGLE OF ATTACK ON LIFT/CRUISE FAN INLET PERFORMANCE

L/H Inlet

$N_F/\sqrt{\theta T_o}$ = 3600 RPM

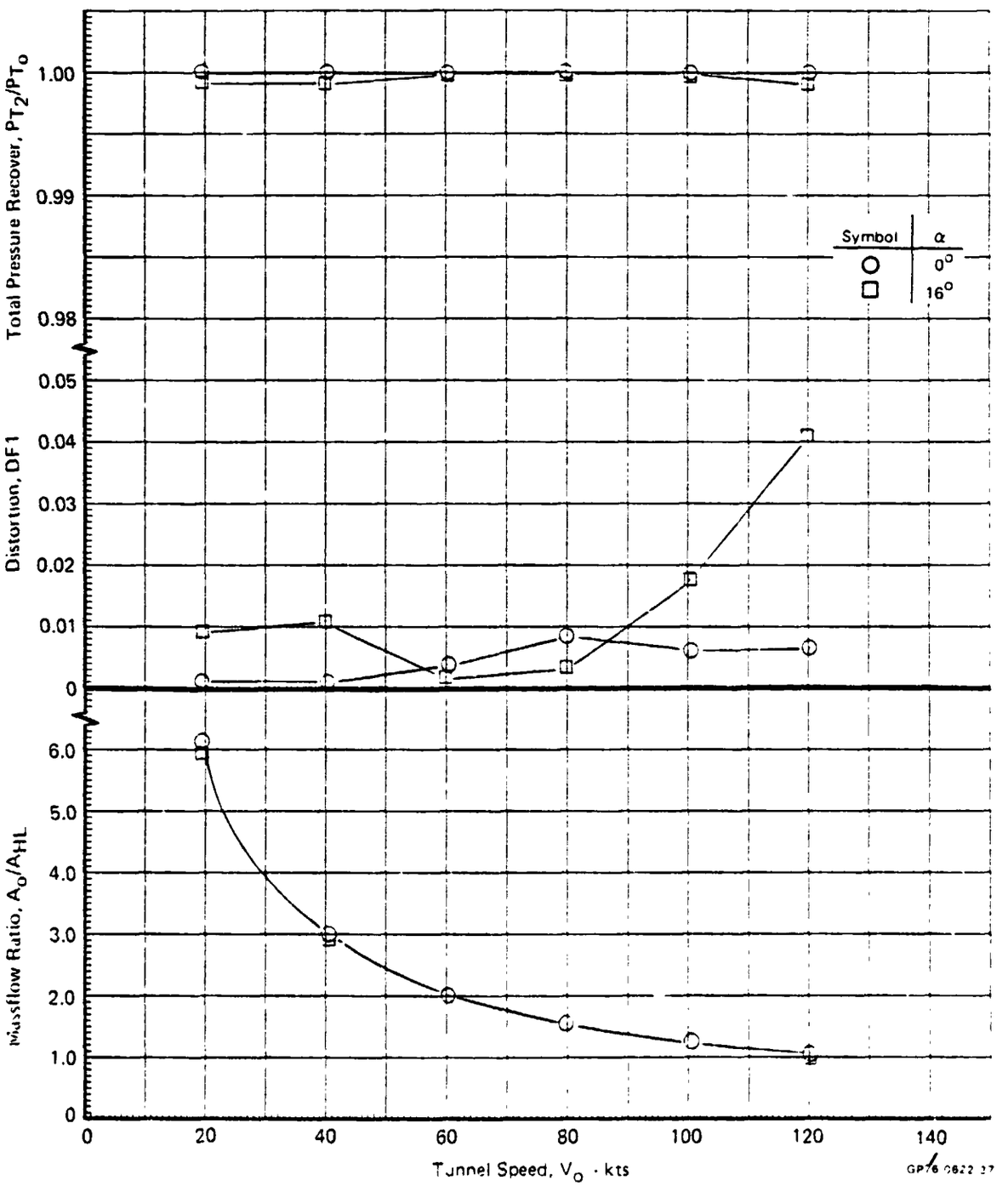

FIGURE 8.8-5
LIFT/CRUISE FAN INLET PERFORMANCE SUMMARY
Nondimensionalized Total Pressure Loss Data
V_o = 103 Knots

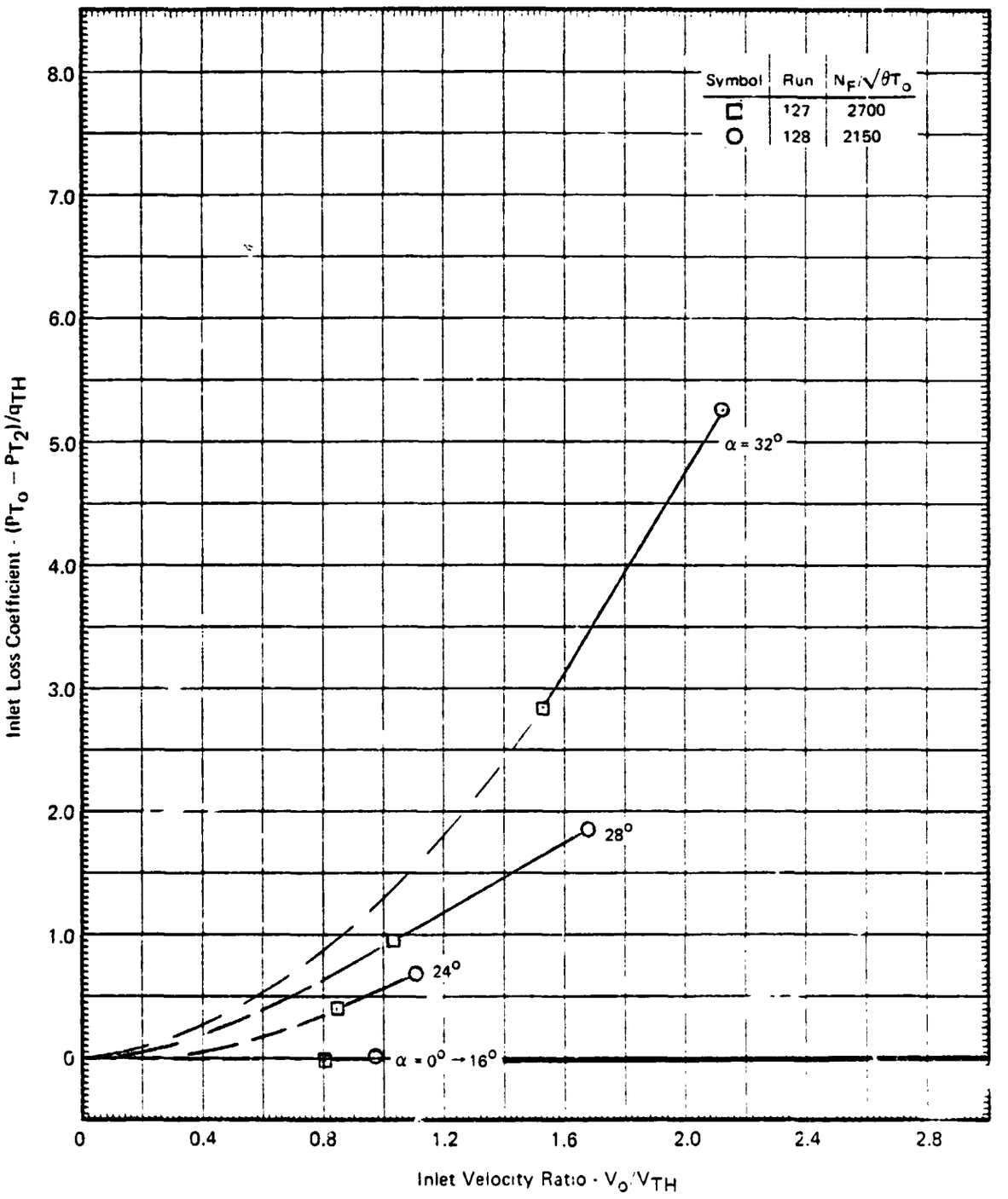

GP76 0622 286

FIGURE 8.8-6
EFFECTS OF ANGLE OF ATTACK AND ENGINE SPEED ON LIFT/CRUISE GAS GENERATOR INLET PERFORMANCE
L/H Inlet
V_o = 103 Kts

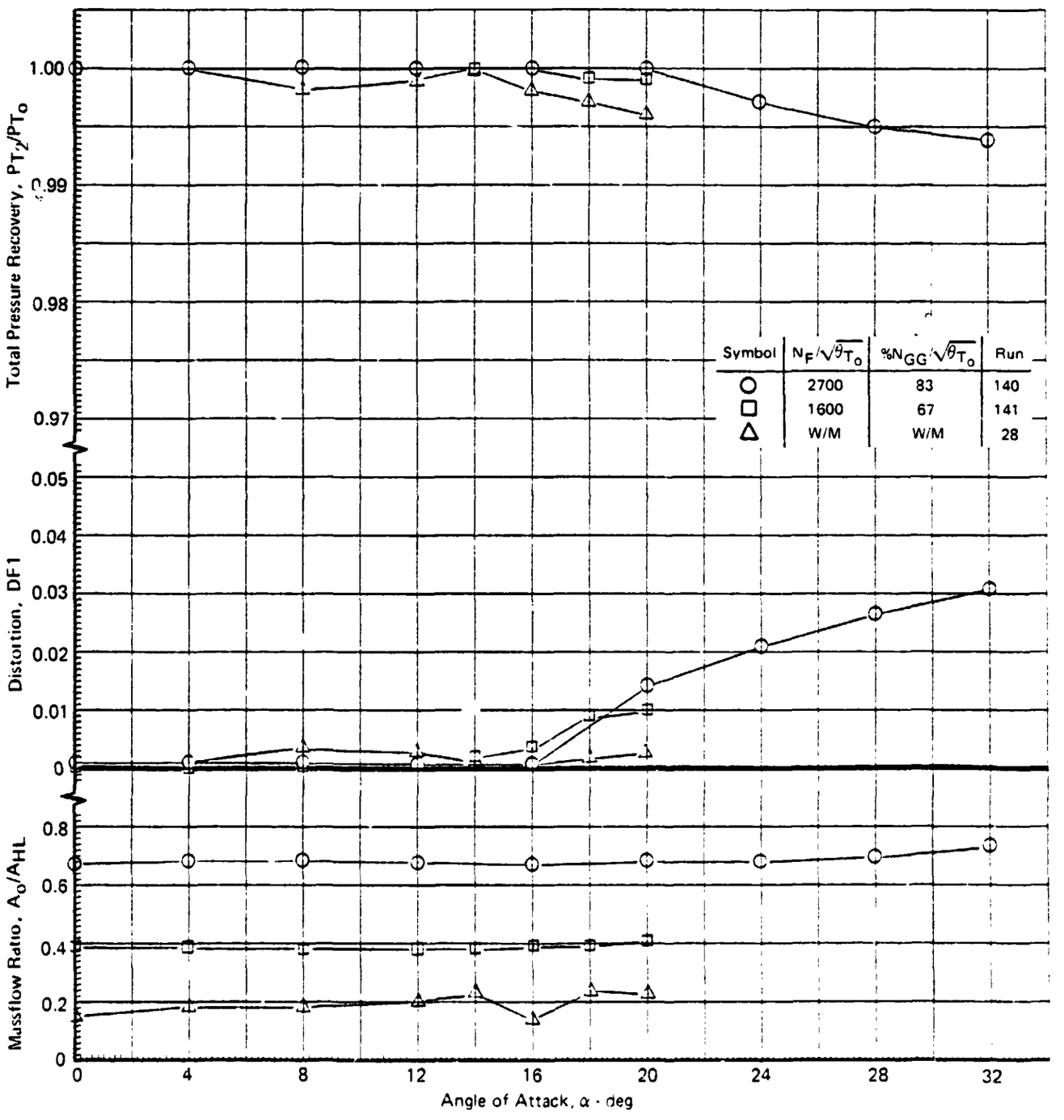

GP76 0622 14

FIGURE 8.8-7
EFFECTS OF ANGLE OF ATTACK AND SIDESLIP ON LIFT/CRUISE GAS GENERATOR INLET PERFORMANCE
L/H Inlet
V_o = 103 Kts $N_F/\sqrt{\theta T_o}$ = 2700 RPM

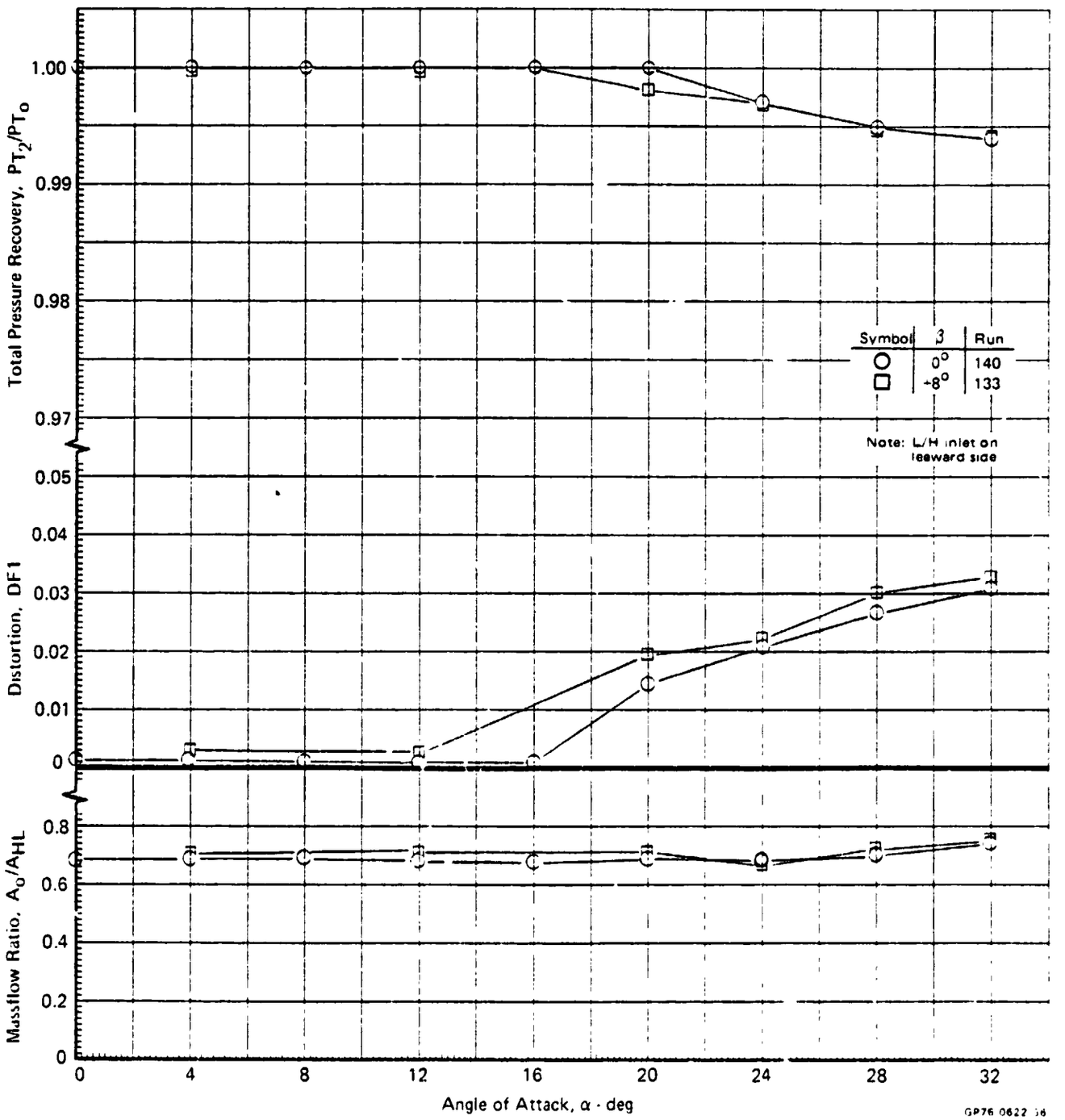

FIGURE 8.8-8
EFFECTS OF ANGLE OF ATTACK AND FAN SPEED ON NOSE FAN INLET PERFORMANCE

V_o = 47 Kts

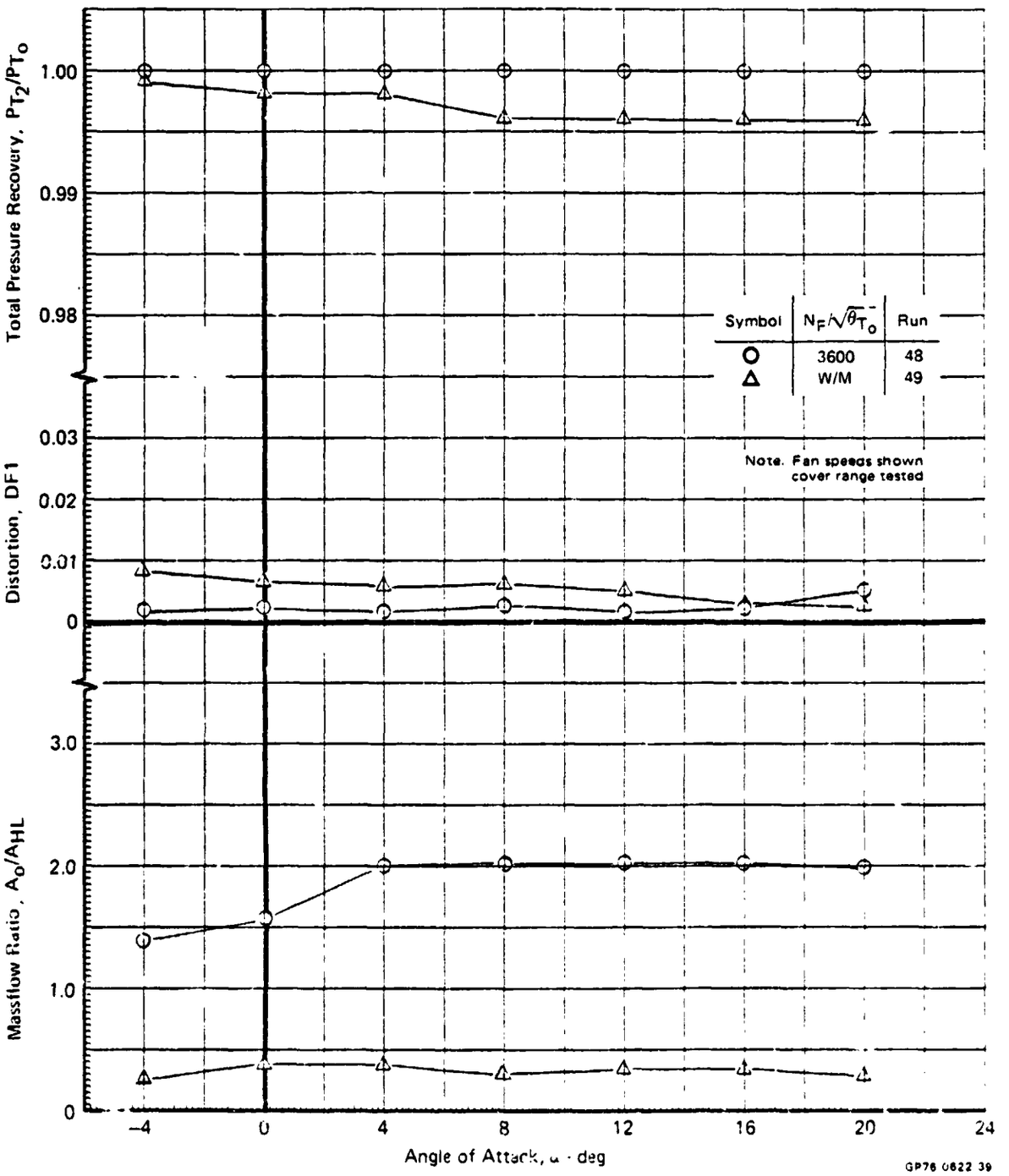

FIGURE 8.8-9
EFFECTS OF ANGLE OF ATTACK AND FAN SPEED ON NOSE FAN INLET PERFORMANCE
V_o = 63 Kts

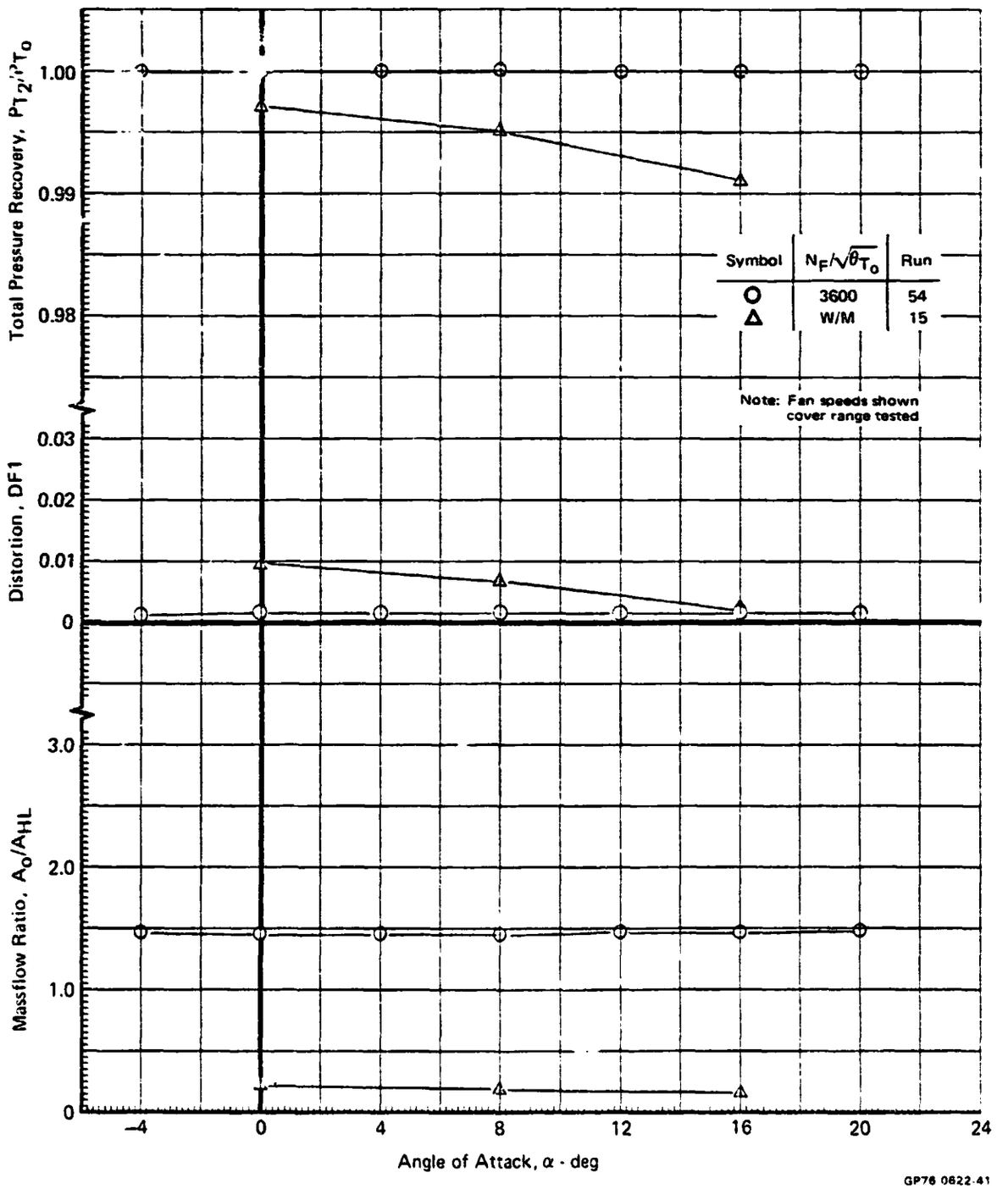

C-4

FIGURE 8.8-10
EFFECTS OF ANGLE OF ATTACK AND FAN SPEED ON NOSE FAN INLET PERFORMANCE
V_o = 78 Kts

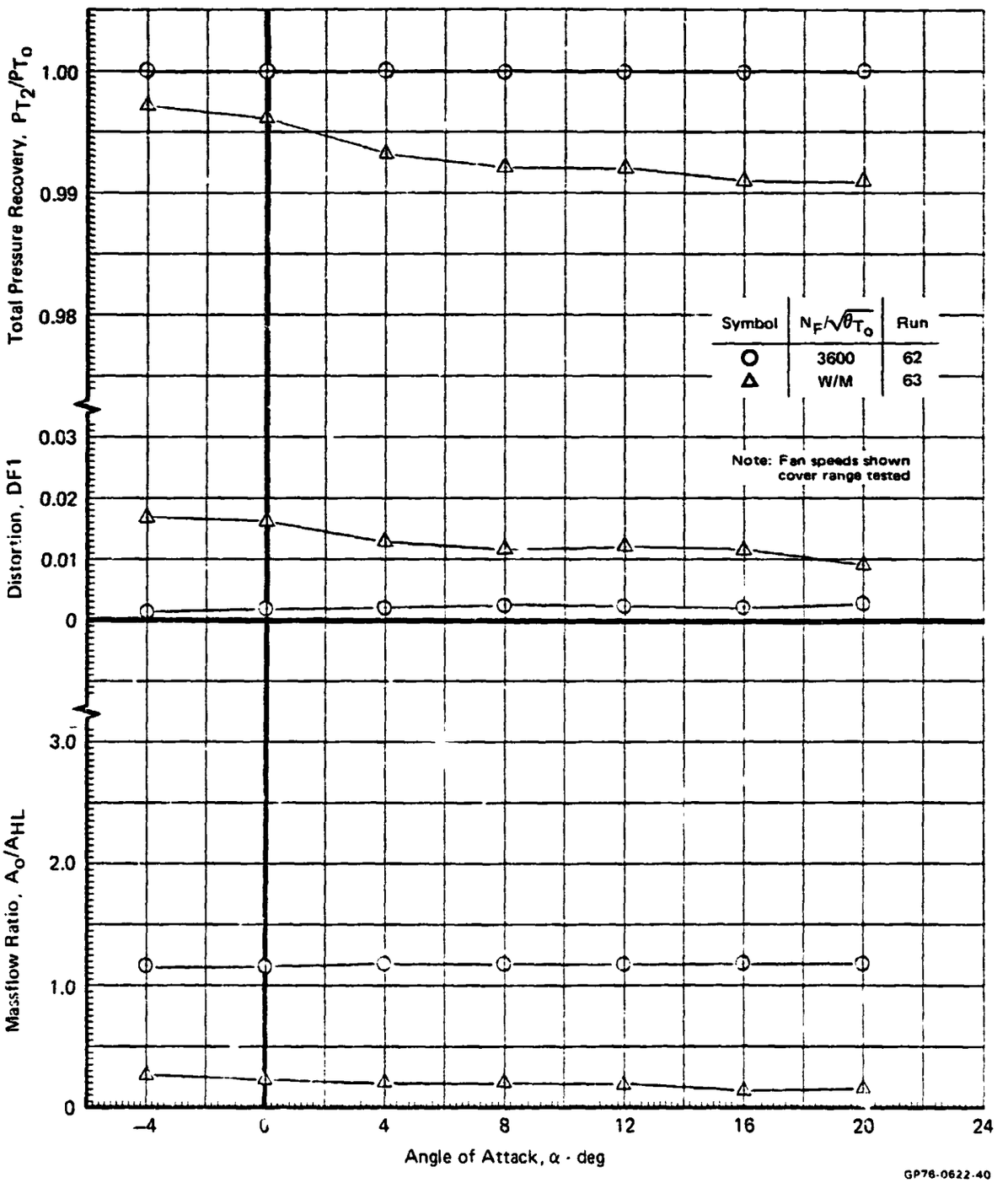

FIGURE 8.8-11
NOSE LIFT UNIT INLET VELOCITY RATIOS

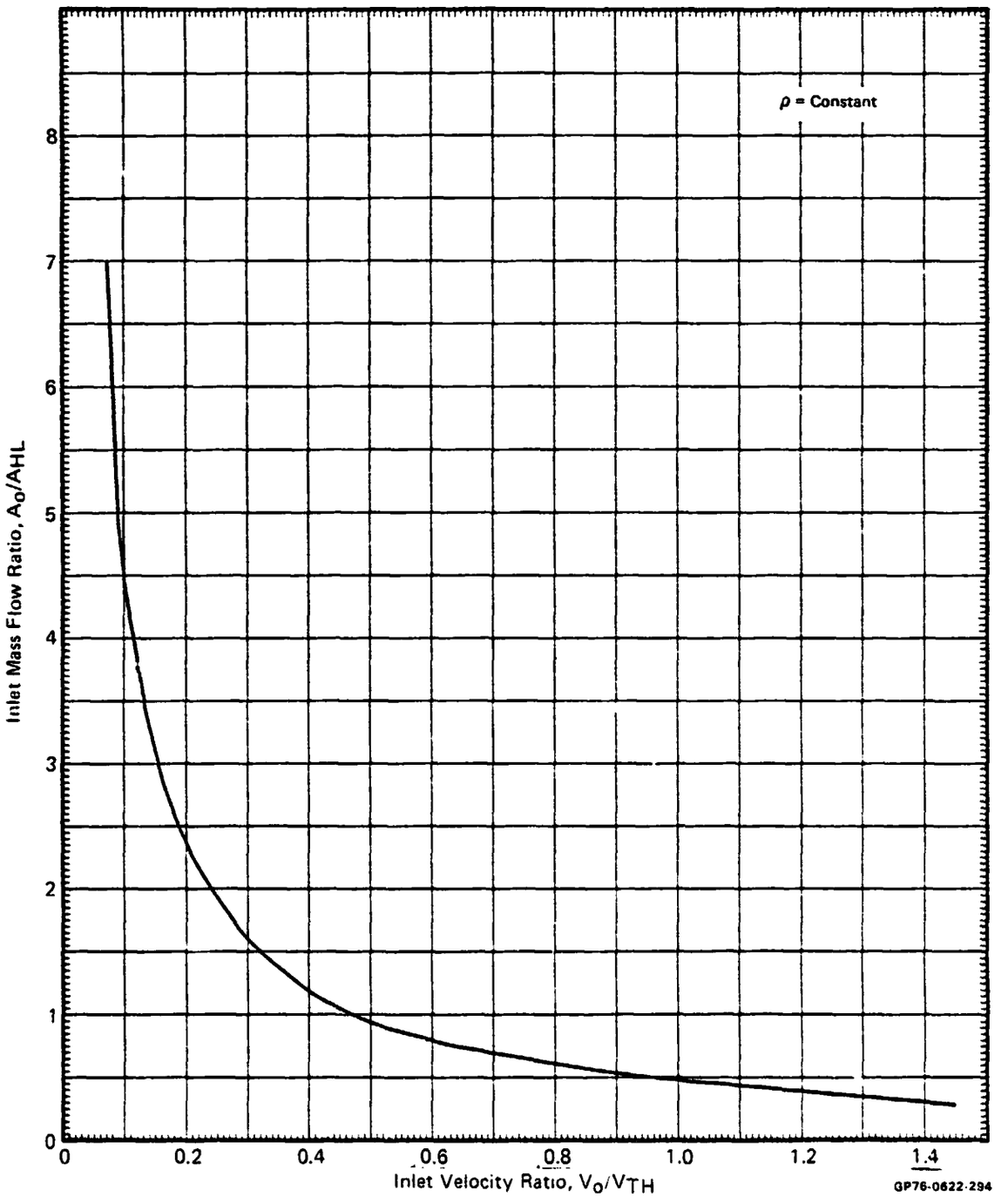

FIGURE 8.8-12
EFFECTS OF SIDESLIP ANGLE ON NOSE FAN INLET PERFORMANCE
$\alpha = 0^o$ V_o = 103 Kts

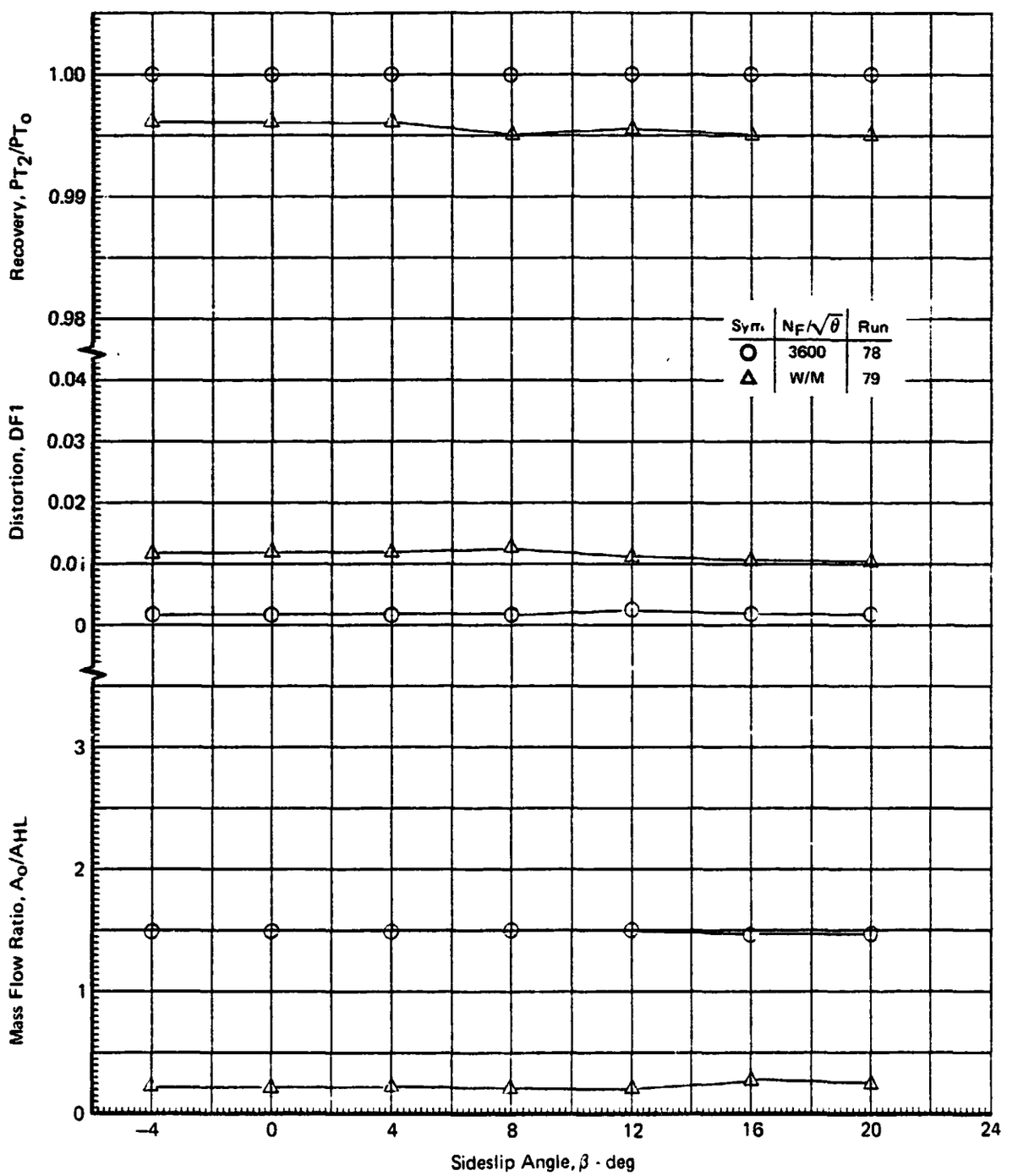

FIGURE 8.8-13
NOSE FAN INLET PERFORMANCE SUMMARY
Nondimensionalized Total Pressure Loss Data
$\alpha = 0^o$

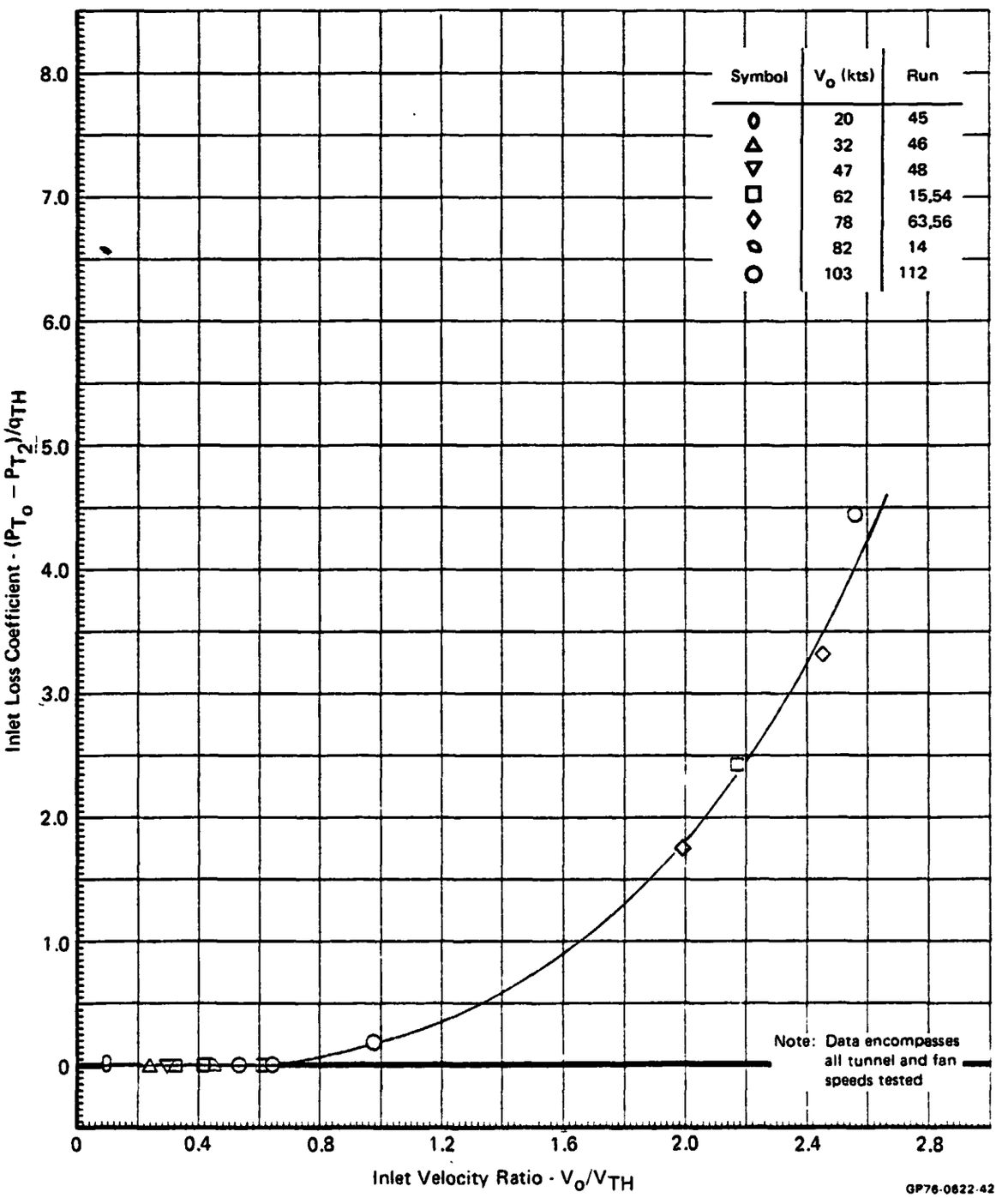

9. OUTSIDE STATIC TEST RESULTS

The results of the outside static test program conducted on the large scale powered model are presented in this section. The discussions cover the propulsion system calibrations, the ground effects on total installed lift, the ground effects on inlet reingestion, and the flow visualization tests.

9.1 PROPULSION SYSTEM CALIBRATIONS

Individual Unit Calibrations

The balance-measured static gross thrust and the rake-measured ideal gross thrusts are presented as a function of fan speed squared for the left and right lift/cruise units in Figures 9-1 and 9-2, respectively. The results are shown for the 90° vector position only, as this was the only vector position tested on the lift/cruise units. For comparison purposes, results of the 40' x 80' wind tunnel static calibrations for each unit are also shown in the figures. Fairly good agreement exists between the two test programs, particularly on the right unit. A rear view of the model showing the lift/cruise vectoring units is given in Figure 9-3. Figure 9-4 presents the balance- and rake-measured thrusts for the forward lift unit at a geometric vector angle of 95°.

Comparisons between the tunnel measured and static test measured nozzle thrust calibration coefficients (C_F) for the left, right and nose lift units are presented in Figures 9-5 and 9-6. As shown in the figures, good agreement exists between the two lift/cruise unit calibrations; however, a shift of approximately 5% was measured on the nose unit. Comparisons of the resultant thrust vector angles for each unit are presented in Figure 9-7 and 9-8, showing good agreement with the 40' x 80' tunnel static calibrations. The absolute level of accuracy of the outside static balance and rake calibration data is of lesser importance to the validity of these test results than the variation in level measured for each height and model configuration tested. These comparisons with the 40' x 80' data are presented herein for reference purposes and as a check on the outside test setup.

Fan Performance Map

The X376B turbotip fan performance map is presented in corrected form in Figures 9-9 and 9-10. The nozzle total pressure ratio in Figure 9-9 and the ideal gross thrust in Figure 9-10 are shown versus the total fan-plus-tip-turbine airflow as a function of various fan speeds for the three alternate nozzle exhaust areas tested. The values in the performance map were calculated using the fan and tip

turbine exit rake data and are presented directly as measured. The fan performance maps are used in evaluating the individual behavior of the three lift units during operation in ground effects. The effects of both nozzle back pressure and inlet hot gas reingestion on fan thrust and airflow rate can be assessed utilizing these fan maps.

FIGURE 9-1
LEFT LIFT/CRUISE UNIT CALIBRATION RESULTS
Static Test Calibrations
$\delta_{LC} = 90^{o}$

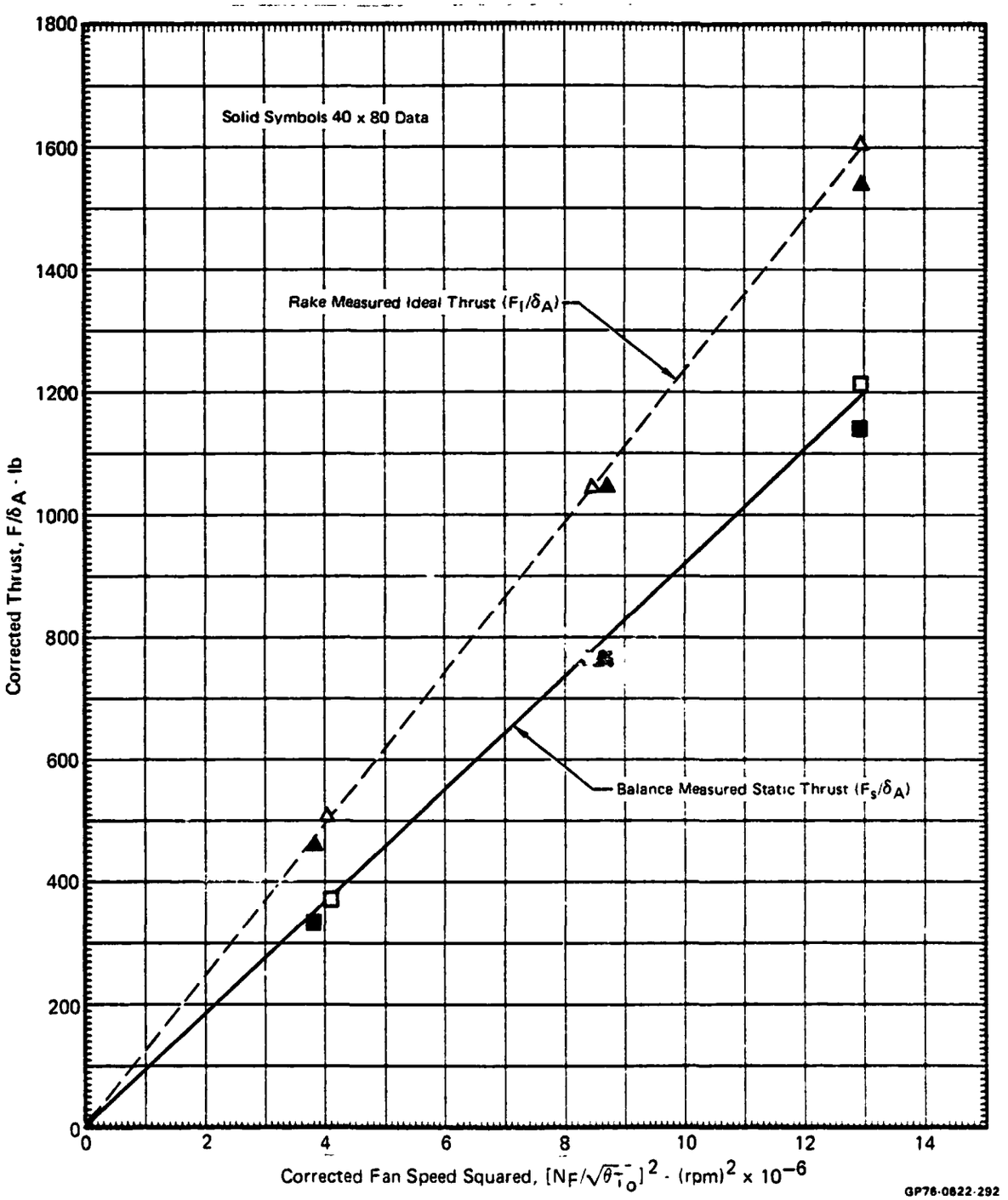

FIGURE 9-2
RIGHT LIFT/CRUISE UNIT CALIBRATION RESULTS
Static Test Calibrations
$\delta_{LC} = 90^{o}$

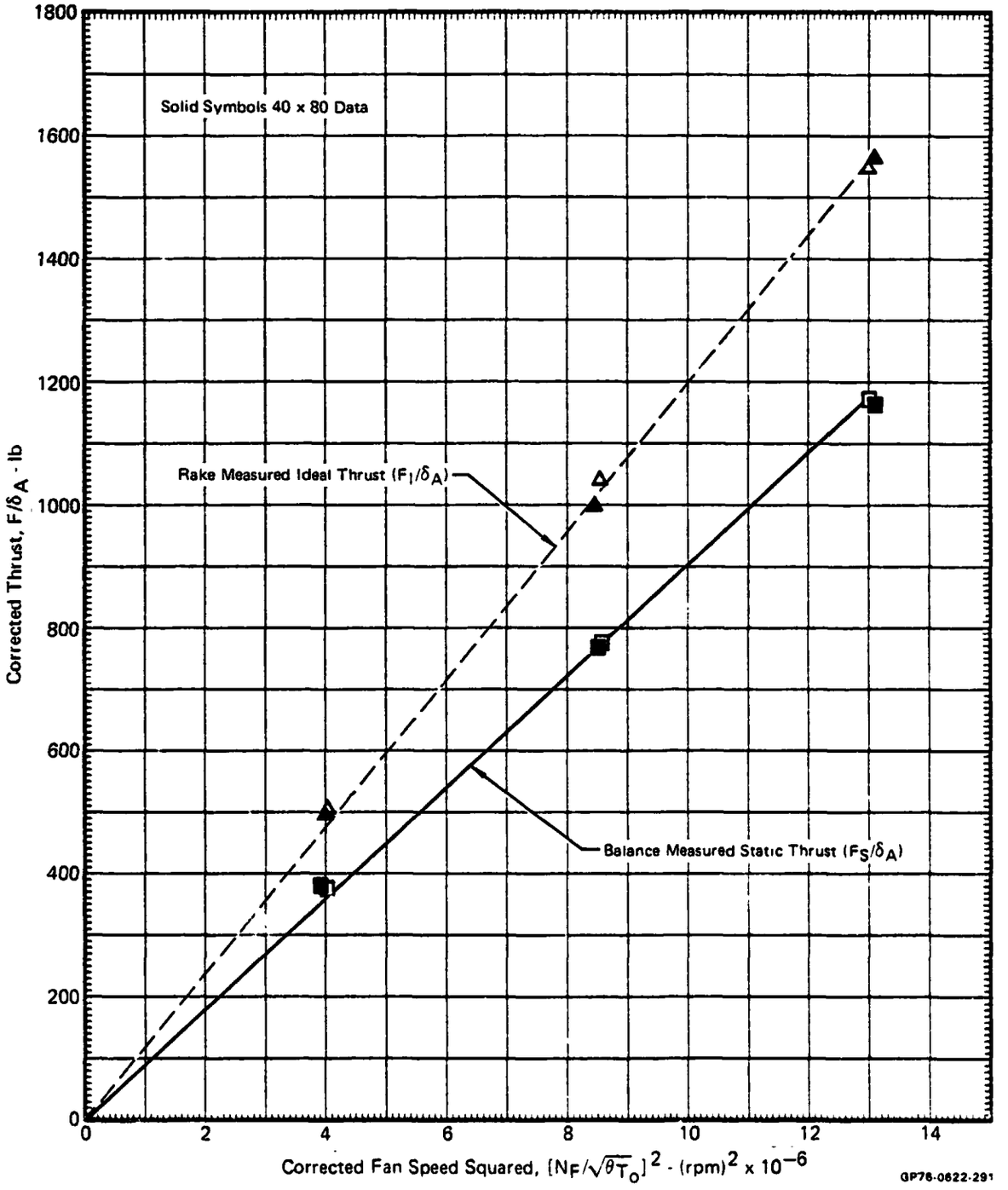

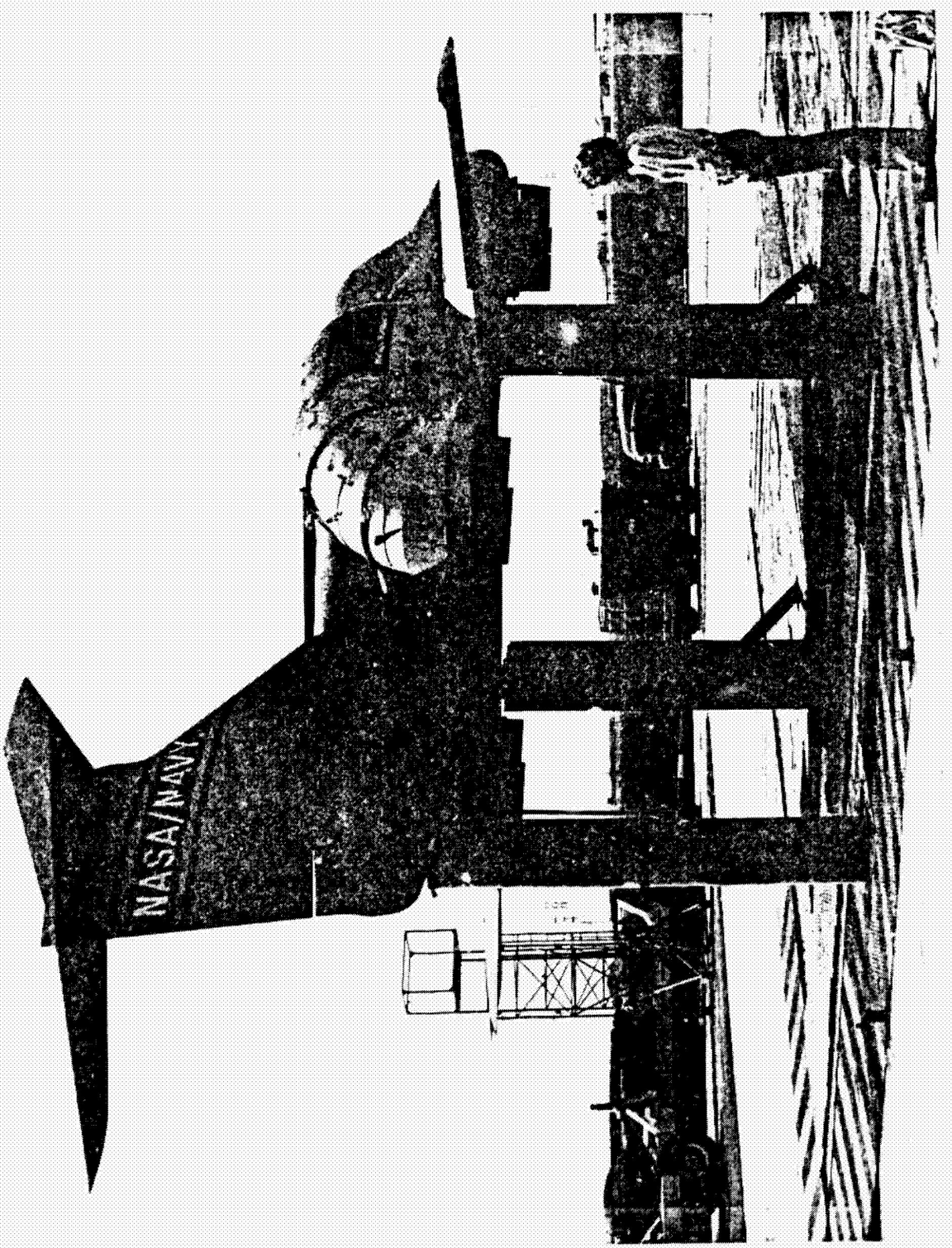

FIGURE 9-3
REAR QUARTER VIEW SHOWING LIFT/CRUISE VECTORING NOZZLES

FIGURE 9-4
NOSE LIFT UNIT CALIBRATION RESULTS
Static Test Calibrations
$\delta_{NL} = 95^{o}$

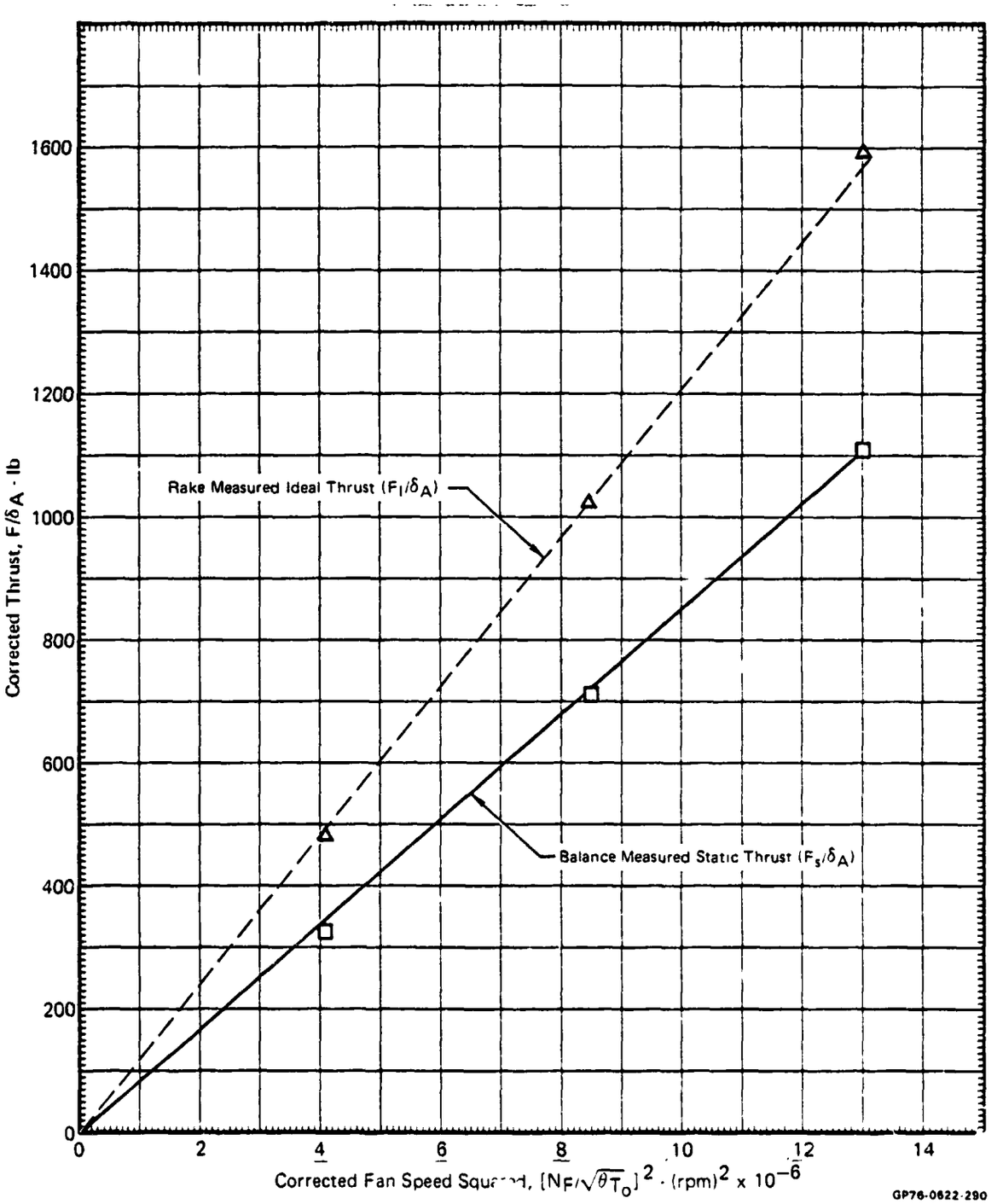

FIGURE 9-5
LIFT/CRUISE UNIT THRUST COEFFICIENT COMPARISON
Propulsion System Calibration Results
$V_o = 0$

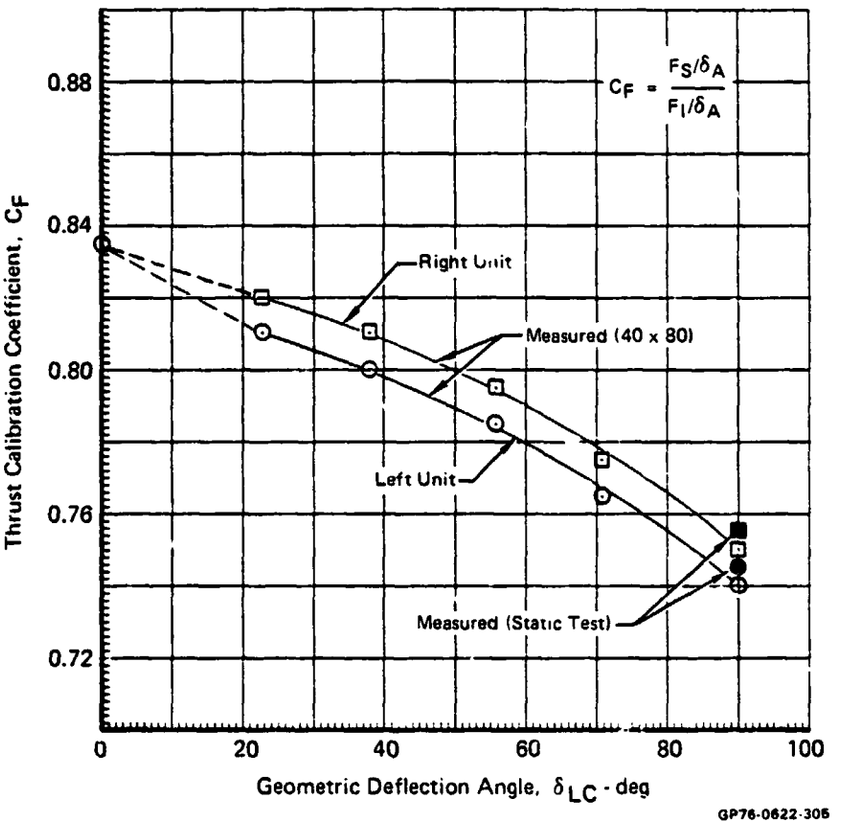

FIGURE 9-6
NOSE LIFT UNIT THRUST COEFFICIENT COMPARISON
Propulsion System Calibration Results
$V_o = 0$

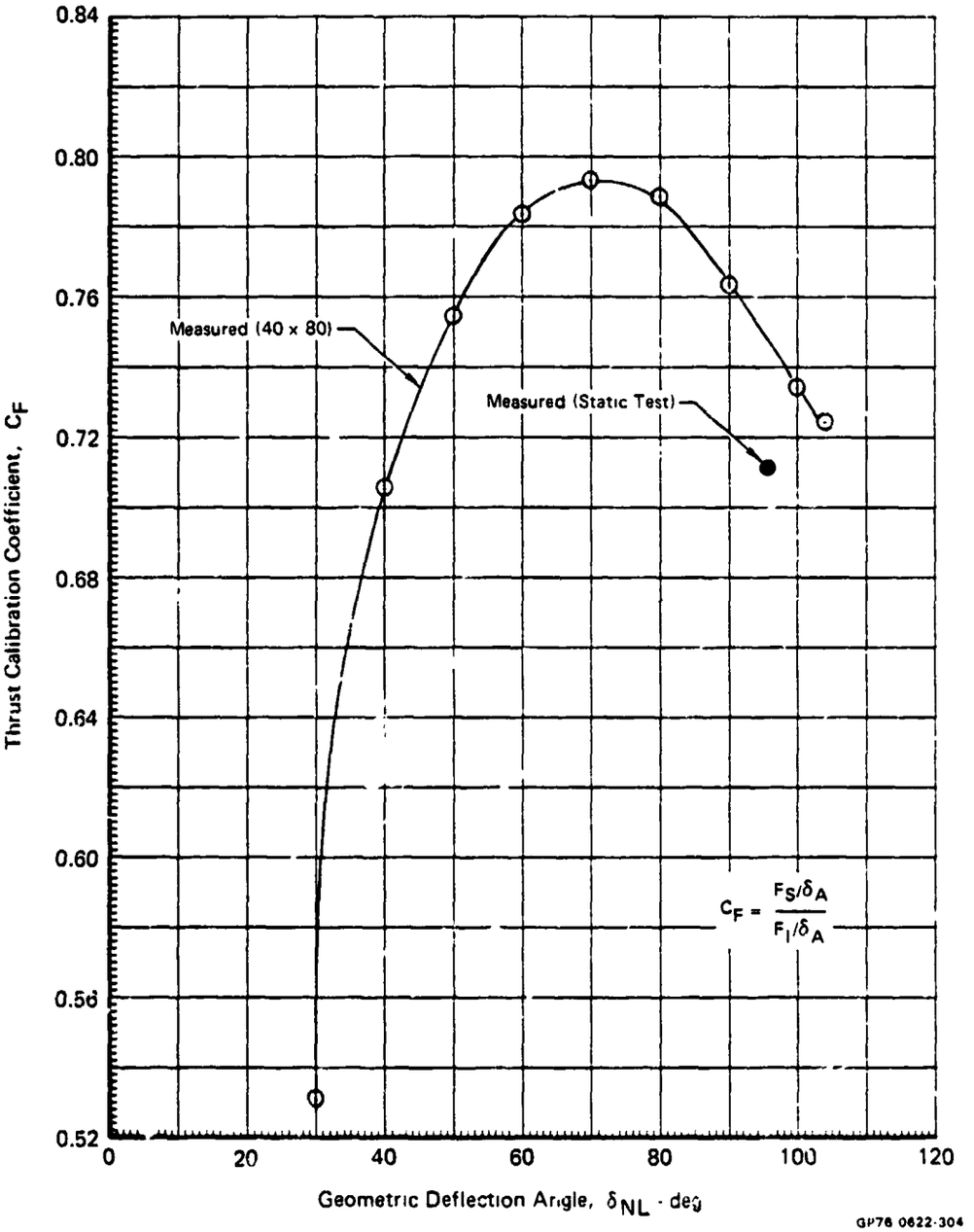

FIGURE 9-7
LIFT/CRUISE UNIT THRUST VECTOR ANGLE COMPARISON
Propulsion System Calibration Results
$V_o = 0$
Left and Right Units

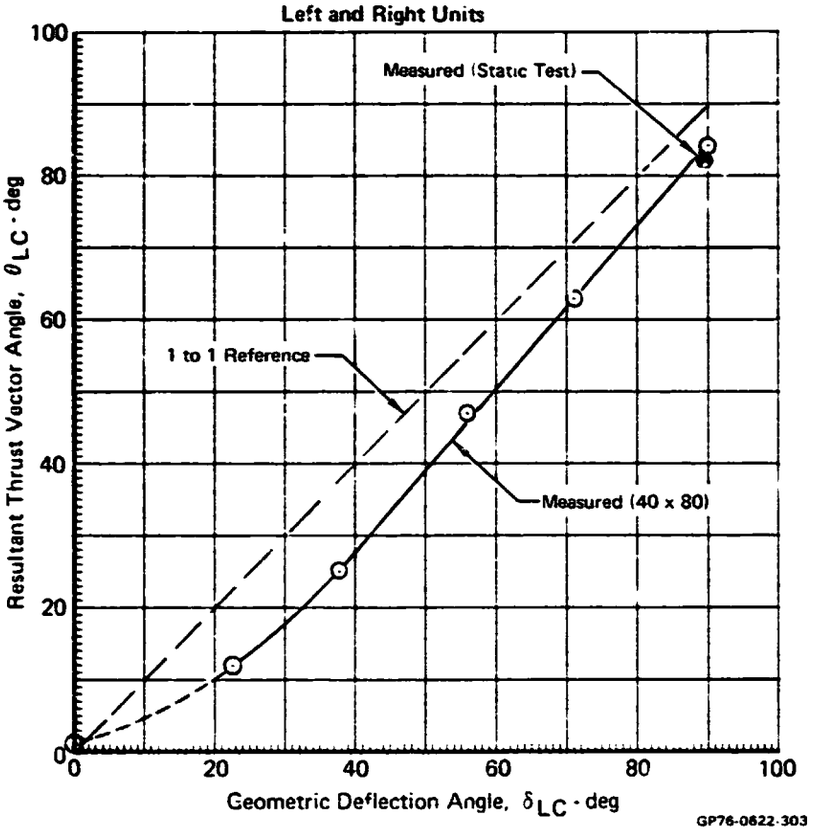

FIGURE 9-8
NOSE LIFT UNIT THRUST VECTOR ANGLE COMPARISON
Propulsion System Calibration Results
$V_o = 0$

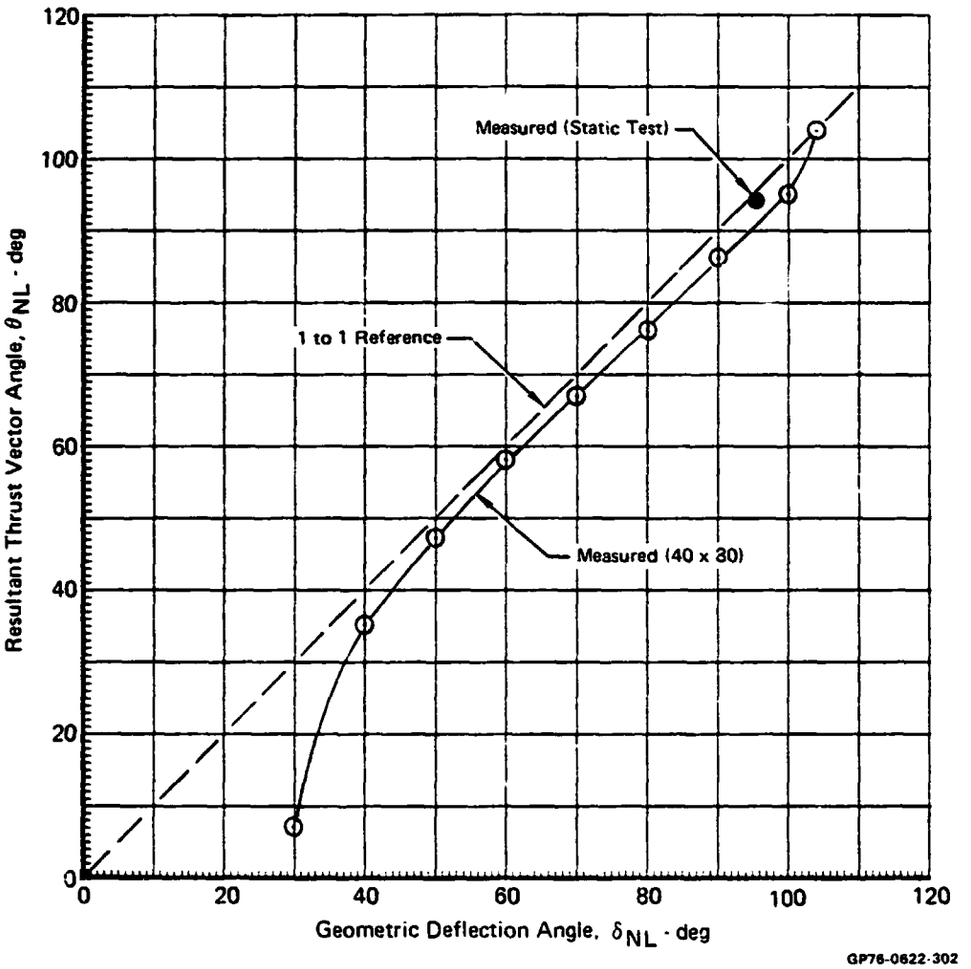

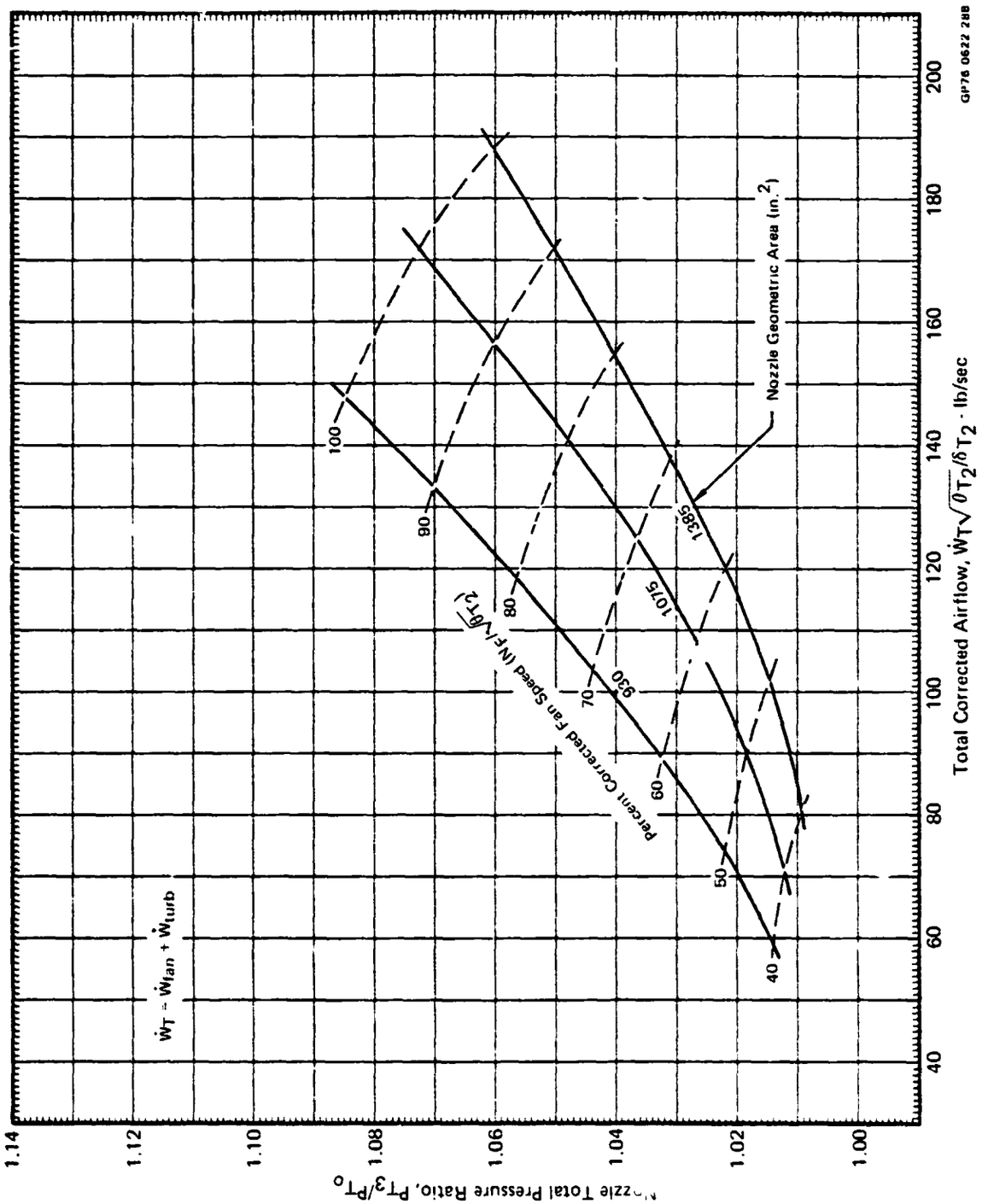

FIGURE 9-9
X376B FAN MAPPING RESULTS
Nozzle Total Pressure Ratio Data

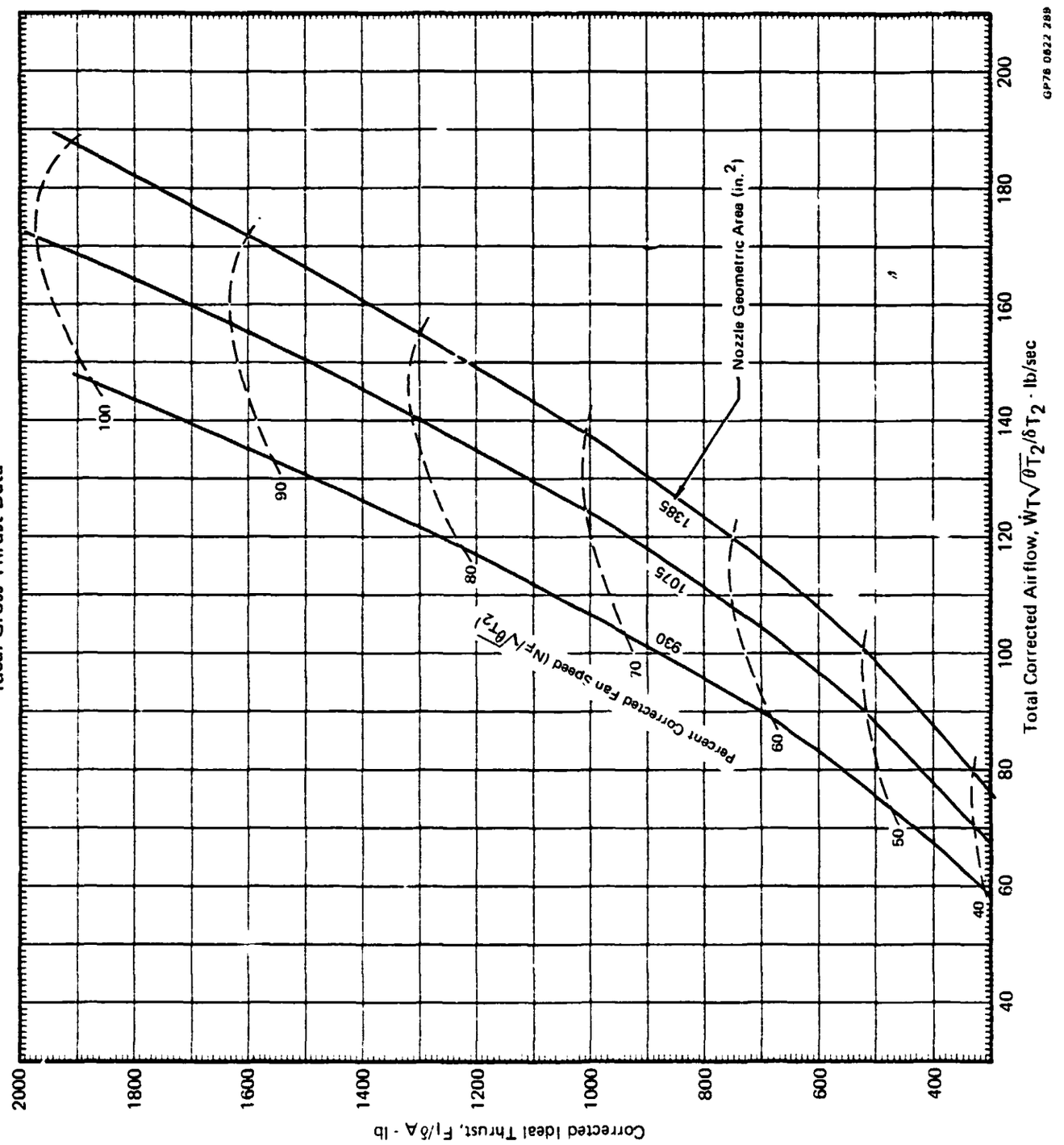

FIGURE 9-10
X376B FAN MAPPING RESULTS
Ideal Gross Thrust Data

9.2 GROUND EFFECTS ON AIRCRAFT LIFT LOSS

The effects of alternate ground heights and selected model variables on the total installed lift during three unit operation, along with the individual unit ground effects test results are given in this section. All data presented are based on steady state measurements obtained with the Vidar data acquisition system.

Three Unit Operation

The balance-measured total lift at the three ground heights tested in this program are presented as a function of fan speed in Figure 9-11. These lift data are plotted versus the average ambient corrected fan speeds (rather than inlet corrected fan speeds) in order to compare at each altitude the combined ground effects including inlet reingestion. The data as presented in the figure include the effects of suckdown plus fountain, fan back pressure, and inlet reingestion as affected by aircraft ground height. As shown by the results in this figure, essentially no net lift loss in ground effects was measured with this aircraft test model, particularly at the higher fan speeds.

The rake-measured ideal thrusts are presented for each lift unit for altitudes of 21.0, 8.3, and 3.3 feet in Figures 9-12, 9-13 and 9-14, respectively, for the same test points as Figure 9-11. The rake-measured ideal thrusts are used to evaluate the thrust variation of the individual units separately from the total net installed lift. The ideal thrust variations shown include the effects of inlet reingestion and back pressure, thereby allowing a comparison with the force data to yield the net propulsion induced ground effects occurring on the aircraft model.

The results of the rake determined individual thrust measurements with all three units operating are presented in Figure 9-15. The relative change in thrust $(\Delta F/F)_{REF}$ versus the model height ratio (H/D) are presented for each unit at a selected corrected fan speed of 3600 rpm. The model height ratio (H/D) for this and all curves presented herein is based on the average exit flow area diameter (D) of all three lift units (D_{AVG} = 39.1"). The reference thrust used in the figure and throughout the report was the value measured at the 21.0 foot model height. The expected deterioration of thrust at the reduced model heights is apparent in the figure as the effects of both inlet temperature reingestion and back pressure are encountered. The sharp rise in the thrust of the nose lift unit as the lower ground heights are reached was found to be the net result of both reduced inlet reingestion and favorable fan back pressure at the lowest ground height. Inspection of the nose fan and gas generator inlet temperature

FIGURE 9-11
EFFECT OF GROUND HEIGHT ON TOTAL MEASURED LIFT
All Units Operating
$\alpha = 0^{o}$

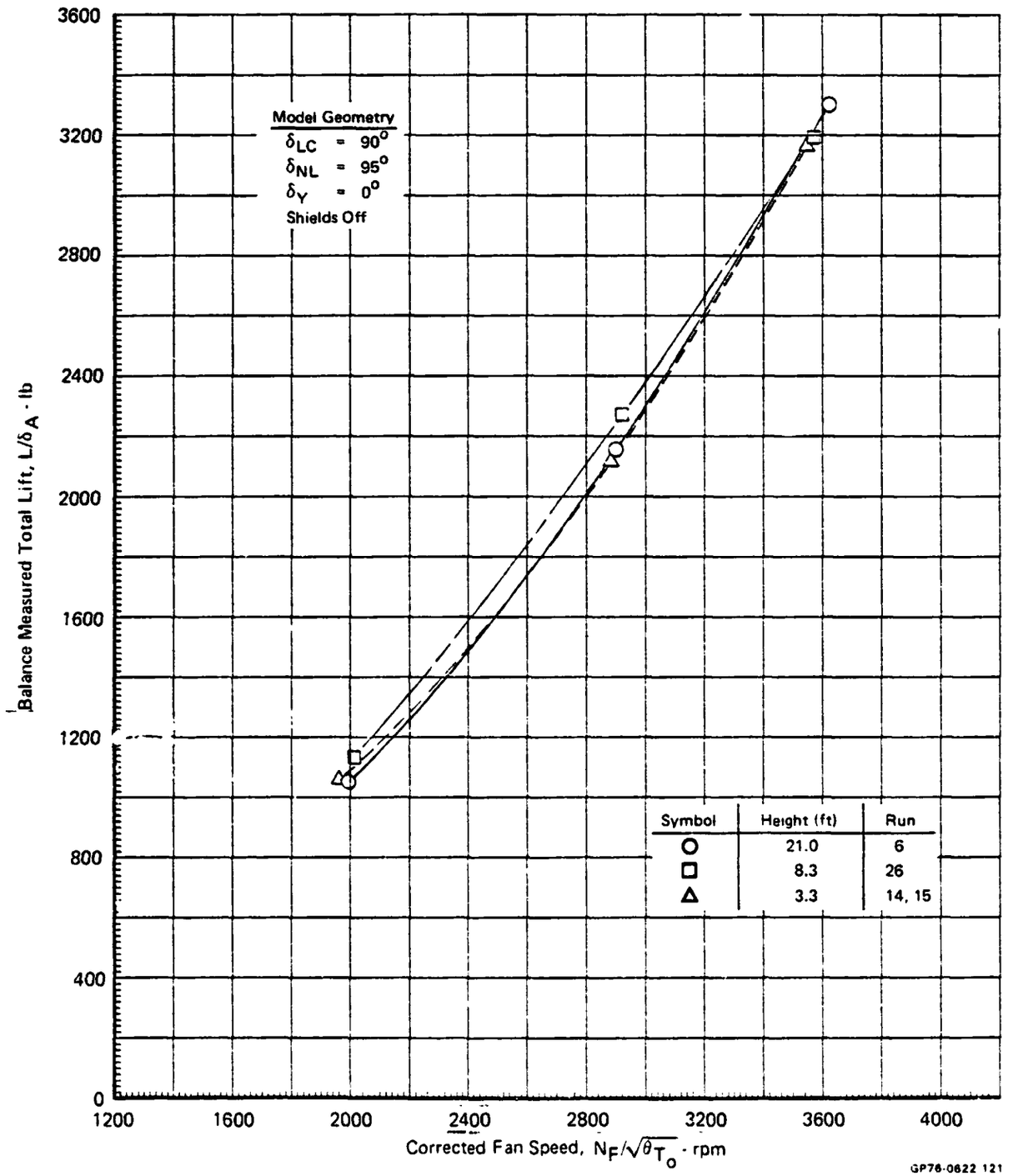

FIGURE 9-12
INDIVIDUAL UNIT IDEAL THRUST MEASUREMENTS
All Units Operating
Model Height = 21.0 Ft

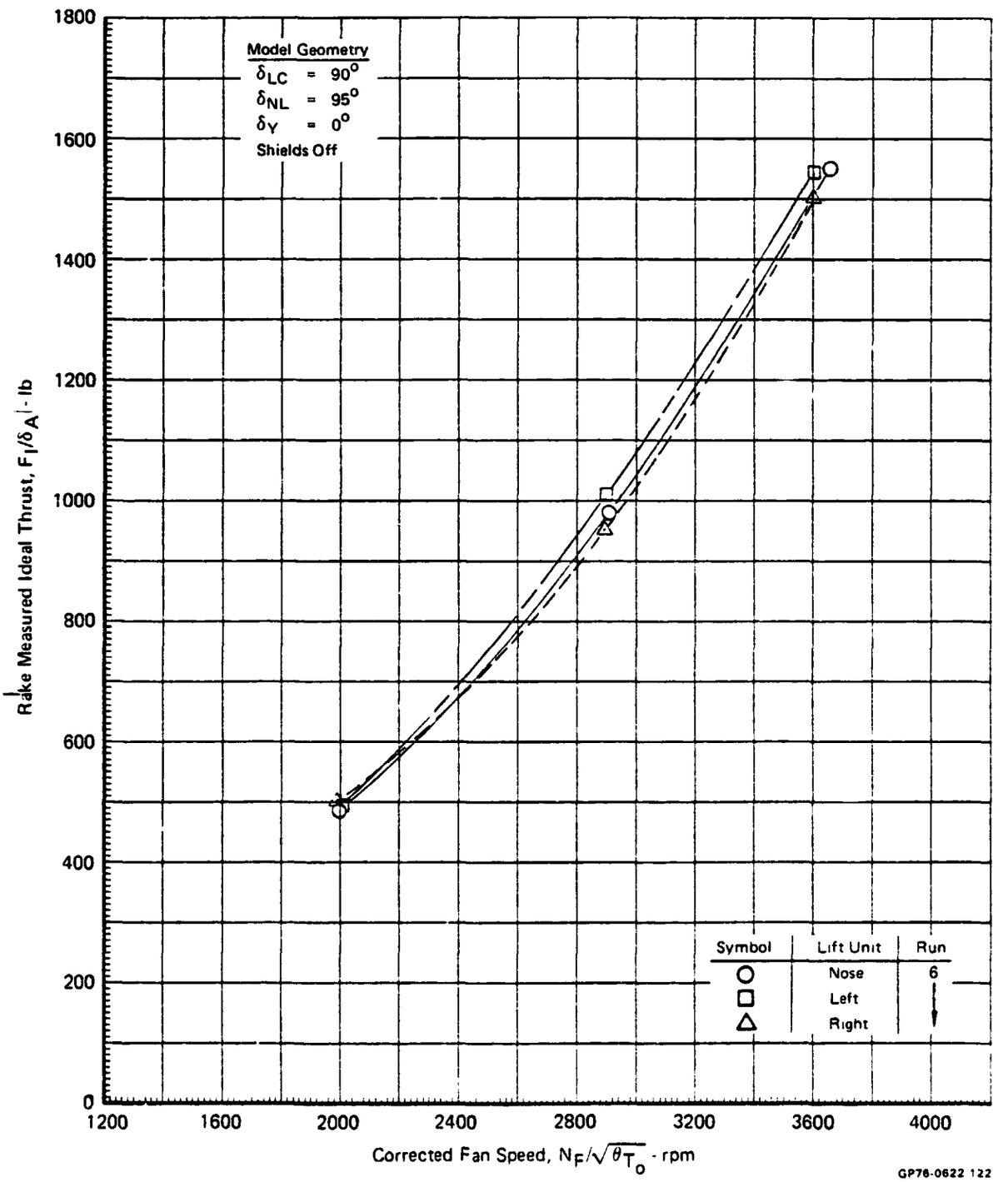

FIGURE 9-13
INDIVIDUAL UNIT IDEAL THRUST MEASUREMENTS
All Units Operating
Model Height = 8.3 Ft

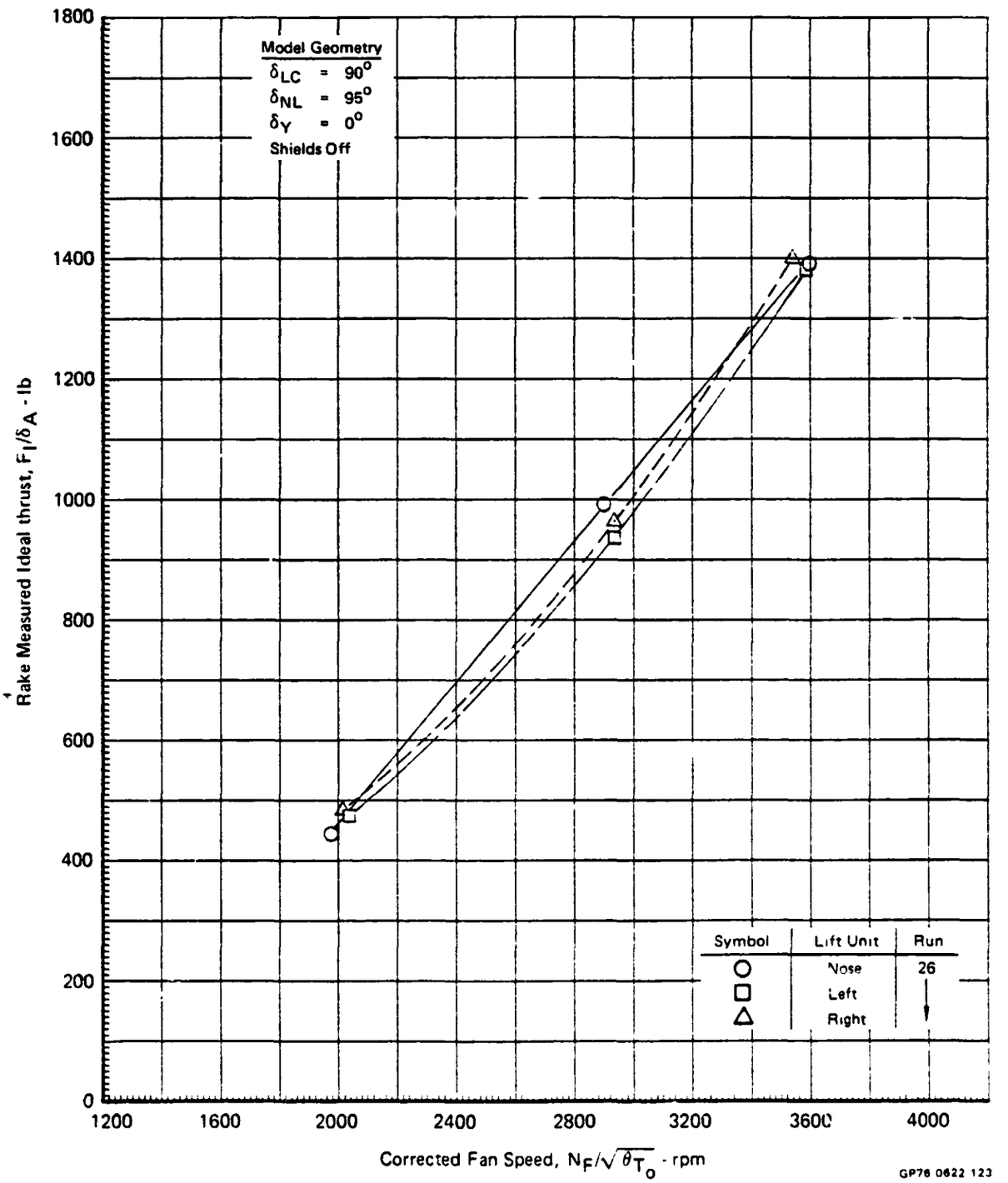

FIGURE 9-14
INDIVIDUAL UNIT IDEAL THRUST MEASUREMENTS
All Units Operating
Model Height = 3.3 Ft

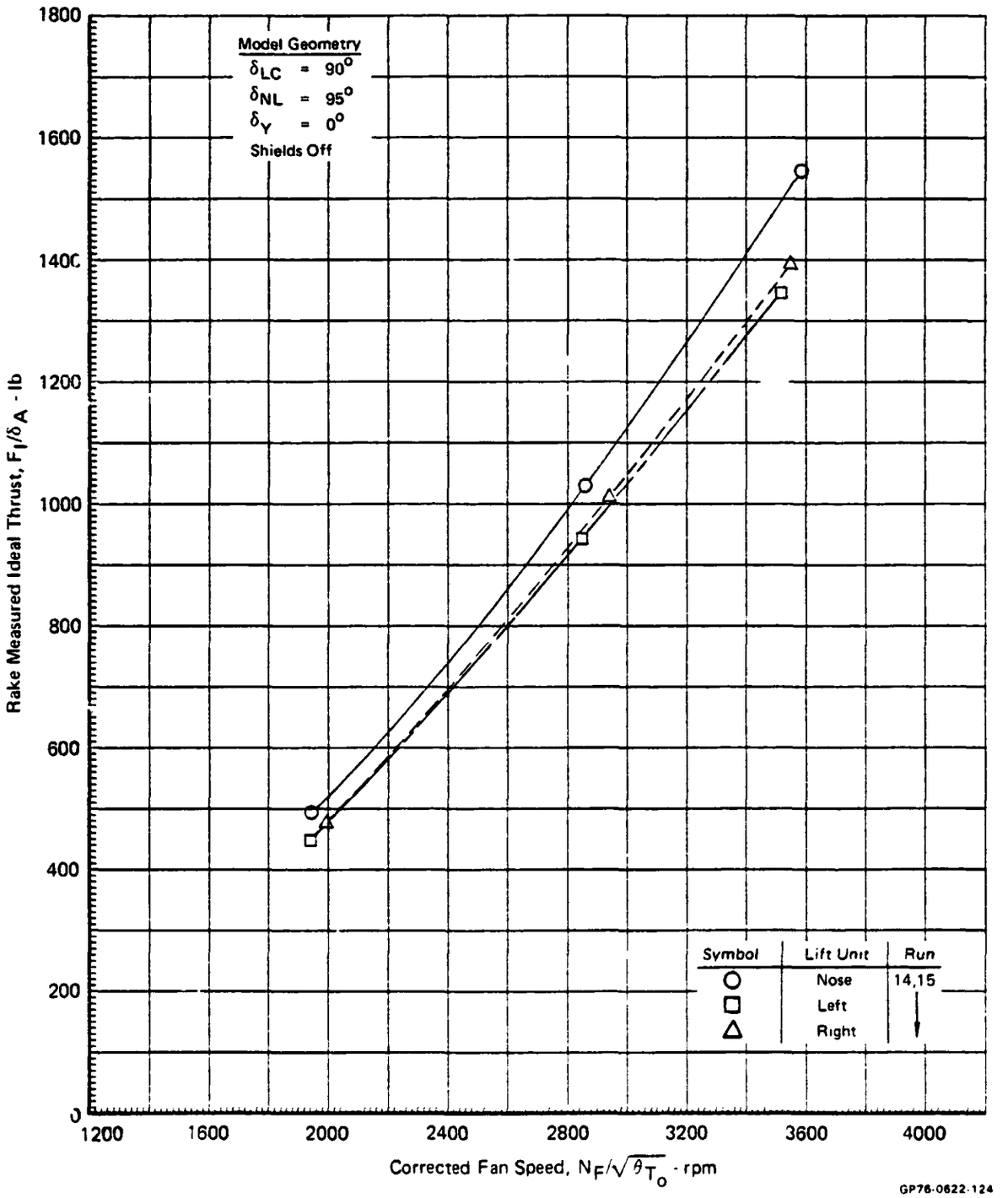

FIGURE 9-15
EFFECT OF GROUND HEIGHT ON THE INDIVIDUAL UNIT THRUST
All Units Operating
Corrected Fan Speed ($N_F/\sqrt{\theta_{T_o}}$) = 3600 RPM

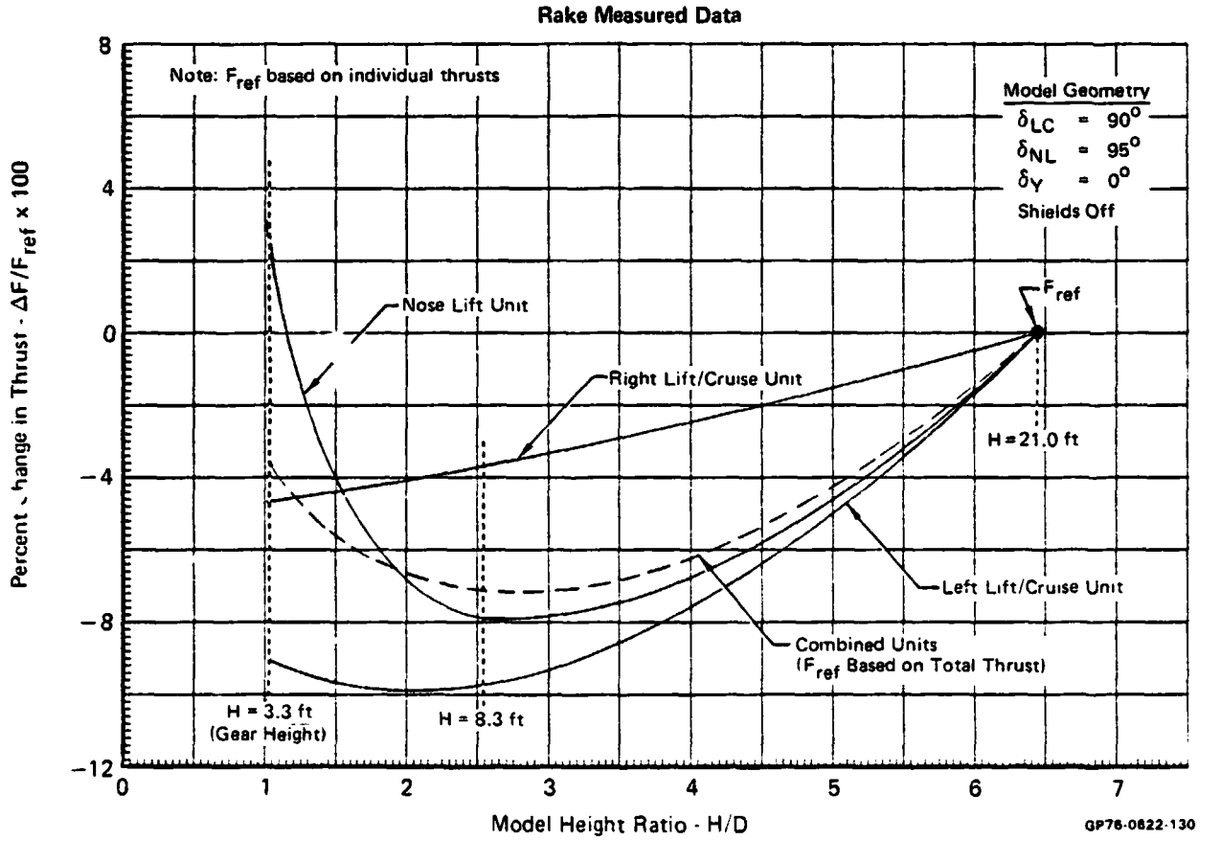

reingestion data in Section 9.3 of this report explains the more favorable reingestion effects. The increased back pressure at the lower ground height caused a reduction in effective nozzle area. The nose fan geometric nozzle area was oversize to start with, therefore the nozzle area match was actually improved at the lower ground height. This moved the fan operating point to a more favorable location on the fan map of Figure 9-10 and thus increased the thrust output. The relative variation of the combined total thrust with height changes is shown by the dashed line in Figure 9-15.

The comparison of the combined total rake-measured thrust variation with the total balance-measured lift variation at a fixed ambient corrected fan speed of 3600 rpm is presented in Figure 9-16. The net balance-measured lift change with ground height (lift loss) was found to decrease less than 1% over the three heights tested. The thrust variation (thrust loss), however, was found to decrease as much as 7% at the intermediate height tested. It is apparent from these data that a net positive induced force is occurring on this model probably due to favorable fountain effects. As was stated previously, both the rake-measured thrust and balance-measured total lift have the effects of reingestion and back pressure in the values presented, therefore indicating that the differences between the two measurements with ground height are due to induced rather than direct thrust forces.

The effects of gas generator inlet shields on the reduction of the gas generator inlet reingestion were found to be favorable and are discussed in Section 9.3. However, as shown in the Figures of 9-17 through 9-19, the effects of inlet shielding on the balance-measured total lift were found to be very small. Figure 9-17 shows essentially no effect for the large shield at a model height of 21.0 ft. A small but apparent positive effect due to the addition of the small shield at the intermediate 8.3 ft altitude is shown in Figure 9-18. A comparison of the large and small inlet shields and their effect on total installed lift loss is shown in Figure 9-19 at the lowest height of 3.3 feet. As shown in the figure, essentially no difference existed between the large and small shields, although a small but negative effect on lift was measured by both shields as compared with the shield off configuration. This negative effect indicates that, although the inlet reingestion is reduced and thrust increased (see Section 9.3), there is a slightly greater lift loss due to an apparent increase in suckdown. Figure 9-20 presents the effect of shield deflection angle (δ_s) on the balance-measured total lift at a corrected fan speed of 2500 rpm at the 3.3 foot model height. This data indicates that an optimum deflection angle exists at approximately 45°,

FIGURE 9-16
EFFECT OF GROUND HEIGHT ON TOTAL LIFT AND THRUST
All Units Operating
Corrected Fan Speed ($N_F/\sqrt{\theta_{T_o}}$) = 3600 RPM

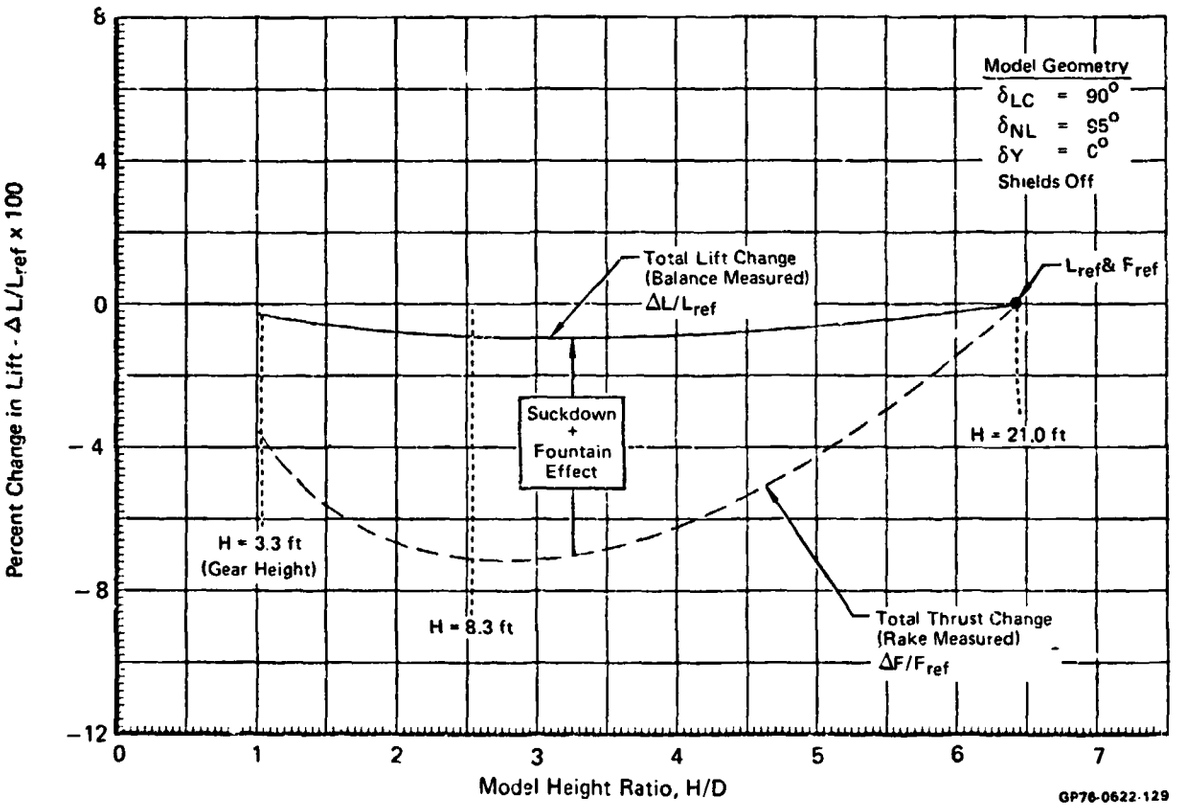

FIGURE 9-17
EFFECT OF INLET SHIELDING ON TOTAL MEASURED LIFT
All Units Operating
Model Height = 21.0 Ft

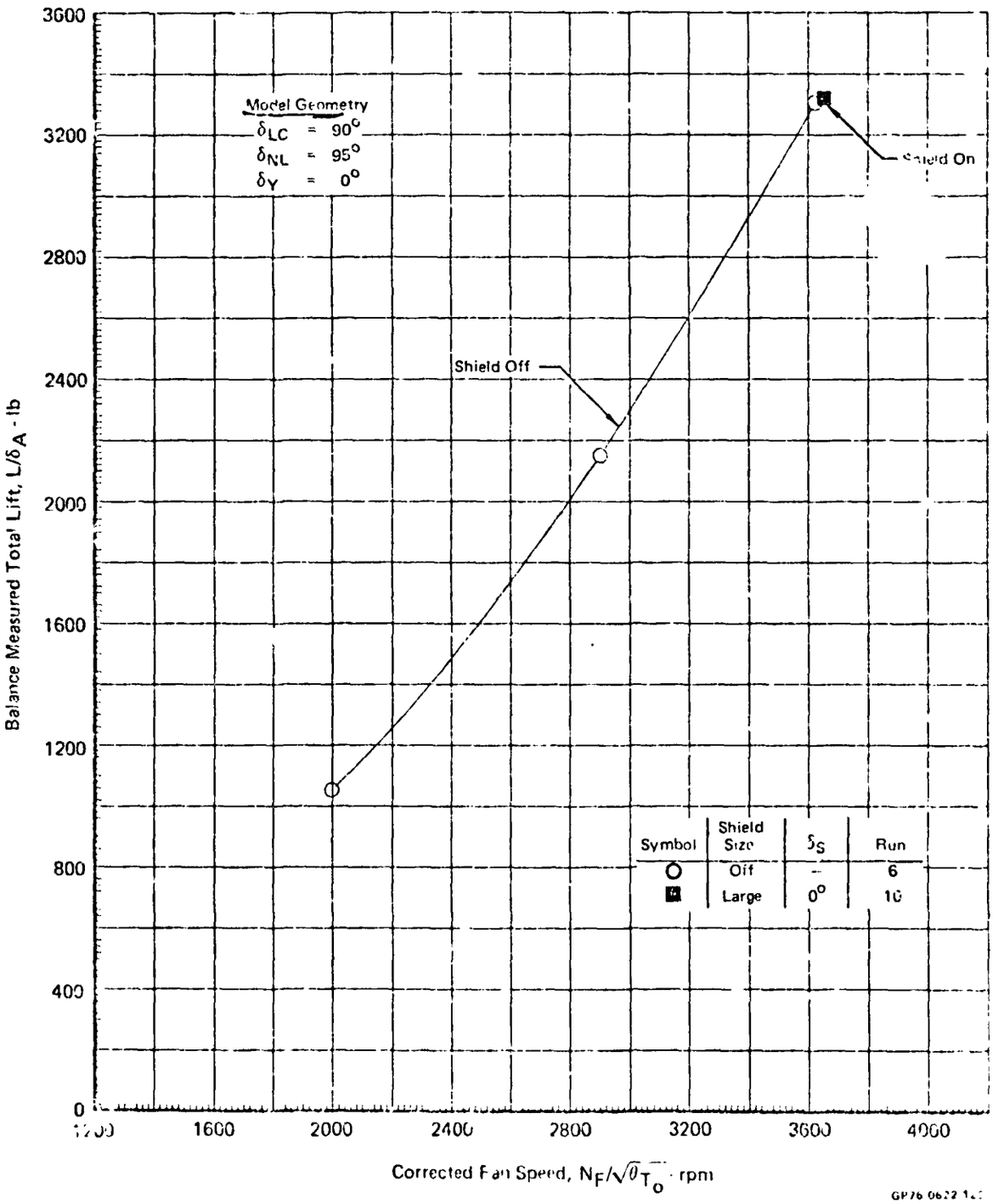

FIGURE 9-18
EFFECT OF INLET SHIELDING ON TOTAL MEASURED LIFT
All Units Operating
Model Height = 8.3 Ft

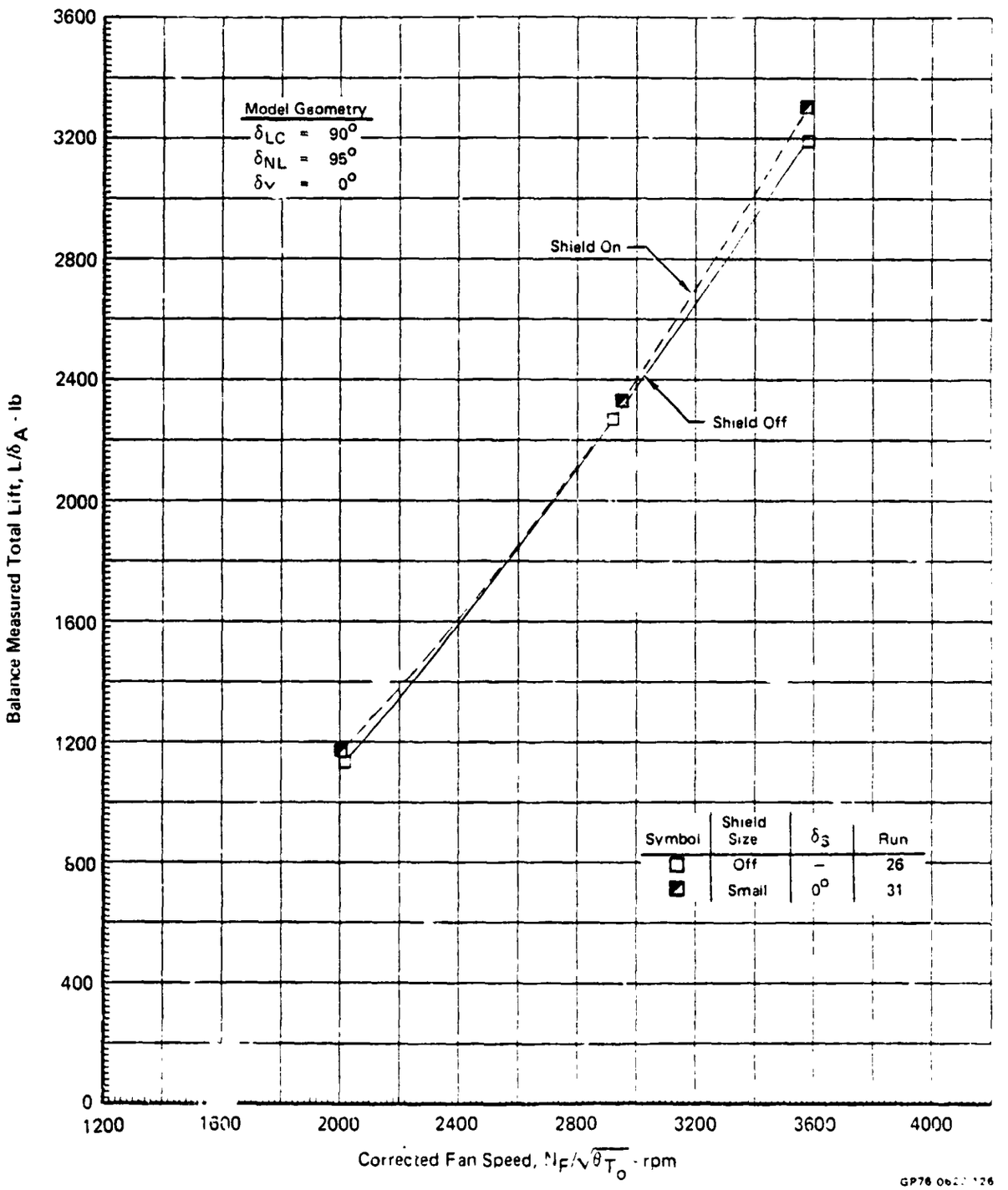

FIGURE 9-19
EFFECT OF INLET SHIELDING ON TOTAL MEASURED LIFT
All Units Operating
Model Height = 3.3 Ft

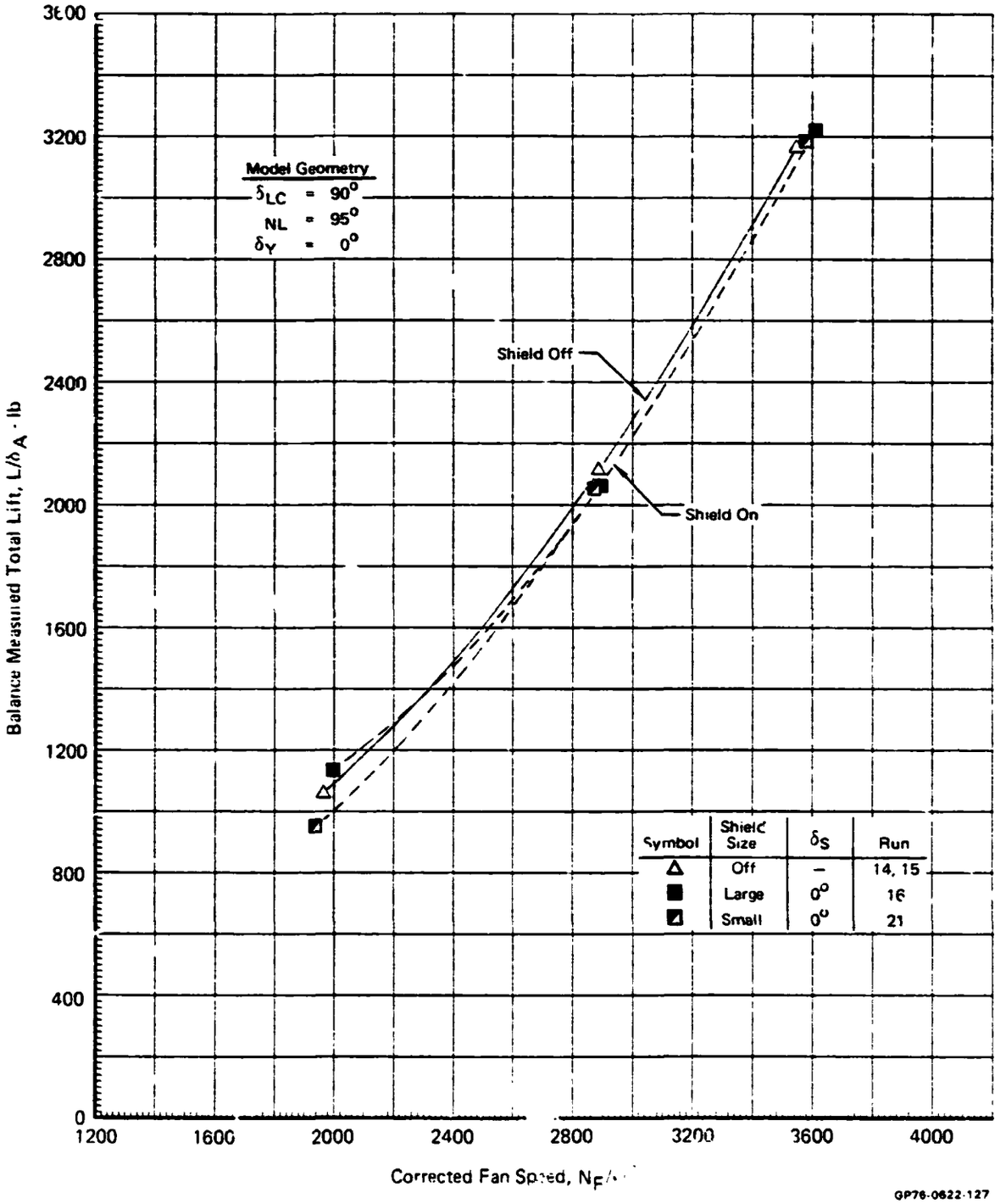

FIGURE 9-2C
EFFECT OF SHIELD DEFLECTION ANGLE ON TOTAL MEASURED LIFT
All Units Operating
Model Height = 3.3 Ft $N_F/\sqrt{\theta_{T_o}}$ **= 2500 RPM**

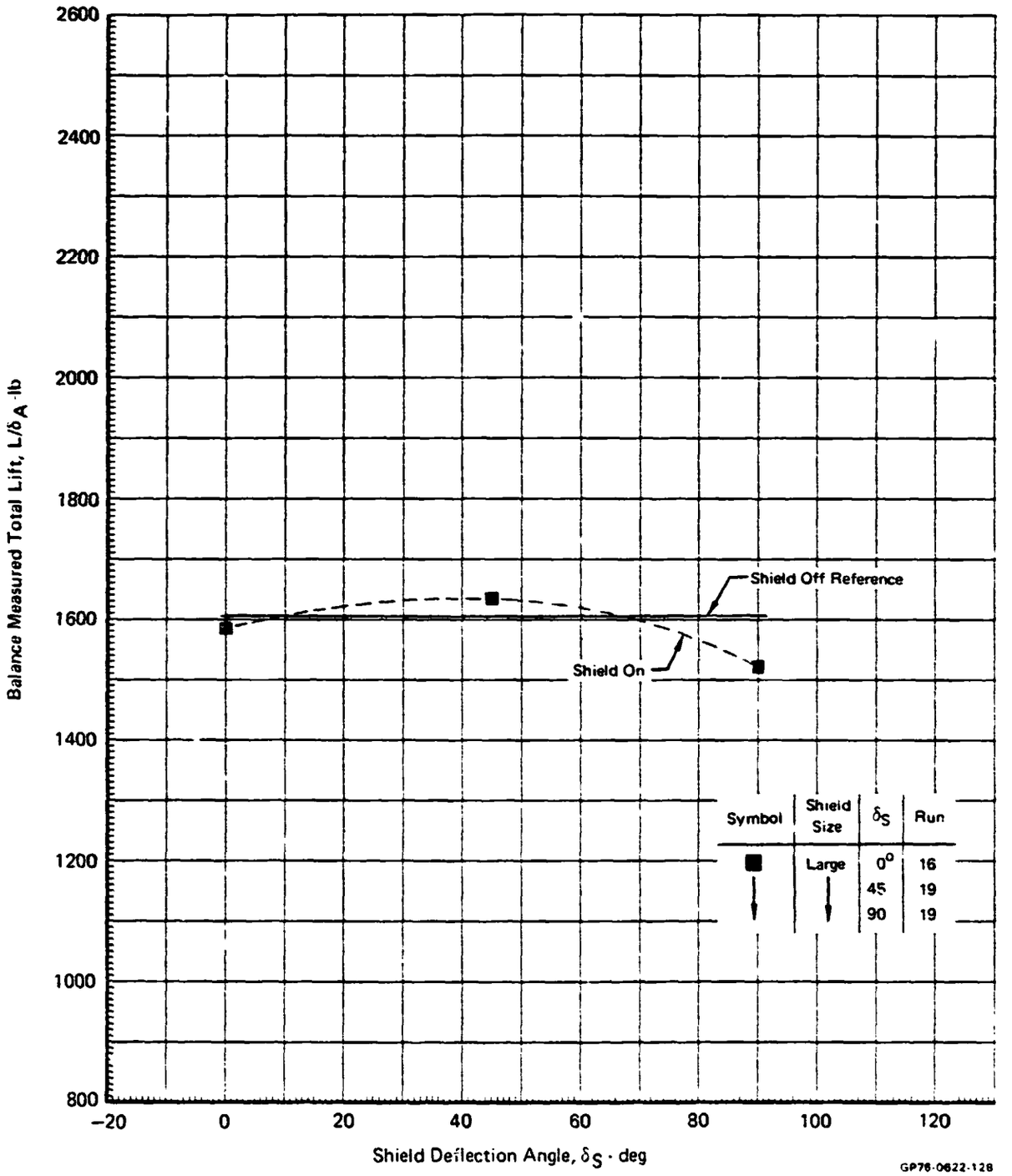

apparently providing a compromise between the opposing inlet reingestion and suckdown effects at this intermediate angle.

Individual Unit Operation

The balance-measured lift of the individual units at three values of ground height are presented in Figures 9-21, 9-22, and 9-23 for the left, right, and nose units, respectively. The data are plotted as a function of ambient corrected fan speed, $N_F/\sqrt{\theta_{TO}}$. The lift loss (or gain) in ground effect is much more apparent for these individual unit runs than for the previously discussed three unit combined runs. The lift/cruise units showed an increasing lift loss as ground height was reduced. The nose lift unit showed the same loss trend as ground heights was reduced until the 8.3 ft level was reached below which the lift began increasing. Inlet reingestion on the individual test runs was minimal, as no fountain or local upwash flow was generated. The lift loss (or gain) as measured by the balance data was therefore due to either increasing fan back pressure, suckdown, or both.

The rake-measured ideal gross thrust for the left, right, and nose units are presented in Figures 9-24, 9-25, and 9-26, respectively, for each ground height tested. These data also are presented versus corrected fan speed and are from the same run as the three balance-measured data figures. All three units exhibited a relatively small change in the rake-measured thrust when altitude was decreased, as shown in the figures. The left and right unit thrust decayed as ground height decreased. However, the nose unit thrust increased with reduced ground heights. Once again, inlet reingestion played an insignificant role in the variation of those rake-measured thrust data, with the thrust variation effects, whether positive or negative, being attributed here to effective nozzle area changing, i.e., back pressure effects.

Comparisons of the balance-measured lift loss data with the rake-measured thrust loss data are presented in Figures 9-27, 9-28, and 9-29 for the left, right, and nose lift units, respectively. The data are presented as a function of model height ratio (H/D) for a fixed corrected fan speed of 3600 rpm. The 21.0 foot model height is used as the reference altitude from which the percentage changes are computed. Note that both lift/cruise units show a thrust decay maximizing at between 3 and 4%, attributable to back pressure. The negative difference between the balance-measured lift and rake-measured thrust data as shown in the figures for the two lift/cruise units is attributed solely to model suckdown. As shown in the two figures, approximately 15% and 20% suckdown force was measured for the two respective units at the gear height of 3.3 feet (H/D = 1.02). The nose

FIGURE 9-21
EFFECT OF GROUND HEIGHT ON INDIVIDUAL UNIT MEASURED LIFT
Left Lift/Cruise Unit Only
$\alpha = 0^{o}$

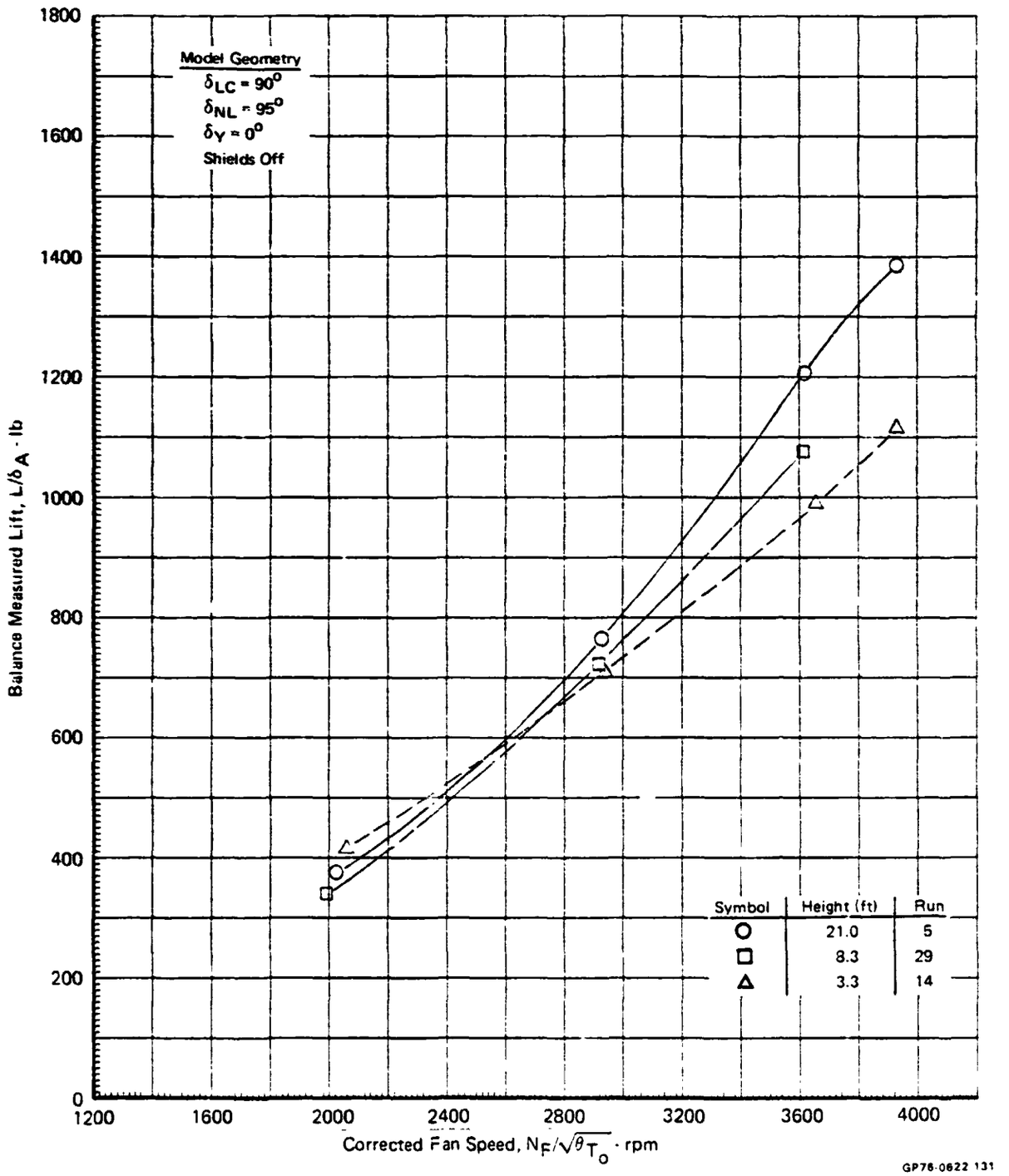

FIGURE 9-22
EFFECT OF GROUND HEIGHT ON INDIVIDUAL UNIT MEASURED LIFT
Right Lift/Cruise Unit Only
$\alpha = 0^{o}$

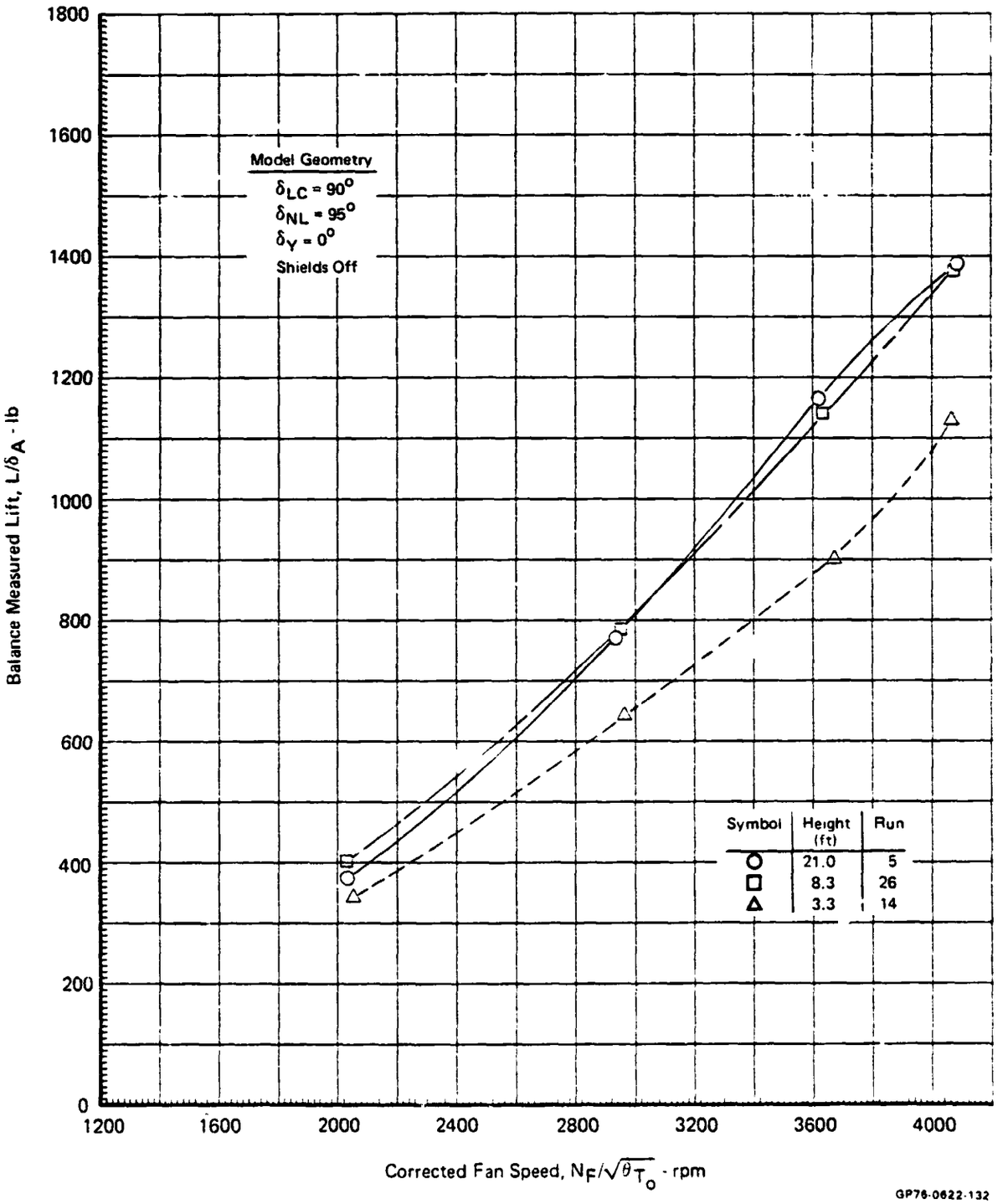

FIGURE 9-23
EFFECT OF GROUND HEIGHT ON INDIVIDUAL UNIT MEASURED LIFT
Nose Lift Unit Only
$\alpha = 0^o$

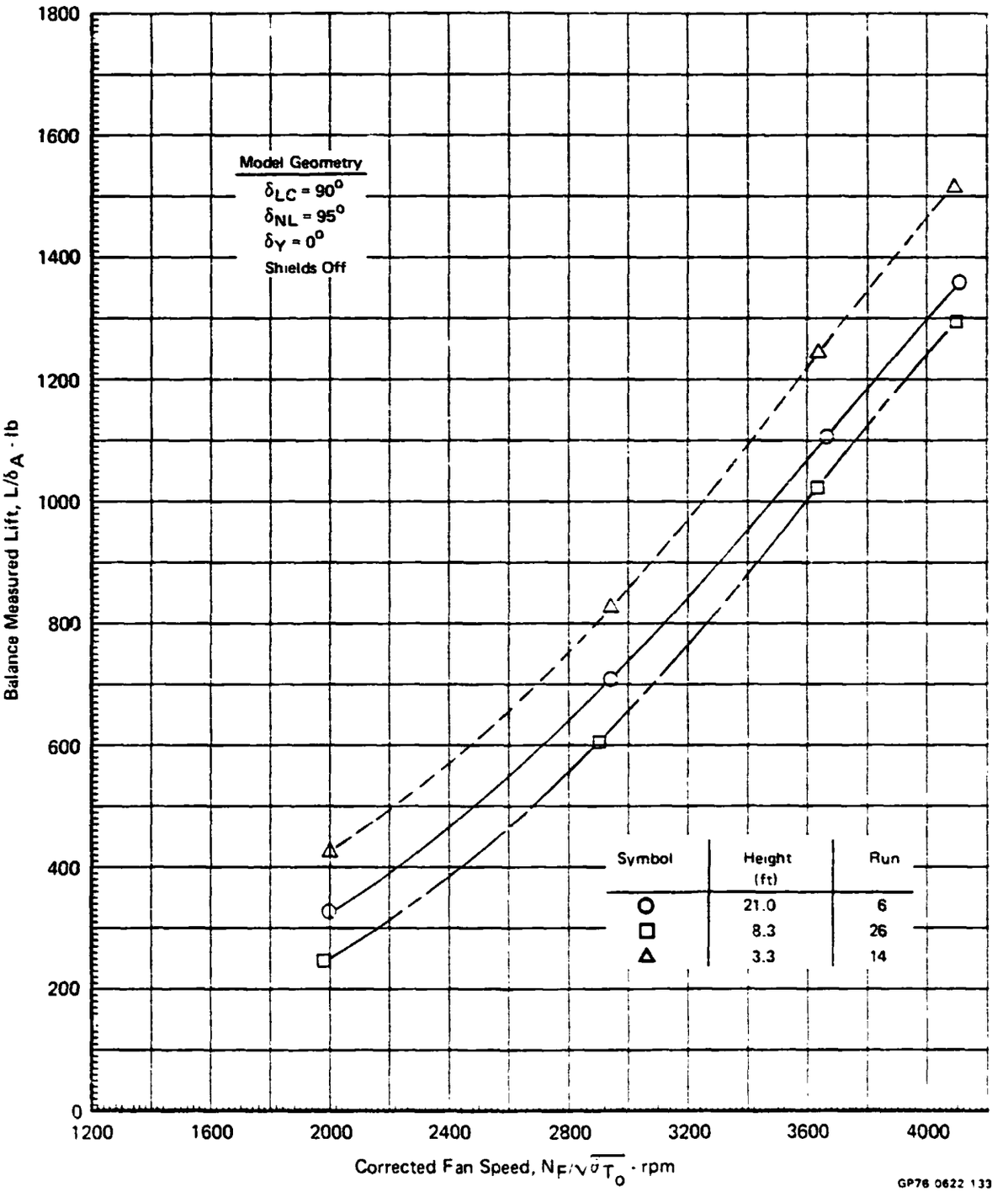

FIGURE 9-24
EFFECT OF GROUND HEIGHT ON INDIVIDUAL UNIT IDEAL THRUST
Left Lift/Cruise Unit Only
$\alpha = 0^{o}$

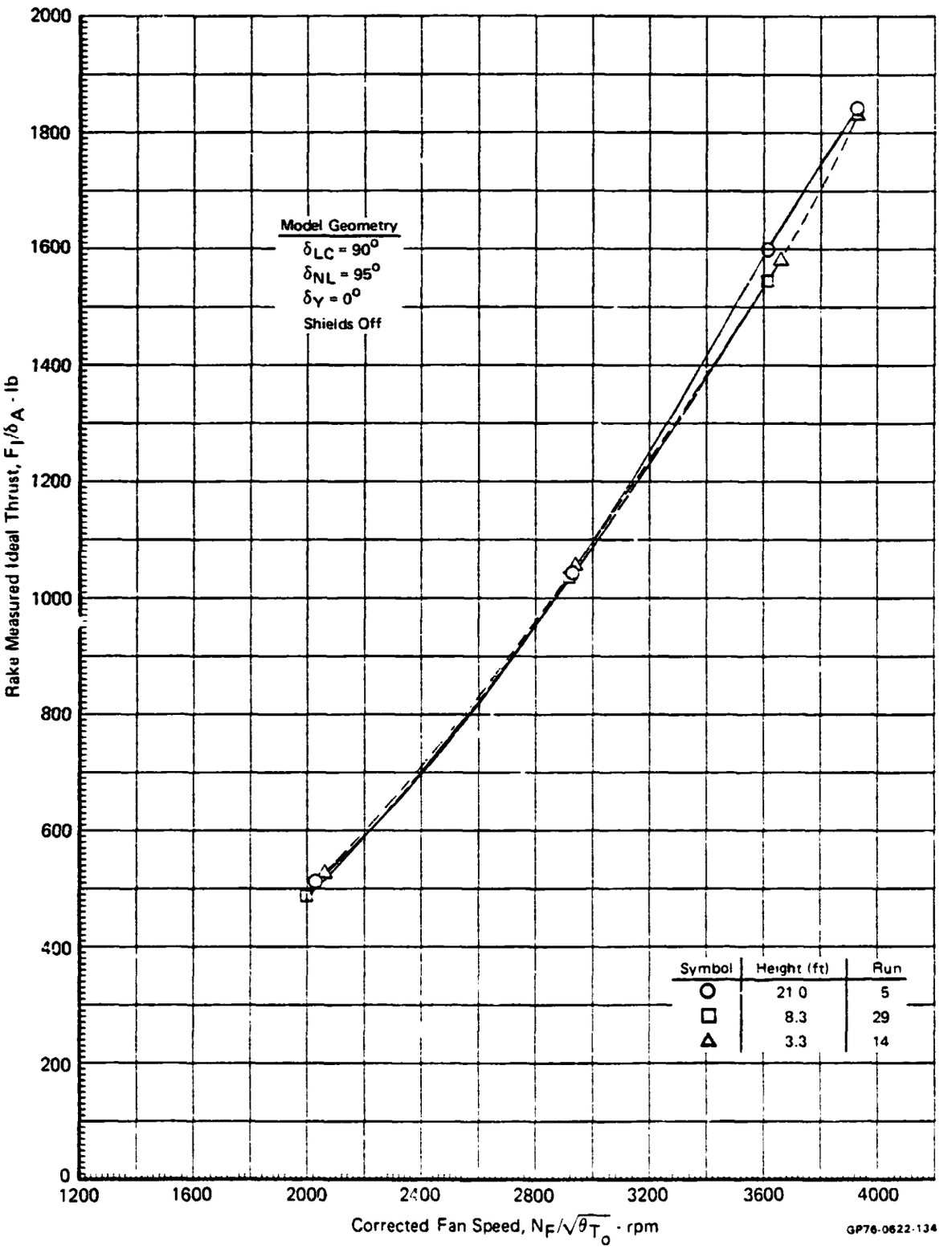

FIGURE 9-25
EFFECT OF GROUND HEIGHT ON INDIVIDUAL UNIT IDEAL THRUST
Right Lift/Cruise Unit Only
$\alpha = 0^{o}$

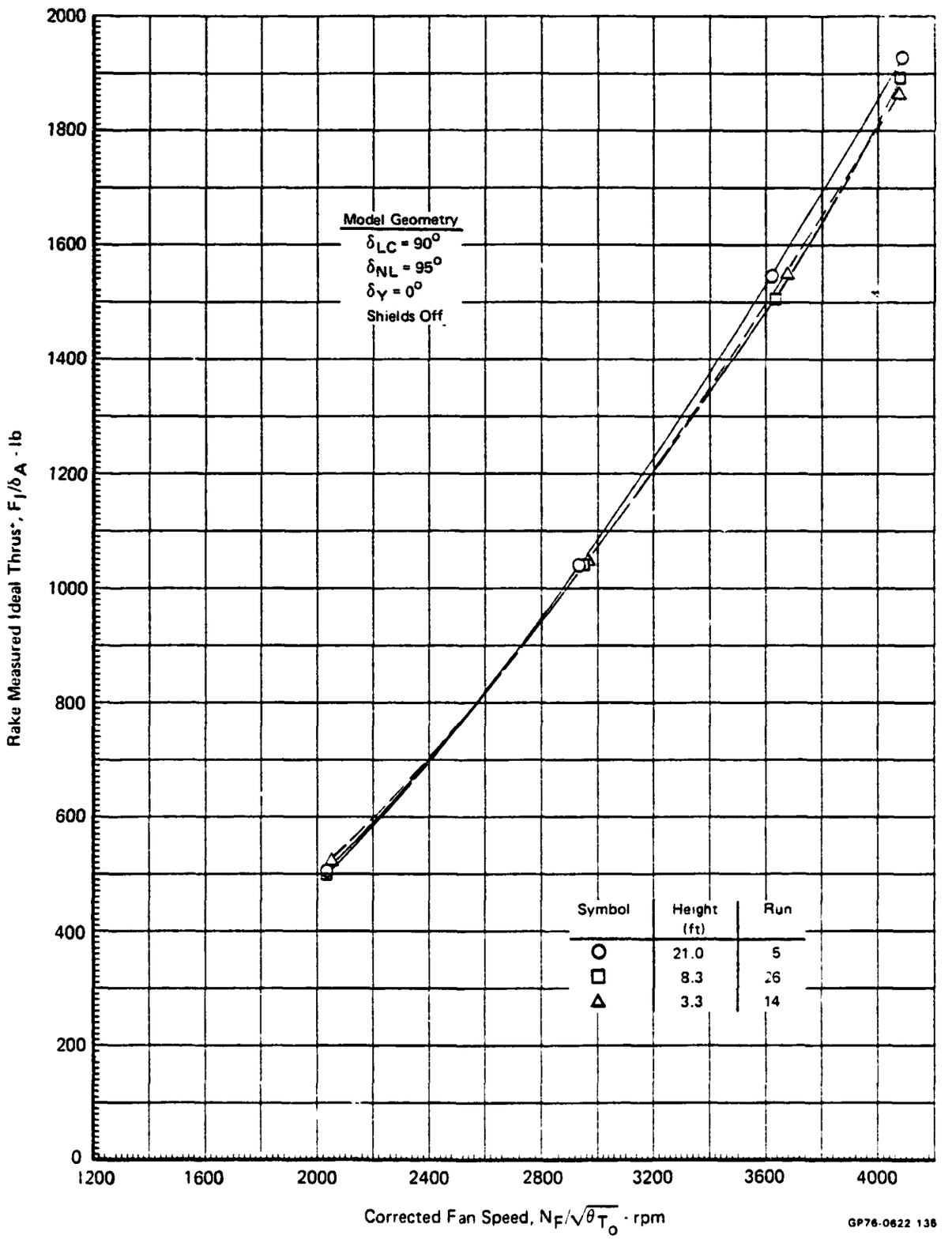

FIGURE 9-26
EFFECT OF GROUND HEIGHT ON INDIVIDUAL UNIT IDEAL THRUST
Nose Lift Unit Only
$\alpha = 0^o$

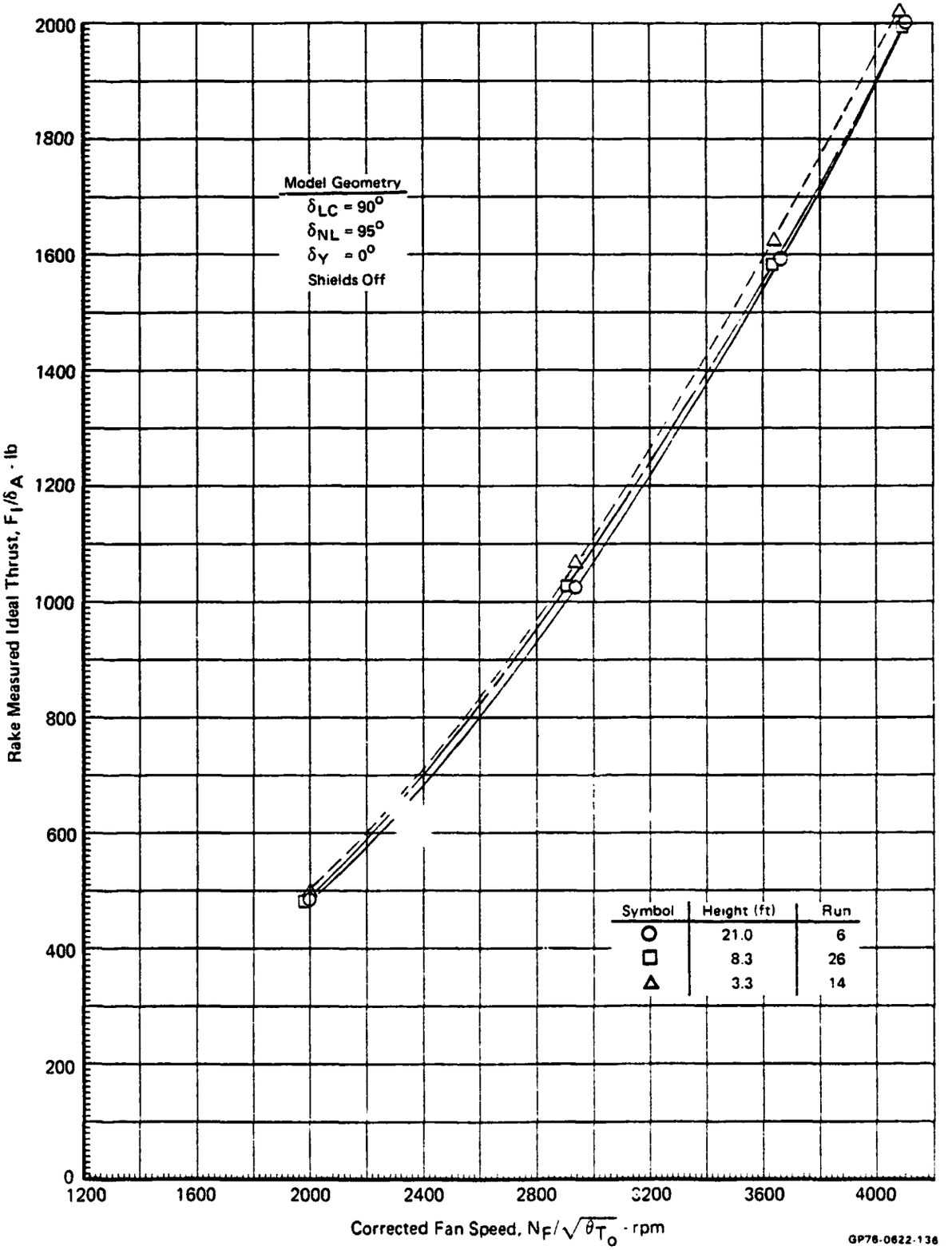

FIGURE 9-27
EFFECT OF GROUND HEIGHT ON INDIVIDUAL UNIT LIFT AND THRUST
Left Lift/Cruise Unit Only
$\alpha = 0^{o}$ $N_F/\sqrt{\theta T_o} = 3600$ RPM

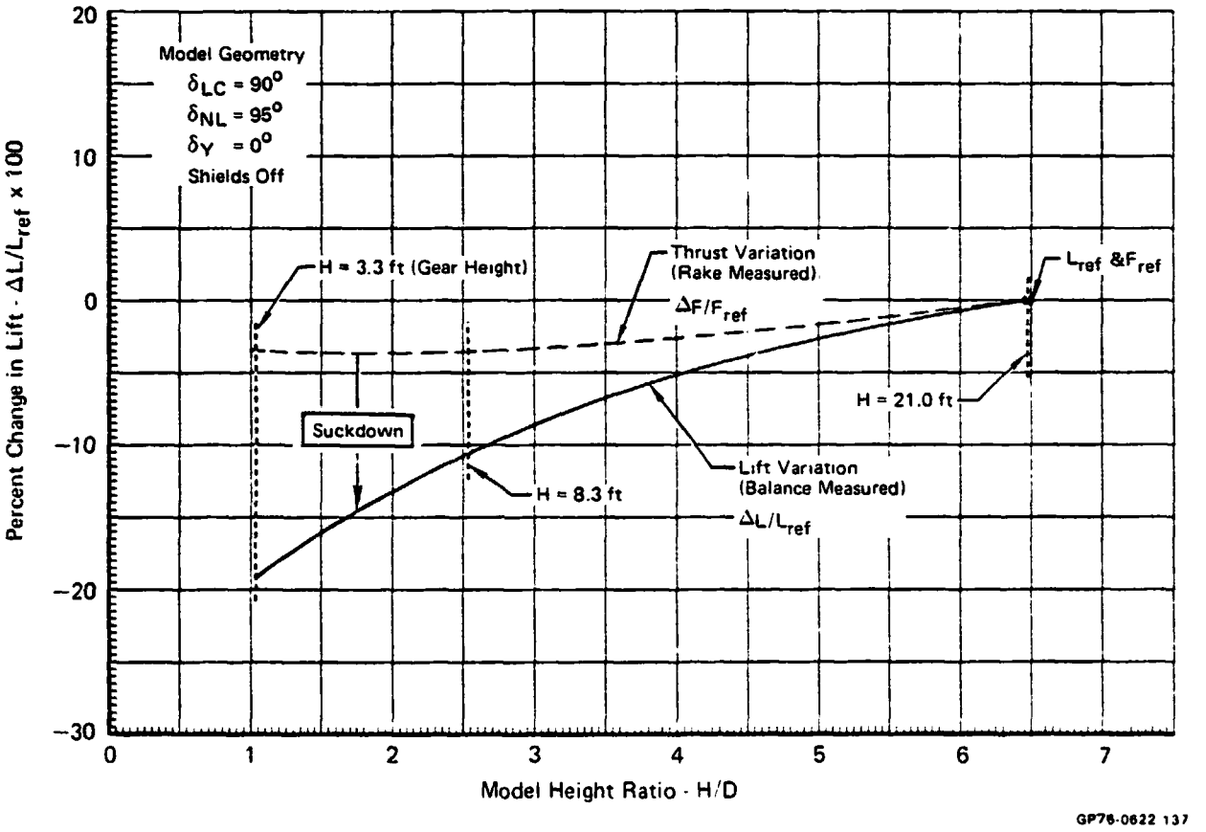

FIGURE 9-28
EFFECT OF GROUND HEIGHT ON INDIVIDUAL UNIT LIFT AND THRUST
Right Lift/Cruise Unit Only
$\alpha = 0^0$ $N_F/\sqrt{\theta T_o} = 3600$ RPM

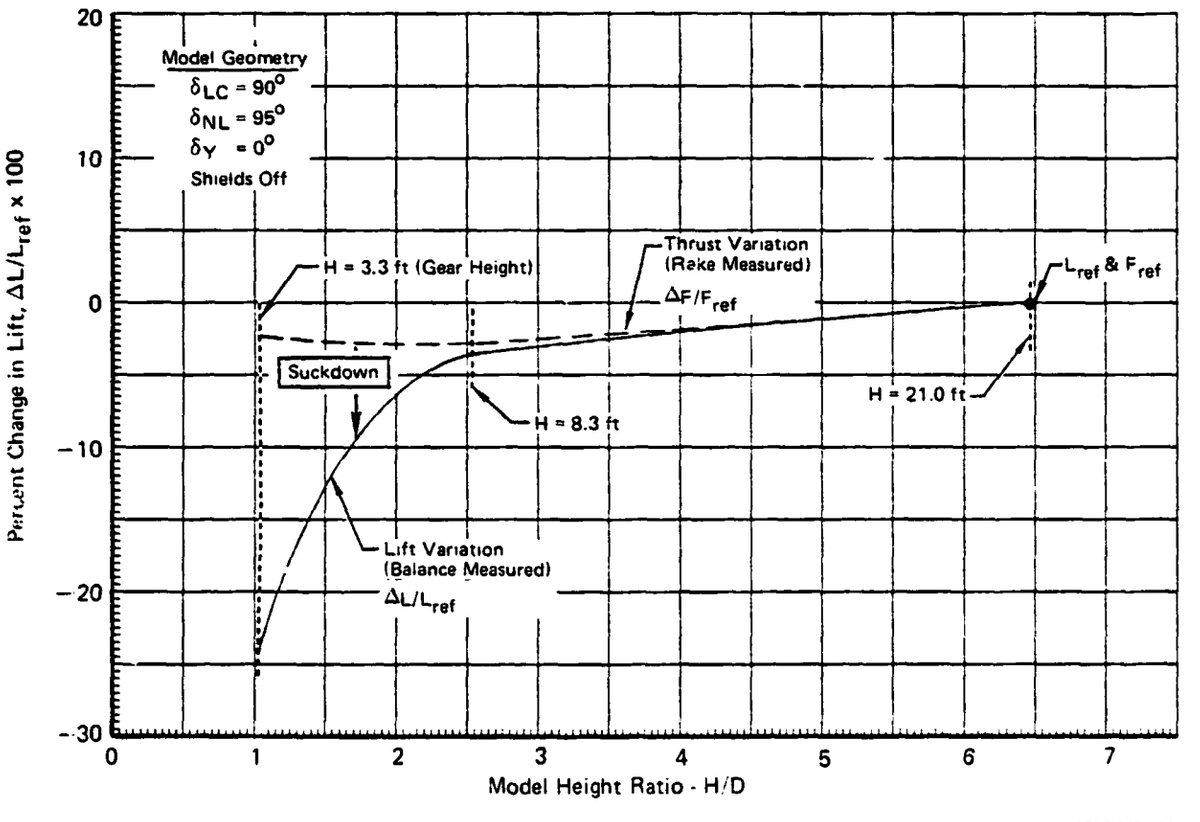

GP76-0622-138

FIGURE 9-29
EFFECT OF GROUND HEIGHT ON INDIVIDUAL UNIT LIFT AND THRUST
Nose Lift Unit Only
$\alpha = 0^{o}$ $N_F/\sqrt{\theta T_o} = 3600$ RPM

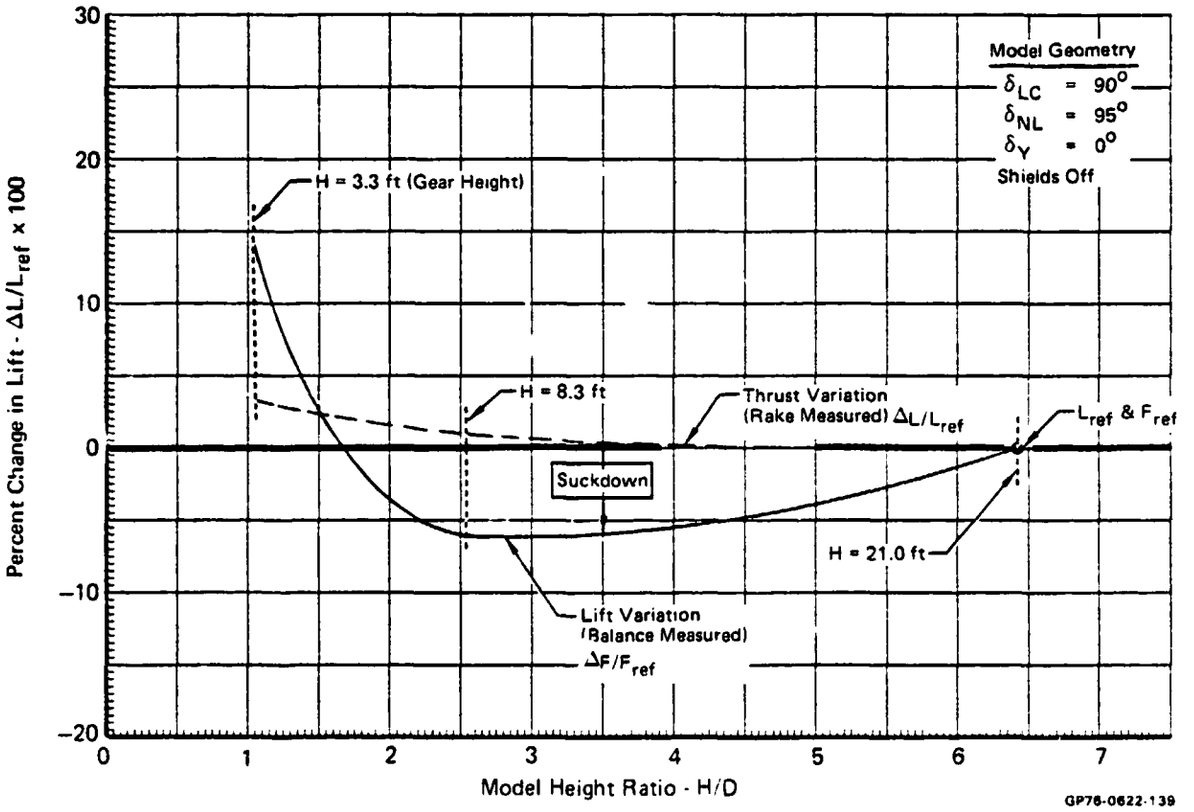

unit data of Figure 9-29 shows an entirely different picture. The rake-measured thrust variation is shown to increase steadily as the ground is approached. This increase is caused by movement to a more favorable operating point on the fan map due to positive back pressure effects. The negative differences between the balance lift and thrust data at the intermediate H/D, like the lift/cruise units, are attributed to suckd .. The positive difference between the lift and thrust data at the lowest H/D i similar to that experienced in small scale model fan tests (Reference 4) at low H/D. The explanation for this phenomenon was that as the horizontally mounted lift fan approach the ground, a higher than ambient base pressure was induced on the exit hub of the lift fan, and a net positive lift was achieved. This same effect is believed to be occurring on the nose unit on this particular model configuration.

Lift Loss Summary

A summary of the balance-measured lift data ($\Delta L/L$) shown on the previous summary plots is presented in Figure 9-30 for both the three unit operation data and the single unit left lift/cruise unit data. The data from this test are plotted on an existing comparison plot of previous multiple-jet model tests as obtained from Reference (6). As shown in the figure, the data trends seen in this test are similar to those shown for the previous tests. It should be noted, however, that the comparison data from this test are shown on this existing summary plot for illustration purposes only, and do not necessarily reflect test data acquired in like manner.

FIGURE 9-30
LIFT LOSS IN GROUND EFFECT COMPARISONS
Figure Reproduced from Reference (6)

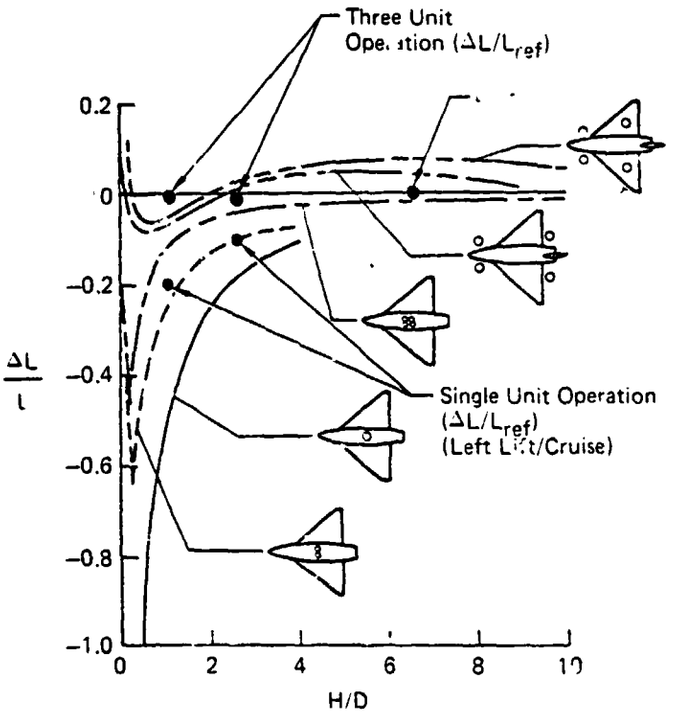

CP76-0622 273

9.3 GROUND EFFECTS ON INLET REINGESTION

The effects of ground height and selected model test variables on inlet temperature reingestion characteristics are presented in this section for the four inlets in operation on this test model as shown in Figure 9-31. The test variables include the model ground height, fan speeds, nose unit vector angle, yaw vane splay angle, inlet shield size and shield deflection angle. Most of the data presented was measured utilizing the Vidar digital data acquisition system and is assumed to be steady state. Selected analog data traces are presented for the more unsteady test runs and comparisons between the digital and analog data for these selected test runs are discussed.

Ground Height Effects

The effects of ground height on inlet temperature reingestion are presented throughout this section in order to provide a basis for comparing the effects of the other test variables. A specific comparison of the inlet temperature rise for each of the four inlets evaluated in the test program is presented as a function of model ground height ratio (H/D) in Figure 9-32. The data shown are presented for a constant ambient corrected fan speed of 3600 rpm. The inlet temperature rise index, $\Delta T_i/\Delta T_j$, is utilized on this and on every figure presented herein in order to non-dimensionalize the reingestion data for direct comparison purposes between runs. The temperature rise index removes from consideration the strong effects of changes in the exhaust jet temperature, which was continually changing over the course of this test program, due both to ambient temperature variations and to the large jet temperature rise associated with large inlet temperature rises. The ΔT_i equals the inlet total temperature rise above ambient ($T_{T_2} - T_{amb.}$), and the ΔT_j equals the three unit mass averaged jet temperature rise above ambient ($T_{T_j} - T_{amb.}$). As shown in Figure 9-32, the peak inlet temperature rise occurred at the intermediate 8.3 foot height tested for all inlets except the left lift/cruise fan inlet. The reason for the lower inlet temperatures at the 3.2 versus the 8.3 foot height is believed to be the stronger upwash dynamic pressure and hence a stronger lateral deflection of the flow field by the aircraft. Also shown in the figure is the inlet which sustains the highest reingestion temperature rise, that of the left gas generator inlet. The approximate location of the lateral fountain (see Figure 9-31) occurs, as expected, in the vicinity of this inlet which is also the only inlet without any form of airframe shielding. The mass average jet temperatures along with the ambient temperatures for each data point are presented in all figures in this section. In general, the ΔT_j value

FIGURE 9-31
POWERED MODEL TEMPERATURE INSTRUMENTED INLETS
Inlet Reingestion Tests

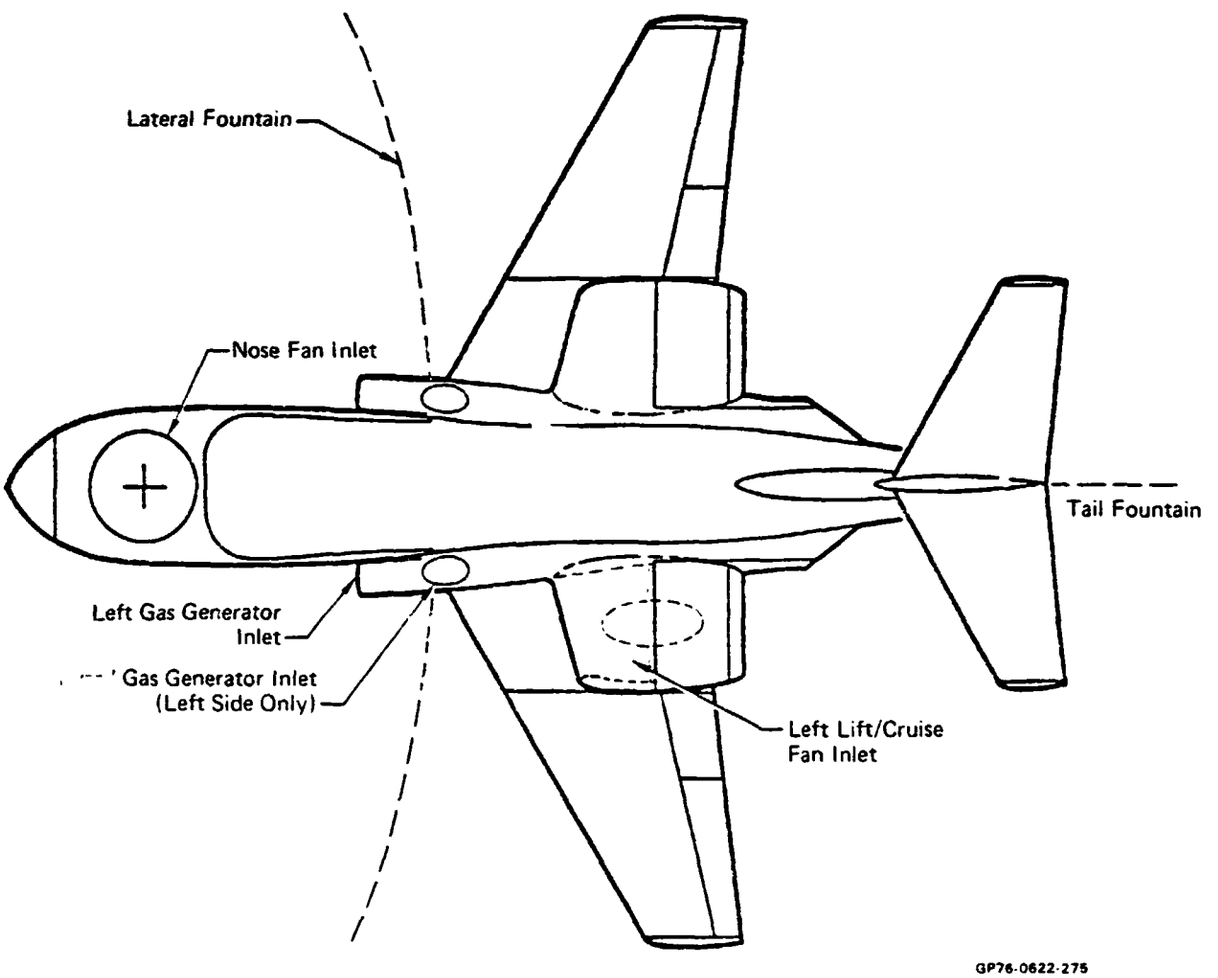

FIGURE 9-32
EFFECT OF GROUND HEIGHT ON INLET REINGESTION

$N_F/\sqrt{\theta_{T_o}}$ = 3600 RPM

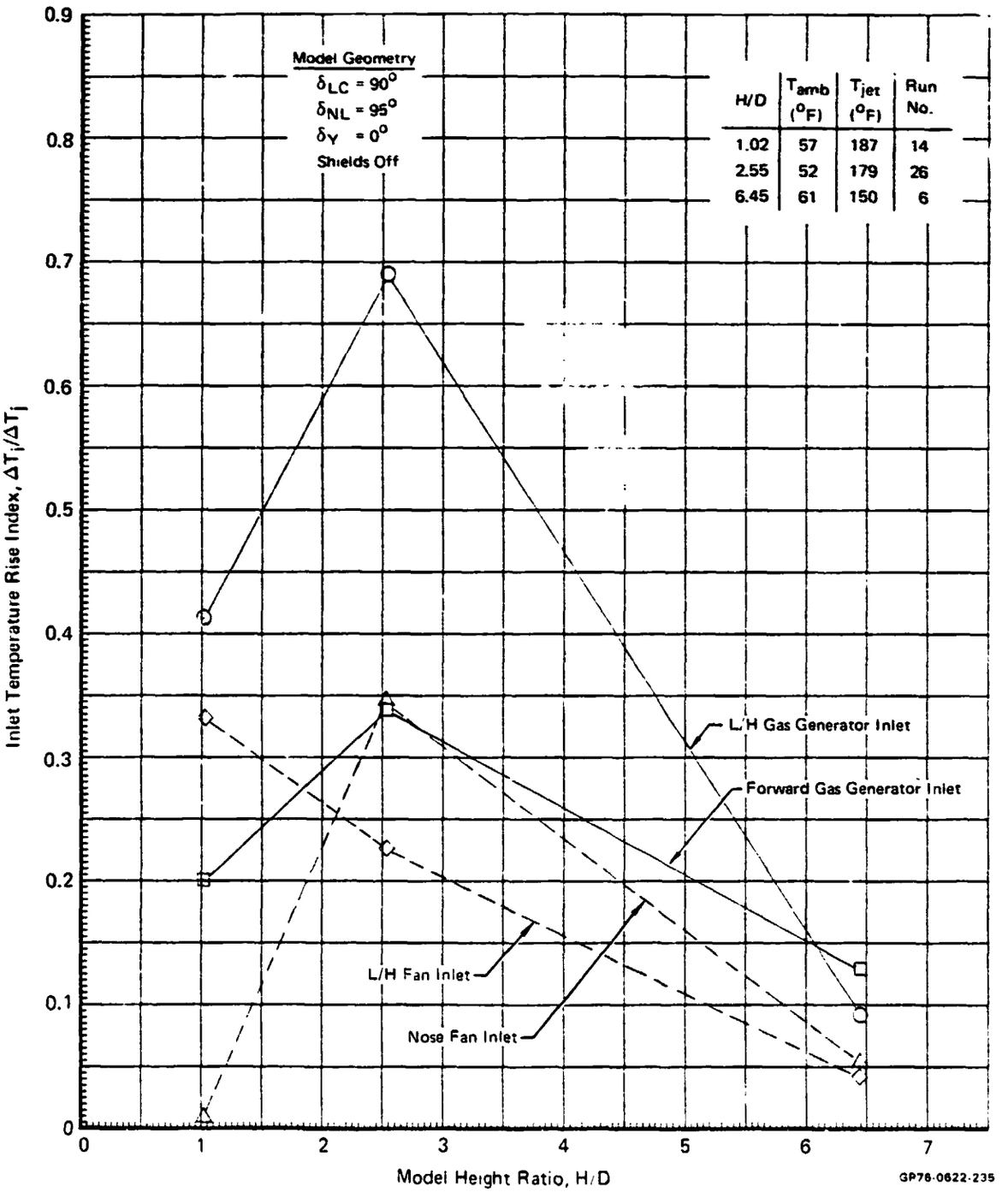

measured in most of the tests was approximately 100 Fahrenheit degrees.

Louver Deflection Effects

The effects of varying nose unit louver deflection angles on inlet reingestion is presented for each inlet in Figures 9-33, 9-34, and 9-35 for ground heights of 3.3, 8.3, and 21.0 feet, respectively. All data are presented for a constant corrected fan speed of 3600 rpm. In general for all inlets at all altitudes, with the exception of the nose fan inlet at the 8.3 foot height, deflecting the louvers from 80° to 102° caused a steadily increasing and significant rise in the inlet temperature levels measured. These characteristics were due to the direct movement of the lateral fountain. Moving it rearward under the wing increased shielding whereas moving it forward away from the wing reduced shielding effects. The sensitivity of inlet temperature rise to louver deflection for the more critical gas generator inlets was shown to be much less as altitude was increased.

Differential Fan Speed E[illegible]s

The effect of nose [illegible]ed variations on reingestion by the four inlets is presented in Figures [illegible] 9-37, and 9-38 for ground heights of 21.0, 8.3 and 3.3 feet, respectively. The nose fan speed was varied below and above a nominal fan speed of 3600 rpm. The effects were found to be most pronounced at the 3.3 foot ground height. Decreasing the nose fan speed and hence its jet dynamic pressure caused the lateral fountain to shift forward from beneath the shielding wing area and therefore increase the reingestion levels of all four inlets. Increasing the nose fan speed moved the fountain rearward and decreased reingestion. Similar characteristics were observed at the 8.3 foot ground height, except that a decrease in fan speed below the nominal 3600 rpm value showed very little effect. Both the nose and lift/cruise fan speed variation effects at the 21.0 foot height, Figure 9-36, showed only minor effects on inlet reingestion.

Nozzle Exhaust Splaying Effects

The effects of splaying the nozzle jet exhausts on inlet reingestion temperature are presented in Figures 9-39 through 9-42 for the four inlets tested. The data are presented versus the ground height ratio (H/D) for a constant corrected fan speed of 3600 rpm.

Splaying was achieved using the manually positioned yaw vanes on each lift unit. The two yaw vanes on each lift cruise unit and the two on the nose unit splayed outboard 12°.

FIGURE 9-33
EFFECT OF NOSE UNIT DEFLECTION ANGLE ON INLET REINGESTION

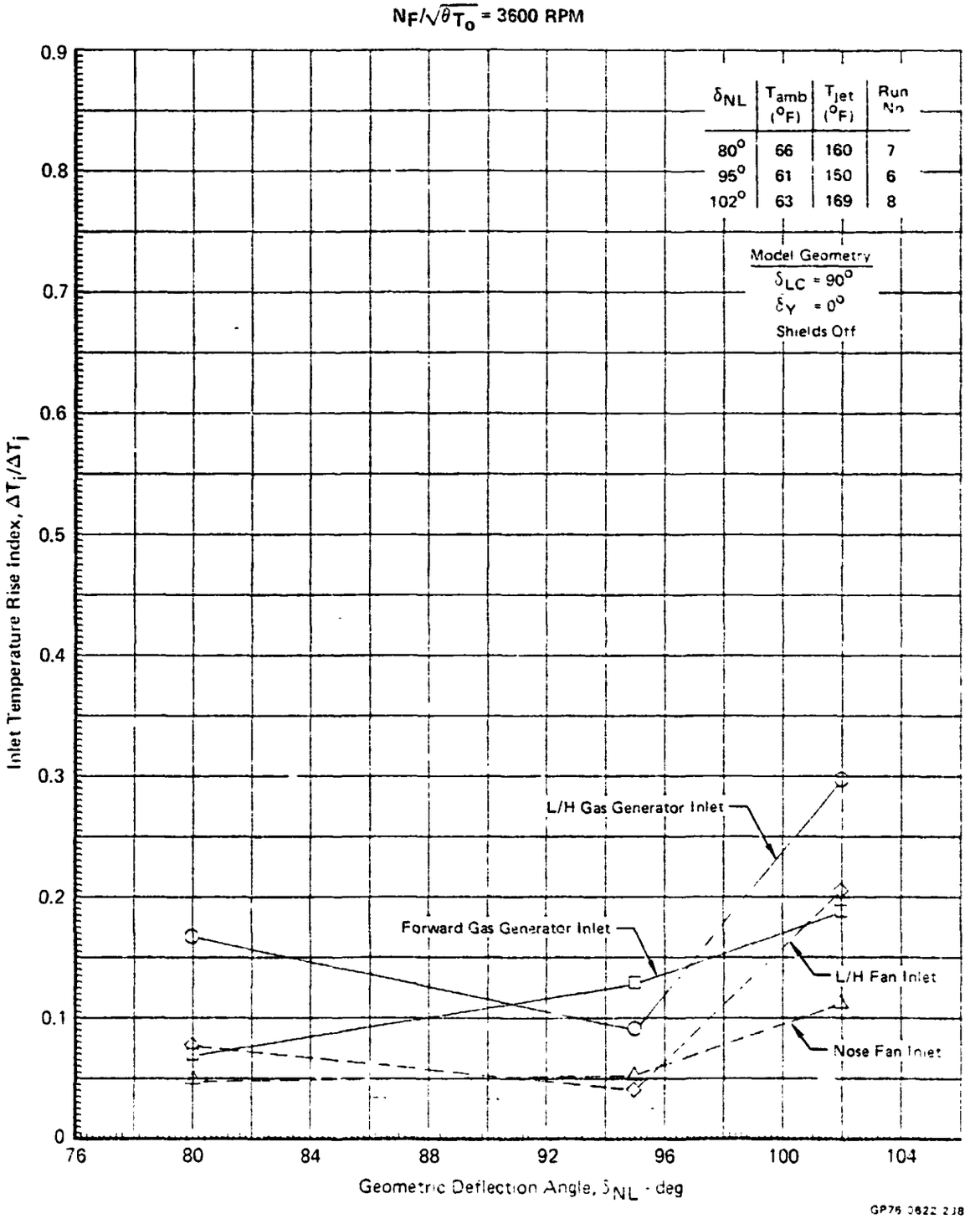

FIGURE 9-34
EFFECT OF NOSE UNIT DEFLECTION ANGLE ON INLET REINGESTION

Model Height = 8.3 ft

$N_F/\sqrt{\theta T_o}$ = 3600 RPM

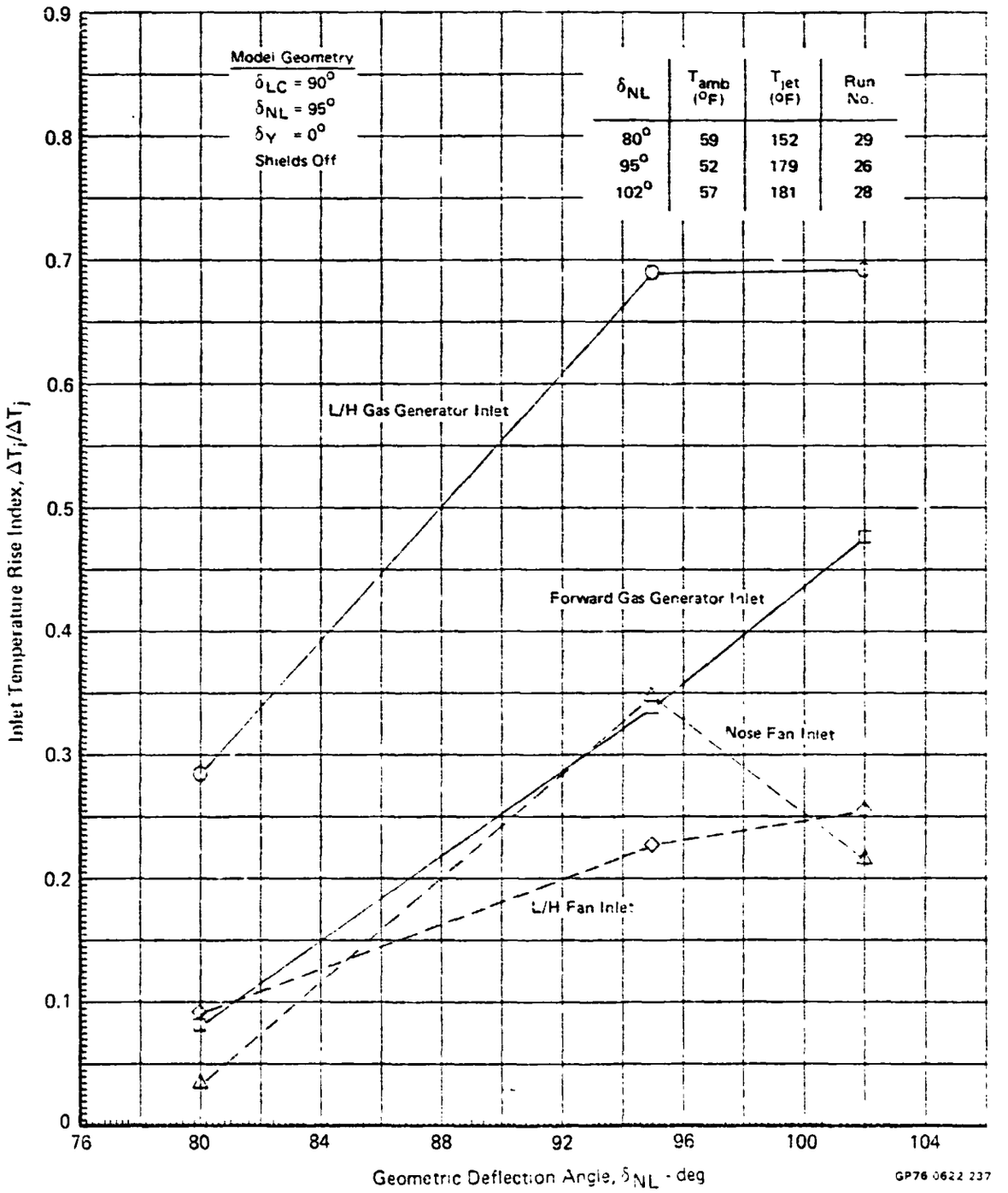

FIGURE 9-35
EFFECT OF NOSE UNIT DEFLECTION ANGLE ON INLET REINGESTION

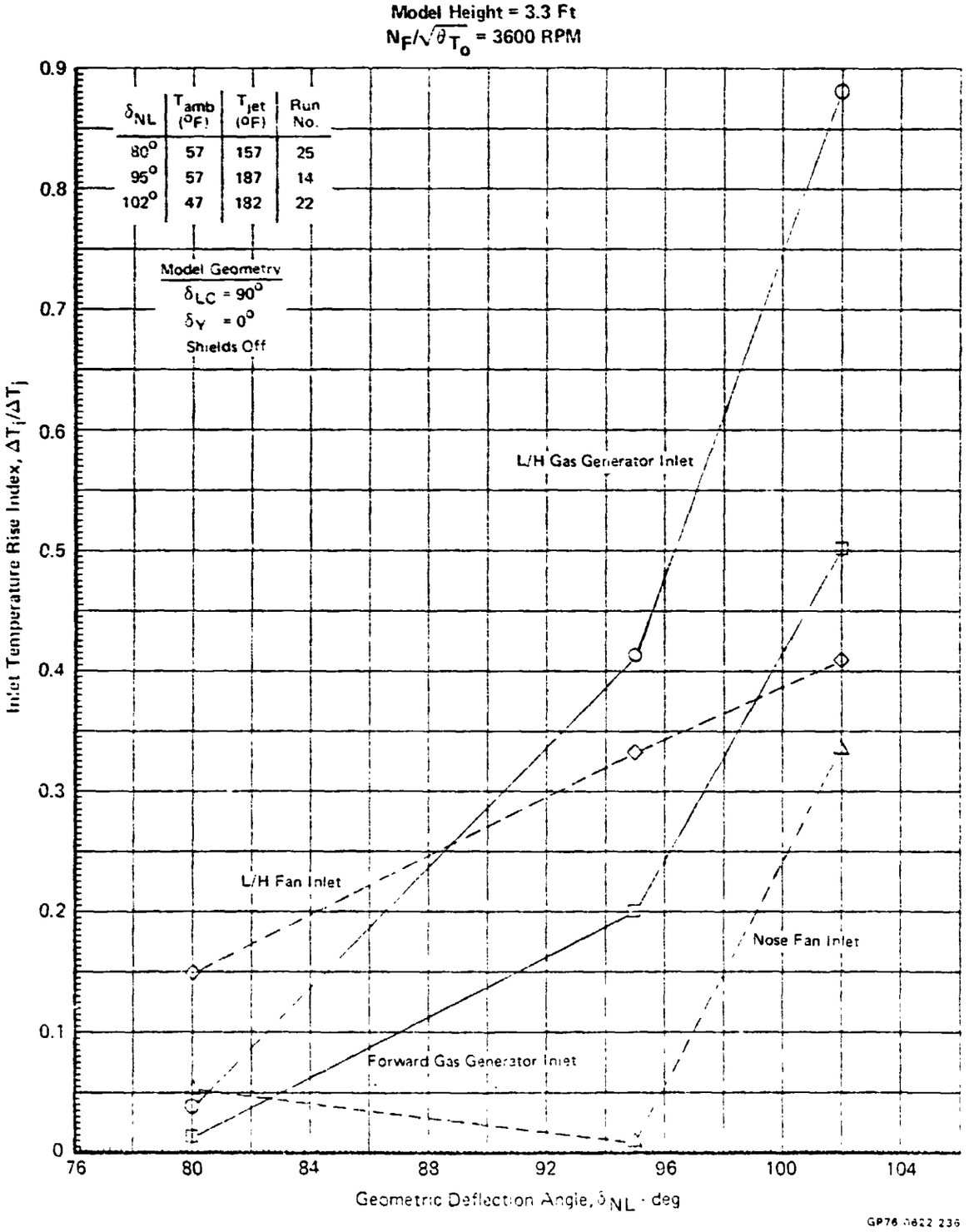

FIGURE 9-36
EFFECT OF FAN SPEED ON INLET REINGESTION

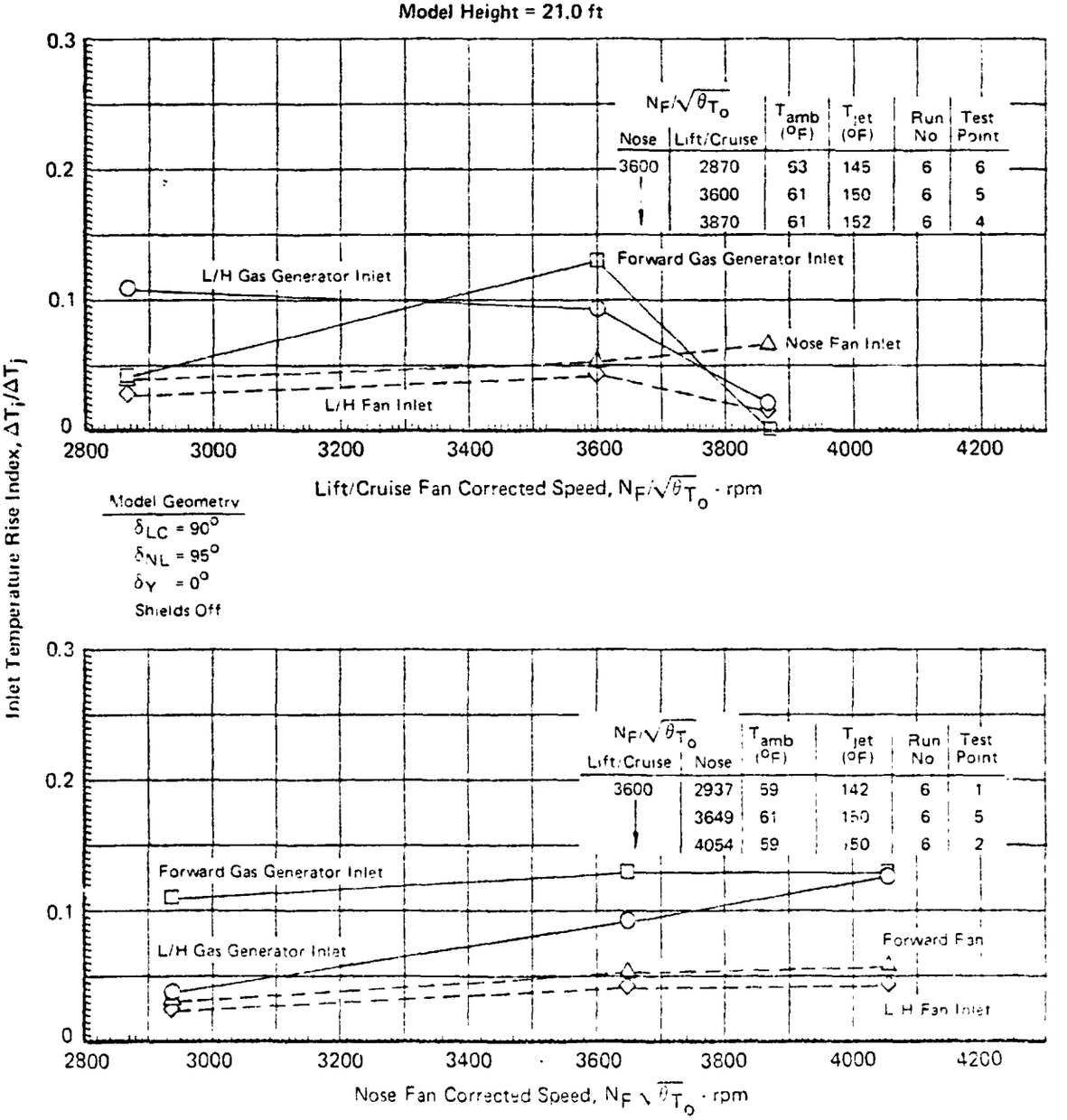

GP76 0522 241

FIGURE 9-37
EFFECT OF NOSE FAN SPEED ON INLET REINGESTION

Model Height = 8.3 ft

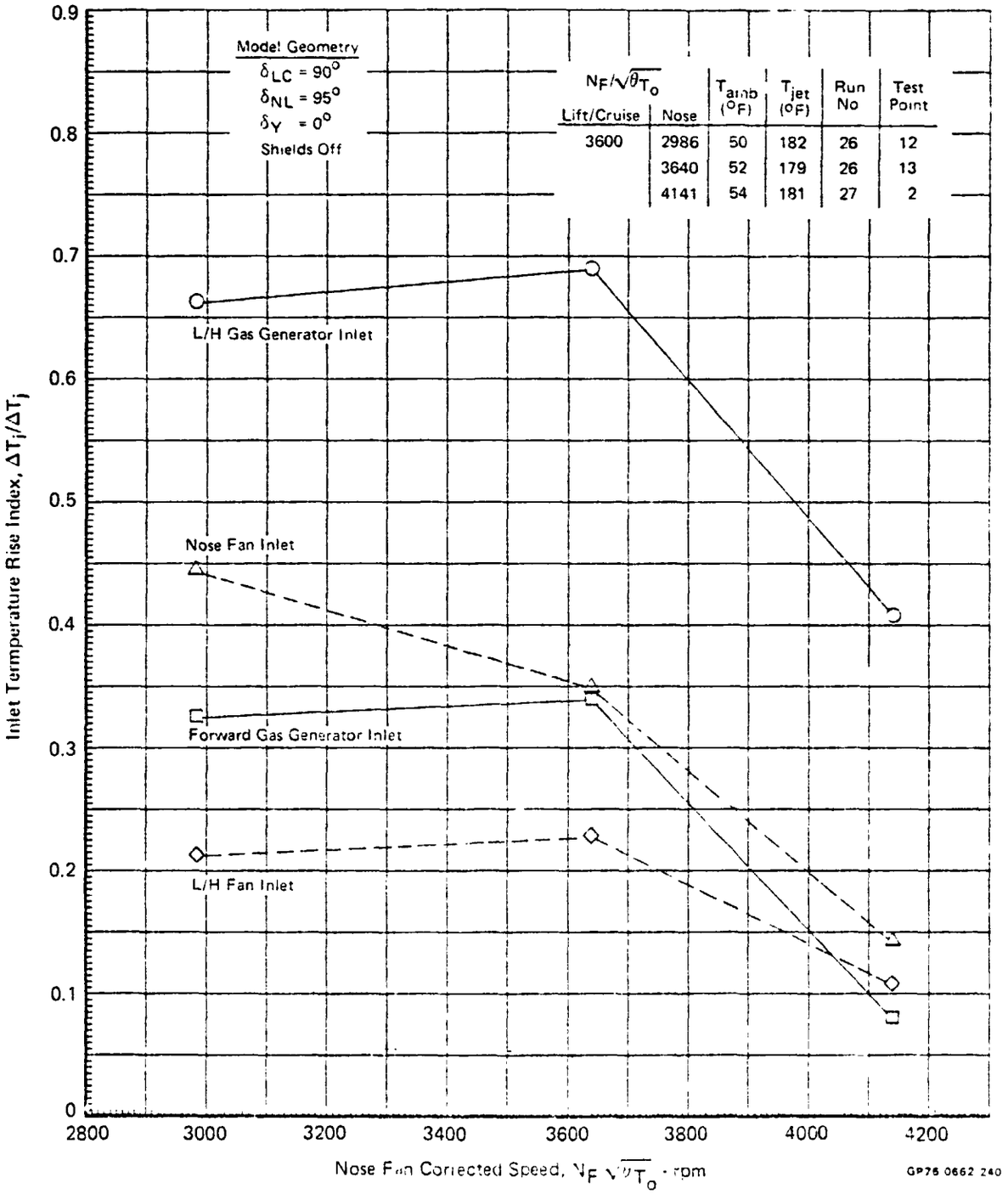

FIGURE 9-38
EFFECT OF NOSE FAN SPEED ON INLET REINGESTION
Model Height = 3.3 ft

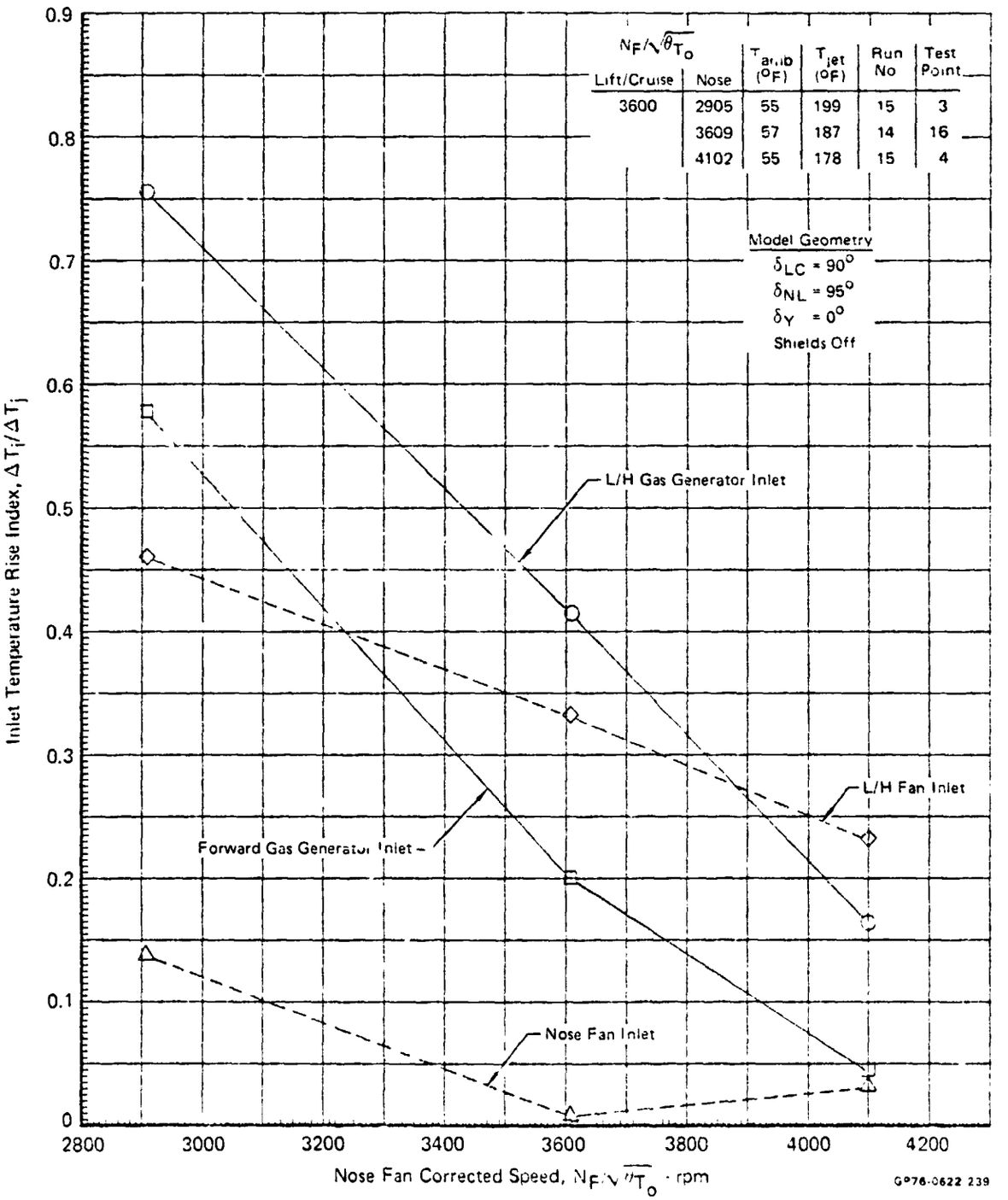

FIGURE 9-39

EFFECT OF NOZZLE EXHAUST SPLAYING ON INLET REINGESTION

Left Gas Generator Inlet

$N_F/\sqrt{\theta T_o}$ = 3600 RPM

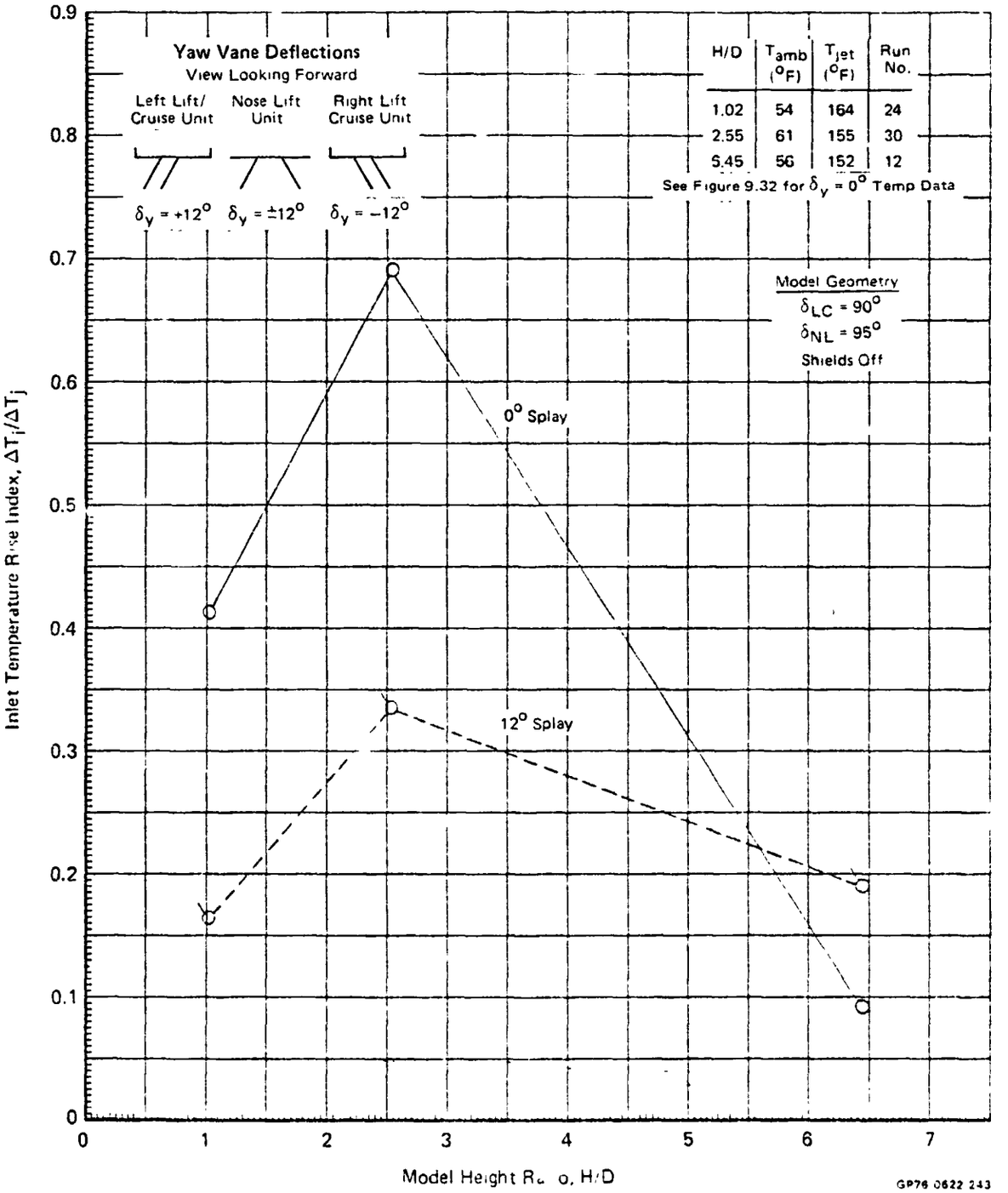

FIGURE 9-40
EFFECT OF NOZZLE EXHAUST SPLAYING ON INLET REINGESTION
Forward Gas Generator Inlet

$N_F/\sqrt{T_o}$ = 3600 RPM

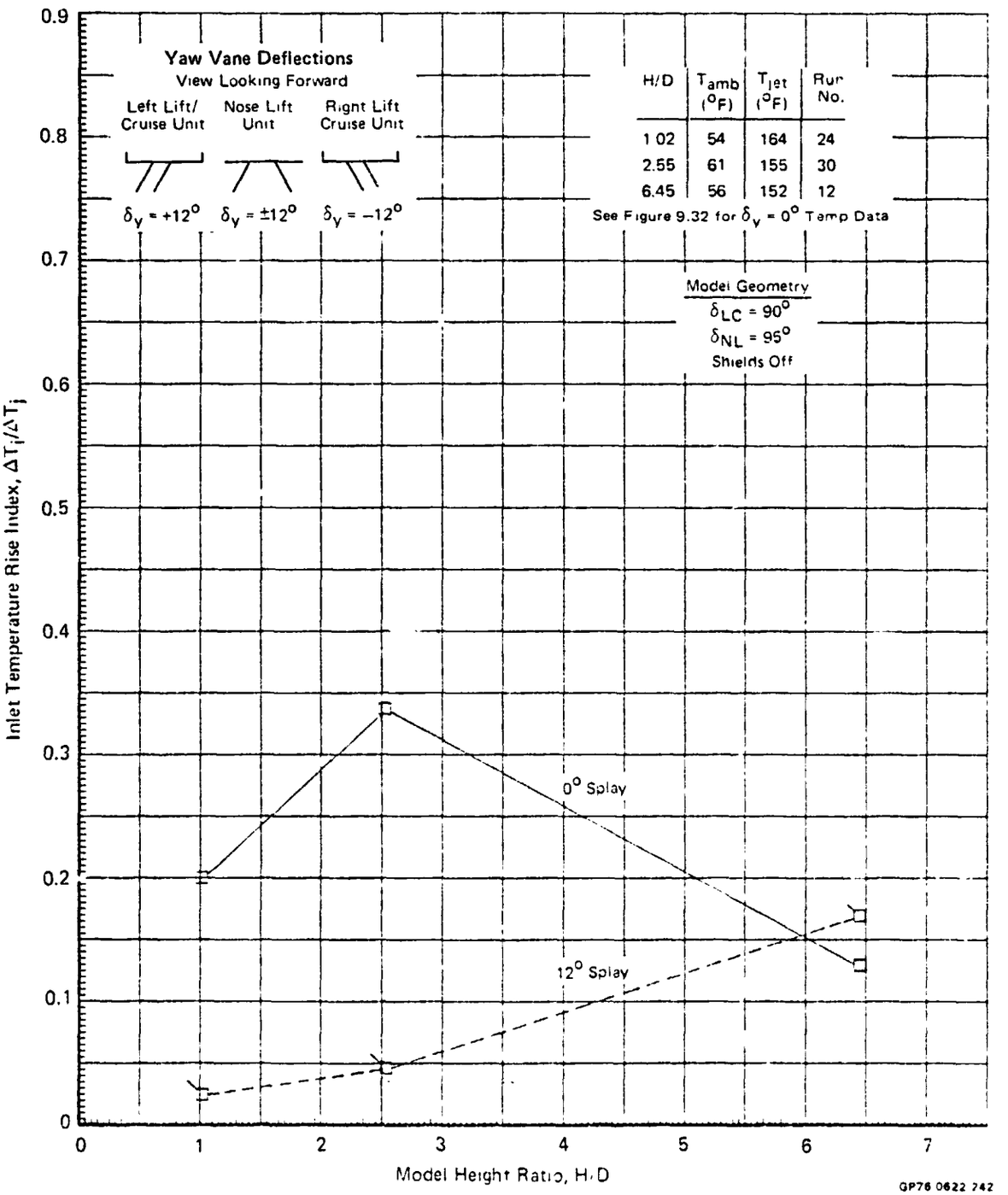

FIGURE 9-41

EFFECT OF NOZZLE EXHAUST SPLAYING ON INLET REINGESTION

L/H Lift/Cruise Fan Inlet

$N_F/\sqrt{\theta}T_0$ = 3600 RPM

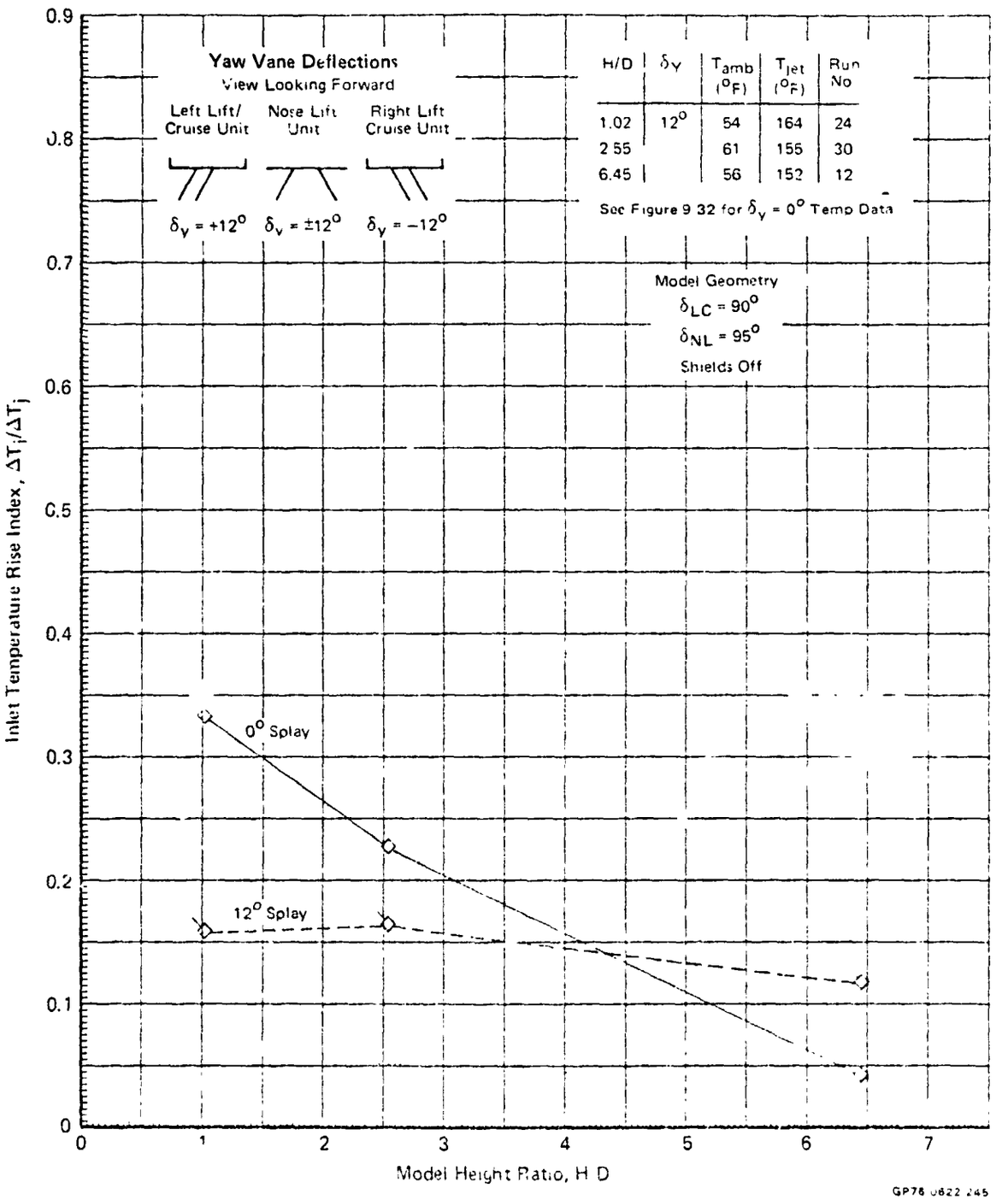

GP78-0822-245

FIGURE 9-42
EFFECT OF NOZZLE EXHAUST SPLAYING ON INLET REINGESTION
Nose Fan Inlet
$N_{F/\sqrt{\theta}T_o}$ = 3600 RPM

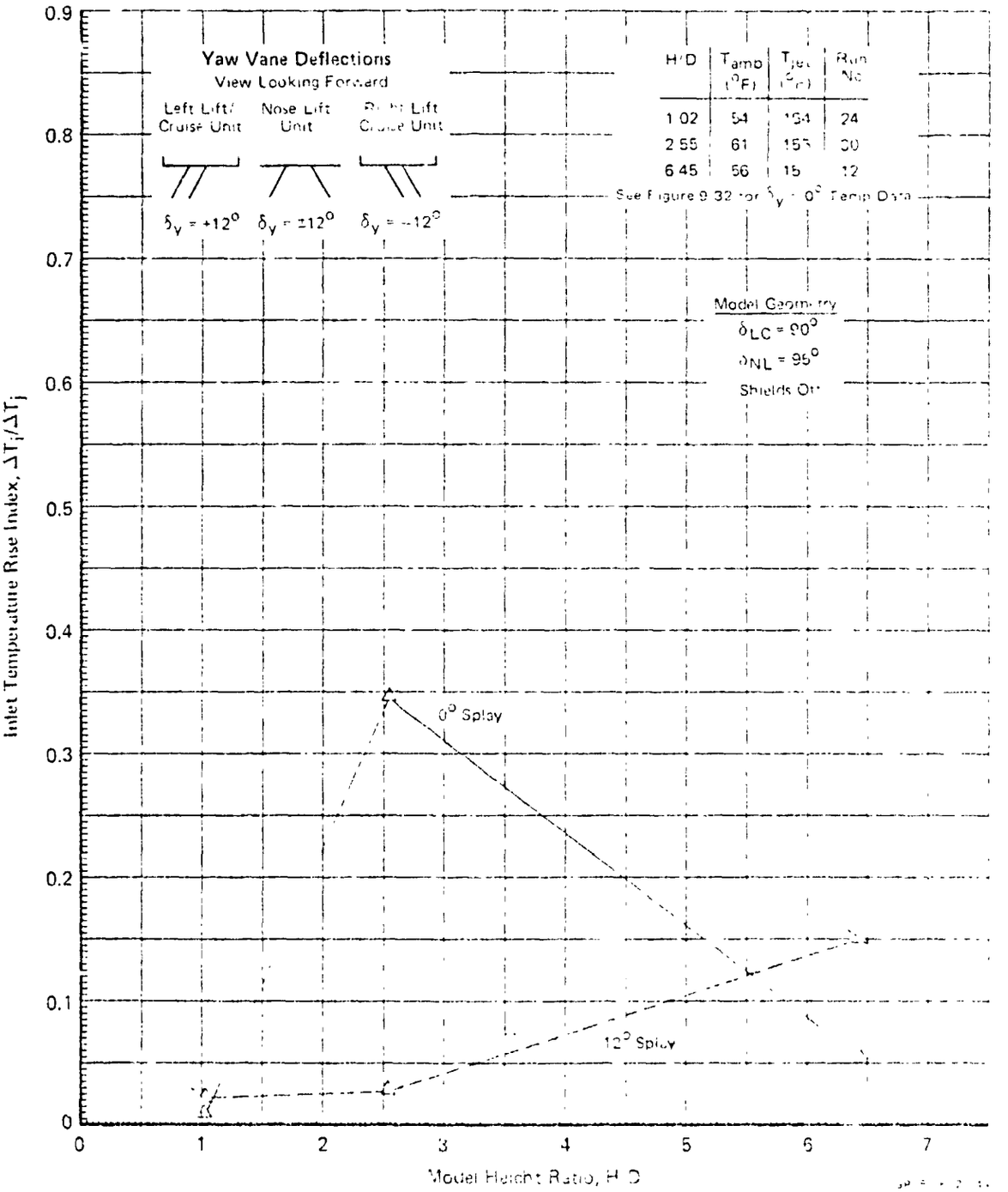

As shown in the figures for each inlet, the effect of splaying was very beneficial in reducing reingestion at the two lower ground heights for all inlets. At the 21.0 foot height, however, splaying was shown to have a negative effect in that the temperature rise on each inlet was increased. This is believed to be due to inducing a stronger far field recirculation flowfield around the model at the higher altitudes.

Effects of Inlet Shielding

The effects of the small gas generator inlet shield on reingestion temperature for tests at the 8.3 foot ground height are presented for the two gas generator inlets in Figure 9-43 and for the two fan inlets in Figure 9-44.

The effects of both large and small gas generator inlet shielding on inlet reingestion temperature for tests at the 3.3 foot ground height are presented for the two gas generators inlets in Figure 9-45 and for the two fan inlets in Figure 9-46. Both shields were found to be very effective in reducing the left gas generator inlet reingestion at the 3.3 foot ground height, as shown in the figure. In Figure 9-46 the gas generator inlet shields were found to have essentially no effect on the reingestion characteristics of both the lift/cruise and nose fan inlets. A photo of the large shield installed on the powered model at the 3.3 foot height is shown in Figure 5-5.

The effects of shield deflection angle (δ_S) on inlet reingestion are presented in Figure 9-47 at a fan speed of 2500 rpm at a ground height of 3.3 feet. Shield deflection angle tests were conducted with the large shield only at this lower ground height. As shown in the figure, a shield deflection angle of 0° was found to provide the best shielding for both gas generator inlets. The effects of shield deflection angle on both fan inlets were found to be minor.

Analog Temperature Data

A representative selection of the continuously recorded analog temperature data measured during the static test program is presented in this section. Individual temperature traces are presented for selected thermocouples located in each of the four inlets in the reingestion tests. Figure 9-48 shows the inlet thermocouple numbering used for identifying the analog traces presented herein.

The purpose of presenting the selected analog data traces is to illustrate the inlet temperature variation during an individual test point, and also to show the deviation from the single scan Vidar system measured inlet temperatures. For all analog data presented, the variations are shown during the complete 90 second time duration of the Vidar digital data acquisition process. During each test point, the model pressures, selected temperatures, fan speeds, and load cell data

are all measured during the initial 85 seconds of the test point. The last 5 seconds are used to measure the inlet temperatures digitally. The inlet reingestion data presented in the previous figures of this report are all based on these digital measurements.

Analog data traces for some thermocouple from each of the four inlets tested are presented in Figures 9-49, 9-50, and 9-51 for the three model ground heights tested of 21.0, 8.3, and 3.3 feet. The temperature variations are shown relative to the digitally measured reference temperature (T_{REF}) for each thermocouple. The time at which the digital T_{REF} is measured is also indicated in each figure for each thermocouple. The particular temperatures selected and shown here are the "worst case" variations for each inlet at these test conditions. As shown, the temperature variations during the three runs and also the deviations from the digitally measured temperature levels were both found to be within $\pm$ 10°F.

The analog temperature data for all thermocouples installed in the more critical left hand gas generator inlet are presented in Figures 9-52, 9-53, and 9-54 for the three model ground heights of 21.0, 8.3, and 3.3 feet. Thermocouple No. 6 on the L/H gas generator inlet was intermittantly inoperative during the static tests, and therefore is not shown. For the seven thermocouple measurements shown in these three figures, the temperature variations during a given run were found to be reasonably stable, and the digitally measured Vidar inlet temperatures are also shown to be very representative measurements of the level of reingestion occurring with this test model.

9.4 FLOW VISUALIZATION TESTS

Flow visualization tests were conducted at the 21.0 and 3.3 foot model heights, utilizing Corvus oil for smoke generation. Flowfield patterns were recorded with high speed (250 to 500 frames/sec) and normal speed (24 frames/sec) movie cameras. Still photos were also taken at selected conditions. Figure 9-48 shows typical still photo comparisons of the flowfield in the vicinity of the L/H gas generator inlet with and without inlet shields installed. Observations made during those tests clearly show when and where inlet reingestion is occurring and likewise support the inlet reingestion trends presented in this report.

FIGURE 9-43
EFFECT OF SHIELDING ON INLET REINGESTION
Model Height = 8.3 ft

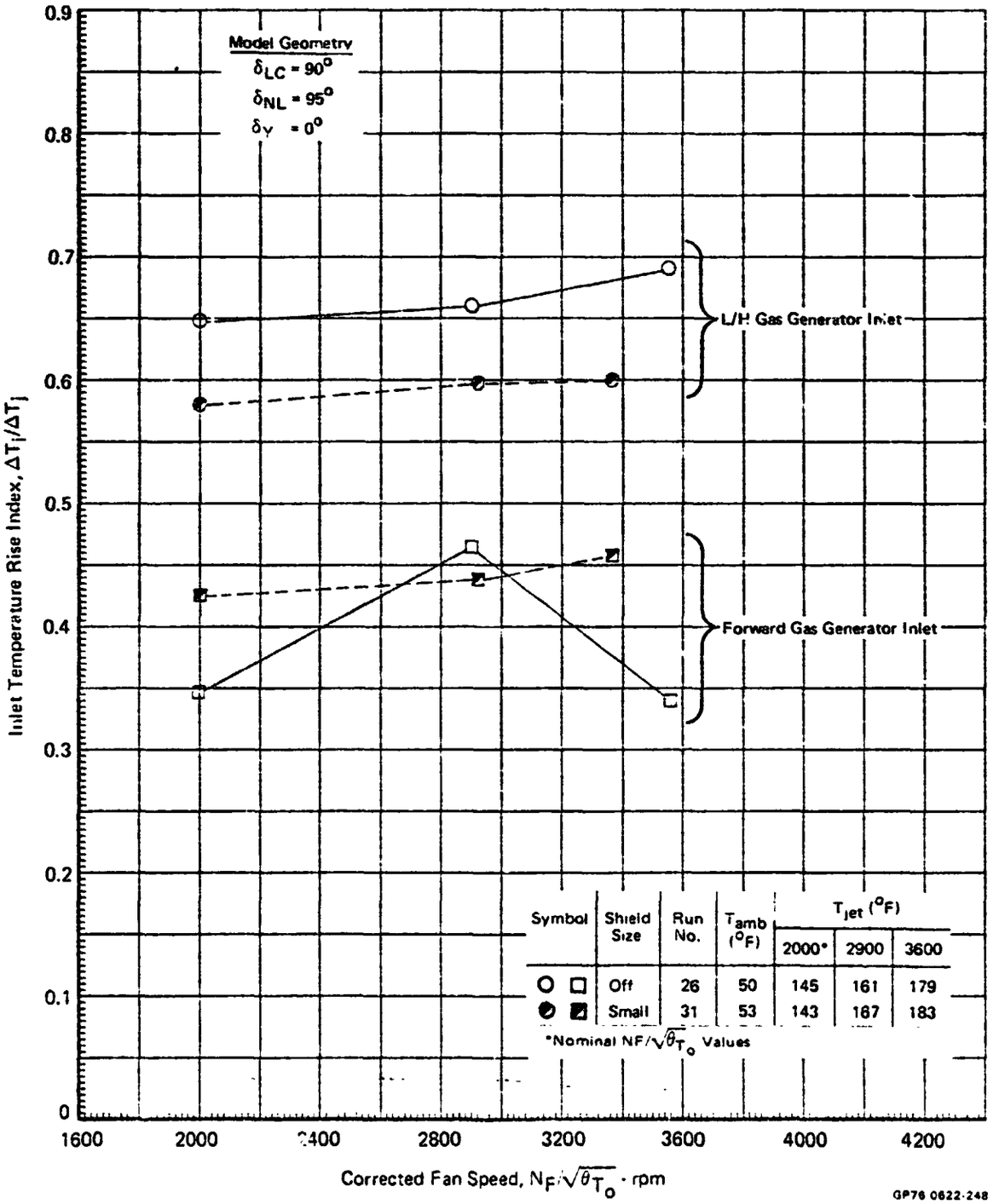

FIGURE 9-44
EFFECT OF SHIELDING ON INLET REINGESTION
Model Height = 8.3 ft

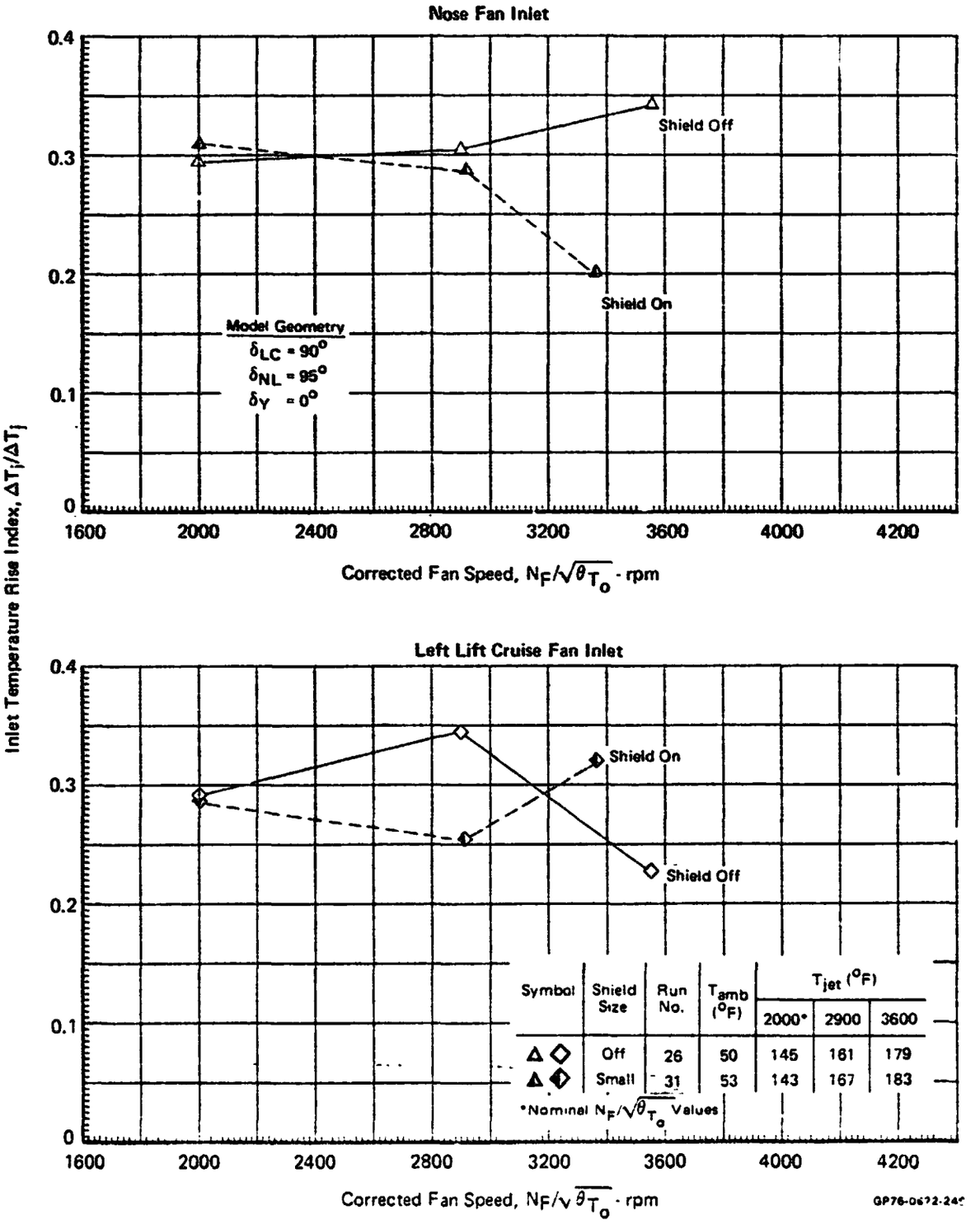

FIGURE 9-45
EFFECT OF SHIELDING ON INLET REINGESTION

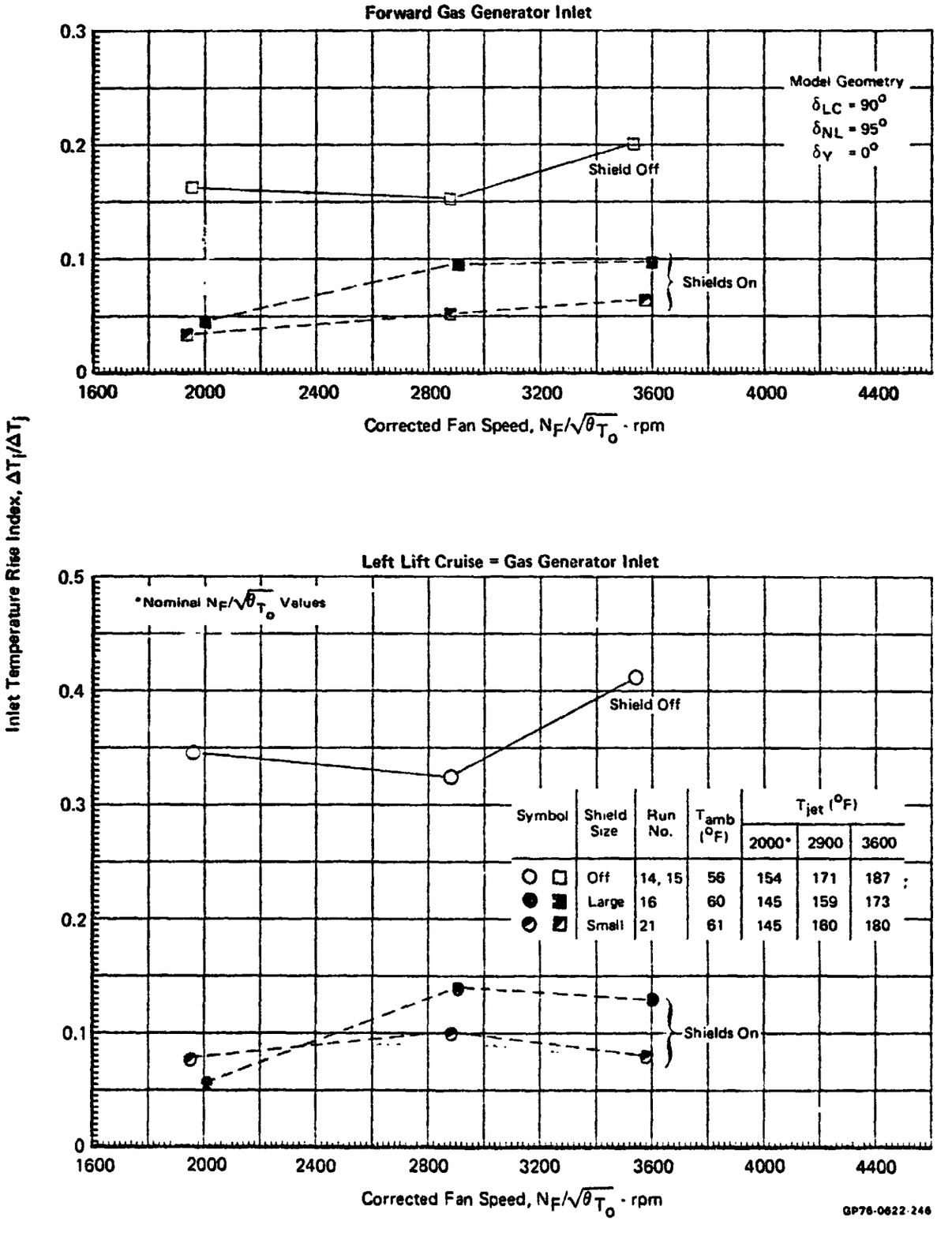

FIGURE 9-46
EFFECT OF SHIELDING ON INLET REINGESTION
Model Height = 3.3 Ft

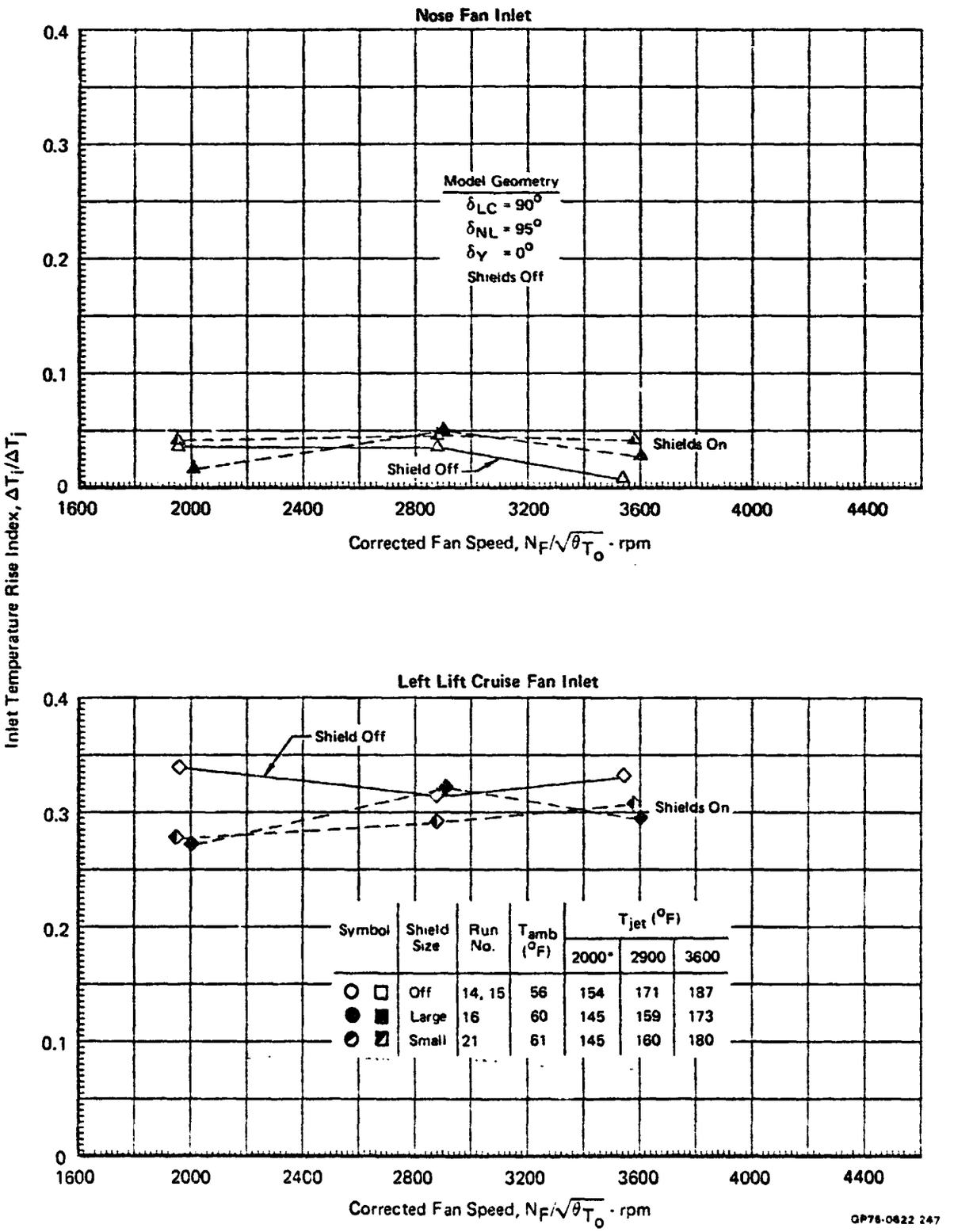

FIGURE 9-47
EFFECTS OF SHIELD DEFLECTION ANGLE ON INLET REINGESTION

Model Height = 3.3 Ft
$N_F/\sqrt{\theta T_o}$ = 2500 RPM

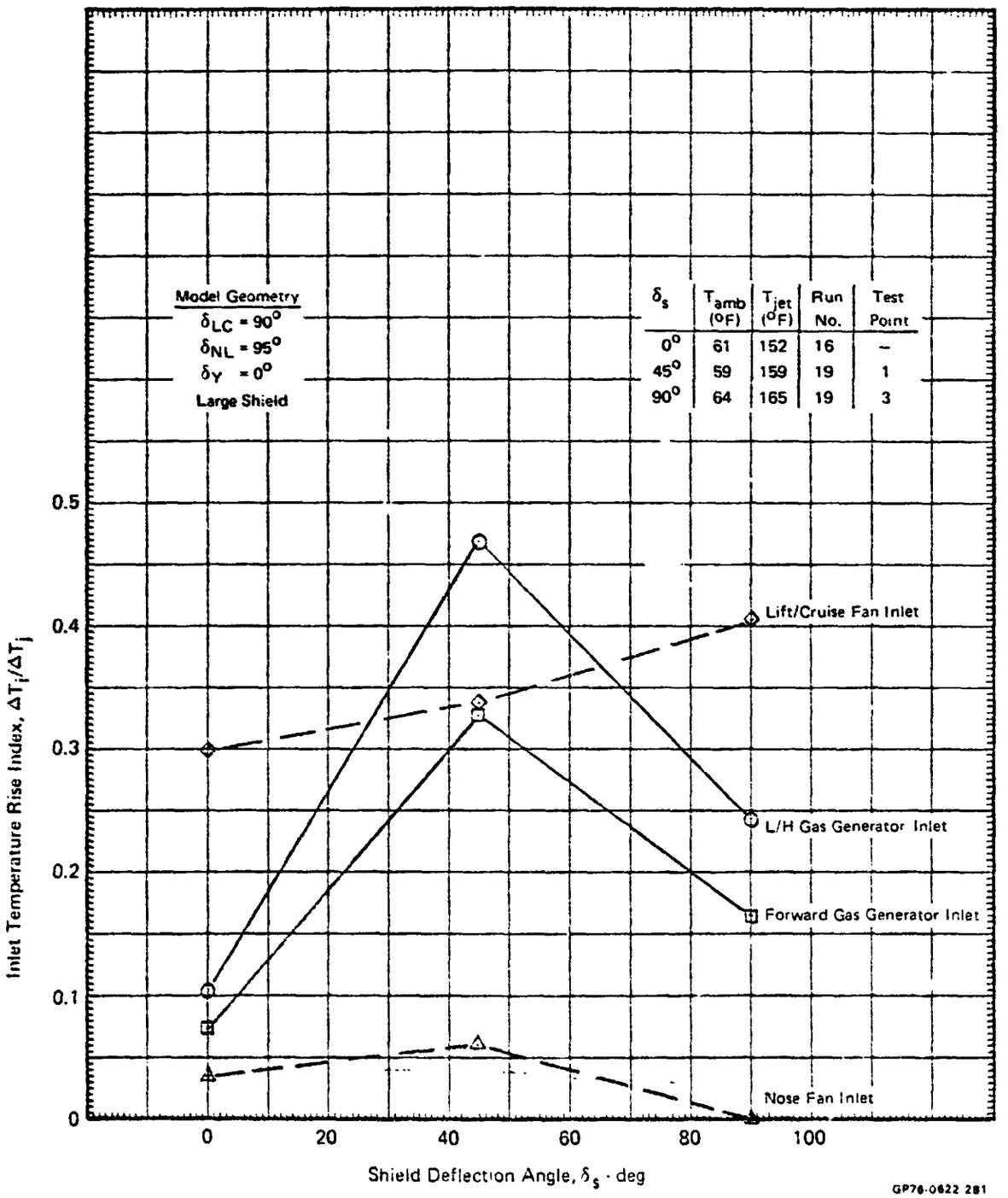

FIGURE 9-48
INLET REINGESTION THERMOCOUPLE IDENTIFICATIONS
Thermocouple (T/C) Numbering Sequence

Nose Fan Inlet

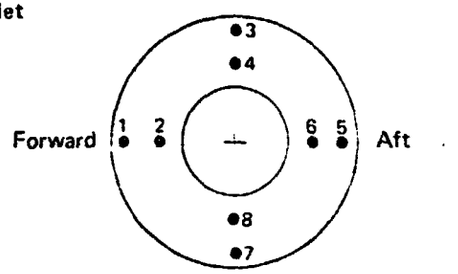

Top View

Left Lift/Cruise Fan Inlet Top

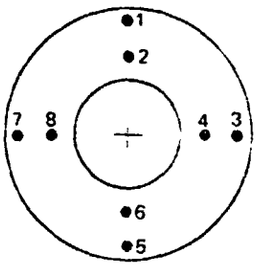

Front View

Forward Gas Generator Inlet Top

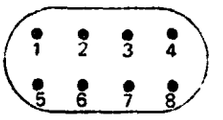

Side View
(L/H Side)

Left Gas Generator Inlet Top

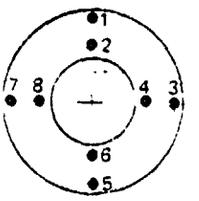

Front View

GP78 0622 312

FIGURE 9-49
INLET REINGESTION ANALOG TEMPERATURE VARIATIONS

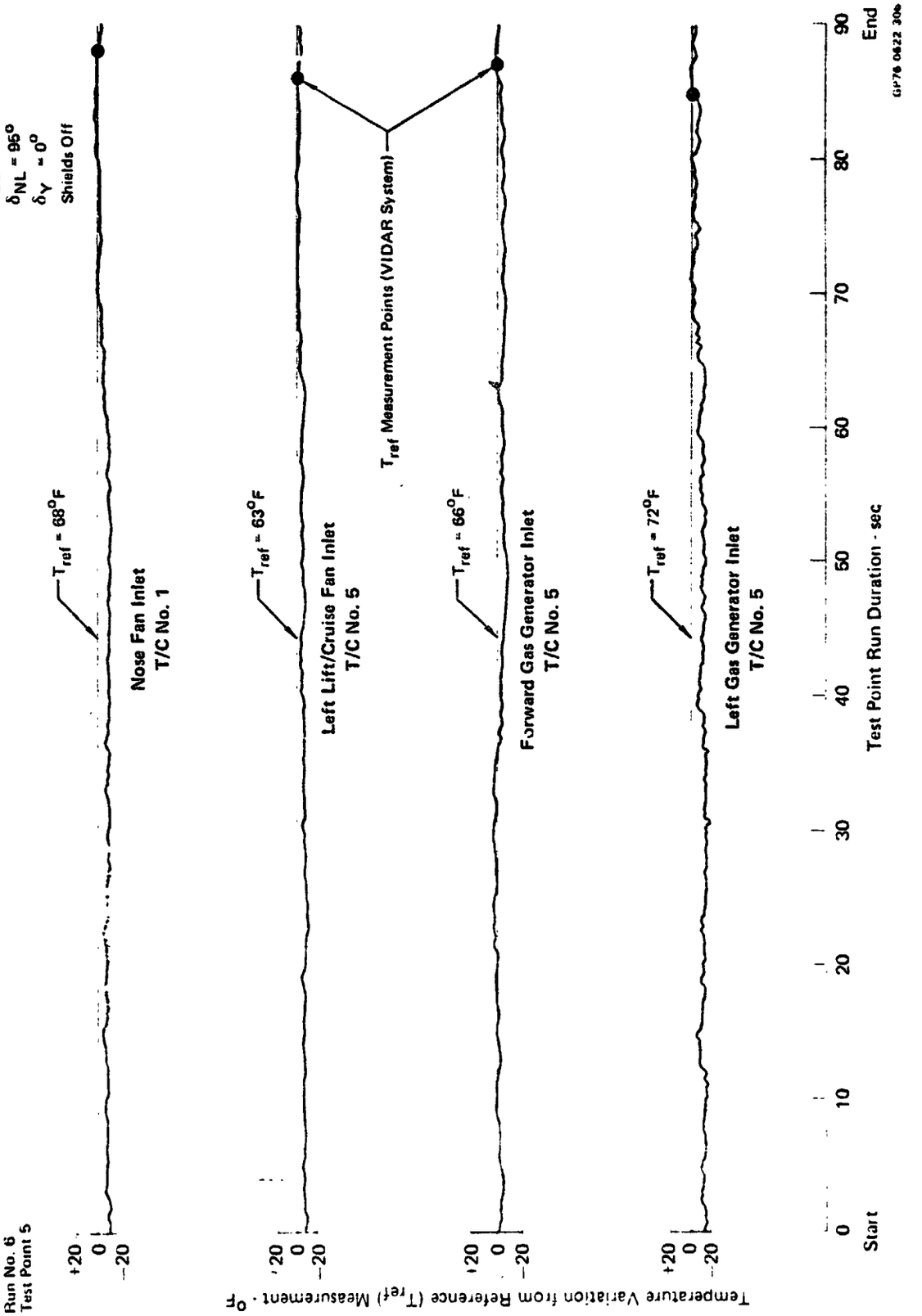

FIGURE 9-50
INLET REINGESTION ANALOG TEMPERATURE VARIATIONS

Model Height = 8.3 Ft
$N_F/\sqrt{\theta}$ T_o = 3600 RPM

Model Geometry
$\delta_{LC} = 90^o$
$\delta_{NL} = 95^o$
$\delta_Y = 0^o$
Shields Off

Run No 26
Test Point 13

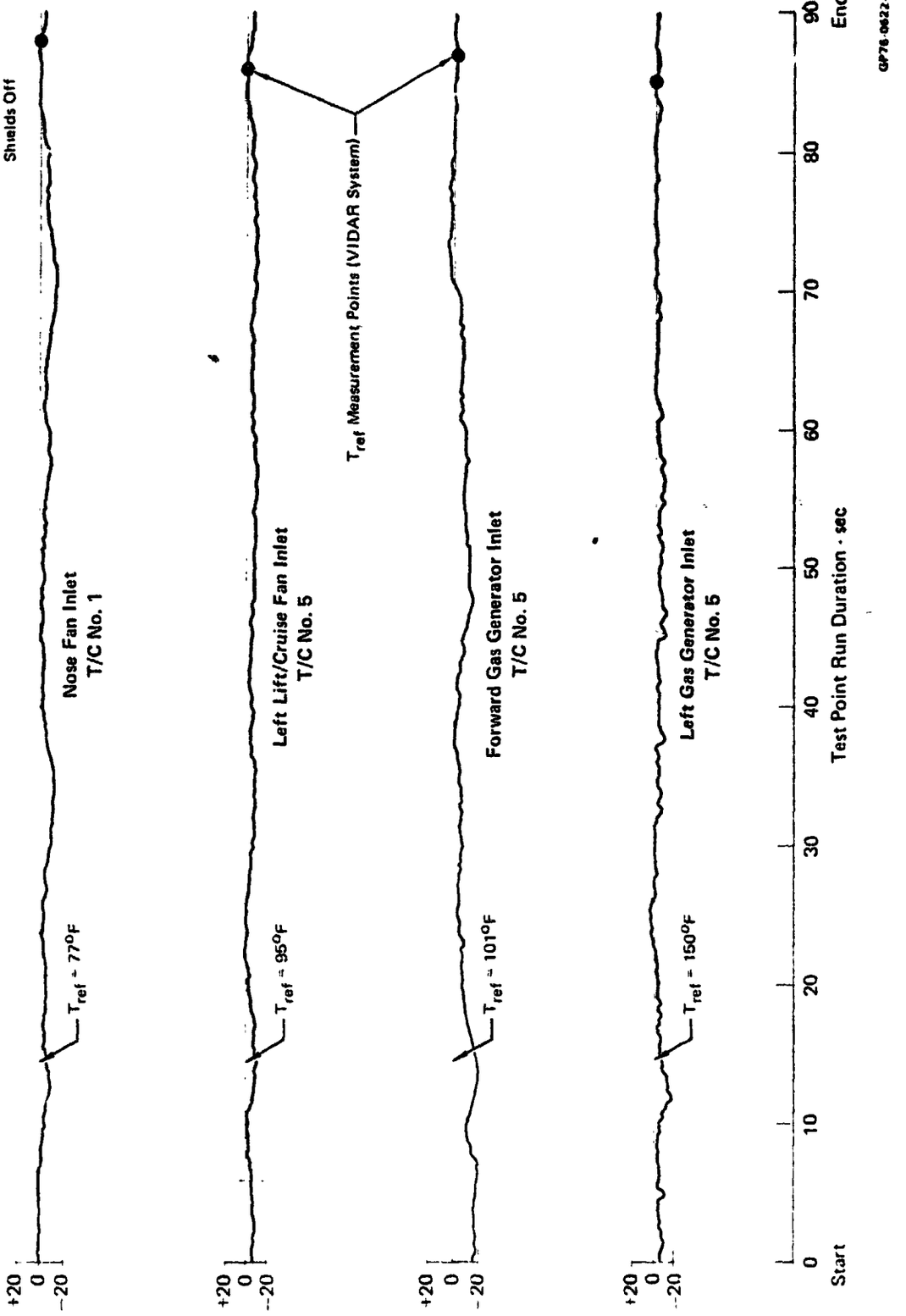

GP76-0422-307

FIGURE 9-51
INLET REINGESTION ANALOG TEMPERATURE VARIATIONS

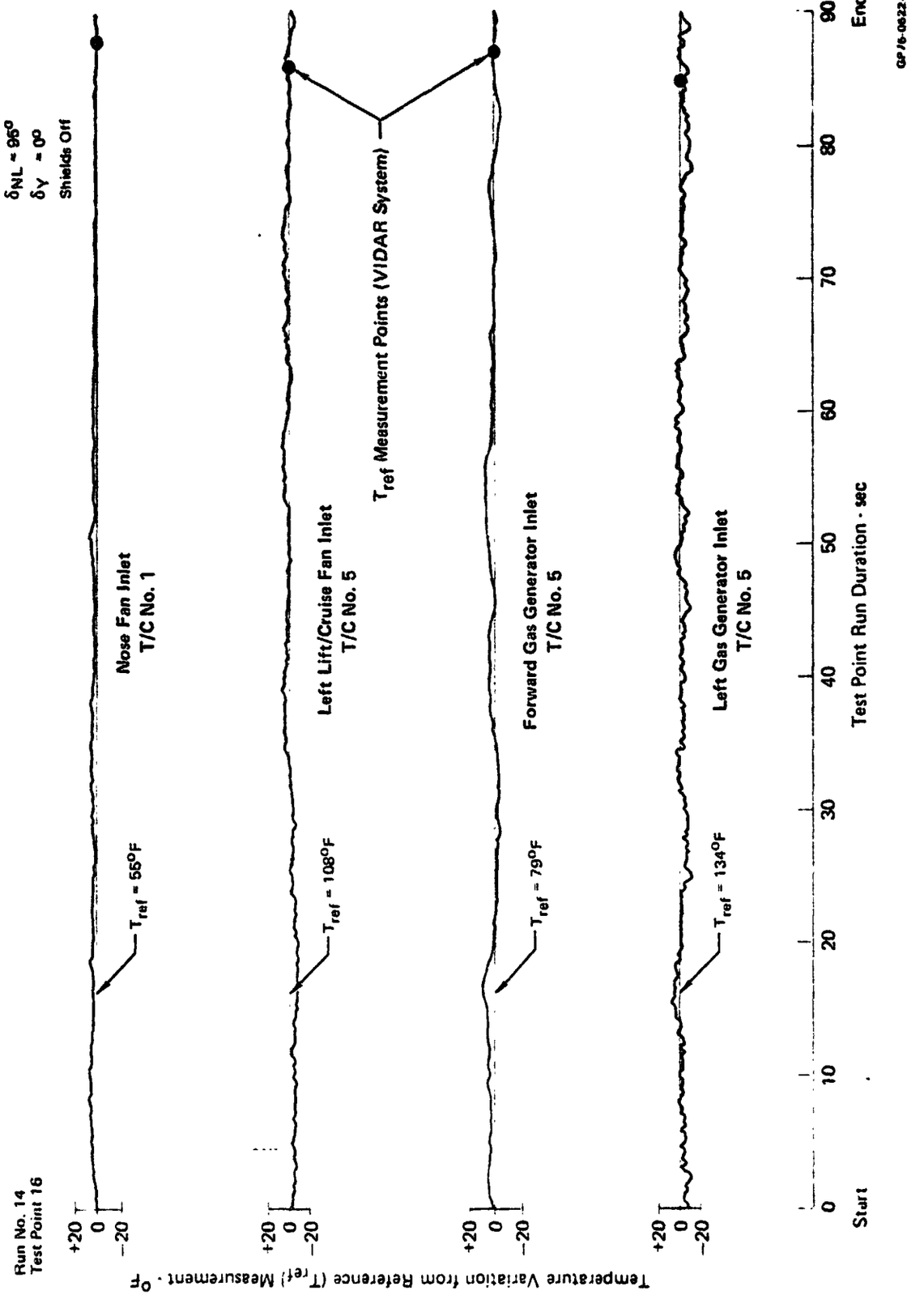

FIGURE 9-52
LEFT GAS GENERATOR INLET ANALOG TEMPERATURE VARIATIONS

Model Height = 21 Ft

$N_F/\sqrt{\theta}T_o$ = 3600 RPM

Model Geometry
δ_{LC} = 90°
δ_{NL} = 95°
δ_γ = 0°
Shields Off

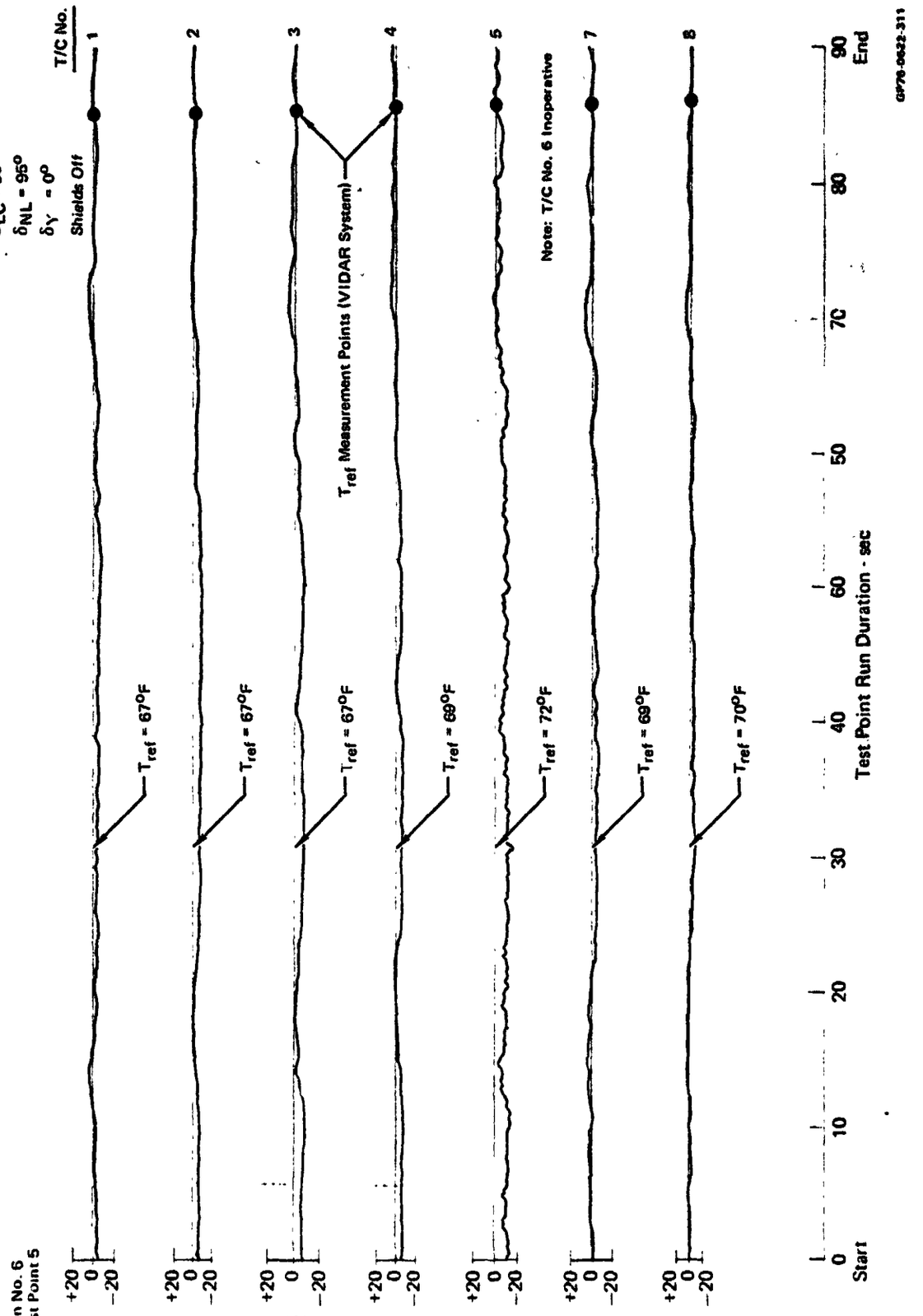

FIGURE 9-53
LEFT GAS GENERATOR INLET ANALOG TEMPERATURE VARIATIONS

Model Height = 8.3 Ft

$N_F/\sqrt{\theta_{T_0}}$ = 3600 RPM

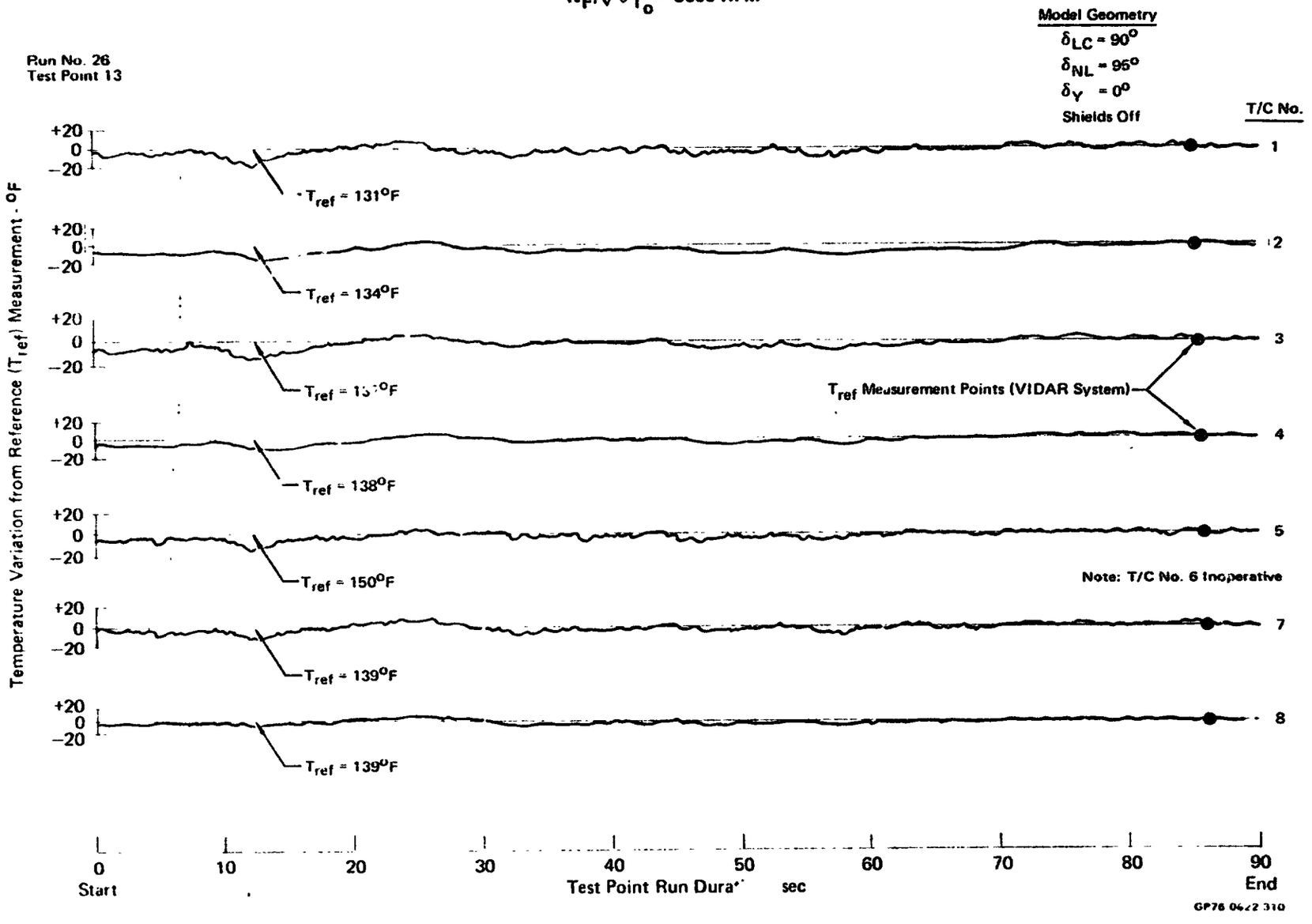

GP76 0642 310

FIGURE 9-54
LEFT GAS GENERATOR INLET ANALOG TEMPERATURE VARIATIONS
Model Height = 3.3 Ft
$N_F/\sqrt{\theta}T_o$ = 3600 RPM

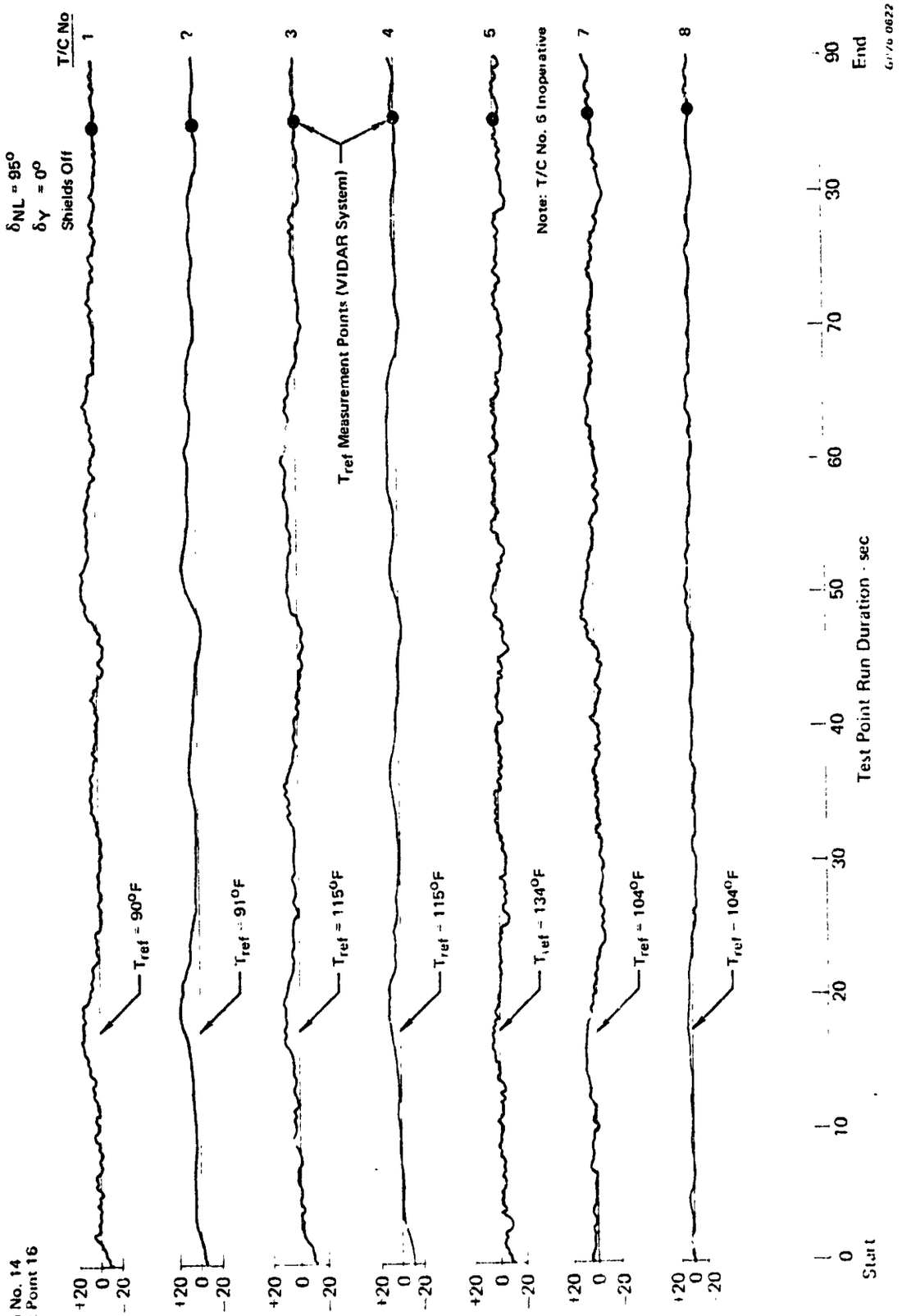

FIGURE 9-55
REPRESENTATIVE FLOW VISUALIZATION TEST RESULTS
Model Height = 3.3 Ft
$N_F/\sqrt{\theta}T_o$ = 2000 RPM

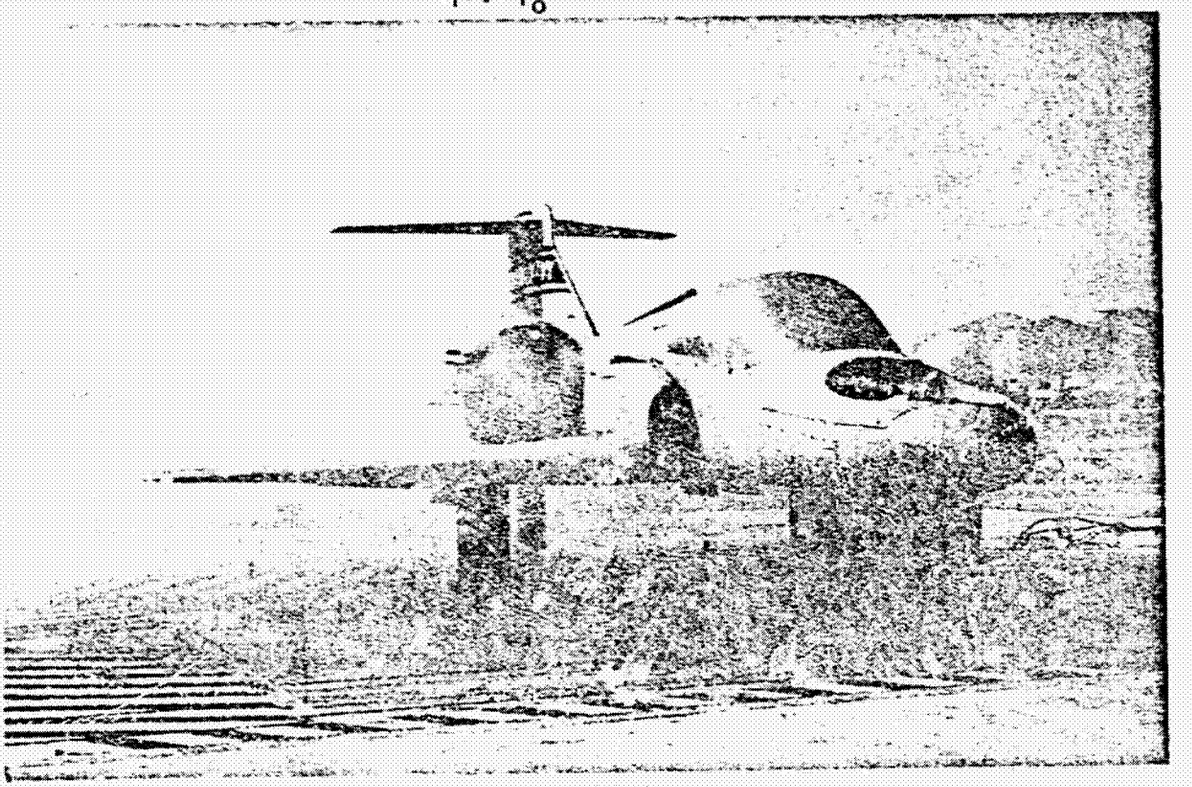

Without Shields

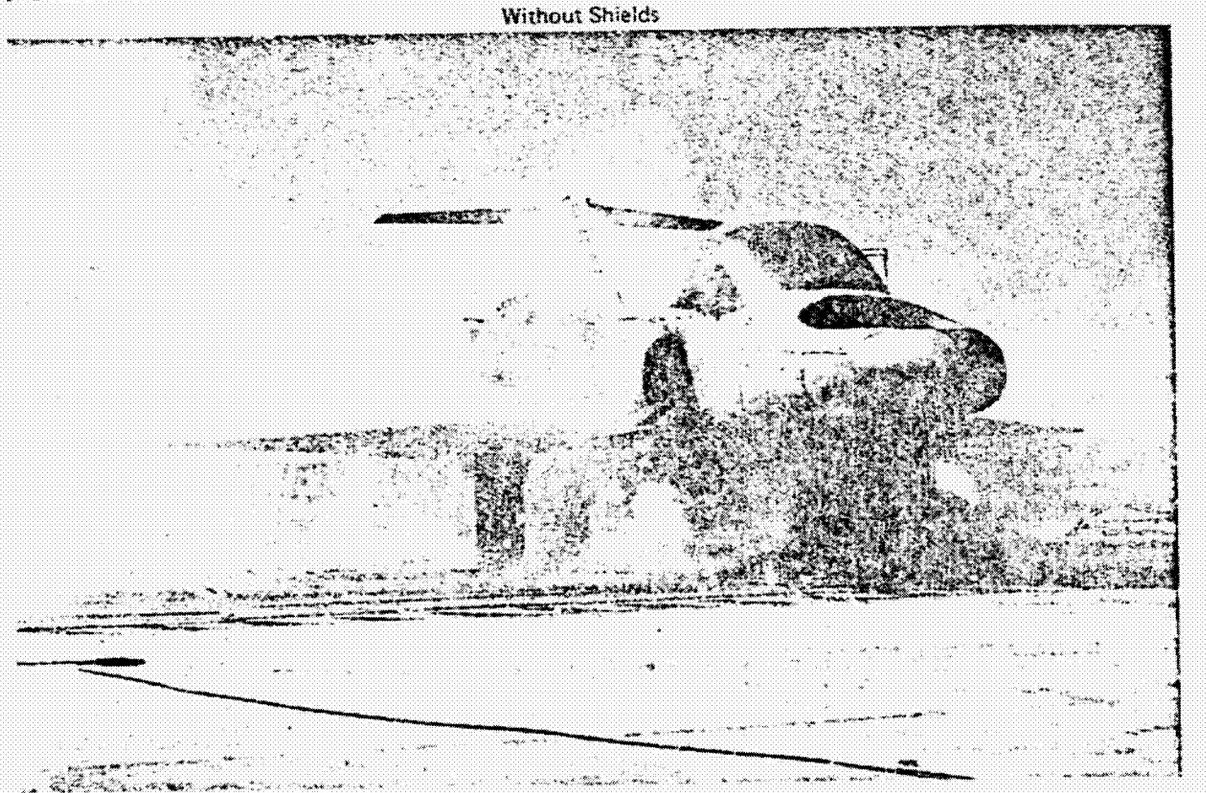

With Large Shields

10. CONCLUSIONS

1. The complete three-fan powered lift configuration exhibits positive induced lift ($\Delta L/F_G$ from 0 to 0.1) for operational combinations of thrust vector angle and jet velocity ratio (V_O/V_J). The corresponding induced drag is generally negative.
2. The two-fan powered lift configuration with the horizontal tail off and the nose lift unit sealed exhibits large positive induced lift values. With the lift/cruise unit at 90°, $\Delta L/F_G$ varies from a nominal 0.1 to 1.7 at jet velocity ratios of 0.1 to 0.7.
3. Operation of the nose lift unit results in a significant adverse effect on induced lift.
4. A comparison of lift and drag data from static tests of three-fan combined operation and three individual fan operations indicates differences in induced aerodynamic forces that may result from a mutual interaction between the propulsion units. Differences in lift range from -5% to +2% of total thrust and differences in drag range from -6% to -3% of total thrust.
5. The three-fan powered lift configuration has unstable directional stability at very low V_O/V_J ratios due to the destabilizing effect of the nose lift unit ram drag. At higher jet velocity ratios, the configuration is stable both directionally and laterally.
6. The aerodynamic lift configuration with horizontal tail on has static longitudinal stability at angles of attack up to wing-stall angle of attack. Horizontal tail control effectiveness is retained through the highest angle of attack tested.
7. The aerodynamic lift configuration has neutral lateral stability and stable directional stability at 0° angle of attack. Above 0° angle of attack the configuration is stable both directionally and laterally through the highest angle of attack tested.
8. The effect of ground height on total lift loss for the model tested was less than 1% while operating at constant fan speeds.
9. Inlet reingestion levels were strongly affected by the model variables tested in this program, including model height, nose vector angle, differential fan speeds, splaying, and inlet shielding.
10. Gas generator inlet shields appear to be effective devices for reducing inlet reingestion levels at low ground heights.

11. The lift/cruise fan, nose fan, and gas generator inlets were all found to exhibit high levels of inlet recovery coupled with low distortion throughout the range of tests performed on this model, particularly at angles of attack less than 20°.

11. LIST OF REFERENCES

1. B. J. Gambucci, K. Aoyagi, L. S. Rolls, "Wind Tunnel Investigation of a Large Scale Model of a Lift/Cruise Fan V/STOL Aircraft," NASA TMS-73, 139 dated May 1976.
2. "Guide for Planning Investigations in the Ames 40- By 80-Foot Wind Tunnel," dated June 1975.
3. J. K. Orr, C. W. Sapp, "Model 260 Low Speed Wind Tunnel Aerodynamic Test Data ASW Configuration," Report MDC B9827-2, dated December 1975.
4. E. J. Phillips, "Model 260 Lift/Cruise Inlet Static and High Speed Performance Test - Series I," Report MDC B9856-2, dated December 1974.
5. "LF460 Detail Design - Fianl Technical Report on Aircraft Support Activity," Report NASA CR-121146, General Electric Co., dated April 1973.
6. Richard J. Margason, "Review of Propulsion-Induced Effects on Aerodynamics of Jet/STOL Aircraft," NASA TN D-5617, dated February 1970.

WIND TUNNEL AND GROUND STATIC INVESTIGATION OF A LARGE SCALE-MODEL OF A LIFT/CRUISE FAN V/STOL AIRCRAFT

APPENDIX A

40' X 80' WIND TUNNEL TEST SCHEDULE AND BALANCE DATA

EXPLANATION OF SYMBOLS FOR RUN SCHEDULE

Symbol	Explanation	Range	Other
RUN	Run Number		
PT	Point Number		
ALPHA	Angle of Attack, α	-4^{o} to 32^{o}	
BETA	Sideslip Angle, β	-4^{o} to 20^{o}	
DLC	Lift/Cruise Unit Geometric Deflection, δ_{LC}	0^{o} to 90^{o}	
DNL	Nose Lift Unit Geometric Deflection, δ_{NL}	0^{o} to 104^{o}	DNL = 99. Indicates the louver system removed and lower fuselage fairing installed
DF	Flap Deflection, δ_f	0^{o} to 30^{o}	
DAL	Left Aileron Deflection, δ_a	-25^{o} to 25^{o}	
DAR	Right Aileron Deflection, δ_a	-25^{o} to 25^{o}	
DH	Horizontal Tail Deflection, δ_H	-20^{o} to 20^{o}	DH = –99. Indicates that the horizontal tail is removed and the flow survey rake installed DH = 99. Indicates that the horizontal tail is removed and the flow survey rake is also removed
DR	Rudder Deflection, δ_R	-20^{o} to 30^{o} (Nominal)	
QC	Corrected Test Section Dynamic Pressure, q_c	0 to 49.2 psf	
FAN 1	Nose Lift Unit Corrected Fan Speed, $N_F/\sqrt{\theta}_{T_o}$	0 to 3600 rpm	
FAN 2	Left Lift/Cruise Unit Corrected Fan Speed, $N_F/\sqrt{\theta}_{T_o}$	0 to 4100 rpm	
FAN 3	Right Lift/Cruise Unit Corrected Fan Speed, $N_F/\sqrt{\theta}_{T_o}$	0 to 4100 rpm	
DYLC	Lift/Cruise Unit Yaw Vane Deflection, δ_{YLC}	-12^{o} to 12^{o}	DYLC = 99. Indicates lift cruise unit yaw vanes removed
DYNL	Nose Lift Unit Yaw Vane Deflection, δ_{YNL}	-12^{o} to 12^{o}	DYNL = 99. Indicates nose lift unit yaw vanes removed.
NOSE GEAR	Code for Nose Gear 1 – Nose Gear Off 2 – Nose Gear On		
NOSE UNIT INLET COVERS	Code for Nose Unit Inlet Covers 1 – Nose Unit Inlets Covered 2 – Nose Unit Inlets Open		

GP76-0622-210

RUN	PT	ALPHA DEG	BETA DEG	DLC DEG	DRL DEG	DF DEG	DAL DEG	DAR DEG	DH DEG	DR DEG	QC PSF	FAN1 RPM	FAN2 RPM	FAN3 RPM	DYLC DEG	DYRL DEG	NOSE GEAR
1	1	0.0	-0.0	90.	0.	30.	15.	15.	-99.	0.	0.00	0.	1962.	16.	0.0	99.0	1
1	2	0.0	-0.0	90.	0.	30.	15.	15.	-99.	0.	0.00	0.	2959.	34.	0.0	99.0	1
1	3	0.0	-0.0	90.	0.	30.	15.	15.	-99.	0.	0.00	0.	3588.	43.	0.0	99.0	1
1	4	0.0	-0.0	90.	0.	30.	15.	15.	-99.	0.	0.00	16.	4127.	54.	0.0	99.0	1
2	1	0.0	-0.0	90.	0.	30.	15.	15.	-99.	0.	0.00	0.	11.	2006.	0.0	99.0	1
2	2	0.0	-0.0	90.	0.	30.	15.	15.	-99.	0.	0.00	0.	12.	2911.	0.0	99.0	1
2	3	0.0	-0.0	90.	0.	30.	15.	15.	-99.	0.	0.00	12.	11.	3615.	0.0	99.0	1
2	4	0.0	-0.0	90.	0.	30.	15.	15.	-99.	0.	0.00	0.	30.	4045.	0.0	99.0	1
3	1	0.0	-0.0	90.	0.	30.	15.	15.	-99.	0.	0.00	0.	2023.	2008.	0.0	99.0	1
3	2	0.0	-0.0	90.	0.	30.	15.	15.	-99.	0.	0.00	0.	2939.	2922.	0.0	99.0	1
3	3	0.0	-0.0	90.	0.	30.	15.	15.	-99.	0.	0.00	14.	3609.	3625.	0.0	99.0	1
4	1	0.0	-0.0	90.	0.	30.	15.	15.	-99.	0.	12.39	0.	3659.	3621.	0.0	99.0	1
4	2	0.0	-0.0	90.	0.	30.	10.	10.	-99.	0.	12.32	12.	3629.	3614.	0.0	99.0	1
4	3	0.0	-0.0	90.	0.	30.	5.	5.	-99.	0.	12.35	0.	3635.	3647.	0.0	99.0	1
4	4	0.0	-0.0	90.	0.	30.	0.	0.	-99.	0.	12.34	24.	3635.	3649.	0.0	99.0	1
4	5	0.0	-0.0	90.	0.	30.	0.	0.	-99.	0.	12.29	11.	552.	553.	0.0	99.0	1
4	6	0.0	-0.0	90.	0.	30.	5.	5.	-99.	0.	12.33	12.	544.	554.	0.0	99.0	1
4	7	0.0	-0.0	90.	0.	30.	10.	10.	-99.	0.	12.32	31.	547.	580.	0.0	99.0	1
4	8	0.0	-0.0	90.	0.	30.	15.	15.	-99.	0.	12.30	17.	544.	567.	0.0	99.0	1
5	1	0.0	-0.0	90.	0.	15.	10.	10.	-99.	0.	1.45	53.	3598.	3603.	0.0	99.0	1
5	2	0.0	-0.0	90.	0.	15.	10.	10.	-99.	0.	5.53	12.	3585.	3596.	0.0	99.0	1
5	3	0.0	-0.0	90.	0.	15.	10.	10.	-99.	0.	12.24	56.	3652.	3675.	0.0	99.0	1
5	4	0.0	-0.0	90.	0.	15.	0.	0.	-99.	0.	12.30	33.	3643.	3623.	0.0	99.0	1
5	5	0.0	-0.0	90.	0.	15.	5.	5.	-99.	0.	12.35	19.	3609.	3669.	0.0	99.0	1
5	6	0.0	-0.0	90.	0.	15.	15.	15.	-99.	0.	12.32	39.	3616.	3671.	0.0	99.0	1
5	7	0.0	-0.0	90.	0.	15.	10.	10.	-99.	0.	21.49	34.	3623.	3634.	0.0	99.0	1
5	8	0.0	-0.0	90.	0.	15.	10.	10.	-99.	0.	34.20	43.	3635.	3645.	0.0	99.0	1
5	9	0.0	-0.0	90.	0.	15.	10.	10.	-99.	0.	49.22	90.	3618.	3624.	0.0	99.0	1
5	10	0.0	-0.0	90.	0.	15.	10.	10.	-99.	0.	49.17	59.	1016.	1074.	0.0	99.0	1
5	11	0.0	-0.0	90.	0.	15.	10.	10.	-99.	0.	12.25	31.	527.	633.	0.0	99.0	1
5	12	0.0	-0.0	90.	0.	15.	0.	0.	-99.	0.	12.25	31.	533.	569.	0.0	99.0	1
5	13	0.0	-0.0	90.	0.	15.	5.	5.	-99.	0.	12.25	28.	521.	552.	0.0	99.0	1
5	14	0.0	-0.0	90.	0.	15.	15.	15.	-99.	0.	12.27	29.	521.	557.	0.0	99.0	1
6	1	0.0	-0.0	56.	0.	15.	10.	10.	-99.	0.	0.00	15.	0.	2007.	0.0	99.0	1
6	2	0.0	-0.0	55.	0.	15.	10.	10.	-99.	0.	0.00	49.	0.	2867.	0.0	99.0	1
6	3	0.0	-0.0	56.	0.	15.	10.	10.	-99.	0.	0.00	0.	36.	3622.	0.0	99.0	1
6	4	0.0	-0.0	55.	0.	15.	10.	10.	-99.	0.	0.00	12.	75.	4060.	0.0	99.0	1
7	1	0.0	-0.0	50.	0.	15.	10.	10.	-99.	0.	0.00	24.	1997.	15.	0.0	99.0	1
7	2	0.0	-0.0	55.	0.	15.	10.	10.	-99.	0.	0.00	12.	2898.	37.	0.0	99.0	1
7	3	0.0	-0.0	55.	0.	15.	10.	10.	-99.	0.	.00	12.	3607.	90.	0.0	99.0	1
7	4	0.0	-0.0	50.	0.	15.	10.	10.	-99.	0.	0.00	15.	4065.	119.	0.0	99.0	1
8	1	0.0	-0.0	56.	0.	15.	10.	10.	-99.	0.	.36	11.	3616.	3626.	0.0	99.0	1
8	2	8.0	-0.0	55.	0.	15.	10.	10.	-99.	0.	.32	0.	3622.	3639.	0.0	99.0	1
8	3	16.0	-0.0	50.	0.	15.	10.	10.	-99.	0.	0.00	22.	3612.	3629.	0.0	99.0	1
9	1	0.0	-0.0	50.	0.	15.	10.	10.	-99.	0.	1.33	13.	3622.	3627.	0.0	99.0	1
9	2	8.0	-0.0	55.	0.	15.	10.	10.	-99.	0.	1.49	15.	3627.	3644.	0.0	99.0	1
9	3	16.0	-0.0	50.	0.	15.	10.	10.	-99.	0.	1.35	22.	3630.	3641.	0.0	99.0	1
9	4	0.0	-0.0	56.	0.	15.	10.	10.	-99.	0.	5.61	30.	3619.	3625.	0.0	99.0	1
10	1	8.0	-0.0	56.	0.	15.	10.	10.	-99.	0.	5.56	0.	3603.	3626.	0.0	99.0	1
10	2	16.0	-0.0	56.	0.	15.	10.	10.	-99.	0.	5.65	24.	3617.	3624.	0.0	99.0	1
10	3	0.0	-0.0	50.	0.	15.	10.	10.	-99.	0.	12.44	0.	3626.	3634.	0.0	99.0	1

GP78-0822-211

ORIGINAL PAGE IS OF POOR QUALITY

FOLDOUT FRAME 1

						BALANCE FORCE AND MOMENT DATA--STABILITY AXES							
FLYNL DEG	NOSE GEAR	NOSE INLET	UNIT COVERS	OTHER	RUN	PT	LIFT (LB)	DRAG (LB)	PITCHING MOMENT (FT-LB)	SIDE FORCE (LB)	ROLLING MOMENT (FT-LB)	YAWING MOMENT (FT-LB)	TUNNEL TOTAL TEMP (DEG F)	AMBIENT PRESSURE (IN HG)
00.0	1		1		1	1	331.	-48.	-2225.	4.	1430.	124.	70.	29.90
00.0	1		1		1	2	760.	-91.	-5363.	15.	3132.	307.	70.	29.90
00.0	1		1		1	3	1127.	-117.	-8119.	8.	4742.	344.	70.	29.90
00.0	1		1		1	4	1484.	-119.	-10868.	24.	6369.	448.	70.	29.90
00.0	1		1		2	1	379.	-55.	-2636.	-3.	-1312.	-221.	70.	29.90
00.0	1		1		2	2	768.	-101.	-5270.	-6.	-3041.	-396.	70.	29.90
00.0	1		1		2	3	1154.	-147.	-8130.	-14.	-4887.	-598.	70.	29.90
00.0	1		1		2	4	1420.	-164.	-10115.	-21.	-6062.	-652.	70.	29.90
00.0	1		1		3	1	643.	-93.	-4624.	14.	-A.	-7.	70.	29.90
00.0	1		1		3	2	1468.	-177.	-10567.	14.	-34.	-153.	70.	29.90
00.0	1		1		3	3	2212.	-248.	-15900.	18.	-268.	-211.	70	29.90
00.0	1		1		4	1	5036.	1202.	-21124.	55.	-237.	-536.	72.	29.90
00.0	1		1		4	2	4945.	1140.	-20669.	65.	-366.	-506.	74.	29.90
00.0	1		1		4	3	4908.	1177.	-20349.	60.	-238.	-513.	74.	29.90
00.0	1		1		4	4	4903.	1174.	-20177.	61.	-193	-567.	74.	29.90
00.0	1		1		4	5	1463.	551.	-4866.	-6.		-49.	73	29.90
00.0	1		1		4	6	1546.	555.	-4973.	-10.		-5.	73.	29.90
00.0	1		1		4	7	1605.	561.	-5141.	-11.		-19.	73.	29.90
00.0	1		1		4	8	1620.	574.	-5360.			-59.	73.	29.90
00.0	1		1		5	1	01.	100.	-15885.				65.	30.03
00.0	1		1		5	2	123.	563.	-17306.	-6.		-41.	66.	30.03
00.0	1		1		5	3	4968.	1113.	-20242.			4	67.	30.03
00.0	1		1		5	4	4764.	1127.	-20019.			6	67.	30.03
00.0	1		1		5	5	4900.	1121.	-20170.			-59	68.	30.03
00.0	1		1		5	6	5003.	1141.	-20541.			-54	68.	30.03
00.0	1		1		5	7	6522.	1767.	-24191.			-174.	68.	30.03
00.0	1		1		5	8	8507.	2481.	-28708.	-71.		1.	69.	30.03
00.0	1		1		5	9	10723.	3301.	-35243.	-24.	-3	560.	69.	30.03
00.0	1		1		5	10	6314.	2110.	-20656.	20.	-63.	-340.	70.	30.03
00.0	1		1		5	11	1591.	525.	-4693.	-6.	21.	-24.	71.	30.03
00.0	1		1		5	12	1443.	516.	-4354.	-5.	41.	10.	71.	30.03
00.0	1		1		5	13	1491.	522.	-4670.	-2.	141.	-12.	71.	30.03
00.0	1		1		5	14	1630.	544.	-5016.	-0.	74.	8.	71.	30.03
00.0	1		1		6	1	274.	-232.	-1684.	-10.	-1201.	-1156.	66.	30.11
00.0	1		1		6	2	566.	-583.	-3630.	-15.	-2303.	-2332.	66.	30.11
00.0	1		1		6	3	918.	-478.	-5476.	-26.	-3847.	-360		30.11
00.0	1		1		6	4	1164.	-1049.	-6408.	-30.	-4965.	-237	66.	30.11
00.0	1		1		7	1	265.	-284.	-1694.	-2.	1110.	109	67.	30.11
00.0	1		1		7	2	533.	-558.	-3443.	3.	2443.	2346.	68.	30.11
00.0	1		1		7	3	920.	-867.	-5593.	5.	3576.	3410	68.	30.11
00.0	1		1		7	4	1167.	-1049.	-6678.	3.	4771.	4271.	68.	30.11
00.0	1		1		8	1	1497.	-1643.	-10489.	-8.	-134.	-92.	70.	30.11
00.0	1		1		8	2	2171.	-1861.	-10246.	-15.	-208.	-87.	71.	30.11
00.0	1		1		8	3	2263.	-1068.	-10452.	-2.	-78.	-85.	71.	30.11
00.0	1		1		9	1	2074.	-1504.	-10263.	-13.	2.	-55.	74.	30.11
00.0	1		1		9	2	2563.	-1154.	-10746.	-5.	-121.	85.	74.	30.11
00.0	1		1		9	3	2878.	-739.	-10895.	-12.	-203.	10.	76.	30.11
00.0	1		1		9	4	2820.	-1075.	-11530.	-1.	-163.	-40.	77.	30.11
00.0	1		1		10	1	3589.	-717.	-11226.	4.	-244.	-56.	66.	30.16
00.0	1		1		10	2	4219.	-67.	-11504.	-13.	-244.	204.	67.	30.16
00.0	1		1		10	3	3774.	-629.	-14264.	-71.	-97.	423.	68.	30.16

MIN	PT	ALPHA DEG	BETA DEG	DLC DEG	DNL DEG	DF DEG	DAL DEG	DAR DEG	DH DEG	DR DEG	QC PSF	FAN1 RPM	FAN2 RPM	FAN3 RPM	DYLC DEG	DYNL DEG	NOSE GEAR	NO INL
10	4	4.0	-0.0	50.	0.	15.	10.	10.	-99.	0.	12.44	11.	3637.	3646.	0.0	99.0	1	1
10	5	16.0	-0.0	50.	0.	15.	10.	10.	-99.	0.	12.36	31.	3626.	3674.	0.0	99.0	1	1
10	6	0.0	-0.0	50.	0.	15.	10.	10.	-99.	0.	21.73	0.	3659.	3664.	0.0	99.0	1	1
10	7	8.0	-0.0	50.	0.	15.	10.	10.	-99.	0.	21.85	66.	3663.	3623.	0.0	99.0	1	1
10	8	16.0	-0.0	50.	0.	15.	10.	10.	-99.	0.	22.02	33.	3619.	3616.	0.0	99.0	1	1
10	9	0.0	-0.0	50.	0.	15.	10.	10.	-99.	0.	34.24	20.	3637.	3634.	0.0	99.0	1	1
10	10	8.0	-0.0	50.	0.	15.	10.	10.	-99.	0.	34.23	47.	3629.	3666.	0.0	99.0	1	1
10	11	16.0	-0.0	50.	0.	15.	10.	10.	-99.	0.	34.32	31.	3622.	3628.	0.0	99.0	1	1
10	12	0.0	-0.0	50.	0.	15.	10.	10.	-99.	0.	49.10	31.	3635.	3624.	0.0	99.0	1	1
10	13	8.0	-0.0	50.	0.	15.	10.	10.	-99.	0.	49.15	28.	3637.	3617.	0.0	99.0	1	1
10	14	16.0	-0.0	50.	0.	15.	10.	10.	-99.	0.	49.14	36.	3603.	3620.	0.0	99.0	1	1
11	1	0.0	-0.0	50.	0.	15.	10.	10.	-99.	0.	44.16	44.	1214.	1246.	0.0	99.0	1	1
11	2	4.0	-0.0	50.	0.	15.	10.	10.	-99.	0.	44.15	56.	1202.	1244.	0.0	99.0	1	1
11	3	16.0	-0.0	50.	0.	15.	10.	10.	-99.	0.	44.16	29.	HAH.	1231.	0.0	99.0	1	1
11	4	0.0	-0.0	50.	0.	15.	10.	10.	-99.	0.	12.30	23.	621.	679.	0.0	99.0	1	1
11	5	8.0	-0.0	50.	0.	15.	10.	10.	-99.	0.	12.33	31.	599.	650.	0.0	99.0	1	1
11	6	16.0	-0.0	50.	0.	15.	10.	10.	-99.	0.	12.24	25.	370.	644.	0.0	99.0	1	1
12	1	0.0	-0.0	50.	104.	15.	10.	10.	-99.	0.	0.00	1988.	14.	31.	0.0	0.0	1	1
12	2	0.0	-0.0	50.	50.	15.	10.	10.	-99.	0.	0.00	2019.	0.	0.	0.0	0.0	1	1
12	3	0.0	-0.0	50.	70.	15.	10.	10.	-99.	0.	0.00	1993.	0.	21.	0.0	0.0	1	1
12	4	0.0	-0.0	50.	50.	15.	10.	10.	-99.	0.	0.00	1994.	0.	22.	0.0	0.0	1	1
12	5	0.0	-0.0	50.	50.	15.	10.	10.	-99.	0.	0.00	2015.	44.	78.	0.0	0.0	1	1
12	6	0.0	-0.0	50.	104.	15.	10.	10.	-99.	0.	0.00	2981.	0.	14.	0.0	0.0	1	1
12	7	0.0	-0.0	50.	104.	15.	10.	10.	-99.	0.	0.00	2948.	0.	26.	0.0	0.0	1	1
12	8	0.0	-0.0	50.	50.	15.	10.	10.	-99.	0.	0.00	2983.	0.	24.	0.0	0.0	1	1
12	9	0.0	-0.0	50.	50.	15.	10.	10.	-99.	0.	0.00	2935.	0.	11.	0.0	0.0	1	1
12	10	0.0	-0.0	50.	70.	15.	10.	10.	-99.	0.	0.00	2938.	0.	17.	0.0	0.0	1	1
12	11	0.0	-0.0	50.	50.	15.	10.	10.	-99.	0.	0.00	2925.	0.	12.	0.0	0.0	1	1
12	12	0.0	-0.0	50.	50.	15.	10.	10.	-99.	0.	0.00	2926.	29.	50.	0.0	0.0	1	1
12	13	0.0	-0.0	50.	50.	15.	10.	10.	-99.	0.	0.00	2944.	36.	65.	0.0	0.0	1	1
12	14	0.0	-0.0	50.	50.	15.	10.	10.	-99.	0.	0.00	2950.	76.	95.	0.0	0.0	1	1
12	15	0.0	-0.0	50.	104.	15.	10.	10.	-99.	0.	0.00	3582.	0.	0.	0.0	0.0	1	1
12	16	0.0	-0.0	50.	104.	15.	10.	10.	-99.	0.	0.00	3574.	0.	11.	0.0	0.0	1	1
12	17	0.0	-0.0	50.	50.	15.	10.	10.	-99.	0.	0.00	3591.	0.	0.	0.0	0.0	1	1
12	18	0.0	-0.0	50.	50.	15.	10.	10.	-99.	0.	0.00	3610.	12.	11.	0.0	0.0	1	1
12	19	0.0	-0.0	50.	70.	15.	10.	10.	-99.	0.	0.00	3596.	16.	49.	0.0	0.0	1	1
12	20	0.0	-0.0	50.	50.	15.	10.	10.	-99.	0.	0.00	3617.	28.	42.	0.0	0.0	1	1
12	21	0.0	-0.0	50.	50.	15.	10.	10.	-99.	0.	0.00	3600.	51.	77.	0.0	0.0	1	1
12	22	0.0	-0.0	50.	50.	15.	10.	10.	-99.	0.	0.00	3587.	55.	84.	0.0	0.0	1	1
12	23	0.0	-0.0	50.	50.	15.	10.	10.	-99.	0.	0.00	3609.	104.	110.	0.0	0.0	1	1
13	1	0.0	-0.0	50.	50.	15.	10.	10.	-99.	0.	0.00	3593.	69.	87.	0.0	0.0	1	1
13	2	0.0	-0.0	50.	35.	15.	10.	10.	-99.	0.	0.00	3613.	94.	104.	0.0	0.0	1	1
13	3	0.0	-0.0	50.	50.	15.	10.	10.	-99.	0.	.59	3602.	3579.	3594.	0.0	0.0	1	1
13	4	8.0	-0.0	50.	50.	15.	10.	10.	-99.	0.	.57	3600.	3590.	3587.	0.0	0.0	1	1
13	5	16.0	-0.0	50.	50.	15.	10.	10.	-99.	0.	.52	3593.	3587.	3561.	0.0	0.0	1	1
13	6	0.0	-0.0	50.	50.	15.	10.	10.	-99.	0.	5.64	3610.	3633.	3624.	0.0	0.0	1	1
13	7	8.0	-0.0	50.	50.	15.	10.	10.	-99.	0.	5.44	3606.	3630.	3621.	0.0	0.0	1	1
13	8	16.0	-0.0	50.	50.	15.	10.	10.	-99.	0.	5.53	3621.	3630.	3619.	0.0	0.0	1	1
13	9	0.0	-0.0	50.	50.	15.	10.	10.	-99.	0.	12.32	3622.	3623.	3616.	0.0	0.0	1	1
13	10	8.0	-0.0	50.	50.	15.	10.	10.	-99.	0.	12.42	3616.	3620.	3611.	0.0	0.0	1	1
13	11	16.0	-0.0	50.	50.	15.	10.	10.	-99.	0.	12.25	3643.	3617.	3627.	0.0	0.0	1	1

DP78-0622-212

FLC DEG	DYNL DEG	NOSE GEAR	NOSE INLET	UNIT COVERS	OTHER	RUN	PT	BALANCE FORCE AND MOMENT DATA--STABILITY AXES LIFT (LB)	DRAG (LB)	PITCHING MOMENT (FT-LB)	SIDE FORCE (LB)	ROLLING MOMENT (FT-LB)	YAWING MOMENT (FT-LB)	TUNNEL TOTAL TEMP. (DEG F)	AMBIENT PRESSURE (IN HG)
0.0	90.0	1		1		10	4	5192.	-170.	-13438.	-51.	56.	287.	69.	30.16
0.0	90.0	1		1		10	5	6222.	725.	-13261.	-56.	-72.	358.	69.	30.16
0.0	90.0	1		1		10	6	5059.	-103.	-17788.	-59.	-134.	208.	70.	30.16
0.0	90.0	1		1		10	7	7349.	432.	-16464.	-46.	70.	417.	70.	30.16
0.0	90.0	1		1		10	8	8964.	1640.	-15779.	-10.	-394.	207.	70.	30.16
0.0	90.0	1		1		10	9	6589.	378.	-22672.	-48.	3.	222.	70.	30.16
0.0	90.0	1		1		10	10	10081.	1120.	-20915.	-33.	167.	106.	71.	30.16
0.0	90.0	1		1		10	11	12287.	2948.	-18231.	-60.	-329.	772.	72.	30.16
0.0	90.0	1		1		10	12	8392.	953.	-24679.	-12.	-349.	-72.	72.	30.16
0.0	90.0	1		1		10	13	13246.	1859.	-25360.	-57.	167.	348.	73.	30.16
0.0	90.0	1		1		10	14	15910.	4334.	-23027.	-115.	-237.	793.	74.	30.15
0.0	90.0	1		1		11	1	5148.	1471.	-18129.	20.	137.	-139.	73.	30.16
0.0	90.0	1		1		11	2	9632.	1471.	-14880.	-39.	625.	233.	73.	30.16
0.0	90.0	1		1		11	3	10891.	3869.	-8887.	117.	-1793.	282.	73.	30.16
0.0	90.0	1		1		11	4	1348.	178.	-4464.	4.	21.	-15.	70.	30.16
0.0	90.0	1		1		11	5	2409.	494.	-3346.	4.	107.	-14.	69.	30.16
0.0	90.0	1		1		11	6	3031.	813.	-2075.	-15.	1010.	309.	68.	30.16
0.0	0.0	1		2		12	1	323.	85.	4109.	-3.	74.	7.	59.	30.22
0.0	0.0	1		2		12	2	363.	-26.	4974.	-3.	32.	3.	59.	30.22
0.0	0.0	1		2		12	3	345.	-145.	4428.	-6.	57.	-50.	59.	30.22
0.0	0.0	1		2		12	4	246.	-248.	4112.	-3.	137.	2.	59.	30.22
0.0	0.0	1		2		12	5	19.	-232.	1291.	-1.	60.	33.	59.	30.22
0.0	0.0	1		2		12	6	697.	173.	8795.	-1.	82.	82.	58.	30.22
0.0	0.0	1		2		12	7	756.	65.	9989.	-11.	96.	-71.	58.	30.22
0.0	0.0	1		2		12	8	741.	-41.	10418.	-4.	100.	-3.	58.	30.22
0.0	0.0	1		2		12	9	779.	-188.	10465.	-8.	57.	-96.	58.	30.22
0.0	0.0	1		2		12	10	754.	-316.	10598.	-3.	27.	-82.	58.	30.22
0.0	0.0	1		2		12	11	687.	-440.	10162.	-5.	81.	-62.	58.	30.22
0.0	0.0	1		2		12	12	577.	-540.	8799.	-1.	76.	18.	58.	30.22
0.0	0.0	1		2		12	13	410.	-600.	6905.	-1.	62.	46.	58.	30.22
0.0	0.0	1		2		12	14	51.	-508.	2847.	11.	-103.	32.	58.	30.22
0.0	0.0	1		2		12	15	1082.	268.	13260.	-9.	-13.	-54.	58.	30.22
0.0	0.0	1		2		12	16	1127.	105.	15029.	0.	3.	-74.	58.	30.22
0.0	0.0	1		2		12	17	1147.	-77.	16120.	-4.	-48.	-30.	59.	30.22
0.0	0.0	1		2		12	18	1144.	-288.	16241.	-7.	-20.	-71.	59.	30.22
0.0	0.0	1		2		12	19	1134.	-478.	15945.	-9.	28.	-121.	60.	30.22
0.0	0.0	1		2		12	20	1048.	-649.	14849.	1.	-35.	-13.	60.	30.22
0.0	0.0	1		2		12	21	880.	-805.	13328.	0.	-4.	10.	60.	30.22
0.0	0.0	1		2		12	22	645.	-901.	10625.	0.	-7.	54.	60.	30.22
0.0	0.0	1		2		12	23	92.	-763.	4191.	16.	-238.	45.	60.	30.22
0.0	0.0	1		2		13	1	616.	-893.	10194.	8.	12.	86.	64.	30.01
0.0	0.0	1		2		13	2	474.	-884.	8432.	8.	60.	104.	64.	30.01
0.0	0.0	1		2		13	3	2651.	-2266.	2862.	-21.	-231.	-47.	65.	30.01
0.0	0.0	1		2		13	4	3014.	-1881.	2953.	-6.	-261.	64.	67.	30.01
0.0	0.0	1		2		13	5	3341.	-1437.	2945.	-1.	-240.	92.	69.	30.01
0.0	0.0	1		2		13	6	3319.	-1643.	1824.	17.	-240.	-107.	73.	30.01
0.0	0.0	1		2		13	7	4163.	-1155.	2480.	32.	-395.	-139.	74.	30.01
0.0	0.0	1		2		13	8	4751.	-390.	2158.	32.	-367.	-47.	74.	30.01
0.0	0.0	1		2		13	9	4095.	-1069.	-365.	-36.	-222.	349.	78.	30.01
0.0	0.0	1		2		13	10	5605.	-462.	162.	23.	-296.	-60.	79.	30.01
0.0	0.0	1		2		13	11	6536.	516.	-74.	32.	-501.	264.	79.	30.01

RUN	PT	ALPHA DEG	BETA DEG	DLC DEG	DNL DEG	DF DEG	DAL DEG	DAR DEG	DH DEG	DR DEG	QC PSF	FAN1 RPM	FAN2 RPM	FAN3 RPM	DYLC DEG	DYNL DEG	NOSE GEAR	IN
13	12	0.0	-0.0	56.	40.	15.	10.	10.	-999.	0.	12.56	3620.	3662.	3671.	0.0	0.0	1	
13	13	0.0	-0.0	56.	45.	15.	10.	10.	-999.	0.	12.37	3613.	3621.	3613.	0.0	0.0	1	
13	14	0.0	-0.0	56.	55.	15.	10.	10.	-999.	0.	12.37	3601.	3622.	3611.	0.0	0.0	1	
13	15	0.0	-0.0	56.	60.	15.	10.	10.	-999.	0.	12.32	3609.	3620.	3607.	0.0	0.0	1	
13	16	0.0	-0.0	56.	50.	15.	10.	10.	-999.	0.	12.42	3390.	3622.	3607.	0.0	0.0	1	
14	1	0.0	-0.0	56.	50.	15.	10.	10.	-999.	0.	21.89	3647.	3621.	3608.	0.0	0.0	1	
14	2	0.0	-0.0	56.	50.	15.	10.	10.	-999.	0.	21.93	3607.	3630.	3678.	0.0	0.0	1	
15	1	16.0	-0.0	56.	56.	15.	10.	10.	-999.	0.	21.93	3599.	3649.	3661.	0.0	0.0	1	
15	2	0.0	-0.0	56.	55.	15.	10.	10.	-999.	0.	34.17	3709.	3634.	3640.	0.0	0.0	1	
15	3	8.0	-0.0	56.	56.	15.	10.	10.	-999.	0.	34.30	3638.	3636.	3683.	0.0	0.0	1	
15	4	16.0	-0.0	56.	56.	15.	10.	10.	-999.	0.	34.15	3628.	3656.	3636.	0.0	0.0	1	
15	5	-4.0	-0.0	56.	56.	15.	10.	10.	-999.	0.	12.27	3635.	3619.	3607.	0.0	0.0	1	
15	6	0.0	-0.0	56.	56.	15.	10.	10.	-999.	0.	12.28	3809.	3625.	3607.	0.0	0.0	1	
15	7	4.0	-0.0	56.	56.	15.	10.	10.	-999.	0.	12.27	3611.	3674.	3717.	0.0	0.0	1	
15	8	8.0	-0.0	56.	56.	15.	10.	10.	-999.	0.	12.39	3612.	3621.	3609.	0.0	0.0	1	
15	9	10.0	-0.0	56.	56.	15.	10.	10.	-999.	0.	12.39	3644.	3629.	3621.	0.0	0.0	1	
15	10	12.0	-0.0	56.	56.	15.	10.	10.	-999.	0.	12.24	3742.	3692.	3695.	0.0	0.0	1	
15	11	14.0	-0.0	56.	56.	15.	10.	10.	-999.	0.	12.42	3620.	3704.	3632.	0.0	0.0	1	
15	12	16.0	-0.0	56.	56.	15.	10.	10.	-999.	0.	12.25	3614.	3733.	3742.	0.0	0.0	1	
15	13	18.0	-0.0	56.	56.	15.	10.	10.	-999.	0.	12.40	3611.	3713.	3640.	0.0	0.0	1	
15	14	20.0	-0.0	56.	56.	15.	10.	10.	-999.	0.	12.25	3621.	3617.	3601.	0.0	0.0	1	
15	15	0.0	-0.0	56.	56.	15.	10.	10.	-999.	0.	12.37	1974.	1970.	1978.	0.0	0.0	1	
15	16	0.0	-0.0	56.	56.	15.	10.	10.	-999.	0.	12.47	2888.	2940.	2933.	0.0	0.0	1	
15	17	0.0	-0.0	56.	56.	15.	10.	10.	-999.	0.	12.37	388.	633.	678.	0.0	0.0	1	
15	18	8.0	-0.0	56.	56.	15.	10.	10.	-999.	0.	12.35	192.	598.	646.	0.0	0.0	1	
15	19	16.0	-0.0	56.	56.	15.	10.	10.	-999.	0.	12.25	68.	471.	644.	0.0	0.0	1	
16	1	0.0	-0.0	0.	90.	15.	10.	10.	-999.	0.	0.00	38.	1983.	27.	99.0	0.0		
16	2	0.0	-0.0	0.	90.	15.	10.	10.	-999.	0.	0.00	62.	2499.	67.	99.0	0.0		
16	3	0.0	-0.0	0.	90.	15.	10.	10.	-999.	0.	0.00	73.	3581.	78.	99.0	0.0		
16	4	0.0	-0.0	0.	90.	15.	10.	10.	-999.	0.	0.00	72.	4046.	97.	99.0	0.0		
17	1	0.0	-0.0	0.	90.	15.	10.	10.	-999.	0.	0.00	52.	34.	1982.	99.0	0.0		
17	2	0.0	-0.0	0.	90.	15.	10.	10.	-999.	0.	0.00	56.	35.	2849.	99.0	0.0		
17	3	0.0	-0.0	0.	90.	15.	10.	10.	-999.	0.	0.00	62.	54.	3612.	99.0	0.0		
17	4	0.0	-0.0	0.	90.	15.	10.	10.	-999.	0.	0.00	71.	73.	4039.	99.0	0.0		
18	1	0.0	-0.0	0.	90.	15.	10.	10.	-999.	0.	.32	98.	3620.	3624.	99.0	0.0		
18	2	0.0	-0.0	0.	70.	15.	10.	10.	-999.	0.	.32	3620.	3617.	3616.	99.0	0.0		
18	3	0.0	-0.0	0.	70.	15.	10.	10.	-999.	0.	.54	3601.	3612.	3611.	99.0	0.0		
18	4	0.0	-0.0	0.	70.	15.	10.	10.	-999.	0.	.54	3588.	3611.	3605.	99.0	0.0		
19	5	0.0	-0.0	0.	55.	15.	10.	10.	-999.	0.	.44	3612.	3616.	3607.	99.0	0.0		
19	1	0.0	-0.0	0.	90.	15.	10.	10.	-999.	0.	1.57	3612.	3611.	3614.	99.0	0.0		
19	2	0.0	-0.0	0.	70.	15.	10.	10.	-999.	0.	1.43	3606.	3612.	3609.	99.0	0.0		
19	3	0.0	-0.0	0.	50.	15.	10.	10.	-999.	0.	1.47	3596.	3605.	3609.	99.0	0.0		
19	4	0.0	-0.0	0.	90.	15.	10.	10.	-999.	0.	5.58	3599.	3612.	3615.	99.0	0.0		
19	5	0.0	-0.0	0.	70.	15.	10.	10.	-999.	0.	5.56	3717.	3611.	3616.	99.0	0.0		
19	6	0.0	-0.0	0.	50.	15.	10.	10.	-999.	0.	5.61	3603.	3605.	3606.	99.0	0.0		
19	7	0.0	-0.0	0.	35.	15.	10.	10.	-999.	0.	5.38	3589.	3603.	3606.	99.0	0.0		
19	8	0.0	-0.0	0.	90.	15.	10.	10.	-999.	0.	12.36	3644.	3609.	3613.	99.0	0.0		
19	9	0.0	-0.0	0.	70.	15.	10.	10.	-999.	0.	12.31	3618.	3615.	3613.	99.0	0.0		
19	10	0.0	-0.0	0.	50.	15.	10.	10.	-999.	0.	12.58	3683.	3618.	3617.	99.0	0.0		
20	1	0.0	-0.0	0.	90.	15.	10.	10.	-999.	0.	21.72	3610.	3713.	3750.	99.0	0.0		
20	2	0.0	-0.0	0.	70.	15.	10.	10.	-999.	0.	22.05	3597.	3611.	3633.	99.0	0.0		

GP76-0622-213

FLC DEG	DYNL DEG	NOSE GEAR	NOSE INLET	UNIT COVERS	OTHER	RUN	PT	BALANCE FORCE AND MOMENT DATA--STABILITY AXES LIFT (LB)	DRAG (LB)	PITCHING MOMENT (FT-LB)	SIDE FORCE (LB)	ROLLING MOMENT (FT-LB)	YAWING MOMENT (FT-LB)	TUNNEL TOTAL TEMP. (DEG F)	AMBIENT PRESSURE (IN HG)
0.0	0.0	1		2		13	12	3853.	-1200.	-5021.	15.	-341.	146.	77.	30.01
0.0	0.0	1		2		13	13	3995.	-1164.	-2443.	6.	-536.	118.	80.	30.01
0.0	0.0	1		2		13	14	4137.	-1003.	309.	-29.	-152.	282.	80.	30.01
0.0	0.0	1		2		13	15	4141.	-909.	859.	-30.	-264.	214.	81.	30.01
0.0	0.0	1		2		13	16	4038.	-989.	-2359.	-47.	-25.	409.	81.	30.01
0.0	0.0	1		2		14	1	5353.	-436.	-4382.	-23.	-528.	-197.	79.	30.05
0.0	0.0	1		2		14	2	7709.	259.	-3467.	-19.	-314.	-172.	81.	30.05
0.0	0.0	1		2		15	1	9149.	1617.	-3490.	-2.	-151.	116.	75.	30.13
0.0	0.0	1		2		15	2	6960.	244.	-8496.	-80.	227.	-215.	77.	30.13
0.0	0.0	1		2		15	3	10461.	1079.	-7680.	-75.	334.	124.	78.	30.13
0.0	0.0	1		2		15	4	12357.	2445.	-5855.	-21.	-389.	573.	80.	30.13
0.0	0.0	1		2		15	5	3310.	-1280.	-585.	-33.	-245.	284.	81.	30.13
0.0	0.0	1		2		15	6	4039.	-1051.	-254.	-13.	-561.	234.	81.	30.13
0.0	0.0	1		2		15	7	4802.	-772.	9.	-9.	-310.	30.	81.	30.13
0.0	0.0	1		2		15	8	5542.	-458.	240.	36.	-671.	-212.	81.	30.13
0.0	0.0	1		2		15	9	5855.	-290.	-15.	83.	-935.	-319.	81.	30.13
0.0	0.0	1		2		15	10	6157.	-110.	62.	59.	-774.	-49.	81.	30.13
0.0	0.0	1		2		15	11	6397.	262.	288.	21.	172.	480.	81.	30.13
0.0	0.0	1		2		15	12	6553.	539.	192.	21.	-629.	112.	81.	30.13
0.0	0.0	1		2		15	13	6894.	884.	-279.	-7.	-265.	210.	82.	30.13
0.0	0.0	1		2		15	14	7085.	1162.	-840.	-18.	-43.	630.	82.	30.13
0.0	0.0	1		2		15	15	2399.	184.	-3153.	-1.	-66.	-146.	82.	30.13
0.0	0.0	1		2		15	16	3244.	-354.	-1802.	-6.	12.	-52.	81.	30.13
0.0	0.0	1		2		15	17	1369.	413.	-4224.	7.	34.	8.	80.	30.13
0.0	0.0	1		2		15	18	2396.	512.	-3214.	13.	-96.	-113.	80.	30.13
0.0	0.0	1		2		15	19	3069.	858.	-2580.	-15.	1029.	300.	79.	30.13
99.0	0.0	1		2		16	1	18.	-401.	-411.	-3.	111.	1707.	70.	30.05
99.0	0.0	1		2		16	2	10.	-458.	-607.	0.	34.	3611.	70.	30.05
99.0	0.0	1		2		16	3	13.	-1329.	-244.	8.	103.	5494.	70.	30.05
99.0	0.0	1		2		16	4	20.	-1688.	-642.	24.	38.	6933.	72.	30.05
99.0	0.0	1		2		17	1	7.	-392.	-602.	-13.	115.	-1589.	72.	30.05
99.0	0.0	1		2		17	2	20.	-861.	-584.	-21.	39.	-3534.	72.	30.05
99.0	0.0	1		2		17	3	9.	-1362.	-9.	-36.	-75.	-5508.	73.	30.05
99.0	0.0	1		2		17	4	33.	-1484.	-535.	-47.	-229.	-6835.	73.	30.05
99.0	0.0	1		2		18	1	0.	-2663.	-853.	-13.	-70.	49.	73.	30.05
99.0	0.0	1		2		18	2	1134.	-2578.	14845.	-58.	-57.	-69.	73.	30.05
99.0	0.0	1		2		18	3	1103.	-2455.	14885.	-27.	-123.	-28.	74.	30.05
99.0	0.0	1		2		18	4	824.	-3326.	13242.	-13.	-139.	54.	75.	30.05
99.0	0.0	1		2		18	5	300.	-3463.	7976.	3.	-107.	269.	75.	30.05
99.0	0.0	1		2		19	1	1412.	-2336.	15237.	-38.	-108.	-109.	79.	30.05
99.0	0.0	1		2		19	2	1316.	-2793.	15571.	-34.	-598.	-223.	80.	30.05
99.0	0.0	1		2		19	3	1047.	-3157.	13323.	-39.	-540.	-262.	81.	30.05
99.0	0.0	1		2		19	4	1661.	-1893.	14671.	11.	211.	466.	83.	30.05
99.0	0.0	1		2		19	5	1599.	-2318.	14979.	-49.	-124.	-233.	84.	30.05
99.0	0.0	1		2		19	6	1330.	-2792.	12413.	-36.	-516.	-114.	84.	30.05
99.0	0.0	1		2		19	7	748.	-2883.	5940.	-30.	-472.	3.	84.	30.05
99.0	0.0	1		2		19	8	1998.	-1360.	13712.	-21.	20.	64.	83.	30.05
99.0	0.0	1		2		19	9	1964.	-1436.	13801.	-70.	136.	-347.	83.	30.05
99.0	0.0	1		2		19	10	1443.	-2223.	11152.	-44.	226.	16.	83.	30.05
99.0	0.0	1		2		20	1	2564.	-784.	11311.	-42.	-203.	-413.	84.	30.05
99.0	0.0	1		2		20	2	2426.	-1267.	11599.	-52.	414.	-569.	84.	30.05

FOLDOUT FRAME 2

MIN	PT	ALPHA DEG	BETA DEG	DLC DEG	DNL DEG	DF DEG	DAL DEG	DAR DEG	DH DEG	DR DEG	QC PSF	FAN1 RPM	FAN2 RPM	FAN3 RPM	DYLC DEG	DYNL DEG	NOSE GEAR	NL INL
20	3	0.0	-0.0	0.	0.	15.	10.	10.	-99.	0.	21.98	3607.	3613.	3622.	99.0	0.0	1	
20	4	0.0	-0.0	0.	0.	15.	10.	10.	-99.	0.	34.19	3625.	3643.	3634.	99.0	0.0	1	
20	5	0.0	-0.0	0.	0.	15.	10.	10.	-99.	0.	34.20	3623.	3649.	3621.	99.0	0.0	1	
20	6	0.0	-0.0	0.	0.	15.	10.	10.	-99.	0.	34.35	3621.	3630.	3620.	99.0	0.0	1	
21	1	8.0	-0.0	0.	0.	15.	10.	10.	-99.	0.	12.32	3607.	3613.	3610.	99.0	0.0	1	
21	2	8.0	-0.0	0.	0.	15.	10.	10.	-99.	0.	12.24	3587.	3602.	3599.	99.0	0.0	1	
21	3	8.0	-0.0	0.	0.	15.	10.	10.	-99.	0.	12.27	3617.	3650.	3633.	99.0	0.0	1	
21	4	8.0	-0.0	0.	0.	15.	10.	10.	-99.	0.	1.35	3611.	3624.	3624.	99.0	0.0	1	
21	5	8.0	-0.0	0.	0.	15.	10.	10.	-99.	0.	1.30	3612.	3622.	3619.	99.0	0.0	1	
21	6	8.0	-0.0	0.	0.	15.	10.	10.	-99.	0.	1.50	3613.	3613.	3618.	99.0	0.0	1	
22	1	0.0	-0.0	0.	0.	15.	10.	10.	-99.	0.	12.35	3604.	655.	692.	99.0	0.0	1	
22	2	0.0	-0.0	0.	0.	15.	10.	10.	-99.	0.	12.18	3602.	652.	688.	99.0	0.0	1	
22	3	0.0	-0.0	0.	0.	15.	10.	10.	-99.	0.	12.29	3612.	659.	698.	99.0	0.0	1	
22	4	0.0	-0.0	0.	0.	15.	10.	10.	-99.	0.	5.52	3644.	437.	471.	99.0	0.0	1	
22	5	0.0	-0.0	0.	0.	15.	10.	10.	-99.	0.	5.56	3606.	435.	463.	99.0	0.0	1	
22	6	0.0	-0.0	0.	0.	15.	10.	10.	-99.	0.	5.53	3604.	436.	467.	99.0	0.0	1	
22	7	0.0	-0.0	0.	0.	15.	10.	10.	-99.	0.	1.42	3600.	223.	257.	99.0	0.0	1	
22	8	0.0	-0.0	0.	0.	15.	10.	10.	-99.	0.	1.29	3614.	196.	220.	99.0	0.0	1	
22	9	0.0	-0.0	0.	0.	15.	10.	10.	-99.	0.	1.45	3605.	215.	233.	99.0	0.0	1	
23	1	0.0	-0.0	0.	0.	15.	10.	10.	-99.	0.	34.25	692.	1041.	1126.	99.0	0.0	1	
23	2	0.0	-0.0	0.	0.	15.	10.	10.	-99.	0.	34.32	666.	1078.	1121.	99.0	0.0	1	
23	3	0.0	-0.0	0.	0.	15.	10.	10.	-99.	0.	34.26	652.	1077.	1121.	99.0	0.0	1	
23	4	0.0	-0.0	0.	0.	15.	10.	10.	-99.	0.	34.15	588.	1079.	1125.	99.0	0.0	1	
23	5	8.0	-0.0	0.	0.	15.	10.	10.	-99.	0.	34.31	275.	1049.	1139.	99.0	0.0	1	
23	6	0.0	-0.0	0.	0.	15.	10.	10.	-99.	0.	12.28	378.	651.	699.	99.0	0.0	1	
23	7	0.0	-0.0	0.	0.	15.	10.	10.	-99.	0.	12.30	400.	655.	692.	99.0	0.0	1	
23	8	0.0	-0.0	0.	0.	15.	10.	10.	-99.	0.	12.30	397.	654.	690.	99.0	0.0	1	
23	9	0.0	-0.0	0.	0.	15.	10.	10.	-99.	0.	12.31	364.	655.	688.	99.0	0.0	1	
24	1	0.0	-0.0	0.	34.	15.	10.	10.	-99.	0.	12.44	3627.	3678.	3674.	99.0	0.0	1	
24	2	8.0	-0.0	0.	34.	15.	10.	10.	-99.	0.	12.27	3598.	3652.	3597.	99.0	0.0	1	
24	3	16.0	-0.0	0.	34.	15.	10.	10.	-99.	0.	12.33	3611.	3630.	3610.	99.0	0.0	1	
24	4	0.0	-0.0	0.	34.	15.	10.	10.	-99.	0.	22.14	3618.	3618.	3626.	99.0	0.0	1	
24	5	8.0	-0.0	0.	34.	15.	10.	10.	-99.	0.	21.49	3607.	3608.	3669.	99.0	0.0	1	
24	6	8.0	-0.0	0.	34.	15.	10.	10.	-99.	0.	34.30	3606.	3611.	3621.	99.0	0.0	1	
24	7	8.0	-0.0	0.	34.	15.	10.	10.	-99.	0.	34.14	3605.	3617.	3616.	99.0	0.0	1	
25	1	0.0	-0.0	0.	0.	15.	10.	10.	-99.	0.	1.35	0.	3608.	3624.	99.0	99.0	1	
25	2	8.0	-0.0	0.	0.	15.	10.	10.	-99.	0.	1.26	0.	3607.	3624.	99.0	99.0	1	
25	3	16.0	-0.0	0.	0.	15.	10.	10.	-99.	0.	1.25	0.	3621.	3604.	99.0	99.0	1	
25	4	0.0	-0.0	0.	0.	15.	10.	10.	-99.	0.	5.51	0.	3618.	3623.	99.0	99.0	1	
25	5	8.0	-0.0	0.	0.	15.	10.	10.	-99.	0.	5.56	0.	3637.	3615.	99.0	99.0	1	
25	6	16.0	-0.0	0.	0.	15.	10.	10.	-99.	0.	5.58	0.	3623.	3612.	99.0	99.0	1	
25	7	0.0	-0.0	0.	0.	15.	10.	10.	-99.	0.	12.35	0.	3605.	3611.	99.0	99.0	1	
25	8	8.0	-0.0	0.	0.	15.	10.	10.	-99.	0.	12.25	0.	3604.	3608.	99.0	99.0	1	
25	9	16.0	-0.0	0.	0.	15.	10.	10.	-99.	0.	12.39	0.	3626.	3629.	99.0	99.0	1	
25	10	0.0	-0.0	0.	0.	15.	10.	10.	-99.	0.	21.83	14.	3617.	3610.	99.0	99.0	1	
25	11	8.0	-0.0	0.	0.	15.	10.	10.	-99.	0.	21.95	14.	3608.	3605.	99.0	99.0	1	
25	12	16.0	-0.0	0.	0.	15.	10.	10.	-99.	0.	21.94	25.	3610.	3614.	99.0	99.0	1	
25	13	0.0	-0.0	0.	0.	15.	10.	10.	-99.	0.	34.25	24.	3613.	3632.	99.0	99.0	1	
25	14	8.0	-0.0	0.	0.	15.	10.	10.	-99.	0.	34.16	22.	3610.	3614.	99.0	99.0	1	
25	15	16.0	-0.0	0.	0.	15.	10.	10.	-99.	0.	34.13	17.	3665.	3644.	99.0	99.0	1	
26	1	-4.0	-0.0	0.	0.	15.	10.	10.	-99.	0.	34.11	35.	2698.	2708.	99.0	99.0	1	

QP7L-0662-214

BALANCE FORCE AND MOMENT DATA--STABILITY AXES

SYLC DEG	DYNL DEG	NOSE GEAR	NOSE INLET	UNIT COVERS	OTHER	RUN	PT	LIFT (LB)	DRAG (LB)	PITCHING MOMENT (FT-LB)	SIDE FORCE (LB)	ROLLING MOMENT (FT-LB)	YAWING MOMENT (FT-LB)	TUNNEL TOTAL TEMP. (DEG F)	AMBIENT PRESSURE (IN HG)
99.0	0.0	1		2		20	3	2139.	-1709.	9361.	-58.	216.	-414.	85.	30.05
99.0	0.0	1		2		20	4	3200.	-170.	8846.	-59.	587.	-824.	85.	30.05
99.0	0.0	1		2		20	5	3144.	-670.	9084.	-22.	790.	-818.	85.	30.05
99.0	0.0	1		2		20	6	2932.	-1156.	7167.	-50.	244.	-450.	84.	30.05
99.0	0.0	1		2		21	1	3442.	-1070.	15444.	-40.	-310.	-324.	84.	30.05
99.0	0.0	1		2		21	2	3387.	-1532.	15099.	-1.	-104.	-38.	87.	30.05
99.0	0.0	1		2		21	3	3103.	-2000.	12524.	-14.	-127.	42.	87.	30.05
99.0	0.0	1		2		21	4	1862.	-2186.	15814.	-27.	12.	7.	86.	30.05
99.0	0.0	1		2		21	5	1826.	-2617.	15867.	-18.	-252.	-50.	89.	30.05
99.0	0.0	1		2		21	6	1601.	-3027.	13339.	-19.	-2	-147.	90.	30.05
99.0	0.0	1		2		22	1	1761.	722.	13182.	40.		57.	87.	30.05
99.0	0.0	1		2		22	2	1654.	250.	13657.	-4.		86.	85.	30.05
99.0	0.0	1		2		22	3	1394.	-147.	10640.	12.	33	58.	84.	30.05
99.0	0.0	1		2		22	4	1436.	401.	14428.	18.	190.		81.	30.05
99.0	0.0	1		2		22	5	1397.	-62.	14930.	-29.	-178.	-173	81.	30.05
99.0	0.0	1		2		22	6	1114.	-430.	12507.	-16.	25.	-168.	81.	30.05
99.0	0.0	1		2		22	7	1254.	141.	15427.	5.	60.	95.	80.	30.05
99.0	0.0	1		2		22	8	1194.	-293.	16020.	1.	-92.	112.	79.	30.05
99.0	0.0	1		2		22	9	945.	-653.	12956.	-11.	-32.	-49.	79.	30.05
99.0	0.0	1		2		23	1	2110.	969.	-7036.	M.	660.	-32.	78.	30. 5
99.0	0.0	1		2		23	2	2094.	961.	-6893.	-3.	1118.	78.	78.	3 3
99.0	0.0	1		2		23	3	2109.	898.	-6454.	9.	809.	-91.	76.	30.05
99.0	0.0	1		2		23	4	2077.	856.	-6953.	9.	603.	-165.	75.	30.05
99.0	0.0	1		2		23	5	4961.	1004.	-5278.	-40.	1037.	76.	76.	30.05
99.0	0.0	1		2		23	6	774.	344.	-2418.	12.	147.	-6.	75.	30.05
99.0	0.0	1		2		23	7	750.	347.	-2398.	M.	212.	-42.	74.	30.05
99.0	0.0	1		2		23	8	770.	34	-2262.	4.	232.	-52.	74.	30.05
99.0	0.0	1		2		23	9	767.	360.	-2372.	2.	306.	-40.	74.	30.05
99.0	0.0	1		2		24	1	1181.	-2408.	6803.	-67.	-181.	74.	75.	30.05
99.0	0.0	1		2		24	2	2734.	-2227.	5867.	-30.	-28.	155.	77.	30.05
99.0	0.0	1		2		24	3	3594.	-1750.	7259.	-10.	-264.	372.	78.	30.05
99.0	0.0	1		2		24	4	1769.	-1906.	3149.	-49.	187.	196.	78.	30.05
99.0	0.0	1		2		24	5	4049.	-1502.	5260.	-24.	448.	279.	79.	30.05
99.0	0.0	1		2		24	6	2461.	-1359.	1313.	-52	435.	106.	79.	30.05
99.0	0.0	1		2		24	7	5792.	-1044.	4168.	-42.	942.	332.	80.	30.05
99.0	99.0	1				25	1	250.	-2488.	-832.	-14.	-353.	-135.	73.	30.09
99.0	99.0	1				25	2	688.	-2461.	-812.	-27.	-33.	-58.	74.	30.09
99.0	99.0	1				25	3	1190.	-2305.	-812.	-18.	-14.	-150.	75.	30.09
99.0	99.0	1				25	4	627.	-2190.	-1296.	-5	-68.	-29.	77.	30.09
99.0	99.0	1				25	5	1474.	-2092.	-722.	-12.	-148.	-17.	78.	30.09
99.0	99.0	1				25	6	2009.	-1921.	-60.	-1.	62.	-98.	79.	30.09
99.0	99.0	1				25	7	1015.	-1807.	-2331.	-42.	211.	6.	79.	30.09
99.0	99.0	1				25	8	2525.	-1691.	-932.	-27.	158.	30.	79.	30.09
99.0	99.0	1				25	9	3562.	-1342.	246.	-140.	2941.	620.	79.	30.09
99.0	99.0	1				25	10	1560.	-1418.	-3949.	-22.	351.	-64.	80.	30.09
99.0	99.0	1				25	11	3934.	-1239.	-2054.	-34.	475.	93.	81.	30.09
99.0	99.0	1				25	12	6063.	-702.	-737.	-93.	2403.	697.	81.	30.09
99.0	99.0	1				25	13	2199.	-966.	-7067.	-31.	1014.	-39.	81.	30.09
99.0	99.0	1				25	14	5730.	-765.	-4001.	-42.	852.	121.	83.	30.09
99.0	99.0	1				25	15	8139.	135.	-433.	75.	-2987.	131.	83.	30.09
99.0	99.0	1				26	1	618.	-665.	-8518.	-1.	705.	-235.	83.	30.09

RUN	PT	ALPHA DEG	BETA DEG	PHI DEG	PSI DEG	DF DEG	DAL DEG	DAR DEG	DM DEG	DH DEG	DC PSF	FAN1 RPM	FAN2 RPM	FAN3 RPM	DYLC DEG	DYNL DEG	NOZZ GEAR	Z
24	2	8.0	-10.0	0.	0.	0.	0.	0.	0.	0.	34.09	29.	2695.	2710.	99.0	99.0	1	
24	3	4.0	-10.0	0.	0.	0.	0.	0.	0.	0.	34.17	31.	2698.	2711.	99.0	99.0	1	
24	4	0.0	-10.0	0.	0.	0.	0.	0.	0.	0.	34.12	30.	2716.	2716.	99.0	99.0	1	
24	5	-4.0	-10.0	0.	0.	0.	0.	0.	0.	0.	34.00	28.	2705.	2707.	99.0	99.0	1	
24	6	-8.0	-10.0	0.	0.	0.	0.	0.	0.	0.	34.10	62.	2705.	2708.	99.0	99.0	1	
24	7	-12.0	-10.0	0.	0.	0.	0.	0.	0.	0.	34.04	43.	2732.	2712.	99.0	99.0	1	
24	8	-16.0	-10.0	0.	0.	0.	0.	0.	0.	0.	34.17	25.	2731.	2745.	99.0	99.0	1	
24	9	12.0	-10.0	0.	0.	0.	0.	0.	0.	0.	34.13	20.	2717.	2723.	99.0	99.0	1	
24	10	8.0	-10.0	0.	0.	0.	0.	0.	0.	0.	34.18	0.	2709.	2726.	99.0	99.0	1	
24	11	4.0	-10.0	0.	0.	0.	0.	0.	0.	0.	34.24	0.	2707.	2712.	99.0	99.0	1	
24	12	0.0	-10.0	0.	0.	0.	0.	0.	0.	0.	34.14	16.	2718.	2723.	99.0	99.0	1	
24	13	-4.0	-10.0	0.	0.	0.	0.	0.	0.	0.	34.08	98.	2770.	2827.	99.0	99.0	1	
24	14	-8.0	-10.0	0.	0.	0.	0.	0.	0.	0.	34.17	42.	1075.	1128.	99.0	99.0	1	
24	15	-12.0	-10.0	0.	0.	0.	0.	0.	0.	0.	34.22	45.	1051.	1105.	99.0	99.0	1	
24	16	-16.0	-10.0	0.	0.	0.	0.	0.	0.	0.	34.14	41.	1032.	1097.	99.0	99.0	1	
24	17	12.0	-10.0	0.	0.	0.	0.	0.	0.	0.	34.17	36.	910.	1090.	99.0	99.0	1	
24	18	8.0	-10.0	0.	0.	0.	0.	0.	0.	0.	34.17	41.	865.	1085.	99.0	99.0	1	
24	19	4.0	-10.0	0.	0.	0.	0.	0.	0.	0.	34.24	51.	729.	1112.	99.0	99.0	1	
27	1	0.0	-10.0	0.	0.	0.	0.	0.	0.	0.	34.21	35.	2715.	2723.	99.0	99.0	1	
27	2	-4.0	-10.0	0.	0.	0.	0.	0.	0.	0.	34.20	34.	2714.	2716.	99.0	99.0	1	
27	3	-8.0	-10.0	0.	0.	0.	0.	0.	0.	0.	34.21	33.	2714.	2719.	99.0	99.0	1	
27	4	-12.0	-10.0	0.	0.	0.	0.	0.	0.	0.	34.09	32.	2711.	2724.	99.0	99.0	1	
27	5	12.0	-10.0	0.	0.	0.	0.	0.	0.	0.	34.17	28.	2711.	2721.	99.0	99.0	1	
27	6	8.0	-10.0	0.	0.	0.	0.	0.	0.	0.	34.19	41.	2754.	2761.	99.0	99.0	1	
27	7	4.0	-10.0	0.	0.	0.	0.	0.	0.	0.	34.19	26.	2722.	2725.	99.0	99.0	1	
27	8	0.0	-10.0	0.	0.	0.	0.	0.	0.	0.	34.22	0.	2724.	2724.	99.0	99.0	1	
27	9	-4.0	-10.0	0.	0.	0.	0.	0.	0.	0.	34.19	0.	2715.	2707.	99.0	99.0	1	
27	10	-8.0	-10.0	0.	0.	0.	0.	0.	0.	0.	34.04	33.	2722.	2708.	99.0	99.0	1	
27	11	-12.0	-10.0	0.	0.	0.	0.	0.	0.	0.	34.23	284.	2721.	2757.	99.0	99.0	1	
27	12	-16.0	-10.0	0.	0.	0.	0.	0.	0.	0.	34.27	35.	2152.	2162.	99.0	[illegible]	1	
27	13	0.0	-10.0	0.	0.	0.	0.	0.	0.	0.	34.18	33.	2148.	2165.	99.0	[illegible]	1	
27	14	4.0	-10.0	0.	0.	0.	0.	0.	0.	0.	34.16	31.	2144.	2158.	99.0	[illegible]	1	
27	15	8.0	-10.0	0.	0.	0.	0.	0.	0.	0.	34.20	25.	2152.	2153.	99.0	99.0	1	
27	16	12.0	-10.0	0.	0.	0.	0.	0.	0.	0.	34.20	30.	2157.	2162.	99.0	99.0	1	
27	17	16.0	-10.0	0.	0.	0.	0.	0.	0.	0.	34.24	33.	2152.	2156.	99.0	99.0	1	
27	18	20.0	-10.0	0.	0.	0.	0.	0.	0.	0.	34.12	87.	2203.	2170.	99.0	99.0	1	
27	19	24.0	-10.0	0.	0.	0.	0.	0.	0.	0.	34.03	0.	2198.	2232.	99.0	99.0	1	
28	1	-4.0	-10.0	0.	0.	0.	0.	0.	0.	0.	34.13	41.	1612.	1649.	99.0	99.0	1	
28	2	0.0	-10.0	0.	0.	0.	0.	0.	0.	0.	34.14	35.	1607.	1622.	99.0	99.0	1	
28	3	4.0	-10.0	0.	0.	0.	0.	0.	0.	0.	34.22	35.	1602.	1618.	99.0	99.0	1	
28	4	8.0	-10.0	0.	0.	0.	0.	0.	0.	0.	34.16	35.	1599.	1616.	99.0	99.0	1	
28	5	12.0	-10.0	0.	0.	0.	0.	0.	0.	0.	34.22	19.	1599.	1640.	99.0	99.0	1	
28	6	16.0	-10.0	0.	0.	0.	0.	0.	0.	0.	34.21	33.	1594.	1623.	99.0	99.0	1	
28	7	20.0	-10.0	0.	0.	0.	0.	0.	0.	0.	34.16	102.	1608.	1625.	99.0	99.0	1	
28	8	24.0	-10.0	0.	0.	0.	0.	0.	0.	0.	34.20	41.	1612.	1643.	99.0	99.0	1	
28	9	28.0	-10.0	0.	0.	0.	0.	0.	0.	0.	34.20	31.	1723.	1741.	99.0	99.0	1	
28	10	32.0	-10.0	0.	0.	0.	0.	0.	0.	0.	34.17	43.	1085.	1128.	99.0	99.0	1	
28	11	36.0	-10.0	0.	0.	0.	0.	0.	0.	0.	34.34	41.	1071.	1119.	99.0	99.0	1	
28	12	40.0	-10.0	0.	0.	0.	0.	0.	0.	0.	34.23	39.	1054.	1118.	99.0	99.0	1	
28	13	8.0	-10.0	0.	0.	0.	0.	0.	0.	0.	34.23	41.	1044.	1099.	99.0	99.0	1	
28	14	12.0	-10.0	0.	0.	0.	0.	0.	0.	0.	34.05	80.	1031.	1133.	99.0	99.0	1	

GP78-0822-218

C	DYNL DEG	NOSE GEAR	NOSE INLET	UNIT COVERS	OTHER	RUN	PT	BALANCE FORCE AND MOMENT DATA--STABILITY AXES LIFT (LB)	DRAG (LB)	PITCHING MOMENT (FT-LB)	SIDE FORCE (LB)	ROLLING MOMENT (FT-LB)	YAWING MOMENT (FT-LB)	TUNNEL TOTAL TEMP. (DEG F)	AMBIENT PRESSURE (IN HG)
.0	90.0	1		1		26	2	2282.	-66.	-7819.	5.	511.	-231.	84.	30.09
.0	90.0	1		1		26	3	3803.	9.	-5671.	-15.	941.	-65.	84.	30.09
.0	90.0	1		1		26	4	5464.	122.	-3949.	-46.	975.	27.	84.	30.09
.0	90.0	1		1		26	5	6277.	231.	-3508.	-9.	572.	111.	84.	30.09
.0	90.0	1		1		26	6	7151.	359.	-3001.	-25.	982.	157.	84.	30.09
.0	90.0	1		1		26	7	8015.	488.	-1932.	-25.	778.	76.	84.	30.09
.0	90.0	1		1		26	8	8377.	869.	-941.	-135.	3153.	764.	84.	30.09
.0	90.0	1		1		26	9	7588.	1283.	674.	-13.	17.	299.	84.	30.09
.0	90.0	1		1		26	10	7653.	1471.	867.	-25.	237.	172.	84.	30.09
.0	90.0	1		1		26	11	8714.	2501.	1404.	13.	284.	-211.	84.	30.09
.0	90.0	1		1		26	12	9358.	3440.	768.	-21.	690.	229.	84.	30.09
.0	90.0	1		1		26	13	9145.	4401.	2105.	-3.	-532.	823.	84.	30.09
.0	90.0	1		1		26	14	2044.	809.	-7442.	3.	1112.	14.	84.	30.09
.0	90.0	1		1		26	15	5109.	997.	-5144.	-12.	714.	70.	82.	30.09
.0	90.0	1		1		26	16	6661.	1207.	-3993.	-9.	598.	133.	82.	30.09
.0	90.0	1		1		26	17	7180.	1407.	-2868.	105.	-2328.	-154.	81.	30.09
.0	90.0	1		1		26	18	7129.	1830.	-1770.	114.	-2937.	214.	81.	30.09
.0	90.0	1		1		26	19	6484.	2149.	-140.	50.	-1741.	323.	81.	30.09
.0	90.0	1		1		27	1	-160.	-151.	-6018.	16.	605.	-310.	70.	30.09
.0	90.0	1		1		27	2	1670.	-182.	-5042.	3.	842.	-183.	71.	30.09
.0	90.0	1		1		27	3	3638.	-135.	-3749.	-12.	600.	-161.	71.	30.09
.0	90.0	1		1		27	4	5052.	-16.	-2544.	-45.	774.	-29.	72.	30.09
.0	90.0	1		1		27	5	6740.	193.	-1120.	-19.	264.	75.	72.	30.09
.0	90.0	1		1		27	6	8042.	623.	383.	-84.	1470.	736.	72.	30.09
.0	90.0	1		1		27	7	7431.	1056.	1590.	12.	-968.	331.	73.	30.09
.0	90.0	1		1		27	8	7407.	1438.	2184.	-14.	327.	-37.	73.	30.09
.0	90.0	1		1		27	9	8258.	2203.	3044.	25.	-116.	-32.	73.	30.09
.0	90.0	1		1		27	10	9035.	3167.	6966.	-11.	197.	244.	73.	30.09
.0	90.0	1		1		27	11	8850.	4131.	3959.	54.	-585.	441.	73.	30.09
.0	90.0	1		1		27	12	-250.	257.	-6062.	34.	343.	-334.	73.	30.09
.0	90.0	1		1		27	13	1543.	214.	-5000.	20.	509.	-260.	73.	30.09
.0	90.0	1		1		27	14	3322.	259.	-4052.	-2.	566.	-92.	73.	30.09
.0	90.0	1		1		27	15	4544.	374.	-2648.	-8.	502.	-22.	73.	30.09
.0	90.0	1		1		27	16	6549.	576.	-1508.	-22.	671.	44.	73.	30.09
.0	90.0	1		1		27	17	7375.	702.	-422.	-3.	331.	171.	73.	30.09
.0	90.0	1		1		27	18	7849.	982.	-267.	-45.	1341.	491.	73.	30.09
.0	90.0	1		1		27	19	7127.	1779.	2219.	-15.	17.	12.	73.	30.09
.0	90.0	1		1		28	1	-324.	524.	-6172.	50.	554.	-304.	73.	30.09
.0	90.0	1		1		28	2	1431.	492.	-5178.	45.	187.	-319.	73.	30.09
.0	90.0	1		1		28	3	3163.	526.	-3886.	37.	76.	-274.	73.	30.09
.0	90.0	1		1		28	4	4754.	634.	-3077.	10.	200.	-114.	73.	30.09
.0	90.0	1		1		28	5	6404.	828.	-1606.	10.	452.	-55.	73.	30.09
.0	90.0	1		1		28	6	7170.	968.	-1122.	21.	-3.	-105.	73.	30.09
.0	90.0	1		1		28	7	7541.	1218.	-667.	-54.	1541.	611.	73.	30.09
.0	90.0	1		1		28	8	7011.	1627.	854.	28.	-1327.	356.	73.	30.09
.0	90.0	1		1		28	9	6838.	2050.	1995.	-47.	1064.	-72.	73.	30.09
.0	90.0	1		1		29	10	-242.	724.	-6168.	75.	282.	-447.	72.	30.09
.0	90.0	1		1		28	11	1412.	689.	-5489.	51.	342.	-295.	72.	30.09
.0	90.0	1		1		28	12	3094.	722.	-4342.	23.	310.	-235.	72.	30.09
.0	90.0	1		1		28	13	4685.	824.	-3215.	-6.	651.	-76.	71.	30.09
.0	90.0	1		1		28	14	6193.	1020.	-2017.	15.	-97.	-66.	71.	30.09

MACH	PT	ALPHA DEG	ETA DEG	DLC DEG	DYL DEG	DF DEG	DAL DEG	DSR DEG	DH DEG	DM DEG	QC PSF	FAN1 RPM	FAN2 RPM	FAN3 RPM	DYLC DEG	DYYL DEG	NOSE GEAR
2M	15	14.0	-0.0	0.	0.	0.	0.	0.	-90.	0.	34.12	37.	922.	1086.	99.0	99.0	1
2M	16	16.0	-0.0	0.	0.	0.	0.	0.	-90.	0.	34.37	260.	801.	1104.	99.0	99.0	1
2M	17	18.0	-0.0	0.	0.	0.	0.	0.	-90.	0.	34.1M	8.	734.	1104.	99.0	99.0	1
2M	18	20.0	-0.0	0.	0.	0.	0.	0.	-90.	0.	34.26	44.	652.	1097.	99.0	99.0	1
3M	1	0.0	-0.0	90.	90.	15.	10.	10.	0.	0.	0.00	3575.	3549.	3581.	12.0	-12.0	2
3M	2	2.0	-0.0	90.	90.	15.	10.	10.	0.	0.	1.1M	3540.	3548.	3578.	12.0	-12.0	2
3M	3	4.0	-0.0	90.	90.	15.	10.	10.	0.	0.	3.24	3507.	3540.	3602.	12.0	-12.0	2
3M	4	6.0	-0.0	90.	90.	15.	10.	10.	0.	0.	6.42	3474.	3487.	3544.	12.0	-12.0	2
3M	1	0.0	-0.0	90.	90.	15.	10.	10.	0.	0.	0.00	39.	0.	0.	0.0	0.0	2
3M	2	0.0	-0.0	90.	90.	15.	10.	10.	0.	0.	0.00	3508.	3606.	3626.	0.0	0.0	2
3M	1	-4.0	-0.0	90.	90.	15.	10.	10.	0.	0.	1.30	3481.	3616.	3606.	0.0	0.0	2
3M	2	0.0	-0.0	90.	90.	15.	10.	10.	0.	0.	1.19	3547.	3601.	3591.	0.0	0.0	2
3M	3	4.0	-0.0	90.	90.	15.	10.	10.	0.	0.	1.40	3590.	3594.	3588.	0.0	0.0	2
3M	4	6.0	-0.0	90.	90.	15.	10.	10.	0.	0.	1.20	3591.	3600.	3596.	0.0	0.0	2
3M	5	12.0	-0.0	90.	90.	15.	10.	10.	0.	0.	1.40	3594.	3607.	3599.	0.0	0.0	2
3M	6	14.0	-0.0	90.	90.	15.	10.	10.	0.	0.	1.42	3597.	3603.	3588.	0.0	0.0	2
3M	7	16.0	-0.0	90.	90.	15.	10.	10.	0.	0.	1.38	3604.	3613.	3618.	0.0	0.0	2
3M	8	20.0	-0.0	90.	90.	15.	10.	10.	0.	0.	1.3M	3596.	3604.	3592.	0.0	0.0	2
3M	1	-4.0	-0.0	90.	90.	15.	10.	10.	0.	0.	7.16	360.	412.	430.	0.0	0.0	2
3M	2	0.0	-0.0	90.	90.	15.	10.	10.	0.	0.	7.16	304.	400.	418.	0.0	0.0	2
3M	3	4.0	-0.0	90.	90.	15.	10.	10.	0.	0.	7.17	219.	356.	399.	0.0	0.0	2
3M	4	8.0	-0.0	90.	90.	15.	10.	10.	0.	0.	7.16	112.	349.	382.	0.0	0.0	2
3M	5	12.0	-0.0	90.	90.	15.	10.	10.	0.	0.	7.14	28.	317.	384.	0.0	0.0	2
3M	6	14.0	-0.0	90.	90.	15.	10.	10.	0.	0.	7.24	0.	159.	386.	0.0	0.0	2
3M	7	16.0	-0.0	90.	90.	15.	10.	10.	0.	0.	7.13	44.	54.	379.	0.0	0.0	2
3M	8	20.0	-0.0	90.	90.	15.	10.	10.	0.	0.	7.15	110.	0.	232.	0.0	0.0	2
3M	1	0.0	-0.0	90.	15.	15.	10.	10.	0.	0.	1.30	3572.	3579.	3563.	0.0	0.0	2
3M	2	0.0	-0.0	90.	90.	15.	10.	10.	0.	0.	1.68	3610.	3606.	3590.	0.0	0.0	2
3M	3	0.0	-0.0	90.	75.	15.	10.	10.	0.	0.	1.22	3635.	3641.	3622.	0.0	0.0	2
3M	1	-4.0	-0.0	90.	90.	15.	10.	10.	0.	0.	3.2M	3626.	3618.	3611.	0.0	0.0	2
3M	2	0.0	-0.0	90.	90.	15.	10.	10.	0.	0.	3.26	3610.	3608.	3614.	0.0	0.0	2
3M	3	4.0	-0.0	90.	90.	15.	10.	10.	0.	0.	3.17	3600.	3604.	3603.	0.0	0.0	2
3M	4	8.0	-0.0	90.	90.	15.	10.	10.	0.	0.	3.28	3605.	3620.	3603.	0.0	0.0	2
3M	5	12.0	-0.0	90.	90.	15.	10.	10.	0.	0.	3.37	3607.	3601.	3623.	0.0	0.0	2
3M	6	14.0	-0.0	90.	90.	15.	10.	10.	0.	0.	3.25	3599.	3600.	3604.	0.0	0.0	2
3M	7	16.0	-0.0	90.	90.	15.	10.	10.	0.	0.	3.24	3597.	3600.	3594.	0.0	0.0	2
3M	8	20.0	-0.0	90.	90.	15.	10.	10.	0.	0.	3.30	3591.	3600.	3598.	0.0	0.0	2
3S	1	0.0	-0.0	90.	100.	15.	10.	10.	0.	0.	3.40	3611.	3610.	3612.	0.0	0.0	2
3S	2	0.0	-0.0	90.	80.	15.	10.	10.	0.	0.	3.22	3593.	3596.	3599.	0.0	0.0	2
3S	3	2.0	-0.0	90.	70.	15.	10.	10.	0.	0.	3.37	3595.	3605.	3611.	0.0	0.0	2
3G	1	-4.0	-0.0	90.	90.	15.	10.	10.	0.	0.	7.19	3627.	3632.	3626.	0.0	0.0	2
3G	2	0.0	-0.0	90.	90.	15.	10.	10.	0.	0.	7.03	3605.	3604.	3600.	0.0	0.0	2
3G	3	4.0	-0.0	90.	90.	15.	10.	10.	0.	0.	6.92	3590.	3615.	3606.	0.0	0.0	2
3G	4	8.0	-0.0	90.	90.	15.	10.	10.	0.	0.	7.24	3643.	3613.	3607.	0.0	0.0	2
3G	5	12.0	-0.0	90.	90.	15.	10.	10.	0.	0.	7.22	3602.	3696.	3733.	0.0	0.0	2
3G	6	14.0	-0.0	90.	90.	15.	10.	10.	0.	0.	7.07	3596.	3631.	3634.	0.0	0.0	2
3G	7	16.0	-0.0	90.	90.	15.	10.	10.	0.	0.	7.09	3591.	3654.	3655.	0.0	0.0	2
3G	8	20.0	-0.0	90.	90.	15.	10.	10.	0.	0.	7.34	3613.	3603.	3691.	0.0	0.0	2
3T	1	0.0	-0.0	90.	100.	15.	10.	10.	0.	0.	7.18	3726.	3638.	3645.	0.0	0.0	2
3T	2	0.0	-0.0	90.	90.	15.	10.	10.	0.	0.	7.03	3601.	3597.	3592.	0.0	0.0	2
3T	3	0.0	-0.0	90.	70.	15.	10.	10.	0.	0.	7.19	3588.	3597.	3599.	0.0	0.0	2

GP78-0822-216

OYLC DEG	OYNL DEG	NOSE GEAR	NOSE INLET	UNIT COVERS	OTHER	RUN	PT	BALANCE FORCE AND MOMENT DATA--STABILITY AXES LIFT (LB)	DRAG (LB)	PITCHING MOMENT (FT-LB)	SIDE FORCE (LB)	ROLLING MOMENT (FT-LB)	YAWING MOMENT (FT-LB)	TUNNEL TOTAL TEMP. (DEG F)	AMBIENT PRESSURE (IN HG)
99.0	99.0	1		1		28	15	6682.	1235.	-1818.	84.	-2067.	-294.	71.	30.09
99.0	99.0	1		1		28	16	6619.	1620.	-367.	133.	-3303.	24.	71.	30.09
99.0	99.0	1		1		28	17	6261.	1477.	1124.	67.	-1440.	244.	71.	30.09
99.0	99.0	1		1		28	18	6134.	2274.	1484.	25.	-548.	205.	71.	30.09
12.0	-12.0	2		2		29	1	3345.	-513.	134.	88.	-980.	-3937.	74.	30.04
12.0	-12.0	2		2		29	2	3709.	-60.	835.	93.	73.	-3575.	74.	30.04
12.0	-12.0	2		2		29	3	4000.	270.	839.	46.	-258.	-3594.	75.	30.04
12.0	-12.0	2		2		29	4	4503.	721.	741.	67.	-434.	-3301.	77.	30.04
0.0	0.0	2		2		30	1	10.	-0.	-244.	1.	10.	-1.	75.	30.04
0.0	0.0	2		2		30	2	3527.	-543.	155.	15.	-234.	-167.	74.	30.04
0.0	0.0	2		2		31	1	3655.	-389.	249.	13.	-175.	41.	74.	30.04
0.0	0.0	2		2		31	2	3734.	-145.	433.	-11.	-108.	-109.	75.	30.04
0.0	0.0	2		2		31	3	3884.	161.	707.	-14.	-107.	-77.	77.	30.04
0.0	0.0	2		2		31	4	3978.	419.	832.	-5.	-162.	-45.	78.	30.04
0.0	0.0	2		2		31	5	4231.	776.	968.	0.	-72.	53.	79.	30.04
0.0	0.0	2		2		31	6	4226.	934.	909.	-17.	10.	177.	79.	30.04
0.0	0.0	2		2		31	7	4188.	1100.	343.	-23.	27.	214.	79.	30.04
0.0	0.0	2		2		31	8	4115.	1432.	38.	-0.	-216.	-1.	79.	30.04
0.0	0.0	2		2		32	1	526.	319.	-1963.	-12.	239.	181.	77.	30.04
0.0	0.0	2		2		32	2	868.	329.	-2328.	-8.	147.	153.	77.	30.04
0.0	0.0	2		2		32	3	1225.	342.	-2557.	-10.	250.	130.	77.	30.04
0.0	0.0	2		2		32	4	1585.	384.	-2957.	-5.	185.	77.	77.	30.04
0.0	0.0	2		2		32	5	1877.	462.	-3134.	4.	12.	70.	76.	30.04
0.0	0.0	2		2		32	6	1852.	517.	-2889.	-7.	633.	391.	75.	30.04
0.0	0.0	2		2		32	7	1863.	592.	-2859.	-12.	884.	339.	73.	30.04
0.0	0.0	2		2		32	8	1875.	664.	-2221.	-6.	272.	73.	73.	30.04
0.0	0.0	2		2		33	1	3764.	455.	-1125.	-36.	320.	190.	69.	30.05
0.0	0.0	2		2		33	2	3861.	60.	-1075.	-6.	-82.	65.	61.	30.05
0.0	0.0	2		2		33	3	3763.	-269.	616.	-3.	-74.	104.	62.	30.05
0.0	0.0	2		2		34	1	3943.	249.	444.	-30.	224.	417.	66.	30.05
0.0	0.0	2		2		34	2	4114.	507.	565.	-23.	117.	460.	66.	30.05
0.0	0.0	2		2		34	3	4321.	801.	580.	-33.	227.	493.	67.	30.05
0.0	0.0	2		2		34	4	4505.	1114.	448.	-38.	443.	464.	67.	30.05
0.0	0.0	2		2		34	5	4615.	1510.	-351.	-49.	584.	514.	69.	30.05
0.0	0.0	2		2		34	6	4693.	1464.	450.	-32.	380.	329.	70.	30.05
0.0	0.0	2		2		34	7	4705.	1453.	653.	-32.	365.	334.	71.	30.05
0.0	0.0	2		2		34	8	4584.	2204.	911.	-6.	-139.	145.	72.	30.05
0.0	0.0	2		2		35	1	4134.	782.	-1009.	-58.	-122.	291.	71.	30.05
0.0	0.0	2		2		35	2	4117.	317.	869.	-33.	-98.	113.	73.	30.05
0.0	0.0	2		2		35	3	4124.	134.	563.	-27.	-422.	-73.	73.	30.05
0.0	0.0	2		2		36	1	4274.	751.	9.	61.	398.	860.	72.	30.05
0.0	0.0	2		2		36	2	4656.	1017.	96.	47.	465.	745.	72.	30.05
0.0	0.0	2		2		36	3	4922.	1346.	-498.	45.	521.	693.	73.	30.05
0.0	0.0	2		2		36	4	5305.	1730.	-222.	58.	184.	615.	73.	30.05
0.0	0.0	2		2		36	5	5515.	2110.	230.	-3.	67.	454.	73.	30.05
0.0	0.0	2		2		36	6	5508.	2259.	649.	-33.	592.	563.	73.	30.05
0.0	0.0	2		2		36	7	5454.	2411.	975.	-9.	349.	285.	73.	30.05
0.0	0.0	2		2		36	8	5357.	2712.	1106.	32.	-447.	-50.	74.	30.05
0.0	0.0	2		2		37	1	4452.	1310.	-1847.	30.	-23.	299.	74.	30.05
0.0	0.0	2		2		37	2	4693.	792.	1112.	3.	89.	94.	74.	30.05
0.0	0.0	2		2		37	3	4616.	589.	655.	11.	188.	70.	74.	30.05

GP78-0022-210

FOLDOUT FRAME

RUN	PT	ALPHA DEG	BETA DEG	DLC DEG	DNL DEG	DF DEG	DAL DEG	DAR DEG	DM DEG	DN DEG	QC PSF	FAN1 RPM	FAN2 RPM	FAN3 RPM	DYLC DEG	DYNL DEG	NOSE GEAR	I
38	1	0.0	-4.0	90.	90.	15.	10.	10.	0.	0.	1.42	3590.	3586.	3580.	0.0	0.0	2	
38	2	0.0	-0.0	90.	90.	15.	10.	10.	0.	0.	1.40	3577.	3605.	3580.	0.0	0.0	2	
38	3	0.0	4.0	90.	90.	15.	10.	10.	0.	0.	1.27	3604.	3621.	3609.	0.0	0.0	2	
38	4	0.0	8.0	90.	90.	15.	10.	10.	0.	0.	1.45	3606.	3630.	3608.	0.0	0.0	2	
38	5	0.0	12.0	90.	90.	15.	10.	10.	0.	0.	1.33	3620.	3626.	3619.	0.0	0.0	2	
39	1	0.0	-0.0	90.	90.	15.	10.	10.	-20.	0.	7.11	3634.	3668.	3659.	0.0	0.0	2	
39	2	0.0	-0.0	90.	90.	15.	10.	10.	-10.	0.	7.21	3609.	3667.	3656.	0.0	0.0	2	
39	3	0.0	-0.0	90.	90.	15.	10.	10.	0.	0.	7.21	3606.	3637.	3607.	0.0	0.0	2	
39	4	0.0	-0.0	90.	90.	15.	10.	10.	10.	0.	7.16	3600.	3530.	3608.	0.0	0.0	2	
39	5	0.0	-0.0	90.	90.	15.	10.	10.	20.	0.	7.09	3621.	3616.	3613.	0.0	0.0	2	
40	1	0.0	-0.0	90.	90.	15.	10.	10.	-20.	0.	1.48	3605.	3610.	3615.	0.0	0.0	2	
40	2	0.0	-0.0	90.	90.	15.	10.	10.	-10.	0.	1.32	3603.	3603.	3602.	0.0	0.0	2	
40	3	0.0	-0.0	90.	90.	15.	10.	10.	0.	0.	1.33	3618.	3622.	3616.	0.0	0.0	2	
40	4	0.0	-0.0	90.	90.	15.	10.	10.	10.	0.	1.35	3616.	3621.	3612.	0.0	0.0	2	
40	5	0.0	-0.0	90.	90.	15.	10.	10.	20.	0.	1.47	3612.	3618.	3609.	0.0	0.0	2	
40	6	0.0	-0.0	90.	90.	15.	10.	10.	-20.	0.	1.28	3614.	3616.	3613.	0.0	0.0	2	
41	1	0.0	-4.0	90.	90.	15.	10.	10.	0.	0.	3.29	3610.	3610.	3609.	0.0	0.0	2	
41	2	0.0	-0.0	90.	90.	15.	10.	0.	0.	0.	3.31	3611.	3607.	3603.	0.0	0.0	2	
41	3	0.0	4.0	90.	90.	15.	10.	10.	0.	0.	3.31	3618.	3635.	3635.	0.0	0.0	2	
41	4	0.0	8.0	90.	90.	15.	10.	10.	0.	0.	3.31	3614.	3631.	3635.	0.0	0.0	2	
41	5	0.0	12.0	90.	90.	15.	10.	10.	0.	0.	3.31	3613.	3622.	3616.	0.0	0.0	2	
42	1	0.0	-4.0	90.	90.	15.	10.	10.	0.	0.	7.16	3612.	3611.	3612.	0.0	0.0	2	
42	2	0.0	-0.0	90.	90.	15.	10.	10.	0.	0.	7.16	3634.	3626.	3621.	0.0	0.0	2	
42	3	0.0	4.0	90.	90.	15.	10.	10.	0.	0.	7.14	3615.	3621.	3623.	0.0	0.0	2	
42	4	0.0	8.0	90.	90.	15.	10.	10.	0.	0.	7.16	3625.	3720.	3750.	0.0	0.0	2	
42	5	0.0	12.0	90.	90.	15.	10.	10.	0.	0.	7.09	3619.	3629.	3625.	0.0	0.0	2	
43	1	8.0	-0.0	90.	90.	15.	10.	10.	10.	0.	.99	3617.	3604.	3610.	0.0	0.0	2	
43	2	8.0	-0.0	90.	90.	15.	10.	10.	20.	0.	1.15	3610.	3609.	3617.	0.0	0.0	2	
43	3	15.0	-0.0	90.	90.	15.	10.	10.	10.	0.	1.10	3608.	3613.	3607.	0.0	0.0	2	
43	4	16.0	-0.0	90.	90.	15.	10.	10.	20.	0.	1.03	3615.	3611.	3611.	0.0	0.0	2	
43	5	0.0	-0.0	90.	90.	15.	10.	10.	-10.	0.	3.26	3610.	3618.	3613.	0.0	0.0	2	
43	6	0.0	-0.0	90.	90.	15.	10.	10.	10.	0.	3.25	3607.	3616.	3613.	0.0	0.0	2	
43	7	0.0	-0.0	90.	90.	15.	10.	10.	20.	0.	3.24	3608.	3612.	3610.	0.0	0.0	2	
43	8	4.0	-0.0	90.	90.	15.	10.	10.	-10.	0.	3.19	3608.	3610.	3605.	0.0	0.0	2	
43	9	4.0	-0.0	90.	90.	15.	10.	10.	10.	0.	3.21	3622.	3611.	3622.	0.0	0.0	2	
43	10	4.0	-0.0	90.	90.	15.	10.	10.	20.	0.	3.19	3606.	3612.	3611.	0.0	0.0	2	
43	11	16.0	-0.0	90.	90.	15.	10.	10.	-10.	0.	3.20	3607.	3621.	3621.	0.0	0.0	2	
43	12	16.0	-0.0	90.	90.	15.	10.	10.	10.	0.	3.21	3608.	3612.	3615.	0.0	0.0	2	
43	13	16.0	-0.0	90.	90.	15.	10.	10.	20.	0.	3.21	3609.	3610.	3613.	0.0	0.0	2	
43	14	8.0	-0.0	90.	90.	15.	10.	10.	-20.	0.	6.97	3609.	3620.	3621.	0.0	0.0	2	
43	15	8.0	-0.0	90.	90.	15.	10.	10.	-10.	0.	7.03	3609.	3618.	3620.	0.0	0.0	2	
43	16	8.0	-0.0	90.	90.	15.	10.	10.	10.	0.	6.97	3615.	3639.	3616.	0.0	0.0	2	
43	17	8.0	-0.0	90.	90.	15.	10.	10.	20.	0.	6.92	3762.	3685.	3673.	0.0	0.0	2	
43	18	16.0	-0.0	90.	90.	15.	10.	10.	-20.	0.	6.96	3619.	3620.	3621.	0.0	0.0	2	
43	19	16.0	-0.0	90.	90.	15.	10.	10.	-10.	0.	6.96	3645.	3620.	3619.	0.0	0.0	2	
43	20	16.0	-0.0	90.	90.	15.	10.	10.	10.	0.	6.94	3739.	3665.	3649.	0.0	0.0	2	
43	21	16.0	-0.0	90.	90.	15.	10.	10.	20.	0.	6.93	3645.	3617.	3617.	0.0	0.0	2	
44	1	0.0	-4.0	90.	90.	15.	10.	10.	0.	0.	6.94	280.	414.	412.	0.0	0.0	2	
44	2	0.0	-0.0	90.	90.	15.	10.	10.	0.	0.	6.97	295.	400.	427.	0.0	0.0	2	
44	3	0.0	4.0	90.	90.	15.	10.	10.	0.	0.	7.04	313.	391.	436.	0.0	0.0	2	
44	4	0.0	8.0	90.	90.	15.	10.	10.	0.	0.	6.88	316.	396.	448.	0.0	0.0	2	

GP78-0822-217

LC	DYNL DEG	NOSE GEAR	NOSE INLET	UNIT COVERS	OTHER	RUN	PT	BALANCE FORCE AND MOMENT DATA--STABILITY AXES LIFT (LM)	DRAG (LM)	PITCHING MOMENT (FT-LB)	SIDE FORCE (LM)	ROLLING MOMENT (FT-LB)	YAWING MOMENT (FT-LB)	TUNNEL TOTAL TEMP. (DEG F)	AMBIENT PRESSURE (IN HG)
.0	0.0					38	1	3756.	232.	-424.	72.	404.	291.	71.	30.14
.0	0.0					38	2	3729.	234.	-411.	-3.	-180.	108.	73.	30.14
.0	0.0					38	3	3791.	207.	-703.	-101.	82.	-120.	75.	30.14
.0	0.0					38	4	3813.	234.	-664.	-159.	-655.	-280.	77.	30.14
.0	0.0					38	5	3837.	203.	-382.	-223.	-404.	-623.	78.	30.14
.0		2				39	1	4606.	1082.	578.	44.	374.	513.	80.	30.14
.0						39	2	4594.	1075.	931.	45.	379.	173.	80.	30.14
.0						39	3	4684.	1012.	19.	40.	507.	407.	81.	30.14
.0						39	4	4807.	1002.	-1827.	23.	306.	344.	82.	30.14
.0						39	5	5045.	1038.	-4147.	24.	663.	591.	82.	30.14
.0						40	1	3736.	244.	329.	-11.	43.	30.	75.	30.07
.0						40	2	3729.	200.	462.	-11.	-57.	27.	76.	30.07
.0						40	3	3734.	202.	460.	-6.	-24.	28.	77.	30.07
.0						40	4	3807.	219.	-173.	-22.	117.	14.	78.	30.07
.0						40	5	3832.	234.	-533.	-13.	46.	16.	79.	30.07
.0						40	6	4015.	804.	715.	-7.	122.	146.	81.	30.07
.0						41	1	4107.	504.	510.	118.	1049.	649.	76.	30.03
.0	0.0					41	2	4096.	512.	181.	-13.	348.	503.	78.	30.03
.0	0.0					41	3	4136.	518.	61.	-148.	261.	380.	78.	30.03
.0	0.0					41	4	4170.	512.	36.	-283.	-142.	187.	80.	30.03
.0	0.0					41	5	4147.	506.	-314.	-400.	-441.	-302.	80.	30.03
.0	0.0					42	1	4562.	1027.	-244.	276.	1240.	1052.	83.	30.03
.0	0.0					42	2	4523.	1047.	-715.	47.	806.	951.	84.	30.03
.0	0.0					42	3	4713.	1029.	-27.	-210.	-546.	633.	84.	30.03
.0	0.0					42	4	4795.	1012.	-709.	-484.	-1582.	485.	84.	30.03
.0	0.0					42	5	4874.	980.	-723.	-734.	-1459.	223.	85.	30.03
.0	0.0					43	1	4001.	757.	-200.	-22.	264.	243.	80.	30.03
.0	0.0					43	2	4064.	799.	-487.	-9.	251.	180.	80.	30.03
.0	0.0					43	3	4030.	1371.	-949.	-7.	153.	170.	81.	30.03
.0	0.0					43	4	4042.	1369.	-1160.	-9.	-52.	191.	81.	30.03
.0	0.0					43	5	4061.	567.	455.	3.	232.	235.	83.	30.03
.0	0.0					43	6	4162.	537.	-712.	-15.	319.	475.	83.	30.03
.0	0.0					43	7	4249.	553.	-1609.	-11.	253.	374.	83.	30.03
.0	0.0					43	8	4364.	1150.	846.	-25.	335.	357.	84.	30.03
.0	0.0					43	9	4517.	1150.	-1018.	-20.	333.	456.	84.	30.03
.0	0.0					43	10	4587.	1183.	-1773.	-29.	492.	603.	84.	30.03
.0	0.0					43	11	4590.	1483.	1415.	-48.	619.	270.	84.	30.03
.0	0.0					43	12	4726.	1914.	-663.	-[illegible]	591.	343.	85.	30.03
.0	0.0					43	13	4758.	1961.	-1149.	-[illegible]	614.	241.	85.	30.03
.0	0.0					43	14	5141.	1756.	760.	[illegible]	103.	717.	85.	30.03
.0	0.0					43	15	5124.	1719.	1785.	12.	376.	684.	85.	30.03
.0	0.0					43	16	5434.	1716.	-2329.	30.	614.	559.	85.	30.03
.0	0.0					43	17	5588.	1765.	-3944.	9.	546.	517.	85.	30.03
.0	0.0					43	18	5368.	2469.	2670.	-15.	502.	186.	85.	30.03
.0	0.0					43	19	5328.	2386.	3355.	-29.	282.	128.	85.	30.03
.0	0.0					43	20	5647.	2475.	-1630.	-16.	104.	146.	85.	30.03
.0	0.0					43	21	5645.	2543.	-1916.	14.	-60.	220.	85.	30.03
.0	0.0					44	1	859.	320.	-2469.	118.	244.	-285.	81.	30.03
.0	0.0					44	2	841.	325.	-2507.	-11.	289.	169.	80.	30.03
.0	0.0					44	3	832.	323.	-2787.	-126.	290.	489.	80.	30.03
.0	0.0					44	4	851.	307.	-2735.	-264.	413.	1035.	80.	30.03

D822-217

FOLDOUT FR[illegible] 2

RUN	PT	ALPHA DEG	BETA DEG	ULC DEG	DAL DEG	AF DEG	UAL DEG	UAR DEG	DH DEG	DR DEG	QC PSF	FAN1 RPM	FAN2 RPM	FAN3 RPM	DYLC DEG	DYNL DEG	NOSE GEAR	NOSE INLET
44	5	0.0	12.0	90.	90.	15.	10.	10.	0.	0.	6.99	304.	362.	449.	0.0	0.0	2	
44	6	0.0	-0.0	90.	90.	15.	10.	10.	-20.	0.	6.97	295.	401.	426.	0.0	0.0		
44	7	0.0	-0.0	90.	90.	15.	10.	10.	-10.	0.	6.99	296.	404.	426.	0.0	0.0		
44	8	0.0	-0.0	90.	90.	15.	10.	10.	10.	0.	7.00	297.	399.	428.	0.0	0.0		
44	9	0.0	-0.0	90.	90.	15.	10.	10.	20.	0.	6.99	296.	399.	430.	0.0	0.0		
45	1	-4.0	-0.0	90.	90.	15.	10.	10.	99.	0.	1.28	3610.	3615.	3616.	0.0	0.0		
45	2	0.0	-0.0	90.	90.	15.	10.	10.	99.	0.	1.27	3608.	3615.	3611.	0.0	0.0		
45	3	4.0	-0.0	90.	90.	15.	10.	10.	99.	0.	1.51	3600.	3606.	3604.	0.0	0.0		
45	4	8.0	-0.0	90.	90.	15.	10.	10.	99.	0.	1.23	3598.	3612.	3616.	0.0	0.0		
45	5	12.0	-0.0	90.	90.	15.	10.	10.	99.	0.	1.28	3602.	3600.	3594.	0.0	0.0		
45	6	14.0	-0.0	90.	90.	15.	10.	10.	99.	0.	1.44	3612.	3605.	3603.	0.0	0.0		
45	7	16.0	-0.0	90.	90.	15.	10.	10.	99.	0.	1.41	3602.	3601.	3601.	0.0	0.0		
45	8	20.0	-0.0	90.	90.	15.	10.	10.	99.	0.	1.20	3610.	3629.	3615.	0.0	0.0		
45	9	32.0	-0.0	90.	90.	15.	10.	10.	99.	0.	1.71	3600.	3626.	3606.	0.0	0.0		
45	10	0.0	-0.0	90.	100.	15.	10.	10.	99.	0.	1.16	3615.	3623.	3622.	0.0	0.0		
45	11	0.0	-0.0	90.	80.	15.	10.	10.	99.	0.	1.31	3611.	3619.	3617.	0.0	0.0		
45	12	0.0	-0.0	90.	70.	15.	10.	10.	99.	0.	1.41	3605.	3641.	3622.	0.0	0.0		
46	1	-4.0	-0.0	90.	90.	15.	10.	10.	99.	0.	3.28	3607.	3627.	3637.	0.0	0.0		
46	2	0.0	-0.0	90.	90.	15.	10.	10.	99.	0.	3.20	3605.	3627.	3638.	0.0	0.0		
46	3	4.0	-0.0	90.	90.	15.	10.	10.	99.	0.	3.46	3609.	3626.	3636.	0.0	0.0		
46	4	8.0	-0.0	90.	90.	15.	10.	10.	99.	0.	3.34	3600.	3620.	3618.	0.0	0.0		
46	5	12.0	-0.0	90.	90.	15.	10.	10.	99.	0.	3.38	3595.	3615.	3614.	0.0	0.0		
46	6	14.0	-0.0	90.	90.	15.	10.	10.	99.	0.	3.37	3593.	3610.	3608.	0.0	0.0		
46	7	16.0	-0.0	90.	90.	15.	10.	10.	99.	0.	3.42	3571.	3601.	3603.	0.0	0.0		
46	8	20.0	-0.0	90.	90.	15.	10.	10.	99.	0.	3.28	3568.	3603.	3594.	0.0	0.0		
47	1	0.0	-0.0	90.	100.	15.	10.	10.	99.	0.	3.29	3563.	3588.	3587.	0.0	0.0		
47	2	0.0	-0.0	90.	80.	15.	10.	10.	99.	0.	3.36	3568.	3584.	3590.	0.0	0.0		
47	3	0.0	-0.0	90.	70.	15.	10.	10.	99.	0.	3.43	3559.	3580.	3586.	0.0	0.0		
47	4	0.0	-0.0	90.	100.	15.	10.	10.	99.	0.	7.08	3577.	3596.	3608.	0.0	0.0		
47	5	0.0	-0.0	90.	80.	15.	10.	10.	99.	0.	7.16	3570.	3579.	3628.	0.0	0.0		
47	6	0.0	-0.0	90.	70.	15.	10.	10.	99.	0.	7.25	3565.	3579.	3581.	0.0	0.0		
48	1	-4.0	-0.0	90.	90.	15.	10.	10.	99.	0.	7.10	3560.	3574.	3567.	0.0	0.0		
48	2	0.0	-0.0	90.	90.	15.	10.	10.	99.	0.	7.23	3561.	3570.	3562.	0.0	0.0		
48	3	4.0	-0.0	90.	90.	15.	10.	10.	99.	0.	7.11	3539.	3564.	3561.	0.0	0.0		
48	4	8.0	-0.0	90.	90.	15.	10.	10.	99.	0.	7.06	3570.	3595.	3647.	0.0	0.0		
48	5	12.0	-0.0	90.	90.	15.	10.	10.	99.	0.	7.24	3544.	3620.	3570.	0.0	0.0		
48	6	14.0	-0.0	90.	90.	15.	10.	10.	99.	0.	7.14	3529.	3571.	3572.	0.0	0.0		
48	7	16.0	-0.0	90.	90.	15.	10.	10.	99.	0.	7.11	3540.	3582.	3599.	0.0	0.0		
48	8	20.0	-0.0	90.	90.	15.	10.	10.	99.	0.	7.14	3573.	3596.	3583.	0.0	0.0		
49	1	-4.0	-0.0	90.	90.	15.	10.	10.	99.	0.	7.09	90.	426.	447.	0.0	0.0		
49	2	0.0	-0.0	90.	90.	15.	10.	10.	99.	0.	7.17	0.	401.	423.	0.0	0.0		
49	3	4.0	-0.0	90.	90.	15.	10.	10.	99.	0.	7.19	0.	357.	402.	0.0	0.0		
49	4	8.0	-0.0	90.	90.	15.	10.	10.	99.	0.	7.21	0.	353.	387.	0.0	0.0		
49	5	12.0	-0.0	90.	90.	15.	10.	10.	99.	0.	7.21	0.	294.	395.	0.0	0.0		
49	6	14.0	-0.0	90.	90.	15.	10.	10.	99.	0.	7.19	0.	97.	390.	0.0	0.0		
49	7	16.0	-0.0	90.	90.	15.	10.	10.	99.	0.	7.14	0.	63.	378.	0.0	0.0		
49	8	20.0	-0.0	90.	90.	15.	10.	10.	99.	0.	7.14	0.	0.	234.	0.0	0.0		
50	1	0.0	-0.0	56.	43.	15.	10.	10.	99.	0.	0.00	3584.	40.	64.	0.0	0.0		
50	2	0.0	-0.0	56.	43.	15.	10.	10.	99.	0.	.57	3617.	3691.	3620.	0.0	0.0		
51	1	-4.0	-0.0	56.	43.	15.	10.	10.	99.	0.	3.31	3599.	3669.	3621.	0.0	0.0		
51	2	0.0	-0.0	56.	43.	15.	10.	10.	99.	0.	3.29	3598.	3657.	3611.	0.0	0.0	2	

GP76-0822-218

BALANCE FORCE AND MOMENT DATA--STABILITY AXES

DYNL DFG	NOSE GEAR	NOSE INLET	UNIT COVERS	OTHER	RUN	PT	LIFT (LB)	DRAG (LB)	PITCHING MOMENT (FT-LB)	SIDE FORCE (LB)	ROLLING MOMENT (FT-LB)	YAWING MOMENT (FT-LB)	TUNNEL TOTAL TEMP. (DEG F)	AMBIENT PRESSURE (IN HG)
0.0	2		2		44	5	842.	288.	-2546.	-363.	255.	1263.	80.	30.03
0.0	2		2		44	6	698.	410.	-392.	1.	59.	117.	80.	30.03
0.0	2		2		44	7	658.	370.	270.	-0.	-40.	175.	80.	30.03
0.0	2		2		44	8	1023.	333.	-4221.	-4.	29.	152.	80.	30.03
0.0	2		2		44	9	1133.	387.	-5287.	-6.	65.	174.	80.	30.03
0.0	2		2		45	1	3728.	-84.	-365.	4.	51.	45.	60.	30.03
0.0	2		2		45	2	3860.	176.	-257.	-20.	264.	180.	60.	30.03
0.0	2		2		45	3	4040.	513.	-697.	-8.	393.	197.	61.	30.03
0.0	2		2		45	4	3989.	760.	-769.	-33.	301.	-44.	61.	30.03
0.0	2		2		45	5	4055.	1078.	-1059.	-25.	278.	64.	62.	30.03
0.0	2		2		45	6	4093.	1267.	-1634.	-46.	426.	271.	62.	30.03
0.0	2		2		45	7	4057.	1387.	-1777.	-44.	349.	239.	63.	30.03
0.0	2		2		45	8	3934.	1615.	-1404.	-25.	229.	31.	64.	30.03
0.0	2		2		45	9	[illegible]	[illegible]	[illegible]	[illegible]	[illegible]	[illegible]	[illegible]	[illegible]
0.0	2		2		45	10	3839.	428.	-1883.	-7.	169.	249.	67.	30.03
0.0	2		2		45	11	3788.	-45.	151.	-7.	120.	90.	69.	30.03
0.0	2		2		45	12	3810.	-213.	-598.	-9.	29.	81.	69.	30.03
0.0	2		2		46	1	4054.	249.	-526.	13.	100.	147.	60.	30.05
0.0	2		2		46	2	4205.	501.	-589.	3.	100.	417.	61.	30.05
0.0	2		2		46	3	4476.	856.	-600.	-12.	175.	340.	62.	30.05
0.0	2		2		46	4	4528.	1137.	-1152.	2.	235.	378.	64.	30.05
0.0	2		2		46	5	4668.	1493.	-1043.	-31.	623.	566.	65.	30.05
0.0	2		2		46	6	4677.	1684.	-1109.	-42.	699.	466.	67.	30.05
0.0	2		2		46	7	4662.	1873.	-1239.	-13.	329.	260.	70.	30.05
0.0	2		2		46	8	4520.	2187.	-884.	10.	-10.	51.	70.	30.05
0.0	2		2		47	1	4046.	762.	-2239.	-12.	258.	441.	72.	30.05
0.0	2		2		47	2	4109.	336.	-357.	5.	-101.	90.	73.	30.05
0.0	2		2		47	3	4080.	152.	-696.	-14.	-306.	-93.	74.	30.05
0.0	2		2		47	4	4617.	1292.	-4040.	47.	-313.	246.	75.	30.05
0.0	2		2		47	5	4821.	801.	-1222.	21.	-117.	72.	76.	30.05
0.0	2		2		47	6	4783.	603.	-1757.	20.	-177.	-64.	77.	30.05
0.0	2		2		48	1	4431.	718.	-1980.	72.	-220.	569.	77.	30.05
0.0	2		2		48	2	4801.	1036.	-2298.	43.	-161.	215.	78.	30.05
0.0	2		2		48	3	5038.	1351.	-2707.	57.	-244.	266.	79.	30.05
0.0	2		2		48	4	5303.	1691.	-2144.	47.	119.	515.	79.	30.05
0.0	2		2		48	5	5539.	2067.	-1219.	-13.	227.	251.	79.	30.05
0.0	2		2		48	6	5474.	2231.	-1386.	-31.	936.	545.	80.	30.05
0.0	2		2		48	7	5414.	2372.	-914.	-0.	78.	180.	80.	30.05
0.0	2		2		48	8	5262.	2569.	-145.	21.	-616.	190.	80.	30.05
0.0	2				49	1	680.	422.	-2891.	-18.	480.	195.	79.	30.05
0.0	2				49	2	969.	331.	-3155.	-12.	391.	209.	77.	30.05
0.0	2				49	3	1268.	146.	-3439.	-10.	344.	149.	77.	30.05
0.0	2				49	4	1587.	389.	-3395.	-11.	368.	118.	77.	30.05
0.0	2				49	5	1825.	437.	-2920.	3.	143.	117.	76.	30.05
0.0	2				49	6	1735.	493.	-2766.	-27.	1062.	589.	75.	30.05
0.0	2				49	7	1784.	567.	-2735.	-14.	1041.	374.	75.	30.05
0.0	2				49	8	1584.	642.	-2082.	-23.	577.	181.	75.	30.05
0.0	2				50	1	675.	-832.	10644.	6.	-33.	23.	65.	29.92
0.0	2				50	2	2423.	-2379.	71.	-2.	-71.	202.	70.	29.92
0.0	2				51	1	2513.	-2152.	-530.	-12.	-111.	90.	80.	29.96
0.0	2				51	2	2850.	-1970.	-395.	8.	-239.	104.	81.	29.96

-0822-218

FOLDOUT FRAME 2

RUN	PT	ALPHA DEG	BETA DEG	DLC DEG	DNL DEG	DF DEG	DAL DEG	DAR DEG	DH DEG	TIR DEG	QC PSF	FAN1 RPM	FAN2 RPM	FAN3 RPM	DYLC DEG	DYNL DEG	NOSE GEAR	NO INL
51	3	4.0	-0.0	50.	43.	15.	10.	10.	99.	0.	3.29	3600.	3666.	3610.	0.0	0.0	2	
51	4	8.0	-0.0	50.	43.	15.	10.	10.	99.	0.	3.32	3595.	3654.	3605.	0.0	0.0	2	
51	5	12.0	-0.0	50.	43.	15.	10.	10.	99.	0.	3.29	3614.	3677.	3634.	0.0	0.0	2	
51	6	14.0	-0.0	50.	43.	15.	10.	10.	99.	0.	3.19	3610.	3681.	3623.	0.0	0.0	2	
51	7	16.0	-0.0	50.	43.	15.	10.	10.	99.	0.	3.24	3616.	3687.	3630.	0.0	0.0	2	
51	8	20.0	-0.0	50.	43.	15.	10.	10.	99.	0.	3.41	3613.	3684.	3631.	0.0	0.0	2	
52	1	0.0	-0.0	50.	38.	15.	10.	10.	99.	0.	3.24	3618.	3673.	3635.	0.0	0.0	2	
52	2	0.0	-0.0	50.	41.	15.	10.	10.	99.	0.	3.29	3660.	3723.	3627.	0.0	0.0	2	
52	3	0.0	-0.0	50.	40.	15.	10.	10.	99.	0.	3.41	3608.	3664.	3627.	0.0	0.0	2	
52	4	0.0	-0.0	50.	35.	15.	10.	10.	99.	0.	3.29	3624.	3662.	3624.	0.0	0.0	2	
52	5	0.0	-0.0	50.	43.	15.	10.	10.	99.	0.	1.90	3618.	3663.	3615.	0.0	0.0	2	
52	6	0.0	-0.0	50.	50.	15.	10.	10.	99.	0.	7.14	3610.	3654.	3621.	0.0	0.0	2	
52	7	0.0	-0.0	50.	45.	15.	10.	10.	99.	0.	7.19	3616.	3755.	3736.	0.0	0.0	2	
52	8	0.0	-0.0	50.	40.	15.	10.	10.	99.	0.	7.16	3657.	3673.	3644.	0.0	0.0	2	
52	9	0.0	-0.0	50.	35.	15.	10.	10.	99.	0.	7.16	3616.	3665.	3615.	0.0	0.0	2	
53	1	-4.0	-0.0	50.	43.	15.	10.	10.	99.	0.	7.19	3606.	3670.	3619.	0.0	0.0	2	
53	2	0.0	-0.0	50.	43.	15.	10.	10.	99.	0.	7.30	3605.	3670.	3612.	0.0	0.0	2	
53	3	4.0	-0.0	50.	43.	15.	10.	10.	99.	0.	7.24	3584.	3665.	3608.	0.0	0.0	2	
53	4	8.0	-0.0	50.	43.	15.	10.	10.	99.	0.	7.11	3550.	3661.	3609.	0.0	0.0	2	
53	5	12.0	-0.0	50.	43.	15.	10.	10.	99.	0.	7.01	3607.	3668.	3613.	0.0	0.0	2	
53	6	14.0	-0.0	50.	43.	15.	10.	10.	99.	0.	7.31	3609.	3679.	3621.	0.0	0.0	2	
53	7	16.0	-0.0	50.	43.	15.	10.	10.	99.	0.	7.19	3640.	3673.	3616.	0.0	0.0	2	
53	8	20.0	-0.0	50.	43.	15.	10.	10.	99.	0.	7.23	3613.	3676.	3621.	0.0	0.0	2	
54	1	-4.0	-0.0	50.	43.	15.	10.	10.	99.	0.	12.32	3623.	3668.	3622.	0.0	0.0	2	
54	2	0.0	-0.0	50.	43.	15.	10.	10.	99.	0.	12.44	3600.	3652.	3617.	0.0	0.0	2	
54	3	4.0	-0.0	50.	43.	15.	10.	10.	99.	0.	12.34	3575.	3653.	3615.	0.0	0.0	2	
54	4	8.0	-0.0	50.	43.	15.	10.	10.	99.	0.	12.51	3599.	3648.	3620.	0.0	0.0	2	
54	5	12.0	-0.0	50.	43.	15.	10.	10.	99.	0.	12.30	3600.	3645.	3613.	0.0	0.0	2	
54	6	14.0	-0.0	50.	43.	15.	10.	10.	99.	0.	12.11	3623.	3644.	3620.	0.0	0.0	2	
54	7	16.0	-0.0	50.	43.	15.	10.	10.	99.	0.	12.40	3605.	3637.	3608.	0.0	0.0	2	
54	8	20.0	-0.0	50.	43.	15.	10.	10.	99.	0.	12.28	3601.	3649.	3617.	0.0	0.0	2	
55	1	0.0	-0.0	50.	30.	15.	10.	10.	99.	0.	12.39	3629.	3652.	3630.	0.0	0.0	2	
55	2	0.0	-0.0	50.	45.	15.	10.	10.	99.	0.	12.40	3574.	3650.	3622.	0.0	0.0	2	
55	3	0.0	-0.0	50.	40.	15.	10.	10.	99.	0.	12.32	3609.	3651.	3620.	0.0	0.0	2	
55	4	0.0	-0.0	50.	35.	15.	10.	10.	99.	0.	12.33	3580.	3650.	3622.	0.0	0.0	2	
56	1	-4.0	-0.0	50.	0.	15.	10.	10.	99.	0.	14.17	51.	758.	822.	0.0	0.0	2	
56	2	0.0	-0.0	50.	0.	15.	10.	10.	99.	0.	14.20	21.	758.	827.	0.0	0.0	2	
56	3	4.0	-0.0	50.	0.	15.	10.	10.	99.	0.	14.15	0.	733.	801.	0.0	0.0	2	
56	4	8.0	-0.0	50.	0.	15.	10.	10.	99.	0.	14.42	0.	731.	797.	0.0	0.0	2	
56	5	12.0	-0.0	50.	0.	15.	10.	10.	99.	0.	14.08	0.	722.	779.	0.0	0.0	2	
56	6	14.0	-0.0	50.	0.	15.	10.	10.	99.	0.	13.25	0.	697.	762.	0.0	0.0	2	
56	7	16.0	-0.0	50.	0.	15.	10.	10.	99.	0.	13.31	0.	504.	793.	0.0	0.0	2	
56	8	20.0	-0.0	50.	0.	15.	10.	10.	99.	0.	13.34	0.	403.	773.	0.0	0.0	2	
57	1	0.0	-0.0	23.	35.	15.	10.	10.	99.	0.	0.00	195.	2000.	448.	0.0	0.0	2	
57	2	0.0	-0.0	23.	35.	15.	10.	10.	99.	0.	0.00	80.	2490.	229.	0.0	0.0	2	
57	3	0.0	-0.0	23.	35.	15.	10.	10.	99.	0.	0.00	200.	3625.	147.	0.0	0.0	2	
57	4	0.0	-0.0	23.	35.	15.	10.	10.	99.	0.	0.00	304.	3936.	120.	0.0	0.0	2	
58	1	0.0	-0.0	23.	35.	15.	10.	10.	99.	0.	0.00	60.	226.	2889.	0.0	0.0	2	
58	2	0.0	-0.0	23.	35.	15.	10.	10.	99.	0.	0.00	71.	102.	3569.	0.0	0.0	2	
58	3	0.0	-0.0	23.	35.	15.	10.	10.	99.	0.	0.00	71.	91.	4010.	0.0	0.0	2	
58	4	0.0	-0.0	23.	35.	15.	10.	10.	99.	0.	0.00	138.	3583.	3602.	0.0	0.0	2	

GP78-0822-219

C	DYNL DEG	NOSE GEAR	NOSE INLET	UNIT COVERS	OTHER	RUN	PT	BALANCE FORCE AND MOMENT DATA--STABILITY AXES LIFT (LB)	DRAG (LB)	PITCHING MOMENT (FT-LB)	SIDE FORCE (LB)	ROLLING MOMENT (FT-LB)	YAWING MOMENT (FT-LB)	TUNNEL TOTAL TEMP. (DEG F)	AMBIENT PRESSURE (IN HG)
0	0.0	N		N		51	3	3204.	-1766.	-285.	-10.	-45.	121.	81.	29.96
0	0.0	N		N		51	4	3524.	-1525.	123.	-11.	-135.	113.	83.	29.96
0	0.0	N		N		51	5	3784.	-1270.	216.	-28.	114.	412.	83.	29.96
0	0.0	N		N		51	6	3896.	-1109.	63.	1.	-205.	274.	83.	29.96
0	0.0	N		N		51	7	4024.	-914.	-208.	22.	-294.	164.	83.	29.95
0	0.0	N		N		51	8	4223.	-607.	-233.	29.	-452.	53.	84.	29.96
0	0.0	N		N		52	1	3089.	-1495.	2281.	-48.	-338.	-112.	85.	29.96
0	0.0	N		N		52	2	2939.	-1465.	524.	-40.	-200.	58.	86.	29.96
0	0.0	N		N		52	3	2788.	-2008.	-1245.	-16.	-336.	156.	87.	29.96
0	0.0	N		N		52	4	2567.	-2006.	-3936.	-2.	-353.	294.	87.	29.96
0	0.0	N		N		52	5	2630.	-2183.	-87.	-19.	-216.	53.	88.	29.96
0	0.0	N		N		52	6	3493.	-1499.	1264.	-4.	-146.	-55.	89.	29.96
0	0.0	N		N		52	7	3384.	-1572.	-365.	14.	-291.	179.	89.	29.96
0	0.0	N		N		52	8	3256.	-1624.	-2479.	57.	-655.	155.	89.	29.95
0	0.0	N		N		52	9	3127.	-1618.	-5010.	-5.	-217.	459.	89.	29.96
0	0.0	N		N		53	1	2829.	-1808.	-2475.	1.	-121.	295.	91.	29.96
0	0.0	N		N		53	2	3343.	-1611.	-2167.	21.	-207.	147.	91.	29.95
0	0.0	N		N		53	3	3865.	-1377.	-2041.	37.	-303.	176.	91.	29.94
0	0.0	N		N		53	4	4322.	-1144.	-1747.	66.	-444.	18.	91.	29.96
0	0.0	N		N		53	5	4745.	-766.	-2495.	19.	422.	507.	91.	29.96
0	0.0	N		N		53	6	4951.	-485.	-2480.	45.	-253.	325.	91.	29.96
0	0.0	N		N		53	7	5061.	-312.	-2707.	63.	-516.	55.	91.	29.96
0	0.0	N		N		53	8	5479.	144.	-3663.	54.	-469.	163.	92.	29.96
0	0.0	N		N		54	1	3300.	-1435.	-4325.	-35.	-91.	708.	94.	29.96
0	0.0	N		N		54	2	4135.	-1206.	-4067.	-29.	-61.	722.	95.	29.96
0	0.0	N		N		54	3	4874.	-958.	-3718.	16.	-320.	494.	95.	29.96
0	0.0	N		N		54	4	5641.	-644.	-3985.	23.	-302.	210.	95.	29.96
0	0.0	N		N		54	5	6267.	-300.	-4080.	67.	-775.	267.	95.	29.96
0	0.0	N		N		54	6	6296.	16.	-4494.	5.	-884.	690.	95.	29.96
0	0.0	N		N		54	7	6638.	379.	-4638.	71.	-573.	315.	95.	29.96
0	0.0	N		N		54	8	7144.	921.	-5029.	19.	-406.	543.	95.	29.96
0	0.0	N		N		55	1	4220.	-1114.	-607.	-21.	-252.	460.	95.	29.96
0	0.0	N		N		55	2	4130.	-1205.	-2714.	-27.	-103.	695.	95.	29.96
0	0.0	N		N		55	3	4051.	-1245.	-4471.	4.	-364.	593.	95.	29.96
0	0.0	N		N		55	4	3899.	-1245.	-7272.	15.	-370.	518.	95.	29.96
0	0.0	N		N		56	1	1272.	517.	-7907.	-16.	342.	226.	89.	29.96
0	0.0	N		N		56	2	2149.	560.	-7276.	-18.	334.	306.	89.	29.96
0	0.0	N		N		56	3	2991.	526.	-6579.	-29.	329.	247.	87.	29.96
0	0.0	N		N		56	4	3824.	748.	-5937.	-18.	233.	252.	85.	29.96
0	0.0	N		N		56	5	4613.	911.	-5641.	-18.	135.	288.	84.	29.96
0	0.0	N		N		56	6	4890.	1065.	-5921.	6.	-74.	204.	84.	29.96
0	0.0	N		N		56	7	4878.	1260.	-6345.	40.	-614.	488.	83.	29.96
0	0.0	N		N		56	8	4437.	1652.	-7551.	32.	-960.	479.	83.	29.96
0	0.0					57	1	85.	-387.	-881.	-1.	541.	1658.	71.	30.07
0	0.0					57	2	180.	-812.	-1547.	-1.	893.	3450.	71.	30.07
0	0.0					57	3	275.	-1285.	-1469.	-2.	1265.	5405.	71.	30.07
0	0.0					57	4	340.	-1493.	-2068.	-4.	1373.	6282.	71.	30.07
0	0.0					58	1	181.	-823.	-1183.	-19.	-767.	-3437.	74.	30.04
0	0.0					58	2	268.	-1270.	-1194.	-26.	-1178.	-5194.	74.	30.04
0	0.0					58	3	334.	-1585.	-1903.	-37.	-1547.	-6558.	74.	30.04
0	0.0	N		N		58	4	550.	-2452.	-3407.	-29.	-135.	-32.	75.	30.04

RUN	PT	ALPHA DEG	BETA DEG	DLC DEG	DNL DEG	DF DEG	DAL DEG	DAR DEG	DM DEG	DP DEG	QC PSF	FAN1 RPM	FAN2 RPM	FAN3 RPM	DYLC DEG	DYNL DEG	NOSE GEAR	INLE
58	5	0.0	-0.0	23.	35.	15.	10.	10.	44.	0.	.32	3621.	3611.	3602.	0.0	0.0	2	
58	6	0.0	-0.0	23.	35.	15.	10.	10.	44.	0.	3.38	3621.	3614.	3602.	0.0	0.0	2	
59	1	0.0	-0.0	23.	40.	15.	10.	10.	44.	0.	0.00	3646.	0.	0.	0.0	0.0	2	
59	2	0.0	-0.0	23.	40.	15.	10.	10.	44.	0.	0.00	3607.	140.	107.	0.0	0.0	2	
59	3	0.0	-0.0	23.	40.	15.	10.	10.	44.	0.	0.00	3621.	178.	104.	0.0	0.0	2	
60	1	-4.0	-0.0	23.	43.	15.	10.	10.	44.	0.	7.09	3616.	3604.	3610.	0.0	0.0	2	
60	2	0.0	-0.0	23.	43.	15.	10.	10.	44.	0.	7.06	3616.	3605.	3599.	0.0	0.0	2	
60	3	4.0	-0.0	23.	43.	15.	10.	10.	44.	0.	7.18	3611.	3604.	3601.	0.0	0.0	2	
60	4	8.0	-0.0	23.	43.	15.	10.	10.	44.	0.	7.09	3612.	3601.	3594.	0.0	0.0	2	
60	5	12.0	-0.0	23.	43.	15.	10.	10.	44.	0.	7.11	3619.	3606.	3608.	0.0	0.0	2	
60	6	16.0	-0.0	23.	43.	15.	10.	10.	44.	0.	7.11	3612.	3603.	3591.	0.0	0.0	2	
60	7	16.0	-0.0	24.	43.	15.	10.	10.	44.	0.	7.11	3613.	3616.	3603.	0.0	0.0	2	
60	8	20.0	-0.0	23.	43.	15.	10.	10.	44.	0.	7.11	3612.	3618.	3614.	0.0	0.0	2	
61	1	-4.0	-0.0	23.	43.	15.	10.	10.	44.	0.	12.44	3606.	3616.	3601.	0.0	0.0	2	
61	2	0.0	-0.0	23.	43.	15.	10.	10.	44.	0.	12.23	3616.	3615.	3621.	0.0	0.0	2	
61	3	4.0	-0.0	23.	43.	15.	10.	10.	44.	0.	12.25	3623.	3629.	3619.	0.0	0.0	2	
61	4	8.0	-0.0	23.	43.	15.	10.	10.	44.	0.	12.28	3639.	3641.	3602.	0.0	0.0	2	
61	5	12.0	-0.0	24.	43.	15.	10.	10.	44.	0.	12.30	3615.	3630.	3616.	0.0	0.0	2	
61	6	16.0	-0.0	23.	43.	15.	10.	10.	44.	0.	12.27	3624.	3619.	3617.	0.0	0.0	2	
61	7	16.0	-0.0	23.	43.	15.	10.	10.	44.	0.	12.19	3624.	3644.	3644.	0.0	0.0	2	
61	8	20.0	-0.0	23.	43.	15.	10.	10.	44.	0.	12.27	3633.	3648.	3659.	0.0	0.0	2	
62	1	-4.0	-0.0	23.	43.	15.	10.	10.	44.	0.	14.23	3609.	3616.	3605.	0.0	0.0	2	
62	2	0.0	-0.0	23.	43.	15.	10.	10.	44.	0.	14.21	3637.	3608.	3608.	0.0	0.0	2	
62	3	4.0	-0.0	23.	43.	15.	10.	10.	44.	0.	14.21	3617.	3634.	3626.	0.0	0.0	2	
62	4	8.0	-0.0	23.	43.	15.	10.	10.	44.	0.	14.43	3650.	3633.	3610.	0.0	0.0	2	
62	5	12.0	-0.0	23.	43.	15.	10.	10.	44.	0.	14.28	3640.	3621.	3601.	0.0	0.0	2	
62	6	16.0	-0.0	23.	43.	15.	10.	10.	44.	0.	14.33	3615.	3617.	3602.	0.0	0.0	2	
62	7	16.0	-0.0	23.	43.	15.	10.	10.	44.	0.	14.25	3633.	3615.	3606.	0.0	0.0	2	
62	8	20.0	-0.0	23.	43.	15.	10.	10.	44.	0.	14.11	3609.	3606.	3593.	0.0	0.0	2	
63	1	-4.0	-0.0	23.	43.	15.	10.	10.	44.	0.	14.27	546.	860.	928.	0.0	0.0	2	
63	2	0.0	-0.0	23.	43.	15.	10.	10.	44.	0.	14.27	495.	855.	927.	0.0	0.0	2	
63	3	4.0	-0.0	23.	43.	15.	10.	10.	44.	0.	14.18	362.	848.	915.	0.0	0.0	2	
63	4	8.0	-0.0	24.	43.	15.	10.	10.	44.	0.	14.23	232.	824.	889.	0.0	0.0	2	
63	5	12.0	-0.0	23.	43.	15.	10.	10.	44.	0.	14.16	98.	820.	895.	0.0	0.0	2	
63	6	16.0	-0.0	23.	43.	15.	10.	10.	44.	0.	14.15	59.	807.	891.	0.0	0.0	2	
63	7	16.0	-0.0	23.	43.	15.	10.	10.	44.	0.	14.22	72.	806.	893.	0.0	0.0	2	
63	8	20.0	-0.0	23.	43.	15.	10.	10.	44.	0.	14.34	144.	851.	962.	0.0	0.0	2	
64	1	0.0	-0.0	23.	43.	15.	10.	10.	0.	0.	3.19	3620.	3640.	3649.	0.0	0.0	2	
64	2	0.0	-0.0	24.	43.	15.	10.	10.	10.	0.	3.23	3617.	3635.	3620.	0.0	0.0	2	
65	1	-4.0	-0.0	23.	43.	15.	10.	10.	0.	0.	7.25	3619.	3619.	3608.	0.0	0.0	2	
65	2	0.0	-0.0	23.	43.	15.	10.	10.	0.	0.	7.11	3618.	3615.	3602.	0.0	0.0	2	
65	3	4.0	-0.0	23.	43.	15.	10.	10.	0.	0.	7.12	3610.	3620.	3605.	0.0	0.0	2	
65	4	8.0	-0.0	23.	43.	15.	10.	10.	0.	0.	7.16	3614.	3631.	3628.	0.0	0.0	2	
65	5	12.0	-0.0	23.	43.	15.	10.	10.	0.	0.	7.26	3665.	3608.	3602.	0.0	0.0	2	
65	6	16.0	-0.0	23.	43.	15.	10.	10.	0.	0.	7.23	3618.	3615.	3606.	0.0	0.0	2	
65	7	16.0	-0.0	23.	43.	15.	10.	10.	0.	0.	7.20	3639.	3611.	3600.	0.0	0.0	2	
65	8	20.0	-0.0	23.	43.	15.	10.	10.	0.	0.	7.14	3611.	3615.	3613.	0.0	0.0	2	
66	1	-4.0	-0.0	23.	43.	15.	10.	10.	0.	0.	12.37	3619.	3639.	3641.	0.0	0.0	2	
66	2	0.0	-0.0	23.	43.	15.	10.	10.	0.	0.	12.25	3612.	3629.	3634.	0.0	0.0	2	
66	3	4.0	-0.0	24.	43.	15.	10.	10.	0.	0.	12.28	3620.	3612.	3603.	0.0	0.0	2	
66	4	8.0	-0.0	23.	43.	15.	10.	10.	0.	0.	12.39	3615.	3612.	3611.	0.0	0.0	2	

GP78-0822-220

ORIGINAL PAGE IS
OF POOR QUALITY

FOLDOUT FRAME

YNL DEG	NOSE GEAR	NOSE INLET	UNIT COVERS	OTHER	RUN	PT	BALANCE FORCE AND MOMENT DATA--STABILITY AXES LIFT (LB)	DRAG (LB)	PITCHING MOMENT (FT-LB)	SIDE FORCE (LB)	ROLLING MOMENT (FT-LB)	YAWING MOMENT (FT-LB)	TUNNEL TOTAL TEMP. (DEG F)	AMBIENT PRESSURE (IN HG)
0.0					58	5	748.	-3267.	3895.	1.	-27.	309.	77.	30.04
0.0					58	6	1094.	-2760.	2403.	4.	-345.	388.	80.	30.04
0.0					59	1	1167.	-55.	15239.	-2.	-46.	-5.	79.	29.97
0.0					59	2	655.	-850.	10522.	3.	-102.	29.	79.	29.97
0.0					59	3	566.	-859.	9704.	8.	-14.	47.	79.	29.97
0.0					60	1	1236.	-2540.	4481.	-23.	-44.	336.	83.	29.97
0.0					60	2	1773.	-2452.	5051.	-37.	-128.	320.	83.	29.97
0.0					60	3	2324.	-2322.	5555.	-13.	-72.	267.	83.	29.97
0.0					60	4	2708.	-2169.	5557.	31.	-305.	342.	83.	29.97
0.0					60	5	3192.	-1985.	5774.	44.	-220.	366.	83.	29.97
0.0					60	6	3355.	-1829.	6328.	-40.	1354.	747.	83.	29.97
0.0					60	7	3447.	-1479.	6102.	9.	561.	565.	83.	29.97
0.0					60	8	3832.	-1401.	6655.	20.	-102.	195.	83.	29.97
0.0					61	1	1435.	-2140.	3643.	-51.	152.	413.	87.	29.79
0.0					61	2	2228.	-2110.	3924.	-36.	43.	431.	87.	29.79
0.0					61	3	3003.	-1977.	4460.	-48.	133.	371.	87.	29.79
0.0					61	4	3702.	-1795.	4996.	-5.	6.	314.	87.	29.79
0.0					61	5	4339.	-1593.	5344.	20.	-124.	265.	87.	29.79
0.0					61	6	4522.	-1407.	5262.	-85.	1881.	1060.	87.	29.79
0.0					61	7	4723.	-1210.	6024.	-94.	2197.	871.	87.	29.79
0.0					61	8	4969.	-762.	5549.	14.	-90.	543.	88.	29.79
0.0					62	1	1702.	-1617.	1779.	-44.	90.	462.	91.	29.97
0.0					62	2	2742.	-1716.	2590.	-26.	144.	350.	91.	29.97
0.0					62	3	3721.	-1559.	3104.	-42.	257.	387.	91.	29.97
0.0					62	4	4802.	-1360.	3758.	-39.	410.	511.	91.	29.97
0.0					62	5	5861.	-1104.	4444.	-42.	258.	533.	91.	29.97
0.0					62	6	6334.	-965.	4504.	-22.	61.	623.	91.	29.97
0.0					62	7	6264.	-603.	4459.	-42.	162.	609.	91.	29.97
0.0					62	8	6541.	-0.	5423.	-44.	109.	841.	91.	29.97
0.0					63	1	548.	496.	-5140.	14.	231.	133.	91.	29.97
0.0					63	2	1447.	495.	-4475.	16.	74.	114.	91.	29.97
0.0					63	3	2277.	524.	-3841.	15.	61.	86.	90.	29.97
0.0					63	4	3089.	546.	-3264.	-5.	301.	197.	90.	29.97
0.0					63	5	3965.	716.	-2569.	-17.	391.	284.	89.	29.97
0.0					63	6	4344.	799.	-2258.	4.	123.	234.	88.	29.97
0.0					63	7	4583.	945.	-2285.	-13.	157.	637.	87.	29.97
0.0					63	8	4064.	1434.	-1236.	-4.	-228.	429.	87.	29.97
0.0					64	1	1296.	-2810.	6868.	-2.	-44.	327.	68.	30.01
0.0					64	2	1411.	-2802.	5966.	-39.	-320.	330.	70.	30.01
0.0					65	1	1144.	-2401.	6325.	-92.	-266.	174.	74.	30.01
0.0					65	2	1648.	-2401.	6296.	-47.	-520.	294.	74.	30.01
0.0					65	3	2276.	-2332.	6011.	-54.	-287.	351.	75.	30.01
0.0					65	4	2822.	-2171.	5670.	-30.	-336.	253.	75.	30.01
0.0					65	5	3340.	-1984.	5729.	3.	-84.	202.	75.	30.01
0.0					65	6	3444.	-1933.	5895.	-64.	1320.	748.	75.	30.01
0.0					65	7	3514.	-1871.	6030.	-16.	133.	358.	76.	30.01
0.0					65	8	3886.	-1394.	6294.	-0.	-134.	261.	76.	30.01
0.0					66	1	1219.	-2181.	5901.	-61.	-111.	435.	78.	30.01
0.0					66	2	2116.	-2105.	5624.	-55.	-155.	385.	78.	30.01
0.0					66	3	2942.	-1974.	5120.	-33.	-117.	335.	78.	30.01
0.0					66	4	3744.	-1784.	4965.	-8.	-201.	350.	78.	30.01

BEST AVAILABLE COPY

RUN	PT	ALPHA DEG	BETA DEG	DLC DEG	DNL DEG	DF DEG	DAL DEG	DAR DEG	DM DEG	DN DEG	QC PSF	FAN1 RPM	FAN2 RPM	FAN3 RPM	DYLC DEG	DYNL DEG	NOSE GEAR	NO INLE
66	5	12.0	-0.0	23.	43.	15.	10.	10.	0.	0.	12.37	3615.	3634.	3628.	0.0	0.0	2	
66	6	14.0	-0.0	23.	43.	15.	10.	10.	0.	0.	12.20	3612.	3647.	3644.	0.0	0.0	2	
66	7	16.0	-0.0	23.	43.	15.	10.	10.	0.	0.	12.37	3651.	3614.	3603.	0.0	0.0	2	
66	8	20.0	-0.0	23.	43.	15.	10.	10.	0.	0.	12.30	3619.	3633.	3635.	0.0	0.0	2	
67	1	-4.0	-0.0	23.	43.	15.	10.	10.	0.	0.	14.28	605.	881.	950.	0.0	0.0	2	
67	2	0.0	-0.0	23.	43.	15.	10.	10.	0.	0.	14.21	500.	838.	908.	0.0	0.0	2	
67	3	4.0	-0.0	23.	43.	15.	10.	10.	0.	0.	14.29	369.	838.	903.	0.0	0.0	2	
67	4	8.0	-0.0	23.	43.	15.	10.	10.	0.	0.	14.27	232.	832.	901.	0.0	0.0	2	
67	5	12.0	-0.0	23.	43.	15.	10.	10.	0.	0.	14.14	103.	806.	883.	0.0	0.0	2	
67	6	14.0	-0.0	23.	43.	15.	10.	10.	0.	0.	14.18	102.	797.	877.	0.0	0.0	2	
67	7	16.0	-0.0	23.	43.	15.	10.	10.	0.	0.	14.23	121.	797.	877.	0.0	0.0	2	
67	8	20.0	-0.0	23.	43.	15.	10.	10.	0.	0.	14.32	104.	821.	877.	0.0	0.0	2	
68	1	-4.0	-0.0	23.	43.	15.	10.	10.	0.	0.	14.19	3616.	3620.	3615.	0.0	0.0	2	
68	2	0.0	-0.0	23.	43.	15.	10.	10.	0.	0.	14.12	3619.	3622.	3610.	0.0	0.0	2	
68	3	4.0	-0.0	23.	43.	15.	10.	10.	0.	0.	14.24	3627.	3620.	3608.	0.0	0.0	2	
68	4	8.0	-0.0	23.	43.	15.	10.	10.	0.	0.	14.16	3614.	3626.	3642.	0.0	0.0	2	
68	5	12.0	-0.0	23.	43.	15.	10.	10.	0.	0.	14.24	3610.	3609.	3597.	0.0	0.0	2	
68	6	14.0	-0.0	23.	43.	15.	10.	10.	0.	0.	14.14	3606.	3640.	3628.	0.0	0.0	2	
68	7	16.0	-0.0	23.	43.	15.	10.	10.	0.	0.	14.01	3605.	3645.	3612.	0.0	0.0	2	
68	8	20.0	-0.0	23.	43.	15.	10.	10.	0.	0.	14.24	3598.	3607.	3599.	0.0	0.0	2	
69	1	0.0	-0.0	23.	43.	15.	10.	10.	-20.	0.	14.23	3623.	3664.	3663.	0.0	0.0	2	
69	2	0.0	-0.0	23.	43.	15.	10.	10.	-10.	0.	14.40	3636.	3642.	3632.	0.0	0.0	2	
69	3	0.0	-0.0	23.	43.	15.	10.	10.	0.	0.	14.21	3615.	3627.	3616.	0.0	0.0	2	
69	4	0.0	-0.0	23.	43.	15.	10.	10.	10.	0.	14.33	3622.	3631.	3619.	0.0	0.0	2	
69	5	0.0	-0.0	23.	43.	15.	10.	10.	20.	0.	14.24	3629.	3641.	3615.	0.0	0.0	2	
69	6	4.0	-0.0	23.	43.	15.	10.	10.	-10.	0.	14.16	3630.	3641.	3616.	0.0	0.0	2	
69	7	4.0	-0.0	23.	43.	15.	10.	10.	0.	0.	14.35	3636.	3643.	3630.	0.0	0.0	2	
69	8	8.0	-0.0	23.	43.	15.	10.	10.	0.	0.	14.14	3617.	3629.	3621.	0.0	0.0	2	
69	9	16.0	-0.0	23.	43.	15.	10.	10.	-10.	0.	14.14	3621.	3626.	3614.	0.0	0.0	2	
69	10	16.0	-0.0	23.	43.	15.	10.	10.	10.	0.	14.11	3617.	3617.	3609.	0.0	0.0	2	
70	1	0.0	4.0	23.	43.	15.	10.	10.	0.	0.	14.17	3654.	3648.	3624.	0.0	0.0	2	
70	2	0.0	-4.0	23.	43.	15.	10.	10.	0.	0.	14.34	3613.	3629.	3608.	0.0	0.0	2	
70	3	0.0	-0.0	23.	43.	15.	10.	10.	0.	0.	14.16	3604.	3613.	3593.	0.0	0.0	2	
70	4	0.0	4.0	23.	43.	15.	10.	10.	0.	0.	14.11	3603.	3615.	3596.	0.0	0.0	2	
70	5	0.0	8.0	23.	43.	15.	10.	10.	0.	0.	14.14	3609.	3627.	3610.	0.0	0.0	2	
70	6	0.0	12.0	23.	43.	15.	10.	10.	0.	0.	14.26	3606.	3614.	3596.	0.0	0.0	2	
71	1	0.0	-0.0	23.	43.	15.	10.	10.	-20.	0.	12.25	3619.	3648.	3642.	0.0	0.0	2	
71	2	0.0	-0.0	23.	43.	15.	10.	10.	-10.	0.	12.41	3617.	3631.	3609.	0.0	0.0	2	
71	3	0.0	-0.0	23.	43.	15.	10.	10.	0.	0.	12.25	3622.	3614.	3599.	0.0	0.0	2	
71	4	0.0	-0.0	23.	43.	15.	10.	10.	10.	0.	12.27	3614.	3625.	3600.	0.0	0.0	2	
71	5	0.0	-0.0	23.	43.	15.	10.	10.	20.	0.	12.23	3622.	3630.	3600.	0.0	0.0	2	
71	6	8.0	-0.0	23.	43.	15.	10.	10.	-10.	0.	12.30	3618.	3627.	3604.	0.0	0.0	2	
71	7	8.0	-0.0	23.	43.	15.	10.	10.	0.	0.	12.20	3609.	3634.	3608.	0.0	0.0	2	
71	8	8.0	-0.0	23.	43.	15.	10.	10.	10.	0.	12.25	3617.	3623.	3597.	0.0	0.0	2	
71	9	8.0	-0.0	23.	43.	15.	10.	10.	20.	0.	12.23	3616.	3628.	3615.	0.0	0.0	2	
71	10	16.0	-0.0	23.	43.	15.	10.	10.	-10.	0.	12.18	3612.	3631.	3620.	0.0	0.0	2	
71	11	16.0	-0.0	23.	43.	15.	10.	10.	10.	0.	12.15	3621.	3632.	3617.	0.0	0.0	2	
72	1	0.0	-4.0	23.	43.	15.	10.	10.	0.	0.	12.40	3643.	3660.	3653.	0.0	0.0	2	
72	2	0.0	-0.0	23.	43.	15.	10.	10.	0.	0.	12.35	3618.	3623.	3613.	0.0	0.0	2	
72	3	0.0	4.0	23.	43.	15.	10.	10.	0.	0.	12.43	3609.	3617.	3602.	0.0	0.0	2	
72	4	0.0	8.0	23.	43.	15.	10.	10.	0.	0.	12.27	3606.	3612.	3594.	0.0	0.0	2	

GP78-0822-221

ORIGINAL PAGE IS
OF POOR QUALITY

FOLDOUT FRAME 1

BALANCE FORCE AND MOMENT DATA--STABILITY AXES

DYNL DEG	NOSE GEAR	NOSE INLET	UNIT COVERS	OTHER	RUN	PT	LIFT (LB)	DRAG (LB)	PITCHING MOMENT (FT-LB)	SIDE FORCE (LB)	ROLLING MOMENT (FT-LB)	YAWING MOMENT (FT-LB)	TUNNEL TOTAL TEMP. (DEG F)	AMBIENT PRESSURE (IN HG)
0.0	2		2		65	5	4550.	-1569.	4670.	10.	-148.	307.	78.	30.01
0.0	2		2		66	6	4642.	-1384.	4978.	-81.	2098.	1010.	78.	30.01
0.0	2		2		66	7	4695.	-1125.	5055.	-1.	-121.	466.	[illegible]	30.01
0.0	2		2		66	8	5146.	-740.	4295.	29.	-176.	496.	[illegible]	30.01
0.0	2		2		67	1	300.	514.	-1523.	20.	160.	64.	77.	30.01
0.0	2		2		67	2	1335.	500.	-2677.	17.	114.	39.	76.	30.01
0.0	2		2		67	3	2313.	530.	-3708.	7.	223.	65.	76.	30.01
0.0	2		2		67	4	3274.	602.	-4499.	-1.	201.	190.	76.	30.01
0.0	2		2		67	5	4210.	742.	-5637.	-14.	274.	236.	77.	30.01
0.0	2		2		67	6	4634.	844.	-6057.	-10.	199.	237.	77.	30.01
0.0	2		2		67	7	4808.	1079.	-6269.	-38.	1052.	851.	77.	30.01
0.0	2		2		67	8	4343.	1527.	-5733.	-12.	100.	612.	77.	30.01
0.0	2		2		68	1	1322.	-1799.	5503.	-62.	202.	491.	63.	30.00
0.0	2		2		68	2	2492.	-1697.	6845.	-35.	-322.	446.	65.	30.00
0.0	2		2		68	3	3662.	-1536.	8194.	-28.	1011.	483.	65.	30.00
0.0	2		2		68	4	4744.	-1333.	9606.	-29.	374.	277.	66.	30.00
0.0	2		2		68	5	5902.	-1052.	11225.	-55.	405.	580.	66.	30.00
0.0	2		2		68	6	6398.	-824.	12428.	-78.	1252.	1343.	67.	30.00
0.0	2		2		69	7	6367.	-519.	12526.	-63.	880.	764.	67.	30.00
0.0	2		2		68	8	6690.	111.	12849.	-67.	474.	743.	68.	30.00
0.0	2		2		69	1	2049.	-1494.	6874.	-43.	364.	267.	70.	30.00
0.0	2		2		69	2	3873.	-1576.	11799.	-51.	156.	545.	70.	30.00
0.0	2		2		69	3	2415.	-1716.	8845.	-32.	114.	322.	71.	30.00
0.0	2		2		69	4	2857.	-1882.	-1168.	-52.	195.	392.	71.	30.00
0.0	2		2		69	5	3210.	-1554.	-5114.	-28.	347.	408.	71.	30.00
0.0	2		2		69	6	4240.	-1484.	10849.	-58.	1888.	505.	72.	30.00
0.0	2		2		69	7	4790.	-1343.	3858.	-33.	234.	407.	72.	30.00
0.0	2		2		69	8	5254.	-1270.	-2373.	-50.	144.	490.	72.	30.00
0.0	2		2		69	9	5748.	-1115.	9346.	-47.	312.	752.	73.	30.00
0.0	2		2		69	10	6651.	-1445.	-3455.	-50.	249.	658.	73.	30.00
0.0	2		2		70	1	2284.	-1700.	4403.	-451.	-77.	445.	74.	30.00
0.0	2		2		70	2	2464.	-1694.	3957.	375.	992.	379.	75.	30.00
0.0	2		2		70	3	2421.	-1691.	4124.	-42.	1529.	249.	76.	30.00
0.0	2		2		70	4	2313.	-1739.	4242.	-416.	-594.	304.	76.	30.00
0.0	2		2		70	5	2463.	-1741.	4239.	-887.	-1301.	463.	76.	30.00
0.0	2		2		70	6	2721.	-1817.	3967.	-1301.	-2474.	536.	76.	30.00
0.0	2		2		71	1	1847.	-1973.	4104.	-9.	194.	267.	79.	30.00
0.0	2		2		71	2	1745.	-2045.	9124.	-19.	-88.	505.	79.	30.00
0.0	2		2		71	3	2081.	-2104.	5161.	-17.	9.	377.	79.	30.00
0.0	2		2		71	4	2391.	-2096.	1237.	-35.	374.	458.	79.	30.00
0.0	2		2		71	5	2556.	-2002.	-911.	-29.	160.	378.	79.	30.00
0.0	2		2		71	6	3464.	-1812.	8789.	-13.	231.	204.	79.	30.00
0.0	2		2		71	7	3716.	-1802.	4705.	14.	153.	274.	79.	30.00
0.0	2		2		71	8	3992.	-1739.	691.	7.	364.	309.	79.	30.00
0.0	2		2		71	9	3943.	-1638.	504.	26.	283.	209.	79.	30.00
0.0	2		2		71	10	4359.	-1719.	8800.	-8.	622.	360.	80.	30.00
0.0	2		2		71	11	4849.	-1050.	1127.	16.	166.	531.	80.	30.00
0.0	2		2		72	1	2117.	-2111.	4424.	235.	-391.	479.	81.	30.00
0.0	2		2		72	2	2090.	-2110.	4949.	-33.	-16.	356.	82.	30.00
0.0	2		2		72	3	2100.	-2116.	4706.	-345.	-767.	386.	82.	30.00
0.0	2		2		72	4	2150.	-2153.	4493.	-641.	-1177.	313.	83.	30.00

FOLDOUT FRAME 2

MACH	PT	ALPHA DEG	BETA DEG	DLC DEG	DL DEG	DF DEG	DEL DEG	DAM DEG	DM DEG	DN DEG	QC PSF	FAN1 RPM	FAN2 RPM	FAN3 RPM	DYLC DEG	DYNL DEG	NOSE GEAR	NOSE INLET	C
72	0	0.0	12.0	56.	43.	15.	10.	10.	0.	0.	12.36	3603.	3621.	3605.	0.0	0.0	2		
73	1	0.0	-8.0	56.	43.	15.	10.	10.	-10.	0.	6.82	3614.	3614.	3601.	0.0	0.0	2		
73	2	0.0	-4.0	56.	43.	15.	10.	10.	-10.	0.	7.03	3607.	3608.	3594.	0.0	0.0	2		
73	3	0.0	-0.0	56.	43.	15.	10.	10.	0.	0.	7.14	3610.	3607.	3596.	0.0	0.0	2		
73	4	0.0	4.0	56.	43.	15.	10.	10.	10.	0.	7.11	3609.	3608.	3610.	0.0	0.0	2		
73	5	0.0	8.0	56.	43.	15.	10.	10.	10.	0.	7.04	3608.	3635.	3620.	0.0	0.0	2		
73	6	8.0	-8.0	56.	43.	15.	10.	10.	-10.	0.	7.04	3608.	3621.	3610.	0.0	0.0	2		
73	7	8.0	-4.0	56.	43.	15.	10.	10.	0.	0.	7.06	3608.	3621.	3606.	0.0	0.0	2		
73	8	8.0	-0.0	56.	43.	15.	10.	10.	10.	0.	7.02	3601.	3615.	3604.	0.0	0.0	2		
73	9	8.0	-0.0	56.	43.	15.	10.	10.	-20.	0.	7.02	3602.	3617.	3624.	0.0	0.0	2		
73	10	16.0	-0.0	56.	43.	15.	10.	10.	-10.	0.	7.01	3600.	3644.	3631.	0.0	0.0	2		
73	11	16.0	-0.0	56.	43.	15.	10.	10.	10.	0.	6.96	3603.	3624.	3612.	0.0	0.0	2		
74	1	0.0	-8.0	56.	43.	15.	10.	10.	-20.	0.	19.23	468.	454.	925.	0.0	0.0	2		
74	2	0.0	-4.0	56.	43.	15.	10.	10.	-10.	0.	19.24	500.	467.	925.	0.0	0.0	2		
74	3	0.0	-0.0	56.	43.	15.	10.	10.	0.	0.	19.24	513.	466.	931.	0.0	0.0	2		
74	4	0.0	4.0	56.	43.	15.	10.	10.	10.	0.	19.23	488.	441.	923.	0.0	0.0	2		
74	5	0.0	8.0	56.	43.	15.	10.	10.	20.	0.	19.17	486.	453.	918.	0.0	0.0	2		
74	6	8.0	-8.0	56.	43.	15.	10.	10.	-10.	0.	19.24	269.	453.	709.	0.0	0.0	2		
74	7	8.0	-4.0	56.	43.	15.	10.	10.	-10.	0.	19.04	264.	437.	698.	0.0	0.0	2		
74	8	16.0	-8.0	56.	43.	15.	10.	10.	-10.	0.	19.27	71.	415.	693.	0.0	0.0	2		
74	9	16.0	-0.0	56.	43.	15.	10.	10.	10.	0.	19.20	82.	799.	891.	0.0	0.0	2		
75	1	0.0	-4.0	56.	43.	15.	10.	10.	0.	0.	19.19	475.	463.	923.	0.0	0.0	2		
75	2	0.0	-0.0	56.	43.	15.	10.	10.	0.	0.	19.30	492.	461.	923.	0.0	0.0	2		
75	3	0.0	4.0	56.	43.	15.	10.	10.	0.	0.	19.29	505.	444.	933.	0.0	0.0	2		
75	4	0.0	8.0	56.	43.	15.	10.	10.	0.	0.	19.15	539.	455.	934.	0.0	0.0	2		
75	5	0.0	12.0	56.	43.	15.	10.	10.	0.	0.	19.30	522.	448.	939.	0.0	0.0	2		
76	1	0.0	-4.0	56.	43.	15.	10.	10.	0.	0.	3.16	3619.	3633.	3615.	0.0	0.0	2		
76	2	0.0	-0.0	56.	43.	15.	10.	10.	0.	0.	3.34	3607.	3632.	3605.	0.0	0.0	2		
76	3	0.0	4.0	56.	43.	15.	10.	10.	0.	0.	3.34	3615.	3654.	3643.	0.0	0.0	2		
76	4	0.0	8.0	56.	43.	15.	10.	10.	0.	0.	3.34	3617.	3624.	3616.	0.0	0.0	2		
76	5	0.0	12.0	56.	43.	15.	10.	10.	0.	0.	3.34	3611.	3621.	3605.	0.0	0.0	2		
76	6	0.0	16.0	56.	43.	15.	10.	10.	0.	0.	3.29	3609.	3619.	3605.	0.0	0.0	2		
76	7	0.0	20.0	56.	43.	15.	10.	10.	0.	0.	3.24	3612.	3627.	3624.	0.0	0.0	2		
77	1	0.0	-4.0	56.	43.	15.	10.	10.	0.	0.	7.06	3624.	3647.	3634.	0.0	0.0	2		
77	2	0.0	-0.0	56.	43.	15.	10.	10.	0.	0.	7.10	3611.	3628.	3615.	0.0	0.0	2		
77	3	0.0	4.0	56.	43.	15.	10.	10.	0.	0.	7.04	3610.	3667.	3657.	0.0	0.0	2		
77	4	0.0	8.0	56.	43.	15.	10.	10.	0.	0.	6.99	3624.	3662.	3613.	0.0	0.0	2		
77	5	0.0	12.0	56.	43.	15.	10.	10.	0.	0.	6.99	3627.	3627.	3609.	0.0	0.0	2		
77	6	0.0	16.0	56.	43.	15.	10.	10.	0.	0.	6.94	3615.	3629.	3605.	0.0	0.0	2		
77	7	0.0	20.0	56.	43.	15.	10.	10.	0.	0.	6.99	3619.	3637.	3609.	0.0	0.0	2		
78	1	0.0	-4.0	56.	43.	15.	10.	10.	0.	0.	12.42	3616.	3640.	3619.	0.0	0.0	2		
78	2	0.0	-0.0	56.	43.	15.	10.	10.	0.	0.	12.42	3609.	3635.	3613.	0.0	0.0	2		
78	3	0.0	4.0	56.	43.	15.	10.	10.	0.	0.	12.30	3637.	3629.	3604.	0.0	0.0	2		
78	4	0.0	8.0	56.	43.	15.	10.	10.	0.	0.	12.20	3613.	3633.	3608.	0.0	0.0	2		
78	5	0.0	12.0	56.	43.	15.	10.	10.	0.	0.	12.21	3607.	3632.	3609.	0.0	0.0	2		
78	6	0.0	16.0	56.	43.	15.	10.	10.	0.	0.	12.23	3617.	3632.	3607.	0.0	0.0	2		
78	7	0.0	20.0	56.	43.	15.	10.	10.	0.	0.	12.24	3615.	3626.	3608.	0.0	0.0	2		
79	1	0.0	-4.0	56.	43.	15.	10.	10.	0.	0.	12.42	380.	660.	706.	0.0	0.0	2		
79	2	0.0	-0.0	56.	43.	15.	10.	10.	0.	0.	12.40	384.	644.	692.	0.0	0.0	2		
79	3	0.0	4.0	56.	43.	15.	10.	10.	0.	0.	12.39	405.	672.	729.	0.0	0.0	2		
79	4	0.0	8.0	56.	43.	15.	10.	10.	0.	0.	12.38	454.	638.	707.	0.0	0.0	2		

GP78-0822-222

C-15

ORIGINAL PAGE IS
OF POOR QUALITY

FOLDOUT FRAME 1

LC	DYNL DEG	NOSE GEAR	NOSE INLET	UNIT COVERS	OTHER	RUN	PT	BALANCE FORCE AND MOMENT DATA--STABILITY AXES LIFT (LB)	DRAG (LB)	PITCHING MOMENT (FT-LB)	SIDE FORCE (LB)	ROLLING MOMENT (FT-LB)	YAWING MOMENT (FT-LB)	TUNNEL TOTAL TEMP. (DEG F)	AMBIENT PRESSURE (IN HG)
0	0.0	2		2		72	5	2262.	-2190.	6745.	-914.	-2102.	21.	62.	30.00
0	0.0	2		2		73	1	1574.	-2467.	7750.	-27.	-963.	425.	63.	30.00
0	0.0	2		2		73	2	1545.	-2391.	8351.	-34.	-989.	550.	63.	30.00
0	0.0	2		2		73	3	1672.	-2433.	6611.	-30.	-1140.	446.	63.	30.00
0	0.0	2		2		73	4	1838.	-2427.	3953.	-24.	-916.	571.	63.	30.00
0	0.0	2		2		73	5	1963.	-2390.	2448.	-29.	-1021.	561.	64.	30.00
0	0.0	2		2		73	6	2054.	-2184.	8157.	-26.	-1070.	504.	64.	30.00
0	0.0	2		2		73	7	2754.	-2147.	5985.	-9.	-736.	346.	64.	30.00
0	0.0	2		2		73	8	2914.	-2157.	3922.	-4.	-808.	397.	64.	30.00
0	0.0	2		2		73	9	2951.	-2145.	3593.	-3.	-819.	423.	64.	30.00
0	0.0	2		2		73	10	3247.	-1714.	4535.	-14.	140.	375.	64.	30.00
0	0.0	2		2		73	11	3624.	-1622.	6148.	-19.	105.	342.	64.	30.00
0	0.0	2		2		74	1	835.	735.	2942.	19.	-1.	89.	68.	29.95
0	0.0	2		2		74	2	732.	589.	6165.	7.	-5.	287.	68.	29.95
0	0.0	2		2		74	3	1297.	507.	-2625.	14.	161.	163.	68.	29.95
0	0.0	2		2		74	4	1744.	528.	-8807.	14.	107.	92.	68.	29.95
0	0.0	2		2		74	5	2070.	478.	-11492.	10.	197.	110.	68.	29.95
0	0.0	2		2		74	6	2747.	506.	1924.	2.	110.	142.	68.	29.95
0	0.0	2		2		74	7	3672.	710.	-10978.	-16.	315.	327.	69.	29.95
0	0.0	2		2		74	8	4341.	1024.	278.	-43.	1146.	800.	69.	29.95
0	0.0	2		2		74	9	5058.	1284.	-10470.	-30.	664.	724.	69.	29.95
0	0.0	2		2		75	1	1305.	492.	-3319.	249.	379.	-335.	69.	29.95
0	0.0	2		2		75	2	1274.	505.	-3360.	16.	351.	74.	69.	29.95
0	0.0	2		2		75	3	1289.	502.	-3342.	-274.	212.	53.	69.	29.95
0	0.0	2		2		75	4	1369.	477.	-3193.	-365.	228.	1012.	69.	29.95
0	0.0	2		2		75	5	1905.	6.	-3282.	-429.	-111.	1293.	69.	29.95
0	0.0	2		2		76	1	2732.	-2012.	515.	100.	-349.	75.	60.	30.02
0	0.0	2		2		76	2	2751.	-1967.	577.	-7.	-314.	-104.	62.	30.02
0	0.0	2		2		76	3	2783.	-2009.	320.	-142.	-256.	-23.	63.	30.02
0	0.0	2		2		76	4	2809.	-2012.	265.	-248.	-972.	-63.	64.	30.02
0	0.0	2		2		76	5	2937.	-2061.	101.	-363.	-989.	-165.	65.	30.02
0	0.0	2		2		76	6	2944.	-2037.	231.	-417.	-1160.	-259.	65.	30.02
0	0.0	2		2		76	7	2934.	-1956.	403.	-510.	-1132.	-1169.	66.	30.02
0	0.0	2		2		77	1	3206.	-1926.	29.	278.	112.	-87.	68.	30.02
0	0.0	2		2		77	2	3215.	-1915.	136.	33.	-321.	44.	68.	30.02
0	0.0	2		2		77	3	3194.	-1837.	79.	-206.	-747.	262.	69.	30.02
0	0.0	2		2		77	4	3260.	-1839.	-18.	-441.	-1384.	516.	69.	30.02
0	0.0	2		2		77	5	3324.	-1867.	-230.	-674.	-2244.	554.	70.	30.02
0	0.0	2		2		77	6	3519.	-1885.	-407.	-742.	-2101.	-454.	70.	30.02
0	0.0	2		2		77	7	3515.	-1690.	-28.	-991.	-2446.	-547.	71.	30.02
0	0.0	2		2		78	1	3835.	-1727.	-492.	307.	436.	130.	72.	30.02
0	0.0	2		2		78	2	3906.	-1628.	-422.	-21.	33.	592.	72.	30.02
0	0.0	2		2		78	3	3787.	-1268.	-583.	-353.	-889.	637.	72.	30.02
0	0.0	2		2		78	4	3875.	-1259.	-664.	-703.	-1800.	1137.	72.	30.02
0	0.0	2		2		78	5	4048.	-1298.	-1320.	-1040.	-2984.	1566.	72.	30.02
0	0.0	2		2		78	6	4316.	-1293.	-1869.	-1237.	-2600.	-209.	72.	30.02
0	0.0	2		2		78	7	4106.	-1318.	-2268.	-1502.	-2972.	-665.	73.	30.02
0	0.0	2		2		79	1	1[illegible].	391.	-3337.	202.	3.	-412.	71.	30.02
0	0.0	2		2		79	2	1234.	394.	-3519.	-1.	121.	178.	70.	30.02
0	0.0	2		2		79	3	1255.	397.	-3709.	-203.	6M.	756.	69.	30.02
0	0.0	2		2		79	4	1285.	383.	-3648.	-415.	190.	1216.	68.	30.02

FOLDOUT FRAME 2

MIN	PT	ALPHA DEG	BETA DEG	DLC DEG	DNL DEG	DF DEG	DFL DEG	DAM DEG	DM DEG	DN DEG	PC PSF	FAN1 RPM	FAN2 RPM	FAN3 RPM	DYLC DEG	DYNL DEG	NOSE GEAR	NOSE INLET
79	5	0.0	12.0	56.	43.	15.	10.	10.	0.	0.	12.37	416.	616.	707.	0.0	0.0	2	
79	6	0.0	16.0	56.	43.	15.	10.	10.	0.	0.	12.32	404.	617.	725.	0.0	0.0	2	
79	7	0.0	20.0	56.	43.	15.	10.	10.	0.	0.	12.15	418.	601.	709.	0.0	0.0	2	
80	1	0.0	-4.0	56.	43.	15.	10.	10.	0.	0.	3.19	3635.	3640.	3632.	0.0	0.0	2	
80	2	0.0	-0.0	56.	43.	15.	10.	10.	0.	0.	3.16	3621.	3639.	3615.	0.0	0.0	2	
80	3	0.0	4.0	56.	43.	15.	10.	10.	0.	0.	3.19	3628.	3634.	3611.	0.0	0.0	2	
80	4	0.0	8.0	56.	43.	15.	10.	10.	0.	0.	3.20	3624.	3624.	3616.	0.0	0.0	2	
80	5	0.0	12.0	56.	43.	15.	10.	10.	0.	0.	3.26	3638.	3624.	3608.	0.0	0.0	2	
80	6	0.0	-4.0	56.	43.	15.	10.	10.	0.	0.	7.02	3628.	3651.	3633.	0.0	0.0	2	
80	7	0.0	-0.0	56.	43.	15.	10.	10.	0.	0.	7.02	3610.	3623.	3604.	0.0	0.0	2	
80	8	0.0	4.0	56.	43.	15.	10.	10.	0.	0.	7.04	3627.	3624.	3624.	0.0	0.0	2	
80	9	0.0	8.0	56.	43.	15.	10.	10.	0.	0.	7.06	3622.	3620.	3618.	0.0	0.0	2	
80	10	0.0	12.0	56.	43.	15.	10.	10.	0.	0.	7.04	3613.	3601.	3605.	0.0	0.0	2	
80	11	0.0	-4.0	56.	43.	15.	10.	10.	0.	0.	12.14	3627.	3625.	3600.	0.0	0.0	2	
80	12	0.0	-0.0	56.	43.	15.	10.	10.	0.	0.	12.23	3606.	3624.	3612.	0.0	0.0	2	
80	13	0.0	4.0	56.	43.	15.	10.	10.	0.	0.	12.30	3623.	3624.	3607.	0.0	0.0	2	
80	14	0.0	8.0	56.	43.	15.	10.	10.	0.	0.	12.37	3615.	3622.	3641.	0.0	0.0	2	
80	15	0.0	12.0	56.	43.	15.	10.	10.	0.	0.	12.35	3613.	3644.	3630.	0.0	0.0	2	
81	1	0.0	-4.0	56.	43.	15.	10.	10.	0.	0.	12.23	104.	654.	675.	0.0	0.0	2	
81	2	0.0	-0.0	56.	43.	15.	10.	10.	0.	0.	12.30	152.	601.	654.	0.0	0.0	2	
81	3	0.0	4.0	56.	43.	15.	10.	10.	0.	0.	12.37	210.	600.	664.	0.0	0.0	2	
81	4	0.0	8.0	56.	43.	15.	10.	10.	0.	0.	12.37	246.	540.	676.	0.0	0.0	2	
81	5	0.0	12.0	56.	43.	15.	10.	10.	0.	0.	12.37	313.	437.	715.	0.0	0.0	2	
82	1	0.0	-0.0	56.	43.	15.	10.	10.	-10.	0.	3.19	3619.	3625.	3612.	0.0	0.0	2	
82	2	0.0	-0.0	56.	43.	15.	10.	10.	0.	0.	3.16	3622.	3612.	3589.	0.0	0.0	2	
82	3	0.0	-0.0	56.	43.	15.	10.	10.	10.	0.	3.21	3649.	3621.	3604.	0.0	0.0	2	
82	4	0.0	-0.0	56.	43.	15.	10.	10.	20.	0.	3.28	3620.	3612.	3592.	0.0	0.0	2	
83	1	0.0	-0.0	56.	43.	15.	10.	10.	-10.	0.	7.09	3626.	3649.	3638.	0.0	0.0	2	
83	2	0.0	-0.0	56.	43.	15.	10.	10.	0.	0.	7.11	3653.	3652.	3642.	0.0	0.0	2	
83	3	0.0	-0.0	56.	43.	15.	10.	10.	10.	0.	7.28	3641.	3657.	3656.	0.0	0.0	2	
83	4	0.0	-0.0	56.	43.	15.	10.	10.	20.	0.	7.15	3643.	3631.	3619.	0.0	0.0	2	
84	1	0.0	-0.0	56.	43.	15.	10.	10.	0.	0.	7.09	3657.	3627.	3611.	0.0	0.0	2	
84	2	0.0	-0.0	56.	43.	15.	10.	10.	0.	0.	7.09	3625.	3632.	3608.	0.0	0.0	2	
84	3	0.0	-0.0	56.	43.	15.	0.	10.	0.	0.	7.11	3700.	3623.	3605.	0.0	0.0	2	
84	4	0.0	-0.0	56.	43.	15.	-15.	10.	0.	0.	7.10	3656.	3620.	3620.	0.0	0.0	2	
84	5	0.0	-0.0	56.	43.	15.	-25.	10.	0.	0.	7.09	3629.	3620.	3605.	0.0	0.0	2	
84	6	0.0	-0.0	56.	43.	15.	-25.	25.	0.	0.	7.11	3617.	3617.	3601.	0.0	0.0	2	
85	1	0.0	-0.0	56.	43.	15.	-25.	-25.	0.	0.	7.28	3617.	3617.	3605.	0.0	0.0	2	
85	2	0.0	4.0	56.	43.	15.	-25.	-25.	0.	0.	7.26	3618.	3635.	3610.	0.0	0.0	2	
85	3	0.0	8.0	56.	43.	15.	-25.	-25.	0.	0.	7.14	3628.	3644.	3615.	0.0	0.0	2	
85	4	0.0	12.0	56.	43.	15.	-25.	-25.	0.	0.	7.09	3611.	3634.	3621.	0.0	0.0	2	
86	1	0.0	-0.0	56.	43.	15.	-25.	10.	0.	0.	12.44	3651.	3650.	3636.	0.0	0.0	2	
86	2	0.0	-0.0	56.	43.	15.	-15.	10.	0.	0.	12.42	3643.	3659.	3658.	0.0	0.0	2	
86	3	0.0	-0.0	56.	43.	15.	0.	10.	0.	0.	2.36	3628.	3648.	3628.	0.0	0.0	2	
86	4	0.0	-0.0	56.	43.	15.	-15.	10.	0.	0.	12.39	3636.	3637.	3624.	0.0	0.0	2	
86	5	0.0	-0.0	56.	43.	15.	-25.	10.	0.	0.	12.39	3642.	3648.	3643.	0.0	0.0	2	
86	6	0.0	-0.0	56.	43.	15.	-25.	25.	0.	0.	12.35	3629.	3634.	3611.	0.0	0.0	2	
87	1	0.0	-0.0	56.	43.	15.	10.	10.	-10.	0.	12.32	407.	649.	689.	0.0	0.0	2	
87	2	0.0	-0.0	56.	43.	15.	10.	10.	0.	0.	12.34	404.	641.	692.	0.0	0.0	2	
87	3	0.0	-0.0	56.	43.	15.	10.	10.	10.	0.	12.37	389.	633.	685.	0.0	0.0	2	
87	4	-0.0	-0.0	56.	43.	15.	10.	10.	20.	0.	12.35	395.	631.	680.	0.0	0.0	2	

GP76-0822-223

ORIGINAL PAGE IS
OF POOR QUALITY

FOLDOUT FRAME 1

C	DYNL DFG	NOSE GEAR	NOSE INLET	UNIT COVERS	OTHER	RUN	PT	BALANCE FORCE AND MOMENT DATA--STABILITY AXES LIFT (LB)	DRAG (LB)	PITCHING MOMENT (FT-LB)	SIDE FORCE (LB)	ROLLING MOMENT (FT-LB)	YAWING MOMENT (FT-LB)	TUNNEL TOTAL TEMP. (DEG F)	AMBIENT PRESSURE (IN HG)
.0	0.0	2		2		79	5	1312.	353.	-3529.	-579.	-23.	1353.	67.	30.02
.0	0.0	2		2		79	6	1321.	340.	-3959.	-730.	21.	1492.	67.	30.02
.0	0.0	2		2		79	7	1321.	325.	-3883.	-854.	441.	1423.	66.	30.02
.0	0.0	2		2		80	1	3389.	-1614.	1042.	85.	35.	-25.	65.	30.02
.0	0.0	2		2		80	2	3392.	-1601.	844.	-10.	-177.	40.	66.	30.02
.0	0.0	2		2		80	3	3428.	-1593.	610.	-112.	-492.	98.	66.	30.02
.0	0.0	2		2		80	4	3485.	-1592.	502.	-227.	-819.	238.	67.	30.02
.0	0.0	2		2		80	5	3517.	-1586.	611.	-311.	-945.	-11.	67.	30.02
.0	0.0	2		2		80	6	4241.	-1153.	-17.	208.	384.	-210.	69.	30.02
.0	0.0	2		2		80	7	4262.	-1147.	217.	55.	-294.	-201.	70.	30.02
.0	0.0	2		2		80	8	4234.	-1139.	78.	-132.	-925.	72.	70.	30.02
.0	0.0	2		2		80	9	4292.	-1144.	-262.	-347.	-1677.	471.	70.	30.02
.0	0.0	2		2		80	10	4346.	-1147.	-462.	-564.	-2118.	887.	71.	30.02
.0	0.0	2		2		80	11	5402.	-665.	-1802.	334.	477.	-164.	71.	30.02
.0	0.0	2		2		80	12	5451.	-644.	-1850.	98.	-392.	-44.	72.	30.02
.0	0.0	2		2		80	13	5437.	-647.	-2203.	-209.	-1266.	256.	72.	30.02
.0	0.0	2		2		80	14	5405.	-674.	-1751.	-582.	-1613.	1275.	72.	30.02
.0	0.0	2		2		80	15	5446.	-703.	-2720.	-904.	-2508.	1807.	72.	30.02
.0	0.0	2		2		81	1	2441.	483.	-4500.	161.	334.	-460.	70.	30.02
.0	0.0	2		2		81	2	2445.	489.	-4599.	-0.	594.	131.	69.	30.02
.0	0.0	2		2		81	3	2459.	491.	-4350.	-195.	434.	879.	69.	30.02
.0	0.0	2		2		81	4	2431.	471.	-4728.	-339.	-268.	1354.	68.	30.02
.0	0.0	2		2		81	5	2363.	446.	-4668.	-445.	-395.	1831.	67.	30.02
.0	0.0	2		2		82	1	2752.	-1048.	1428.	17.	-356.	-33.	66.	30.04
.0	0.0	2		2		82	2	2770.	-1470.	1243.	15.	-382.	-58.	65.	30.04
.0	0.0	2		2		82	3	2872.	-1494.	324.	9.	-278.	50.	66.	30.04
.0	0.0	2		2		82	4	2931.	-1497.	-747.	14.	-288.	27.	67.	30.04
.0	0.0	2		2		83	1	3102.	-1502.	2038.	61.	-496.	54.	69.	30.04
.0	0.0	2		2		83	2	3141.	-1506.	1001.	67.	-534.	27.	69.	30.04
.0	0.0	2		2		83	3	3354.	-1497.	-1119.	72.	-520.	-55.	70.	30.04
.0	0.0	2		2		83	4	3527.	-1505.	-3112.	82.	-467.	2.	70.	30.04
.0	0.0	2		2		84	1	3217.	-1594.	787.	66.	-333.	-57.	72.	30.04
.0	0.0	2		2		84	2	3141.	-1604.	427.	56.	-370.	-22.	72.	30.04
.0	0.0	2		2		84	3	3140.	-1606.	1042.	64.	-414.	-11.	73.	30.04
.0	0.0	2		2		84	4	3053.	-1605.	1160.	64.	-1355.	-80.	73.	30.04
.0	0.0	2		2		84	5	2974.	-1594.	1612.	82.	-1407.	-240.	73.	30.04
.0	0.0	2		2		84	6	2930.	-1576.	1367.	61.	-2065.	-143.	73.	30.04
.0	0.0	2		2		85	1	2974.	-1571.	1391.	33.	1331.	130.	75.	30.04
.0	0.0	2		2		85	2	3043.	-1582.	495.	-236.	977.	426.	75.	30.04
.0	0.0	2		2		85	3	3120.	-1612.	255.	-486.	-144.	834.	76.	30.04
.0	0.0	2		2		85	4	3272.	-1625.	-186.	-684.	63.	662.	77.	30.04
.0	0.0	2		2		86	1	3794.	-1192.	-321.	22.	323.	254.	78.	30.04
.0	0.0	2		2		86	2	3780.	-1211.	-244.	26.	-159.	426.	78.	30.04
.0	0.0	2		2		86	3	3640.	-1218.	-27.	41.	-444.	610.	78.	30.04
.0	0.0	2		2		86	4	3586.	-1208.	445.	37.	-1913.	230.	78.	30.04
.0	0.0	2		2		86	5	3405.	-1190.	565.	34.	-2581.	-97.	78.	30.04
.0	0.0	2		2		86	6	3536.	-1174.	527.	36.	-3017.	151.	79.	30.04
.0	0.0	2		2		87	1	874.	467.	1703.	-2.	129.	140.	78.	30.04
.0	0.0	2		2		87	2	1177.	403.	-2571.	3.	125.	80.	77.	30.04
.0	0.0	2		2		87	3	1540.	407.	-6518.	4.	15.	123.	77.	30.04
.0	0.0	2		2		87	4	1730.	505.	-8924.	-4.	124.	151.	77.	30.04

FOLDOUT FRAME 2

RUN	PT	ALPHA DEG	BETA DEG	DLC DEG	DNL DEG	DE DEG	DAL DEG	DAR DEG	DR DEG	DR DEG	QC PSF	FAN1 RPM	FAN2 RPM	FAN3 RPM	DYLC DEG	DYNL DEG	NOSE GEAR	NOSE INLET	UNI COVE
88	1	0.0	-0.0	56.	43.	15.	10.	10.	-20.	0.	12.49	3622.	3649.	3661.	0.0	0.0	2		2
88	2	0.0	-0.0	56.	43.	15.	10.	10.	-15.	0.	12.32	3630.	3628.	3619.	0.0	0.0	2		2
88	3	0.0	-0.0	56.	43.	15.	10.	10.	-10.	0.	12.45	3640.	3637.	3620.	0.0	0.0	2		2
88	4	0.0	-0.0	56.	43.	15.	10.	10.	-5.	0.	12.47	3616.	3632.	3619.	0.0	0.0	2		2
88	5	0.0	-0.0	56.	43.	15.	10.	10.	0.	0.	12.47	3618.	3627.	3621.	0.0	0.0	2		2
88	6	0.0	-0.0	56.	43.	15.	10.	10.	5.	0.	12.47	3615.	3635.	3625.	0.0	0.0	2		2
88	7	0.0	-0.0	56.	43.	15.	10.	10.	10.	0.	12.47	3614.	3627.	3613.	0.0	0.0	2		2
88	8	0.0	-0.0	56.	43.	15.	10.	10.	15.	0.	12.37	3614.	3637.	3631.	0.0	0.0	2		2
88	9	0.0	-0.0	55.	43.	15.	10.	10.	20.	0.	12.44	3614.	3626.	3609.	0.0	0.0	2		2
89	1	0.0	-0.0	56.	43.	15.	10.	10.	0.	0.	19.26	3648.	3644.	3634.	0.0	0.0	2		2
89	2	0.0	-0.0	55.	43.	15.	10.	10.	0.	0.	19.25	2916.	3617.	3610.	0.0	0.0	2		2
89	3	0.0	-0.0	56.	43.	15.	10.	10.	0.	0.	19.33	2008.	3634.	3636.	0.0	0.0	2		2
90	1	8.0	-0.0	56.	43.	15.	10.	10.	-10.	0.	3.43	3617.	3622.	3617.	0.0	0.0	2		2
90	2	8.0	-0.0	56.	43.	15.	10.	10.	0.	0.	3.42	3615.	3636.	3630.	0.0	0.0	2		2
90	3	8.0	-0.0	56.	43.	15.	10.	10.	10.	0.	3.41	3609.	3618.	3614.	0.0	0.0	2		2
90	4	8.0	-0.0	56.	43.	15.	10.	10.	20.	0.	3.26	3608.	3610.	3614.	0.0	0.0	2		2
91	1	8.0	-0.0	56.	43.	15.	10.	10.	-20.	0.	7.28	3618.	3622.	3610.	0.0	0.0	2		2
91	2	8.0	-0.0	56.	43.	15.	10.	10.	0.	0.	7.11	3602.	3608.	3601.	0.0	0.0	2		2
91	3	8.0	-0.0	56.	43.	15.	10.	10.	10.	0.	7.04	3616.	3606.	3595.	0.0	0.0	2		2
91	4	8.0	-0.0	56.	43.	15.	10.	10.	20.	0.	7.04	3615.	3621.	3608.	0.0	0.0	2		2
92	1	8.0	-0.0	56.	43.	15.	10.	10.	-10.	0.	12.62	3629.	3621.	3615.	0.0	0.0	2		2
92	2	8.0	-0.0	56.	43.	15.	10.	10.	0.	0.	12.32	3619.	3634.	3610.	0.0	0.0	2		2
92	3	8.0	-0.0	56.	43.	15.	10.	10.	10.	0.	12.25	3632.	3615.	3604.	0.0	0.0	2		2
92	4	8.0	-0.0	56.	43.	15.	10.	10.	20.	0.	12.25	3615.	3618.	3608.	0.0	0.0	2		2
93	1	8.0	-0.0	56.	43.	15.	10.	10.	-10.	0.	12.42	160.	613.	648.	0.0	0.0	2		2
93	2	8.0	-0.0	56.	43.	15.	10.	10.	0.	0.	12.31	162.	613.	652.	0.0	0.0	2		2
93	3	8.0	-0.0	56.	43.	15.	10.	10.	10.	0.	12.32	178.	602.	654.	0.0	0.0	2		2
93	4	8.0	-0.0	56.	43.	15.	10.	10.	20.	0.	12.30	154.	595.	649.	0.0	0.0	2		2
93	5	8.0	-0.0	56.	43.	15.	10.	10.	0.	0.	14.10	194.	744.	804.	0.0	0.0	2		2
94	1	16.0	-0.0	56.	43.	15.	10.	10.	-10.	0.	3.26	3607.	3631.	3606.	0.0	0.0	2		2
94	2	16.0	-0.0	56.	43.	15.	10.	10.	0.	0.	3.24	3641.	3621.	3611.	0.0	0.0	2		2
94	3	16.0	-0.0	56.	43.	15.	10.	10.	10.	0.	3.24	3618.	3614.	3609.	0.0	0.0	2		2
94	4	16.0	-0.0	56.	43.	15.	10.	10.	20.	0.	3.23	3644.	3611.	3605.	0.0	0.0	2		2
95	1	16.0	-0.0	55.	43.	15.	10.	10.	-10.	0.	7.04	3619.	3631.	3619.	0.0	0.0	2		2
95	2	16.0	-0.0	55.	43.	15.	10.	10.	0.	0.	7.06	3629.	3625.	3615.	0.0	0.0	2		2
95	3	16.0	-0.0	55.	43.	15.	10.	10.	10.	0.	7.18	3612.	3654.	3645.	0.0	0.0	2		2
95	4	16.0	-0.0	55.	43.	15.	10.	10.	20.	0.	7.15	3647.	3641.	3620.	0.0	0.0	2		2
96	1	16.0	-0.0	56.	43.	15.	10.	10.	-10.	0.	12.28	3635.	3638.	3619.	0.0	0.0	2		2
96	2	16.0	-0.0	56.	43.	15.	10.	10.	0.	0.	12.39	3630.	3658.	3642.	0.0	0.0	2		2
96	3	16.0	-0.0	56.	43.	15.	10.	10.	10.	0.	12.25	3625.	3656.	3637.	0.0	0.0	2		2
96	4	16.0	-0.0	56.	43.	15.	10.	10.	20.	0.	12.18	3620.	3628.	3612.	0.0	0.0	2		2
97	1	16.0	-0.0	56.	43.	15.	10.	10.	-10.	0.	12.25	46.	485.	657.	0.0	0.0	2		2
97	2	16.0	-0.0	56.	43.	15.	10.	10.	0.	0.	12.32	56.	466.	656.	0.0	0.0	2		2
97	3	16.0	-0.0	56.	43.	15.	10.	10.	10.	0.	12.33	88.	443.	662.	0.0	0.0	2		2
97	4	16.0	-0.0	56.	43.	15.	10.	10.	20.	0.	12.23	63.	431.	651.	0.0	0.0	2		2
98	1	-4.0	-0.0	56.	43.	15.	10.	10.	0.	0.	3.22	3605.	3618.	3594.	0.0	0.0	2		2
98	2	-4.0	-0.0	56.	43.	15.	10.	10.	0.	0.	7.12	3645.	3625.	3608.	0.0	0.0	2		2
98	3	-4.0	-0.0	56.	43.	15.	10.	10.	0.	0.	12.30	3625.	3647.	3619.	0.0	0.0	2		2
99	1	12.0	-0.0	56.	43.	15.	10.	10.	0.	0.	3.24	3675.	3640.	3634.	0.0	0.0	2		2
99	2	12.0	-0.0	56.	43.	15.	10.	10.	0.	0.	7.11	3645.	3629.	3614.	0.0	0.0	2		2
99	3	12.0	-0.0	56.	43.	15.	10.	10.	0.	0.	12.31	3617.	3632.	3618.	0.0	0.0	2		2

GP78-0822-224

ORIGINAL PAGE IS
OF POOR QUALITY

FOLDOUT FRAME 1

BALANCE FORCE AND MOMENT DATA--STABILITY AXES

DYNL DEG	NOSE GEAR	NOSE INLET	UNIT COVERS	OTHER	RUN	PT	LIFT (LB)	DRAG (LB)	PITCHING MOMENT (FT-LB)	SIDE FORCE (LB)	ROLLING MOMENT (FT-LB)	YAWING MOMENT (FT-LB)	TUNNEL TOTAL TEMP. (DEG F)	AMBIENT PRESSURE (IN HG)
0.0	2		2		98	1	3577.	-1053.	1487.	25.	-338.	251.	76.	30.08
0.0	2		2		88	2	3647.	-1086.	1149.	26.	-364.	351.	77.	30.08
0.0	2		2		88	3	3579.	-1106.	2436.	12.	-421.	427.	77.	30.08
0.0	2		2		88	4	3544.	-1178.	2507.	24.	-468.	399.	78.	30.08
0.0	2		2		88	5	3663.	-1194.	501.	39.	-472.	427.	79.	30.08
0.0	2		2		88	6	3816.	-1194.	-1533.	8.	-140.	363.	79.	30.08
0.0	2		2		88	7	3995.	-1174.	-3541.	7.	-83.	342.	78.	30.08
0.0	2		2		88	8	4162.	-1151.	-5474.	2.	-214.	198.	78.	30.08
0.0	2		2		88	9	4324.	-1110.	-7148.	9.	-294.	390.	79.	30.08
0.0	2		2		89	1	4525.	-743.	-1244.	13.	12.	75.	80.	30.08
0.0	2		2		89	2	4414.	-913.	-5051.	3.	-20.	-11.	80.	30.08
0.0	2		2		89	3	4414.	-319.	-8416.	-17.	68.	72.	81.	30.08
0.0	2		2		90	1	3384.	-1524.	2015.	-7.	-304.	7.	75.	30.08
0.0	2		2		90	2	3442.	-1538.	1219.	-7.	-264.	-14.	76.	30.08
0.0	2		2		90	3	3524.	-1530.	344.	-4.	-281.	9.	77.	30.08
0.0	2		2		90	4	3547.	-1512.	-332.	-13.	-286.	-19.	78.	30.08
0.0	2		2		91	1	4059.	-1067.	3008.	62.	-620.	-11.	80.	30.08
0.0	2		2		91	2	4186.	-1116.	1048.	74.	-554.	-208.	81.	30.08
0.0	2		2		91	3	4357.	-1085.	-1141.	74.	-468.	-210.	82.	30.08
0.0	2		2		91	4	4470.	-1023.	-2519.	65.	-543.	-278.	82.	30.08
0.0	2		2		92	1	5061.	-608.	2603.	28.	-459.	257.	83.	30.08
0.0	2		2		92	2	5321.	-629.	-1092.	68.	-495.	-187.	83.	30.08
0.0	2		2		92	3	5648.	-579.	-5133.	60.	-524.	-44.	83.	30.08
0.0	2		2		92	4	5823.	-471.	-6961.	43.	-284.	33.	83.	30.08
0.0	2		2		93	1	2174.	484.	183.	-4.	305.	96.	83.	30.08
0.0	2		2		93	2	2434.	491.	-3710.	-3.	184.	99.	82.	30.08
0.0	2		2		93	3	2784.	550.	-7424.	-13.	363.	187.	81.	30.08
0.0	2		2		93	4	2719.	554.	-7438.	-2.	245.	107.	81.	30.08
0.0	2		2		93	5	3814.	754.	-6035.	-4.	175.	196.	0.	30.08
0.0	2		2		94	1	3847.	-935.	1455.	23.	-364.	98.	1.	30.08
0.0	2		2		94	2	3930.	-926.	1106.	24.	-365.	-44.	82.	30.08
0.0	2		2		94	3	3991.	-898.	4.	21.	-370.	-1.	83.	30.08
0.0	2		2		94	4	4041.	-867.	-604.	32.	-414.	60.	83.	30.08
0.0	2		2		95	1	4748.	-340.	1419.	79.	-521.	-89.	85.	30.08
0.0	2		2		95	2	4834.	-323.	-54.	94.	-604.	-331.	85.	30.08
0.0	2		2		95	3	5163.	-242.	-2354.	90.	-584.	-285.	86.	30.08
0.0	2		2		95	4	5211.	-181.	-3334.	93.	-621.	-297.	86.	30.08
0.0	2		2		96	1	6124.	290.	2134.	34.	-508.	84.	87.	30.08
0.0	2		2		96	2	6474.	305.	-2235.	44.	-469.	-134.	87.	30.08
0.0	2		2		96	3	6704.	434.	-5849.	16.	-53.	17.	87.	30.08
0.0	2		2		96	4	6749.	575.	-7341.	52.	-564.	-11.	87.	30.08
0.0	2		2		97	1	2915.	439.	-172.	-13.	657.	309.	85.	30.08
0.0	2		2		97	2	3260.	462.	-4401.	-34.	1312.	540.	86.	30.08
0.0	2		2		97	3	3430.	494.	-7478.	-16.	1217.	344.	85.	30.08
0.0	2		2		97	4	3378.	1072.	-6880.	-8.	950.	380.	85.	30.08
0.0	2		2		98	1	2351.	-2116.	884.	-2.	-231.	84.	63.	29.96
0.0	2		2		98	2	2486.	-1792.	471.	71.	-475.	-125.	64.	29.96
0.0	2		2		98	3	2492.	-1401.	233.	16.	94.	702.	67.	29.96
0.0	2		2		99	1	3695.	-1306.	1332.	-16.	171.	222.	69.	29.96
0.0	2		2		99	2	4614.	-773.	-275.	56.	347.	224.	69.	29.96
0.0	2		2		99	3	6195.	-290.	-2122.	46.	-69.	114.	71.	29.96

0822-224

FOLDOUT FRAME 2

RUN	PT	ALPHA DEG	BETA DEG	DLC DEG	DNL DEG	DF DEG	DAL DEG	DAR DEG	DM DEG	DR DEG	QC PSF	FAN1 RPM	FAN2 RPM	FAN3 RPM	DYLC DEG	DYNL DEG	NOSE GEAR	NOSE INLET	UN COV
100	1	12.0	-0.0	56.	43.	15.	10.	10.	0.	0.	12.37	81.	554.	645.	0.0	0.0	2		2
101	1	0.0	-0.0	56.	43.	15.	10.	10.	0.	0.	7.09	3628.	3623.	3629.	0.0	0.0	1		1
101	2	0.0	-0.0	56.	43.	15.	10.	10.	0.	0.	3.33	3629.	3633.	3617.	0.0	0.0	1		1
101	3	0.0	-0.0	56.	43.	15.	10.	10.	0.	0.	12.23	3605.	3620.	3613.	0.0	0.0	1		1
101	4	0.0	-0.0	56.	43.	15.	10.	10.	0.	0.	19.21	3631.	3625.	3607.	0.0	0.0	1		1
102	1	0.0	-0.0	56.	43.	15.	10.	10.	0.	0.	3.38	3629.	3614.	3621.	0.0	0.0	2		2
102	2	0.0	-0.0	56.	43.	15.	10.	10.	0.	0.	7.16	3626.	3634.	3622.	0.0	0.0	2		2
102	3	0.0	-0.0	56.	43.	15.	10.	10.	0.	0.	12.35	3626.	3665.	3657.	0.0	0.0	2		2
102	4	0.0	-0.0	56.	43.	15.	10.	10.	0.	0.	19.01	3652.	3611.	3617.	0.0	0.0	2		2
103	1	-4.0	-0.0	38.	43.	15.	10.	10.	0.	0.	12.29	3618.	3619.	3615.	0.0	0.0	2		2
103	2	0.0	-0.0	38.	43.	15.	10.	10.	0.	0.	12.30	3631.	3613.	3608.	0.0	0.0	2		2
103	3	4.0	-0.0	38.	43.	15.	10.	10.	0.	0.	12.31	3627.	3612.	3607.	0.0	0.0	2		2
103	4	8.0	-0.0	38.	43.	15.	10.	10.	0.	0.	12.30	3626.	3643.	3646.	0.0	0.0	2		2
103	5	12.0	-0.0	38.	43.	15.	10.	10.	0.	0.	12.37	3631.	3621.	3610.	0.0	0.0	2		2
103	6	14.0	-0.0	38.	43.	15.	10.	10.	0.	0.	12.44	3630.	3637.	3624.	0.0	0.0	2		2
103	7	16.0	-0.0	38.	43.	15.	10.	10.	0.	0.	12.32	3624.	3648.	3627.	0.0	0.0	2		2
103	8	20.0	-0.0	38.	43.	15.	10.	10.	0.	0.	12.37	3640.	3649.	3632.	0.0	0.0	2		2
104	1	0.0	-0.0	38.	43.	15.	10.	10.	-10.	0.	12.32	3614.	3623.	3606.	0.0	0.0	2		2
104	2	0.0	-0.0	38.	43.	15.	10.	10.	0.	0.	12.35	3618.	3608.	3594.	0.0	0.0	2		2
104	3	0.0	-0.0	38.	43.	15.	10.	10.	10.	0.	12.44	3626.	3614.	3608.	0.0	0.0	2		2
104	4	0.0	-0.0	38.	43.	15.	10.	10.	20.	0.	12.32	3636.	3616.	3606.	0.0	0.0	2		2
105	1	-4.0	-0.0	38.	43.	15.	10.	10.	0.	0.	19.19	3626.	3669.	3659.	0.0	0.0	2		2
105	2	0.0	-0.0	38.	43.	15.	10.	10.	0.	0.	19.19	3640.	3683.	3664.	0.0	0.0	2		2
105	3	4.0	-0.0	38.	43.	15.	10.	10.	0.	0.	19.28	3639.	3631.	3618.	0.0	0.0	2		2
105	4	8.0	-0.0	38.	43.	15.	10.	10.	0.	0.	19.21	3626.	3638.	3614.	0.0	0.0	2		2
105	5	12.0	-0.0	38.	43.	15.	10.	10.	0.	0.	19.22	3615.	3629.	3629.	0.0	0.0	2		2
105	6	14.0	-0.0	38.	43.	15.	10.	10.	0.	0.	19.32	3635.	3629.	3620.	0.0	0.0	2		2
105	7	16.0	-0.0	38.	43.	15.	10.	10.	0.	0.	19.16	3638.	3656.	3639.	0.0	0.0	2		2
105	8	20.0	-0.0	38.	43.	15.	10.	10.	0.	0.	19.28	3600.	3635.	3633.	0.0	0.0	2		2
106	1	0.0	-0.0	38.	43.	15.	10.	10.	-10.	0.	19.35	3614.	3628.	3617.	0.0	0.0	2		2
106	2	0.0	-0.0	38.	43.	15.	10.	10.	0.	0.	19.39	3614.	3652.	3658.	0.0	0.0	2		2
106	3	0.0	-0.0	38.	43.	15.	10.	10.	10.	0.	19.23	3627.	3627.	3608.	0.0	0.0	2		2
106	4	0.0	-0.0	38.	43.	15.	10.	10.	20.	0.	19.24	3624.	3640.	3619.	0.0	0.0	2		2
107	1	-4.0	-0.0	38.	43.	15.	10.	10.	0.	0.	7.16	3635.	3645.	3622.	0.0	0.0	2		2
107	2	0.0	-0.0	38.	43.	15.	10.	10.	0.	0.	7.16	3627.	3649.	3639.	0.0	0.0	2		2
107	3	4.0	-0.0	38.	43.	15.	10.	10.	0.	0.	7.14	3622.	3634.	3613.	0.0	0.0	2		2
107	4	8.0	-0.0	38.	43.	15.	10.	10.	0.	0.	7.07	3625.	3631.	3609.	0.0	0.0	2		2
107	5	12.0	-0.0	38.	43.	15.	10.	10.	0.	0.	7.11	3619.	3626.	3602.	0.0	0.0	2		2
107	6	14.0	-0.0	38.	43.	15.	10.	10.	0.	0.	7.16	3615.	3631.	3611.	0.0	0.0	2		2
107	7	16.0	-0.0	38.	43.	15.	10.	10.	0.	0.	7.04	3619.	3633.	3618.	0.0	0.0	2		2
107	8	20.0	-0.0	38.	43.	15.	10.	10.	0.	0.	7.21	3618.	3668.	3638.	0.0	0.0	2		2
108	1	0.0	-0.0	38.	43.	15.	10.	10.	-10.	0.	7.16	3630.	3646.	3633.	0.0	0.0	2		2
108	2	0.0	-0.0	38.	43.	15.	10.	10.	0.	0.	7.23	3623.	3642.	3630.	0.0	0.0	2		2
108	3	0.0	-0.0	38.	43.	15.	10.	10.	10.	0.	7.26	3622.	3626.	3615.	0.0	0.0	2		2
108	4	0.0	-0.0	38.	43.	15.	10.	10.	20.	0.	7.14	3614.	3628.	3617.	0.0	0.0	2		2
109	1	-4.0	-0.0	38.	43.	15.	10.	10.	0.	0.	19.28	568.	848.	920.	0.0	0.0	2		2
109	2	0.0	-0.0	38.	43.	15.	10.	10.	0.	0.	19.25	527.	836.	905.	0.0	0.0	2		2
109	3	4.0	-0.0	38.	43.	15.	10.	10.	0.	0.	19.24	357.	826.	895.	0.0	0.0	2		2
109	4	8.0	-0.0	38.	43.	15.	10.	10.	0.	0.	19.28	191.	813.	872.	0.0	0.0	2		2
109	5	12.0	-0.0	38.	43.	15.	10.	10.	0.	0.	19.25	91.	789.	868.	0.0	0.0	2		2
109	6	16.0	-0.0	38.	43.	15.	10.	10.	0.	0.	19.35	93.	669.	871.	0.0	0.0	2		2

GP76-0622-228

HALANCE FORCE AND MOMENT DATA--STABILITY AXES

DYNL DEG	NOSE GEAR	NOSE INLET	UNIT COVERS	OTHER	RUN	PT	LIFT (LH)	DRAG (LH)	PITCHING MOMENT (FT-LH)	SIDE FORCE (LH)	ROLLING MOMENT (FT-LH)	YAWING MOMENT (FT-LH)	TUNNEL TOTAL TEMP. (DEG F)	AMBIENT PRESSURE (IN HG)
0.0	2		2		100	1	3086.	-607.	-4325.	1.	103.	131.	71.	29.96
0.0	2		2		101	1	2624.	-2183.	639.	9.	-491.	-9.	67.	29.96
0.0	2		2		101	2	2742.	-2004.	581.	-13.	-167.	-29.	69.	29.96
0.0	2		2		101	3	3615.	-1232.	196.	17.	-440.	144.	70.	29.96
0.0	2		2		101	4	4541.	-784.	-1474.	-13.	493.	235.	71.	29.96
0.0	2		2	LIFT CRUISE THRUST MODULATION PORTS OPEN	102	1	2510.	-1799.	1218.	-35.	-374.	133.	64.	29.96
0.0	2		2		102	2	2973.	-1363.	727.	-90.	-144.	423.	63.	29.96
0.0	2		2		102	3	3425.	-970.	-377.	25.	-196.	289.	65.	29.96
0.0	2		2		102	4	4234.	-505.	-1466.	-34.	537.	306.	66.	29.96
0.0	2		2		103	1	1791.	-2004.	3799.	56.	-133.	-102.	77.	29.86
0.0	2		2		103	2	2624.	-1482.	3531.	45.	-40.	-125.	78.	29.86
0.0	2		2		103	3	3521.	-1061.	2982.	29.	-117.	-96.	79.	29.86
0.0	2		2		103	4	4414.	-1644.	2620.	22.	46.	-113.	79.	29.86
0.0	2		2		103	5	5273.	-1184.	2427.	29.	-150.	-82.	80.	29.86
0.0	2		2		103	6	5434.	-904.	1783.	-54.	1919.	619.	81.	29.86
0.0	2		2		103	7	5444.	-643.	1816.	37.	-66.	45.	81.	29.86
0.0	2		2		103	8	5931.	-144.	1252.	32.	-124.	125.	82.	29.86
0.0	2		2		104	1	2437.	-1776.	6187.	6.	-29.	158.	84.	29.86
0.0	2		2		104	2	2644.	-1456.	3633.	41.	-29.	41.	84.	29.86
0.0	2		2		104	3	2984.	-1438.	-427.	14.	123.	9.	84.	29.86
0.0	2		2		104	4	3261.	-1772.	-3695.	26.	150.	116.	85.	29.86
0.0	2		2		105	1	2093.	-1644.	3316.	3.	647.	133.	84.	29.86
0.0	2		2		105	2	3297.	-1493.	2565.	-3.	414.	210.	87.	29.86
0.0	2		2		105	3	4575.	-1262.	1431.	-24.	750.	179.	87.	29.86
0.0	2		2		105	4	5727.	-783.	1078.	-6.	422.	-10.	87.	29.86
0.0	2		2		105	5	6441.	-634.	-195.	7.	361.	103.	87.	29.86
0.0	2		2		105	6	7321.	-350.	-303.	-67.	1796.	800.	87.	29.86
0.0	2		2		105	7	7141.	-27.	-102.	15.	-127.	144.	88	29.86
0.0	2		2		105	8	7701.	704.	-481.	11.	-556.	740.	85.	29.86
0.0	2		2		106	1	2913.	-1350.	8119.	-17.	15.	495.	89.	29.86
0.0	2		2		106	2	3234.	-1471.	2973.	7.	578.	39.	89.	29.86
0.0	2		2		106	3	3434.	-1449.	-3530.	-14.	837.	154.	90.	29.86
0.0	2		2		106	4	4207.	-1332.	-8045.	13.	373.	92.	90.	29.86
0.0	2		2		107	1	1554.	-2483.	4869.	4.	-470.	-49.	90.	29.86
0.0	2		2		107	2	2124.	-2286.	4101.	4.	-35.	-212.	91.	29.86
0.0	2		2		107	3	2732.	-2057.	4132.	-17.	171.	29.	91.	29.86
0.0	2		2		107	4	3373.	-1867.	4066.	5.	1.	2.	92.	29.86
0.0	2		2		107	5	3949.	-1650.	4035.	50.	-332.	-176.	93.	29.86
0.0	2		2		107	6	4072.	-1553.	4101.	-1.	1122.	293.	93.	29.86
0.0	2		2		107	7	4144.	-1262.	4135.	66.	-183.	-4.	93.	29.86
0.0	2		2		107	8	4540.	-805.	3422.	95.	-633.	-174.	94.	29.86
0.0	2		2		108	1	2094.	-2184.	5495.	54.	-254.	140.	94.	29.86
0.0	2		2		108	2	2147.	-2235.	4157.	74.	-231.	-35.	94.	29.86
0.0	2		2		108	3	2334.	-2232.	2198.	94.	-379.	-44.	94.	29.85
0.0	2		2		108	4	2556.	-2195.	470.	85.	-214.	61.	94.	29.86
0.0	2		2		109	1	495.	527.	-1952.	7.	509.	140.	93.	29.86
0.0	2		2		109	2	1494.	519.	-3112.	9.	375.	93.	93.	29.85
0.0	2		2		109	3	2532.	557.	-4228.	-0.	461.	144.	91.	29.86
0.0	2		2		109	4	3441.	651.	-5045.	-6.	373.	115.	91.	29.86
0.0	2		2		109	5	4429.	811.	-6046.	-5.	222.	150.	91.	29.86
0.0	2		2		109	6	4916.	1181.	-6811.	4.	65.	714.	90.	29.86

622-226

FOLDOUT FRAME 2

MIN	PT	ALPHA DEG	BETA DEG	DLC DEG	DSL DEG	DF DEG	DAL DEG	DAR DEG	DH DEG	DR DEG	QC PSF	FAN1 RPM	FAN2 RPM	FAN3 RPM	DYLC DEG	DYNL DEG	NOSE GEAR	NOSE INLET
109	7	20.0	-0.0	34.	43.	15.	10.	10.	0.	0.	19.14	200.	506.	889.	0.0	0.0	2	
110	1	0.0	-0.0	34.	43.	15.	10.	10.	0.	23.	0.00	71.	117.	3624.	0.0	0.0		
110	2	0.0	-0.0	34.	43.	15.	10.	10.	0.	23.	.26	121.	3638.	3629.	0.0	0.0		
110	3	0.0	-0.0	34.	43.	15.	10.	10.	0.	23.	.37	3642.	3672.	3652.	0.0	0.0		
111	1	0.0	-0.0	34.	43.	15.	10.	10.	0.	24.	7.23	3631.	3647.	3622.	0.0	0.0		
111	2	8.0	-0.0	34.	43.	15.	10.	10.	0.	24.	7.11	3621.	3622.	3616.	0.0	0.0		
111	3	12.0	-0.0	34.	43.	15.	10.	10.	0.	23.	7.11	3609.	3617.	3606.	0.0	0.0		
111	4	16.0	-0.0	34.	43.	15.	10.	10.	0.	23.	7.02	3613.	3640.	3616.	0.0	0.0		
111	5	20.0	-0.0	34.	43.	15.	10.	10.	0.	24.	7.06	3619.	3640.	3636.	0.0	0.0		
111	6	0.0	-0.0	34.	43.	15.	10.	10.	0.	24.	12.36	3616.	3650.	3628.	0.0	0.0		
111	7	8.0	-0.0	34.	43.	15.	10.	10.	0.	23.	12.33	3613.	3621.	3607.	0.0	0.0		
111	8	12.0	-0.0	34.	43.	15.	10.	10.	0.	24.	12.32	3642.	3623.	3612.	0.0	0.0		
111	9	16.0	-0.0	34.	43.	15.	10.	10.	0.	24.	12.32	3630.	3627.	3619.	0.0	0.0		
111	10	20.0	-0.0	34.	43.	15.	10.	10.	0.	24.	12.25	3615.	3626.	3608.	0.0	0.0		
112	1	0.0	-0.0	34.	43.	15.	10.	10.	0.	23.	34.17	3612.	1113.	1202.	0.0	0.0		
112	2	0.0	-0.0	34.	43.	15.	10.	10.	0.	23.	34.24	2893.	1107.	1194.	0.0	0.0		
112	3	0.0	-0.0	34.	43.	15.	10.	10.	0.	23.	34.19	1968.	1098.	1186.	0.0	0.0		
112	4	16.0	-0.0	34.	43.	15.	10.	10.	0.	23.	34.22	3626.	1094.	1188.	0.0	0.0		
112	5	16.0	-0.0	34.	43.	15.	10.	10.	0.	24.	34.34	2937.	1012.	1186.	0.0	0.0		
112	6	16.0	-0.0	34.	43.	15.	10.	10.	0.	24.	34.16	2010.	989.	1188.	0.0	0.0		
112	7	16.0	-0.0	34.	43.	15.	10.	10.	0.	24.	34.22	91.	956.	1157.	0.0	0.0		
112	8	0.0	-0.0	34.	43.	15.	10.	10.	0.	24.	34.19	662.	1126.	1218.	0.0	0.0		
113	1	0.0	-0.0	71.	35.	15.	10.	10.	0.	0.	0.00	69.	81.	3624.	0.0	0.0		
113	2	0.0	-0.0	71.	35.	15.	10.	10.	0.	0.	0.00	146.	3651.	3639.	0.0	0.0		
113	3	0.0	-0.0	71.	35.	15.	10.	10.	0.	0.	.25	3627.	3634.	3610.	0.0	0.0		
114	1	0.0	-0.0	71.	35.	15.	10.	10.	0.	0.	1.55	3633.	3637.	3635.	0.0	0.0		
114	2	8.0	-0.0	71.	35.	15.	10.	10.	0.	0.	1.34	3608.	3634.	3596.	0.0	0.0		
114	3	16.0	-0.0	71.	35.	15.	10.	10.	0.	0.	1.35	3613.	3640.	3600.	0.0	0.0		
114	4	0.0	-0.0	71.	35.	15.	10.	10.	-10.	0.	3.21	3632.	3678.	3632.	0.0	0.0		
114	5	0.0	-0.0	71.	35.	15.	10.	10.	10.	0.	3.33	3614.	3634.	3617.	0.0	0.0		
114	6	0.0	-0.0	71.	35.	15.	10.	10.	20.	0.	3.53	3626.	3634.	3634.	0.0	0.0		
115	1	-4.0	-0.0	71.	35.	15.	10.	10.	0.	0.	3.41	3627.	3663.	3629.	0.0	0.0		
115	2	0.0	-0.0	71.	35.	15.	10.	10.	0.	0.	3.27	3623.	3629.	3617.	0.0	0.0		
115	3	8.0	-0.0	71.	35.	15.	10.	10.	0.	0.	3.24	3623.	3653.	3634.	0.0	0.0		
115	4	12.0	-0.0	71.	35.	15.	10.	10.	0.	0.	3.36	3653.	3633.	3611.	0.0	0.0		
115	5	14.0	-0.0	71.	35.	15.	10.	10.	0.	0.	3.29	3646.	3627.	3606.	0.0	0.0		
115	6	16.0	-0.0	71.	35.	15.	10.	10.	0.	0.	3.21	3603.	3631.	3612.	0.0	0.0		
115	7	20.0	-0.0	71.	35.	15.	10.	10.	0.	0.	3.51	3610.	3634.	3613.	0.0	0.0		
115	8	0.0	-0.0	71.	35.	15.	10.	10.	0.	0.	7.21	3615.	3621.	3601.	0.0	0.0		
116	1	-4.0	-0.0	0.	99.	0.	0.	0.	0.	0.	34.20	93.	2711.	2719.	99.0	99.0		
116	2	0.0	-0.0	0.	99.	0.	0.	0.	0.	0.	34.33	129.	2708.	2722.	99.0	99.0		
116	3	2.0	-0.0	0.	99.	0.	0.	0.	0.	0.	34.27	89.	2702.	2718.	99.0	99.0		
116	4	4.0	-0.0	0.	99.	0.	0.	0.	0.	0.	34.23	99.	2710.	2716.	99.0	99.0		
116	5	6.0	-0.0	0.	99.	0.	0.	0.	0.	0.	34.20	90.	2713.	2707.	99.0	99.0		
116	6	8.0	-0.0	0.	99.	0.	0.	0.	0.	0.	34.12	96.	2715.	2702.	99.0	99.0		
116	7	10.0	-0.0	0.	99.	0.	0.	0.	0.	0.	34.14	88.	2745.	2751.	99.0	99.0		
116	8	12.0	-0.0	0.	99.	0.	0.	0.	0.	0.	34.12	98.	2732.	2739.	99.0	99.0		
116	9	14.0	-0.0	0.	99.	0.	0.	0.	0.	0.	34.18	96.	2722.	2718.	99.0	99.0		
116	10	15.0	-0.0	0.	99.	0.	0.	0.	0.	0.	34.15	121.	2733.	2731.	99.0	99.0		
116	11	18.0	-0.0	0.	99.	0.	0.	0.	0.	0.	34.21	107.	2739.	2742.	99.0	99.0		
116	12	20.0	-0.0	0.	99.	0.	0.	0.	0.	0.	34.14	87.	2754.	2756.	99.0	99.0	1	

GP76-0822-228

DYNL DEG	NOSE GEAR	NOSE INLET	UNIT COVERS	OTHER	RUN	PT	BALANCE FORCE AND MOMENT DATA--STABILITY AXES LIFT (LB)	DRAG (LB)	PITCHING MOMENT (FT-LB)	SIDE FORCE (LB)	ROLLING MOMENT (FT-LB)	YAWING MOMENT (FT-LB)	TUNNEL TOTAL TEMP. (DEG F)	AMBIENT PRESSURE (IN HG)
0.0	2		2		109	7	4349.	1604.	-6148.	7.	-200.	266.	69.	29.86
0.0	2		2		110	1	554.	-1705.	-2809.	-22.	-2437.	-4925.	79.	29.90
0.0	2		2		110	2	1068.	-2554.	-6474.	-2.	-29.	-5.	79.	29.90
0.0	2		2		110	3	1695.	-3170.	5811.	25.	-211.	264.	79.	29.90
0.0	2		2		111	1	2324.	-2224.	4460.	214.	715.	-1696.	79.	29.90
0.0	2		2		111	2	3453.	-1487.	4297.	222.	199.	-1454.	79.	29.90
0.0	2		2		111	3	4010.	-1527.	3995.	214.	1.	-1911.	79.	29.90
0.0	2		2		111	4	4160.	-1240.	4327.	234.	-246.	-1885.	79.	29.90
0.0	2		2		111	5	4539.	-857.	3675.	276.	-719.	-2030.	79.	29.90
0.0	2		2		111	6	2743.	-1437.	3503.	365.	1077.	-2936.	80.	29.90
0.0	2		2		111	7	4464.	-1424.	3045.	329.	685.	-3073.	80.	29.90
0.0	2		2		111	8	5342.	-1157.	2617.	330.	222.	-3094.	80.	29.90
0.0	2		2		111	9	5555.	-601.	1674.	352.	-505.	-3195.	81.	29.90
0.0	2		2		111	10	5904.	-142.	1409.	344.	-321.	-3246.	81.	29.90
0.0	2		2		112	1	2974.	413.	5150.	604.	2674.	-6622.	81.	29.90
0.0	2		2		112	2	2817.	-23.	1598.	529.	2481.	-6416.	80.	29.90
0.0	2		2		112	3	2711.	-91.	-1898.	604.	2686.	-6822.	80.	29.90
0.0	2		2		112	4	8476.	2142.	-540.	566.	182.	-6013.	80.	29.90
0.0	2		2		112	5	8405.	2266.	-3865.	546.	298.	-5968.	80.	29.90
0.0	2		2		112	6	8170.	2272.	-7046.	477.	1230.	-5162.	80.	29.90
0.0	2		2		112	7	8004.	2298.	-10041.	564.	-1795.	-5654.	80.	29.90
0.0	2		2		112	8	2658.	1004.	-5510.	620.	2491.	-6530.	79.	29.90
0.0	2		2		113	1	1049.	-555.	-6630.	-30.	-4553.	-2153.	60.	29.91
0.0	2		2		113	2	2038.	-1052.	-13244.	25.	-67.	40.	60.	29.91
0.0	2		2		113	3	3034.	-1774.	1601.	1.	-34.	56.	60.	29.91
0.0	2		2		114	1	3311.	-1404.	1812.	-37.	-103.	-91.	60.	29.91
0.0	2		2		114	2	3600.	-974.	2008.	-21.	-194.	7.	63.	29.91
0.0	2		2		114	3	3925.	-399.	1623.	-14.	-311.	60.	64.	29.91
0.0	2		2		114	4	3513.	-1153.	2042.	-46.	-257.	-263.	65.	29.91
0.0	2		2		114	5	3592.	-1140.	870.	-64.	-424.	-5.	67.	29.91
0.0	2		2		114	6	3682.	-1125.	21.	-60.	-393.	-5.	67.	29.91
0.0	2		2		115	1	3238.	-1493.	1881.	-66.	-418.	14.	69.	29.91
0.0	2		2		115	2	3550.	-1177.	2103.	-70.	-410.	-70.	69.	29.91
0.0	2		2		115	3	4072.	-650.	1525.	-41.	-455.	47.	67.	29.91
0.0	2		2		115	4	4293.	-291.	1467.	-62.	-59.	411.	70.	29.91
0.0	2		2		115	5	4357.	-139.	1514.	-40.	-210.	347.	70.	29.91
0.0	2		2		115	6	4411.	38.	1788.	-34.	-469.	183.	70.	29.91
0.0	2		2		115	7	4579.	449.	1879.	-13.	-508.	213.	71.	29.91
0.0	2		2		115	8	3958.	-714.	1330.	-.	-71.	42.	71.	29.91
90.0	1		1		116	1	-558.	-193.	-672.	-16.	214.	177.	63.	29.95
90.0	1		1		116	2	1485.	-240.	-2697.	-20.	411.	268.	63.	29.95
90.0	1		1		116	3	2662.	-225.	-3414.	-32.	583.	290.	65.	29.95
90.0	1		1		116	4	3435.	-194.	-4274.	-30.	593.	300.	65.	29.95
90.0	1		1		116	5	4550.	-115.	-4793.	-44.	843.	343.	66.	29.95
90.0	1		1		116	6	5258.	-55.	-5700.	-52.	624.	453.	65.	29.95
90.0	1		1		116	7	6159.	50.	-6798.	-44.	550.	442.	67.	29.95
90.0	1		1		116	8	7224.	184.	-7143.	-41.	523.	469.	67.	29.95
90.0	1		1		116	9	8128.	384.	-7948.	-60.	590.	771.	67.	29.95
90.0	1		1		116	10	8232.	744.	-7919.	-151.	2120.	952.	68.	29.95
90.0	1		1		116	11	7802.	1222.	-7162.	-62.	304.	787.	68.	29.95
90.0	1		1		116	12	7814.	1582.	-5722.	-31.	197.	581.	69.	29.95

FOLDOUT FRAME 3

RUN	PT	ALPHA DEG	BETA DEG	DLC DEG	DNL DEG	PL DEG	DAL DEG	DAR DEG	DR DEG	DM DEG	QC PSF	FAN1 RPM	FAN2 RPM	FAN3 RPM	DYLC DEG	DYNL DEG	NOSE GEAR
116	13	24.0	-0.0	0.	99.	0.	0.	0.	0.	0.	34.22	85.	2693.	2714.	99.0	99.0	1
116	14	28.0	-0.0	0.	99.	0.	0.	0.	0.	0.	34.14	125.	2708.	2745.	99.0	99.0	1
116	15	32.0	-0.0	0.	99.	0.	0.	0.	0.	0.	34.31	146.	2732.	2725.	99.0	99.0	1
117	1	-4.0	-0.0	0.	99.	0.	0.	0.	0.	0.	34.24	19.	2146.	2153.	99.0	99.0	1
117	2	0.0	-0.0	0.	99.	0.	0.	0.	0.	0.	34.16	20.	2142.	2150.	99.0	99.0	1
117	3	2.0	-0.0	0.	99.	0.	0.	0.	0.	0.	34.25	18.	2151.	2148.	99.0	99.0	1
117	4	4.0	-0.0	0.	99.	0.	0.	0.	0.	0.	34.20	19.	2167.	2160.	99.0	99.0	1
117	5	6.0	-0.0	0.	99.	0.	0.	0.	0.	0.	34.15	18.	2163.	2154.	99.0	99.0	1
117	6	8.0	-0.0	0.	99.	0.	0.	0.	0.	0.	34.15	55.	2148.	2152.	99.0	99.0	1
117	7	10.0	-0.0	0.	99.	0.	0.	0.	0.	0.	34.17	19.	2145.	2152.	99.0	99.0	1
117	8	12.0	-0.0	0.	99.	0.	0.	0.	0.	0.	34.17	21.	2176.	2189.	99.0	99.0	1
117	9	14.0	-0.0	0.	99.	0.	0.	0.	0.	0.	34.07	21.	2176.	2152.	99.0	99.0	1
117	10	16.0	-0.0	0.	99.	0.	0.	0.	0.	0.	34.20	17.	2180.	2192.	99.0	99.0	1
117	11	18.0	-0.0	0.	99.	0.	0.	0.	0.	0.	34.16	30.	2185.	2189.	99.0	99.0	1
117	12	20.0	-0.0	0.	99.	0.	0.	0.	0.	0.	34.27	21.	2148.	2173.	99.0	99.0	1
117	13	24.0	-0.0	0.	99.	0.	0.	0.	0.	0.	34.17	51.	2195.	2181.	99.0	99.0	1
117	14	28.0	-0.0	0.	99.	0.	0.	0.	0.	0.	34.12	23.	2151.	2174.	99.0	99.0	1
117	15	32.0	-0.0	0.	99.	0.	0.	0.	0.	0.	34.15	38.	2172.	2149.	99.0	99.0	1
118	1	-4.0	-0.0	0.	99.	0.	0.	0.	0.	0.	34.17	44.	1592.	1591.	99.0	99.0	1
118	2	0.0	-0.0	0.	99.	0.	0.	0.	0.	0.	34.23	41.	1615.	1612.	99.0	99.0	1
118	3	2.0	-0.0	0.	99.	0.	0.	0.	0.	0.	34.11	49.	1614.	1619.	99.0	99.0	1
118	4	4.0	-0.0	0.	99.	0.	0.	0.	0.	0.	34.25	20.	1604.	1604.	99.0	99.0	1
118	5	6.0	-0.0	0.	99.	0.	0.	0.	0.	0.	34.15	56.	1600.	1603.	99.0	99.0	1
118	6	8.0	-0.0	0.	99.	0.	0.	0.	0.	0.	34.15	20.	1627.	1630.	99.0	99.0	1
118	7	10.0	-0.0	0.	99.	0.	0.	0.	0.	0.	34.15	17.	1600.	1605.	99.0	99.0	1
118	8	12.0	-0.0	0.	99.	0.	0.	0.	0.	0.	34.01	48.	1607.	1608.	99.0	99.0	1
118	9	14.0	-0.0	0.	99.	0.	0.	0.	0.	0.	34.00	64.	1589.	1590.	99.0	99.0	1
118	10	16.0	-0.0	0.	99.	0.	0.	0.	0.	0.	34.25	28.	1620.	1632.	99.0	99.0	1
118	11	18.0	-0.0	0.	99.	0.	0.	0.	0.	0.	34.35	27.	1609.	1633.	99.0	99.0	1
118	12	20.0	-0.0	0.	99.	0.	0.	0.	0.	0.	34.13	15.	1595.	1626.	99.0	99.0	1
118	13	24.0	-0.0	0.	99.	0.	0.	0.	0.	0.	34.27	19.	1630.	1713.	99.0	99.0	1
119	1	0.0	-0.0	0.	99.	0.	0.	-20.	0.	0.	34.15	52.	2730.	2719.	99.0	99.0	1
119	2	8.0	-0.0	0.	99.	0.	0.	-20.	0.	0.	34.18	33.	2707.	2706.	99.0	99.0	1
119	3	16.0	-0.0	0.	99.	0.	0.	-20.	0.	0.	34.29	25.	2747.	2766.	99.0	99.0	1
119	4	24.0	-0.0	0.	99.	0.	0.	-20.	0.	0.	34.02	18.	2673.	2772.	99.0	99.0	1
119	5	28.0	-0.0	0.	99.	0.	0.	-20.	0.	0.	34.24	54.	2729.	2733.	99.0	99.0	1
119	6	32.0	-0.0	0.	99.	0.	0.	-20.	0.	0.	34.20	40.	2706.	2701.	99.0	99.0	1
120	1	0.0	-0.0	0.	99.	0.	0.	-20.	0.	0.	34.23	32.	2153.	2173.	99.0	99.0	1
120	2	4.0	-0.0	0.	99.	0.	0.	-20.	0.	0.	34.22	50.	2154.	2141.	99.0	99.0	1
120	3	16.0	-0.0	0.	99.	0.	0.	-20.	0.	0.	34.12	18.	2176.	2173.	99.0	99.0	1
120	4	24.0	-0.0	0.	99.	0.	0.	-20.	0.	0.	34.24	24.	2159.	2151.	99.0	99.0	1
120	5	28.0	-0.0	0.	99.	0.	0.	-20.	0.	0.	34.24	61.	2196.	2195.	99.0	99.0	1
120	6	32.0	-0.0	0.	99.	0.	0.	-20.	0.	0.	34.24	69.	2183.	2175.	99.0	99.0	1
121	1	0.0	-0.0	0.	99.	0.	0.	-10.	0.	0.	34.24	20.	2742.	2735.	99.0	99.0	1
121	2	8.0	-0.0	0.	99.	0.	0.	-10.	0.	0.	34.22	26.	2755.	2718.	99.0	99.0	1
121	3	16.0	-0.0	0.	99.	0.	0.	-10.	0.	0.	34.05	22.	2733.	2725.	99.0	99.0	1
121	4	24.0	-0.0	0.	99.	0.	0.	-10.	0.	0.	34.19	25.	2785.	2723.	99.0	99.0	1
121	5	28.0	-0.0	0.	99.	0.	0.	-10.	0.	0.	34.26	38.	2719.	2739.	99.0	99.0	1
121	6	32.0	-0.0	0.	99.	0.	0.	-10.	0.	0.	34.29	51.	2754.	2737.	99.0	99.0	1
122	1	0.0	-0.0	0.	99.	0.	0.	0.	0.	0.	0.00	67.	1630.	463.	99.0	99.0	1
122	2	0.0	-0.0	0.	99.	0.	0.	0.	0.	0.	0.00	83.	2172.	112.	99.0	99.0	1

GP78-0621-227

BALANCE FORCE AND MOMENT DATA--STABILITY AXES

FAN3 RPM	DYLC DEG	DYNL DEG	NOSE GEAR	NOSE INLET	UNIT COVERS	OTHER	RUN	PT	LIFT (LB)	DRAG (LB)	PITCHING MOMENT (FT-LB)	SIDE FORCE (LB)	ROLLING MOMENT (FT-LB)	YAWING MOMENT (FT-LB)	TUNNEL TOTAL TEMP. (DEG F)	AMBIENT PRESSURE (IN HG)
[illegible]14.	99.0	99.0	1		1		116	13	872[illegible].	2360.	-3972.	-26.	450.	284.	69.	29.95
[illegible]45.	99.0	99.0	1		1		116	14	9286.	3324.	-2397.	-53.	210.	804.	70.	29.95
725.	99.0	99.0	1		1		116	15	8926.	4187.	1860.	-9.	-209.	856.	71.	29.95
[illegible]53.	99.0	99.0	1		1		117	1	-574.	197.	-[illegible].	4.	468.	[illegible]	[illegible]7.	29.94
[illegible]50.	99.0	99.0	1		1		117	2	1382.	146.	-3017.	-1.	363.	167.	68.	29.94
[illegible]48.	99.0	99.0	1		1		117	3	2572.	170.	-3736.	-8.	399.	188.	68.	29.94
[illegible]60.	99.0	99.0	1		1		117	4	3317	185.	-4561.	-10.	352.	194.	68.	29.94
156.	99.0	99.0	1		1		117	5	4439.	263.	-5671.	-34.	559.	350.	69.	29.94
152.	99.0	99.0	1		1		117	6	5174.	331.	-6536.	-34.	442.	372.	69.	29.94
152.	99.0	99.0	1		1		117	7	6114.	431.	-7105.	-24.	351.	385.	70.	29.94
18[illegible].	99.0	99.0	1		1		117	8	7093.	561.	-8100.	-29.	175.	395.	70.	29.94
152.	99.0	99.0	1		1		117	9	7914.	707.	-8523.	-12.	[illegible].	4[illegible].	7[illegible].	29.94
192.	99.0	99.0	1		1		117	10	8138.	1129.	-8845.	-166.	3503.	1232.	71.	29.94
189.	99.0	99.0	1		1		117	11	7605.	15[illegible].	-7699.	-45.	306.	885.	71.	29.94
173.	99.0	99.0	1		1		117	12	7605.	1957.	-6057.	-26.	397.	402.	72.	29.94
181.	99.0	99.0	1		1		117	13	8199.	2732.	-4333.	-20.	967.	140.	72.	29.94
174.	99.0	99.0	1		1		117	14	804[illegible].	3507.	-1108.	-18.	-258.	592.	73.	29.94
149.	99.0	99.0	1		1		117	15	7740.	415[illegible].	[illegible]635.	34.	-491.	538.	73.	29.94
591.	99.0	99.0	1		1		118	1	-714.	488.	-1082.	29.	492.	-13.	73.	29.94
[illegible]12.	99.0	99.0	1		1		118	2	1307.	423.	-3471.	14.	499.	128.	74.	29.94
619.	99.0	99.0	1		1		118	3	2511.	430.	-4132.	7.	437.	158.	74.	29.94
509.	99.0	99.0	1		1		118	4	3267.	460.	-5025.	-2.	495.	207.	74.	29.94
603.	99.0	99.0	1		1		118	5	4317.	530.	-5863.	-45.	552.	383.	74.	29.94
630.	99.0	99.0	1		1		118	6	4955.	591.	-6706.	-26.	556.	348.	74.	29.94
605.	99.0	99.0	1		1		118	7	5888.	686.	-7452.	-31.	531.	419.	74.	29.94
608.	99.0	99.0	1		1		118	8	6730.	808.	-8298.	-38.	475.	415.	74.	29.94
590.	99.0	99.0	1		1		118	9	7640.	955.	-9222.	-1.	275.	316.	74.	[illegible]
[illegible]32.	99.0	99.0	1		1		118	10	7942.	1438.	-9488.	-130.	3163.	1299.	74.	
633.	99.0	99.0	1		1		118	11	7493.	1787.	-8249.	-23.	45[illegible].	483.	74.	
526.	99.0	99.0	1		1		118	12	7277.	2179.	-6383.	-40.	599.	1[illegible].	74.	[illegible]
713.	99.0	99.0	1		1		118	13	7381.	2913.	-34[illegible].	-2.	544.	[illegible]34.	74.	[illegible]
719.	99.0	99.0	1		1		119	1	491.	165.	9915.	-19.	208.	326.	74	29.94
706.	99.0	99.0	1		1		119	2	3735.	153.	14286.	-84.	754.	727.	75.	29.94
766.	99.0	99.0	1		1		119	3	6533.	334.	13988.	-92.	917.	1104.	75	29.94
772.	99.0	99.0	1		1		119	4	7275.	1999.	15825.	-5.	13.	461.	75.	29.94
733.	99.0	99.0	1		1		119	5	8009.	2909.	[illegible]145.	-45.	247.	735.	75.	29.94
701.	99.0	99.0	1		1		119	6	7454.	3446.	14342.	32.	-467.	705.	76.	29.94
173.	99.0	99.0	1		1		120	1	364.	558.	9311.	23.	454.	-195.	77.	29.94
181.	99.0	99.0	1		1		120	2	3648.	537.	13949.	-32.	447.	443.	77.	29.94
173.	99.0	99.0	1		1		120	3	6470.	935.	14725.	-187.	3270.	1676.	77.	[illegible]
151.	99.0	99.0	1		1		120	4	6744.	2379.	15549.	-37.	664.	410.	77	[illegible]
195.	99.0	99.0	1		1		120	5	6984.	3165.	15202.	-16.	-51.	549.	7[illegible]	[illegible]
175.	99.0	99.0	1		1		120	6	7127.	3963.	12192.	-24.	-484.	902.	[illegible]	[illegible]
[illegible]35.	99.0	99.0	1		1		121	1	530.	-139.	9072.	-29.	431.	374.	[illegible]	[illegible]
[illegible]18.	99.0	99.0	1		1		121	2	4365.	-76.	5740.	-56.	615.	453.	[illegible]	[illegible]
[illegible]25.	99.0	99.0	1		1		121	3	7415.	616.	3954.	-170.	3385.	1332.	[illegible]	[illegible]
[illegible]23.	99.0	99.0	1		1		121	4	7971.	2129.	5361.	-16.	267.	400.	79.	29.94
[illegible]39.	99.0	99.0	1		1		121	5	8633.	3029.	7869.	-8.	358.	481.	79.	29.94
[illegible]37.	99.0	99.0	1		1		121	6	8519.	3969.	8086.	-0.	-304.	804.	79.	29.94
463.	99.0	99.0	1		1		122	1	19.	-259.	-555.	0.	25.	1099.	72.	29.90
112.	99.0	99.0	1		1		122	2	24.	-479.	-386.	1.	-32.	2017.	72.	29.90

GP76 0622-227

FOLDOUT FR[illegible]

RUN	PT	ALPHA DEG	BETA DEG	DLC DEG	DNL DEG	DF DEG	DAL DEG	DAR DEG	DH DEG	DR DEG	QC PSF	FAN1 RPM	FAN2 RPM	FAN3 RPM	DYLC DEG	DYNL DEG	NOSE GEAR	NOSE INLET
122	3	0.0	-0.0	0.	99.	0.	0.	0.	0.	0.	0.00	123.	2733.	117.	99.0	99.0	1	
123	1	0.0	-0.0	0.	99.	0.	0.	0.	-10.	0.	34.27	85.	2160.	2163.	99.0	99.0	1	
123	2	8.0	-0.0	0.	99.	0.	0.	0.	-10.	0.	34.27	79.	2188.	2169.	99.0	99.0	1	
123	3	16.0	-0.0	0.	99.	0.	0.	0.	-10.	0.	34.29	80.	2187.	2186.	99.0	99.0	1	
123	4	24.0	-0.0	0.	99.	0.	0.	0.	-10.	0.	34.31	84.	2178.	2186.	99.0	99.0	1	
123	5	28.0	-0.0	0.	99.	0.	0.	0.	-10.	0.	34.16	79.	2172.	2160.	99.0	99.0	1	
123	6	32.0	-0.0	0.	99.	0.	0.	0.	-10.	0.	34.22	105.	2212.	2218.	99.0	99.0	1	
124	1	0.0	-0.0	0.	99.	0.	0.	0.	10.	0.	34.08	89.	2729.	2723.	99.0	99.0	1	
124	2	8.0	-0.0	0.	99.	0.	0.	0.	10.	0.	34.07	91.	2740.	2750.	99.0	99.0	1	
124	3	16.0	-0.0	0.	99.	0.	0.	0.	10.	0.	34.20	94.	2714.	2714.	99.0	99.0	1	
124	4	24.0	-0.0	0.	99.	0.	0.	0.	10.	0.	34.28	88.	2744.	2735.	99.0	99.0	1	
124	5	28.0	-0.0	0.	99.	0.	0.	0.	10.	0.	34.18	157.	2702.	2714.	99.0	99.0	1	
124	6	32.0	-0.0	0.	99.	0.	0.	0.	10.	0.	34.26	95.	2727.	2722.	99.0	99.0	1	
125	1	0.0	-0.0	0.	99.	0.	0.	0.	0.	0.	0.00	63.	432.	1646.	99.0	99.0	1	
125	2	0.0	-0.0	0.	99.	0.	0.	0.	0.	0.	0.00	55.	445.	2178.	99.0	99.0	1	
125	3	0.0	-0.0	0.	99.	0.	0.	0.	0.	0.	0.00	71.	142.	2704.	99.0	99.0	1	
125	4	0.0	-0.0	0.	99.	0.	0.	0.	0.	0.	0.00	72.	1582.	1609.	99.0	99.0	1	
125	5	0.0	-0.0	0.	99.	0.	0.	0.	0.	0.	0.00	85.	2718.	2715.	99.0	99.0	1	
126	1	0.0	-0.0	0.	99.	0.	0.	0.	10.	0.	34.34	71.	2158.	2169.	99.0	99.0		
126	2	8.0	-0.0	0.	99.	0.	0.	0.	10.	0.	34.17	81.	2184.	2187.	99.0	99.0	1	
126	3	16.0	-0.0	0.	99.	0.	0.	0.	10.	0.	34.10	90.	2159.	2175.	99.0	99.0	1	
126	4	24.0	-0.0	0.	99.	0.	0.	0.	10.	0.	34.04	79.	2143.	2158.	99.0	99.0	1	
126	5	28.0	-0.0	0.	99.	0.	0.	0.	10.	0.	34.16	68.	2201.	2192.	99.0	99.0	1	
126	6	32.0	-0.0	0.	99.	0.	0.	0.	10.	0.	34.03	146.	2182.	2150.	99.0	99.0	1	
127	1	0.0	-0.0	0.	99.	0.	0.	0.	20.	0.	34.05	90.	2716.	2709.	99.0	99.0	1	
127	2	8.0	-0.0	0.	99.	0.	0.	0.	20.	0.	34.25	109.	2716.	2717.	99.0	99.0	1	
127	3	16.0	-0.0	0.	99.	0.	0.	0.	20.	0.	34.17	116.	2712.	2726.	99.0	99.0	1	
127	4	24.0	-0.0	0.	99.	0.	0.	0.	20.	0.	34.11	133.	2741.	2745.	99.0	99.0	1	
127	5	28.0	-0.0	0.	99.	0.	0.	0.	20.	0.	34.17	102.	2736.	2706.	99.0	99.0	1	
127	6	32.0	-0.0	0.	99.	0.	0.	0.	20.	0.	34.19	139.	2726.	2707.	99.0	99.0	1	
128	1	0.0	-0.0	0.	99.	0.	0.	0.	20.	0.	34.01	84.	2194.	2193.	99.0	99.0	1	
128	2	8.0	-0.0	0.	99.	0.	0.	0.	20.	0.	34.12	86.	2150.	2163.	99.0	99.0	1	
128	3	16.0	-0.0	0.	99.	0.	0.	0.	20.	0.	34.11	89.	2153.	2154.	99.0	99.0	1	
128	4	24.0	-0.0	0.	99.	0.	0.	0.	20.	0.	34.15	109.	2192.	2188.	99.0	99.0	1	
128	5	28.0	-0.0	0.	99.	0.	0.	0.	20.	0.	34.28	89.	2172.	2225.	99.0	99.0	1	
128	6	32.0	-0.0	0.	99.	0.	0.	0.	20.	0.	34.29	94.	2195.	2205.	99.0	99.0	1	
129	1	0.0	-0.0	0.	99.	0.	0.	0.	0.	0.	34.31	91.	2728.	2727.	99.0	99.0	1	
129	2	0.0	-0.0	0.	99.	0.	0.	0.	0.	0.	34.22	85.	2733.	2721.	99.0	99.0	1	
129	3	0.0	4.0	0.	99.	0.	0.	0.	0.	0.	34.10	100.	2708.	2733.	99.0	99.0	1	
129	4	0.0	8.0	0.	99.	0.	0.	0.	0.	0.	34.02	103.	2710.	2711.	99.0	99.0	1	
129	5	0.0	12.0	0.	99.	0.	0.	0.	0.	0.	34.18	109.	2716.	2716.	99.0	99.0	1	
129	6	0.0	-4.0	0.	99.	0.	0.	0.	0.	0.	34.13	79.	1624.	1625.	99.0	99.0	1	
129	7	0.0	-8.0	0.	99.	0.	0.	0.	0.	0.	34.20	67.	1597.	1621.	99.0	99.0	1	
129	8	0.0	-4.0	0.	99.	0.	0.	0.	0.	0.	34.03	57.	1597.	1617.	99.0	99.0	1	
129	9	0.0	4.0	0.	99.	0.	0.	0.	0.	0.	34.13	57.	1637.	1639.	99.0	99.0	1	
129	10	0.0	12.0	0.	99.	0.	0.	0.	0.	0.	33.98	83.	1611.	1622.	99.0	99.0	1	
130	1	4.0	-4.0	0.	99.	0.	0.	0.	0.	0.	34.22	91.	2745.	2744.	99.0	99.0	1	
130	2	4.0	-8.0	0.	99.	0.	0.	0.	0.	0.	34.18	84.	2714.	2714.	99.0	99.0	1	
130	3	4.0	4.0	0.	99.	0.	0.	0.	0.	0.	34.17	95.	2729.	2730.	99.0	99.0	1	
130	4	8.0	4.0	0.	99.	0.	0.	0.	0.	0.	34.12	97.	2728.	2731.	99.0	99.0	1	
130	5	8.0	12.0	0.	99.	0.	0.	0.	0.	0.	34.12	98.	2725.	2705.	99.0	99.0	1	

GP78-0822-228

BALANCE FORCE AND MOMENT DATA--STABILITY AXES

DYNI DEG	NOSE GEAR	NOSE INLET	UNIT COVERS	OTHER	RUN	PT	LIFT (LB)	DRAG (LB)	PITCHING MOMENT (FT-LB)	SIDE FORCE (LB)	ROLLING MOMENT (FT-LB)	YAWING MOMENT (FT-LB)	TUNNEL TOTAL TEMP. (DEG F)	AMBIENT PRESSURE (IN HG)
00.0	1		1		122	3	24.	-751.	-616.	1.	1.	3[illegible]1.	72.	29.90
00.0	1		1		123	1	516.	253.	8620.	-14.	369.	325.	72.	29.90
00.0	1		1		123	2	4393.	295.	4854.	-25.	667.	411.	72.	29.90
00.0	1		1		123	3	7364.	1031.	2439.	-138.	2621.	1025.	73.	29.90
00.0	1		1		123	4	7571.	2524.	5547.	-23.	781.	194.	73.	29.90
00.0	1		1		123	5	7548.	3304.	6793.	-7.	-111.	474.	74.	29.90
00.0	1		1		123	6	7544.	4032.	7829.	36.	-340.	525.	74.	29.90
00.0	1		1		124	1	2296.	-220.	-13894.	-18.	534.	201.	74.	29.90
00.0	1		1		124	2	6235.	97.	-17400.	-49.	417.	704.	75.	29.90
00.0	1		1		124	3	8622.	1151.	-15589.	-81.	981.	593.	75.	29.90
00.0	1		1		124	4	9422.	2750.	-13359.	-16.	317.	272.	75.	29.90
00.0	1		1		124	5	9818.	3704.	-11343.	-47.	[illegible].	474.	74.	29.90
00.0	1		1		124	6	9298.	4405.	-9907.	8.	-149.	514.	75.	29.90
00.0	1		1		125	1	-16.	-266.	-77.	-8.	34.	-1104.	65.	29.92
00.0	1		1		125	2	-4.	-475.	-214.	-14.	89.	-1985.	65.	29.92
00.0	1		1		125	3	-17.	-754.	-174.	-16.	-125.	-3117.	65.	29.92
00.0	1		1		125	4	-21.	-903.	-217.	-6.	3.	-2.	66.	29.92
00.0	1		1		125	5	-38.	-1490.	73.	-16.	-74.	41.	66.	29.92
00.0	1		1		126	1	2253.	188.	-14066.	6.	404.	1[illegible]1.	66.	29.92
00.0	1		1		126	2	6032.	449.	-17803.	-33.	345.	665.	66.	29.92
00.0	1		1		126	3	8468.	1476.	-15453.	-124.	2713.	864.	67.	29.92
00.0	1		1		126	4	8704.	3114.	-13534.	-42.	936.	256.	69.	29.92
00.0	1		1		126	5	8479.	3786.	-6554.	8.	44.	381.	69.	29.92
00.0	1		1		126	6	7494.	4304.	-433.	1.	-404.	722.	70.	29.92
00.0	1		1		127	1	2775.	62.	-18208.	-1.	411.	-22.	71.	29.92
00.0	1		1		127	2	5982.	404.	-16736.	-10.	307.	284.	72.	29.92
00.0	1		1		127	3	8224.	1327.	-10964.	-94.	1503.	704.	72.	29.92
00.0	1		1		127	4	9066.	2908.	-9008.	-11.	-80.	376.	73.	29.92
00.0	1		1		127	5	8781.	4059.	-10851.	-44.	67.	605.	73.	29.92
00.0	1		1		127	6	9418.	4725.	-6010.	-27.	-74.	735.	74.	29.92
00.0	1		1		128	1	2670.	652.	-18607.	17.	343.	-34.	73.	29.92
00.0	1		1		128	2	5 [illegible]6.	781.	-16327.	-22.	501.	249.	73.	29.92
00.0	1		1		128	3	8121.	1944.	-10749.	-115.	2115.	753.	73.	29.92
00.0	1		1		128	4	8547.	3367.	-10141.	-5.	347.	153.	74.	29.92
00.0	1		1		128	5	8547.	4149.	-8829.	-36.	-214.	461.	74.	29.92
00.0	1		1		128	6	8128.	4568.	-2520.	20.	-387.	610.	74.	29.92
00.0	1		1		129	1	1345.	-254.	-2842.	483.	-24.	-993.	74.	29.92
00.0	1		1		129	2	1413.	-249.	-2451.	12.	20.	145.	75.	29.92
00.0	1		1		129	3	1341.	-254.	-3451.	-475.	-33.	1431.	75.	29.92
00.0	1		1		129	4	1439.	-304.	-3739.	-958.	-720.	2735.	75.	29.92
00.0	1		1		129	5	1447.	-372.	-4064.	-1430.	-634.	3960.	75.	29.92
00.0	1		1		129	6	1334.	411.	-3737.	443.	243.	-925.	75.	29.92
00.0	1		1		129	7	1274.	424.	-3599.	25.	114.	46.	75.	29.92
00.0	1		1		129	8	1242.	413.	-3711.	-408.	-458.	1277.	75.	29.92
00.0	1		1		129	9	1244.	389.	-3660.	-863.	-67.	2558.	75.	29.92
00.0	1		1		129	10	1265.	368.	-4312.	-1285.	-7.	3635.	75.	29.92
00.0	1		1		130	1	5252.	-56.	-6499.	443.	406.	-1099.	74.	29.92
00.0	1		1		130	2	5144.	-50.	-6099.	4.	-663.	241.	74.	29.92
00.0	1		1		130	3	5223.	-69.	-6402.	-471.	-1232.	1696.	74.	29.92
00.0	1		1		130	4	5218.	-112.	-6584.	-945.	-2031.	3098.	74.	29.92
00.0	1		1		130	5	5169.	-157.	-7603.	-1413.	-2593.	4489.	74.	29.92

FOLDOUT FRAME 2

RUN	PT	ALPHA DEG	BETA DEG	DLC DEG	DNL DEG	DF DEG	DAL DEG	DAR DEG	DH DEG	DR DEG	QC PSF	FAN1 RPM	FAN2 RPM	FAN3 RPM	DYLC DEG	DYNL DEG	NOSE GEAR	NOSE INLET
130	4	4.0	-4.0	0.	99.	0.	0.	0.	0.	0.	34.17	61.	1645.	1624.	99.0	99.0	1	
130	7	8.0	-0.0	0.	99.	0.	0.	0.	0.	0.	34.15	72.	1613.	1622.	99.0	99.0	1	
130	8	8.0	4.0	0.	99.	0.	0.	0.	0.	0.	34.12	64.	1612.	1618.	99.0	99.0	1	
130	9	8.0	8.0	0.	99.	0.	0.	0.	0.	0.	34.16	65.	1609.	1637.	99.0	99.0	1	
130	10	8.0	12.0	0.	99.	0.	0.	0.	0.	0.	34.10	80.	1585.	1612.	99.0	99.0	1	
131	1	16.0	-4.0	0.	99.	0.	0.	0.	0.	0.	34.20	25.	2741.	2736.	99.0	99.0	1	
131	2	16.0	-0.0	0.	99.	0.	0.	0.	0.	0.	34.13	22.	2699.	2694.	99.0	99.0	1	
131	3	16.0	4.0	0.	99.	0.	0.	0.	0.	0.	34.25	17.	2715.	2702.	99.0	99.0	1	
131	4	16.0	8.0	0.	99.	0.	0.	0.	0.	0.	34.22	37.	2708.	2717.	99.0	99.0	1	
131	5	16.0	12.0	0.	99.	0.	0.	0.	0.	0.	34.29	16.	2699.	2720.	99.0	99.0	1	
132	1	16.0	-4.0	0.	99.	0.	0.	0.	0.	0.	34.11	33.	1601.	1637.	99.0	99.0	1	
132	2	16.0	-0.0	0.	99.	0.	0.	0.	0.	0.	34.22	24.	1582.	1606.	99.0	99.0	1	
132	3	16.0	4.0	0.	99.	0.	0.	0.	0.	0.	34.12	12.	1590.	1615.	99.0	99.0	1	
132	4	16.0	8.0	0.	99.	0.	0.	0.	0.	0.	34.21	19.	1589.	1622.	99.0	99.0	1	
132	5	16.0	12.0	0.	99.	0.	0.	0.	0.	0.	34.30	14.	1581.	1624.	99.0	99.0	1	
133	1	4.00	8.0	0.	99.	0.	0.	0.	0.	0.	34.19	38.	2745.	2739.	99.0	99.0	1	
133	2	12.0	8.0	0.	99.	0.	0.	0.	0.	0.	34.26	26.	2711.	2714.	99.0	99.0	1	
133	3	20.0	8.0	0.	99.	0.	0.	0.	0.	0.	34.17	23.	2722.	2727.	99.0	99.0	1	
133	4	24.0	8.0	0.	99.	0.	0.	0.	0.	0.	34.22	24.	2710.	2745.	99.0	99.0	1	
133	5	28.0	8.0	0.	99.	0.	0.	0.	0.	0.	34.30	28.	2749.	2740.	99.0	99.0	1	
133	6	32.0	8.0	0.	99.	0.	0.	0.	0.	0.	34.22	54.	2717.	2746.	99.0	99.0	1	
134	1	8.0	-0.0	0.	99.	0.	0.	0.	-10.	0.	34.21	21.	2732.	2740.	99.0	99.0	1	
134	2	8.0	-0.0	0.	99.	0.	0.	0.	10.	0.	34.31	15.	2742.	2739.	99.0	99.0	1	
134	3	8.0	-0.0	0.	99.	0.	0.	0.	0.	0.	34.24	14.	2712.	2713.	99.0	99.0	1	
134	4	8.0	-0.0	0.	99.	0.	0.	0.	0.	0.	34.20	31.	2726.	2730.	99.0	99.0	1	
134	5	16.0	-0.0	0.	99.	0.	0.	0.	0.	0.	34.07	20.	2714.	2709.	99.0	99.0	1	
134	6	24.0	-0.0	0.	99.	0.	0.	0.	0.	0.	34.24	16.	2714.	2719.	99.0	99.0	1	
134	7	32.0	-0.0	0.	99.	0.	0.	0.	0.	0.	34.19	28.	2703.	2697.	99.0	99.0	1	
135	1	0.0	-0.0	0.	99.	0.	0.	0.	-10.	0.	34.23	30.	1604.	1632.	99.0	99.0	1	
135	2	0.0	-0.0	0.	99.	0.	0.	0.	10.	0.	34.18	51.	1596.	1624.	99.0	99.0	1	
135	3	0.0	-0.0	0.	99.	0.	0.	0.	0.	0.	34.24	27.	1622.	1614.	99.0	99.0	1	
135	4	8.0	-0.0	0.	99.	0.	0.	0.	0.	0.	34.17	17.	1623.	1618.	99.0	99.0	1	
135	5	16.0	-0.0	0.	99.	0.	0.	0.	0.	0.	34.31	26.	1615.	1621.	99.0	99.0	1	
135	6	24.0	-0.0	0.	99.	0.	0.	0.	0.	0.	34.20	24.	2160.	2163.	99.0	99.0	1	
135	7	24.0	-0.0	0.	99.	0.	0.	0.	0.	0.	34.33	17.	2175.	2186.	99.0	99.0	1	
135	8	32.0	-0.0	0.	99.	0.	0.	0.	0.	0.	34.16	53.	2190.	2218.	99.0	99.0	1	
136	1	0.0	-0.0	0.	99.	0.	25.	-25.	0.	0.	34.26	23.	2705.	2702.	99.0	99.0	1	
136	2	0.0	-0.0	0.	99.	0.	25.	0.	0.	0.	34.22	21.	2707.	2712.	99.0	99.0	1	
136	3	0.0	-0.0	0.	99.	0.	25.	25.	0.	0.	34.25	23.	2711.	2736.	99.0	99.0	1	
136	4	0.0	-0.0	0.	99.	0.	0.	-25.	0.	0.	34.18	27.	2700.	2705.	99.0	99.0	1	
136	5	0.0	-0.0	0.	99.	0.	-15.	0.	0.	0.	34.12	20.	2731.	2706.	99.0	99.0	1	
136	6	0.0	-0.0	0.	99.	0.	-25.	0.	0.	0.	34.11	17.	2695.	2705.	99.0	99.0	1	
136	7	0.0	-0.0	0.	99.	0.	-25.	25.	0.	0.	34.24	14.	2699.	2711.	99.0	99.0	1	
137	1	0.0	-0.0	0.	99.	0.	25.	-25.	0.	0.	34.14	27.	1593.	1627.	99.0	99.0	1	
137	2	0.0	-0.0	0.	99.	0.	25.	0.	0.	0.	34.21	25.	1586.	1619.	99.0	99.0	1	
137	3	0.0	-0.0	0.	99.	0.	15.	0.	0.	0.	34.29	26.	1590.	1627.	99.0	99.0	1	
137	4	0.0	-0.0	0.	99.	0.	0.	0.	0.	0.	34.35	59.	1587.	1624.	99.0	99.0	1	
137	5	0.0	-0.0	0.	99.	0.	-15.	0.	0.	0.	34.21	47.	1586.	1636.	99.0	99.0	1	
137	6	0.0	-0.0	0.	99.	0.	-25.	0.	0.	0.	34.19	21.	1604.	1620.	99.0	99.0	1	
137	7	0.0	-0.0	0.	99.	0.	-25.	25.	0.	0.	34.10	47.	1599.	1633.	99.0	99.0	1	
138	1	8.0	-0.0	0.	99.	0.	-25.	25.	0.	0.	34.23	53.	2722.	2719.	99.0	99.0	1	

GP78-0822-229

BALANCE FORCE AND MOMENT DATA--STABILITY AXES

DYNL DEG	NOSE GEAR	NOSE INLET	UNIT COVERS	OTHER	RUN	PT	LIFT (LB)	DRAG (LB)	PITCHING MOMENT (FT-LB)	SIDE FORCE (LB)	ROLLING MOMENT (FT-LB)	YAWING MOMENT (FT-LB)	TUNNEL TOTAL TEMP. (DEG F)	AMBIENT PRESSURE (IN HG)
99.0	1		1		130	6	4931.	555.	-7000.	430.	-28.	-1198.	75.	29.92
99.0	1		1		130	7	4960.	592.	-6779.	[illegible]	-517.	243.	75.	29.92
99.0	1		1		130	8	4972.	575.	-7359.	-452.	-490.	1803.	75.	29.92
99.0	1		1		130	9	4935.	535.	-7742.	-88.	-1650.	3120.	75.	29.92
99.0	1		1		130	10	4886.	462.	-8463.	-1354.	-2033.	4563.	75.	29.92
99.0	1		1		131	1	8141.	821.	-8425.	175.	8796.	227.	65.	29.93
99.0	1		1		131	2	8169.	519.	-8543.	-177.	4073.	945.	65.	29.93
99.0	1		1		131	3	8067.	529.	-8403.	-485.	-2866.	2209.	67.	29.93
99.0	1		1		131	4	7750.	864.	-8520.	-754.	-9158.	3224.	67.	29.93
99.0	1		1		131	5	7771.	793.	-9465.	-1026.	-12586.	3902.	67.	29.93
99.0	1		1		132	1	7679.	1379.	-9252.	124.	7461.	-125.	69.	29.93
99.0	1		1		132	2	7966.	1354.	-10064.	-163.	3341.	1382.	70.	29.93
99.0	1		1		132	3	7741.	1365.	-9422.	-462.	-2212.	2366.	70.	29.93
99.0	1		1		132	4	7383.	1430.	-10054.	-670.	-8724.	3241.	70.	29.93
99.0	1		1		132	5	7027.	1425.	-9975.	-693.	-13124.	4519.	71.	29.93
99.0	1		1		133	1	3423.	-265.	-5390.	-996.	-535.	3100.	73.	29.93
99.0	1		1		133	2	7170.	132.	-8247.	-1028.	-1319.	3816.	75.	29.93
99.0	1		1		133	3	8256.	1561.	-7496.	-831.	-6097.	4622.	76.	29.93
99.0	1		1		133	4	6878.	2301.	-5433.	-856.	-3851.	4096.	76.	29.93
99.0	1		1		133	5	9108.	3334.	-3712.	-724.	-4875.	4811.	76.	29.93
99.0	1		1		133	6	9025.	4132.	488.	-517.	-5505.	5705.	76.	29.93
99.0	1		1		134	1	503.	-64.	9197.	546.	3071.	-6327.	67.	29.93
99.0	1		1		134	2	2241.	-134.	-13637.	522.	3011.	-6113.	67.	29.93
99.0	1		1		134	3	1347.	-166.	-2027.	557.	3097.	-6527.	75.	29.93
99.0	1		1		134	4	5160.	22.	-5653.	498.	1497.	-6184.	76.	29.93
99.0	1		1		134	5	8196.	871.	-7371.	437.	2336.	-5823.	77.	29.93
99.0	1		1		134	6	8701.	2445.	-4350.	530.	-741.	-6175.	78.	29.93
99.0	1		1		134	7	8835.	4215.	2018.	165.	-1888.	-3105.	78.	29.93
99.0	1		1		135	1	166.	501.	4986.	566.	2455.	-6368.	80.	29.93
99.0	1		1		135	2	2224.	526.	-14376.	565.	2100.	-6245.	80.	29.93
99.0	1		1		135	3	1240.	494.	-2822.	588.	2781.	-6553.	81.	29.93
99.0	1		1		135	4	4594.	652.	-6682.	501.	1885.	-6102.	80.	29.93
99.0	1		1		135	5	7940.	1413.	-9330.	430.	2452.	-5561.	80.	29.93
99.0	1		1		135	6	8134.	1167.	-8572.	393.	16.	-5582.	80.	29.93
99.0	1		1		135	7	8245.	2788.	-4319.	552.	-500.	-5360.	80.	29.93
99.0	1		1		135	8	7754.	4186.	3696.	306.	-1121.	-2228.	80.	29.93
99.0	1		1		136	1	1130.	-125.	-2347.	-168.	9284.	601.	76.	29.93
99.0	1		1		136	2	1714.	-166.	-4075.	-59.	3776.	-107.	76.	29.93
99.0	1		1		136	3	1602.	-194.	-3992.	-77.	2880.	126.	77.	29.93
99.0	1		1		136	4	1341.	-234.	-3043.	-38.	414.	371.	77.	29.93
99.0	1		1		136	5	950.	-223.	-1968.	21.	-3122.	40.	78.	29.93
99.0	1		1		136	6	719.	-188.	-1424.	61.	-5304.	-540.	78.	29.93
99.0	1		1		136	7	1125.	-116.	-2442.	75.	-8325.	191.	79.	29.93
99.0	1		1		137	1	912.	539.	-2738.	-120.	9326.	416.	80.	29.93
99.0	1		1		137	2	1586.	499.	-4681.	-37.	3371.	-372.	80.	29.93
99.0	1		1		137	3	1445.	467.	-4128.	-32.	2734.	-12.	80.	29.93
99.0	1		1		137	4	1202.	434.	-3569.	-1.	379.	239.	81.	29.93
99.0	1		1		137	5	835.	441.	-2433.	62.	-3503.	-129.	81.	29.93
99.0	1		1		137	6	570.	475.	-1764.	79.	-5502.	-546.	81.	29.93
99.0	1		1		137	7	889.	547.	-2718.	137.	-8611.	-34.	81.	29.93
99.0	1		1		138	1	4936.	40.	-5190.	121.	-8777.	1259.	81.	29.93

RUN	PT	ALPHA DEG	BETA DEG	DLC DEG	DNL DEG	DE DEG	DAL DEG	DAR DEG	DH DEG	DH DEG	QC PSF	FAN1 RPM	FAN2 RPM	FAN3 RPM	DYLC DEG	DYNL DEG	NOSE GEAR	NOSE INLET	CO
138	2	16.0	-0.0	0.	99.	0.	-25.	25.	0.	0.	34.17	2M.	2717.	2743.	99.0	99.0	1		1
138	3	24.0	-0.0	0.	99.	0.	-25.	25.	0.	0.	34.1M	24.	2712.	2717.	99.0	99.0	1		1
138	4	32.0	-0.0	0.	99.	0.	-25.	25.	0.	0.	34.1M	25.	2721.	2721.	99.0	99.0	1		1
139	1	8.0	-0.0	0.	99.	0.	-25.	25.	0.	0.	34.26	25.	1625.	1644.	99.0	99.0	1		1
139	2	16.0	-0.0	0.	99.	0.	-25.	25.	0.	0.	34.21	14.	1588.	1629.	99.0	99.0	1		1
139	3	16.0	-0.0	0.	99.	0.	-25.	25.	0.	0.	34.24	43.	2185.	2189.	99.0	99.0	1		1
139	4	24.0	-0.0	0.	99.	0.	-25.	25.	0.	0.	34.25	44.	2139.	2176.	99.0	99.0	1		1
139	5	32.0	-0.0	0.	99.	0.	-25.	25.	0.	0.	34.31	20.	2207.	2208.	99.0	99.0	1		1
140	1	-4.0	-0.0	0.	99.	0.	0.	0.	99.	0.	34.22	29.	2734.	2755.	99.0	99.0	1		1
140	2	0.0	-0.0	0.	99.	0.	0.	0.	99.	0.	34.31	16.	2724.	2754.	99.0	99.0	1		1
140	3	2.0	-0.0	0.	99.	0.	0.	0.	99.	0.	34.35	25.	2719.	2741.	99.0	99.0	1		1
140	4	4.0	-0.0	0.	99.	0.	0.	0.	99.	0.	34.21	20.	2744.	2747.	99.0	99.0	1		1
140	5	6.0	-0.0	0.	99.	0.	0.	0.	99.	0.	34.19	40.	2713.	2718.	99.0	99.0	1		1
140	6	M.0	-0.0	0.	99.	0.	0.	0.	99.	0.	34.27	2M.	2718.	2715.	99.0	99.0	1		1
140	7	10.0	-0.0	0.	99.	0.	0.	0.	99.	0.	34.23	22.	2724.	2718.	99.0	99.0	1		1
140	M	12.0	-0.0	0.	99.	0.	0.	0.	99.	0.	34.22	3M.	2704.	270M.	99.0	99.0	1		1
140	9	14.0	-0.0	0.	99.	0.	0.	0.	99.	0.	34.12	20.	2707.	2715.	99.0	99.0	1		1
140	10	15.0	-0.0	0.	99.	0.	0.	0.	99.	0.	34.12	20.	2717.	2726.	99.0	99.0	1		1
140	11	18.0	-0.0	0.	99.	0.	0.	0.	99.	0.	34.22	30.	2747.	2738.	99.0	99.0	1		1
140	12	20.0	-0.0	0.	99.	0.	0.	0.	99.	0.	34.30	54.	2718.	2717.	99.0	99.0	1		1
140	13	24.0	-0.0	0.	99.	0.	0.	0.	99.	0.	34.34	26.	2704.	2716.	99.0	99.0	1		1
140	14	24.0	-0.0	0.	99.	0.	0.	0.	99.	0.	34.30	20.	2723.	2714.	99.0	99.0	1		1
140	15	32.0	-0.0	0.	99.	0.	0.	0.	99.	0.	34.24	34.	2746.	2747.	99.0	99.0	1		1
141	1	-4.0	-0.0	0.	99.	0.	0.	0.	99.	0.	34.24	14.	1609.	1614.	99.0	99.0	1		1
141	2	0.0	-0.0	0.	99.	0.	0.	0.	99.	0.	34.37	15.	1603.	1622.	99.0	99.0	1		1
141	3	2.0	-0.0	0.	99.	0.	0.	0.	99.	0.	34.23	30.	1623.	1623.	99.0	99.0	1		1
141	4	4.0	-0.0	0.	99.	0.	0.	0.	99.	0.	34.32	68.	1594.	1616.	99.0	99.0	1		1
141	5	5.0	-0.0	0.	99.	0.	0.	0.	99.	0.	34.17	21.	1590.	1612.	99.	99.0	1		1
141	6	M.0	-0.0	0.	99.	0.	0.	0.	99.	0.	34.14	14.	1631.	1650.	99.0	99.0	1		1
141	7	10.0	-0.0	0.	99.	0.	0.	0.	99.	0.	34.22	19.	1593.	1600.	99.0	99.0	1		1
141	M	12.0	-0.0	0.	99.	0.	0.	0.	99.	0.	34.19	16.	1594.	1601.	99.0	99.0	1		1
141	9	14.0	-0.0	0.	99.	0.	0.	0.	99.	0.	34.26	32.	1604.	[illegible]	99.0	99.0	1		1
141	10	15.0	-0.0	0.	99.	0.	0.	0.	99.	0.	34.17	91.	1595.	1.	99.0	99.0	1		1
141	11	18.0	-0.0	0.	99.	0.	0.	0.	99.	0.	34.2M	3M.	1626.	6.	99.0	99.0	1		1
141	12	20.0	-0.0	0.	99.	0.	0.	0.	99.	0.	34.17	42.	1654.	1674.	99.0	99.0	1		1

GP76-0622-230

TAIL FLAG	NOSE GEAR	NOSE INLET	UNIT COVERS	OTHER	RUN	PT	BALANCE FORCE AND MOMENT DATA--STABILITY AXES LIFT (LB)	DRAG (LB)	PITCHING MOMENT (FT-LB)	SIDE FORCE (LB)	ROLLING MOMENT (FT-LB)	YAWING MOMENT (FT-LB)	TUNNEL TOTAL TEMP. (DEG F)	AMBIENT PRESSURE (IN HG)
0.0	1		1		138	2	8145.	835.	-7773.	-63.	-3311.	3033.	82.	29.93
0.0	1		1		138	3	8683.	2620.	-6472.	31.	-3260.	2424.	83.	29.93
0.0	1		1		138	4	8727.	4203.	1914.	-1.	-3443.	3544.	83.	29.93
0.0	1		1		139	1	4650.	692.	-4274.	134.	-1585.	1019.	83.	29.93
0.0	1		1		139	2	7771.	1382.	-9022.	-54.	-2983.	3303.	83.	29.93
0.0	1		1		139	3	7852.	1202.	-8634.	-33.	-3155.	2955.	83.	29.93
0.0	1		1		139	4	8047.	2753.	-6249.	26.	-3122.	2152.	84.	29.93
0.0	1		1		139	5	7565.	4158.	5163.	41.	-3378.	3366.	84.	29.93
0.0	1		1		140	1	-132.	-225.	-6181.	8.	322.	114.	73.	29.87
0.0	1		1		140	2	1653.	-253.	-5272.	-2.	204.	213.	73.	29.87
0.0	1		1		140	3	2728.	-230.	-4245.	17.	-156.	174.	73.	29.87
0.0	1		1		140	4	3385.	-201.	-4142.	-5.	224.	240.	73.	29.87
0.0	1		1		140	5	4455.	-143.	-3117.	-15.	370.	344.	74.	29.87
0.0	1		1		140	6	5107.	-75.	-2414.	-24.	399.	460.	74.	29.87
0.0	1		1		140	7	5988.	16.	-1685.	-32.	1[illegible].	447.	74.	29.87
0.0	1		1		140	8	6744.	140.	-1671.	-46.	472.	514.	75.	29.87
0.0	1		1		140	9	7641.	207.	-978.	-69.	141.	555.	75.	29.87
0.0	1		1		140	10	7640.	484.	434.	-121.	1387.	541.	75.	29.87
0.0	1		1		140	11	7302.	1117.	911.	-47.	-1[illegible].	477.	76.	29.87
0.0	1		1		140	12	7327.	1454.	1623.	-1.	-775.	643.	77.	29.87
0.0	1		1		140	13	8331.	2231.	2241.	-32.	174.	455.	77.	29.87
0.0	1		1		140	14	8940.	3216.	1984.	-55.	-27.	725.	77.	29.87
0.0	1		1		140	15	8842.	4156.	3761.	-15.	-172.	774.	77.	29.87
0.0	1				141	1	-324.	451.	-6576.	16.	533.	73.	77.	29.87
0.0	1		1		141	2	1401.	421.	-5525.	5.	458.	124.	77.	29.87
0.0	1		1		141	3	2477.	433.	-4560.	-2.	403.	181.	77.	29.87
0.0	1		1		141	4	3143.	458.	-4315.	-4.	324.	203.	77.	29.87
0.0	1				141	5	4137.	514.	-3405.	-24.	293.	299.	77.	29.87
0.0	1				141	6	4763.	567.	-3372.	-42.	659.	345.	77.	29.87
0.0	1		1		141	7	5574.	650.	-2665.	-18.	541.	336.	77.	29.87
0.0	1		1		141	8	6376.	756.	-1909.	-33.	333.	374.	77.	29.87
0.0	1		1		141	9	7124.	880.	-1292.	-1.	20.	372.	77.	29.87
0.0	1		1		141	10	7350.	1348.	-6[illegible].	-147.	322[illegible].	1334.	77.	29.87
0.0	1		1		141	11	6941.	1459.	321.	-2[illegible].	-59.	662.	77.	29.87
0.0	1		1		141	12	6729.	2034.	1906.	-50.	920.	421.	77.	29.87

WIND TUNNEL AND GROUND STATIC INVESTIGATION OF A LARGE SCALE-MODEL OF A LIFT/CRUISE FAN V/STOL AIRCRAFT

APPENDIX B

OUTSIDE STATIC TEST RUN SUMMARY

OUTSIDE STATIC TEST RUN SUMMARY

RUN NUMBER	NUMBER OF DATA POINTS No.	LIFT/CRUISE UNIT - LEFT SIDE					LIFT/CRUISE UNIT - RIGHT SIDE					FORWARD FAN UNIT			A/C POSITION		MODEL CONFIGURATION				RUN PURPOSE
		NOZZLE VECTOR ANGLE (DEG.)	YAW VANE DEFLECTION (DEG.)	SPOILAGE PORT OPENING (%)	NOZZLE EXIT CONFIGURATION	FAN SPEED SCHEDULE	NOZZLE VECTOR ANGLE (DEG.)	YAW VANE DEFLECTION (DEG.)	SPOILAGE PORT OPENING (%)	NOZZLE EXIT CONFIGURATION	FAN SPEED SCHEDULE	LOUVER VECTOR ANGLE (DEG.)	YAW VANE DEFLECTION (DEG.)	FAN SPEED SCHEDULE	MODEL HEIGHT (FT)	ANGLE OF ATTACK (DEG.)	AILERON DEFLECTION (δ_A) (DEG.)	FLAP DEFLECTION (δ_F) (DEG.)	STABILATOR DEFLECTION (δ_H) (DEG.)	INLET SHIELD CONFIGURATION	
1	1	0	OFF	0	1075	1620									21	0				OFF	FAN MAPPING
	2					2030															
	3					2435															
	4					2840															
	5					3250															
	6					3655															
	7					3910					Y										
	8					2000					2000										
	9					2900					2900										
	10					3600					3600										
	11					0					2000										
	12										2900										
	13				Y						3600										
2	1	0	OFF	0	1075	1630					0	90	0	0							FLOW VIZ
	2					2445															
	3					3260															
	4				Y	1570															
3	1					1030															
	2					3665															
	3					3260															
	4					2445															
4	1				Y	1630				Y	Y	102	Y	Y							
	2					3260					0										
	3					3920															
	4					3260															
	5					2900															
	6					3650					3600										
	7					1640					1640										

RUN NUMBER	~~REJECTED~~ POINT # n/a	LIFT/CRUISE UNIT - LEFT SIDE							LIFT/CRUISE UNIT - RIGHT SIDE							FORWARD FAN UNIT			A/C POSITION		MODEL CONFIGURATION				RUN PURPOSE
		NOZZLE VECTOR ANGLE (DEG.)	YAW VANE DEFLECTION (DEG.)	SPOILAGE PORT OPENING (%)	NOZZLE EXIT CONFIGURATION	FAN SPEED SCHEDULE	NOZZLE VECTOR ANGLE (DEG.)	YAW VANE DEFLECTION (DEG.)	SPOILAGE PORT OPENING (%)	NOZZLE EXIT CONFIGURATION	FAN SPEED SCHEDULE	LOUVER VECTOR ANGLE (DEG.)	YAW VANE DEFLECTION (DEG.)	FAN SPEED SCHEDULE	MODEL HEIGHT (FT)	ANGLE OF ATTACK (DEG.)	AILERON DEFLECTION (δ_A) (DEG.)	FLAP DEFLECTION (δ_F) (DEG.)	STABILIZATION DEFLECTION (δ_H) (DEG.)	INLET SHIELD CONFIGURATION	
4	7	90	0	0	1190	0	90	0	0	1190	0	102	0	0	21	0	10	15	0	OFF	
	8					2000					2000			0							
	9					2900					2900			2000							
	10					3600					3600			2900							
5	1					4074					4074	60		3600							
	2					2000					0			4074							
	3					3200					2900			2000							
	4					3600					3600			2900							
	5					2900					3600			3600							
	6					3600					4074			4074							
	7					0					0			1							
	8													2000							
	9													2900							
	10													3600							
	11													2900							
6	12													4074							
	1					3600					0			1							
	2					1					1			2000							
	3					2000					2000			2900							
	4					2700					3600			3600							
	5					3600					2900										
	6					2900					1			2900							
	7					1					0			2000							
	8					0								2200							
	9													3600							
	10													4074							
	11																				

RUN NUMBER	NUMBER OF TEST POINTS	LIFT/CRUISE UNIT - LEFT SIDE						LIFT/CRUISE UNIT - RIGHT SIDE						FORWARD FAN UNIT			A/C POSITION		MODEL CONFIGURATION					RUN-PURPOSE COMMENTS
		NOZZLE VECTOR ANGLE (DEG.)	YAW VANE DEFLECTION (DEG.)	SPOILAGE PORT OPENING (%)	NOZZLE EXIT CONFIGURATION	FAN SPEED SCHEDULE		NOZZLE VECTOR ANGLE (DEG.)	YAW VANE DEFLECTION (DEG.)	SPOILAGE PORT OPENING (%)	NOZZLE EXIT CONFIGURATION	FAN SPEED SCHEDULE		LOUVER VECTOR ANGLE (DEG.)	YAW VANE DEFLECTION (DEG.)	FAN SPEED SCHEDULE	MODEL HEIGHT (FT)	ANGLE OF ATTACK (DEG.)	AILERON DEFLECTION (δ_A) (DEG.)	FLAP DEFLECTION (δ_F) (DEG.)	STABILIATOR DEFLECTION (δ_H) (DEG.)	INLET SHIELD CONFIGURATION		
7	1	90	0	0	1190	3600		90	0	0	1190	3600		80	0		21	0	10	15	0	OFF		
	2					0						0												
	3						2900						2900											
	4						2000						2000											
8	1					3600						3600		102										
	2					0						0												
	3																							
9	1													90										
	2																							
10	1					3600						3600		95		2900					51-90			
	2															3600								
	3															1074								
	4															3600		+4						
	5																	-4						
11	1													102				0						
12	1		+12						-12					95	±12									
	2																							
	3					0						3600				3600								
	4					3600										1400								
	5					1400						1400												
1	6		1			0			1			0				0					1			
13	1		0						0							0	33					OFF	WIND ~ 10 KTS	
	2					1						1				1900								
	3					2900						2900												
	4					3600						3600				0								
	5					0						0												
	6																							
	7																							

RUN NUMBER	NUMBER OF TEST POINTS	LIFT/CRUISE UNIT - LEFT SIDE						LIFT/CRUISE UNIT - RIGHT SIDE						FORWARD FAN UNIT			A/C POSITION		MODEL CONFIGURATION				PURPOSE COMMENTS
		NOZZLE VECTOR ANGLE (DEG.)	YAW VANE DEFLECTION (DEG.)	SPOILAGE PORT OPENING (%)	NOZZLE EXIT CONFIGURATION	FAN SPEED SCHEDULE	NOZZLE VECTOR ANGLE (DEG.)	YAW VANE DEFLECTION (DEG.)	SPOILAGE PORT OPENING (%)	NOZZLE EXIT CONFIGURATION	FAN SPEED SCHEDULE	LOUVER VECTOR ANGLE (DEG.)	YAW VANE DEFLECTION (DEG.)	FAN SPEED SCHEDULE		MODEL HEIGHT (FT)	ANGLE OF ATTACK (DEG.)	AILERON DEFLECTION (δ_A) (DEG.)	FLAP DEFLECTION (δ_F) (DEG.)	STABILIATOR DEFLECTION (δ_H) (DEG.)	INLET SHIELD CONFIGURATION	
13	8	90	0	0	1190	2400	90	0	0	1190	2400	95	0	0		3.3	0	10	15	0	OFF	WIND ~ 10 KTS
1	9					3600					3600			2000								
14	1					0					0			2000								REPEAT OF P13
1	2													2900								
1	3					1								3600								
1	4													4000								
1	5					2000								0								REPEAT OF R13
1	6					2900																
1	7					3900																
1	8					3600					1											
1	9					2000					2000											
1	10					3600					3600											
1	11					0					2000											
1	12										2900											
1	13					1					3200			1								
1	14										4000											
1	15					2900					2900											
1	16					3600					3600			1								
15	1					2000					2000			2000								
1	2					2900					2900			2900								
1	3					3500					3500			1								
1	4					1					1			4000								
16	1					2000					2000			2000								
	2					2900					2900			2900								
	3					3600					3600			2100								
	4													2900								
1	5					1					1			1900								
	6																					
	7																					
	8																					
	9																					
	10																					
	11																					
	12																					
	13																					
	14																					
	15																					
	16																					
	17																					
	18																					
	19																					
	20																					

RUN NUMBER	NUMBER OF TEST POINTS	LIFT/CRUISE UNIT - LEFT SIDE					LIFT/CRUISE UNIT - RIGHT SIDE					FORWARD FAN UNIT		A/C POSITION		MODEL CONFIGURATION		RUN PURPOSE
		NOZZLE VECTOR ANGLE (DEG.)	YAW VANE DEFLECTION (DEG.)	SPOILAGE PORT OPENING (%)	NOZZLE EXIT CONFIGURATION	FAN SPEED SCHEDULE	NOZZLE VECTOR ANGLE (DEG.)	YAW VANE DEFLECTION (DEG.)	SPOILAGE PORT OPENING (%)	NOZZLE EXIT CONFIGURATION	FAN SPEED SCHEDULE	LOUVER VECTOR ANGLE (DEG.)	YAW VANE DEFLECTION (DEG.)	FAN SPEED SCHEDULE	MODEL HEIGHT (FT)	ANGLE OF ATTACK (DEG.)	AILERON DEFLECTION (δ_A) (DEG.)	FLAP DEFLECTION (δ_F) (DEG.)	STABILIZER DEFLECTION (δ_H) (DEG.)	INLET SHIELD CONFIGURATION	
17	1	90	0	0	1190	2900	90	0	0	1190	2900	95	0	2400	3.3	0	10	15	0	S1-0°	
	2					4000					4000										
18	3					3600					3600										
	1																				
	2																				
19	1													2500						S1-45°	
	2					2500					2500			2000						S1-90°	
	3					2000					2000			2500							
	4					2500					2500			2900							
20	1					2900					2900			3600						S1-0°	
21	1		+12			3600		-12			3600		±12	2400						S2-0°	
	2		0			2000		0			2000		0	2900							
	3					2900					2900			3600							
22	1					3600					3600			2400						1	
	2					3500					3500	102		3500						OFF	
23	1		Y			0		1			0	80	0	3600							
	2		+12			3600		-12			3600			0							
	3					0					3600			2400							
24	1					0					0	95	±12	3600							
	2		1			2400		1			3600		1	2400							
	3		0			2000		0			2000	80	0	2000							
25	1					0					0			2400							
	2					2400					2400			2700							
	3					2400					2400			3600							
	4					2400					3600			3600							
	5	Y				2400					2400			3600							
1	1																				FLOW VIS.

RUN NUMBER	NUMBER OF TEST POINTS	LIFT/CRUISE UNIT - LEFT SIDE					LIFT/CRUISE UNIT - RIGHT SIDE					FORWARD FAN UNIT			A/C POSITION		MODEL CONFIGURATION				RUN PURPOSE
		NOZZLE VECTOR ANGLE (DEG.)	YAW VANE DEFLECTION (DEG.)	SPOILAGE PORT OPENING (%)	NOZZLE EXIT CONFIGURATION	FAN SPEED SCHEDULE	NOZZLE VECTOR ANGLE (DEG.)	YAW VANE DEFLECTION (DEG.)	SPOILAGE PORT OPENING (%)	NOZZLE EXIT CONFIGURATION	FAN SPEED SCHEDULE	LOUVER VECTOR ANGLE (DEG.)	YAW VANE DEFLECTION (DEG.)	FAN SPEED SCHEDULE	MODEL HEIGHT (FT)	ANGLE OF ATTACK (DEG.)	AILERON DEFLECTION (δ_A) (DEG.)	FLAP DEFLECTION (δ_F) (DEG.)	STABILIATOR DEFLECTION (δ_H) (DEG.)	INLET SHIELD CONFIGURATION	
26	1	90	0	0	1190	0	90	0	0	1190	0	95	0	0	8.3	0	10	15	0	OFF	
	2					2000					2000			2000							
	3					2700					2700			2900							
	4					3600					3600			3600							
	5					4000					4050			4050							
	6					3600					3600			3600							
	7					0					2000			1050							
	8					↓					2700			3600							
	9										4050			↓							
	10										2000			3600							
	11										2900			↓							
	12										3600			0							
	13										↓			↓							
	14										0			2000							
	15										↓			2900							
	16										↓			3600							
	17										↓			4050							
27	1										2900			3600							
	2										3600	↓		1050							
28	1										0	102		3600							
	2										3600	↓		↓							
29	1										0	80		0							
	2										↓	↓		↓							
	3										↓	↓		3600							
	4										↓	↓		↓							
	5										0	↓		2000							
	6										↓	↓		2700							
	7	↓	↓	↓	↓	↓	↓	↓	↓	↓	↓	↓	↓	3600	↓	↓	↓	↓	↓	↓	↓

RUN NUMBER	NUMBER OF TEST POINTS	LIFT/CRUISE UNIT - LEFT SIDE						LIFT/CRUISE UNIT - RIGHT SIDE						FORWARD FAN UNIT			A/C POSITION		MODEL CONFIGURATION			RUN PURPOSE
		NOZZLE VECTOR ANGLE (DEG.)	YAW VANE DEFLECTION (DEG.)	SPOILAGE PORT OPENING (%)	NOZZLE EXIT CONFIGURATION	FAN SPEED SCHEDULE		NOZZLE VECTOR ANGLE (DEG.)	YAW VANE DEFLECTION (DEG.)	SPOILAGE PORT OPENING (%)	NOZZLE EXIT CONFIGURATION	FAN SPEED SCHEDULE		LOUVER VECTOR ANGLE (DEG.)	YAW VANE DEFLECTION (DEG.)	FAN SPEED SCHEDULE	MODEL HEIGHT (FT)	ANGLE OF ATTACK (DEG.)	AILERON DEFLECTION (δ_A) (DEG.)	FLAP DEFLECTION (δ_F) (DEG.)	STABILATOR DEFLECTION (δ_H) (DEG.)	INLET SHIELD CONFIGURATION	
30	1	90	+12	0	1170	0	3600	90	-12	0	11.0	0	3600	95	+12	3400	8.3	0	10	15	0	OFF	
	2																						
	3																						
	4																						
	5																						
31	1		0			2000			0			2000			0	2000						S2-0	
	2					2900						2900				2900							
	3					3400						3400				3400							
	4															4174							
	5															3400							
	6					2900																	
32	1					3400								80									
33	1													102									
	2					0						0		90		2700							
	3															3400							
	4		Y													1800							
34	1		+12	1	1	3400		1	-12	1	1	3400		85	+12	2400							

F.O.T.